Journal of The Iron and Steel Institute

JANUARY 1957
Vol. 185 Part 1

Published Monthly

Editorial contents copyright by
The Iron and Steel Institute

EDITOR
K. Headlam-Morley

MANAGING EDITOR
E. R. Mort, B.SC., F.I.M.

PRODUCTION EDITOR
H. F. Cleere, B.A.

ASSISTANT EDITOR
Elizabeth S. Fairhurst

EDITORIAL AND ADVERTISEMENT OFFICES

4 Grosvenor Gardens, London, S.W.1
SLOane 0061
Telegrams - - Irosamente, Sowest

SUBSCRIPTIONS

Members Free - Extra Copies Prices on application
Non-members - £10.0.0 per annum
Single Copies £1 each
Packing and Postage 1s. per copy

NOTE

The Institute as a body is not responsible for statements made or opinions expressed in papers, articles, or discussions appearing in the Journal of The Iron and Steel Institute.

Contents

PROCEEDINGS OF THE INSTITUTE

Report of Special Meeting in France, 1956 1

THE IRON AND STEEL INSTITUTE

The Study of Fracture Surface Markings *by C. F. Tipper* 4

The Formation of Carbide in Low-carbon Chromium–Vanadium Steels at 700°C *by S. W. K. Shaw and A. G. Quarrell* 10

Investigation of the Behaviour of Metals under Deformation at High Temperatures *by C. H. M. Jenkins and E. A. Jenkinson* 23

The Direct Measurement of the Total Heat in Open-hearth Furnaces *by A. M. Godridge and G. G. Thurlow* 46

Thermodynamics of Slag Systems *by P. T. Carter and T. G. Macfarlane*
Part I: The Thermodynamic Properties of $CaO–Al_2O_3$ Slags 54
Part II: The Thermodynamic Properties of $CaO–SiO_2$ Slags 62

Observations on the Mechanical Behaviour of Heat-treated Steels at High Hardness Levels *by N. H. Polakowski* 67

An Investigation of the System $2FeO.SiO_2–3Na_2O.P_2O_5–Na_2O.2SiO_2$ *by C. Bodsworth and W. R. Maddocks* 75

The Laboratory Production of Cylindrical Crucibles of 5½ Litres Capacity *by V. H. Stott* 82

LETTERS TO THE EDITOR

The Identification of Microscopic Spherical Inclusions in Electric Furnace Steel *by R. M. Glaister* 103

Rapid Solution of Oxygen in Molten Iron Oxide Slags *by E. T. Turkdogan and D. J. Goodwin* 104

AFFILIATED LOCAL SOCIETIES

Production Control Quantometer for Steelworks Analysis *by D. Manterfield and W. Sykes* 105

BRITISH IRON AND STEEL RESEARCH ASSOCIATION

Sinter-plant Assessment Trials at Margam, Steel Company of Wales Limited *by C. Lang and H. Bates* 86

The Alcoholic-Iodine Method for the Extraction of Inclusions from Steels *by J. E. Garside, T. E. Rooney, and J. J. J. Belli* 95

NEWS 114 **ABSTRACTS** 118

THE IRON AND STEEL INSTITUTE, 4 GROSVENOR GARDENS, LONDON, S.W.1

Wellman-Galusha Gas Producers

A battery of seven 10′ 0″ diameter Wellman-Galusha Gas Producers, for gasifying Natal anthracite coal—under construction at Vereeniging, Transvaal, South Africa. The installation is one of the most extensive gas producer plants to be erected initially as one battery in the British Commonwealth.

Wellman-Galusha Gas Producers can be supplied in 6′ 0″, 8′ 0″ or 10′ 0″ diameters and will produce an ideal gas for all industrial purposes.

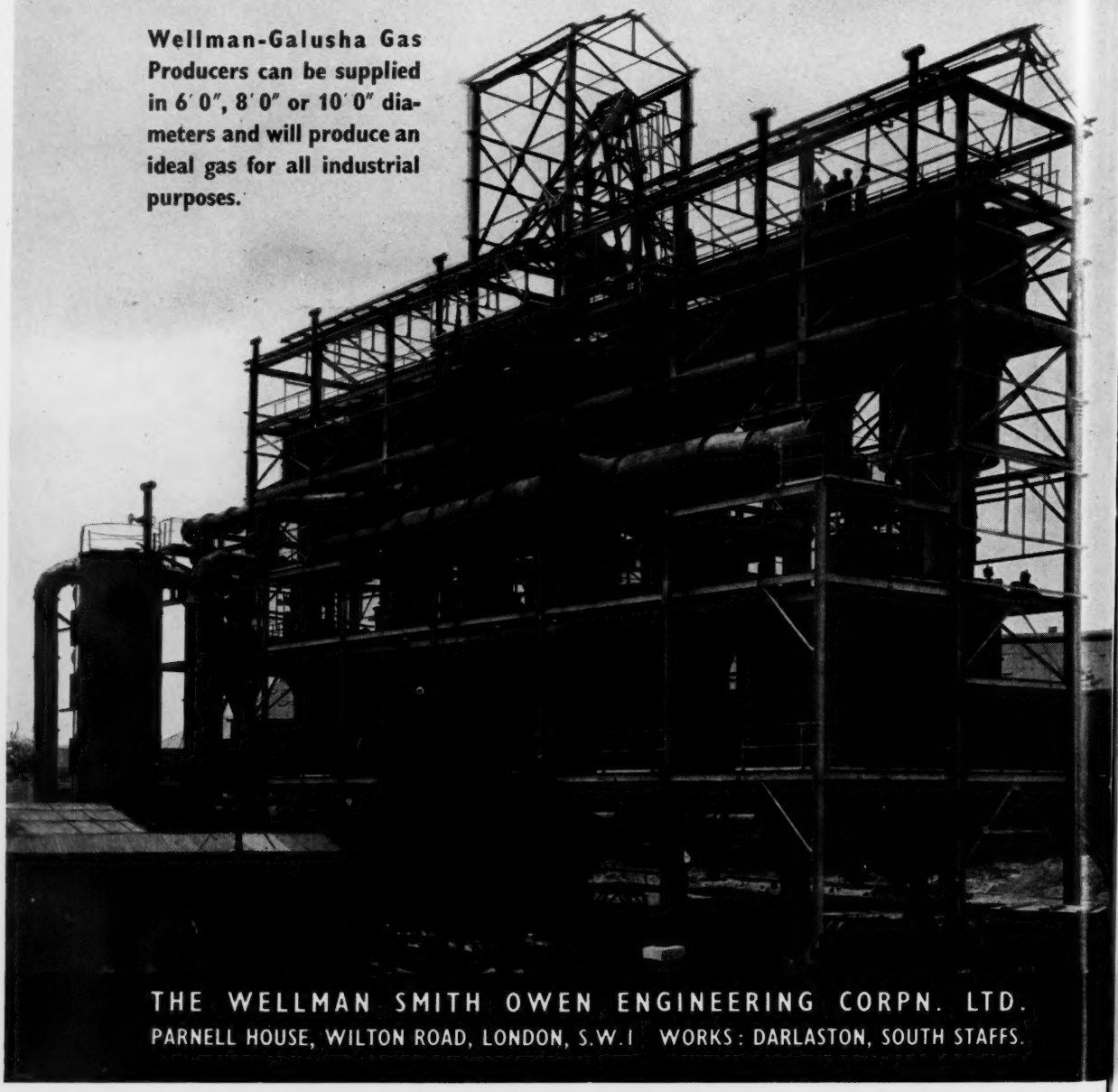

THE WELLMAN SMITH OWEN ENGINEERING CORPN. LTD.
PARNELL HOUSE, WILTON ROAD, LONDON, S.W.1 WORKS: DARLASTON, SOUTH STAFFS.

H. H. UTLEY, A.M.I.Mech.E., A.I.M.

HERBERT HENRY UTLEY was educated at Rotherham Grammar School and the Applied Science Department of Sheffield University. His career began as an engineering apprentice with the United Steel Companies Ltd., at their Rothervale works. After a period as assistant to the Engineer, he transferred in 1931 to the Companies' Central Fuel Department. In 1940 Mr. Utley took up an appointment with the Skinningrove Iron Co., Ltd., as Night Superintendent; nearly two years later he became Assistant Works Manager. He left Skinningrove in 1945 to join Dorman Long and Co., Ltd., as Assistant Works Manager of their Cleveland works, and he was promoted to Works Manager in 1954.

Mr. Utley, who has been a Member of The Iron and Steel Institute since 1941, is an Associate Member of the Institution of Mechanical Engineers, a Fellow of the Institute of Fuel, and an Associate Member of the Institution of Metallurgists. He is a member of several committees of the British Standards Institution, a member of council of the Cleveland Scientific and Technical Institution, and a member of the Advisory Committee of the Eston Technical School. A member of council of the Cleveland Institution of Engineers since 1945, Mr. Utley was elected President for the 1955–1956 session; as such, he served as an Honorary Member of Council of The Iron and Steel Institute during his term of office.

H. H. Utley, A.M.I.Mech.E., A.I.M.

Honorary Member of Council, 1955–1956

PROCEEDINGS OF

THE INSTITUTE

Reports of Council · Meetings · Notices

Special Meeting in France, 1956

A SPECIAL MEETING of The Iron and Steel Institute was held in France from Tuesday, 5th June, to Thursday, 14th June, 1956, by invitation of the Chambre Syndicale de la Sidérurgie Française and the Société Française de Métallurgie.

The programme consisted of six days in Paris, followed by two alternative tours to Central France and to Lorraine. Two Technical Sessions were held in Paris on the mornings of Wednesday and Friday, 6th and 8th June, 1956. A number of social functions were arranged, and a special programme provided for the Ladies.

ORGANIZATION

A RECEPTION COMMITTEE was formed in Paris, of which Monsieur Jean Raty, President of the Chambre Syndicale de la Sidérurgie Française, acted as Chairman, and Baron Walckenaer, President of the Société Française de Métallurgie, as Vice-Chairman. A Ladies Committee was also formed with Madame Raty as Chairman and Baronne Walckenaer as Vice-Chairman. Detailed arrangements were made in France by Dr. E. Dupuy, Past President and Honorary General Secretary of the Société Française de Métallurgie, and Monsieur Maurice de Courcel, Administrative Secretary of the French Society, and by Monsieur P. Gouge, Honorary Secretary of the Société Métallurgique de Normandie.

A detailed Programme of the Meeting with biographies of the principal French hosts is given on pp. 15–18 of the May, 1956, *Journal*.

OPENING SESSION

A Plenary Opening Session was held in the Grand Amphithéâtre of the Sorbonne on the afternoon of Tuesday, 5th June. Monsieur Jean Raty, Chairman of the Reception Committee, was in the Chair. Monsieur Raty welcomed the Members and Ladies of The Iron and Steel Institute on behalf of the Reception Committee, and the President, Dr. H. H. Burton, C.B.E., replied.

Baron Walckenaer and Dr. H. H. Burton, C.B.E., announced the following awards:

By the Société Française de Métallurgie

Dr. **H. H. Burton,** C.B.E. (President) and Mr. **K. Headlam-Morley** (Secretary) to be Honorary Members. Silver Medals of the Society were also presented to them.

By The Iron and Steel Institute

Monsieur **Jean Raty**, Président de la Chambre Syndicale de la Sidérurgie Française, and Monsieur **Henri Malcor**, Président de l'Institut de Recherches de la Sidérurgie, to be Honorary Members.

Baron **Walckenaer**, Président de la Société Française de Métallurgie, and Dr. **Eugène L. Dupuy**, Past-President and Honorary General Secretary of the Société Française de Métallurgie, to be Honorary Vice-Presidents.

Greetings from the American Institute of Mining, Metallurgical and Petroleum Engineers and the American Society of Metals were read by Dr. Howard Biers, Honorary Member. The texts of the messages are given on p. 433 of the August, 1956, *Journal*.

The President also presented a coloured reproduction of the portrait of Sir Henry Bessemer, F.R.S., by Rudolf Lehmann to Professor A. M. Portevin, Honorary Member of the Institute and Bessemer Gold Medallist.

The Session closed with a Lecture on "Sir Henry Bessemer" by Monsieur G. Delbart, Director of the Institut de Recherches de la Sidérurgie. The text is given on pp. 190–195 of the June, 1956, *Journal*.

TECHNICAL SESSIONS

Two Technical Sessions were held jointly with the Société Française de Métallurgie on the mornings of Wednesday and Friday, 6th and 8th June, at the Chambre Syndicale de la Sidérurgie Française, 25, Rue de Madrid, Paris. The papers presented at these Sessions are listed on pp. 15–17 of the May, 1956, *Journal*, and a report of the discussions will be published later.

PROGRAMME IN PARIS

The Meeting began on Tuesday, June 5th, with a Reception for the Members and Ladies, given by the Chamber of Commerce of Paris at 27, Avenue Friedland. This was followed by lunch on board a 'Bateau Mouche' on the River Seine. Members and Ladies had interesting views in excellent weather of the Seine bridges and of

the many beautiful and historic buildings of Paris. The afternoon was devoted to the Plenary Opening Session at the Sorbonne. In the evening Members and Ladies attended a reception and buffet at the Louvre, many of the art treasures of which were illuminated.

On Wednesday, 6th June, in the morning there was a Technical Session. In the afternoon, Members were able to visit one of the following works—Régie Nationale des Usines Renault, Billancourt Works; Société Nationale d'Étude et de Construction de Moteurs d'Aviation, Kellermann Works; Centre Technique des Industries de la Fonderie, Sèvres; Institut de Recherches de la Sidérurgie (IRSID), St. Germain-en-Laye; Société Industrielle de Mécanique et de Carosserie Automobile (SIMCA), Poissy Works; Centre d'Études Nucléaires du Commissariat à l'Energie Atomique de la France; and Central Arrighi de l'Electricité de France—or to visit the Supreme Headquarters Allied Powers in Europe (SHAPE), where they heard a lecture from General A. Gruenther, the Supreme Commander.

The Ladies had the morning free and in the afternoon were the guests of Madame Charles Schneider at a reception and tea at her house at 25, Rue Octave Feuillet, Paris.

In the evening many Members and Ladies attended a performance of Verdi's opera " Otello " at the Opera House.

On Thursday, 7th June, Members could either visit the works of the Société Métallurgique de Normandie at Mondeville, near Caen, all day, or the laboratories of the Institut de Recherches de la Sidérurgie (IRSID), St. Germain-en-Laye, in the morning, and the Flins Works of the Régie Nationale des Usines Renault in the afternoon. Ladies were able either to travel to Caen with the Members, or to visit St. Germain-en-Laye for lunch with Members in the Pavillon Henri IV, and go to Malmaison during the afternoon.

Members and Ladies who visited Caen also had the opportunity of seeing the ' Mulberry Harbour ' Museum of Arromanches and the Tapestries at Bayeux.

On Friday, 8th June, the second Technical Session was held in the morning, and in the afternoon there were alternative visits to the following works—Régie Nationale des Usines Renault, Billancourt Works; Société Industrielle de Mécanique et de Carosserie Automobile (SIMCA), Nanterre Works; Société des Tréfileries et Laminoirs du Havre, St. Maurice Cable Works; Institut de Recherches de la Sidérurgie (IRSID), St. Germain-en-Laye; Station d'Essais de la Recherche Scientifique, Vitry Laboratory; and Centre National de Calculateurs Electroniques.

The Ladies had the morning free and in the afternoon attended a Fashion Parade by invitation of Monsieur Christian Dior. In the evening Members and Ladies were guests of the Reception Committee at a banquet and dance in the Orangerie of the Palace of Versailles. Baron Walckenaer was in the Chair and welcomed Members and Ladies on behalf of the Committee. Dr. H. H. Burton, C.B.E., President of the Institute, replied. A speech of welcome was also made on behalf of the French Government. Arrangements had been made for Members and Ladies to see the Spectacle de Son et Lumière in the Palace Gardens. Owing to the weather, it was only possible for part of this performance to be given. At the Dinner all the staff were dressed in costume of the time of Louis XV, including the Toastmaster, who was dressed in the uniform of the Grand Chamberlain. The floodlit 18th century Orangerie was a wonderful spectacle. It was only sad that the full enjoyment of this unique occasion was marred by very cold and wet weather.

On Saturday, 9th June, Members and Ladies were able to visit either the Château of Chantilly, the Cathedral of Chartres, or the Palace and Forest of Fontainebleau. Special guides for Chartres and Fontainebleau were provided by the Ministry of Fine Arts. These expeditions were greatly enjoyed.

On Sunday, 10th June, an excursion was arranged to Chantilly race course to see the Prix du Jockey Club de France (the French Derby). Owing to the very inclement weather only a few dozen Members and Ladies attended.

The Meeting in Paris concluded on Sunday, 10th June. The general impression was one of great enjoyment. Hospitality was boundless, the technical interest agreeably high, and the distinction of Paris can surmount weather which would have been more readily accepted on the other side of the Channel.

Many Members and Ladies left the Meeting at this point, but others took part in excursions to Central and Eastern France. An excursion to Northern France with visits to three Works near Lille—Union Sidérurgique du Nord de la France (USINOR), Denain Works; Compagnie de Fives-Lille pour Constructions Mécaniques et Entreprises; and Etablissements Arbel—did not take place.

EXCURSIONS TO CENTRAL AND EASTERN FRANCE

Central France

Members and Ladies left Paris by train on the afternoon of Sunday, 10th June, and spent the night at Chalon-sur-Saône.

On Monday, 11th June, Members visited the works of Société des Forges et Ateliers du Creusot, and were the guests of the Company throughout the day. The Ladies visited Beaune and the wine-growing districts of Burgundy and Autun. They joined the Members for tea at Le Creusot, where they were most hospitably entertained by Monsieur and Madame Charles Schneider at La Verrerie. In the evening Members and Ladies travelled by special train from Le Creusot to Lyons where they spent the night. On Tuesday, 12th June, Members visited the works of Compagnie des Ateliers et Forges de la Loire at Firminy, Unieux, and St. Chamond with lunch and tea at the Château de Jarez. The Ladies visited Bourg and Nantua and joined the Members for tea. Members and Ladies had dinner at St. Etienne and took the night train back to Paris where they dispersed.

Members and Ladies who took part in this excursion are grateful to all who attended to their welfare, and particularly to Monsieur and Madame Charles Schneider, the staff of Le Creusot, and Monsieur and Madame Henri Malcor and their colleagues at Firminy.

Eastern France

Members and Ladies left Paris by train on the morning of Monday, 11th June, and travelled to Metz where they spent two nights. They were received at lunch by the Chambre Syndicale de la Sidérurgie de la Moselle. In the afternoon Members visited the Rombas Works of the Union Sidérurgique de Lorraine (SIDELOR), and the Ladies visited Douaumont and Verdun.

On Tuesday, 12th June, Members visited the Works of Société Lorraine de Laminage Continu (SOLLAC) with lunch at the works. The Ladies visited Metz Cathedral and other places of historic interest in Metz and joined the Members for lunch at SOLLAC. In the afternoon the Members and Ladies visited the workmen's housing estates at SOLLAC.

In the evening there was an informal dance at the Globe Hotel, Metz, where Members and Ladies were able

to return some of the hospitality offered to them in Lorraine.

On Wednesday, 13th June, Members were able to visit one of the following works at Longwy—Société Anonyme des Hauts Fourneaux de la Chiers; Société Anonyme des Hauts Fourneaux, Forges, Fonderies et Usines de la Providence, Réhon Works; or Société Lorraine-Escaut, Mont-St-Martin Works. They were entertained to lunch by the Union des Mines et de la Métallurgie de Longwy, and in the afternoon visited the Central Power Station and Tonnage Oxygen plant at Herserange, near Longwy. The Ladies visited Longuyon and Avioth and joined the Members for tea at Longwy. Members and Ladies had dinner in the hotels at Metz and returned either to Paris, or by special sleeping-car train to Calais for London.

All Members and Ladies who took part in the Meeting will remember the generous hospitality provided by the French hosts, the great technical progress made in many of the works, and the beauty of much they were shown. Despite the inclement weather, those who attended will look back on the Meeting with interest, gratitude and pleasure.

The President and Council of the Institute wish to express their thanks to the Presidents and Council of the Chambre Syndicale de la Sidérurgie Française and of the Société Française de Métallurgie: to the Chairmen, Vice-Chairmen, and Members of the Reception and Ladies Committees; to the President of the Chamber of Commerce of Paris; to the Chambre Syndicale de la Sidérurgie de la Moselle and the Union des Mines et de la Métallurgie de Longwy; to Dr. E. Dupuy, Past President and Honorary General Secretary of the Société Française de Métallurgie and to Monsieur P. Gouge, Honorary General Secretary of the Société Métallurgique de Normandie; to General A. Gruenther and Staff of Supreme Headquarters Allied Powers in Europe; to the managements of the works and other establishments in France who kindly invited Members and Ladies to visit them; and to the authors of papers and all others who collaborated in organizing the Meeting.

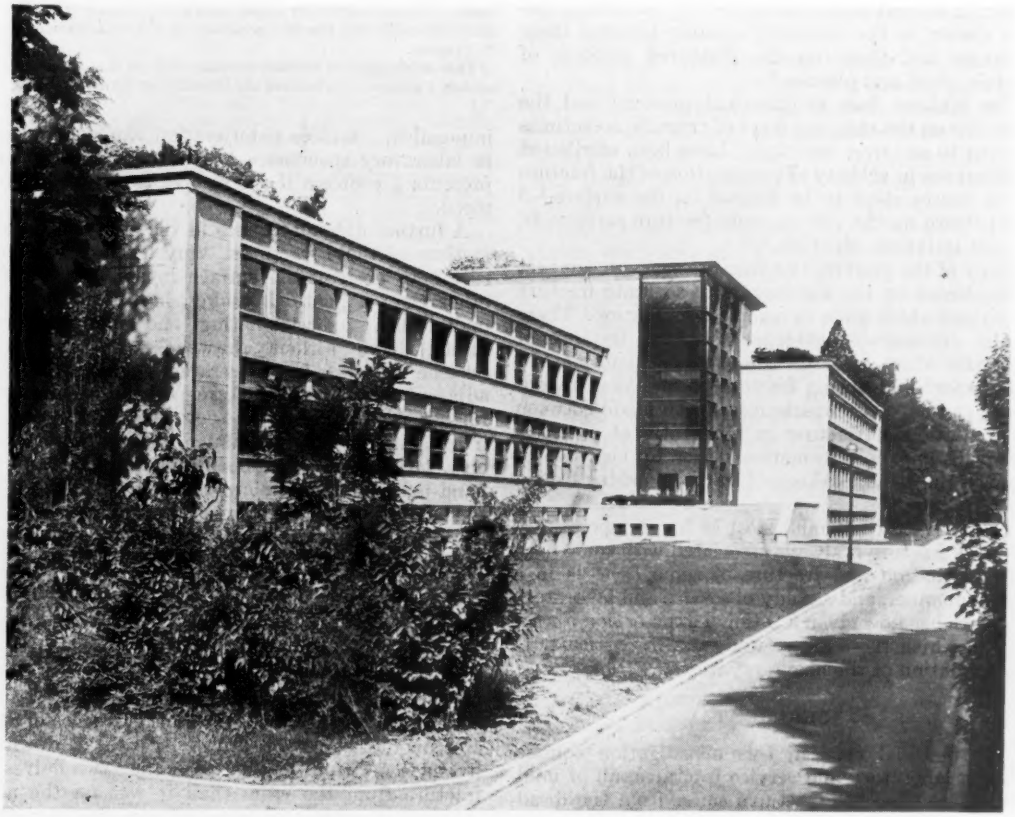

General view of the laboratories of the Institut de Recherches de la Sidérurgie (IRSID) at Saint Germain-en-Laye

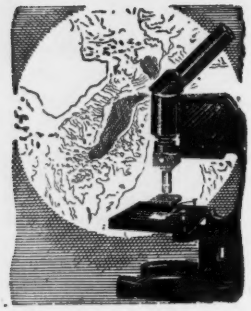

PAPERS AND REPORTS ON RESEARCH AND PRACTICE

Metallurgy • Plant Operation • Research

The Study of Fracture Surface Markings

By C. F. Tipper, Sc.D.

SYNOPSIS

A detailed investigation of a fractured plate from an oil-storage tank has shown that the surface markings are due to the arrest and re-initiation of the fracture. Cracks which are approximately parallel and staggered are joined by shear of the bridges of metal separating them. Discontinuities, or steps, are left on the fractured surfaces since the individual fracture zones are at different levels and tend to overlap.

This mechanism of breakdown can occur on a microscopic scale and on a gross scale wherever the fractures are chiefly brittle. 1202

THE CHARACTERISTIC PATTERN, always present to some degree on the fractured surfaces of structural mild steel which has broken in a ' brittle ' manner—the so-called ' chevron pattern '—has been discussed in several publications.[1, 2, 4, 5] Attention has been drawn to the similarity existing between these markings and those on the fractured surfaces of crystals, glass, and plastics.[2]

The Wallner lines in glass and plastics[7] and the striations on the cleavage faces of crystals, sometimes referred to as ' river markings,' have been attributed to difference in velocity of propagation of the fracture which causes steps to be formed on the surface.[2, 3] The pattern on the two opposite fracture surfaces is, in most instances, identical.[5, 6]

Many of the markings on fracture surfaces can best be explained on the assumption of separate fracture initiations which unite to complete separation. There is also considerable evidence that the fracture of materials which undergo some plastic deformation, both before and during fracture, is always a discontinuous process. Comparison has been made between the initiation of fracture in the centre of a tensile test-piece and hole formation either by cleavage or shear in the neighbourhood of fractures arising from a notch.

In the fracture of mild steel at low temperatures, cleavage fracture is always associated with some plastic deformation and fracture of some crystals in a normal manner, and a study of service and laboratory fractures has now given a rational explanation for the way in which these are related, and in particular to the formation of the chevron pattern.

EXPERIMENTAL

The material used in this investigation consists of both laboratory and service fractures, all of mild-steel plate. Service fractures suffer from the disadvantage that they are usually badly rusted and corroded, and even when both halves of a fracture are recoverable, exact registration of a particular region is impossible. Surface deterioration can be prevented in laboratory specimens, but exact registration still presents a problem if the sample is completely fractured.

A further difficulty arises in the study of polished sections of these fractures. Any attempt to remove rust may destroy the surface layers, and cleaning, other than a gentle brushing, has been considered undesirable. Electroplating and mounting in a plastic have serious drawbacks since solutions become trapped in the cracks running into, and adjacent to, the main fracture, and cause staining and further rusting. All the sections prepared for this investigation were unmounted. They were ground on a surface grinder, rubbed down on lead laps, and hand-polished. Photomicrographs show that, although some detail of the fracture edges may have been lost, the damage was slight and gross irregularities were unaffected.

MACROSTRUCTURE OF CHEVRON MARKINGS

Examination of a number of service and laboratory fractures has now confirmed the following observations. Some of these were facilitated by making plaster casts of the fractured surfaces. The cast accentuates the gross pattern at the expense of detail. Moreover, the plaster was easily rubbed down and it was found to be easier to ' match ' two halves of a fracture from the casts than it was on the actual

Manuscript received on 3rd August, 1955.

Dr. Tipper is Reader in the Department of Engineering, Cambridge University.

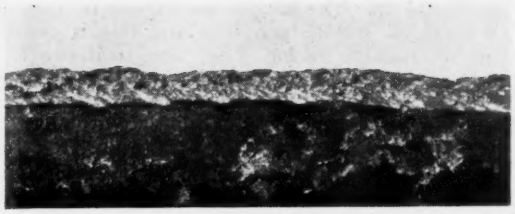

Fig. 1—Plate from fractured oil-storage tank showing chevron pattern and waviness on plate surface

steel specimens. The observations enumerated below are illustrated by photographs.

(1) Some reduction in thickness of the plates near the fracture, sometimes extending to $\frac{1}{2}$ in. from the surface, is usually observed: it may be as much as 5%

(2) The extreme edge is wavy. Figure 1, which is a photograph from a service fracture, shows how the waviness of the edge is related to the chevron pattern. Figures 2*a* and *b* give two views of plaster casts made from a test-piece broken in the laboratory. When the chevron pattern is very marked, the waviness is pronounced. It is often difficult to identify, but it is always present (cf. Fig. 3). Figure 4 is a photomicrograph of the fractured edge of a polished test-piece, broken at such a low temperature that a surface chevron pattern was not visible to the naked eye. The irregularities are here only a few crystals in extent, but they show how the pattern is composed of alternating ductile and brittle zones

(3) Depressions on one face coincide with protuberances on the other. This is very clearly shown in Figs. 2*a* and *b*

(4) Surface markings are due to differences in level and consist of a series of intermittent ridges running approximately parallel with the plate faces in the centre of the plate and curving outwards towards the surfaces to form the characteristic chevron pattern. It follows from (3) that the chevron pattern gives rise to steps, some of which are steps 'up', with corresponding steps 'down' in respect to the direction of fracture propagation. It has been observed that there is a tendency for all the steps to face the same way over a length of fracture, but they may also face one way towards one surface and in the opposite direction towards the other. This has always been noticed in plates which were slightly bent.

MICROSTRUCTURE

Internal cracks have been observed in many fractures to a depth of 0·3 in. from the surface. Some of these are clearly running in from the main fracture, and nearly parallel to it, for up to $\frac{1}{2}$ in. Most of the crystals have broken by cleavage, alternating with some plastic deformation and failure by shear. Intercrystalline failure is rare, but cracks have been observed starting from, and following round, non-metallic inclusions.

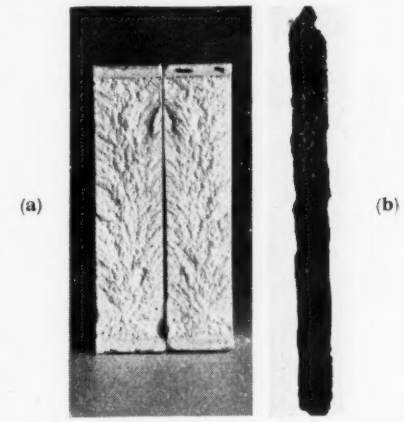

Fig. 2—Plaster casts made from plate fractured in the laboratory: (*a*) shows the two surfaces, (*b*) the side view

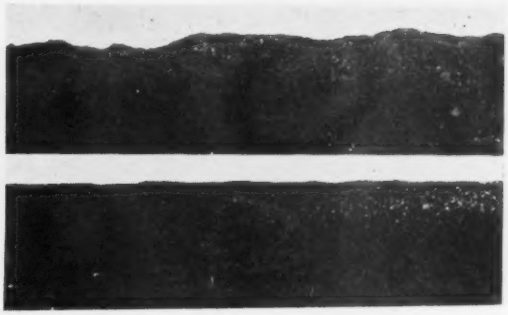

Fig. 3—Irregularities of fracture surfaces as seen from plate surfaces; upper plate 0·82 in., lower 0·57 in.

EXAMINATION OF A SERVICE FRACTURE

A sample of plate, nominal thickness $\frac{31}{32}$ in., from an oil-storage tank which had failed in service was selected, in order to relate macrostructure with microstructure.

The actual plate thickness, about $\frac{1}{2}$ in. from the fractured surface, was 0·94 in. A sample about 1 in. × 0·8 in., in the direction of fracture, showed marked irregularities, some running parallel with the plate surface, some forming both types of chevrons. The cut faces perpendicular to the fractured surface were ground parallel and the face furthest from the origin, referred to as face 1, was prepared as described earlier. After measurement with a micrometer, a tracing of the fractured edge was made at a magnification of 10 and, after a metallographic polish, at a magnification of 100. The lower magnification was sufficient to give the general outline, but the higher magnification was required to show detail, and finer cracks were looked for and examined at still higher magnifications.

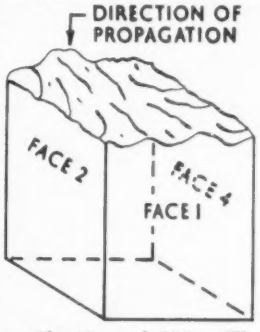

After tracing and photographing where desirable, the surface was reground. The process was repeated, the amount removed by each successive grinding being recorded with the corresponding tracings. Figure 5 shows the series of tracings obtained from face 1. The amount of material removed by each operation is shown vertically and the direction is towards the fracture origin.

After 0·045 in. had been removed, sufficient to show the change in crack distribution, both faces 2 and 4 were treated similarly. Figures 6 and 7 show the fracture contours as the material was removed by

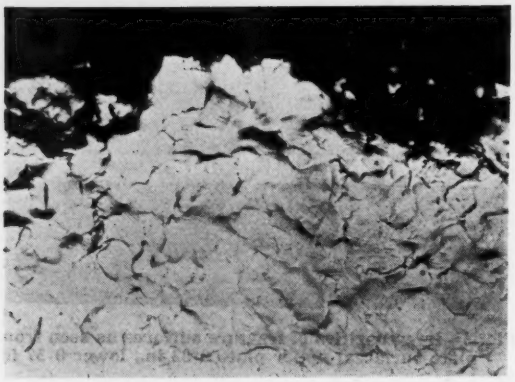

Fig. 4—Notched test-piece polished before fracture. Note alternate zones of cleavage and plastic deformation × 500

grinding parallel with faces 2 and 4, and the position of each tracing is indicated by the numbered vertical lines marked on Fig. 5. The fracture direction is now indicated by means of an arrow.

The tracings show the general trend in the gross surface irregularities as material is removed in the direction of fracture propagation and perpendicular to it. The magnification is insufficient to show details which could be fully studied in the tracings made at a magnification of 100. As it is impossible to reproduce the larger tracings, special details are illustrated by means of a few photomicrographs, and the general trend as revealed by repeated examination described.

DESCRIPTION AND SUMMARY OF FRACTURE SECTIONS

Face 1

Figure 5 shows that there was considerable local drawing-down of the plate thickness without an appreciable lip. The sample was chosen because of the depth of surface markings and this is clearly brought out in the tracing. There were small cleavage cracks at intervals along the surface and large groups of cracks and holes situated at varying distances below the surface.

Reference has been made to the two forms of 'steps' made by the chevrons, and the object of sectioning was to ascertain whether the steps resulted from the fracture running in and stopping, or whether cracks originated below the surface and ran out. If the first, each succeeding layer removed, taking the section *towards* the origin, should show the groups of cracks increasing and the holes becoming larger. Conversely, cracks originating below the surface and growing out would tend to decrease in extent and to be removed. In fact, both types were observed, but by far the larger number increased in size, indicating that most of the subsidiary cracks were due to branches from the main fracture running in and stopping.

The structure was confused by the number of branching cracks that must have spread transverse to the main direction of propagation. The highest concentration of cracks occurred in the centre of the plate, where the cracks also occurred to a greater depth. These observations are in agreement with what is known of the stress distribution across the plate thickness. The relative freedom of the outer layers from internal fracture (no cracks were observed to run out to the surfaces) is in accordance with what is known of the properties of free surfaces. Cleavage cracks in the surface layers have been observed in more brittle material, an example being shown in Fig. 4.

Faces 2 and 4

Figures 6 and 7 are the tracings made by removing successive layers from the two plate surfaces, i.e. perpendicular to face 1.

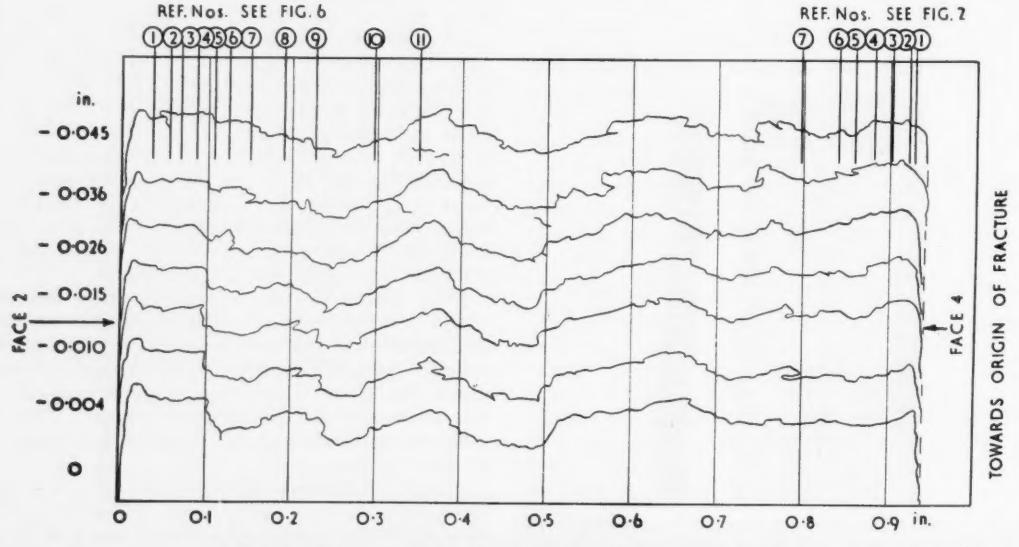

Fig. 5—Tracings of sections through fracture: face 1

Face 2 contained a large step where the section cuts one arm of a ' chevron ', and the tracings show clearly how such a step may be caused. It also shows how the deep branching crack running into the metal below the main fracture is smoothed out towards the surface of the plate.

Towards the plate centre (Nos. 9, 10, and 11, where the ridges run parallel with the plate surfaces) both types of step occur, i.e. those facing towards and away from the direction of fracture propagation.

On face 4, the largest chevrons were representative of those turned away from the direction of propagation. These are clearly marked and their smoothing-out towards the surfaces is also brought out in the successive tracings.

In addition to the gross irregularities, there are numerous smaller ones which can be regarded as sections through chevrons in miniature.

Microstructure

Details of the original surface were partly obliterated by damage and rust, but Figs. 8–12 are characteristic of the structure. Cleavage alternates with distorted grains, cleavage cracks running in from the surface at various angles, but chiefly inclined at an angle facing towards the main direction of propagation. Thus a directional effect is conferred, such as is shown specially in Fig. 8. Moreover, most of the cracks and groups of cracks are related to the main fracture in the same pattern. Individual cracks and groups take up positions roughly parallel with the main fracture, but inclined to it at relatively small angles. Small parallel cracks may occur in individual crystals (Fig. 10) or groups of cracks spread over a number (Figs. 9–11), and at more advanced stages of fracture they develop into large holes (Fig. 11), opening eventually into the main fracture. Severe

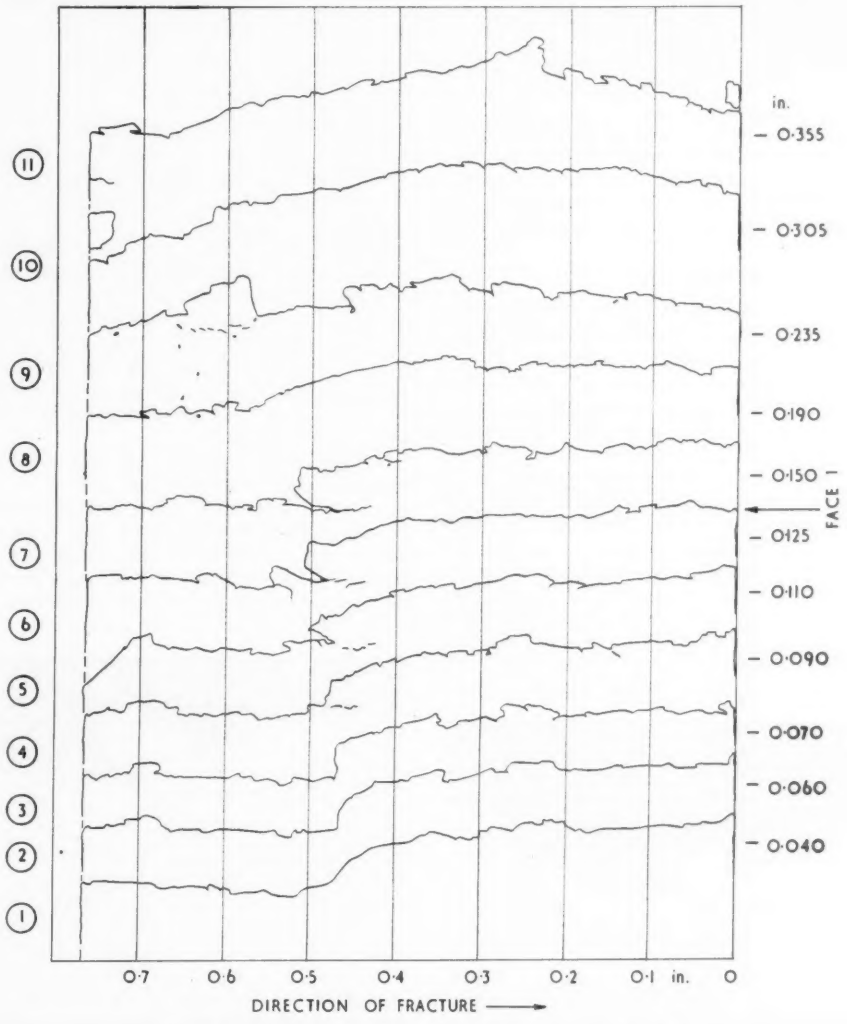

Fig. 6—Tracings of sections through fracture: face 2

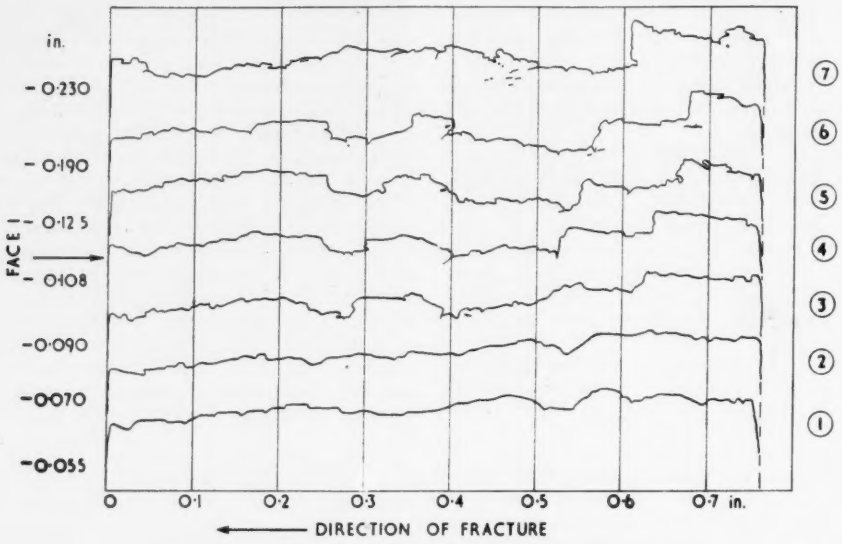

Fig. 7—Tracings of sections through fracture: face 4

local surface deformation has always been found in the faces of the ridges making the chevron, and Fig. 12, taken on face 4, stage 5, shows how extensive it may be.

It is now possible to put forward an explanation of the mechanism of propagation of this fracture.

CONCLUSIONS

The discontinuous theory of fracture propagation has received considerable support from these results.

Starting from the smallest cracks, such as are shown in Fig. 9, up to large-scale overrunning cracks, and even to service fractures, where overlapping fractures are not uncommon,[8] the same processes are involved in propagation. Unless the cracks occur end-to-end, so that they can unite by the simple process of extension in the manner envisaged by Griffith, they must join by the breaking-down of the material separating them, either by secondary cleavage, in the case of single crystals, or by shear. Failure by shear seems to be the usual mode of breakdown of the bridges between cracks. An example was shown in Fig. 11 of an earlier paper[5] of the interruption and re-initiation of fracture in silicon–iron crystals analogous to the breakdown which appears to have occurred in many fractures of polycrystalline mild steel. Such a process inevitably leaves a step, and these steps cause the markings left on the cleavage faces of crystals, or give rise to striations and chevrons in polycrystalline metals and plastics.

It might be expected that the mean path of fracture should be maintained perpendicular to the principal tensile stress, and that secondary fractures deviating from this direction would be arrested in a ductile material. Branching of fractures in glass and plastics is characteristic of high-velocity propagation, but the opposite appears to follow where branching leads to a greater amount of plastic deformation such as occurs in ductile metals.

Figures 13*a* and *b* show diagrammatically how these fractures may progress and produce the structure described. The tendency for fracture to continue into the metal and form under-surface cracks is always greatest in the direction in which the fracture is moving. This tendency is indicated by dotted lines. Some cracks have been observed at the base of the sharp discontinuities facing away from the fracture

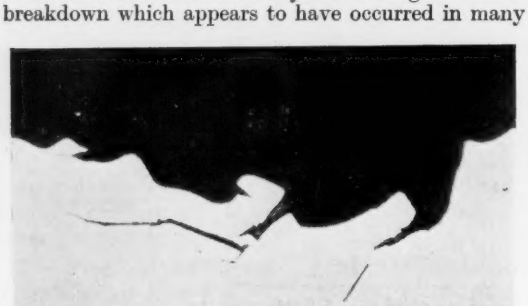

Fig. 8—Edge of fracture, face 2. Direction of propagation from right to left × 150

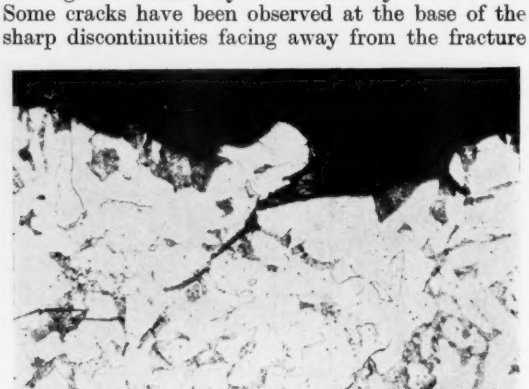

Fig. 9—Edge of fracture, face 2. Direction of propagation from right to left × 150

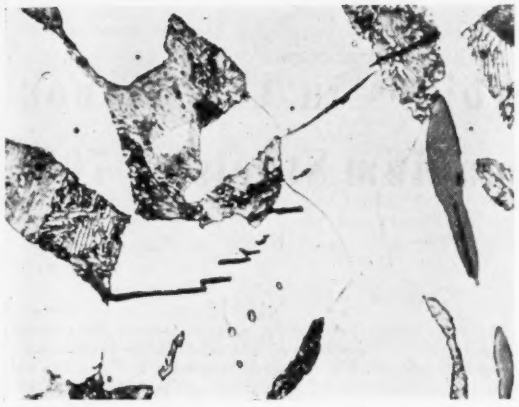

Fig. 10—Typical groups of microscopic cracks × 800

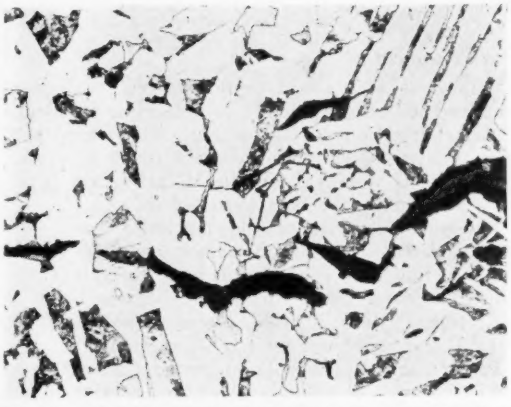

Fig. 11—Typical groups of cracks in various stages of enlargement × 150

origin, but these are far less extensive, so that a directional structure is imparted to the fractures. Centres of possible new origins are marked ×. They probably occur at positions of maximum tensile stress and the fracture spreads in both directions as indicated by the small arrows, but their exact location has not yet been ascertained. Shaded regions show where failure occurs by shear.

As already noted, internal cracks also spread in a transverse direction. The direction of spread was not equal towards both surfaces, in agreement with the asymmetry of the chevron markings. Attention has been drawn to this characteristic in previous publications,[1] and it is probably due in this instance to the bending of the plates before the construction of the tank. The curvature of the chevrons outward towards the surfaces of the plates, however, seems to be accounted for by assuming that plastic flow increases towards the surfaces with a corresponding retardation of velocity of propagation. Arrested fractures generally show that the centre of the plate has fractured ahead of the surfaces, the extent of advance depending upon the relative velocity of propagation in the two directions of the plate. It is well known that a laminated plate and one containing certain types of non-metallic inclusions often shows high

Fig. 12—Plastic deformation on surface of step made by a chevron intersecting on face 4 (Fig 7: 5.) Direction of propagation from left to right × 150

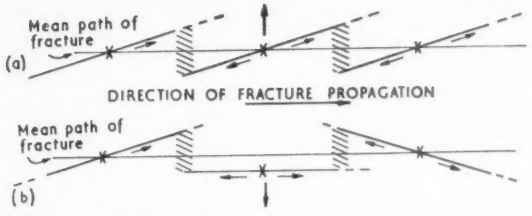

Fig. 13—Diagram showing method of progress of fracture

energy absorption in notch tests, attributable to the difficulty which the fracture encounters in traversing those barriers.

Acknowledgments

This work was carried out in the Engineering Department, Cambridge University, under the direction of Professor J. F. Baker, O.B.E., SC.D., with funds received from the Admiralty.

Lloyd's Register of Shipping, Mr. A. H. Goodger, and Messrs. Whessoe have kindly provided the service fractures which have been investigated.

References

1. G. M. Boyd: *Engineering*, 1953, vol. 175, pp. 65–69, 100–102.
2. J. A. Kies, A. M. Sullivan, and G. R. Irwin: *J. Appl. Phys.*, 1950, vol. 21, pp. 716–720.
3. H. Schardin: *Kunststoffe*, 1954, vol. 44, pp. 48–55.
4. C. F. Tipper: Admiralty Ship Welding Committee Report No. R.3: 1948, London, H.M.S.O.
5. C. F. Tipper and A. M. Sullivan: *Trans. Amer. Soc. Metals*, 1951, vol. 43, pp. 906–934.
6. C. F. Tipper and E. O. Hall: *J. Iron Steel Inst.*, 1953, vol. 175, pp. 9–15.
7. H. Wallner: *Zeitschrift für Physik*, 1939, vol. 114, p. 368.
8. M. L. Williams and G. A. Ellinger: *Weld. J.*, 1953, vol. 18, pp. 498–527.

ANDREW CARNEGIE SCHOLARSHIP REPORT

The Formation of Carbides in Low-Carbon, Chromium–Vanadium Steels at 700°C

By S. W. K. Shaw and A. G. Quarrell

SYNOPSIS

X-ray and chemical analyses of carbides extracted from suitably heat-treated steels have been used to establish the constitution of the carbide phase at 700° C in steels containing 0·2% carbon with up to 12% chromium and 2% vanadium, and to study the approach to equilibrium in selected steels. The constitutional diagram was based on heat-treatments of 500 to 2000 h. It is shown that the extraction technique may give misleading results if a change in carbide type occurs at a late stage in the tempering. 1235

IT HAS BEEN REALIZED for some time that the creep properties of ferritic steels are dependent upon the nature and distribution of the carbide phase.[1] Detailed investigations have been made of particular steels of industrial importance[2–5] but it is nevertheless true that background knowledge of the carbide phase in ferritic steels is very meagre.

Crafts and Lamont[6] have investigated the tempering process in a small number of chromium–vanadium steels of constant carbon content of about 0·25%. The investigation was mainly concerned with softening and secondary hardening during tempering in a range of temperatures, and with the application of the Holloman-Jaffe relationship for the equivalence of time and temperature. They extracted the carbides from all specimens of one of their steels, identified them by X-ray diffraction, and examined them by electron microscopy.

The present work was undertaken as a first step in a larger programme intended to throw light upon the constitution of the carbides in ferritic steels in equilibrium at typical service temperatures, and upon changes that occur in the carbides during the approach to equilibrium at such temperatures. In the first instance, a systematic study has been made of the structures and compositions of the carbides that occur at 700° C in low-carbon steels containing up to 12% chromium and up to 2% vanadium. A carbon content of 0·2% has been aimed at throughout as typical of present practice in high-temperature ferritic steels.

The techniques adopted are already well established. Steels within the range of compositions mentioned above were suitably heat-treated and an electrolytic method was used for the extraction of the carbides. These were then examined by X-ray and chemical methods.

EXPERIMENTAL

In all, over 100 experimental steels of the compositions given in Table I were made in an h.f. furnace from boiler plate scrap, Swedish white iron, and ferro-alloys. All melts were deoxidized with ferro-silicon and ferro-manganese. For the most part,* each melt provided a 7-lb ingot tapering from 2 in. square at the top to about 1½ in. at the bottom. The hot top ensured that the ingot itself was sound. The ingots were forged to 1 in. round from 1250° C, usually with two intermediate heatings.

Heat Treatment

Transverse sections of representative steels were examined metallographically to determine the depth of decarburization during forging. The forged bars were then machined to a sufficient depth to ensure the complete removal of the decarburized layer. After machining, the bars were ½–¾ in. dia.

Three-inch lengths of the machined bars were heat-treated in an argon atmosphere for 4 h at 1200° C and O.Q. Steels of high chromium and vanadium contents in which δ-ferrite was likely to be retained were furnace cooled from 1200° to 1100° C and held there for ½ h before quenching.

Preliminary experiments suggested that 500 h at 700° C would be adequate for the attainment of equilibrium in the O.Q. specimens. This treatment was therefore adopted as standard, but in addition some 30 specimens were tempered for 2000 h and a further 15 specimens for 1000 h. No difference was observed between the carbide phases present after 500 and 2000 h respectively, except in three steels which will be referred to later.

All the long-time tempering treatments were done in a lead bath of large capacity and a coal gas atmosphere was maintained above the lead to prevent oxidation. For treatments up to 100 h, a salt bath was used. All specimens were water quenched from the tempering temperature.

Extraction of Carbides

After heat treatment, typical specimens were examined metallographically. All specimens were then machined to a sufficient depth to ensure the complete removal of any decarburized or contaminated surface layer. The carbides were extracted electrolytically using a 5% aqueous solution of hydrochloric acid and a current density of 0·025 A/cm². With specimens of standard size, two runs of 36 h each were normally necessary to yield sufficient

* At first, 15-lb ingots were used and the results were in conformity with those for the smaller ingots which were found to be adequate and were used in all the later work.

Paper received 30th September, 1955.

Mr. Shaw is with The National Gas Turbine Establishment, Ministry of Supply. Professor Quarrell is Head of the Department of Metallurgy, University of Sheffield.

extract for X-ray and chemical analyses. The carbides were filtered from the electrolyte using a No. 4 sintered glass filter, washed with distilled water followed by alcohol and ether and then heated to 40° C to drive off any residual liquid.

Examination of Carbides

In general, the yield of extract was less than to be expected from the carbon content of the steel. It tended to increase as tempering progressed. X-ray analysis was used to identify the types of carbides present.

For the most part, structures quoted by Goldschmidt[7] were assumed as:

Fe_3C–orthorhombic with 16 atoms per unit cell;
$a = 4{\cdot}5144$ kX, $b = 5{\cdot}0787$ kX, $c = 6{\cdot}7297$ kX
Cr_7C_3–hexagonal with 80 atoms per unit cell;
$a = 13{\cdot}98$ kX, $c/a = 0{\cdot}324$
$Cr_{23}C_6$–face-centred cubic with 116 atoms per unit cell;
$a = 10{\cdot}638$ kX
V_4C_3–NaCl-type cubic structure;
$a = 4{\cdot}15 \pm 0{\cdot}05$ kX

The composition of the stable vanadium carbide has been reported both as VC and as V_4C_3. Goldschmidt comments "It is probable that a solid solution VC–V_4C_3 exists (defect lattice, carbon atoms being omitted from the ideal NaCl cell), and that the values 4·30 and 4·13 kX apply to approximately the two ends of the range. In steels, the carbide V_4C_3 is liable to appear." The cubic vanadium carbide identified in the present work had lattice parameters ranging from $a = 4{\cdot}137$ kX to $a = 4{\cdot}151$ kX. In view of this, and since the practice has been adopted in other relevant papers[1, 2] vanadium carbide has been referred to as V_4C_3 throughout the rest of this paper.

All the carbide types observed in this work showed solubility for the principal alloying elements in the steel. For example, where reference is made to Cr_7C_3 it should be understood that the carbide has the structure of Cr_7C_3, but that the composition is better represented as $(Cr, V, Fe)_7C_3$. Specimens for examination in a 9-cm X-ray powder camera were made by mixing the carbides with gum tragacanth and moulding into a thin cylinder. Unfiltered chromium radiation was used throughout and exposures were about 5 mAh. Diffraction patterns were identified by direct comparison with those of known carbides. In addition, the pattern of at least one specimen from each phase field was measured and analysed in detail.

When the extract consisted of a mixture of carbides, the proportions were estimated by visual comparison of the X-ray patterns with those of synthetic mixtures of two known carbides in controlled proportions. If the extract contained three carbides, the proportions were estimated by comparison with two of the synthetic mixtures. This procedure makes no allowance either for change in composition or particle size of the carbide phase within a given phase field which may cause variations in the relative intensities of the diffraction lines, and it is appreciated that the results are correspondingly approximate.

For chemical analysis, the carbides were taken into solution by fusion with sodium peroxide and sodium bicarbonate in a nickel crucible. Standard wet methods of analysis were used. For the most part the analyses for iron, chromium, and vanadium* plus the theoretical carbon content totalled 80–85%.

Earlier work in this laboratory has shown that it is difficult to make reliable analyses of the carbon contents of carbides, particularly during the early stages of formation, but that the ratios of the metallic elements in the carbides can be satisfactorily determined. In what follows, the results are expressed as metal-atom ratios, i.e. the fraction of metal atoms in the carbide which consist of the particular metal. Thus the chromium atom ratio is equal to Cr%/(Fe% + Cr% + V%). The ratios were calculated from weight percentages in view of the relatively small differences in atomic weight.

The concept of metal-atom ratio proves particularly helpful in considering the transformation from one type of carbide to another.

Detailed results are given in Table I.

RESULTS

Carbide Constitution at 700° C

The phases observed after long-time tempering at 700° C are shown in Fig. 1. For the most part, the experimental points correspond to 500 h, but where results for 1000 or 2000 h are known they have been taken into account. Over all, some 40% of the results are for 1000 or 2000 h; most of the steels treated for these longer times were the more highly alloyed ones in which the changes were likely to be more sluggish. The numbers and positions of the experimental points are such that the phase boundaries have been determined with some certainty, subject to the following observations.

(i) The extract from steel 424 (7·02% Cr; 0·17% V), the result for which is shown in Fig. 1 on the $Cr_7C_3/(Cr_7C_3 + Cr_{23}C_6)$ phase boundary, contained only Cr_7C_3 after 500 h but contained 12% $Cr_{23}C_6$ after 2000 h.

(ii) On the other side of the two-phase field, the extract from steel 413 (8·30% Cr; 0·60% V), contained both chromium carbides after 500 h but only $Cr_{23}C_6$ after 2000 h.

(iii) The points defining the three-phase field $(V_4C_3 + Cr_7C_3 + Cr_{23}C_6)$ all correspond to 500 h at 700° C. After this time the extract from steel 460 (6·91% Cr; 1·16% V) contained only V_4C_3 and Cr_7C_3 but after 2000 h all three phases were present. The proportions of the phases were:

Treatment/Carbide	V_4C_3	Cr_7C_3	$Cr_{23}C_6$
500 h at 700° C	65	35	...
2000 h at 700° C	77	14	9

Thus the position of the three-phase field in Fig. 1 may not represent true equilibrium, but only the constitution after 500 h at

*Work by Mr. R. Smith has shown that manganese is usually 2% or more of the extract and that there is a loss of 3% by wt. on evacuation and another 30% on heating to 250° C *in vacuo*. Oxygen and nitrogen probably account for most of the remainder.

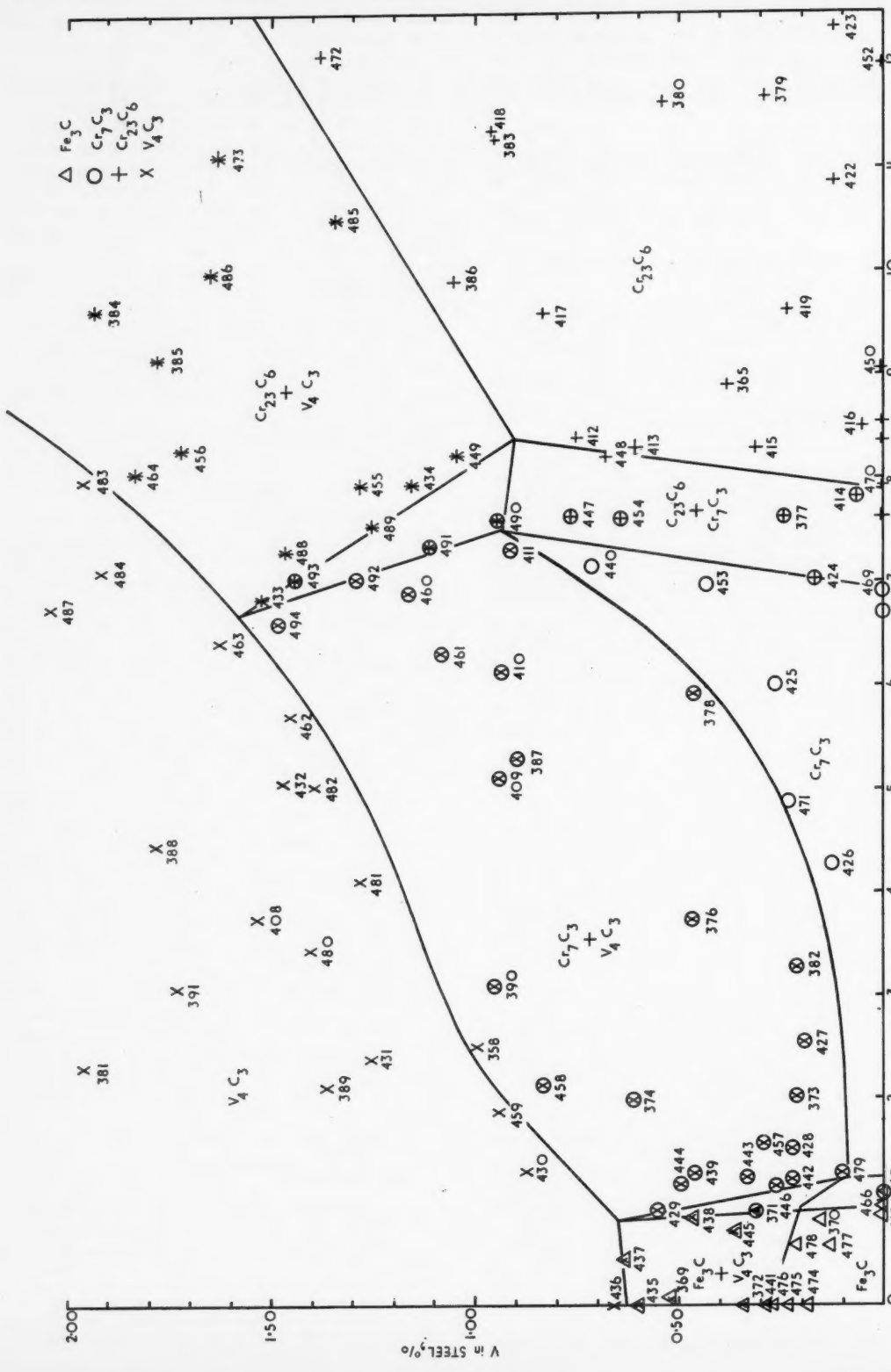

Fig. 1—Carbide constitution, at 700° C in 0·20% carbon, chromium–vanadium steels

Table I

DETAILS OF EXPERIMENTAL STEELS AND EXTRACTED CARBIDES

Experimental steels*					Carbide extract						
					Metal-atom ratios					Lattice parameters in kX	
Steel No.	C, %	Cr, %	V, %	No. of h at 700° C	Fe	Cr	V	Carbide phases present	Ratios of Carbides	Cr_7C_3 (a, c/a)	$Cr_{23}C_6$ (a)
358	0·20	2·52	0·99	1	0·078	0·186	0·736	$V_4C_3 + Cr_7C_3$	80 : 20		
				2	0·071	0·166	0·763		95 : 5		
				4	0·079	0·163	0·758		90 : 10		
				8	0·073	0·169	0·758		85 : 15		
				24	0·072	0·192	0·736		85 : 15		
				48	0·079	0·199	0·722		80 : 20		
				96	0·092	0·194	0·714		85 : 15		
				192	0·105	0·188	0·707		75 : 25		
365	0·21	8·91	0·38	1	0·227	0·365	0·408	No diffraction lines			
				2	0·227	0·481	0·292	Cr_7C_3		13·995 : 0·32121	
				4	0·200	0·559	0·241	Cr_7C_3		13·987 : 0·32169	
				7	0·197	0·608	0·195	Cr_7C_3		13·987 : 0·32161	
				24	0·164	0·665	0·171	$Cr_7C_3 + Cr_{23}C_6$	90 : 10	13·987 : 0·32173	10·582
				48	0·191	0·683	0·126	$Cr_7C_3 + Cr_{23}C_6$	55 : 45	13·989 : 0·32191	10·582
				96	0·265	0·621	0·114	$Cr_{23}C_6 + Cr_7C_3$	90 : 10		10·582
				190	0·298	0·619	0·083	$Cr_{23}C_6$			10·584
				1000	0·286	0·648	0·066	$Cr_{23}C_6$			10·585
368	0·22	0·05	0·24	500	0·875	0·010	0·115	Fe_3C			
369	0·21	0·07	0·52	500	0·592	0·008	0·400	$Fe_3C + V_4C_3$	50 : 50		
				680	0·707	0·016	0·277	$Fe_3C + V_4C_3$	70 : 30		
370	0·21	0·82	0·16	1000	0·742	0·165	0·093	Fe_3C			
371	0·21	0·91	0·31	1000	0·526	0·238	0·236	$Cr_7C_3 + Fe_3C$ V_4C_3			
372	0·21	...	0·34	1000	0·732	...	0·268	$Fe_3C + V_4C_3$	60 : 40		
				680	0·886	...	0·114	$Fe_3C + V_4C_3$	95 : 5		
373	0·23	2·02	0·21	1000	0·376	0·440	0·184	$Cr_7C_3 + V_4C_3$	85 : 15		
374	0·25	1·99	0·61	1000	0·327	0·368	0·305	$Cr_7C_3 + V_4C_3$	70 : 30		
376	0·20	3·74	0·46	1000	0·256	0·556	0·188	$Cr_7C_3 + V_4C_3$	80 : 20		
377	0·20	7·63	0·24	1000	0·235	0·718	0·047	$Cr_7C_3 + Cr_{23}C_6$	60 : 40		10·578
378	0·20	5·93	0·46	1000	0·168	0·737	0·095	$Cr_7C_3 + V_4C_3$	95 : 5		
379	0·21	11·69	0·29	500	0·273	0·648	0·080	$Cr_{23}C_6$			
380	0·24	11·67	0·54	500	0·284	0·624	0·092	$Cr_{23}C_6$			10·587
381	0·21	2·34	1·96	500	0·050	0·007	0·943	V_4C_3			
382	0·22	3·27	0·21	1000	0·340	0·570	0·090	$Cr_7C_3 + V_4C_3$	95 : 5		
383	0·26	11·29	0·95	1000	0·246	0·642	0·112	$Cr_{23}C_6$ $Cr_{23}C_6$			10·598
384	0·27	9·64	1·93	500							
385	0·24	9·18	1·78	1000	0·133	0·377	0·490	$V_4C_3 + Cr_{23}C_6$	80: 20		
386	0·16	9·92	1·05	1000	0·235	0·587	0·178	$Cr_{23}C_6 + V_4C_3$	90 : 10		10·594
387	0·20	5·30	0·89	1000	0·093	0·293	0·614	$V_4C_3 + Cr_7C_3$	80 : 20		
388	0·21	4·49	1·78	500	0·040	0·042	0·918	V_4C_3			
389	0·21	2·14	1·36	500	0·048	0·028	9·924	V_4C_3			
390	0·20	3·11	0·95	1000	0·043	0·086	0·871	$V_4C_3 + Cr_7C_3$	90 : 10		
391	0·22	3·08	1·73	500	0·070	0·072	0·858	V_4C_3			
408	0·23	3·76	1·53	500	0·026	0·045	0·929	V_4C_3			
409	0·21	5·13	0·94	500	0·119	0·282	0·599	$V_4C_3 + Cr_7C_3$	70 : 30	14·008 : 0·32084	
				2000	0·104	0·375	0·521	$V_4C_3 + Cr_7C_3$	60 : 40	14·005 : 0·32093	
410	0·20	6·15	0·93	500	0·145	0·426	0·429	$Cr_7C_3 + V_4C_3$	50 : 50	14·015 : 0·32051	
				2000	0·134	0·492	0·374		60 : 40	14·016 : 0·32060	
411	0·20	7·43	0·91	500	0·148	0·528	0·324	$Cr_7C_3 + V_4C_3$	70 : 30	14·025 : 0·32033	
				2000	0·162	0·559	0·279		75 : 25	14·026 : 0·32054	
412	0·21	8·41	0·75	0·5	0·208	0·473	0·319	Cr_7C_3		13·996 : 0·32085	
				2	0·201	0·603	0·196			14·016 : 0·32047	
				12	0·183	0·629	0·188			14·018 : 0·32057	
				50	0·169	0·648	0·183			14·022 : 0·32048	
				110	0·172	0·622	0·206	$Cr_7C_3 + Cr_{23}C_6$	85 : 15	14·026 : 0·32057	10·588
				190	0·183	0·647	0·170	$Cr_7C_3 + Cr_{23}C_6$	75 : 25	14·025 : 0·32070	10·587
				240	0·177	0·643	0·180	$Cr_7C_3 + Cr_{23}C_6$	80 : 20	14·025 : 0·32064	10·588
				500	0·263	0·598	0·139	$Cr_{23}C_6$			10·588
				2000	0·288	0·604	0·108	$Cr_{23}C_6$			10·587
413	0·20	8·30	0·60	500	0·284	0·625	0·091	$Cr_{23}C_6 + Cr_7C_3$	70 : 30		10·585
				2000	0·310	0·624	0·066	$Cr_{23}C_6$			10·582
414	0·20	7·82	0·06	1·5	0·198	0·796	0·006	Cr_7C_3		13·951 : 0·32270	
				6	0·200	0·795	0·005			13·952 : 0·32278	
				24	0·188	0·807	0·005			13·959 : 0·32282	
				100	0·180	0·814	0·006	$Cr_7C_3 + Cr_{23}C_6$	97 : 3	13·960 : 0·32274	
				279	0·174	0·816	0·010		95 : 5	13·960 : 0·32276	10·574
				500	0·280	0·705	0·015	$Cr_{23}C_6 + Cr_7C_3$	65 : 35	13·963 : 0·32277	10·573
				2000	0·283	0·714	0·003	$Cr_{23}C_6 + Cr_7C_3$	75 : 25	13·963 : 0·32276	10·572
415	0·21	8·29	0·31	500	0·304	0·643	0·053	$Cr_{23}C_6$			10·579
				2000	0·311	0·649	0·040				10·579
416	0·20	8·50	0·05	1·5	0·182	0·810	0·008	Cr_7C_3		13·957 : 0·32275	
				6	0·173	0·822	0·005	$Cr_7C_3 + Cr_{23}C_6$	65 : 35	13·953 : 0·32258	10·572
				24	0·222	0·772	0·006	$Cr_{23}C_6 + Cr_7C_3$	95 : 5		10·578
				100	0·282	0·711	0·007				10·576
				500	0·302	0·698	...	$Cr_{23}C_6$			10·577
				2000	0·303	0·691	0·001				10·575
417	0·21	9·161	0·93	500	0·252	0·627	0·121	$Cr_{23}C_6$			10·595
				2000	0·253	0·621	0·126	$Cr_{23}C_6$			10·594
418	0·20	11·38	0·96	500	0·238	0·641	0·121	$Cr_{23}C_6$			10·599
419	0·20	9·62	0·23	500	0·274	0·685	0·041	$Cr_{23}C_6$			10·584
420	0·21	7·62	...	500	0·284	0·716	...	$Cr_{23}C_6 + Cr_7C_3$	75 : 25	13·969 : 0·32248	10·572
				2000	0·286	0·714	...		75 : 25	13·963 : 0·32268	10·573
421	0·24	8·36	...	500	0·329	0·680	...	$Cr_{23}C_6$			10·574
422	0·19	10·87	0·12	500	0·260	0·722	0·018	$Cr_{23}C_6$			10·586
				2000	0·238	0·740	0·022	$Cr_{23}C_6$			10·588
423	0·20	12·39	0·12	500	0·222	0·751	0·027	$Cr_{23}C_6$			10·589
424	0·18	7·02	0·17	1·5	0·232	0·624	0·144	Cr_7C_3		13·976 : 0·32147	
				6	0·225	0·665	0·110			13·975 : 0·32171	
				24	0·209	0·690	0·101			13·977 : 0·32201	
				100	0·196	0·711	0·093			13·982 : 0·32202	
				500	0·181	0·724	0·095			13·983 : 0·32192	
				2000	0·186	0·730	0·084	$Cr_7C_3 + Cr_{23}C_6$	88 : 12	13·982 : 0·32204	10·578

* For steels Nos. 358 to 415 the mean manganese content was 0·20%; for the remaining steels it was 0·36%

Fig. 1—Carbide constitution, at 700° C in 0·20% carbon, chromium–vanadium steels

Table I—(*continued*)

Experimental steels*					Carbide extract						
Steel No.	C, %	Cr, %	V, %	No. of h at 700° C	Metal-atom ratios			Carbide phases present	Ratios of Carbides	Lattice parameters in kX	
					Fe	Cr	V			Cr_7C_3 (a, c/a)	$Cr_{23}C_6$ (a)
425	0·20	6·01	0·26	500	0·199	0·723	0·078	Cr_7C_3		13·976 : 0·32200	
426	0·22	4·38	0·12	500	0·264	0·663	0·073	Cr_7C_3		13·957 : 0·32220	
427	0·20	2·57	0·19	500	0·380	0·565	0·055	Cr_7C_3 + V_4C_3	97 : 3	13·914 : 0·32293	
428	0·19	1·52	0·22	500	0·454	0·416	0·130	Cr_7C_3 + V_4C_3	85 : 15	13·881 : 0·32350	
429	0·17	0·88	0·55	1000	0·264	0·179	0·557	V_4C_3 + Cr_7C_3	55 : 45		
				680	0·352	0·213	0·435	Cr_7C_3 + V_4C_3	55 : 45		
430	0·18	1·31	0·87	500	0·026	0·014	0·960	V_4C_3			
				680	0·165	0·156	0·679	V_4C_3 + Cr_7C_3	80 : 20		
431	0·16	2·41	1·25	500	0·036	...	0·964	V_4C_3			
432	0·20	5·08	1·47	500	0·023	0·009	0·968	V_4C_3			
433	0·21	6·85	1·52	500	0·029	0·053	0·918	} V_4C_3 + $Cr_{23}C_6$	95 : 5		
				2000	0·091	0·153	0·756		90 : 10		
434	0·19	7·95	1·15	0·5	0·134	0·425	0·441	Cr_7C_3 + V_4C_3	80 : 20		
				2	0·140	0·442	0·418	Cr_7C_3 + V_4C_3	50 : 50	14·035 : 0·31994	
				12	0·141	0·477	0·382	Cr_7C_3 + V_4C_3	50 : 50	14·035 : 0·32013	
				50	0·136	0·450	0·414	V_4C_3 + Cr_7C_3	60 : 40	14·041 : 0·31995	
				110	0·117	0·290	0·593	V_4C_3 + $Cr_{23}C_6$ + Cr_7C_3 + 2	63 : 21 : 16	14·042 : 0·31995	10·592
				240	0·151	0·311	0·538	V_4C_3 + $Cr_{23}C_6$	60 : 40		10·592
				500	0·192	0·419	0·389	} $Cr_{23}C_6$ + V_4C_3	55 : 45		10·592
				2000	0·211	0·461	0·328		60 : 40		10·594
435	0·18	...	0·60	500	0·136	...	0·864	V_4C_3			
				680	0·645	...	0·355	Fe_3C + V_4C_3	50 : 50		
436	0·13	...	0·66	500	0·054	...	0·946	V_4C_3			
				680	0·155	...	0·845	V_4C_3 + Fe_3C	97 : 3		
437	0·20	0·45	0·67	500	0·531	0·123	0·346	} Fe_3C + V_4C_3	60 : 40		
				680	0·450	0·114	0·435		50 : 50		
438	0·20	0·87	0·47	500	0·595	0·141	0·263	Fe_3C + V_4C_3	50 : 50		
				680	0·667	0·155	0·178	Fe_3C + V_4C_3 + Cr_7C_3	47 : 47 : 6		
439	0·25	1·28	0·46	500	0·444	0·316	0·240	Cr_7C_3 + V_4C_3	65 : 35		
440	0·21	7·15	0·71	500	0·168	0·675	0·158	Cr_7C_3		14·010 : 0·32092	
				2000	0·170	0·673	0·158	Cr_7C_3		14·012 : 0·32103	
441	0·20	...	0·27	500	0·804	...	0·197	Fe_3C + V_4C_3	50 : 50		
				680	0·900	0·004	0·096	Fe_3C			
442	0·20	1·22	0·22	500	0·544	0·356	0·101	Cr_7C_3 + V_4C_3	85 : 15	13·861 : 0·32429	
443	0·18	1·25	0·33	500	0·465	0·348	0·187	Cr_7C_3 + V_4C_3	75 : 25	13·869 : 0·32386	
444	0·19	1·17	0·49	500	0·291	0·278	0·432	Cr_7C_3 + V_4C_3	50 : 50	13·884 : 0·32377	
				680	0·408	0·256	0·336	Cr_7C_3 + V_4C_3	70 : 30		
445	0·20	0·73	0·36	500	0·641	0·144	0·216	Fe_3C + V_4C_3	70 : 30		
				680	0·694	0·118	0·189	Fe_3C + V_4C_3	80 : 20		
446	0·17	1·15	0·26	500	0·497	0·380	0·123	Cr_7C_3 + V_4C_3	85 : 15	13·871 : 0·32401	
447	0·20	1·65	0·76	500	0·219	0·577	0·205	Cr_7C_3 + $Cr_{23}C_6$	80 : 20	14·021 : 0·32063	10·586
				2000	0·204	0·645	0·151	Cr_7C_3 + $Cr_{23}C_6$	55 : 45	14·024 : 0·32075	10·586
448	0·20	8·21	0·68	500	0·304	0·614	0·083	$Cr_{23}C_6$			10·586
				2000	0·299	0·632	0·069				10·585
449	0·18	8·24	1·04	500	0·230	0·480	0·290	} $Cr_{23}C_6$ + V_4C_3	75 : 25		10·591
				2000	0·241	0·541	0·218		75 : 25		10·592
450	0·19	9·06	...	500	0·317	0·684	...	$Cr_{23}C_6$			10·577
451	0·20	8·54	...	500	0·327	0·673	...	$Cr_{23}C_6$			10·575
452	0·23	12·00	...	1·5	0·262	0·738	...	Cr_7C_3		13·974 : 0·32208	
				2	0·242	0·758	...	$Cr_{23}C_6$			10·581
				12	0·269	0·731	...	$Cr_{23}C_6$			10·583
				50	0·279	0·721	...	$Cr_{23}C_6$			10·583
				500	0·261	0·739	...	$Cr_{23}C_6$			10·590
				2000	0·228	0·772	...	$Cr_{23}C_6$			10·590
453	0·22	6·97	0·43	500	0·186	0·695	0·119	} Cr_7C_3		13·997 : 0·32139	
				2000	0·175	0·721	0·104			13·997 : 0·32153	
454	0·19	7·61	0·64	500	0·203	0·627	0·169	Cr_7C_3 + $Cr_{23}C_6$	70 : 30		
				2000	0·248	0·640	0·114	$Cr_{23}C_6$ + Cr_7C_3	70 : 30		
455	0·19	7·95	1·28	500	0·120	0·306	0·574	V_4C_3 + $Cr_{23}C_6$	60 : 40		10·593
				2000	0·183	0·414	0·404	$Cr_{23}C_6$ + V_4C_3	60 : 40		10·592
456	0·20	8·30	1·72	500	0·029	0·214	0·757	} V_4C_3 + $Cr_{23}C_6$	70 : 30		
				2000	0·151	0·338	0·511		50 : 50		
457	0·17	1·57	0·29	500	0·425	0·364	0·212	Cr_7C_3 + V_4C_3	85 : 15	13·884 : 0·32343	
458	0·17	2·14	0·83	500	0·065	0·172	0·762	V_4C_3 + Cr_7C_3	85 : 15	13·950 : 0·32205	
				2000	0·053	0·057	0·890	V_4C_3 + Cr_7C_3	97 : 3		
459	0·18	1·90	0·94	500	0·031	0·031	0·939	} V_4C_3			
				2000	0·049	0·050	0·900				
				680	0·053	0·008	0·940				
460	0·18	6·91	1·16	500	0·069	0·308	0·623	V_4C_3 + Cr_7C_3	65 : 35	14·037 : 0·32005	
				2000	0·132	0·328	0·541	V_4C_3 + Cr_7C_3 + $Cr_{23}C_6$	77 : 14 : 9	14·034 · 0·32010	
461	0·22	6·33	1·08	500	0·077	0·309	0·613	} $_4C_3$ + Cr_7C_3	70 : 30	14·024 : 0·32042	
				2000	0·102	0·321	0·578		70 : 30	14·025 : 0·32046	
462	0·17	5·72	1·45	500	0·029	0·020	0·950	} $_4C_3$			
				2000	0·043	0·024	0·933				
463	0·18	6·43	1·62	500	0·030	0·022	0·947	} V_4C_3			
				2000	0·042	0·021	0·938				
464	0·20	8·08	1·83	500	0·036	0·084	0·881	} V_4C_3 + $Cr_{23}C_6$	90 : 10		
				2000	0·066	0·108	0·827		88 : 12		
465	0·20	0·84	...	500	0·779	0·221	...	Fe_3C			
466	0·18	0·95	...	500	0·802	0·198	...	Fe_3C			
467	0·19	1·08	...	500	0·691	0·309	...	Fe_3C + Cr_7C_3	70 : 30		
468	0·20	6·70	...	500	0·181	0·820	...	Cr_7C_3		13·960 : 0·32277	
469	0·18	6·91	...	500	0·181	0·820	...	Cr_7C_3			
470	0·19	7·92	...	500	0·317	0·678	0·004	$Cr_{23}C_6$			10·574
471	0·19	4·88	0·23	500	0·240	0·670	0·090	Cr_7C_3			
472	0·16	12·10	1·38	500	0·213	0·620	0·167	$Cr_{23}C_6$			10·606
473	0·19	11·10	1·63	500	0·193	0·505	0·302	$Cr_{23}C_6$ + V_4C_3	90 : 10		10·605
474	0·18	...	0·23	500	0·908	...	0·092	Fe_3C			
				680	0·941	...	0·059	Fe_3C			

* For steels Nos. 358 to 415 the mean manganese content was 0·20% ; for the remaining steels it was 0·36%

Table I—(*continued*)

Experimental steels*					Carbide extract						
Steel No.	C, %	Cr, %	V, %	No. of h at 700° C	Metal-atom ratios			Carbide phases present	Ratios of Carbides	Lattice parameters in kX	
					Fe	Cr	V			Cr_7C_3 (a, c/a)	$Cr_{23}C_6$ (a)
475	0·18	...	0·19	500	0·945	...	0·055	Fe_3C			
				680	0·935	...	0·063	Fe_3C			
476	0·18	...	0·27	500	0·901	...	0·099	Fe_3C			
				680	0·837		0·163	$Fe_3C + V_4C_3$	97 : 3		
477	0·21	0·57	0·13	500	0·766	0·123	0·110	Fe_3C			
478	0·15	0·59	0·22	500	0·706	0·121	0·173	Fe_3C			
479	0·17	1·28	0·10	500	0·545	0·379	0·076	$Cr_7C_3 + V_4C_3$	90 : 10		
480	0·19	3·46	1·40	500	0·030	0·024	0·946	V_4C_3			
481	0·15	4·12	1·28	500	0·035	0·034	0·932	V_4C_3			
482	0·16	5·04	1·39	500	0·049	0·031	0·920	V_4C_3			
483	0·19	8·00	1·96	500	0·036	0·029	0·935	V_4C_3			
484	0·18	7·13	1·92	500	0·028	0·028	0·945	V_4C_3			
485	0·18	10·51	1·34	500	0·215	0·570	0·215	$Cr_{23}C_6 + V_4C_3$	85 : 15		10·601
486	0·17	9·99	1·65	500	0·179	0·474	0·347	$Cr_{23}C_6 + V_4C_3$	65 : 35		
487	0·18	6·78	2·04	500	0·026	0·030	0·944	V_4C_3			
488	0·22	7·31	1·46	500	0·120	0·245	0·634	$V_4C_3 + Cr_{23}C_6$	60 : 40		
489	0·19	7·56	1·25	500	0·175	0·384	0·441	$V_4C_3 + Cr_{23}C_6$	50 : 50		
490	0·21	7·61	0·94	500	0·184	0·548	0·268	$Cr_{23}C_6 + Cr_7C_3 + V_4C_3$	38 : 38 : 25	14·032 : 0·32033	10·588
491	0·20	7·36	1·11	500	0·141	0·432	0·427	$Cr_7C_3 + V_4C_3 + Cr_{23}C_6$	44 : 44 : 12	14·036 : 0·32024	10·588
492	0·21	7·03	1·28	500	0·090	0·287	0·623	$V_4C_3 + Cr_7C_3$	75 : 25		
493	0·14	7·06	1·44	500	0·074	0·191	0·735	$V_4C_3 + Cr_7C_3 + Cr_{23}C_6$	78 : 14 : 9	14·042 : 0·31972	10·591
494	0·21	6·62	1·48	500	0·048	0·066	0·887	$V_4C_3 + Cr_7C_3$	97 : 3		

* For steels Nos. 358 to 415 the mean manganese content was 0·20% ; for the remaining steels it was 0·36%

700° C. Fortunately the bottom left-hand corner of the three-phase field has been fairly well established, for the carbides extracted from steel 411 (7·43% Cr; 0·91% V) consisted of $Cr_7C_3 + V_4C_3$ in similar proportions after both 500 and 2000 h. It is likely therefore that any effect of increased tempering time will be to rotate the three-phase field anti-clockwise about a point close to the left-hand bottom corner of the triangle.

(iv) The results given in Fig. 1 for steels containing vanadium but no chromium correspond to 680° C instead of 700° C. This is because the Ac_1 temperature for such steels is about 690° C, and it was considered desirable that sub-critical tempering should be used throughout. When specimens of the vanadium steels were tempered at 700° C, austenite was observed in the grain boundaries of some. In accordance with the iron–vanadium–carbon diagram, tempering at 700° C, i.e. slightly above the Ac_1 line, gave a carbide extract containing only V_4C_3. On the other hand, after tempering at 680° C, Fe_3C was found up to about 0·6% vanadium, with a trace suspected at 0·65% vanadium.

The general form of Fig. 1 calls for little comment except that $Cr_{23}C_6$ occurs at lower chromium contents than would be expected from the published data.[8] As will be seen later, this is probably due to the longer tempering times used for the present work.

The hardness (V.P.N.) of a number of the specimens tempered for 500 h, and a few tempered for 1000 h, appear in Fig. 2 which shows the general level of hardness of the specimens after long-time tempering at 700° C. Some discrepancies between neighbouring points in Fig. 2 may be due to differences in carbon content shown in Table I. In what follows, a V.P.N. of less than 155 has been termed ' very soft '; 155–170 ' soft '; 170–185 ' intermediate ' ; and greater than 185 ' hard.' Steels containing only small additions of chromium and vanadium which are insufficient to cause the formation of alloy carbides are ' very soft,' and additions of vanadium alone up to 0·65% do not increase the hardness to above 170. Chromium alone does not cause an appreciable increase in hardness until 9% has been added and the chromium carbide present is $Cr_{23}C_6$. Above 9% the hardness increases progressively to about 190 at 12% chromium. In the Cr_7C_3 single-phase field, the hardness of the steel increases with increasing vanadium content while in the $Cr_{23}C_6$ single-phase field, the hardness does not appear to be related to the vanadium content of the steel; an $8\frac{1}{2}$% Cr steel is still ' soft ' with up to 0·75% V. The ' hard ' region at the left-hand end of the $Cr_7C_3 + V_4C_3$ field agrees with the high creep resistance of alloys based on this composition. On the other hand, the results suggest that after long-time tempering at 700° C, steels then containing only V_4C_3 are not as hard as those containing V_4C_3 plus a chromium carbide.

From the results in Table I that refer to single-phase regions of Fig. 1, it is clear that the various carbides differ considerably in their ability to dissolve other metal atoms. The extremes of carbide compositions observed in the present work are summarized in Table II.

Figure 3 shows how the metal-atom ratios of the equilibrium carbides vary with composition of the steel when no V_4C_3 is present. As might be expected in the Cr_7C_3 phase field, the higher the chromium content of the steel the lower the iron ratio of the carbide. There is a marked increase in iron ratio in the two-phase field, followed by a progressive decline in the $Cr_{23}C_6$ region as the chromium content of the steel is increased still further.

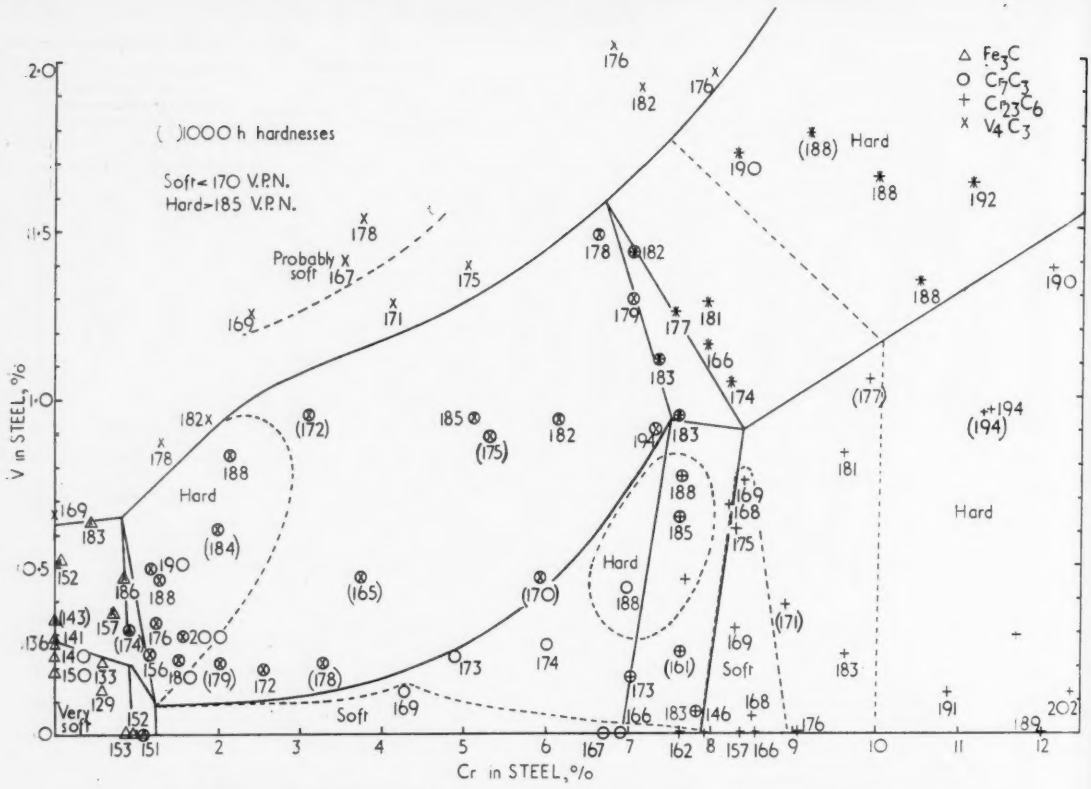

Fig. 2—Hardness (V.P.N.) of specimens tempered for 500 and 1000 h

If the chromium ratio is plotted against chromium content of the steel, a curve can be drawn which is approximately the inverse of the iron ratio curve, but the scatter is very much greater. The results for vanadium ratio in the carbide show no relationship to the chromium content of the steel, yet when combined with those for the chromium ratio they lead to a distribution of points with surprisingly little scatter about the curve drawn in Fig. 3. Thus it would seem that chromium and vanadium are virtually interchangeable in the chromium carbides formed in ferritic steels.

As shown in Fig. 1, the boundaries of the $Cr_7C_3 + Cr_{23}C_6$ field occur at increasing chromium content as the vanadium content of the steel is increased. To allow for this effect the change from Cr_7C_3 to $Cr_{23}C_6$ is represented in Fig. 3 by a broken line for steels free from vanadium and by a full line for those containing vanadium.

Lattice Parameters of Cr_7C_3 and $Cr_{23}C_6$

The lattice parameters of Cr_7C_3 and $Cr_{23}C_6$ are reported in Table I for a number of extracts which contain these carbides. The lattice parameter of Cr_7C_3 was observed to range from $a = 13{\cdot}861$kX and $c/a = 0{\cdot}3243$, to $a = 14{\cdot}042$kX and $c/a = 0{\cdot}3197$; and of $Cr_{23}C_6$ from $a = 10{\cdot}572$kX to $a = 10{\cdot}606$kX. If the lattice parameters of the carbides occurring in single carbide phase fields are in each case plotted against chromium ratio and the vanadium ratio noted for each point, it is possible to draw a family of parallel straight lines of equal vanadium ratio through the experimental points. These graphs are not reproduced as the number and accuracy of the experimental points is insufficient to prove the relationship or the exact direction of the lines but it may be said that the experimental points are consistent with a linear lattice parameter composition relationship, and the lattice parameter increases about twice as rapidly with vanadium ratio as with chromium ratio for both carbides. Further, the variation of axial ratio c/a for Cr_7C_3 appears to be consistent with a linear relationship between composition and c/a; the family of parallel straight lines of equal axial ratio lie at a slightly smaller angle to the composition axis than do the lines of equal vanadium ratio. It would therefore seem possible that the composition of Cr_7C_3 in chromium–vanadium steels might be obtained from X-ray data alone, even when other carbides are present.

In Fig. 4 the lattice parameters of $Cr_{23}C_6$ with a vanadium ratio of less than $0{\cdot}015$ are plotted against chromium content of the steel. The results are compatible with the $Cr_7C_3 + Cr_{23}C_6/Cr_{23}C_6$ boundary occurring at $7{\cdot}9\%$ chromium.

Tempering: Approach to Equilibrium

Eight steels were selected for studying the effect of

Table II

VARIATIONS IN COMPOSITION OF DIFFERENT CARBIDE TYPES OBSERVED IN STEELS TEMPERED FOR 500 h AT 700° C

Carbide type	Steel No.	Metal-atom ratio			Comments
		Fe	Cr	V	
Fe_3C	465	0·779	0·221	...	Max. Cr in binary carbide
	476	0·901	...	0·099	Max. V in binary carbide
	478	0·706	0·121	0·173	Min. Fe in ternary carbide
	469	0·180	0·820	...	Only two steels examined gave carbide free from V; both of this composition. Additional Cr in steel produced second chromium carbide
Cr_7C_3	426	0·264	0·663	0·073	Max. Fe in single phase field but note that no suitable steel of lower Cr content was examined*
	440	0·168	0·675	0·158	Max. V
$Cr_{23}C_6$	451	0·327	0·673	...	Max. Fe in binary carbide
	472	0·213	0·620	0·167	Max. V
	412–1	0·263	0·598	0·139	Min. Cr
	423	0·222	0·751	0·027	Max. Cr
V_4C_3	432	0·023	0·009	0·968	Min. Fe; max. V in ternary
	381	0·050	0·007	0·943	Min. Cr in ternary
	391	0·070	0·072	0·858	Max. Cr; min. V in ternary
	435	0·136	...	0·864	Max. Fe in binary (Note: Except in steels 391 and 435, all V_4C_3 extracts had V at a ratio of 0·90 more)

* It should be noted that in steel 479, which contains only 1·28% Cr, the carbide extract had an iron atom ratio of 0·545. The extract contained a little V_4C_3, but since this carbide usually has a very low iron content it is almost certain that the maximum iron atom ratio for Cr_7C_3 is much higher than is suggested by Table II.

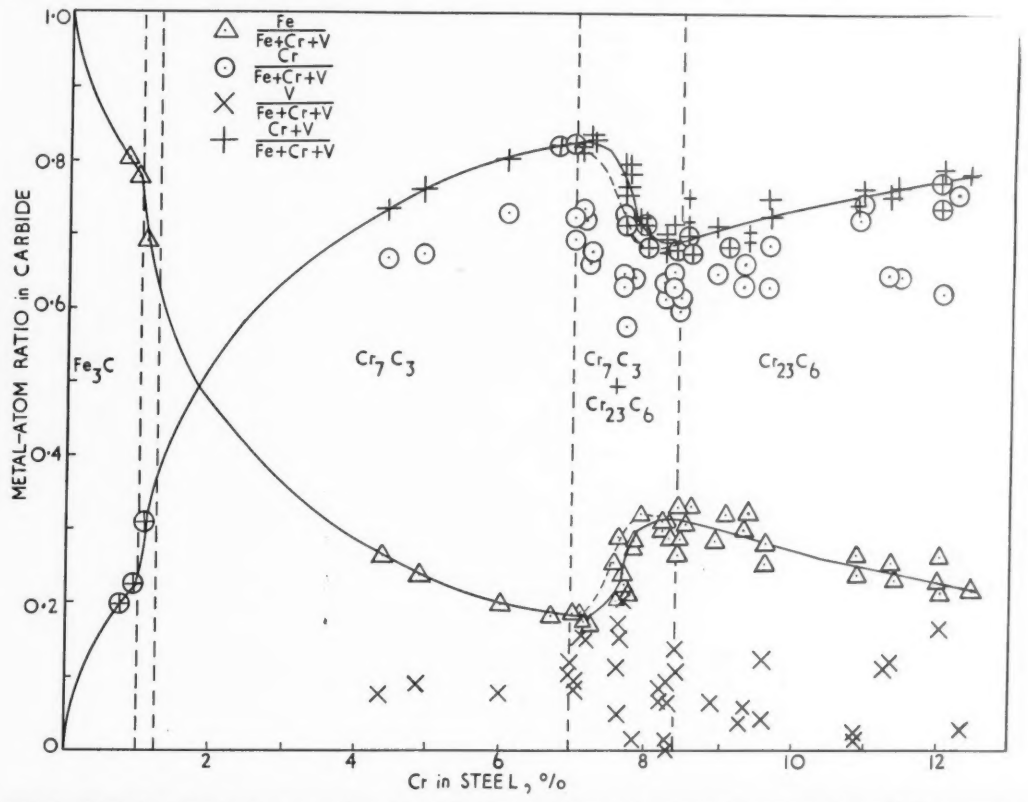

Fig. 3—Variation of metal-atom ratios of equilibrium carbides with composition of steels, no V_4C_3 present

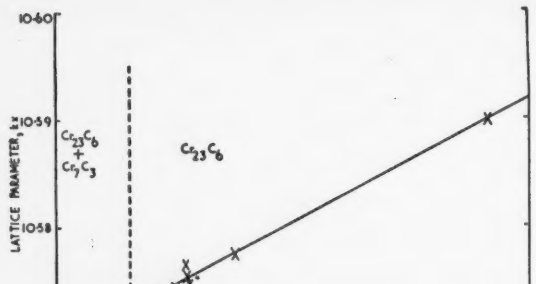

Fig. 4—Change in lattice parameter of (Cr, Fe)$_{23}C_6$ with chromium content of steel

time of tempering at 700° C. Six of the steels cover the range 7–9% chromium, 0–1·2% vanadium. The two steels falling outside this range contained 12·0% chromium–0·0% vanadium, and 2·5% chromium–1·0% vanadium respectively.

The results of the tempering experiments are shown in Figs. 5–12, with the corresponding V.P.N. hardness numbers.

In the series formed by Figs. 5–10 inclusive, only chromium carbides were observed. It is possible that other carbide types were formed in the early stages of tempering, but not observed because the shortest treatment given was half an hour at 700° C.

The simplest results are those for steels 424 (7·0% Cr; 0·17% V) and 452 (12% Cr; 0% V) (Figs. 5 and 8). Both show a transition from Cr_7C_3 to $Cr_{23}C_6$ type carbides between 500 and 2000 h and between 1·5 and 2·0 h respectively. There is no sudden variation in the proportion of chromium present in the carbides; indeed, there is only a small and gradual variation in the chromium ratio during the whole of the tempering time.

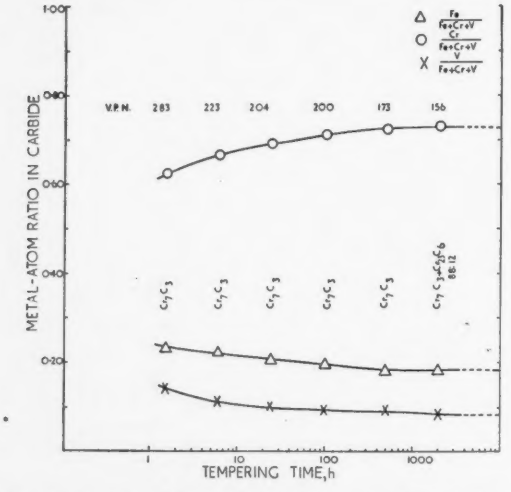

Fig. 5—Result of tempering test, steel 424 (0·18% C, 7·02% Cr, 0·27% V)

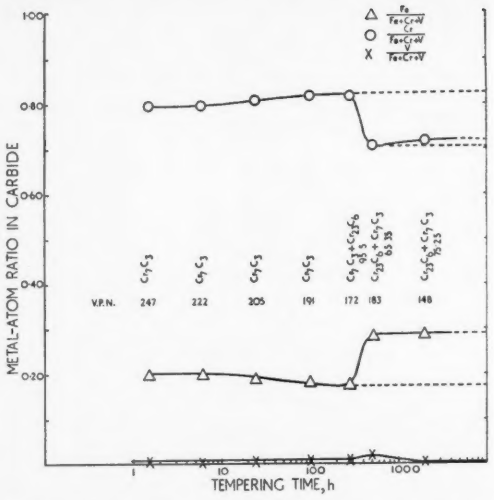

Fig. 6—As Fig. 5, steel 414 (0·20% C; 17·82% Cr; 0·06% V)

For the other steels 414, 416, 412, and 365 (Figs. 6, 7, 9, and 10) in which only chromium carbides were observed, the transition from Cr_7C_3 to $Cr_{23}C_6$ type carbide was accompanied by a drop in chromium ratio and an equally marked rise in iron ratio. On the logarithmic plots, the transition appears to be very rapid, but in all cases takes 100–200 h at 700° C for apparent completion. For steels of low vanadium contents (steels 414 and 416, Figs. 6 and 7) the change from Cr_7C_3 to $Cr_{23}C_6$ was accompanied by a drop in chromium ratio from 0·82 to 0·70. Approximately similar values were observed for the (Cr + V) ratios for vanadium-bearing steels 412 and 365 (Figs. 9 and 10) in which the change in chromium-carbide was observed without V_4C_3 formation.

It is noteworthy that the carbide extracts from steels 412 (8·41% Cr; 0·75% V) and 365 (8·9% Cr;

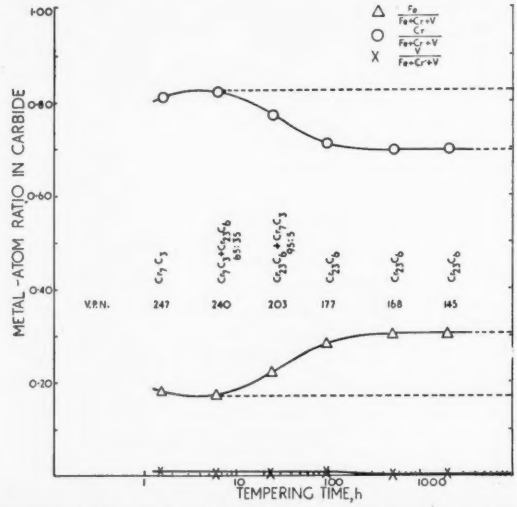

Fig. 7—As Fig. 5, steel 416 (0·20% C; 8·50% Cr; 0·05% V)

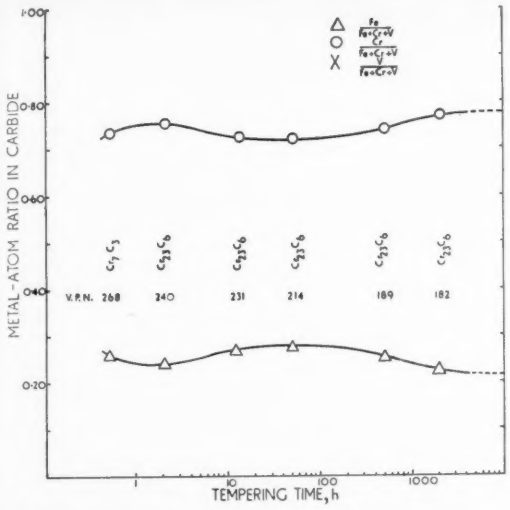

Fig. 8—As Fig. 5, steel 452 (0·23% C; 12·00% Cr; 0·0% V)

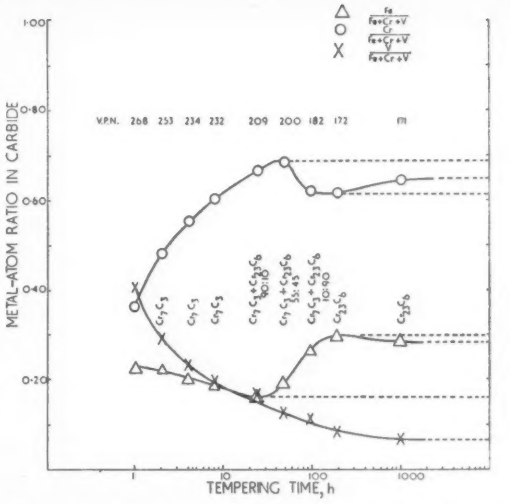

Fig. 10—As Fig. 5, steel 365 (0·21% C; 8·91% Cr; 0·38% V)

0·38% V) had high vanadium ratios after ½ h at 700° C, but that increased tempering led to a fairly rapid reduction in vanadium ratio, a more gradual reduction in iron ratio, and a corresponding increase in chromium ratio. The fact that the curves of vanadium and iron ratios are so different indicates that these effects are not simply due to dilution caused by an increasing percentage of chromium diffusing into the carbides. It would seem that in this range of composition, vanadium plays an important part in nucleating Cr_7C_3; the examination of specimens tempered for shorter times would clearly be of value.

The carbides extracted from steels 358 and 434 (respectively 2·52% Cr–0·99% V (Fig. 11) and 7·95% Cr–1·15% V (Fig. 12)) consisted of a mixture of vanadium- and chromium-type carbides after all treatments given. Steel 358 with the lower chromium content gave V_4C_3 and Cr_7C_3 in approximately constant proportions, but the chromium carbide in steel 434 transformed as tempering proceeded. After tempering for a few hours at 700° C, the extract was a mixture of V_4C_3 and Cr_7C_3 and then as tempering proceeded, $V_4C_3 + Cr_7C_3 + Cr_{23}C_6 + Z$ which in turn gave place to $V_4C_3 + Cr_{23}C_6$. As will be seen from Fig. 12, the transition stage was associated with high vanadium and low chromium ratios. The Z-phase was attributed to an unidentified transition structure. Strongest unidentified diffractions correspond to spacings of 2·514 and 1·478kX respectively.

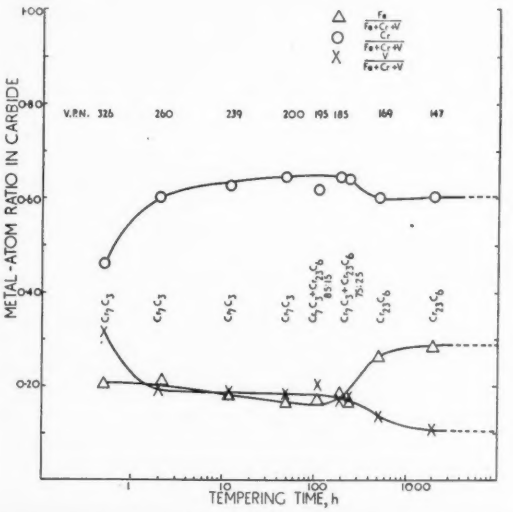

Fig. 9—As Fig. 5, steel 412 (0·21% C; 8·41% Cr; 0·75% V)

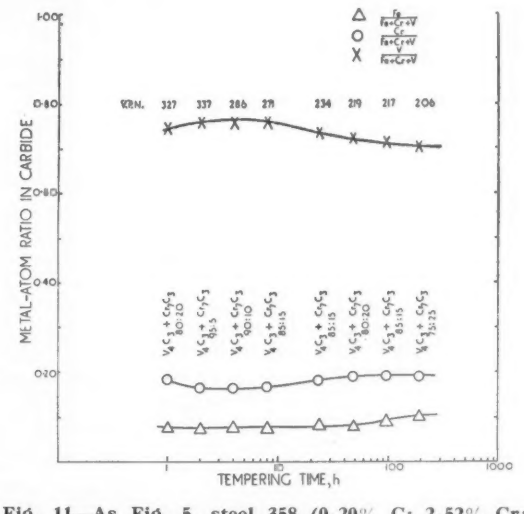

Fig. 11—As Fig. 5, steel 358 (0·20% C; 2·52% Cr; 0·99% V)

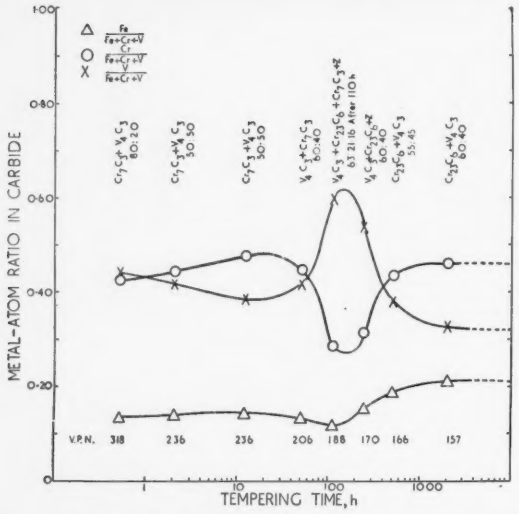

Fig. 12—As Fig. 5, steel 434 (0·19% C; 7·95% Cr; 1·15% V)

The abnormal vanadium and chromium ratios during the transition might have been attributed to experimental error had not the scatter of the results generally in this work been so low and had not repeat analyses given similar results. Moreover, a colleague, Mr. R. Smith, has repeated this part of the work, making two further steels of compositions close to that of steel 434. The results for both of these steels confirm those reported above for 434. In each case there is a pronounced peak in the vanadium ratio and a corresponding minimum in the chromium ratio after tempering for 200–300 h at 700° C but, as will be seen from Table III, the maximum does not occur quite so soon as in steel 434. There are, however, differences of composition between the steels that might account for this.

There appears to be no simple relationship between the nature of the carbides extracted and the rate of softening of the steels. Thus steel 358 (Fig. 11) shows secondary hardening and delayed softening that might be attributed to the presence of about 1·0% vanadium but steel 434 (Fig. 12) of equal vanadium and higher chromium content than steel 358 is apparently no more resistant to softening in 2000 h than, for example, steel 424 (Fig. 5) containing slightly less chromium and only 0·17% vanadium. However, in steel 358 the proportion of vanadium carbide is almost twice that in steel 434 throughout the tempering and only the Cr_7C_3 type of chromium carbide is present. It is likely that the size and distribution of the carbides will be more important than their structures in determining the softening behaviour and an electron micrographic study of this aspect is being undertaken by Professor Honeycombe and Mr. Seal at Sheffield University.

DISCUSSION

The results show that even after several hundred hours at 700° C, changes of carbide structure as well as of composition may occur in alloy steels of the type examined.

No such change was reported by Crafts and Lamont [6] in their 0·26% carbon, 4·69% chromium, 1·03% vanadium steel, but it will be seen from Fig. 1 that with this composition no changes in carbide are likely to occur late in the tempering process. Their observation that in this steel Cr_7C_3 and V_4C_3 occurred in about equal proportions fits in with the results now reported for steel 409. For a steel containing 1% chromium and 1·04% vanadium they reported only V_4C_3, which is in agreement with Fig. 1.

The present work has not been concerned with the earliest stages of tempering, but by consideration of the results as a whole it is possible to build up a tentative picture of the tempering process in this type of steel. When precipitation of carbide first occurs it is likely to be at a large number of nuclei where carbon atoms have associated with those metal atoms that are the strongest carbide formers. Nucleation will occur preferentially at those regions of the lattice where, on an atomic scale, there happen to be local concentrations of carbide-forming elements. Carbon atoms will diffuse to the nuclei more rapidly than can the strong carbide-forming elements, and therefore that type of carbide will tend to be formed which can accommodate the highest proportion of other metallic elements. Under these conditions, fewer metal atoms will need to diffuse over long distances to the growing particle, since it can take into its structure more of the metal atoms that are by chance adjacent to it in the matrix. From the results reported above, particularly those for short tempering times, the Cr_7C_3 type of carbide seems to be able to accommodate more vanadium and iron than can the $Cr_{23}C_6$ type. Indeed, the results for steel 365 (Fig. 10) show that in the early stages of tempering the Cr_7C_3 may contain less chromium than vanadium; after one hour at 700° C only about one metal atom site in three appears to be occupied by chromium.

Most of the present work is concerned with the 'over-ageing' or spheroidization stage of tempering, during which the smaller particles redissolve in the matrix and the larger particles grow in size. This stage is slow compared with the initial formation of carbides for the rate-controlling process is the diffusion of carbide-forming elements to the growing carbide particles. As tempering proceeds the compositions of the carbides will approach more closely to the equilibrium values. This tendency is well shown in Fig. 10, where the chromium ratio for the Cr_7C_3 type carbide rises from 0·36 to 0·69 between 1 and 50 h and there is a corresponding reduction in vanadium ratio.

Except in steel 452 (12·0% Cr; 0·0% V) the change from Cr_7C_3 to $Cr_{23}C_6$ occurs after many hours at 700° C when the spheroidization has reached an advanced stage, and when the chromium and vanadium ratios for the Cr_7C_3 have approached, if not reached, their limiting values. Formation of $Cr_{23}C_6$ might occur by re-solution of the Cr_7C_3 and subsequent nucleation and growth of the second carbide, but it seems much more likely that the transition occurs by the interaction of the Cr_7C_3 with

Table III

ATOM RATIOS DURING THE CHROMIUM-CARBIDE TRANSITION

Steel	Time at 700° C, h	Fe ratio	Cr ratio	V ratio	Carbides
434 (0·19% C, 7·95% Cr, 1·15% V)	12	0·141	0·477	0·382	$V_4C_3 + Cr_7C_3$
	50	0·136	0·450	0·414	$V_4C_3 + Cr_7C_3$
	110	0·117	0·290	0·593	$V_4C_3 + Cr_7C_3 + Cr_{23}C_6 + Z$
	240	0·151	0·311	0·538	$V_4C_3 + Cr_{23}C_6$
	500	0·192	0·419	0·389	$Cr_{23}C_6 + V_4C_3$
RS.1 (0·23% C, 7·86% Cr, 1·14% V)	50	0·136	0·456	0·408	$V_4C_3 + Cr_7C_3$
	150	0·135	0·487	0·378	$V_4C_3 + Cr_7C_3$
	300	0·144	0·355	0·501	$V_4C_3 + Cr_7C_3 + Cr_{23}C_6$
	385	0·133	0·298	0·569	$V_4C_3 + Cr_7C_3 + Cr_{23}C_6$
	500	0·164	0·486	0·350	$V_4C_3 + Cr_7C_3 + Cr_{23}C_6$
	1000	0·210	0·502	0·288	$V_4C_3 + Cr_{23}C_6 + Cr_7C_3$ (trace)
RS.2 (0·20% C, 7·66% Cr, 1·27% V)	30	0·172	0·502	0·320	$V_4C_3 + Cr_7C_3$
	100	0·190	0·490	0·320	$V_4C_3 + Cr_7C_3$
	150	0·111	0·347	0·543	$V_4C_3 + Cr_7C_3 + Cr_{23}C_6$ (trace)
	215	0·108	0·379	0·514	$V_4C_3 + Cr_7C_3 + Cr_{23}C_6$
	300	0·152	0·383	0·465	$V_4C_3 + Cr_7C_3 + Cr_{23}C_6$
	600	0·194	0·391	0·417	$V_4C_3 + Cr_{23}C_6$

the adjacent matrix. Diffusion of the carbide-forming metals through the matrix will be the rate-controlling process no matter which mechanism operates. This is self evident for the first mechanism and may be deduced for the second as follows.

When the transformation occurs, each six carbon atoms become associated with 23 metal atoms in $Cr_{23}C_6$ instead of with 14 as in Cr_7C_3. If the $Cr_{23}C_6$ could not dissolve a higher proportion of iron atoms than existed in the Cr_7C_3 from which it was formed there would be no change in the atom ratios of the extracted carbides, and the transformation would occur at a rate which was governed by the rate of diffusion of chromium and vanadium to maintain these ratios in the new carbide. On the other hand, if the flexibility of composition of the carbide were such that the change occurred almost instantaneously by interaction with the immediately adjacent matrix of average composition, then the drop in chromium ratio would be very much greater than that actually observed. Thus, in steel 416 the chromium ratio would drop from 0·81 to 0·52 instead of to the observed value of 0·70, whilst the iron ratio would rise from 0·18 to 0·47 instead of to the observed value of 0·30.

The experimental observations suggest that there may be a minimum chromium (or chromium + vanadium) ratio below which the $Cr_{23}C_6$ structure is not stable. If this were so, the first-formed $Cr_{23}C_6$ would have the composition corresponding to this ratio, and diffusion of further chromium would be necessary to enable this ratio to be maintained. On completion of the transformation, further chromium would diffuse into the carbide and the chromium ratio would increase towards the equilibrium value. This tendency may be observed in several of the curves, notably Figs. 6 and 10.

The results for steel 434 call for special comment. After 110 h at 700° C the extract contains at least three carbide phases and the formation of the $Cr_{23}C_6$ appears to be associated with the formation of more V_4C_3 and a very much higher vanadium ratio in the extract. It is difficult to understand how a sudden increase followed by a decrease in the V_4C_3 content can occur at a late stage in the tempering, but the apparent increase in this carbide and in the vanadium ratio might be due to the manner in which the chromium-carbide transformation takes place. Thus, if the transformation of the Cr_7C_3 to $Cr_{23}C_6$ occurs by the diffusion of metal atoms inwards through the carbide particles, the $Cr_{23}C_6$ is hardly likely to be coherent with the Cr_7C_3 from which it has formed. In the early stages of the transformation it is likely to have a fine grain size and to be of imperfect structure. As a result, some of the $Cr_{23}C_6$ may be lost during the extraction process, and that which is extracted may make a relatively small contribution to the X-ray diffraction pattern. If either or both of these effects occur, the results of X-ray and chemical analysis shown in Fig. 12 may be reconciled.

If it is assumed that no new V_4C_3 is formed in the later stages of tempering, the V_4C_3/Cr_7C_3 ratio may be taken as a measure of the progress of the chromium-carbide transformation. One part of Cr_7C_3 gives rise to 1·6 parts of $Cr_{23}C_6$, and if the transformation commences at 12 h when V_4C_3 and Cr_7C_3 are in the ratio 50 : 50, then the relationship between the number of parts of Cr_7C_3 transformed (x) and the V_4C_3/Cr_7C_3 ratio (R) is: $x = 50 - (50/R)$. After tempering for 110 h at 700° C: $R = (63/16) \simeq 4$.

Whence $x = 37{\cdot}5$, and the $Cr_{23}C_6$ formed $= 37{\cdot}5 \times 1{\cdot}6 = 60$ parts. The new $V_4C_3 : Cr_7C_3 : Cr_{23}C_6$ ratios should therefore be: 50 : 12·5 : 60 or, about 12 : 3 : 15. The values recorded experimentally (X-ray analysis) were: 63 : 16 : 21 or, about 12 : 3 : 4.

Thus the calculated and observed ratios could be reconciled if about three-quarters of the $Cr_{23}C_6$ formed from Cr_7C_3 were (*a*) lost during extraction, or (*b*) too fine to contribute to the X-ray pattern. The over-all metal-atom ratios determined by chemical analysis of the extract may be used to decide between these alternatives, but it is necessary

Table IV
CALCULATED OVERALL RATIOS

Assumed carbide ratios V_4C_3 :	Cr_7C_3 :	$Cr_{23}C_6$	Metal-atom ratios of mixed carbides Fe :	Cr :	V
12	3	15	0·167	0·385	0·448
12	3	4	0·113	0·261	0·626
Experimentally observed			0·117	0·290	0·593
12	3	5	0·121	0·277	0·602

to assume metal-atom ratios for the individual carbides during the $Cr_7C_3 \rightarrow Cr_{23}C_6$ transformation. The assumed values can be based on the present work as follows:

V_4C_3: Normally about 90% of the metal is vanadium, and chromium and iron are in roughly equal proportions. Hence assume 0·05 Fe, 0·05 Cr, 0·9 V.

Cr_7C_3: The tempering curves show a build-up in chromium until the transformation occurs. To compare with steel 434 we may take steel 412 which is of high vanadium content but contains no vanadium carbide. The Cr_7C_3 extracted from this steel is likely to contain about as much vanadium as that from steel 434. Hence assume, 0·17 Fe, 0·65 Cr, 0·18 V.

$Cr_{23}C_6$: Steel 412 is a good basis of comparison.* Hence assume 0·26 Fe, 0·60, Cr, 0·14 V.

Assuming the above metal-atom ratios for the individual carbides, the calculated overall ratios are shown in Table IV.

Thus, on the basis of the metal-atom ratios of the extract it appears that the more probable explanation of the anomalous peak on the curves for steel 434 is that much of the $Cr_{23}C_6$ produced by transformation of the Cr_7C_3 is lost during extraction. On the basis of the chemical analyses, the ratios of the carbides in the collected extract are likely to be 12 : 3 : 5, instead of the 12 : 3 : 4, indicated by the X-ray analysis.

Further confirmation for this explanation may be derived from the results for the yields of extract that were recorded as a matter of routine during this work, though they did not prove particularly interesting except in this respect. From the above, 100 parts of carbide after 12 h at 700° C should correspond to 122·5 parts after 110 h at 700° C, assuming that there is no loss of extract.

* Substantially the same conclusions are arrived at if the metal-atom ratios for $Cr_{23}C_6$ are based upon the results for steel 416 (Fig. 7).

The observed yield after 12 h was 1·71 g/100 g steel, so that the theoretical yield after 100 h assuming no loss, would be $1·71 \times 1·225 = 2·1$ g/100 g steel. It was shown above that the observed metal-atom ratios of the extract could be explained if about one-third of the total extract were lost. On this basis, the theoretical yield after 110 h would be $\frac{2}{3} \times 2·1 = 1·4$ g/100 g steel compared with an observed yield of 1·3 g/100 g steel.

Bearing in mind the assumptions made and the limitations of the experimental methods, this agreement must be regarded as good. The explanation advanced for the shape of the metal-atom ratio curves for steel 434 in the three-phase region is self-consistent and seems to be satisfactory. It is clear that the extraction process is likely to give misleading results not only during the early stages of tempering, which is well appreciated, but also during the transformation from one carbide to another even when this occurs after many hours at 700° C. The metal-atom ratios of the extract are most likely to be affected but new phases may be missed in the early stages. One must therefore be careful not to attribute to the tempering process effects which may be due to limitations of the extraction technique.

Acknowledgments

The authors are grateful to many colleagues in the department for helpful discussions, and especially to Mr. R. Smith for some of the experimental work to elucidate the tempering process in the 8% chromium, 1% vanadium steel 434. A Robert Styring Postgraduate Scholarship and a grant from the Andrew Carnegie Research Fund have enabled Mr. Shaw to devote his whole time to this research. Grateful thanks are due respectively to the University of Sheffield and to the Council of The Iron and Steel Institute for this financial assistance.

References

1. E. Colbeck and J. R. Rait: "Symposium on High-Temperature Steels and Alloys for Gas Turbines", *Iron Steel Inst. Spec. Rep.* No. 43, pp. 107–124, 1951.
2. G. Wood and J. R. Rait: *Iron Coal Trades Rev.*, 1949, vol. 158, pp. 221–228, pp. 281–288.
3. H. J. Goldschmidt: *J. Iron Steel Inst.*, 1948, vol. 160, pp. 345–362.
4. W. Crafts and C. M. Offenhauer: *Trans. Amer. Inst. Min. Met. Eng.*, 1943, vol. 154, pp. 361–373.
5. Kehsin Kuo: *J. Iron Steel Inst.*, 1953, vol. 173, pp. 363–375.
6. W. Crafts and J. L. Lamont: *Trans. Amer. Inst. Min. Met. Eng.*, 1950, vol. 188, pp. 561–574.
7. H. J. Goldschmidt: *Loc. cit.*
8. W. D. Forgeng, in "Metals Handbook," p. 1248: 1948, Cleveland, Ohio, Amer. Soc. Metals

Investigation of the Behaviour of Metals under Deformation at High Temperatures

By C. H. M. Jenkins, D.Sc., A.R.S.M., and E. A. Jenkinson, M.Sc.

Part III—THE DEFORMATION, MICROSTRUCTURE, AND FORM OF CARBIDES IN A 0·15% C, 0·5% Mo STEEL IN CREEP TESTS

SYNOPSIS

Vacuum tests in the temperature range 450–850° C for times ranging from a few minutes to 13,470 h have been used to trace the extent of transcrystalline and intercrystalline cracking. The limits are shown in stress/temperature and time temperature diagrams.

A minimum ductility was observed at about 550° C in about 2000 h after which recovery was noted, a phenomenon not apparent in tests made in air. In many specimens cavities were formed which might be related to processes associated with 'dislocation' phenomena. The relationship of these cavities to the further deformation of the specimen and to transcrystalline and intercrystalline cracking is discussed. High local deformation appears to accelerate some of the changes observed.

Recrystallization, spheroidization, and graphitization changes take place less rapidly than in carbon steels. The strength of carbon and molybdenum steels is compared at high temperatures.

The alcoholic iodine method gave reasonable solution of the steel leaving the carbides undissolved and suitable for identification by the X-ray method. The changes in the carbides have had a marked effect on creep resistance. Three carbides have been identified, namely Fe_3C, Mo_2C, and $(Fe_{21}Mo_2)C_6$. The first named carbide is present initially in the steel. The two latter appear after long exposure to temperatures of 530° C and 630° C respectively and their formation removes molybdenum from the ferrite, thus causing a reduction in the creep strength. 1201

Introduction

THIS INVESTIGATION is a continuation of earlier work[1, 2] on the nature of the changes in microstructure of iron and carbon steels when subjected to deformation at high temperatures. It is well known that hot rolled or normalized steels containing 0·5% of molybdenum have creep properties superior to those of low-carbon steels.[3, 4] This and further development by alloying with Cr, V, etc. has led to extensive industrial use in the range 500–600° C. This type of alloy[6–9] has been made into pipes, tubes, and other parts for steam power plant. The investigation of utilizable creep properties of these materials forms a part of the work of the J/E Committee of the British Electrical and Allied Industries Research Association but some of the more general properties are studied in this laboratory.

The effect of deformation and of high temperatures on the changes in microstructure of a 0·5% Mo low-carbon steel (reference mark *HNA*) has been studied by creep and short time tensile tests in the range 450–850° C. The conditions of testing are more severe in regard to stress than normally experienced in the service life of this material. A number of tests have been taken to rupture giving a range of life from a few minutes to more than 10,000 h. These tests have given sufficient information to trace the mode of deformation and the extent to which transcrystalline and intercrystalline cracks occurred in the fractured specimens. To prevent interference by oxidation the vacuum was maintained below 0·0002 mm of Hg by means of a high vacuum mercury diffusion pump attached to each unit. The highly polished test specimens could be maintained in good order free from pitting and available for repeated microscopical examination without repolishing. Preferential attack along the grain boundaries was also prevented.

The comparison has been made with the results of an earlier investigation[5] carried out at this laboratory on a Mo steel *FZW* and a Mo–V steel *HKD* 12. These steels were tested in long time creep tests on specimens in air. In the present vacuum tests some recovery, i.e. improvement in ductility in long time tests, is now recorded; whereas this effect was not noted in the earlier series of tests which were carried on for even longer times.

The work on the nature of the carbides reported at the end of this paper shows that exposure to high temperatures for long times brings about changes in their constitution which affect the properties disclosed by creep tests.

Manuscript received 3rd August, 1955.

Dr. Jenkins and Mr. Jenkinson are in the Metallurgy Division at the National Physical Laboratory.

Table I

COMPARISON OF *HNA* WITH OTHER STEELS

Steel Mark	Mode of Preparation, etc.	Size of Bar	Ref. Paper No.	Chemical Composition, %									
				C	Si	S	P	Mn	Ni	Cr	Mo	V	Cu
HNA	Acid H.F. Induction	1-in. dia. bar	—	0·15	0·20	0·021	0·031	0·52	0·16	0·23	0·52	nil	0·065
FZW	Acid H.F. Induction	1⅛-in. „ „	5	0·09	0·24	0·025	0·026	0·66	0·06	0·28	0·49	<0·01	0·05
MSS	B.O.H.	Steampipe 13-in. O.D. 1·95-in. wall	9	0·09	0·22	0·034	0·023	0·52	0·26	0·08	0·50	<0·01	0·07
HKD 12	Acid H.F. Induction	1-in. dia. bar	5	0·14	0·16	0·016	0·020	0·47	0·07	0·10	0·49	0·27	0·055
STS	Basic Arc Furnace	Steampipe 9·5-in. O.D. 0·75-in. wall	8	0·10	0·11	0·012	0·020	0·54	0·14	0·09	0·54	0·21	0·16
M	A.O.H.	1-in. dia. bar	2	0·17	0·13	0·018	0·025	0·68	0·06	nil	—	—	0·044
NGK	B.O.H.	„ „ „	2	0·17	0·05	0·032	0·016	0·63	0·03	0·01	<0·01	<0·01	0·09
*GBE*1–7	A.O.H.	1-in. plate	2	0·40	0·21	0·037	0·035	0·58	0·02	0·01	<0·01	<0·01	0·06
DB	EF (Crucible Steel Quality)	⅝-in. dia. bar	2	0·90	0·12	0·023	0·021	0·68	nil	nil	—	—	0·013
NKE	EF (Crucible Steel Quality)	„ „ „	2	0·86	0·12	0·015	0·027	0·22	nil	nil	—	—	0·002
Swedish *S*	Swedish (Lancashire) Hearth	1-in. dia. bar	1	0·017	0·05	0·003	0·036	0·005	nil	nil	—	—	nil
Armco '*A*'	Ingot Iron (E.F.)	„ „ „	1	0·016	0·006	0·017	0·003	0·030	0·03	nil	—	—	0·07
Carbonyl *C*	Unmelted product (Sintered powder followed by considerable amount of hot working)	⅛-in. plate	1	0·015	<0·02	<0·001	<0·001	<0·005	0·011	nil	—	—	<0·002

Materials Examined

The principal material selected for the present work was an 0·15% C, 0·5% Mo steel rolled into 1-in. dia. bars. The chemical analysis and certain details of manufacture are given below:

Details of Manufacture of Steel *HNA*

Type of furnace in which steel was melted:	High frequency induction
Character of lining:	Acid
Method of deoxidation:	Additions of ferro-manganese and of ferro-silicon. No aluminium
Weight of charge cast:	1 ton 19 cwt
Number and size of ingots:	One top cast ingot of 25 cwt
Details of rolling and of intermediate reheating:	First pass on 1-in. dia. bars, 1090–1120° C. Finished at 925–955° C
Form in which supplied and amount of reduction:	Billets 3-in. square reduced to 1-in. dia. bars
General observations:	A good cast—tapped hot at 1640° C to ensure making some castings alongside ingot

Longitudinal and transverse sections of the bar were polished and examined for sulphur and phosphorus segregation. In the test for the latter a faint square pattern was found in the transverse section and this indicated a normal ingot structure.

Tables I and II contain the results of chemical analysis on the steels considered: many of them are referred to in earlier papers.[1, 2, 5] These tables provide additional information on these steels which had not been given previously.

The present steel *HNA* contains high oxygen and low total aluminium content which agrees with the details of manufacture given above. On the other hand, steel *FZW* discussed in the earlier report[5] has a low oxygen and a high aluminium content. *FZW* is 'abnormal' in grain size, according to the McQuaid-Ehn test, the grain size being 5–8 on the A.S.T.M. chart, whereas the size of *HNA* is 1–3. Figure 8*a* shows the distribution of the variously sized grains after this test and indicates the degree of incompleteness of the grain boundaries. Confirmation that *HNA* shows 'normal grain size' characteristics has been obtained from a test on a series of specimens heat treated and quenched from temperatures varying every 25° C between 900° and 1100° C inclusive. For the normalizing treatment 925° C was selected as at higher temperatures such as 950° and 975° C coarser structures were developed.

The coarser structures had, however, greater creep resistance. The tensile strength is also greater (*see* Table III). No sudden grain growth was observed at the higher temperatures of treatment such as characterize 'abnormal' steels. Steel *HNA* appears

Table II

ANALYSES OF STEELS FOR ALUMINIUM, OXYGEN, HYDROGEN AND NITROGEN

Steel	Analyses for Aluminium, Oxygen, Hydrogen, and Nitrogen (for methods see Ref. 3)				
	Al (soluble)	Al (insoluble)	Vacuum Fusion (Carbon Reduction)		
			O_2	N_2	H_2
HNA	0·003	<0·001	0·019	0·004	0·00004
FZW	0·039	0·005	0·003	0·006	0·00003
MSS	0·001	0·006	0·011	0·003	<0·00001
*HKD*12	0·004	0·003	0·017	0·004	0·00004
STS	0·001	0·006	0·005	0·008	<0·00001
*M**	0·001	<0·001	0·005	0·007	0·00004
*NGK**	0·004	0·003	0·022	0·003	0·00006
*GBE*1–7*	0·001	<0·001	0·003	0·003	0·00003
*DB**	0·006	0·007	0·004	0·005	0·00002
*NKE**	0·008	0·008	0·005	0·005	0·00013

* The aluminium contents recorded in Refs. 1 and 2 for the above materials should be cancelled. Ref. 3 refers to a superior method by which the present determinations were made.

Table III

ROOM TEMPERATURE PROPERTIES OF STEEL *HNA* IN AIR

Condition of Material (1-in. dia. hot rolled bar)	Limit of Proportionality, tons/in²	Yield Point, tons/in²	U.T.S., tons/in²	Elongation on 4√ area, %	Reduction in area, %	Modulus of Elasticity (10^6 lb/in²)
As received	13·0	20·7	31·6	39·5	66	29·8
	15·4	21·5	32·1	40·5	66	29·2
Normalized 925° C 15 min. Air cooled*	—	(Not definite)	30·7	36	64	—
	9·4	18·95	30·8	38	61	29·6
Normalized 975° C 30 min. Air cooled	9·6	(Not definite)	37·5	27·5	61	29·5

* This treatment was adopted for most tests in this work.

to behave in a similar manner to a 'normal' carbon steel in regard to the effect of aluminium and oxygen on the grain size characteristics.[3]

SHORT TIME (TENSILE) TESTS OF Mo STEEL *HNA*

Tensile tests were carried out *in vacuo* in a special unit (*see* Fig. 3, Ref. 1) and the stress was applied to the specimens in an Amsler testing machine. Measurements of total extension and reduction in area of testpieces were taken after their removal from the testing unit. The properties at room temperature of the material in the as-received, i.e. the hot-rolled, condition and after normalizing are given in the Table III. Some of the data are plotted in Figs. 1 and 2 together with data obtained at elevated temperature (Table IV).

In the tensile tests there is a significant lowering of the limit of proportionality on normalizing (Table III). This fact has been reported by Tapsell and Ridley[6] in tests on three Mo steels which were in the form of superheater tube, steampipe, and superheater header. (Figures for the limit of proportionality on these three steels were respectively 6·7, 14·5, and 14·5 tons/in²).

The highest tensile strength, 37·4 tons/in², is observed at 250° C, and above this temperature there is a steady fall in tensile strength until the $\alpha \rightarrow \gamma$ transformation range (just below 750° C) is reached. This is similar to that observed in carbon steel[1, 2] where the transformation occurs at about 720° C.

Hardness measurements along the central axis of the testpiece gave figures higher after tensile tests at 350° C and 440° C than after a 250° C test although the tensile strength had fallen from 37·4 tons/in² at 250° C to 31·3 tons/in² at 440° C (Table IV).

In Fig. 1 the tensile properties of four carbon steels are compared with steel *HNA*. It is apparent that the 0·5% Mo steel is stronger between 500° C and 750° C than the carbon steels containing up to 0·4% C; but is weaker than the 0·9% C steel, *DB* up to 650° C. It is of considerable interest that above 500° C for the same tensile strength steel *HNA* is 100° C superior to the carbon steels, *NGK* and *M*, which incidentally have a similar carbon content.

A marked increase in ductility is shown at 650° C and above in tensile tests in both the molybdenum steel (Table IV) and in the carbon steels.[1, 2]

Table IV

SHORT TIME TENSILE TESTS *IN VACUO* ON STEEL *HNA*

Specimen letter and number	Temperature of test, °C	U.T.S., tons/in²	Elongation on 4√ area, %	Reduction in area, %	Time to fracture, min	Diamond Pyramid Hardness (10 kg load)		
						Close to fracture	½ in. from fracture	½ in. from fracture
HNA 534	Room temperature	30·7	36	64	2·5	233	232	219
4A2	,,	30·8	38	61	—			
535	250	37·4	23	44	3·0	251	249	221
536	350	35·0	35	53	3·25	268	259	238
533	440	31·3	29	53	2·75	263	243	219
515	550	24·4	33	74	4·0	243	227	199
514	650	13·7	69	85	7·0	200	186	179
516	750	5·1	129	95	18·0	*	*	*
531	850	4·5	77	55	11·0	*	*	*
532	950	3·2	57	42	4·75	*	*	*

* Passed through $\gamma \rightarrow \alpha$ transformation
(*a*) No yield point was observed in these tests
(*b*) The specimens were machined from 1-in. bar which had been normalized at 925° C for 15 min and air cooled
(*c*) The tests at 15°, 250° and 350° were in air. All other tests *in vacuo*.

It is also of interest that the carbon steel, *NGK*, containing 0·17% C was the weakest steel in the ferritic condition but the strongest in the austenitic state (Fig. 1). At 950° C the tensile strengths of the steels shown in this figure are in the reverse order of their carbon contents. It is furthermore clear that at this temperature when the steels are in the austenitic condition the addition of 0·5% Mo has not increased the strength (compare steels *HNA* and *NGK*).

CREEP TESTS OF Mo STEEL *HNA*

The vacuum creep tests were carried out in the special units erected for the earlier work on commercial irons and carbon steels.[1, 2] The diameter of the standard testpiece used in the work was 0·357 in., but where loads in excess of 10 tons/in² were required the diameter of the test specimen was reduced to 0·282 or 0·226 in. to keep the load on the creep machine below one ton.

The stresses and temperatures imposed on the creep and tensile specimens are shown in Figs. 2–5 which record the rupture life, elongation, and reduction in area.

The load/life relationship for the material in the temperature range 450–850° C is plotted in Fig. 3. The curves for the relationship at 550° C and 650° C are markedly different in shape. It should be noted that at 550° C, a load of 21 tons/in² will cause rupture in a specimen after 33 h. This is only 3·4 tons/in² less than the tensile strength of the material. The reduction in area of the specimen has fallen markedly from 74 to 42% but the value of elongation less sharply from 33 to 27%. Two further tests at 20 tons/in² and 18 tons/in² at this temperature lasting for 60 and 125 h gave reductions in area of 21 and 18%, and elongation of 16 and 13% respectively. These results show a fairly rapid reduction of ductility. No evidence was obtained that intercrystalline cracking occurred although there was

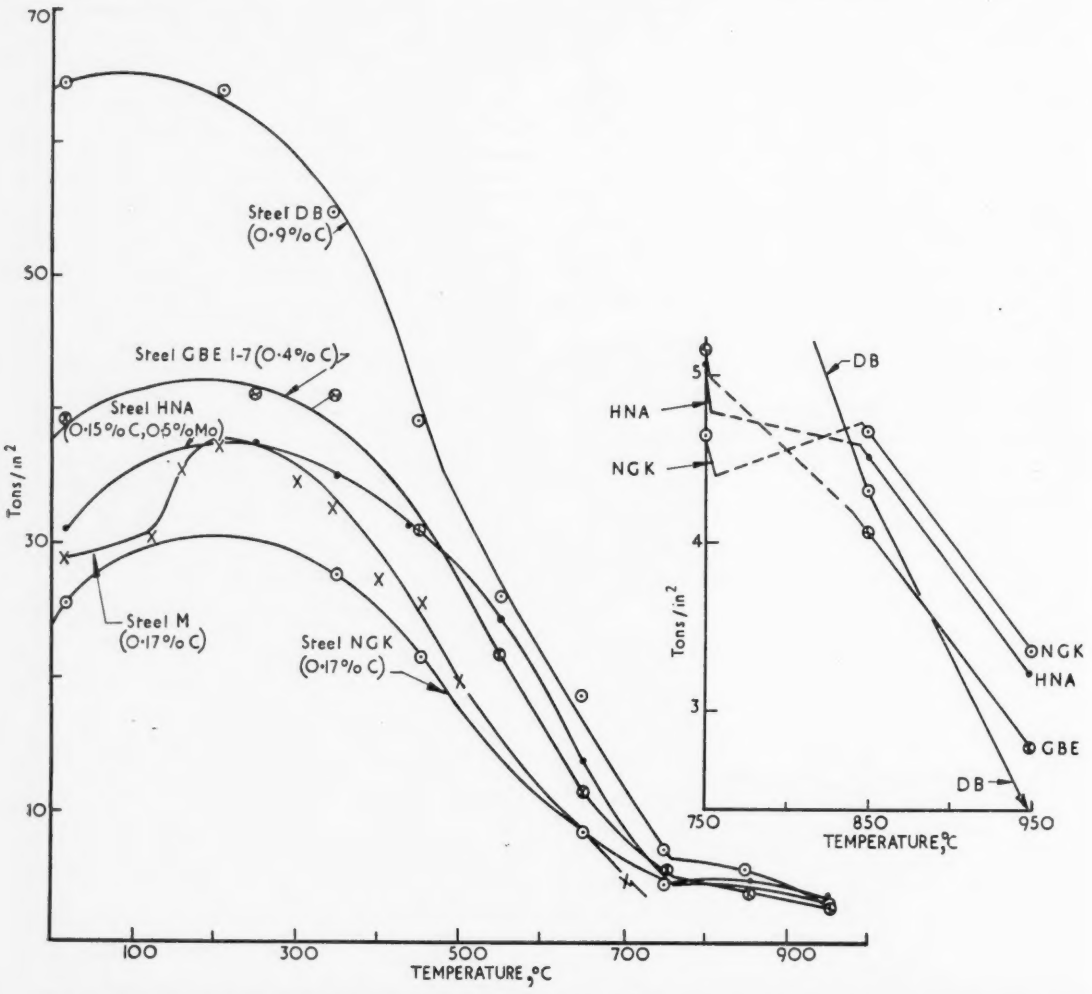

Fig. 1—Tensile strength of the 0·5% Mo steel *HNA* compared with carbon steels containing 0·17–0·90% C

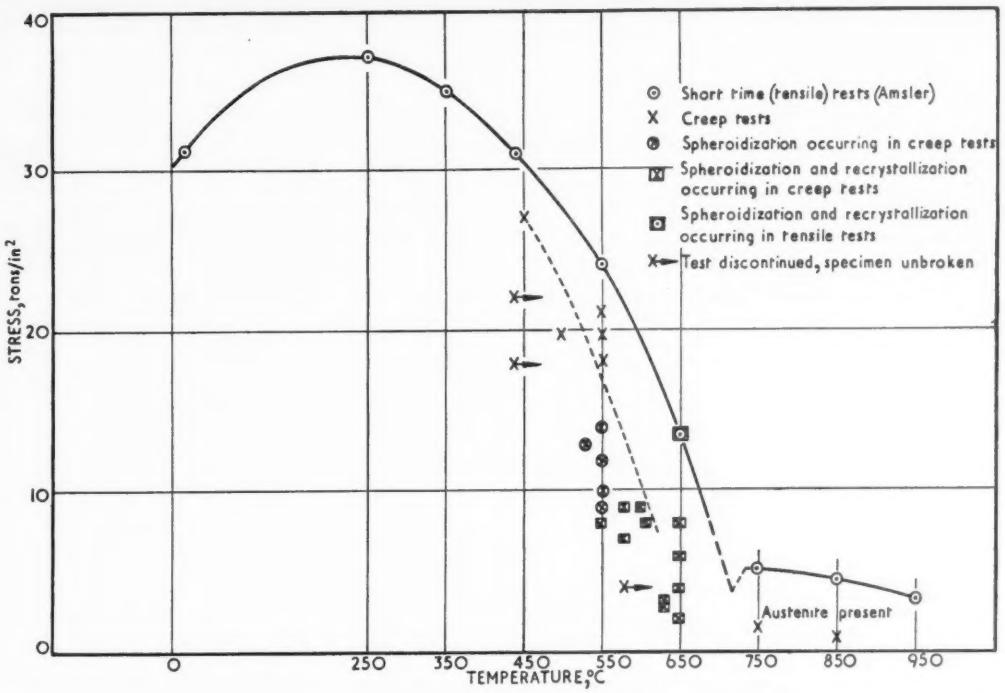

Fig. 2—Boundary of transcrystalline and intercrystalline fracture in short time (tensile) and creep tests in 0·5% Mo steel *HNA*

evidence of the development of cavities some of which were elongated during the course of testing. In a longer time creep test at the same temperature lasting 330 h, intercrystalline cracks were however developed but recrystallization was not observed (*see* Fig. 16*c*, and the discussion on this specimen in the section on microstructure).

At 650° C the short time tensile testpiece showed spheroidization and recrystallization without intercrystalline cracking. Although the duration of loading was 0·07 h, the furnace was maintained at a constant temperature before test following a heating

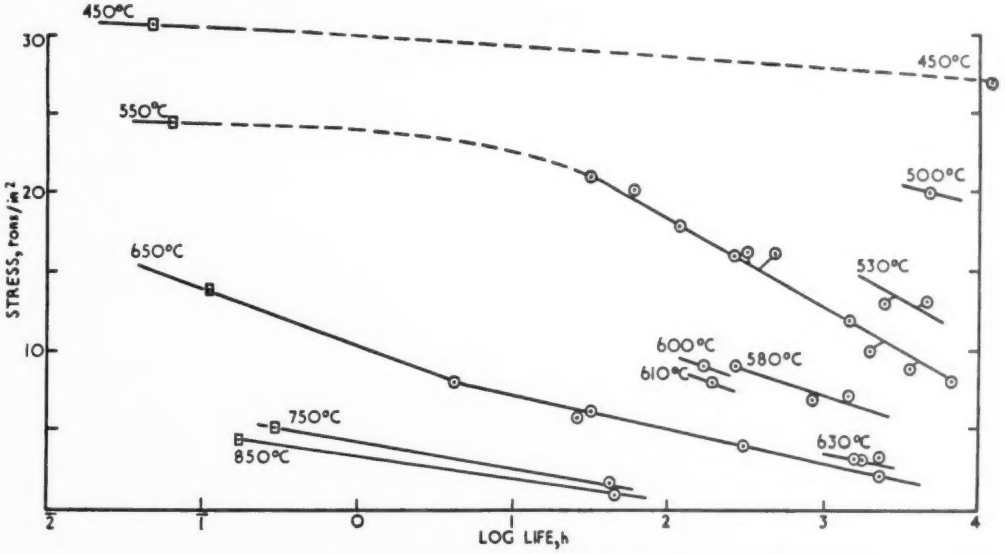

Fig. 3—Load/life relationship for steel *HNA* in tests *in vacuo*

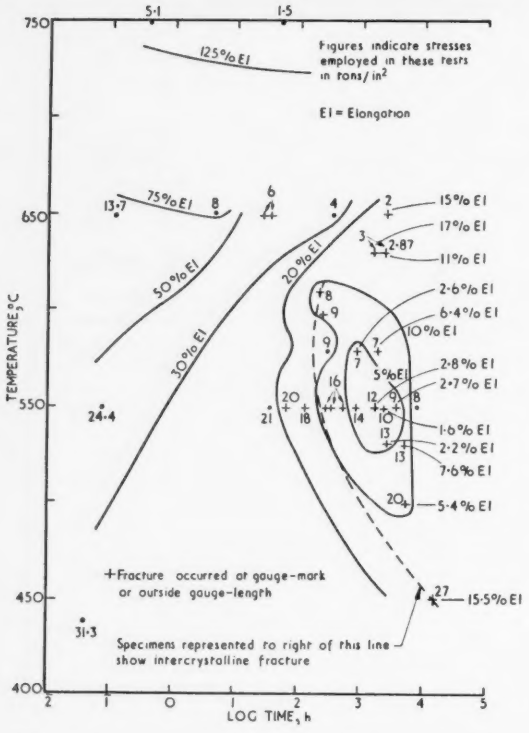

Fig. 4—Relationship of elongation to intercrystalline fracture

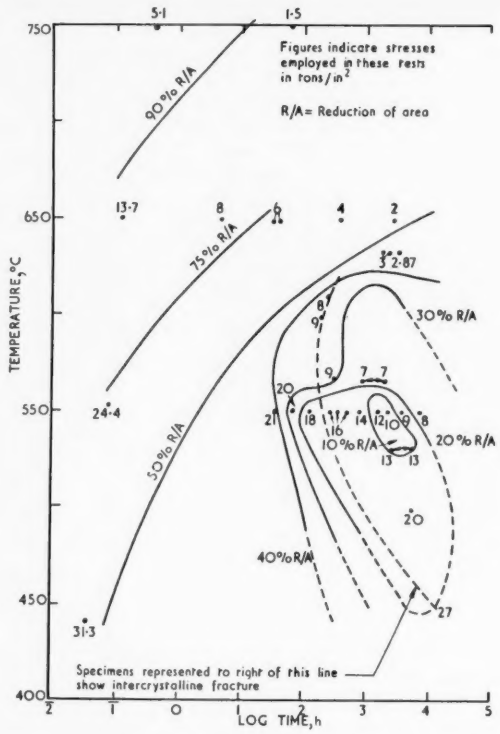

Fig. 5—Relationship of reduction in area to intercrystalline fracture

period of 2–3 h. The specimen after a test at 2 tons/in² at 650° C showed that much recrystallization was present. The line of rupture followed the new set of grain boundaries formed during the recrystallization.

The elongation and reduction in area figures of the specimens are plotted in Figs. 4 and 5. The direction of the contours in these figures shows that a minimum value in the properties occurs at 550° C in about 2000 h. A test specimen under 9 tons/in² broke in 3768 h with an elongation of 2·7% and a reduction in area of 13%; a further specimen under a stress of 8 tons/in² which lasted for 6825 h showed improvement in the degree of elongation and also in its reduction in area, the values being 15 and 28%, respectively.

A broken line is shown in Figs. 2, 4, and 5, to show the boundary of transcrystalline and intercrystalline rupture as determined by microscopic examination of the specimens.

COMPARISON OF CREEP PROPERTIES OF STEEL *HNA* WITH OTHER MOLYBDENUM AND CARBON STEELS

Comparisons of the tensile strength and stress to rupture in 300 and 3000 h in molybdenum steels, carbon steels, and commercial irons are given in Table V. The creep data for rupture at 300 and at 3000 h are plotted in Figs. 6 and 7.

Above 550° C it is apparent that the Mo–V steel *HKD*12, containing 0·27% V, is stronger than the plain Mo steels, *HNA* and *FZW*. These latter are in turn superior to the carbon steels which are themselves appreciably stronger than the com-

KEY TO TABLE V

* = at 625° C
† = at 567° C
e = extrapolated value from tests at different stresses at the temperature given
f = at 4 tons/in² the creep rate at 200 h is 1·5 millionths/h

Steel	McQuaid-Ehn test	A.S.T.M. Grain-size	Creep rate at 550° C under 9 tons/in² at 8 days in millionths/h: N. at 925° C	N. at 975° C	A.C. from 1100° C
HNA	N.	1–3	5·8	1·2	1·4
FZW	AbN.	5–8	21·0	4·3	2·1

Table V

COMPARISON OF THE TENSILE STRENGTH AND STRESS TO RUPTURE IN 300 AND 3000 h

Steel letter and number	Heat treatment before test	Creep or tensile tests in vacuum (V) or air (A)	Ultimate tensile strength, 1 Stress for 300 h rupture life, 2 Stress for 3000 h rupture life, 3 tons/in²	Temperature of test, °C														Paper Reference
				R.T.	250	350	450	500	530	550	580	600	630	650	750	850	950	
Mo Steels																		
HNA 95	N.925° C	V	1	30·7	37·4	35·0	31·3	—	—	24·4	—	—	—	13·7	5·1	4·5	3·2	For creep rate in air see ref. 7 pp. 167 and 171
			2	—	—	—	28·2	—	—	16·0	8·8*f*	—	4·6*e*	4·0	0·6*e*	0·85*e*	—	
			3	—	—	—	27·4	20·6	13·4	10·1	—	—	2·5*e*	1·8	—	—	—	
FZW 13	N.975° C	A	1	30·5	—	—	—	—	—	—	—	—	—	—	—	—	—	5
			2	—	—	—	—	—	—	13·0	10·8*e*	—	—	2·9*e*	—	—	—	
			3	—	—	—	—	—	—	8·7	5·0*e*	3·5	—	—	—	—	—	
MSS 92	N.975° C	A	1	27·0	—	—	25·0	—	—	—	—	—	—	—	—	—	—	6 and 9
			2	—	—	—	—	—	—	—	—	—	—	—	—	—	—	
			3	—	—	—	—	—	—	—	6·0†	—	—	—	—	—	—	
Mo–V Steels																		
*HKD*12 24	N.1000° C	A	1	37·8	—	—	—	—	—	—	—	—	—	—	—	—	—	5
			2	—	—	—	—	—	—	18·0*e*	16·4	—	10·6	7·3	—	—	—	
			3	—	—	—	—	—	18·6*e*	15·2	10·2	8·5*e*	6·0	—	—	—	—	
STS 129	N.950–980° C +T.670–690° C	A	1	—	—	—	—	—	—	—	—	—	—	—	—	—	—	8
			2	—	—	—	—	—	—	—	—	—	8–9*	—	—	—	—	
			3	—	—	—	—	—	—	—	—	—	—	—	—	—	—	
Cr–Mo Steel																		
SEV 128	N.930° C	A	1	—	—	—	—	—	—	—	—	—	—	—	—	—	—	8
			2	—	—	—	—	—	—	—	—	—	6–7*	—	—	—	—	
			3	—	—	—	—	—	—	—	—	—	—	—	—	—	—	

Carbon Steels				R.T.	250	300	350	400	450	500	550	650	750	850	950			Ref.
NGK 97	N.950° C	V	1	25·4	26·0	—	27·7	—	21·3	—	13·7	8·2	4·6	4·7	3·35			1 and 2
			2	—	—	—	—	20·0	13·0	—	5·0	1·3*e*	0·5*e*	0·85	0·50			
			3	—	—	—	—	15·0*e*	8·0*e*	—	2·2*e*	—	—	—	—			
M —	N. by Makers	A (tensile) V (creep)	1	28·7	37·3	—	32·7	—	25·5	—	15·0	7·5	—	—	—			1 and 2
			2	—	—	—	23·8	—	17·5	10·0	5·2	2·0	0·5*e*	—	—			
			3	—	—	—	—	—	12·5*e*	7·3*e*	2·2*e*	—	—	—	—			
*GBE*1 14	N.900° C	V	1	39·0	41·0	—	40·8	—	31·0	—	21·7	11·2	5·3	4·1	2·77			1 and 2
			2	—	—	—	—	—	16·8	—	6·1	2·0	1·0	1·4	0·59			
			3	—	—	—	—	—	13·2	—	4·0	—	—	—	—			
DA —	N.950° C+ N.875° C	V	1	46·6	52·5	—	45·2	—	34·4	—	23·4	13·3	6·8	4·3	2·58			2
			2	—	—	—	—	—	16·0	—	6·2	2·0	1·0	0·85*e*	0·45*e*			
			3	—	—	—	—	—	12·4*e*	—	—	—	—	—	—			
DB	N.900° C+ N.850° C	V	1	64·4	63·6	—	54·4	—	38·1	—	25·9	18·7	7·1	4·3	2·33			2
			2	—	—	—	—	—	19·8	—	6·4	2·1	1·25	0·85*e*	0·41*e*			
			3	—	—	—	—	—	15·0*e*	—	—	—	—	—	—			
NKE —	N.790° C	V	1	53·2*	—	—	—	—	—	—	—	—	—	—	—			2
			2	—	—	—	—	—	13·7*e*	8·15*e*	5·6*e*	1·8	1·18	0·6*e*	0·12*e*			
			3	—	—	—	—	—	12·2*e*	—	—	—	—	—	—			
DC —	N.950° C+ N.900° C	V	1	58·2	63·0	—	57·9	—	44·0	—	30·5	15·0	8·7	4·1	2·17			2
			2	—	—	—	—	—	19·8	—	6·2	1·9	1·0	0·65	0·39			
			3	—	—	—	—	—	14·7	—	—	—	—	—	—			
Commercial Irons																		
S — (Swedish Iron)	As received, hot rolled bar	V	1	19·7	—	—	25·7	—	16·2	—	10·4	5·3	2·8	1·55	3·33			1
			2	—	—	—	16·4	10·2	6·5	3·9*e*	2·5	1·05	—	0·2*e*	0·40			
			3	—	—	—	—	—	4·2*e*	—	—	—	—	—	—			
A — (Armco Iron)	As received, hot rolled bar	V	1	20·4	—	—	23·5	—	15·1	—	8·6	5·2	3·2	2·3	3·17			1
			2	—	—	16·2	12·9	9·8	6·2	—	2·6*e*	1·3	0·8	0·15*e*	0·25			
			3	—	—	—	—	—	5·0*e*	—	—	—	—	—	—			
C — (Carbonyl Iron)	As received plate	V	1	18·2	—	—	13·7	—	11·6	—	7·4	3·8	2·5	0·9	2·51			1
			2	—	—	—	7·3*e*	5·6	3·5*e*	—	2·2*e*	0·66	—	—	0·25			
			3	—	—	—	—	—	—	—	—	—	—	—	—			

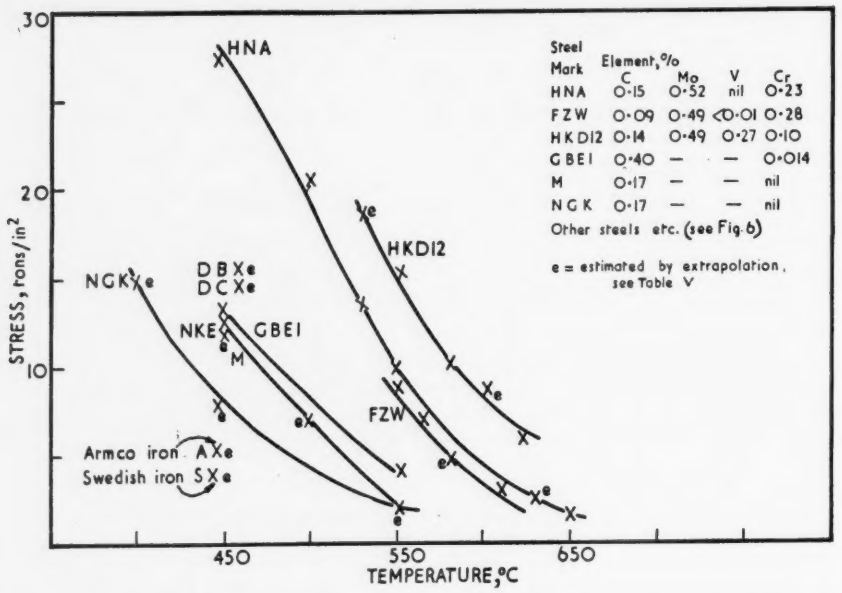
STRESS, tons/in²
TEMPERATURE, °C
HNA
HKD12
NGK
DBXe
DCXe
NKE
GBE1
M
FZW
Armco iron AXe
Swedish iron SXe
Steel Mark | Element, % C | Mo | V | Cr
HNA | 0·15 | 0·52 | nil | 0·23
FZW | 0·09 | 0·49 | <0·01 | 0·28
HKD12 | 0·14 | 0·49 | 0·27 | 0·10
GBE1 | 0·40 | — | — | 0·014
M | 0·17 | — | — | nil
NGK | 0·17 | — | — | nil
Other steels etc. (see Fig. 6)
e = estimated by extrapolation, see Table V

Fig. 6—Comparison of steel *HNA* with several other materials. Curves of stress to rupture in 300 h (Refs. 1, 2, 3)

mercial irons (Swedish, Armco, and Carbonyl irons). Two additional points for a Mo–V and a Cr–Mo steel *STS* and *SEV* respectively are given in Fig. 6 for an estimated rupture life of 300 h. The greater strength of the Mo–V steel is confirmed whereas the Cr–Mo steel shows agreement with the plain Mo steels.

The elongation and reduction in area of steel *HNA* has been compared with that of the carbon steels. (The data for the reduction in area may be more informative than that for the elongation which may include elongation due to the widening of cracks which is not shown in the reduction in area values. In addition the effect of local necking at the point of fracture is clearly shown in the values for the reduction in area but not well shown in those for elongation.) In creep tests of steel *HNA* (Fig. 2), the elongation and reduction in area in tests at

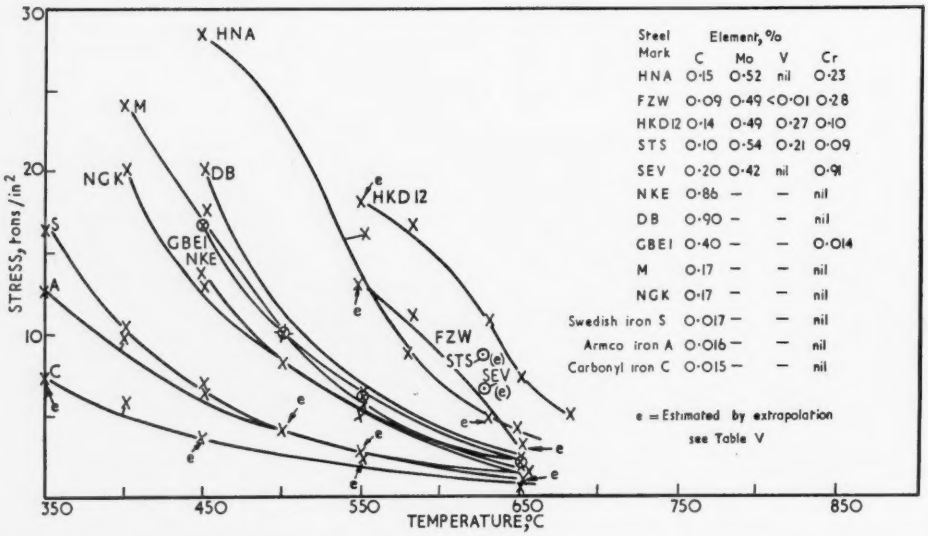
STRESS, tons/in²
TEMPERATURE, °C
HNA
M
NGK
DB
GBE1
NKE
HKD12
FZW
STS
SEV
Steel Mark | Element, % C | Mo | V | Cr
HNA | 0·15 | 0·52 | nil | 0·23
FZW | 0·09 | 0·49 | <0·01 | 0·28
HKD12 | 0·14 | 0·49 | 0·27 | 0·10
STS | 0·10 | 0·54 | 0·21 | 0·09
SEV | 0·20 | 0·42 | nil | 0·91
NKE | 0·86 | — | — | nil
DB | 0·90 | — | — | nil
GBE1 | 0·40 | — | — | 0·014
M | 0·17 | — | — | nil
NGK | 0·17 | — | — | nil
Swedish iron S | 0·017 | — | — | nil
Armco iron A | 0·016 | — | — | nil
Carbonyl iron C | 0·015 | — | — | nil
e = Estimated by extrapolation see Table V

Fig. 7—Comparison of steel *HNA* with several other materials. Curves of stress to rupture in 3000 h (Refs. 1, 2, 3)

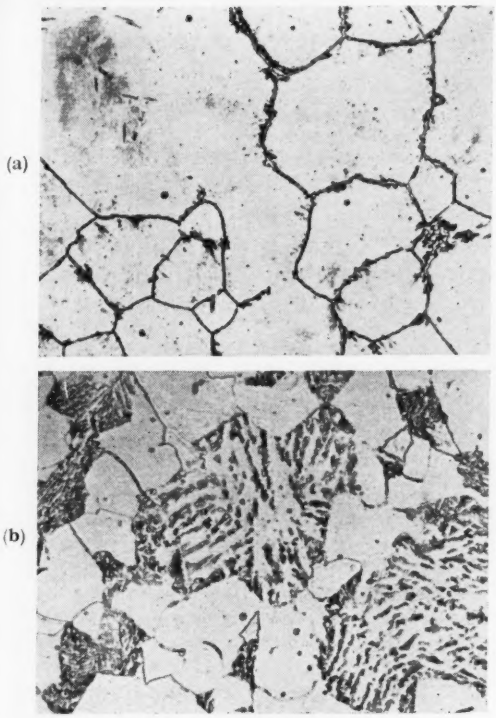

Fig. 8—(*a*) Steel ***HNA***. McQuaid-Ehn test. A.S.T.M. Grain size 1–3 × 150
(*b*) Steel ***HNA***. Material before test. Normalized 925° C, 15 min A.C. × 500

450°, 530°, and 550° C, is low whereas in carbon steels[2], at 450° C and 550° C the ductility is good except for the elongation values for some high carbon steels[2] e.g. steel *DB* containing 0·90% C at 450° C which falls to 6·5%.

In some previous work from the laboratory[5] creep tests in air were made on steels *FZW* and *HKD* 12 at stresses of between 3 and 17 tons/in² and temperatures between 530° C and 700° C. This earlier work (*see* Fig. 9 of the previous paper) shows a minimum

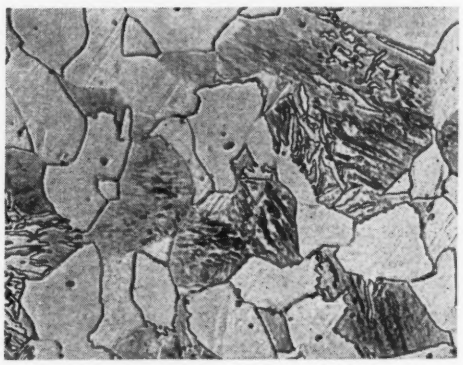

Fig. 9—Microstructure of 1-in. dia. bar. Heat treated N. 925° C, 15 min A.C. to 550° C then W.Q. × 500

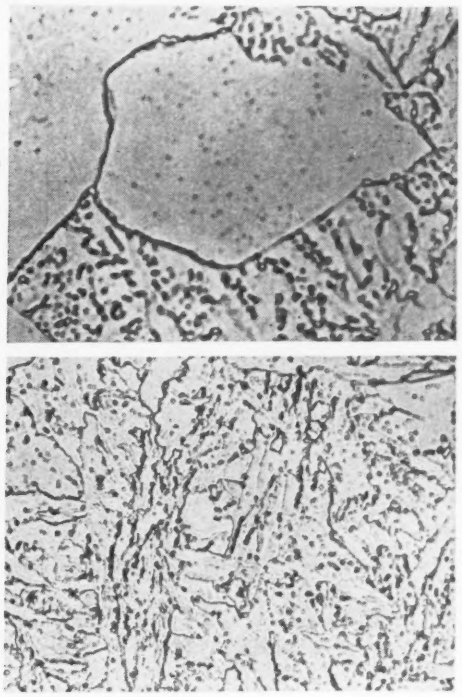

Fig. 10—(*a*) Steel ***HNA***, 925° C. 15 min A.C. + 14 days 625° C A.C. × 1500
(*b*) Steel ***HNA***, 1100° C. 15 min A.C. + 60 days 650° C A.C. × 500

value for the elongation occurring in the Mo steel in about 2000 h at 550° C (this is very similar in time to the occurrence of minimum ductility in steel *HNA* as discussed above and also shown in Fig. 4). In that work, the long time tests were affected by oxidation e.g. a test on steel *FZW* at 5 tons/in² ruptured after 19,600 h at 550° C with only 4·5% elongation whereas 15% elongation was obtained on steel *HNA* after 6825 h. A sample of Mo–V steel *HKD*12 which at 550° C lasted 5383 h in a test in air under a stress of 13 tons/in² showed low extension (4·0%) after fracture and little improvement was noted at 600° C after 1000 h in air (*see* Fig. 16 of Ref. (5)).

MICROSTRUCTURE

A treatment, consisting of heating to 925° C for 15 min followed by air-cooling, was given to the steel before testing in the creep or tensile units. The resulting microstructure (Fig. 9) shows ferrite and bainite together with a pearlitic type of constituent which consists of needles of ferrite which precipitated from the austenite during cooling in the range 700–650° C. Under the microscope the carbide particles are less well resolved than in a carbon steel. Figure 30 shows the appearance under the electron microscope of a bainitic area and a portion of a carbide-free ferrite grain. After long time annealing at 625–650° C (Figs. 10*a* and *b*), the carbide particles can be resolved clearly and lie in the same areas

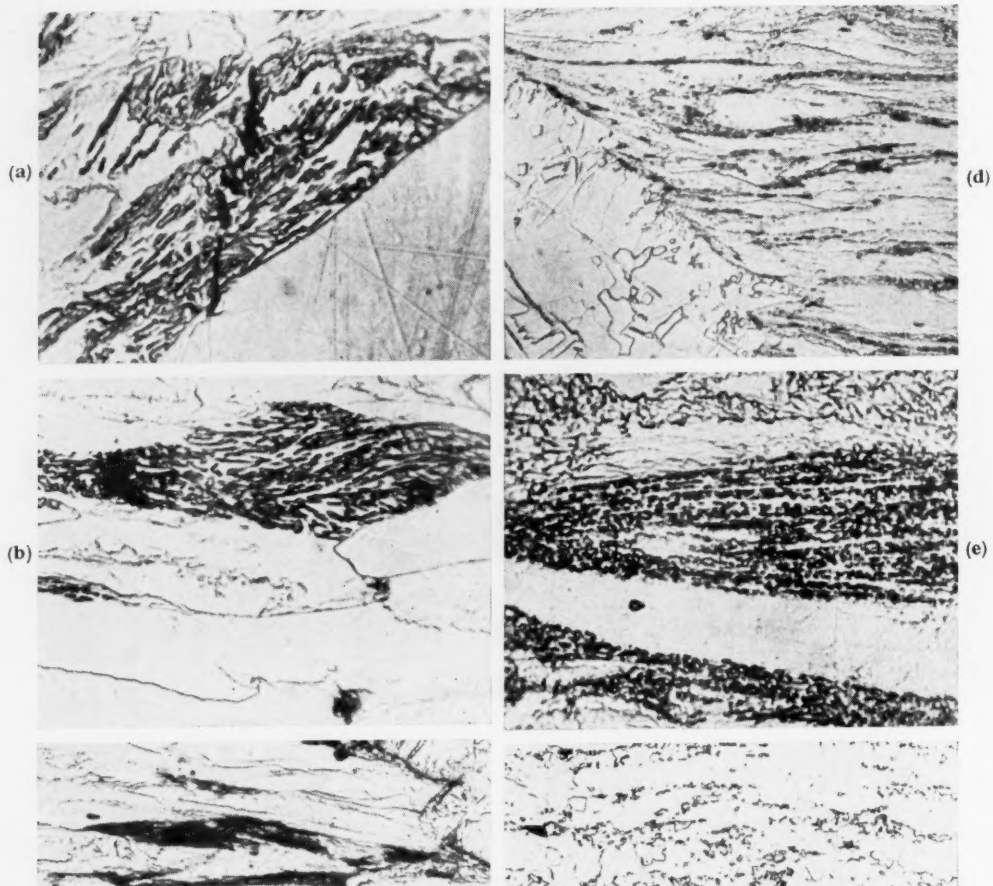

Fig. 11—(*a*) Short time (tensile) test 350° C, section close to fracture. 35 tons/in². El. 35%. R/A 53% × 1500
(*b*) Short time (tensile) test. 440° C. Section close to fracture. 31·3 tons/in². El. 29%. R/A 53% × 1500
(*c*) Short time (tensile) test. 550° C. Section at iron-plated fracture. 24·4 tons/in². El. 33%. (*See* Fig. 12). R/A 74% × 500
(*d*) Short time (tensile) test. 650° C. Section at iron-plated fracture. 13·7 tons/in². El. 69%. R/A 85% × 500
(*e*) Details as for (*d*). Section close to fracture × 1500
(*f*) Short time (tensile) test. 750° C. Section ¼ in. from fracture. 5·1 tons/in². El. 129%. R/A 95% × 1500
(*g*) Short time (tensile) test. 850° C. Section ¼ in. from fracture. 4·5 tons/in². El. 77%. R/A 55% × 1500

Table VI

GRAPHITE FORMATION IN MOLYBDENUM STEELS *HNA* AND *FZW*

Steel	Atmosphere during test	Temperature of creep test, °C	Load, tons/in²	Life, h	Elongation, %	Reduction in area, %	Graphite† (by micro-chemical analysis), %
HNA	Vacuum	550	10	2043	1·6*	11	<0·005
FZW	Air	550	7	7010	7·2	—	0·005
,,	,,	550	5	19600	4·5	—	0·005
HNA	Vacuum	580	7	1513	6·4*	28	nil
FZW	Air	580	7	1032	6·5	—	0·01
,,	,,	580	5	2900	10·5	—	0·009
,,	,,	580	3	9000(U)	2·5	—	0·008
,,	,,	610	3	3250	23	—	0·03
HNA	Vacuum	630	3·0	1676	67	48	nil
,,	,,	630	2·87	2294	11*	43	nil
FZW	Air	640	3·0	505	31	—	0·01
HNA	Vacuum	650	4·0	315	32	60	0·01
,,	,,	650	2·0	2359	15*	55	<0·005

* Specimen fractured on or outside gauge mark
† Specimen for analysis out close to and includes fracture: (except where specimen is unbroken. Here a specimen from the parallel portion of testpiece has been taken).

which were formerly occupied by the bainite and pearlite. Thermal curve determinations on cooling and microscopic examination of a sample indicate that the bainite was formed at a temperature of 530° C. The structure of a sample quenched from 550° C, as shown in Fig. 9, consists of ferrite, pearlite, and some austenite. This confirms that the bainite was formed on cooling just below this temperature. An attempt to eliminate the bainitic condition and obtain a ferrite pearlite structure similar to that observed in a carbon steel was made by slowly cooling a sample from the normalizing temperature at 100° C/h. The resulting ferrite showed no tendency to separate in an acicular or needle-shaped form. Thus the habit of crystallization of the final austenitic areas was very different and a relatively fine ferrite carbide eutectoid structure resulted. Specimens containing this fine eutectoid structure are relatively weak (*see* Table VII). It is shown below by the X-ray examination that the carbide formed by the slow cooling just referred to is $(Fe_{21}Mo_2)C_6$ and not Fe_3C as in the steel in the bainitic condition. It is clear that the crystallization habit is dependent on the nature of the carbide separating from the austenite.

In this paper comparison is made with another Mo steel *FZW*. This steel contains little bainite in the condition as tested, i.e. normalized, from 975° C (*see* Ref. (5), Fig. 17).

The fractured test specimens were mounted in soft electro-deposited iron coatings[1, 2] and subsequently sectioned longitudinally to reveal the nature of the deformation at the fracture and at the surface. In the present work the length of the test specimens is represented in the photographs of the microstructures by the longer direction. In the following sections various aspects in the microstructure of tensile and creep specimens are discussed.

Microstructures of Tensile Test Specimens

The examination of the microstructures of tensile test specimens shows the nature of the changes produced by the deformation (Figs. 11*a–g*, 12*a*, 13). At 250° C the steel shows very little distortion of the ferrite and pearlite which is in line with diminution in the degree of elongation and reduction in area. Figure 11*a* shows a section close to the fracture in a short time tensile specimen at 350° C and indicates the deformation of the pearlite grains. The rigidity of the pearlite has prevented continuous deformation with the ferrite and in consequence high internal stress has been developed. To relieve this stress, cracks have developed and have spread through the pearlite grains. The tensile specimen at 440° C has behaved similarly (Fig. 11*b*). In this micrograph slip can be traced in the ferrite grains and cracking has proceeded right through a large but elongated pearlite grain. Later this crack has developed into a cavity under the action of deformation. This type of distortion in the ferrite probably caused by slip in more than one direction in the crystal should be compared with the contorted structure (' woody ' structure) developed in carbonyl iron (*see* earlier work on low-carbon irons and steels—Ref. (1), Figs. 102 and 108). At 550° C the ferrite and pearlite appear capable of receiving greater deformation and there is increased ductility as is evident from the banded structure shown in Fig. 11*c*. Figure 12*a* shows the structure of the steel at a low magnification (16·6 diameters). This photograph indicates the local necking at the fracture and the nature of the elongated longitudinal cavities. Strain lines were observed in carbon steels at 450° C (instead of slip lines at lower temperatures), i.e. 100° C lower in temperature than in the present Mo steel. Strain lines were first observed in the Mo steel at 550° C and are shown in Fig. 11*c* (cf. Fig. 31 of Ref. (1)). Figure 41 of Ref. (1) is also of interest as it shows

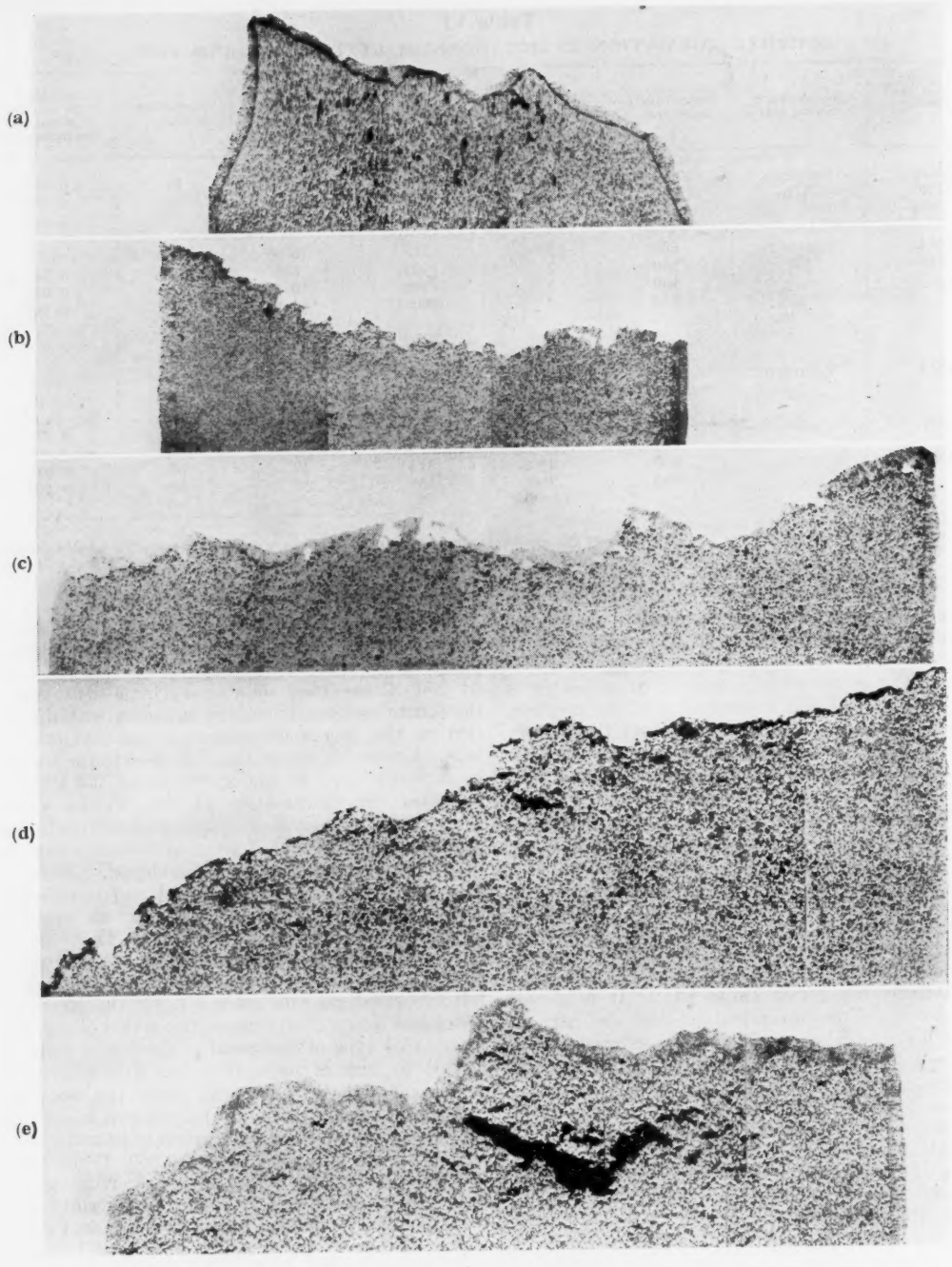

Fig. 12—Iron-plated fractures after sectioning. Specimens tested at 550° C × 50 reduced $\frac{1}{3}$

§ Indicates specimens broken at or outside gauge marks in this and subsequent figures

(*a*) Short time tensile test U.T.S. 24·4 tons/in². El. 33%. R/A 74%, dia. 0·226 in.
(*b*) Creep test specimen 16 tons/in². 330 h to rupture. El. 10%. R/A 14% of 0·226 in.
(*c*) Creep test specimen 16 tons/in². 496 h to rupture. El. 9%. R/A 13%. Specimen 0·357 in.§
(*d*) Creep test specimen 9 tons/in². 3768 h to rupture. El. 2·7%. R/A 13%. Specimen 0·357 in.§
(*e*) Creep test specimen 8 tons/in². 6825 h to rupture. El. 15%. R/A 28%. Specimen 0·357 in.

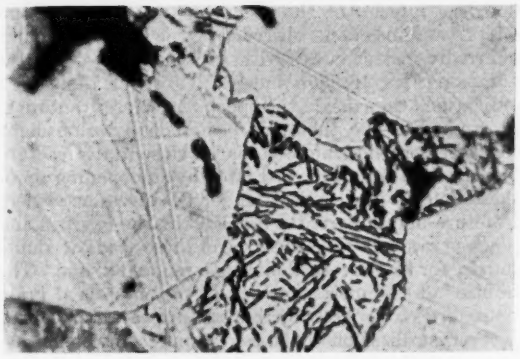

Fig. 13—Short time (tensile) test 950° C. Section close to fracture. 3·2 tons/in². El. 57%. R/A 42% × 1500

Fig. 15—Creep test. 13 tons/in², 530° C. Section close to fracture. 2509 h. El. 2·2%§. R/A 9% × 1500

in the carbon steel at 450° C a similar degree of deformation as in the Mo steel at 550° C. In the tests so far described the fractures are transcrystalline, the rupture occurring across the pearlite grains and without tending to follow the ferrite grain boundaries. Intercrystalline cracking was not observed in any tensile tests on this steel at the range 250–750° C. Deformation has been considerable at 650° C accompanied by recrystallization in the ferrite grains and spheroidization within the elongated pearlite grains (Figs. 11*d* and *e*). The deformation of the pearlite appears to accelerate spheroidization. At 750° C the changes in the steel are rapid under the action of deformation accompanying stress. Complete recrystallization of the ferrite has taken place. The carbide particles have not been taken into solution to form austenite but have remained as discrete particles in the ferrite (Fig. 11*f*). The heavy distortion, recrystallization and spheroidization in tensile tests at 650° C and 750° C appear to have suppressed the tendency to intercrystalline cracking. The specimens tested at these two temperatures show elongated holes in the region of fracture. These have been developed from small rounded cavities at the points of weakness of grain boundaries, such as occur at the junction of grains or at dislocations and other types of faults in the body of the ferrite and pearlite grains.

At temperatures of 850° C and 950° C the steel had been changed to austenite, and the structures depicted in Figs. 11*g* and 13 are the result of cooling down in the furnace of the creep unit at the conclusion of the test. It is apparent that the cracks do not lie in the grain boundaries although they bear some resemblance to intercrystalline cracks. Yet there is little trace of the high ductility of the test-piece. The grain boundary system might have been altered on cooling through the transition range.

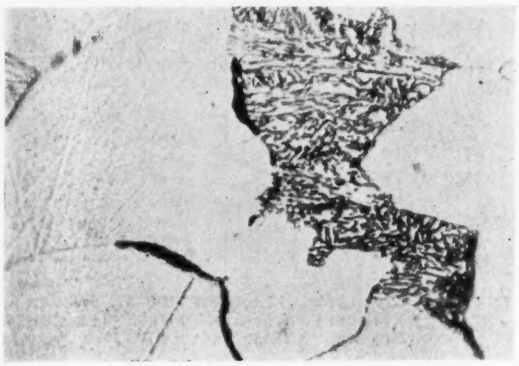

Fig. 14—Creep test. 27 tons/in², 450° C. Section close to fracture. 13,470 h. El. 15·5%§. R/A 20% × 1500

Microstructures of Creep Test Specimens

The microstructure of creep specimens has been studied after testing at temperatures of 450° C and upwards. In a test at 450° C and 27 tons/in² which lasted 13,470 h (Fig. 14), little change is apparent in the character of the carbide in the pearlite grains. Cracking has developed in the grain boundaries between the ferrite and pearlite grains, and also in those between adjacent ferrite grains. At the higher temperature of 530° C under a load of 13 tons/in² (Fig. 15) the pearlite is beginning to show slight spheroidization, but cracking is definitely intercrystalline, and the material at this temperature shows little elongation. In this temperature range 450–530° C, all the fractured test pieces have been in long-time tests of between 2509 h and 13,470 h; and in contradistinction to the short-time tensile tests show typical intercrystalline cracks which are being opened up into longer transverse cracks by the continued stressing. The microstructures of the fracture of the tensile test specimen and four of the creep test specimens at 550° C (reduced from an original magnification of 50 diameters) are shown in Fig. 12. The tensile specimen was discussed above and the considerable elongation of the grains and the formation of longitudinal cavities were noted (Fig. 12*a*). The three creep specimens which fractured in 330, 496, and 3768 h at 550° C show little elongation of the ferrite and pearlite grains (Figs. 12*b–d*), but more elongation is apparent in the longest time test, 6825 h at this temperature (Fig. 12*e*). The unrepolished surfaces of all the creep test specimens after test at 550° C show slip in the ferrite grains and intercrystalline cracking: an example is shown in Fig. 25. The specimen which ruptured in 6825 h under a load of 8 tons/in² was examined on the surface prior to fracture at 5006 and 6727 h. After exposure for

5006 h, when the specimen had stretched 1·4%, 'widening' of the grain boundaries (previously seen in carbon steels and in the various irons[1, 2]) was observed. After 6727 h the specimen had elongated 8·4% (the surface in this case was repolished to obtain a smooth surface and showed a network of intercrystalline cracks (Fig. 18*a* and *b*)). On sectioning this specimen after fracture had occurred in 6825 h with 15% extension, the interior of the specimen did not show the intercrystalline cracks observed on the surface or found internally in test pieces with rupture lives of shorter duration (Figs. 16*c*, 17*a* and *b*). However, there were indications that inside the specimen whose fracture is shown in Fig. 12*e*, there had been initially some slight separation at the grain boundaries close to the fracture but this had been followed later by the opening up of these defects into cavities under the stressing action. Fracture had apparently initiated at the cavities and holes so formed. The presence of these voids accounts in part for the increased elongation noted above. The failure* of the initial cracking of the crystals at grain boundaries to progress further also appears to be caused by recrystallization of the ferrite under local deformation at the ends of the cracks. Recrystallization has also been facilitated by the lowering of the Mo content of the ferrite phase arising from the precipitation of the molybdenum carbide Mo_2C. After isolation by chemical extraction, this carbide as well as Fe_3C and $Fe_{21}Mo_2C_6$ has been identified by X-ray examination as described in this paper.

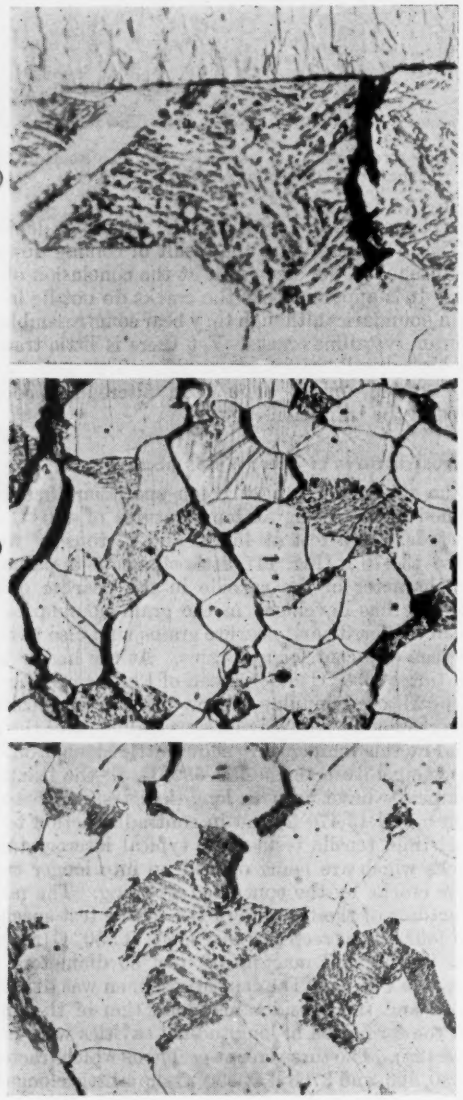

Fig. 16—(*a*) Creep test. 16 tons/in², 550° C. Section at iron-plated surface. 270 h. El. 5·1% R/A 14% × 1500
(*b*) Creep test. 16 tons/in², 550° C. Surface after test ¼ in. from fracture. 330 h. El. 10%§. (*See* Fig. 12). R/A 14% × 500
(*c*) Creep test. 16 tons/in², 550° C. Section close to fracture. 330 h. El. 10%§ (*See* Fig. 12). R/A 14% × 500

* The interruption of the spread of intercrystalline cracks laterally by recrystallization of the matrix has been noted by the authors in a previous paper.[12] The tests in this instance had been made on a copper alloy containing 2·4% Ni and 0·6% Si.

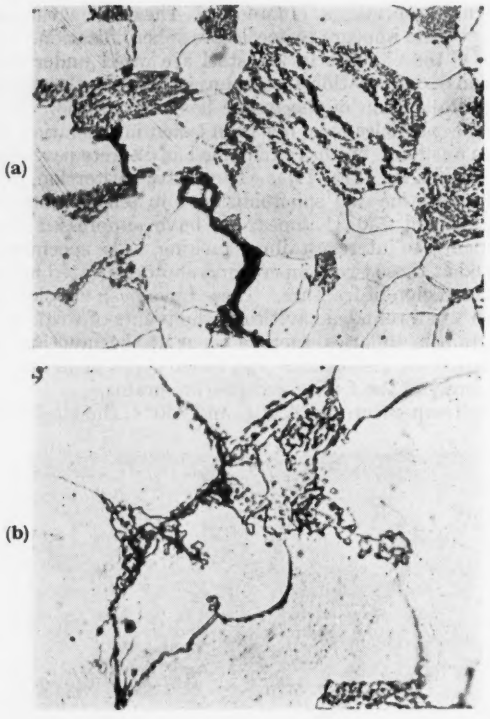

Fig. 17—(*a*) Creep test. 12 tons/in², 550° C. Section at iron-plated fracture. 1518 h. El. 2·8%§. R/A 10% × 500
(*b*) Creep test. 12 tons/in², 550° C. Section close to fracture. 1518 h. El. 2·8%§. R/A 10% × 1500

Table VII—X-RAY EXAMINATION OF RESIDUES FROM STEEL *HNA* FOR CARBIDES

Condition of Material				Diamond Pyramid Hardness (10 kg)			X-ray Analysis						Micro-structure (Fig. No.)	Creep Rate (at 8 days in a test at 550° C 9 tons/in², 10^{-6} in./in./h
							Alcoholic Iodine Reagent for Solution of Iron in Steel			Either (*a*) Citric Acid, I, HCl bath, or (*b*) 10% HCl in Alcohol Bath used electrolytically for Solution of Iron in Steel				
Heat-Treatment and Duration of Test (h)	Creep Test													
	Load, tons/in²	Elong. ($4\sqrt{A}$), %	Red. in A., %	Unstressed	‡ in. from fracture	Close to fracture	Residue,* %	Carbides Identified	Notes	Residue,* %	Carbides Identified	Notes		
(1)	(2)	(3)	(4)	(5)	(6)	(7)	(8)	(9)	(10)	(11)	(12)	(13)	(14)	(15)
As-received hot-rolled bar	Unstressed			166	—	—	0·81	Fe_3C	—	(*a*) 0·63	no X-ray pattern	—	—	3·7
A.R. + 925° C, 15 min, A.C. (referred to as *N*)	Unstressed			147	—	—	2·61	Fe_3C	—	(*a*) 1·26	no X-ray pattern	—	8*b*	5·8
A.R. + 925° C, 15 min, then slowly cooled in 6 h at 100° C/h	Unstressed			128	—	—	—‡	$M_{23}C_6+Fe_3C$	Fe_3C weak	(*a*) 0·36	no X-ray pattern	—	—	13
A.R. + 1100° C, 15 min, A.C.	Unstressed			175	—	—	2·0	Fe_3C	weak pattern	(*a*) 0·55	no X-ray pattern	—	—	1·4
N + 13470 h 450° C	27	15·5†	28	148	253	254	1·6	Fe_3C	—	(*a*) 0·42	no X-ray pattern	—	14	—
N + 2509 h 530° C	13	2·2†	9	156	164	166	2·28	Fe_3C+Mo_2C	Mo_2C v. weak	(*b*) 0·50	no X-ray pattern	—	15	—
N + 4634 h 530° C	13	7·6†	10	154	180	184	2·32	Fe_3C+Mo_2C	Mo_2C v. weak	(*b*) 0·30	no X-ray pattern	—	—	—
N + 125 h 550° C	18	13	18	142	156	208	2·08	Fe_3C	—				—	—
N + 1518 h 550° C	12	2·8†	10	158	155	160	2·76	Fe_3C+Mo_2C	Mo_2C v. weak				17*a*, *b*	—
N + 2043 h 550° C	10	1·6†	11	139	149	139	2·21	Fe_3C+Mo_2C	Mo_2C v. weak				—	—
N + 3768 h 550° C	9	2·7†	13	142	142	137	2·09	Fe_3C+Mo_2C	Mo_2C weak	(*b*) 1·33	Fe_3C	weak pattern	—	—
N + 6825 h 550° C	8	15	28	136	135	120	>1·3‡	Fe_3C+Mo_2C	Mo_2C weak	(*b*) 0·48	Fe_3C+Mo_2C		18*c*	—
N + „ „ „	Screw thread of test piece				—	—	1·85	Fe_3C+Mo_2C	Mo_2C weak	(*b*) 0·70	Mo_2C		—	—
N + „ „ „	Shoulder of test piece				—	—	2·63	Fe_3C+Mo_2C	Mo_2C weak	(*b*) 1·09	Mo_2C		—	—
N + 336 h 625° C	Unstressed			147	—	—	1·50	Fe_3C+Mo_2C	—	(*a*) 1·46	Fe_3C		10*a*	107
N + 2294 h 630° C	2·87	11†	43	122	118	95	2·44	$M_{23}C_6+Mo_2C+Fe_3C$	—	(*a*) 1·25	Fe_3C		23*a*, *b*	—
N + 0·11 h 650° C	13·7	69	85	—	179	200	2·3	Fe_3C	—				11*d*	—
N + 315 h 650° C	4	32	60	130	126	104	2·45	$Fe_3C+Mo_2C+M_{23}C_6$	$M_{23}C_6$ weak	(*a*) 1·26	Fe_3C+Mo_2C	Mo_2C weak	—	—
1100° C 15 min A.C. + 1440 h 650° C	Unstressed			153 111	—	—	1·90	Fe_3C+Mo_2C	—	(*b*) 0·64 (*a*) 0·69	Mo_2C+Fe_3C Mo_2C+Fe_3C		— —	122 180
N + 2359 h 650° C	2	15†	55	115	107	81	2·24	$M_{23}C_6+Fe_3C+Mo_2C$	Mo_2C weak	(*a*) 1·42	$Fe_3C+M_{23}C_6+Mo_2C$	Mo_2C weak	27*a*, *b*	—
N + „ „ „	Unstressed			115	—	—	2·58	$Fe_3C+M_{23}C_6+Mo_2C$	—	(*b*) 1·51	$M_{23}C_6$		—	—
N + 2500 h 675° C	Unstressed			115	—	—	1·02	$M_{23}C_6+Mo_2C+Fe_3C$	Fe_3C weak	(*a*) 0·66	$M_{23}C_6+Mo_2C$		—	—
N + 315 h 650° C + 24 h 675° C	Unstressed after the 315 h at 650° C			128	—	—	2·50	$Fe_3C+Mo_2C+M_{23}C_6$	$M_{23}C_6$ v. weak	(*b*) 0·57	Mo_2C+Fe_3C	Fe_3C weak	—	—
N + 315 h 650° C + 24 h 700° C	Unstressed after the 315 h at 650° C			125	—	—	1·72	$Fe_3C+Mo_2C+M_{23}C_6$	$M_{23}C_6$ v. weak	(*b*) 0·42	Mo_2C+Fe_3C	Fe_3C weak	—	—

* = Sections of creep specimens taken close to fracture:
$M_{23}C_6$, maybe $(Fe_{21}Mo_2)C_6$
† = Fracture at a gauge mark
‡ = Some lost in extraction

In addition to this precipitation at 550° C, spheroidization of the primary carbide Fe_3C has proceeded (Figs. 17*a* and *b*, 18*b* and *c*). However, this latter change does not alter the Mo content of the ferrite as little of the molybdenum is associated with this carbide. Kuo[19] reports that 1–2% Mo may be dissolved in Fe_3C, and Goldsmidt[18] records only 0·5%. Incidentally, these authors report a solubility for chromium in Fe_3C of 18% and 15% respectively, which gives an opportunity for retention of some of the chromium. If some is retained it would increase the stability of the Fe_3C and tend to prevent graphitization.

In tests at 580° C, an examination of the surface of specimens shows slip to be present in the ferrite grains but the intercrystalline cracks present at the surface have not extended laterally as at lower temperatures (compare Fig. 19*a* with Fig. 16*b*). At this temperature recrystallization is most marked in a test of short duration, namely 277 h, but little is seen in the longer time tests of 872 and 1573 h, i.e. tests at a lower rate of deformation (Figs. 19*b* and 20*a–c*). Spheroidization of the carbide in the pearlite grains is proceeding considerably faster at temperatures of 580° and 600° C than in the tests at 550° C (compare Fig. 16*a* with Figs. 19*b* and 21). At 630° C the spheroidized carbide particles spread beyond the area of the original pearlite grains into the surrounding ferrite (Figs. 22*a* and *b*, and 23*a*). The carbide particles in the grain boundaries show considerable growth (Figs. 22*a* and 23*b*). There is also precipitation of fine particles of molybdenum carbide, Mo_2C, in the tests lasting 1676, 1819 and 2294 h as shown by the microstructures in

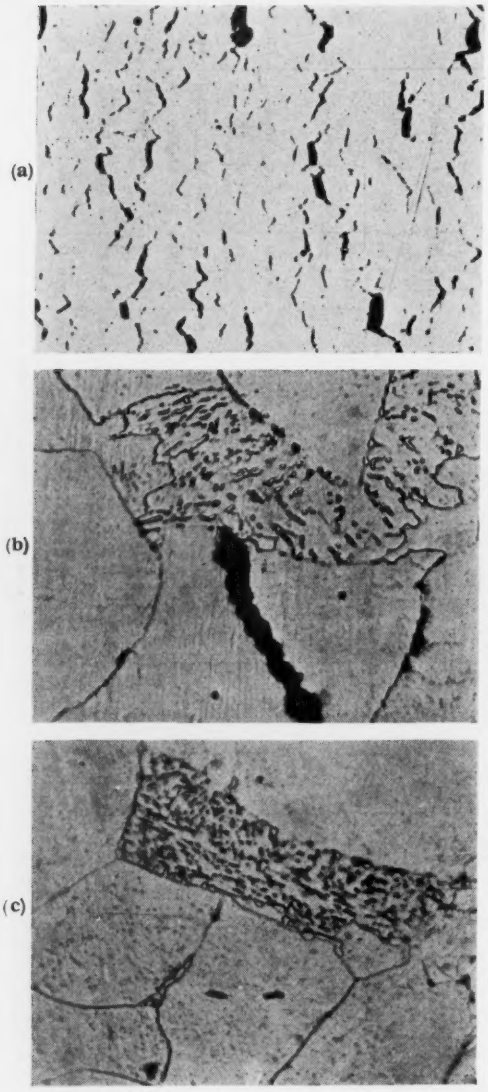

Fig. 18—(*a*) Creep test. 8 tons/in², 550° C. Surface of unbroken test piece (repolished) after 6727 h. El. 8·4% (*See* Fig. 12) × 150
(*b*) Creep test. 8 tons/in², 550° C. Surface of unbroken test piece (etched) after 6727 h. El. 8·4% (*See* Fig. 12) × 1500
(*c*) Creep test. 8 tons/in², 550° C. Section ¼ in. from fracture. 6825 h. El. 15% (*See* Fig. 12) R/A 28% × 1500

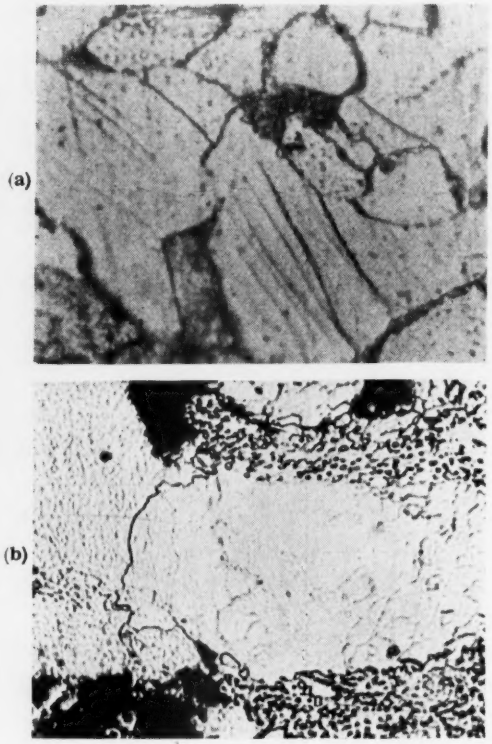

Fig. 19—(*a*) Creep test. 9 tons/in², 580° C. Surface after test ¾ in. from fracture. 277 h. El. 23%. R/A 37% × 1000
(*b*) Creep test. 9 tons/in², 580° C. Section close to fracture. 277 h. El. 23%. R/A 37% × 1500

Figs. 22*a*, 23*a* and *b*. Figure 31 shows an electron micrograph at a magnification of 5000 diameters of spheroidized particles of residual Fe_3C and smaller parallel-sided ones of Mo_2C. The largest particles are $M_{23}C_6$. The deformation/time curves of these tests did not show any abrupt or gradual alteration in shape which could be related to the change in strength on the formation of molybdenum carbide, but creep tests carried out on material so as to produce this

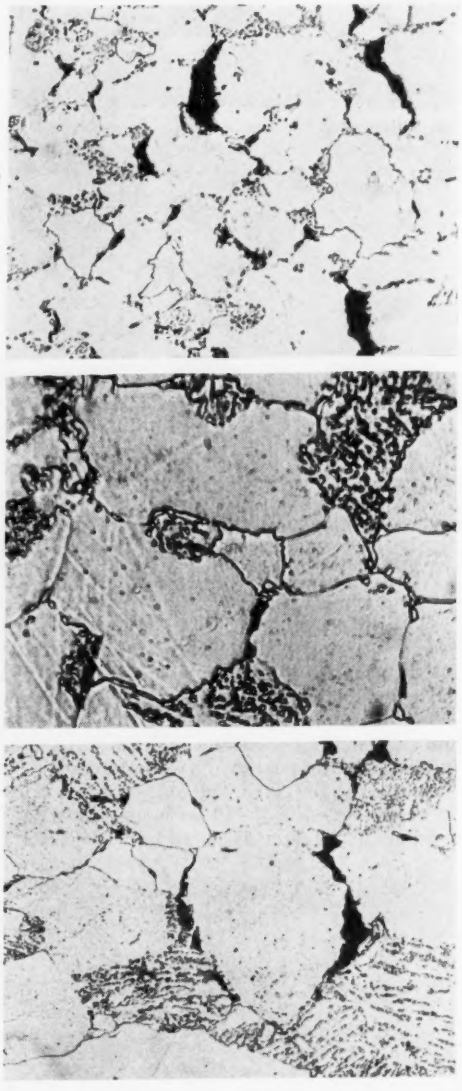

Fig. 20—(*a*) Creep test. 7 tons/in², 580° C. Section close to fracture. 872 h. El. 2·6%§. R/A 21% × 500
(*b*) Creep test. 7 tons/in², 580° C. Section ¼ in. from fracture. 872 h. El. 2·6%§. R/A 21% × 1500
(*c*) Creep test. 7 tons/in², 580° C. Section close to fracture. 1513 h. El. 6·4%. R/A 28% × 1500

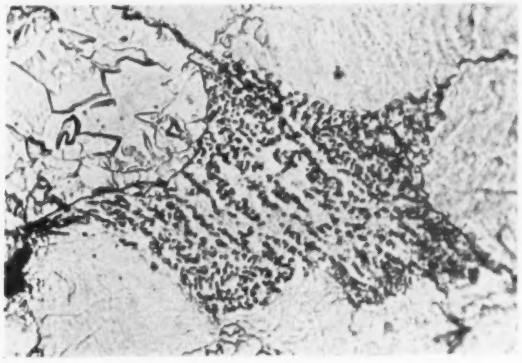

Fig. 21—Creep test. 9 tons/in², 600° C. Section at iron-plated fracture. 175 h. El. 5·5%§. R/A 32% × 1500

carbide (Mo_2C) before the test began, show a marked reduction in strength (*see* column 15 of Table VII). Sub-crystallization (or polygonization)[1, 2] of the ferrite appears in these specimens (*see* Fig. 22*a* which represents the structure 0·25 in. from a fracture and Fig. 23*a* close to a fracture). This form of recrystallization in creep specimens is discussed in a later section.

The changes at 650° C are more marked than at lower temperatures. Spheroidization is proceeding rapidly and, with longer periods of testing, the pearlite areas are becoming less sharply defined (compare Fig. 25 with Figs. 24, 26, and 27). Both coarse and fine carbide particles are present in Figs. 26*b* and 27, the coarser being $(Fe_{21}Mo_2)C_6$ which was formed from Fe_3C, and the finer Mo_2C precipitated in the ferrite as mentioned previously. Recrystallization has occurred in the ferrite. In tests which lasted a few hundred hours some rounded holes occur close to the fracture in a similar manner to those first noted for the specimen shown in Fig. 12*e* at 550° C after 6825 h. In the longer time test of 2359 h (Fig. 27*e*) some intercrystalline cracks which had apparently developed earlier in the test appear to have been prevented from spreading by marked recrystallization as noted at lower temperatures (550° and 580° C).

The temperature of test (750° C), was close to that of the transformation temperature, and to ensure that the steel was above the lower critical point during the test, the creep specimen was heated to 850° C for 1 h in the testing unit before testing. The temperature was then lowered to 750° C, and the load put on. (The tensile specimen tested at this temperature discussed previously was not so treated.) A high elongation has resulted in the creep test, and the material appears to have completely recrystallized. The grains of pearlite formed on cooling from the austenite present a rounded appearance (Fig. 28) probably because the softer ferrite grains have flowed around the harder austenitic grains.

The fracture of the test specimen at 850° C shows intergranular type cracking but it should be remembered that the steel was in the austenitic condition at the temperature of test and changed to ferrite on cooling (Fig. 29).

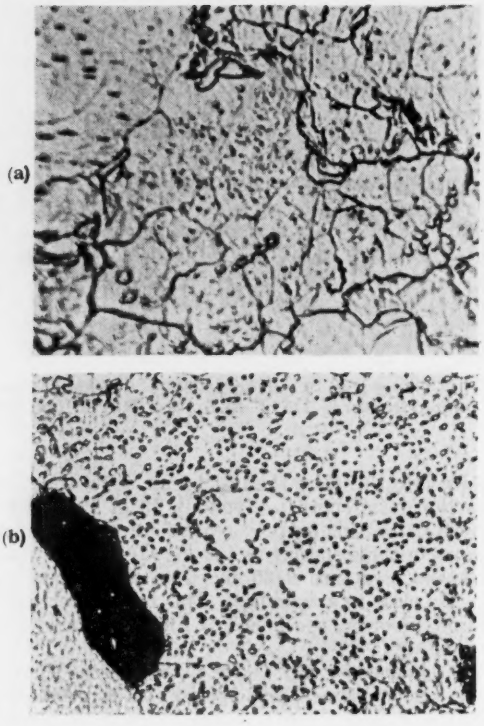

Fig. 22—(*a*) Creep test. 3 tons/in², 630° C. Section ¼ in. from fracture. 1676 h. El. 67%. R/A 48% × 1500
(*b*) Creep test. 3 tons/in², 630° C. Section close to fracture. 1819 h. El. 17%. R/A 32% × 1500

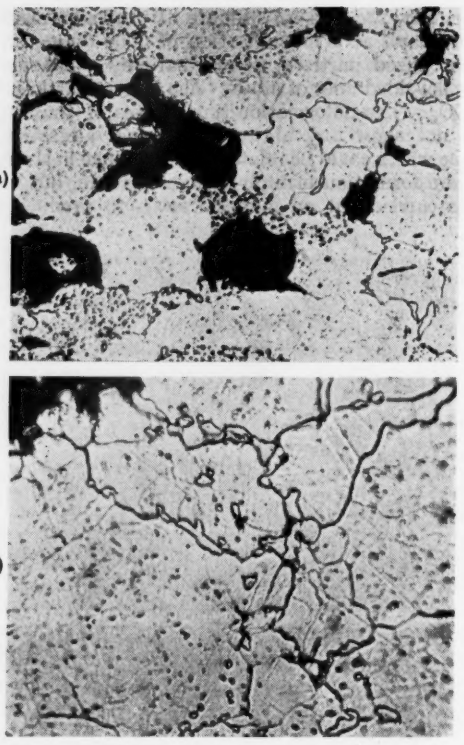

Fig. 23—(*a*) Creep test. 2·87 tons/in², 630° C. Section close to fracture. 2294 h. El. 11%§. R/A 43% × 500
(*b*) Creep test. Details as for (*a*). Section close to fracture × 1500

Spheroidization of Carbide

The incidence of spheroidization in creep tests and in one of the tensile tests is traced in Fig. 2. This effect is first seen under the microscope on sections of specimens in creep tests at 530° C lasting 2509 and 4634 h (Fig. 19*b*). At higher temperatures the rate increases, and after a testing time of 721 h at 550° C the change begins to be visible. In longer time tests at 550° C, i.e. those for times of 3768 and 6825 h, more progress has occurred. In the latter case, where the deformation is greater, namely 15%, the degree of spheroidization has increased. Movement of carbide particles from the pearlite into the ferrite grains has not occurred at 550° C though long particles of carbide have accumulated in the grain boundaries (Fig. 18*c*). After tests at 580° for 277 h and at 600° C for 175 h

Fig. 24—Creep test. 8 tons/in², 650° C. Section at iron-plated fracture. 4 h. El. 78%. R/A 76% × 150

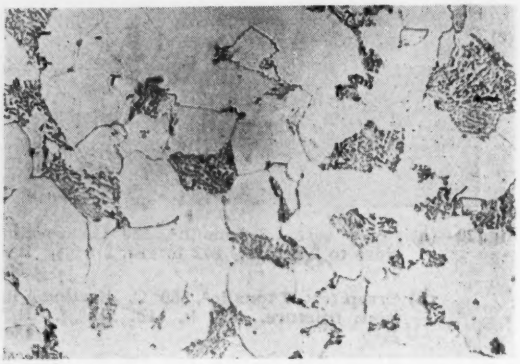

Fig. 25—Unstressed material. 650° C. 4 h × 500

(Figs. 19*b* and 21), spheroidization of the pearlite is more marked.

The above-named features agree with those previously reported in earlier work from this Laboratory for a 0·5% Mo steel (*MSS*)[6] after 5270 h at 580° C and in another Mo steel (*FZW*)[5] tested in creep in the temperature range 535° C and above. In the present work the effect of deformation on spheroidization is quite appreciable; for example, in the tensile test at 650° C spheroidization occurs close to the fracture, but is not to be found where the deformation is less (0·25 in. away). Also in the creep tests lasting 315 and 2359 h, spheroidization, dispersion of the spheroidized carbide into the surrounding ferrite grains, and growth of carbide particles have all occurred close to the fracture (Figs. 27*a* and *b*). In contrast, the degree of spheroidization in unstrained material at 625° C and 650° C is shown in Figs. 10*a* and *b*, for times of exposure of 336 and 1440 h respectively (compare with Figs. 23*b* and 27*b*). Figure 10*a* shows a trace of the ferritic needle structure of the Widmanstätten type remaining after fairly full spheroidization of the carbide. This tendency can be shown more clearly in a sample coarsened in the austenitic condition at 1100° C, and subsequently spheroidized by more severe heat treatment (Fig. 10*b*). Comparison with Fig. 22*b*, which shows the microstructure of the steel given a creep test of comparable magnitude of exposure to high temperatures, indicates that stress has removed the needle structure by recrystallization of the ferrite. The recrystallization is type 1 (p. 43), the conditions not having caused 'full' recrystallization. Spheroidization occurs in creep tests[1, 2] in carbon steels at lower temperatures than in those containing molybdenum. At 450° C the 0·17% C steels, *M* and *NGK*, both show considerable spheroidization in creep test specimens in the regions adjacent to fracture.

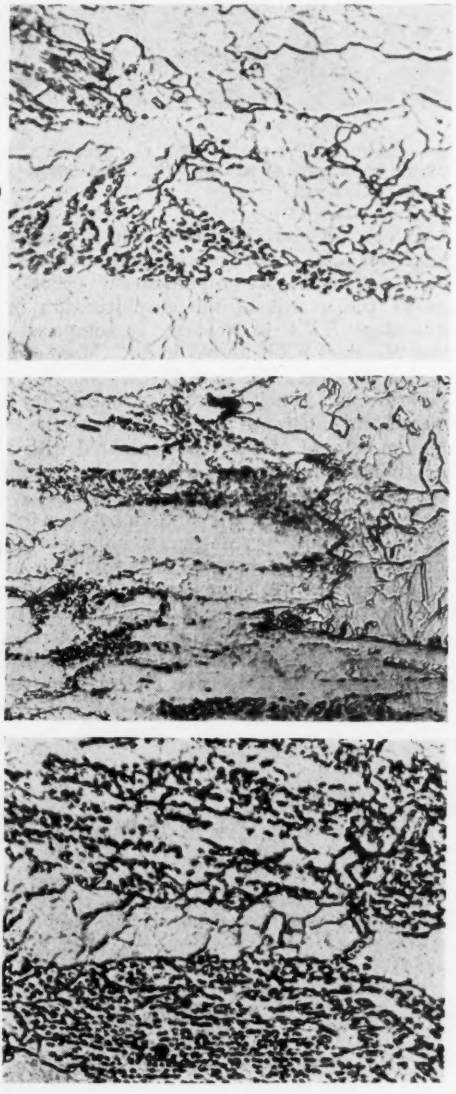

Fig. 26—(*a*) Creep test. 6 tons/in², 650° C. Section close to fracture. 28 h. El. 30%§. R/A 67% × 1500

(*b*) Creep test. 6 tons/in², 650° C. Section at iron-plated fracture. 33 h. El. 17%. R/A 71% × 500

(*c*) Creep test. 6 tons/in², 650° C. Section close to fracture. 33 h. El. 17%§. R/A 71% × 1500

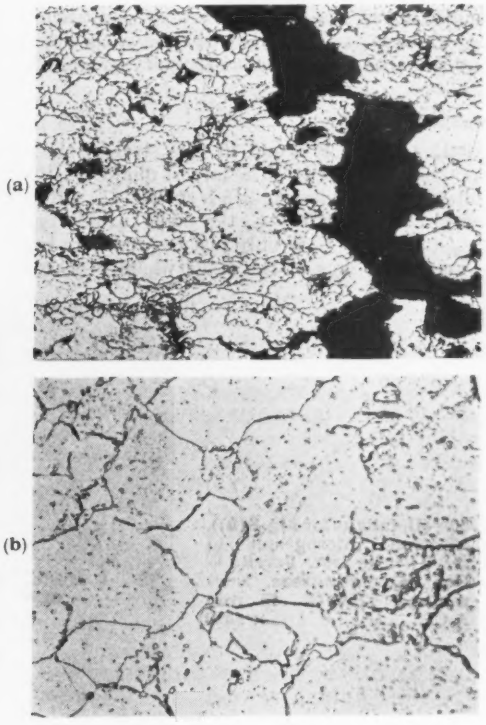

Fig. 27—(*a*) Creep test. 2 tons/in², 650° C. Section close to fracture. 2359 h. El. 15%§. R/A 55% × 150

(*b*) Creep test. 2 tons/in², 650° C. Section ½ in. from fracture. 2359 h. El. 15%§. R/A 55% × 500

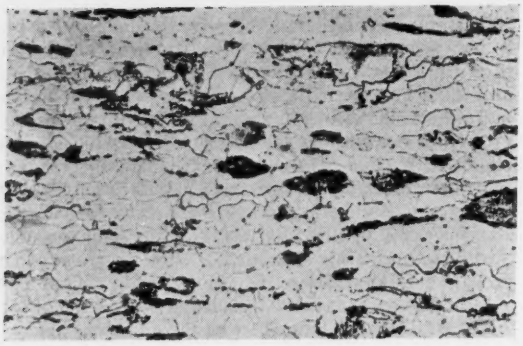

Fig. 28—Creep test. 1·5 tons/in², 750° C. Section close to fracture. 44 h. El. 141%. R/A 86% × 500

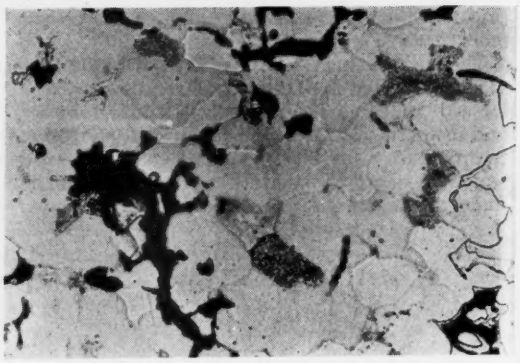

Fig. 29—Creep test. 1 ton/in², 850° C. Section at iron-plated fracture. 46 h. El. 67%. R/A 50% × 500

In a recent paper by Sinnott, Rohrig, Freeman, and Rush[21] there is an account published of the results of 100,000 h tests on a 0·13% C, 0·60–0·62% Mo steel steam pipe in service at 482° C. The steel was fine grained (A.S.T.M. grain size 5–8), i.e. an abnormal creep rate steel. Examination showed that spheroidization associated with massive carbide in the grain boundaries had taken place. There was also a fine general precipitation in the ferrite grains. The steel appeared to be transforming faster than the 'normal' steel *HNA* now discussed in the present work but the precipitation in the ferrite grains was apparently of Mo_2C which is similar to that isolated in specimens in this series after creep tests at temperatures of 530° C and above.

Graphitization

Little graphite is found in this steel in the tests carried out (Table VI). The largest quantity, 0·01%, results from a test lasting 315 h at 650° C. After this interval of time at 650° C, the main carbide present is Fe_3C; $(Fe_{21}Mo_2)C_6$ is only just beginning to replace the Fe_3C, and thus at the stage where Fe_3C can be detected as undergoing graphitization is prior to its change to $(Fe_{21}Mo_2)C_6$ and it is likely that at this stage a maximum rate of graphitization occurs. In Table VI the extent of the graphitization in the present steel *HNA* in vacuum is compared with another Mo steel *FZW* tested in air. More graphite is found in the steel *FZW* at 610° C, a somewhat lower temperature; but in neither steel is the quantity large. The significant difference is perhaps due to the higher aluminium content of *FZW* as compared with *HNA* rather than to differences in the testing conditions such as testing in air as compared with that in vacuum. Both steels, *HNA* and *FZW* contain between 0·2 and 0·3% Cr which may be sufficient to influence the rate of graphitization. Further, as is shown later in this paper, the carbides are themselves changing composition during test. The effect of annealing is to reduce the Mo content of the ferrite phase and increase the amount in the carbides, and the higher Mo content in the carbide may be a decisive factor in preventing graphitization in Mo steel.

Fig. 30—(Details as for Fig. 8 (*b*)). Electron micrograph of steel before test. Ferrite + Fe_3C in bainitic areas. Normalized 925% C. 15 min A.C. × 5000

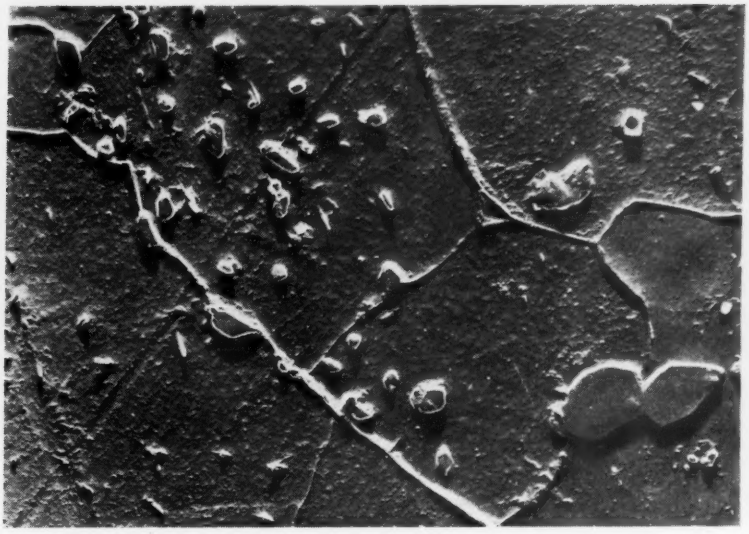

Fig. 31—(Details as for Fig. 23). Electron micrograph of steel. 2·87 tons/in², 630° C. 2294 h. Close to fracture. Showing Fe_3C as spheroidized carbide and Mo_2C as parallel sided particles. The largest particles which tend to be polygonal are of $M_{23}C_6$ type × 5000

Graphite has been found in carbon steels[2] in considerable amounts in creep test specimens in the temperature range 450–650° C, especially where the Mn–Si ratio is low. In the present two Mo steels this ratio is not low enough to be a factor accelerating graphitization.

Recrystallization

The recrystallization changes recorded in the following paragraphs are in line with the deductions made in earlier papers.[1, 2, 5, 11, 12, 14] As set forth in the paper published in 1935[1] the deformation under creep stress at high temperature may lead to:

(1) Grain growth
(2) Generation of new crystals by full recrystallization
(3) Division of existing crystals into smaller units: sub-crystallization.[1, 2, 5, 12] The terms polygonization and sub-crystallization have been introduced in recent years for similar phenomena in high purity aluminium.[13]

Recrystallization occurs to a small degree close to the fracture in the longest time test, 6825 h at 550° C. It will be remembered[1, 2] that carbon steels show marked recrystallization at about 1000 h at 450° C. At temperatures of 580° C and 600° C, polygonization of the ferrite is clearly revealed. An example is shown in Fig. 19*b*. In addition slight general recrystallization is observed close to the fracture in the sample tested at 600° C. In contrast the lightly deformed specimens at 580° C which lasted for 872 and 1513 h (i.e. with low extensions of 2·6 and 6·4% respectively) did not show recrystallization (Figs. 20*a* and *b* and compare with Fig. 19*b*, elongation 23%.) At 630° C in three tests lasting 1676, 1819, and 2294 h, polygonization of the ferrite has occurred (Figs. 22*a* and 23). Unstressed material exposed to similar or longer times at 630° C does not show either general recrystallization or polygonization. Recrystallization is also found in both tensile and creep specimens, but not in unstressed specimens, at 650° C (Figs. 11*d* and *e*, 25, 26, 27*a*, and 10*b*).

NATURE OF CARBIDES ISOLATED FROM TEST SPECIMENS OF STEEL *HNA*

X-ray examinations have been carried out on the residues obtained from the creep and tensile specimens by chemical or electrolytic solution attack of the steel. Three methods have been used to extract the carbides. These in some cases are contaminated by other materials depending on the efficacy of the separation.

(*a*) Citric acid, iodine, HCl bath
(*b*) 10% HCl in alcohol bath
(*c*) Alcoholic iodine reagent

In (*a*) and (*b*) the residues have been obtained by electrolysis while in (*c*) there has been simple solution of the matrix in the iodine reagent.

The electrolytic baths (*a*) and (*b*) have been used by a number of earlier workers[16, 17, 19] who have all pointed out that the results must be carefully examined since the carbides may be affected by the chemical or electrolytic action. In the case of the present steel *HNA*, while residues have been obtained in every case using baths (*a*) and (*b*) the quantity extracted has been small compared with what was to be expected. Assuming all the carbon in the steel (0·15% in this case) to be present as the carbide, Fe_3C, about 2·25% of carbide residue should be obtained. The results given in Table VIII show that using baths (*a*) and (*b*) the residues obtained from the various creep test and heat-treated specimens range from 0·30–1·51%, more being obtained in general where long heat treatment had taken place and at the higher temperatures of test. The results of the X-ray examination of the residues obtained by baths (*a*) and (*b*) are shown in columns 12 and 13 of Table VII. The residues extracted from the material as normalized or from creep test specimens which had been tested at 450° C for a period of 13,470 h or at 530° C for periods of 2509 and 4634 h, or at 550° C for shorter times than 3768 h all failed to give X-ray patterns. It appeared that the carbides were attacked by the reagents used in baths (*a*) and (*b*). In the longer time tests at 550° C, X-ray patterns of Fe_3C and Mo_2C were ob-

tained, while in tests at 630° C and above, a further carbide of the $M_{23}C_6$ type $(Fe_{21}Mo_2)C_6$[18,19,22] was found but these compounds were identified in residues which were deficient in quantity.

The failure to obtain satisfactory X-ray patterns from certain of the residues referred to above, a fact also noted by previous investigators on C–Mo steels, led to the use of another reagent (*c*) alcoholic iodine, which had been used in the Laboratory[15] for the analysis of oxides in steel. Its use especially at room temperature instead of hot (for oxide analyses) has led to the recovery of much larger residues approximating in weight to that which would be expected if most of the carbon was present as carbide. The use of reagent (*c*) shows an all-round improvement in the amount of carbide extracted (compare column 8 with column 11 in Table VII). The X-ray results obtained by this method (*c*) are given in columns 9 and 10. There has been in most cases little breakdown of the carbide residues but the percentage extracted from the 'as received' sample is still low, but X-ray examination has given good patterns from all the residues.

The results of the general examination of the extracted carbides suggest that three carbides Fe_3C, Mo_2C, and $(Fe_{21}Mo_2)C_6$ are present in the creep test specimens, depending on the temperature and time of test; perhaps in some cases these carbide changes have been accelerated by the deformation given to the material. It appears that the material shows different resistance to creep and behaviour at different temperatures, depending on the carbides that are present.

The microstructure of steel *HNA* before test, i.e. as normalized from 925° C, consists of ferrite, pearlite, and some bainite, as discussed earlier; the carbide of the pearlite and bainite is shown by X-ray examination to consist of cementite (Fe_3C). If slower cooling rates such as 100° C/h are used from the austenitic range Fe_3C is not formed but the carbide $(Fe_{21}Mo_2)C_6$ is identified as the chief constituent, as a result of the higher temperature of transformation induced by this slower rate of cooling.

The partition of molybdenum between the ferrite and the carbide in Fe–C–Mo steels has been referred to by Bowman, Parke, and Herzig,[10] in steels isothermally transformed at 1200° F (649° C), 1100° F (593° C), and 1000° F (538° C). They mention that at the highest temperature $(FeMo)_{23}C_6$ is formed, but at 593° C, Fe_3C appears in addition while at 538° C, Fe_3C is produced alone. They have studied the redistribution of the molybdenum between the ferrite and the carbide resulting from the peritectic type of reaction by which Fe_3C is formed. The alloys discussed have a higher carbon content (0·40%), and the time of reaction has probably been insufficient for Mo_2C to be formed from the ferrite.

Kuo[19] and Hultgren[20] report proportions of molybdenum partitioned between the carbide and the ferrite amounting to 8 : 1. Bowman, Parke, and Herzig,[10] in their work at 1200° F (649° C) on an iron alloy containing a 0·78% C, 0·54% Mo, find an even higher partition ratio.

Crafts and Offenhauer[16] also investigated the peritectic type of reaction by which Fe_3C is formed but consider that at higher temperatures such as 700° C the compound formed is Mo_2C and not $(FeMo)_{23}C_6$. These authors had adopted quenching and tempering for times up to 64 h of their alloys before study of the identity of the compound. Bowman, Parke, and Herzig[10] used isothermally transformed material which showed $(FeMo)_{23}C_6$ to be produced but their longest time of treatment was 2 h and probably was insufficient for full diffusion of molybdenum to occur; and thus Mo_2C was not produced although isothermal transformation might assist the attainment of equilibrium. It is interesting that Kuo[19] adopting an intermediate time of 24 h at 700° C found in a 0·23% C, 0·80% Mo steel that both Mo_2C and $(Fe_{21}Mo_2)C_6$ were present.

In the sample of *HNA* cooled at 100° C/h, conditions were not dissimilar to those in Bowman and his co-worker's experiments, and confirmation was obtained that the major compound in these circumstances is $(Fe_{21}Mo_2)C_6$ ($M_{23}C_6$ type). The present work also confirms the possibility of changes in the nature of the carbides below the temperature of decomposition of the austenite, but no claim is made that equilibrium conditions have been attained. These changes might be due to the existence of peritectic reactions as suggested by other authors. Further reference should also be made to the work of Kuo[19] discussed below who considers MoC to be the final product in the alloys with which he dealt, but many of his steels have either higher carbon or higher molybdenum contents. Goldschmidt[18] also considers that this compound may be present in Fe–Mo–C alloys after a 700° C treatment.

In short-time tests up to a temperature of 650° C and in the long-time test, 13,470 h at 450° C, the single carbide Fe_3C was present. At 530° C and 550° C, in addition to Fe_3C, the carbide Mo_2C appeared as a precipitated phase in the ferrite provided the test has proceeded for a sufficiently long time. Thus 2509 and 4634 h at 530° C, and 1518 and 2043 h at 550° C, were sufficient for Mo_2C to be detected in the X-ray patterns. In tests lasting 3768 and 6825 h at 550° C, much stronger X-ray patterns of Mo_2C have been observed. The presence of this carbide, Mo_2C, has led to the weakening of the ferrite by loss of molybdenum, and this has resulted in increased ductility as given by the elongation of a test specimen. For example (as previously discussed earlier in this paper), in the test at 550° C, which lasted 6825 h, the elongation at the end of the test had reached 15%, while the specimen which lasted 2043 h at this temperature gave only 1·6% elongation.

At temperatures of 630° C and above, in addition to the carbides, Fe_3C and precipitated Mo_2C, the carbide $(Fe_{21}Mo_2)C_6$ was present. This last replaced the cementite, Fe_3C, and was formed by a re-arrangement of the cementite lattice by inclusion of additional iron and molybdenum atoms.[18] In creep specimens tested at 630° C and 650° C, the carbide $(Fe_{21}Mo_2)C_6$ appeared as the major constituent and formed more readily in the heavily deformed areas adjacent to the fractures of the creep specimens.

Steel *HNA* contains 0·15% C and the maximum proportion of Fe_3C which could be formed in a normalized steel would not be sufficient to remove more than a small proportion of the molybdenum. The greater proportion of the molybdenum is therefore to be found in the ferrite and its presence there is the

principal cause of the improvement in creep properties on adding molybdenum to a carbon steel. However, when Mo_2C forms the ferrite loses molybdenum and the creep rate increases as is indicated in column 15, Table VII. Similarly when $(Fe_{21}Mo_2)C_6$ forms from Fe_3C, molybdenum is required and is obtained mostly from the ferrite and in consequence the creep strength tends to be diminished.

CONCLUSIONS

The steel showed normal McQuaid-Ehn characteristics and a good creep resistance. It was tested in the air-cooled condition as 1-in. round bars, normalized from 925° C. After this treatment the molybdenum and to some extent the carbon content were both held in solid solution in the ferrite. During normalizing the γ–α change was not however complete until the steel had cooled to below 550° C.

Testing in vacuum confirmed the loss of ductility which is well known to be the result of exposure to 500–550° C for long periods of time in air. In these experiments a minimum value, less than 3% elongation and 10–13% reduction in area, was observed at about 1500–3700 h at 550° C. In a longer time test in which rupture occurred at 6825 h the material showed a marked recovery to 15% elongation and 28% reduction in area. The results of previous tests carried out in air showed rupture in 7010 h at this temperature, the elongation being 7·2% and in a second specimen at a lower stress rupture occurred at 19·600 h with an elongation of 4·5%. These reduced values are the result of oxidation which had penetrated along the intercrystalline cracks and prevented the recovery of ductility.

A comparison has been made of the results known for molybdenum steels at temperatures up to 950° C with the published results of various carbon steels tested in vacuum and in air. The molybdenum steel is superior in strength in the ferritic state, having creep strength at 550° C not unlike that found in carbon steels at 450° C. This is probably due to the strengthening effect caused by molybdenum and to a lesser extent carbon held in solid solution in the ferrite. Molybdenum does not however improve the strength of low-carbon steel in the austenitic condition at 850° C. Comparison is also made with some published results of the other molybdenum and complex molybdenum steels.

Earlier published work on carbon steels shows that deformation accelerates structural changes such as the spheroidization of the cementite present in the pearlite. In the present work similar changes are observed in molybdenum steel. These are found to proceed at considerably slower rates than in carbon steels and this reduction may be due to structural changes in the carbides. In this connection the carbides produced after long exposure to high temperatures may be somewhat more stable than cementite in regard to graphitization in the region of 600° C and above. But it should be remembered that manganese, silicon, and aluminium have a marked influence on controlling the rate of graphitization. A study of the methods available for dissolving the matrix by various reagents has been necessary as some reagents appeared to attack the carbides and in certain cases no compound identifiable by X-ray methods was left behind. Some of the more stable compounds found in titanium, niobium, and vanadium bearing molybdenum steels are not subject to this attack. Eventually the alcoholic iodine method was adopted to isolate the compounds for subsequent X-ray identification. No change in the cementite phase was observed at 450° C in a rupture test under a high stress, namely 27 tons/in², in which considerable deformation (15·5%) was given to the specimen, but long exposure to 500° C is likely to show the beginning of changes in both the cementite and the ferrite.

Although there has not been sufficient time to attain final equilibrium, the results summarized in Table VII lead to certain conclusions in samples heat treated after cooling through the transformation range but not in those *isothermally* transformed.

(1) Fe_3C is the predominating phase in normalized samples and in many of the samples given creep tests up to 625° C. Kuo and Goldschmidt both consider that this compound has, however, a small molybdenum content. The Fe_3C formed on normalizing is not necessarily saturated and may increase in molybdenum content during the progress of creep tests.

(2) Mo_2C, after long-time exposures at 530° C, separates from the ferrite which appears to have a higher carbon content (due to the presence of molybdenum) than that found in carbon steels. The formation at 450° C was too slow to be observed in the one long-time creep test at this temperature.

The particles of Mo_2C (whose formation appears to be controlled by the diffusion rate of molybdenum in the ferrite) do not appear to be preferentially associated with the grain boundaries. The formation of particles of Mo_2C appears to coincide with the return of ductility in the steel in long-time tests at 550° C. In consequence the removal of molybdenum from the ferrite crystals reduces the strength of these and allows deformation to occur to a greater extent within the grains rather than at grain boundaries.

(3) In the times of creep testing described, $(Fe_{21}Mo_2)C_6$ begins to replace Fe_3C at 630° C and above. The former compound is identifiable by its sooty black appearance on being etched in 4% nital, whereas Fe_3C remains relatively unattacked. $(Fe_{21}Mo_2)C_6$ also makes its appearance in samples which are slowly cooled (100° C/h) from the normalizing temperature.

The structural changes, namely recrystallization, spheroidization, and carbide phase changes, have all led to a reduction in strength. However, before ultimate failure occurs in long-time tests internal cavities develop in the steel. These cavities form in the grain boundaries as well as in the interior of the grains. The cavities seem to originate from the enlargement of minute imperfections, some being submicroscopic, which lie in the grain boundaries of the crystals or in the crystals themselves. Dislocation theory might perhaps afford an explanation of the

mechanism of cavity formation. It is thought that the initiation of the minute imperfections referred to above occurs at sites where there has been an accumulation of dislocations. With continued deformation, the imperfections develop into cavities, and dependent upon the properties of the material they either spread along grain boundaries to form intercrystalline cracks or enlarge into holes elongated in the direction of the applied stress.

In a test at 450° C, development of intercrystalline cracking was not clearly marked after 13,470 h under a stress of 27 tons/in². The specimen was probably a borderline case in which both transcrystalline and intercrystalline cracking occurred. The present investigation shows the development of intercrystalline cracking in all specimens with a life of more than about 5 days. This differs from the previous work on carbon steel in which transcrystalline ruptures were observed but it would appear that the addition of 0·5% Mo has hardened up the ferrite without a corresponding increase in the strength at the grain boundaries. At higher temperatures and at relatively longer times the development of intercrystalline cracking is arrested by the increased ductility in the steel resulting from the precipitation of Mo_2C. This greater ductility allows the steel to recrystallize and thus grain boundary tearing is hindered. The importance of recrystallization is to be noted as a means of limiting the degree of intercrystalline cracking at high temperatures. Above 550° C a rigid classification of the type of fracture is difficult on account of spheroidization, recrystallization, carbide separation, and carbide changes which have taken place. However, a tentative boundary line has been drawn in figures graphically relating stress with temperature, thus indicating the change from transcrystalline to intercrystalline cracking.

Acknowledgments

This work formed a part of the General Research Programme of the National Physical Laboratory and is published with the permission of the Director.

The authors wish to acknowledge the help of Mr. H. R. Sullivan for his chemical extraction of the carbides and the subsequent chemical and X-ray analyses of the residues obtained. This has involved considerable development of new methods.

References

1. C. H. M. Jenkins and G. A. Mellor: *J. Iron Steel Inst.*, 1935, vol. 132, pp. 179–227.
2. C. H. M. Jenkins, G. A. Mellor, and E. A. Jenkinson: *Ibid.*, 1942, vol. 145, pp. 51P–86P.
3. C. H. M. Jenkins and H. J. Tapsell: *Ibid.*, 1952, vol. 171, pp. 359–371. (For further work on grain size *see* Report J/T 139 British Electrical and Allied Industries Research Association.)
4. C. H. M. Jenkins, *et al.*: *Transactions of the Chemical Engineering Congress of the World Power Conference*, London, 1936, vol. 1, pp. 122–159.
5. H. J. Tapsell, C. A. Bristow, and C. H. M. Jenkins: *Proc. Inst. Mech. Eng.*, 1941, vol. 146, pp. 208–222.
6. H. J. Tapsell and R. W. Ridley: *Ibid.*, 1945, vol. 153, pp. 181–192.
7. A. E. Johnson and H. J. Tapsell: *Ibid.*, 1948, vol. 159, pp. 165–171.
8. E. A. Jenkinson and D. C. Herbert: *Engineering*, 1952, vol. 173, pp. 345–347.
9. R. W. Ridley: *Proc. Inst. Mech. Eng.*, 1952–53, vol. 1*B* No. 11, pp. 511–515.
10. F. E. Bowman, R. M. Parke, and A. J. Herzig: *Trans. Amer. Soc. Metals*, 1943, vol. 31, pp. 487–495; 1944, vol. 33, pp. 481–495; 1945, vol. 35 pp. 112–125.
11. C. H. M. Jenkins: *Journal of Rheology*, 1932, vol. 3, pp. 289–297.
12. C. H. M. Jenkins, E. H. Bucknall, and E. A. Jenkinson: *J. Inst. Metals*, 1944, vol. 70, pp. 57–79.
13. R. W. Cahn: "The Strength of Solids," pp. 136–137, 1948, London, The Physical Society; P. Lacombe: *Ibid.*, pp. 91–94.
14. C. H. M. Jenkins: N.P.L. Conference on Creep, 1954, H.M.S.O. Paper No. 13, 1956, pp. 287–298.
15. T. E. Rooney and A. G. Stapleton: *J. Iron Steel Inst.*, 1935, vol. 131, pp. 249–262.
16. W. Crafts and C. M. Offenhauer: *Trans. Amer. Inst. Min. Met. Eng.*, 1942, vol. 150, p. 275; 1943, vol. 154, pp. 361–373.
17. D. J. Blickwede and M. Cohen: *Ibid.*, 1949, vol. 185, p. 578.
18. H. J. Goldschmidt: *J. Iron Steel Inst.*, 1948, vol. 160, pp. 345–362.
19. K. Kuo: *Ibid.*, 1953, vol. 173, pp. 363–375.
20. A. Hultgren *et al.*: *Proceedings of the Royal Swedish Academy of Science*, 1953, vol. 4, p. 3.
21. R. J. Sinnott *et al.*: A.S.M.E. Advance Copy, New York Meeting, November-December, 1954, Paper No. 54-A-73.
22. A. Westgren, G. Phragmen, and T. Negresco: *J. Iron Steel Inst.*, 1928, vol. 117, 383–400.

The Direct Measurement of the Total Heat in Open-hearth Furnaces

By A. M. Godridge and G. G. Thurlow

SYNOPSIS

The total heats of the preheat and waste gases in an oil- and a producer-gas-fired open-hearth furnace have been measured directly using a calorimeter method. The results obtained have been compared with values estimated from temperature readings and found to agree up to about 1700° C. Whilst the total heat meter operated consistently at temperatures higher than this, measurements of waste-gas temperatures above 1700° C by the suction pyrometer were not reliable.

It was possible to obtain continuous readings with the total heat meter over the major part of two typical melts on the producer-gas-fired furnace and the results are presented and discussed. Some tentative conclusions are drawn as to the significance of these results and possible future uses of the instrument. 1234

THE OUTPUT and efficiency of open-hearth furnaces are related to the preheated air and waste-gas temperatures. The heat content of the pre-heated air forms a large part of the heat input to the furnace whilst, by governing the temperature of the flame, it will have an effect on the rate of combustion and the heat-transfer processes in the furnace. The heat content of the waste gases is that not transferred in

Manuscript first received on 10th October, 1955, and in its final form on 11th February, 1956.

Mr. Godridge and Mr. Thurlow are with the British Coal Utilisation Research Association.

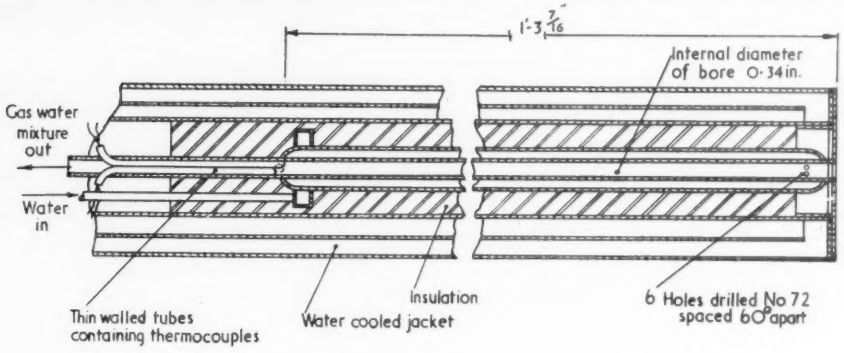

Fig. 1—Calorimeter unit of total heat meter (turbulence promoter not shown)

the furnace and, though a large part of this heat is recovered in the regenerators, its value gives an indication as to whether the combustion rate in the furnace is satisfactory and combustion is complete before the gases reach the downtake. The difference between the heat input from pre-heat and fuel and the heat in the waste gas is simply related, to a reasonable degree of accuracy, to the heat given to the bath. These two measurements are, in fact, together with routine observations, sufficient to give a good account of the performance of the open-hearth, irrespective of the actual combustion and heat-transfer processes in the furnace itself.

It will be noted, though, that it is the total heat, rather than the temperature of the gas, which is required. The total heat consists of the sensible heat (a product of temperature and specific heat) and the latent heat of any constituent which changes state between the gas temperature and datum. In practice, datum is taken as 32° F and the only constituent which has to be considered is water vapour.

Two other factors could conceivably increase the total heat significantly: dissociation and the heat content of the dust burden.

Dissociation will have an insignificant effect under stable conditions up to about 1700° C, but above this may become appreciable. For example, in the case of the waste gas from a heavy fuel-oil flame of composition 14%$CO_2 + SO_2$, 11½%H_2O, the latent heat of dissociation expressed as a percentage of the total heat content increases from just under 2% at 1700° C to 5% at 1900° C and 10½% at 2100° C. For a producer-gas flame (18% CO_2, 8%H_2O), the equivalent percentages are 2·2%, 5·5%, and 11%.[1] There is a possibility, however, that dissociated products formed in the flame may persist for a while at lower temperatures and so pass out of the furnace.

Such effects as these, if they occur, can best be observed by direct measurement of the total heat, and the present paper describes an instrument for doing this and some tests with it on open-hearth furnaces. At the same time, it is shown that this instrument has advantages over many existing methods and can give continuous readings for prolonged periods over the complete preheat–waste gas cycle.

THE TOTAL HEAT METER

Principle

The form of total heat meter* discussed here was initially developed at the British Coal Utilisation Research Association by R. H. Baulk.[2,3]

The principle of all total heat meters requires that a known quantity of the flue gas be sampled and passed through a calorimeter system where heat is extracted from it and measured. Any appreciable unmeasured heat losses must be avoided, and this implies that the calorimeter must be small and compact. For this reason, simple heat exchangers with heat flow across a wall dividing flue gas and the coolant are at a disadvantage and, in the instrument discussed here, a spray calorimeter is used. The gases are sucked into a calorimeter, installed at the end of a water-cooled probe inserted into the gas stream, and are intimately mixed with water sprayed in from jets round the periphery of the sampling tube. Advantage is taken of both the heat required to raise the temperature of the water in the liquid phase and the latent heat of vaporization. High rates of heat transfer are obtained and the calorimeter length can be kept short.

At the exit from the calorimeter, two distinct sets of conditions can occur, dependent on the heat content of the gases and the relative quantities of water and flue gas. If sufficient water is injected to give excess liquid at equilibrium, a condition, termed by Baulk 'partial vaporization', occurs. If, however, all the added water is evaporated, a state of 'total vaporization' exists.

It has been found that total vaporization is very difficult to achieve and it is recommended that this condition should not be used in practice. Expressions for obtaining the total heat of the gas and the equivalent gas temperature for the condition of partial vaporization are derived in the Appendix.

* There is some room for controversy as to whether the instrument described here should be termed a total or sensible heat meter. This is mainly a question of definition but as, in fact, the instrument does measure a change in total heat it is thought justified to term it a total heat meter. Where the expression ' total heat ' is used, however, it should be understood to refer to a change above a datum temperature, not necessarily above absolute zero.

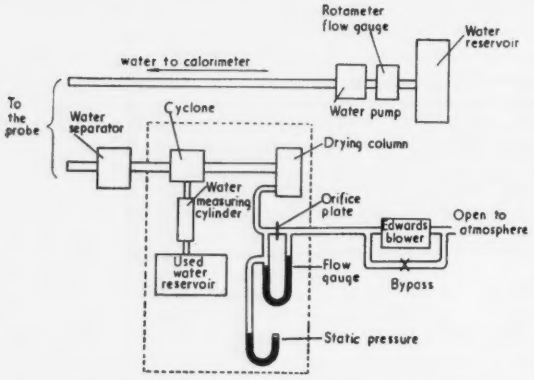

Fig. 2—Block diagram of auxiliary equipment for total heat meter

The Probe and Calorimeter

The spray calorimeter illustrated in Fig. 1 is housed in one end of a water-cooled probe of 2 in. external diameter, which serves both to shield the calorimeter from heat other than that in the sampled gases and to enable it to be inserted at appropriate points in the furnace. On leaving the calorimeter, the gas–water mixture passes through auxiliary equipment where it is dried and metered.

The water which is sprayed into the gas is delivered to the calorimeter through a tube passing up the centre of the probe, whilst the mixture from the calorimeter is carried to the cold end of the probe by a second tube. A third tube leads to a static pressure tapping at the exit end of the calorimeter. Two chromel/alumel thermocouples, situated at the calorimeter exit, measure the temperature of the mixture leaving the calorimeter, the four leads being also led down the centre of the probe and out through the cold end. Two thermocouples are used as a precautionary measure.

Multi-junction thermocouples may be used to enable the same accuracy of reading as with a single thermocouple to be obtained with a less accurate potentiometer. Experience has shown that the water inlet temperature can be measured by a thermometer at the exit from the water reservoir. The added water passes through an annulus surrounding the mixing chamber over the whole length of the calorimeter unit and is then sprayed into the centre core, down which the gases are sucked, at a point $\frac{3}{16}$ in. from the entrance. Six spray holes (72 drill) spaced at 60° intervals are used.

The inner core of the calorimeter is 0·34 in. dia. and is fitted with a turbulence promoter consisting of a twisted strip of tungsten steel. The thermocouples are contained in thin-bore copper tubing closed at one end and brazed in the inner tube as shown. The calorimeter unit is thermally insulated from the water-cooled walls, and it is so designed that it can be slid forward out of the water-cooled jacket for examination and repair.

Auxiliary Equipment

The apparatus necessary for metering the water and gas flows to and from the calorimeter is shown in block diagram form in Fig. 2.

The water to be mixed with the hot sampled gases is fed from the bottom of an aluminium storage container through a rotameter to an accurately machined meshed-gear metering pump. This pump has an output of 1 cm³ per revolution and, driven by a geared synchronous motor, gives a resultant flow of about 23 cm³ ($0{\cdot}815 \times 10^{-3}$ ft³) per minute. Though this output is dependent on the mains frequency, it is found that changes in frequency are normally insufficient to give a significant change in flow during a test.

On leaving the probe, the gas–water mixture is immediately sucked through a simple water separator (Fig. 3) before passing on to a water-extracting cyclone and drying column in order to pass dry gas through the orifice plate and blower. The cyclone, shown in Fig. 4 and described elsewhere,[4] has been shown to operate using water–air mixtures at an efficiency better than 99·8% at room temperature under the relevant conditions. Water extracted by the cyclone enters a reservoir forming the bottom of the box holding the equipment.

The drying column consists of a thin-wall brass tube having an overall length of 14 in. and an inside diameter of approximately 2 in. packed with medium-sized calcium chloride or silica gel. The gas passes up the column against gravity.

The suction unit is a vane-type pump with by-pass connection to control the flow. This gives a maximum flow rate of about 2 ft³/min (cold flow). In use, this flow is adjusted to ensure that the mixture leaving the calorimeter is in a state of partial vaporization, i.e. that the temperature is below 100° C. The temperature measurement becomes very critical at temperatures approaching 100° C and it has been found best to work in the range 70–90° C where a reading to 0·1° C gives reasonable accuracy. The actual mixture temperature obtained, however, is dependent on that of the gas.

The orifice plate is of the sharp-edged type with corner tappings and was calibrated against a gas meter which had itself been checked by a direct displacement method.

It was hoped initially that it would be possible to meter the water extracted from the gas and so find, by difference, the water content of the gas as sampled. This procedure, however, gave inaccurate results, apparently owing to the gases leaving the cyclone being incompletely saturated. Tests carried out at room temperature tended to confirm that complete saturation of the gases leaving the cyclone is not achieved. The water content of the gases in the following work has therefore been determined by independent means. If similar conditions occur at

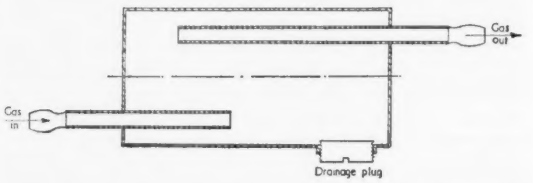

Fig. 3—Water separator

the calorimeter exit, the total heats given by direct calculation from the total heat meter readings will tend to be high, and a direct calibration of the instrument has been carried out to find the magnitude of any such effect.

CALIBRATION

It was necessary to carry out the calibration of the total heat meter under conditions where the true total heat of the gases could be accurately determined. A down-jet-fired coke furnace was used as it was possible to control the temperature of the waste gases very accurately over a wide temperature band, the gases being clean (except for a fine silica dust) and effectively dry. This absence of any appreciable moisture is particularly advantageous in so far as it simplifies calculations of the total heat (*see* Appendix) and, further, makes the possibilities of any appreciable dissociation in the flames extremely remote. The firing rate of the furnace was approximately 50 lb of coke per hour and, hence, the weight of flue gas was about 700 lb/h.

The total heat meter was compared with a suction pyrometer of a type previously described.[5] It consists of a 2-in. outside dia. water-cooled probe with a $1\frac{3}{8}$-in. dia. central bore. A Pt/Pt–13% Rh thermocouple encased in a steel sheath passes up the centre of this. The metal sheath finishes at the hot end about 8 in. inside the water-cooling and is replaced by a refractory tube, closed at one end.

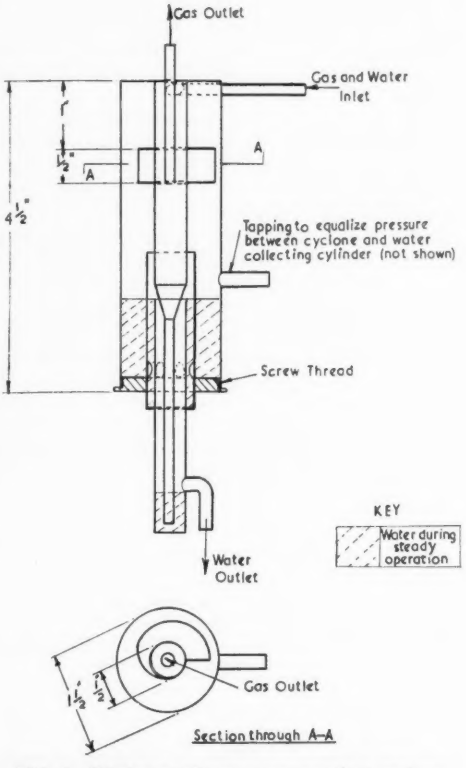

Fig. 4—Diagram of water-separating cyclone

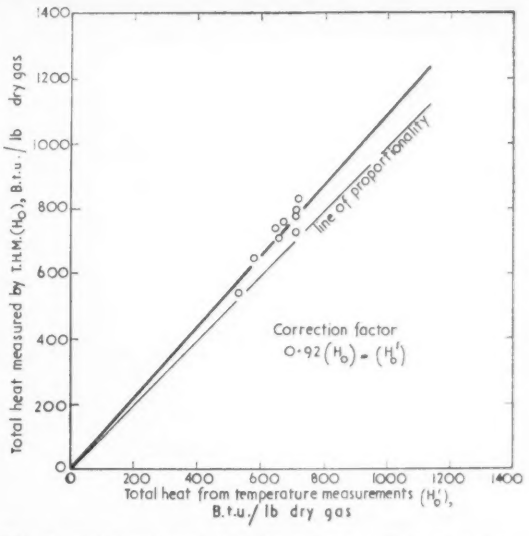

Fig. 5—Calibration of total heat meter: tests on down-jet furnace

Various forms of refractory radiation shields have been developed for use with this instrument. For the tests on the down-jet furnace, a head comprising two concentric refractory shields as described previously[5] was used. It has been shown that this gives readings close to the true temperature and, in addition, correction factors are available which enable the observed reading to be brought even nearer to the true temperature.

The difference between the reading given by this instrument at full and no suction in the down-jet furnace was about 200° C and, with corrections applied, it is thought that the temperature readings are accurate to about 10° C. The volume of gas sucked through the pyrometer was about one-seventh of the total flue gas but tests showed that the flow through either instrument had no measurable effect on the reading given by the other.

The result of the comparison between the two instruments is shown in Fig. 5. As a result of this, a correction factor of 0·92 has been applied to the calculated heat contents given by the total heat meter on the open-hearth.

TESTS ON OPEN-HEARTH FURNACES

Comparison between Total Heat Meter and Temperature Readings

A series of tests was carried out in the uptake of an open-hearth furnace on both waste and preheat gases during charging, melting, and refining to compare the total heats given by the total heat meter with values estimated from temperature measurements. The latter were measured in this case by a suction pyrometer fitted with a water-cooled refractory head, as recently developed by B.I.S.R.A. and Land Pyrometers Ltd.

A report on this latter instrument, in which the radiation shields consist of a multi-shield extruded refractory set inside the water-cooled jacket, has

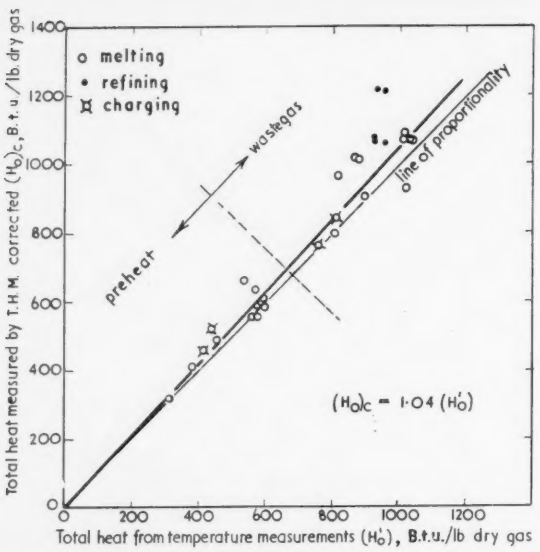

Fig. 6—Comparison between total heat readings and estimations from temperature readings: tests on open-hearth furnace

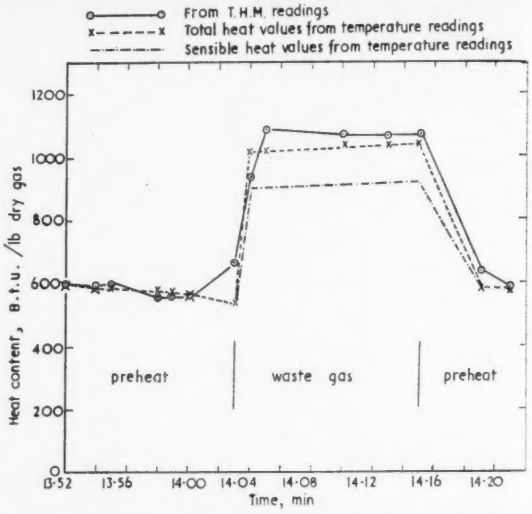

Fig. 7—Change in heat content of the gases in an oil-fired open-hearth furnace uptake, during melting period

been published elsewhere.[6] The chief practical advantage of the design is its robustness whilst, at least on the preheated gases, it gives readings to within about 20° C of the true temperature. The position on the waste-gas cycle is less satisfactory. The accuracy of the reading at high temperatures, especially when deposits form on the refractory heads, cannot be estimated with certainty, whilst the present authors have found that, at the high waste-gas temperatures described in the next section, some damage due to thermal shock occurred. Active research is proceeding elsewhere to try and solve these problems and it is indeed unfair to generalize as a result of the limited experience described here.

Correction factors of 20° C for the preheat and 40° C for the waste-gas temperatures have been applied to the observed suction-pyrometer readings.

The total heat meter and the suction pyrometers were inserted side by side about 2 ft above stage level into the single uptake of an oil-fired open-hearth furnace. The hot end of each instrument projected into the hot gases for a distance of 2 ft from the inside wall of the uptake. Air infiltration was restricted to a minimum by plugging the area around the probes.

Values of the water contents in the gases were calculated from fuel and air data and are summarized in Table I. The correction discussed in Section 3 has been applied to the total heat meter values.

The total heats obtained by both methods are compared in Fig. 6. This diagram shows that there is no large discrepancy in the total heat determined by the two methods. In particular, the agreement of the two methods for preheat, which one would expect, is repeated for the waste gases where any discrepancy between the methods would be most likely to occur.

The slight deviation from proportionality and the scatter are probably partly due to the fact that, although the readings were taken simultaneously, the different speed of response of the two instruments would tend to make the observations slightly out of phase. The limited observations made during charging and refining do not make it possible to determine any change in this agreement between these stages—except in so far as it would not appear to be large.

It should be noted that the temperatures throughout these trials were rather low, 1500° C being the maximum attained. As stated earlier, this is well below the temperature at which appreciable dissociation can occur under stable conditions.

The readings of both instruments over one preheat and waste-gas cycle are shown in Fig. 7. The relative shape of the curves at the change from preheat to waste gas is probably explained by the response of the instruments just referred to. The suction pyrometer has an appreciable initial lag but, when once it starts to respond, approaches equilibrium rapidly. The response to the total heat meter has not been fully investigated but it appears quicker than the pyrometer and it is probable that its curve is more representative of the actual temperature changes.

Table I

WATER CONTENT OF GASES, lb/lb of dry gas

Period	Preheat Air	Additional Moisture in Waste Gases		Total Moisture in Waste Gases
		From Oil	From Steam	
1	0·012	0·077	0·032	0·121
2	0·012	0·053	0·028	0·093
3	0·012	0·077	0·032	0·121

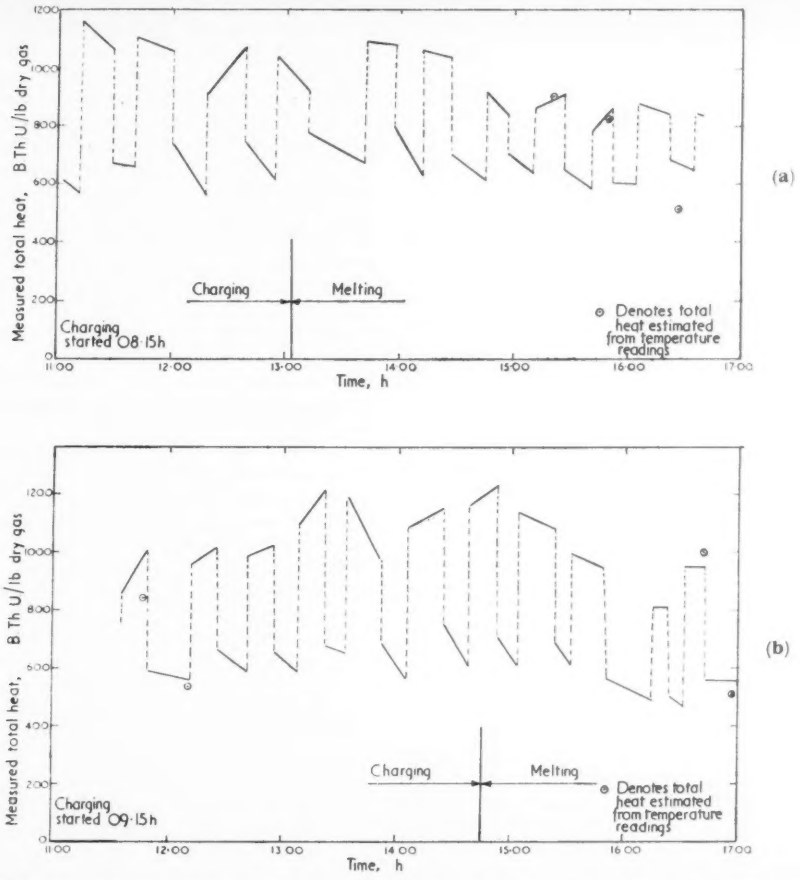

Fig. 8—Variation of total heat in the preheat and waste gases of a producer-gas-fired open-hearth furnace

The sensible-heat curve has been included to illustrate the magnitude of the latent heat in the water vapour in the waste gases and to emphasize that the waste-gas temperature alone must not be taken as a measure of total heat.

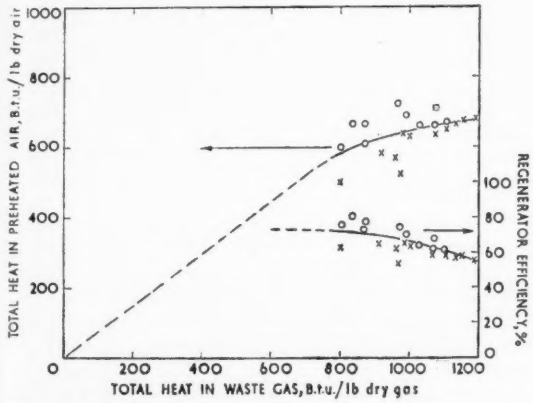

Fig. 9—Relationship between heat in waste gases entering and in air leaving the regenerator of a producer-gas-fired open-hearth furnace

The Variation of Total Heat over a Melt

Continuous readings of the variation in total heat over the middle period of two melts on a producer-gas-fired furnace were obtained to test the instrument in continuous operation. The required flow rates and temperatures were all recorded and the variations in total heat, calculated from these, are given in Figs. 8*a* and *b*. Minor fluctuations in total heat during a reversal period are not shown. The tests were carried out during normal operation of the furnace and no special care was taken to ensure regular, or even representative, conditions. No undue significance should be attached to these results, therefore, concerning furnace operation or performance, even though it is of interest to consider them further and to try to relate them to temperature.

There were no signs of blockage of the instrument during these runs, the water injected washing the dust through the probe and into the separators.

Attempts to measure the temperature of the waste gases by suction pyrometry in these tests were not, as mentioned earlier, very successful. A few spot readings obtained are shown in Fig. 8.

It will be seen from Fig. 8 that the total heat of the preheated air always falls over a reversal cycle, as is to be expected, though the change in that of the waste

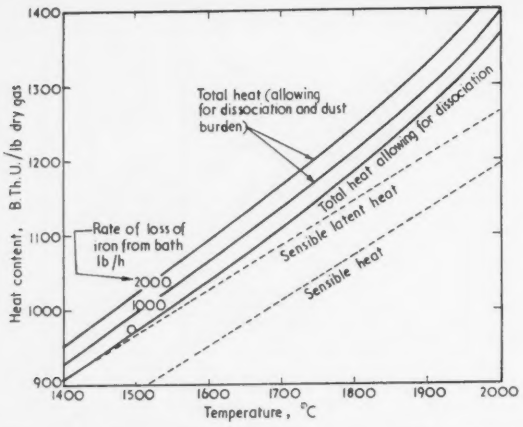

Fig. 10—Relation between gas temperature and the heat content of the waste gas (80-ton producer-gas-fired open-hearth furnace)

gases is dependent on whether the temperature level as a whole is rising or falling. A similar observation has been reported by Burton,[6] who has measured the variation of preheat and waste gas temperatures over a number of reversals.

As readings were only made at one end of the open-hearth, it is not possible to relate the results to overall furnace performance. It is, however, possible to make observations on the regenerator. The degree of preheat attained by the air is dependent, among other things, on the heat content of the waste gases entering the regenerator. Figure 9 shows the relationship between the mean total heat of the air over a half-cycle and that of the waste gas over the previous half-cycle. A mean curve through the results of both test series has been drawn, even though it appears probable that the values obtained during the second series are displaced slightly relative to the first.

It is possible from this curve to get an indication of the regenerator efficiency. On a gas-fired furnace, it is reasonable to assume that the gas and air mass flows through the regenerator are roughly equal. If the air is assumed to enter the regenerator at datum temperature (32° F), the heat content of the air leaving it is equal to the heat transferred. The heat content of the gas entering the regenerator is the heat input. It can be argued that, in practice, the latent heat of the water vapour in the waste gas is not available for transfer, but it seems more logical to include it, especially if it is intended to compare this efficiency with other components of the furnace. The ratio of the heat content of the preheated air to that of the waste gas, therefore, gives, to a fair degree of approximation, the regenerator efficiency, as shown by the subsidiary curve in Fig. 9.

In order to interpret the total heat values given in Fig. 8, it is necessary to consider the possible influence of dissociation and the heat content of the dust burden. The comparison shown in Fig. 6 suggests that, at temperatures below 1500° C, these terms have no large effects. Dissociation, however, will have an increasing influence with temperature, though it is not possible to define the magnitude of the effect accurately. There is a possibility that dissociation products will persist at a temperature lower than that at which they are in equilibrium long enough to be present at the furnace exit. At the same time, the quenching to which the gases are subjected when sucked into the total heat meter may not allow re-association to be completed and hence liberate all the available heat in the calorimeter. If we assume any effect due to these two causes to cancel out and take the dissociation as that at equilibrium at the gas temperature, the influence of dissociation on the total heat readings can be found from published tables.[1]

Figure 10 shows calculated relationships between heat content and temperature for the waste gases examined in these tests. The relative amounts of sensible heat, latent heat, and heat due to dissociation are shown.

The influence of the dust in the waste gases is even more difficult to allow for. Assuming the dust is all ferrous oxide with a specific heat (at about 1500° C) of 0·6 B.t.u./° C per lb of oxide, the additional heat due to any given concentration of dust can be found. This has been related back to the loss of iron from the bath, taking average gas flows, etc., and the resulting values are also shown in Fig. 10. Some idea of the average annual iron loss from the furnace is known (about 3%), but how much of this is lost as dust is uncertain, whilst this loss is clearly not uniform, varying very much with the type of scrap and being much larger during charging and melting than refining. Losses at the rate of 1000 lb/h are probably quite common. This is equivalent to a concentration of the order of 0·02 lb of dust per lb of dry gas.

Assuming a dust burden due to an iron loss of this order, it will be found that the gas temperature equivalent to the maximum heat contents of about 1200 B.t.u./lb measured on this producer-gas-fired furnace is of the order of 1750–1800° C.

CONCLUSIONS

The total heat meter is capable of giving continuous readings of the total heat of both the waste gases and the preheated air in an open-hearth furnace. It is unlikely to be found suitable for routine use owing to its inherent complexity and the difficulty of making it give a direct reading of total heat, though such a modification is not impossible. It should, however, be a valuable research instrument for experimental investigations into open-hearth operations and lead to useful data on the heat input to and heat taken from both furnace and regenerator.

Acknowledgments

The experimental work on open-hearth furnaces was carried out at Steel, Peech and Tozer, Rotherham, and the authors' thanks are due to this company and its staff, especially Mr. J. Chapman, for their co-operation and help.

Mr. R. Holland, of B.C.U.R.A., assisted in the experimental work. Permission to publish this paper has been given by the Director-General of the B.C.U.R.A.

References

1. H. M. SPIERS (Ed.): "Technical Data on Fuel," 5th Ed., p. 440: 1950, London, British National Committee, World Power Conference.
2. R. H. BAULK: Thesis, University of Sheffield.
3. R. H. BAULK: *J. Inst. Fuel*, 1950, vol. 23, pp. 77–85.
4. A. M. GODRIDGE and G. G. THURLOW: *J. Sci. Instruments*, 1954, vol. 31, p. 258.
5. R. BARBER *et al.*: *J. Inst. Fuel*, 1954, vol. 27, pp. 408–416.
6. E. J. BURTON: *J. West Scotland Iron Steel Inst.*, 1953/4, vol. 61, pp. 208–216.

APPENDIX

The Principle of the Total Heat Meter (Partial Vaporization)

Evaluation of Heat Content

The heat content of the gas–liquid mixture leaving the calorimeter can be divided, in this case, into three parts.

(1) *The heat content of the* '*dry gas*'—

$$= W_g C'_p (T_p - T_0) \quad \ldots\ldots\ldots\ldots\ldots\ldots (1)$$

where T_p and T_0 = temperature of gas leaving calorimeter and the datum temperature respectively (°F); W_g = rate of suction of dry flue gas (lb/s); C'_p = mean specific heat at constant pressure of dry gas mixture between temperatures T_p and T_0. The specific heat is defined by the expression $H_s = \int c dT$, where H_s is the change in *sensible* heat content (i.e. without change of state) of the gas and c is the instantaneous specific heat. It has been found by experiment that the pressure drop down the calorimeter is small and such changes in the total or partial pressure as occur in the system will not significantly affect the specific heats.

(2) *The heat content of the vapour*—The gas may be assumed to be saturated as excess water is present. The total heat content Q of the water vapour which combines with unit weight of dry gas to give saturated gas can be found from standard tables. Hence the heat content of the water vapour

$$= W_g Q_p \quad \ldots\ldots\ldots\ldots\ldots\ldots (2)$$

where suffix 'p' denotes conditions at temperature T_p.

(3) *The heat content of the liquid*—The total water in the system may be found by addition of that injected and that present in the flue gas. Hence the heat content of the liquid, with the specific heat of water equal to unity,

$$= W_g\left(\frac{w}{W_g} + \rho - x\right)(T_p - T_0) \quad \ldots\ldots\ldots\ldots (3)$$

where w = weight of metered water added, ρ = water content of hot gas per unit weight dry gas (lb/lb), and x = weight of water vapour per unit weight dry gas giving saturated gas at temperature T_p. Where the specific heats of the sampled gases are not widely different from air, it is possible to combine (1) and (2), using the relationship given in standard tables between the total heat of saturated air and temperature. Then the total heat of the gas phase

$$= W_g K_p \quad \ldots\ldots\ldots\ldots\ldots\ldots (4)$$

where K_p = the total heat content of saturated air containing unit weight of dry air at a temperature T_p (B.t.u./lb).

The summation of these three terms may be equated to the heat content of the gas and water entering the system. If the change in heat content of the sampled (i.e. wet) gas per unit weight of dry gas between its temperature as sampled and the datum temperature T_0 is H_0, we may write

$$W_g H_0 + w(T_w - T_0) = W_g C'_p (T_p - T_0) + W_g Q_p + W_g\left(\frac{w}{W_g} + \rho - x\right)(T_p - T_0) \quad \ldots\ldots\ldots (5)$$

where T_w is the temperature of the metered water, from which

$$H_0 = C'_p (T_p - T_0) + Q_p + \frac{w}{W_g}(T_p - T_w) + (\rho - x)(T_p - T_0) \quad \ldots\ldots\ldots\ldots\ldots\ldots (6)$$

Evaluation of Temperature

It is assumed that the heat content of the dust in the gas, etc. is negligible. Now, the total heat of the hot gas sampled H_0 may also be expressed in terms of its heat content up to the water dewpoint temperature (i.e. that temperature at which the gas, on cooling, is first saturated) of these gases and the heat added between the dewpoint and gas temperatures, viz.:

$$H_0 = \underbrace{C'_d (T_d - T_0) + Q_d}_{\text{heat content of gas mixture between } T_0 \text{ and } T_d} + \underbrace{(1+\rho)(C_g T_g - C_d T_d)}_{\text{heat content of gas mixture between } T_g \text{ and } T_d} \quad \ldots (7)$$

where T_d = dewpoint temperature of the sampled gas

T_g = temperature of the hot gases

C_g = mean specific heat of the wet gas between T_g and T_0

C'_d = mean specific heat of the dry gas between T_d and T_0

To be strictly accurate, the heat content of the gas mixtures between

$$T_g \text{ and } T_d \text{ is } (1+\rho)\int_{T_d}^{T_g} \frac{c dT}{T_d}$$

It can, however, be approximated to

$$(1+\rho)(C_g[T_g - T_0] - C_d[T_d - T_0]),$$

which is equal to

$$(1+\rho)(C_g T_g - C_d T_d) \text{ as } (C_g - C_d)\, T_0$$

is insignificant compared to the total heat content. If C_g and C_d are evaluated on the same basis, any error due to uncertainty in their estimations will be small. Thus, evaluating the specific heats of a mixed gas in the usual manner from the mean specific heats of its components (assuming the composition does not change above datum temperature) will give reasonable results. At the percentages of water vapour in furnace gases, the difference between C_d and C'_d is small.

As before, the first expression may be simplified, assuming the gas is air, to

$$C'_d (T_d - T_0) + Q_d = K_d \quad \ldots\ldots\ldots\ldots (8)$$

By equating and rearranging equations (6) and (7), the product of gas temperature and mean specific heat,

$$T_g C_g = \frac{1}{1+\rho}\left\{(Q_p - Q_d) + (C'_p T_p) + \frac{w}{W_g}(T_p - T_w) + (\rho - x)(T_p - T_0) + \rho (C_d T_d)\right\} \quad \ldots\ldots\ldots\ldots (9)$$

Or, for air,

$$= \frac{1}{1+\rho}\left\{(K_p - K_d) + \frac{w}{W_g}(T_p - T_w) + (\rho - x)(T_p - T_0) + C_d T_d (1+\rho)\right\} \quad \ldots\ldots\ldots\ldots (10)$$

These equations can be simplified if there is no appreciable water in the hot gases (i.e. $\rho = 0$). Then, equations 9 and 10 become respectively

$$T_g C_g = Q_p + C'_p T_p + \frac{w}{W_g}(T_p - T_w) - x(T_p - T_0) \quad \ldots (11)$$

$$T_g C_g = K_p + \frac{w}{W_g}(T_p - T_w) - x(T_p - T_0) + C'_d T_0 \quad \ldots (12)$$

Thermodynamics of Slag Systems

By P. T. Carter, B.Sc., Ph.D., F.I.M., and T. G. Macfarlane, B.Sc., A.R.T.C.

PART I—THE THERMODYNAMIC PROPERTIES OF CaO–Al_2O_3 SLAGS

SYNOPSIS

The sulphur equilibrium between CaO–Al_2O_3 slags and CO–CO_2–SO_2 gas mixtures at 1500° C has been investigated and the results used to determine the activity of lime and alumina in these melts. Approximate values for the free energies of formation of $3CaO.Al_2O_3$, $12CaO.7Al_2O_3$, and $CaO.Al_2O_3$ from their constituent oxides have been derived. The sulphur absorbed by a given slag depends on $\sqrt{\frac{p_{S_2}}{p_{O_2}}}$, which, for the gas compositions investigated, decreased with rise of temperature. 1187

IN RECENT YEARS, the sulphur burden in both the blast-furnace and the open-hearth furnace has shown a steady increase, in the former case mainly owing to the increasing quantity of sulphur in coal, and consequently in coke, in the latter case to the increasing sulphur contents of the gaseous and liquid fuels. Sulphur removal in both processes is controlled mainly by slag–metal reactions, although in the open-hearth furnace, reactions of both slag and metal with the furnace gases may also be important, for large amounts of sulphur enter with the fuel gases. Most investigations of the desulphurizing power of slags have used the results of slag–metal experiments.[1–5]

The difficulty of finding a refractory container to withstand the corrosive action of both slag and metal has usually resulted in the formation of relatively complex slags, and the data obtained have been correspondingly difficult to interpret. A study of gas–slag equilibria simplifies the problem in two important ways. Firstly, the elimination of the metal phase permits the use of metallic containers for the slag. (In the present work, platinum was found to be quite suitable for slag-gas experimental work.) Secondly, if the thermodynamic properties of the components of the gas phase are known, partial pressures calculated therefrom can be equated to activities (fugacities), since it can reasonably be assumed that ideality will obtain at the high temperatures used. Even when these thermodynamic properties are not accurately known, useful comparative results can be obtained by equilibrating different slags with the same gas mixture at the same temperature. Such studies may therefore provide knowledge of slag activities applicable to the consideration of slag–metal reactions in both the blast-furnace and the open-hearth furnace. They should also give some indication of the importance of gas–slag reactions in open-hearth steelmaking, and of the direction in which sulphur transfer may be expected to proceed.

The amount of data at present available on reactions of the slag with the furnace atmosphere is small compared with that available from slag–metal studies. Apart from important recent contributions by Fincham and Richardson,[6,7] laboratory investigations have been confined mainly to studies of oxygen transfer between the gas phase and slags containing iron oxides.[8–12] Whereas in the present work a detailed study has been made of the equilibrium between CO–CO_2–SO_2 gas mixtures and CaO–Al_2O_3 slags at 1500° C, Fincham and Richardson, using H_2–CO_2–SO_2–N_2 gas mixtures, investigated only a small number of CaO–Al_2O_3 slags. On the other hand, they made a detailed study of the effect of temperature, the oxygen potential of the gas phase, and different basic oxides on the gas–slag sulphur equilibrium. Their results will be considered later with those of the present work.

Manuscript received 7th July, 1955.

Dr. Carter is with the Department of Metallurgy, Royal Technical College, Glasgow. Mr. Macfarlane was formerly of the same department.

THEORETICAL CONSIDERATIONS

The reactions by which a lime-containing slag absorbs sulphur from a gas containing CO, CO_2, and SO_2 may be represented by the equations

$$(CaO) + SO_2 + 3CO = (CaS) + 3CO_2 \quad \ldots(1)$$
$$(CaO) + SO_2 + CO_2 = (CaSO_4) + CO \quad \ldots(2)$$

where brackets denote reactants dissolved in the slag phase. It is more convenient to describe the reactions in terms of oxygen and sulphur pressures, namely,

$$(CaO) + \tfrac{1}{2}S_2 = (CaS) + \tfrac{1}{2}O_2 \quad \ldots\ldots\ldots\ldots\ldots(3)$$
$$(CaO) + \tfrac{1}{2}S_2 + \tfrac{3}{2}O_2 = (CaSO_4) \quad \ldots\ldots\ldots\ldots\ldots(4)$$

It is clear that sulphide formation will be favoured by reducing conditions, whereas sulphate formation will occur more readily under oxidizing conditions. The oxygen pressures used in the present work ranged from $\sim 10^{-9}$–10^{-8} atm, and resulted in the formation of sulphide only. This is in agreement with the results of Fincham and Richardson, who showed that when p_{O_2} was less than $\sim 10^{-5}$ atm, sulphur transfer took place almost entirely by sulphide formation ; whereas under more oxidizing conditions ($p_{O_2} > 10^{-3}$ atm), sulphate formation predominated. Consequently only reaction (3) need be considered here. No direct determination of its standard free energy change has been made, but by combining the results of Rosenqvist[13] for the reaction

$$CaO(s) + H_2O = CaS(s) + H_2O \quad \ldots\ldots\ldots\ldots(5)$$

with the free energies of formation of H_2O and H_2S, the value

$$\Delta G = 23{,}020 - 1{\cdot}25T$$

can be derived for the reaction

$$CaO(s) + \tfrac{1}{2}S_2 = CaS(s) + \tfrac{1}{2}O_2 \quad \ldots\ldots\ldots\ldots\ldots(6)$$

This value should be applicable to the gas equilibrium with a slag simultaneously saturated with CaO

and CaS, but in the case of unsaturated slags, a knowledge of activities in the liquid state is required. No direct determinations of a_{CaO} or a_{CaS} have hitherto been made. The results of the present investigation have been used in the following manner to estimate a_{CaO}:

the equilibrium constant for reaction (3) is given by

$$K = \frac{(a_{CaS})\ {}^{p}O_2^{\frac{1}{2}}}{(a_{CaO})\ {}^{p}S_2^{\frac{1}{2}}} \quad \ldots\ldots(7)$$

If the sulphurizing power of the gas is denoted by A, where $A = (p_{S_2}/p_{O_2})^{\frac{1}{2}}$, then

$$a_{CaO} = \frac{(a_{CaS})}{K.A} \quad \ldots\ldots(8)$$

If a slag of unit CaO activity, and CaS activity $= (a^{\circ}_{CaS})$is in equilibrium with a gas whose sulphurizing power $= A^{\circ}$, then $K = \frac{a^{\circ}_{CaS}}{A^{\circ}}$ and for any other slag,

$$(a_{CaO}) = \frac{\frac{(a_{CaS})}{A}}{\frac{(a^{\circ}_{CaS})}{A^{\circ}}} \quad \ldots\ldots(9)$$

The activity of CaS in a slag cannot be determined from the present study. However, if it is assumed that for slags sufficiently far removed from sulphide saturation, the activity coefficient of CaS does not vary significantly with slag composition or sulphur concentration, CaO activities can be obtained by substituting weight percentages of S for CaS activities in equation (9),

i.e.

$$a_{CaO} = \frac{\frac{\%S}{A}}{\frac{\%S^{\circ}}{A^{\circ}}} \quad \ldots\ldots(10)$$

The following assumptions are also implicit in the above procedure:

(i) a_{CaO} is not lowered significantly by the substitution of small amounts of sulphide for oxide. This should hold for low sulphur concentrations.

(ii) No appreciable amount of sulphur is present in the slag as aluminium or silicon sulphide, i.e. linked to Al or Si atoms. This is evident from the experimental results, and has also been demonstrated by Fincham and Richardson.

Table I
SOLUBILITY OF CaS IN SLAG, % S

Investigators	Approximate slag Compositions				T °C	%S
	CaO	Al_2O_3	SiO_2	MgO		
McCaffery and Oesterle[14]	Range of Compositions				1500	8–11
Glaser[15]	48	—	52	—	1500	5·5
Filer and Darken[16]	41	15	37	7	1500	3·5–4·5
Taylor and Stobo[17]	29	45	26	—	1500	1
	39	19	37	5	1475	4
Fincham and Richardson[6]	41	52	7	—	1500	~2
Martin, Glockler, and Wood[19]	46	13	41	—	1425	3·6
Present Work	52	48	—	—	1500	~2·7

Table II
COMPARISON OF FREE ENERGY DATA

Reaction	ΔG°_{1773} °K (kcal)	
	Kelley	Richardson and Jeffes
$S_2 + 2O_2 = 2SO_2$	− 112	− 112
$SO_2 = S + O_2$	− 83	+ 68
$SO_2 = SO + \frac{1}{2}O_2$	− 47	+ 29
$SO_2 + CO = COS + O_2$	− 66	+ 66

Solubility of CaS in CaO-containing Slags

No accurate values for the solubility of CaS in slags are available, but the approximate data presented in Table I indicate solubilities, expressed as sulphur, of the order of 2–5% at 1500° C in CaO–Al_2O_3–SiO_2 slags. Although the figures given by McCaffery and Oesterle[14] are probably high, their conclusion that the solubility is greater for more basic compositions and higher temperatures is probably correct. They also concluded that temperature affected the solubility of CaS more than changes in slag composition.

Fincham and Richardson attributed certain abnormally high sulphur contents to the occurrence of saturation with CaS. A value less than 1·9% S for saturation can be calculated from their results, assuming that γ_{CaS} does not change appreciably with sulphur concentration. As a slight decrease in γ_{CaS} might be expected as saturation is approached, because sulphide–silicate systems exhibit liquid immiscibility and should therefore give activity-composition curves of the type calculated by Rosenqvist[13] for blast-furnace slags, the true saturation value may be slightly higher than the above 'estimate' but lower than the observed content (4·2% S). Certain abnormally high sulphur contents obtained in the present work also appeared to be due to saturation with CaS having been reached, the slag having a peculiar bulbous appearance instead of being glassy or minutely crystalline. Thus in Table IV, expt. 23, S-contents of 4·5 and 6·1% were obtained instead of 2·9% calculated by assuming a sulphur absorption proportional to the sulphurizing power of the gas. The CaS solubility should therefore correspond to less than 2·9% S. Similar observations in experiments with CaO–Al_2O_3–SiO_2 slags low in SiO_2 suggested a solubility between 2·5 and 2·9% S for this slag.

It is obvious that slag sulphur contents below the CaS saturation value must be aimed at in the gas–slag experiments. Gas compositions were accordingly adjusted to obtain sulphur contents well below the expected saturation value.

Choice of Standard Slag

Although no liquid slag in the CaO–Al_2O_3 system is in equilibrium with solid CaO at 1500° C, a small part of the 1500° C isotherm in the CaO–Al_2O_3–SiO_2 system passes through the primary phase field of CaO. A composition on this part of the isotherm (60·6% CaO, 32·4% Al_2O_3, 7·0% SiO_2) was chosen as the standard slag, of unit CaO activity.

Table III

RESULTS OF PRELIMINARY EXPERIMENTS USING SLAG CA5

Expt. No.	Inlet gas CO/CO_2	Inlet gas SO_2%	Inlet gas A_K	Time, h	Slag S, %	$\frac{(S\%)}{A_K} \times 10^4$	Remarks
1	1·48	0·82	340	2½	0·394 0·363	11·1	Normal procedure
2	1·52	0·83	357	3½	0·446	12·5	Normal procedure
3	1·49	0·83	346	3½	0·417	12·1	Normal procedure
4	1·51	0·78	340	4	0·408 0·408	12·0	Normal procedure
5	1·49	0·84	348	4½	0·401 0·423	11·9	Normal procedure
6	1·50	0·77	330	4	0·428 0·400	12·6	Furnace cooled
7	1·51	0·77	334	3½	0·318 0·320	9·6	Cooled in furnace in air
8	1·47	0·82	336	3½	0·391 0·388	11·6	Gas flows: 65 ml/min
9	1·52	0·83	356	¾	(1)0·275 (2)0·640		0·8% S added to (2)
10	1·55	0·84	367	3½	(1)0·439 (2)0·439	12·0	0·3% S added to (1) 0·5% S added to (2)
11	1·50	0·85		3½	0·372		T = 1513° C
12	1·50	0·86		3½	0·332 0·371		T = 1525° C

Mean Value of $\frac{(S\%)}{A_K} \times 10^4$ from expts. 2, 3, 4, 5, 8 and 10 = 12·0

Determination of the Sulphurizing Power of the Gas

To calculate A, the sulphurizing power of the gas, the data required are :

(i) the free energy change for the reaction

$$2CO + O_2 = 2CO_2$$

for which Richardson and Jeffes[19] give

$$\Delta G^\circ = -135{,}100 + 41{\cdot}5T \text{ cal}$$

(ii) the free energy changes for the formation of the gaseous compounds of S, C, and O, from SO_2 and CO. These were initially obtained from Kelley,[20] but later, data collected by Richardson and Jeffes[21] became available. Both sets of data indicate that within the range of gas compositions used, the amounts of S_6, S_8, CS, CS_2, and SO_3 formed could be ignored. Significant differences exist between the two sets of free energy data for the remaining S-compounds, as can be seen from Table II.

The differences originate in the choice of the dissociation energy of S_2 into normal atoms from spectroscopic data. According to Gaydon,[22] the dissociation energy can be 101, 83, or 76 kcal. Gaydon and Kelley favour the highest value, whereas Richardson and Jeffes prefer the lowest. Recently, as a result of experiments in which lime–iron oxide slags were equilibrated with SO_2–CO gas mixtures, St. Pierre and Chipman[23] have chosen the intermediate value. However, preliminary experiments in which the same slag was equilibrated with gases of different sulphurizing power have indicated a preference for the highest value, and Kelley's data will therefore be used here. Sulphurizing powers calculated from them will be denoted by A_K.

EXPERIMENTAL

Figure 1 shows the arrangement used for the production of a steady flow of the required CO–CO_2–SO_2 gas mixture and its chemical analysis, and the furnace and reaction chamber.

Control and Analysis of the Gas Mixture

CO_2 and SO_2 were obtained from commercial liquids. Analysis showed that $(O_2 + N_2)$ was less than 0·05%, which should have negligible effect on the CO/CO_2 ratio of the gas mixture at 1500° C. CO was obtained by passing dry CO_2 over dried (pre-heated in CO_2 at 1100° C for 2–3 h) powdered electrode graphite at 1100–1150° C. Soda asbestos was used to remove unchanged CO_2. It was shown by passing the resultant gas over heated copper oxide and through a **U**-tube

Table IV

RESULTS OF GAS–SLAG EQUILIBRIA USING CaO–Al_2O_3 SLAGS

Expt. No.	Slag No.	Slag Composition, % CaO	Slag Composition, % Al_2O_3	M.P. (°C)	Inlet Gas CO/CO_2	Inlet Gas SO_2, %	Inlet Gas A_K	Slag, S%	$\frac{(S\%)}{A_K} \times 10^4$	a_{CaO}
13	*CA*1	42·0	58·0	1500	1·52	0·80	347	0·136	3·92	0·074
14	*CA*2	43·0	57·0	1480	1·49	0·72	311	0·147	4·73	0·090
15	*CA*3	45·0	55·0	1450	1·52	0·83	356	0·232	6·5	0·123
16	*CA*4	47·8	52·2	1450	1·06	0·72	168	0·196	11·7	0·224
17					1·51	0·30	165	0·196	11·9	
18	*CA*5*	48·2	51·8	1450			336–357		12·0	0·23
19	*CA*6	50·0	50·0	1400	1·52	0·83	356	0·570	16·0	0·305
20	*CA*7	52·0	48·0	1430	1·50	0·83	351	0·804	22·9	0·44
21	*CA*8	54·0	46·0	1460	1·50	0·86	358	1·02	28·4	0·54
22	*CA*9	54·4	45·6	1470	1·06	0·72	168	0·462	27·5	0·525
23					3·22	0·95	980	4·5 6·1		
24	*CA*10	56·0	44·0	1490	1·52	0·80	347	1·25	36·0	
25					1·49	0·85	349	1·29	37·0	0·69
26					1·51	0·78	337	1·23	36·4	
27	*CA*11	58·0	42·0	1520	1·50	0·86	358	1·60	44·8	0·855
28	Standard		SiO_2	1500	1·52	0·77	340	1·79	52·7	1·00
29	Slag	60·6	32·4 7·0		1·06	0·72	168	0·88	52·4	

* Mean Value for experiments 2–5, 8, and 10
Time of experiments: 3½–4 h. Gas flow = 140–150 ml/min. Temperature = 1500° C

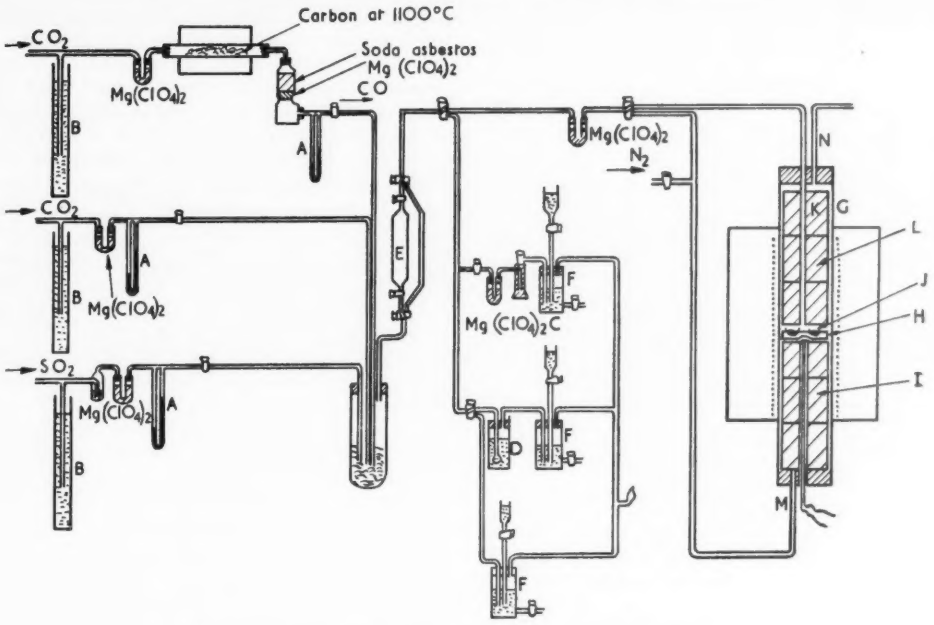

Fig. 1—Apparatus for gas–slag equilibrium experiments

containing $MgClO_4$ that no measurable amount of H_2 was present.

The dried gases were passed through capillary flowmeters (*A*), the flow during an experimental run being maintained constant by adjustable bleeder valves (*B*). The flowmeter readings were only used to indicate a constant flow during a run, the gas mixture being always analysed immediately before a run. The weight of ($CO_2 + SO_2$) flowing per minute was determined by absorption in soda asbestos (*C*). The SO_2 flow was determined by absorption in 5-volume H_2O_2 (*D*) and subsequent titration with N/20 NaOH. The end point could be obtained within 0·1 ml, representing less than 1% error. The gas sample in bulb *E* was analysed to obtain the ratio $\frac{CO}{CO_2 + SO_2}$ by flushing it with purified nitrogen through a soda asbestos absorption tube followed by copper oxide at 400–500° C and a second soda asbestos absorption tube. A second copper oxide tube in the furnace followed by a third absorption tube showed that conversion of CO to CO_2 had been complete. The data so obtained were used to calculate the volumetric CO/CO_2 ratio and SO_2% in the gas mixture. Flows during gas analysis were maintained unaltered by adjustable water columns (*F*).

The Furnace and Reaction Chamber

All the experimental runs were carried out in a platinum-wound resistance furnace, in which was inserted a 30-in. long mullite tube (*G*). The hot zone at 1500° C was constant to within 5° C over a length of about 2 in. The power input to the furnace was controlled by a Variac autotransformer and Sunvic energy regulator. The temperature, which could be maintained within ± 2° C, was measured by a Pt/Pt–13% Rh thermocouple, calibrated against the melting points of Au (1063° C) and Pd (1555° C). The thermocouple sheath fitted into a depression in the base of the alundum reaction tray (*H*), which was supported in the centre of the hot zone by alundum stools (*I*). By comparison with another thermocouple placed in the reaction tray, a slight temperature correction, never more than 5° C, was usually necessary.

Depressions in the reaction tray held small hemispherical crucibles cold-pressed from platinum foil, which could contain 0·25–0·40 g of slag (*J*). The gas mixture entered the reaction chamber via an alumina tube *K*, $\frac{1}{8}$ in. int. dia., which supported a series of alundum stools (*L*), the lowest being cemented in position. The gap between the lowest stool and the reaction tray was not more than 0·5 in., and this gap together with the reaction tray, which was 0·4–0·5 in. deep, may conveniently be termed the reaction chamber.

Thermal Diffusion

The possibility of errors arising from thermal diffusion was considered. Preliminary experiments (Table III) showed that alteration of the linear velocity of gas flow by decreasing the flow rate from 140–150 ml to 65 ml per min, or by using a gas inlet tube $\frac{1}{16}$ in. int. dia., thereby giving a fourfold increase in linear velocity, gave results agreeing, within the limits of experimental error, with those obtained using the normal gas flow. This was in agreement with the expected effects of thermal diffusion, which should be negligible since the ratios of the densities of CO, CO_2, and SO_2 are not large, the percentages of SO_2 were small, the gas would be pre-heated in travelling down the alumina inlet tube *K*, and the reaction chamber was contained entirely within the hot zone.

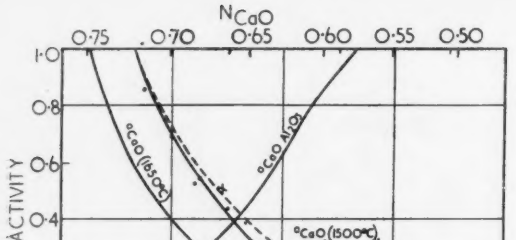

Fig. 2—Activities in CaO–Al_2O_3 slags at 1500° C

Preparation of Slag Mixtures

Three master slags were prepared by melting *AR* $CaCO_3$ (previously calcined) and Al_2O_3 in graphite crucibles using induction heating, with subsequent crushing and calcination at 1100° C to oxidize carbon picked up during melting. These were analysed by standard chemical methods. Further slags were prepared by mixing the master slags in the required proportions, with small additions of one of the components in one or two cases.

Experimental Procedure

After insertion of the reaction tray, crucibles, and slag, the furnace was flushed out with nitrogen. The gas mixture was made to by-pass the furnace and, after at least 1 h, analysed as previously described. When constant analyses were obtained, and the furnace was at the desired temperature, the gas mixture was allowed to enter the furnace via tube *M* in the lower bung, in order to remove nitrogen completely. After 30 min, the gas was led in via tube *K*. In each case the gases left the furnace via tube *N* in the upper bung. After a time sufficient for the attainment of equilibrium, the gas flow was stopped, the power switched off, and the reaction tray lowered about 3 in. It was then slowly removed over a period of about 10 min to prevent spalling of the tube. Owing to the small slag bulk, cooling was rapid and usually resulted in glass formation.

Attainment of Equilibrium

The results for slag *CA5* given in Table III indicate that equilibrium was attained within 3 h. Approaching equilibrium from both sides during the same run showed that true equilibrium was being attained (Table III, expt. 10).

Effect of Method of Cooling

A comparison of the results of experiments 4, 5, and 6 (Table III) shows that if the slag is allowed to cool in the furnace after shutting off the power and gas supply, the sulphur content obtained is slightly higher but almost within the experimental error of that obtained with normal cooling. During furnace cooling the slag would tend towards the equilibrium S-content at the temperature of solidification. This would suggest that the S-content of a slag in equilibrium with a gas of given initial composition increased with fall of temperature. Low results were obtained when the reaction tray was allowed to cool in the hot zone in air, showing that atmospheric oxygen had reacted with some of the sulphur before solidification was completed (Table III, expt. 7).

Analysis of Slags for Sulphur

Because of the small sample weights and low sulphur contents of certain of the slags, the gravimetric procedure was not sufficiently accurate. In the early stages of the present work, no stoichiometric combustion method was available, and the evolution method used by Kitchener, Liberman, and Spratt[24] for steels, suitably modified for use with slags, was considered more accurate. This consisted of solution of the slag in 1 : 1 HCl and absorption of the evolved H_2S in alkaline hypochlorite solution. Analysis of the residual solution showed that no sulphate was present, as expected from thermodynamic considerations.

RESULTS

The results obtained are summarized in Tables III and IV. Of the preliminary experiments in Table III only those showing the effect of temperature have not yet been considered. If experiments 11 and 12 had been carried out at 1500° C, S-contents of 0·425 and 0·427%, respectively, would have been obtained. Thus the S-content of a slag in equilibrium with a gas of given initial composition decreases with rise of temperature. This confirms the conclusion reached earlier for furnace-cooled samples. At first sight this may appear to contradict the results of Fincham and Richardson, who showed for a gas of constant equilibrium p_{O_2} and a given SO_2 input, that the equilibrium S-content increased with rise of temperature. However, the present results cannot be directly compared with those of Fincham and Richardson, since at different temperatures, gases of the same equilibrium p_{O_2} and initial SO_2 content are initially of different compositions. To facilitate comparison, it is necessary to calculate the initial gas composition which at 1500° C would have the same p_{O_2} values as those used in experiments 11 and 12 at 1513° and 1525° C. In the former case this is found to be $CO/CO_2 = 1{\cdot}31$, $SO_2 = 0{\cdot}85\%$, for which $A_K = 282$. Slag *CA5* at equilibrium with this gas would contain 0·339% S. Thus, using gases of constant p_{O_2} and the same initial SO_2 content increases the sulphur content of the melt from 0·339 to 0·372%, which agrees qualitatively with the findings of Fincham and Richardson. Also, if it is assumed that a_{CaO} and γ_{CaS} do not vary significantly between 1500° and 1525° C, it can be calculated from the change in A_K and the equilibrium constant of reaction (6) with temperature, that the equilibrium S-content of slag *CA5* at 1513° and 1525° C would be 0·375 and 0·344% respectively, in good agreement with the observed values.

All the data given in Table IV were obtained at 1500° C, using a total gas flow of 140–150 ml/min. Duplicate results were obtained for most of the slags, but only the mean S% is reported. The agreement between duplicates was within ± 3%. The melting

points of the slags used were obtained from the relevant phase diagrams.[25] It should be noted that although the melting point of slag *CA*11 is 1520° C, sulphur absorption caused the resultant slag to be completely liquid at 1500° C. In expt. 28, the standard slag ($^{a}CaO = 1$) was used, for which $S\%/A_K$ was found to be $52{\cdot}7 \times 10^{-6}$. The activity in each slag, which is proportional to $S\%/A_K$ was calculated using this value.

The standard slag was also equilibrated with a gas of lower sulphurizing power ($A_K = 168$, expt. 29). The results show that the sulphur content of the slag is proportional to A_K. Assuming the correctness of the gas thermodynamic data and the various assumptions made, this indicates that γ_{CaS} is constant up to 1·8% S. A similar result was obtained by Fincham and Richardson.[6] However, if the slag compositions are recalculated on a CaS-free basis, the results indicate a slight (~ 5%) decrease in γ_{CaS} with increase in S-content of the slag from 0·9–1·8%. This change in γ_{CaS} is in the expected direction.

Activities in $CaO–Al_2O_3$ Slags

Activities of CaO at 1500° C obtained using gases of approximately constant composition ($A_K = 350 \pm 15$) are plotted against wt-% CaO in Fig. 2. The curve indicates $a_{CaO} = 1$ at 58·5% CaO, which agrees well with the value obtained by extrapolating the CaO liquidus of the $CaO–Al_2O_3$ system to 1500° C (Fig. 3). The greatest uncertainty in the a_{CaO} curve originates in the assumption that γ_{CaS} is the same in all the slags investigated. As the solubility of CaS is generally believed to decrease with acidity, i.e. increase of Al_2O_3 content, γ_{CaS} would be expected to show a corresponding increase. This would cause the calculated values of a_{CaO} to be progressively lower than the true values as Al_2O_3 increased. The curve shown in Fig. 2 therefore indicates minimum values of a_{CaO}. The magnitude of the change in γ_{CaS} cannot be assessed from known data, but is unlikely to be as much as two-fold over the range of compositions investigated. A curve for a_{CaO}, assuming such a two-fold increase, is shown in Fig. 2 but will not be used in the subsequent discussion.

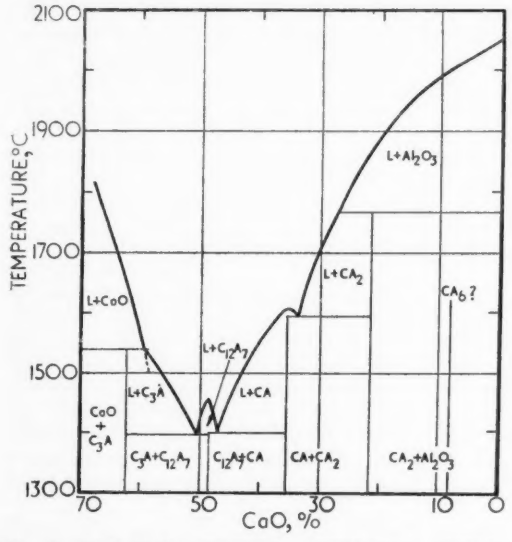

Fig. 3—$CaO–Al_2O_3$ thermal equilibrium diagram ($C = CaO$, $A = Al_2O_3$)

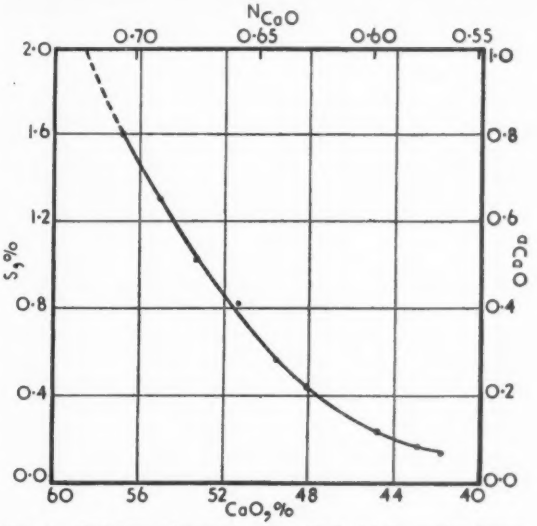

Fig. 4—Sulphur absorption by $CaO–Al_2O_3$ melts from $CO–CO_2–SO_2$ gas mixture ($A_K = 358$) at 1500° C. Slag composition calculated to CaS-free basis

The a_{CaO} values shown in Fig. 2 are independent of the thermodynamic data used to calculate the sulphurizing power of the gas phase. Two values obtained using gases of slightly different composition ($A_K = 165–168$) also show satisfactory agreement with the curve. These results suggest that the replacement of small amounts of oxygen in the slag by sulphur does not greatly alter the activity of lime in the slag. Ideally, it would be necessary to equilibrate each slag with a series of gases of progressively decreasing sulphurizing power and extrapolate to zero S-content to eliminate any error arising from this assumption. This procedure is limited by the difficulty of determining accurately the low sulphur contents which would result from the use of such gases. However, the magnitude of the error may be estimated by calculating the final slag compositions to a CaS-free

Table V

ACTIVITIES OF CaO IN $CaO–Al_2O_3$ SLAGS

Slag No.	Composition calculated to CaS-free basis		a_{CaO}
	CaO	Al_2O_3	
*CA*1	41·8	58·2	0·070
*CA*2	42·8	57·2	0·085
*CA*3	44·8	55·2	0·117
*CA*5	48·0	52·0	0·215
*CA*6	49·5	50·5	0·285
*CA*7	51·3	48·7	0·41
*CA*8	53·2	46·8	0·51
*CA*10	55·0	45·0	0·65
*CA*11	56·8	43·2	0·80
	58·5	41·5	1·00

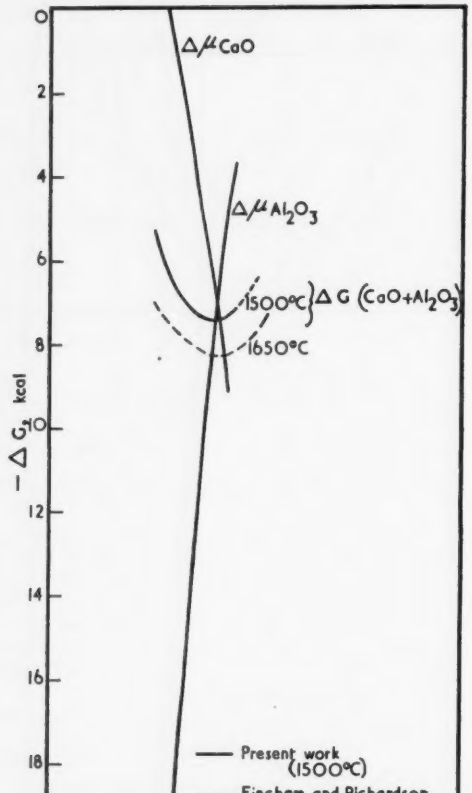

Fig. 5—Free energies of formation and chemical potentials of CaO–Al_2O_3 melts at 1500° C

basis, and plotting S% for a constant gas sulphurizing power ($A_K = 358$ was chosen) against the slag composition so obtained, as shown in Fig. 4. The S-content at 58·5% CaO (' saturation ' with CaO at 1500° C) is 2·0% compared with 1·9% ($A_K = 358$) for the standard slag. It should be noted, however, that as a result of sulphur absorption from the gas phase, the ' standard ' slag is unlikely to remain saturated with CaO. The activity of CaO in the sulphur-containing slag should therefore be slightly less than unity ; a value of $\frac{1{\cdot}9}{2{\cdot}0} = 0{\cdot}95$ appears reasonable.

Values of a_{CaO} calculated on this basis (i.e. by dividing the sulphur absorption from a gas of sulphurizing power $A_K = 358$, by 2·0) are little different from those shown in Fig. 2, being slightly higher for CaO contents above 49% and slightly lower for lower CaO contents. The deviations are well within experimental error. The recalculated a_{CaO} values are summarized in Table V. In order to avoid confusion they have not been plotted in Fig. 2. They are shown in Fig. 4 and will be used in subsequent calculations.

No direct determinations of a_{CaO} in CaO–Al_2O_3 melts have previously been carried out. Approximate values were obtained by Fincham and Richardson by combining their gas–slag results (obtained at 1650° C) with the free energy change for reaction (3), and assuming $\gamma_{CaS} = 5$, the value obtained for silicate melts. These values are also included in Fig. 2. Since CaO–Al_2O_3 melts are saturated with lime at 62% CaO at 1650° C, a curve has been drawn through their points to pass through $a_{CaO} = 1$ at this composition. Although the position of the curve depends on the choice of thermodynamic data for the gaseous sulphur compounds, it is not inconsistent with that of the a_{CaO} curve obtained in this investigation. A value of a_{CaO} at 1500° C calculated from the approximate CaS saturation limit is also in good agreement with the present results. Whether or not the a_{CaO} curves for 1650° and 1500° C cross at low N_{CaO} values depends on the shape of the ΔH ($CaO + Al_2O_3$) curve. No reliable data on this are available.

If the saturation limit for slag *CA*9 (Table I) is taken as 2·7% S (corresponding to $\gamma_{CaS} = 16{\cdot}5$), a value of 21·6 kcal can be calculated for ΔG° of reaction (3) at 1500° C, compared with 20·8 kcal calculated from the free energy equation given earlier. In view of the assumptions made in the present work, the agreement can be regarded as most satisfactory.

In spite of the relatively high lime activity in melt *CA*9 the value of γ_{CaS} used above is considerably greater than that obtained by Fincham and Richardson for CaO–SiO_2 melts at 1600° C ($\gamma_{CaS} = 5$). This would suggest that the solubility of sulphur is less in CaO–Al_2O_3 melts than in CaO–SiO_2 melts of comparable basicity (i.e. lime activity) ; or else that the effect of temperature on the solubility of sulphur is unusually large.

The activity of Al_2O_3 in CaO–Al_2O_3 melts could be calculated if a_{CaO} were known in a slag in equilibrium with solid Al_2O_3 at 1500° C. No such slag exists, and a reliable extrapolation of the Al_2O_3 liquidus curve to 1500° C is not possible since its position is not known accurately. Nevertheless, because existing knowledge of the thermodynamic properties of the CaO–Al_2O_3 system is so meagre, a tentative extrapolation has been carried out, which indicated ~35% CaO as the most probable value of ' Al_2O_3 saturation ' at 1500° C.* This led to a value of $a_{Al_2O_3} = \sim 0{\cdot}2$ for the melt saturated in $CaO.Al_2O_3$ (CaO = 42·5%) which appears reasonable, and is consistent with a value of ~0·25 which can be derived from the results of Fincham and Richardson for the same composition at 1650° C. The $a_{Al_2O_3}$ curve obtained using the Gibbs-Duhem relationship is shown in Fig. 2. The a_{CaO} and $a_{Al_2O_3}$ curves have been used to calculate the corresponding chemical potentials and the free energy of formation of one mole of melt from solid CaO and Al_2O_3 at 1500° C (Fig. 5). If $a_{Al_2O_3}$ were 0·1 or 0·4 at 42·5% CaO, the free energy curve would be lowered or raised respectively by 0·5–0·75 kcal. Error limits of ± 1 kcal may therefore be reasonably assigned to this curve. The free energy curve obtained by Fincham and Richardson for 1650° C is also shown. Although the difference between the two curves is only

* Use was made of the extension of the 1500° C isotherm in the Al_2O_3 field of the CaO–Al_2O_3–SiO_2 system to the CaO–Al_2O_3 binary system in making this extrapolation.

about 1 kcal, and is in the expected direction, it is greater than might be anticipated, and leads to an improbable ΔH curve. However, the limits of error of both ΔG curves* are too great to justify the calculation of ΔH values.

Thermodynamic Properties of Compounds of CaO and Al_2O_3

The work of Shepherd *et al.*[25] on the CaO–Al_2O_3 system established the existence of four compounds, namely, $3CaO.Al_2O_3$, $5CaO.3Al_2O_3$, $CaO.Al_2O_3$, and $3CaO.5Al_2O_3$. The X-ray investigations of Büssem and Eitel[26] indicated that the correct composition of $5CaO.3Al_2O_3$ is $12CaO.7Al_2O_3$, and Tavasci[27] has suggested $CaO.2Al_2O_3$ instead of $3CaO.5Al_2O_3$. The CaO–Al_2O_3 phase diagram, including these modifications, is shown in Fig. 3. The existence of 3CaO.$16Al_2O_3$ and $CaO.6Al_2O_3$ has also been suggested[28, 29] but the evidence for them is uncertain. Little is known of the thermodynamic properties of the above compounds, and the small amount of data available has been summarized by Richardson, Jeffes, and Withers,[30] who derived from them the following free energy equations :

$$3CaO(s) + Al_2O_3(s) = 3CaO.Al_2O_3(s)$$
$$\Delta G^\circ_{298\,^\circ K} = -3700 \text{ cal} \pm 10 \text{ kcal}$$
$$\Delta H^\circ_{298\,^\circ K} = -2700 \text{ cal}$$
$$5CaO(s) + 3Al_2O_3(s) = 5CaO.3Al_2O_3(s)$$
$$\Delta G^\circ_{298\,^\circ K} = 0 \pm >10 \text{ kcal}$$

The results of the present work have therefore been used to supplement the existing data. The free energy formation of $12CaO.7Al_2O_3$ (liquid) from solid CaO and Al_2O_3 can be obtained directly from the ΔG curve of Fig. 5. The free energies of formation of solid $3CaO.Al_2O_3$ and $CaO.Al_2O_3$ can be obtained by applying the activity product relationship to the values of a_{CaO} and $a_{Al_2O_3}$ at the respective saturation limits at 1500° C. The values so obtained are :

$$12CaO(s) + 7Al_2O_3(s) = 12CaO.7Al_2O_3(l) \quad \ldots(11)$$
$$\Delta G^\circ_{1773\,^\circ K} = -140 \text{ kcal}$$

The uncertainty is considerable on account of the large multiplication factor used.

$$3CaO(s) + Al_2O_3(s) = 3CaO.Al_2O_3(s) \quad \ldots\ldots\ldots(12)$$
$$\Delta G^\circ_{1773\,^\circ K} = -22{\cdot}3 \pm 4 \text{ kcal}$$
$$CaO(s) + Al_2O_3(s) = CaO.Al_2O_3(s) \quad \ldots\ldots\ldots(13)$$
$$\Delta G^\circ_{1773\,^\circ K} = -14{\cdot}3 \pm 2 \text{ kcal}$$

A check for $12CaO.7Al_2O_3$ which eliminates part of the error arising from the assumption made regarding $a_{Al_2O_3}$ can be obtained by constructing the $a_{CaO.Al_2O_3}$ curve (*see* Fig. 2), since a_{CaO} is known for the melt saturated with $CaO.Al_2O_3$. From the $\Delta\mu$ CaO and $\Delta\mu$ $CaO.Al_2O_3$ curves, the free energy change for the reaction

$$5CaO(s) + 7(CaO.Al_2O_3)(s) = 12CaO.7Al_2O_3(l) \quad \ldots(14)$$

was calculated to be

$$\Delta G^\circ_{1773\,^\circ K} = -39{\cdot}2 \text{ kcal}$$

Combination of this with the above data for $CaO.Al_2O_3$ yields

$$\Delta G^\circ_{1773\,^\circ K} = -139{\cdot}3 \text{ kcal}$$

for equation (11). This value is almost the same as that given above.

The minimum in the free energy curve shown in Fig. 5 occurs at $N_{Al_2O_3} \cong 0{\cdot}4$, i.e. at a composition between $12CaO.7Al_2O_3$ and $CaO.Al_2O_3$. Richardson[31] found a minimum occurred at a similar composition in the CaO–B_2O_3 system, though at a greater (negative) ΔG value, corresponding to much lower CaO activities. CaO activities in the CaO–Al_2O_3 system are also considerably higher than those in the CaO–SiO_2 system (*see* Part II), on account of the lower stability of calcium aluminates as compared with calcium silicates.

* Fincham and Richardson estimate the uncertainty in their ΔG curve to be about $\pm$ 2 kcal.

Acknowledgments

The authors wish to record their appreciation of the helpful advice and criticism of Professor R. Hay. They would also like to thank B.I.S.R.A. for financial support of the investigation. One of the authors (T.G.M.) wishes to thank the Ferguson Bequest Fund for financial assistance.

References

1. P. Bardenheur and W. Geller: *Mitteilungen aus dem Kaiser-Wilhelm Institut für Eisenforschung*, 1934, vol. 16, No. 7, pp. 77–91.
2. K. L. Fetters and J. Chipman: *Trans. Amer. Inst. Min. Met. Eng.*, 1941, vol. 145, pp. 95–112.
3. N. J. Grant and J. Chipman: *Ibid.*, 1946, vol. 167, pp. 134–154.
4. G. G. Hatch and J. Chipman: *Ibid.*, 1949, vol 185, pp. 274–284.
5. R. Rocca, N. J. Grant, and J. Chipman: *Ibid.*, 1951, vol. 191, pp. 319–326.
6. C. J. B. Fincham and F. D. Richardson: *Proc. Roy. Soc.*, Series *A*, 1954, vol. 223, pp. 40–62.
7. F. D. Richardson and C. J. B. Fincham: *J. Iron Steel Inst.*, 1954, vol. 178, pp. 4–15.
8. J. White: *Iron Steel Inst.*, Carnegie Scholarship Memoir, 1938, vol. 27, pp. 1–75.
9. L. S. Darken and R. W. Gurry: *J. Amer. Chem. Soc.*, 1945, vol. 67, pp. 1398–1412.
10. H. Larson and J. Chipman: *Trans. Amer. Inst. Min. Met. Eng.*, 1953, vol. 197, pp. 1089–1096.
11. R. Schuhmann Jr. and P. J. Ensio: *Ibid.*, 1951, vol. 191, pp. 401–411.
12. E. J. Michal and R. Schuhmann Jr.: *Ibid.*, 1952, vol. 194, pp. 723–728.
13. T. Rosenqvist: *Ibid.*, 1951, vol. 191, pp. 535–540 ; Tatsuji Uno: *Ibid.*, 1951, vol. 191, p. 1048.
14. R. S. McCaffery and J. F. Oesterle: *Ibid.*, 1923, vol. 69, p. 606.
15. O. Glaser: *Zeitschrift für Mineralogie, Geologie und Paläontologie*, 1926, *A*, pp. 81–96.
16. E. W. Filer and L. S. Darken: *Trans. Amer. Inst. Min. Met. Eng.*, 1952, vol. 194, pp. 253–257.
17. J. Taylor and J. J. Stobo: *J. Iron Steel Inst.*, 1954, vol. 178, pp. 360–367.
18. A. E. Martin, G. Glockler, and C. E. Wood: *U.S. Bur. Mines, Rep. Invest.*, 1941, No. 3552.
19. F. D. Richardson and J. H. E. Jeffes: *J. Iron Steel Inst.*, 1948, vol. 160, pp. 261–270.
20. K. K. Kelley: *Bull. U.S. Bur. Mines*, 1937, No. 406.
21. F. D. Richardson and J. H. E. Jeffes: *J. Iron Steel Inst.*, 1952, vol. 171, pp. 165–175.
22. A. G. Gaydon: " Dissociation Energies and Spectra of Diatomic Molecules," p. 194: 1947, Chapman and Hall, London.
23. G. St. Pierre and J. Chipman: *J. Amer. Chem. Soc.*, 1954, vol. 76, pp. 4787–4791.
24. J. A. Kitchener, A. Liberman, and D. A. Spratt: *Analyst*, 1951, vol. 76, pp. 509–516.
25. E. S. Shepherd, G. A. Rankin, and F. E. Wright: *Amer. J. Sci.*, 1909, 4th series, vol. 28, pp. 293–333. G. A. Rankin and F. E. Wright: *Amer. J. Sci.*, 1915, 4th Series, vol. 39, pp. 1–79.
26. W. Büssem and A. Eitel: *Zeitschrift für Kristallographie*, 1936, vol. 95, pp. 175–188.
27. B. Tavasci: *La Chimica e l'Industria*, 1935, vol. 17, pp. 461–471.

28. K. LAGERQVIST, S. WALLMARK, and A. WESTGREN: *Zeitschrift für anorganische und allgemeine Chemie*, 1937, vol. 234, pp. 1–16.
29. N. E. FILONENKO: *Doklady Akademii Nauk*, 1949, vol. 64, pp. 529–532.
30. F. D. RICHARDSON, J. H. E. JEFFES, and G. WITHERS: *J. Iron Steel Inst.*, 1950, vol. 166, pp. 213–234.
31. F. D. RICHARDSON: "The Physical Chemistry of Melts," pp. 75–95: 1953, Institute of Mining and Metallurgy, London.

Part II—THE THERMODYNAMIC PROPERTIES OF CaO–SiO_2 SLAGS

SYNOPSIS

Results on the equilibrium between CaO–SiO_2 slags and CO–CO_2–SO_2 gas mixtures at 1500° C have been used to obtain values for the activity of CaO and SiO_2 in these melts, and the free energies of formation of $CaSiO_3$ and Ca_2SiO_4 from their constituent oxides.

1217

THE CHEMICAL behaviour of the complex slags encountered in metallurgical processes will only be fully understood when more complete data on the simpler component systems are available. Because of the importance of the CaO–SiO_2 system, it has been the subject of several recent studies, both theoretical and experimental, which have provided data on the thermodynamic properties of CaO–SiO_2 melts.

Survey of Previous Work

The available, but relatively incomplete, thermodynamic data pertaining to the formation of $CaO.SiO_2$, $2CaO.SiO_2$, and $3CaO.SiO_2$ from CaO and SiO_2 have been critically summarized by Richardson, Jeffes, and Withers.[1] Richardson[2] later used them to determine the heats and free energies of formation of CaO–SiO_2 melts from solid CaO and SiO_2, and the activities of CaO and SiO_2 in these melts. A free energy curve was also derived by Darken[3] from the experimental results of Taylor and Chipman[4] on the system CaO–SiO_2–FeO, but even when allowance is made for the different standard states adopted by Darken for CaO and SiO_2*, the agreement with the curve obtained by Richardson is not good. A different theoretical approach was adopted by Rey,[5] who derived silica activities from the characteristics of the silica liquidus curve. The method was somewhat empirical, except near silica saturation, but gave useful qualitative information.

A number of direct experimental determinations of activities in CaO–SiO_2 slags have been carried out but the agreement can hardly be regarded as satisfactory. The earliest of note was that of White,[6] who studied the effect of CaO and SiO_2 additions on the dissociation of iron oxides. A formal treatment of the results in terms of the dissociation of the compounds assumed to be present in liquid slags enabled Murray and White[1] to calculate values for a_{CaO} and a_{SiO_2} in CaO–SiO_2 slags. Chang and Derge[8] investigated the electrochemical behaviour of these slags, and obtained values for a_{SiO_2} in fair agreement with those of Murray and White.

Sanbongi and Ohtani[9] studied the reduction of silica by hydrogen in slag–metal equilibrium experiments, according to the reaction:

$$(SiO_2) + 2H_2 = \underline{Si} + 2H_2O \quad \ldots\ldots\ldots\ldots\ldots\ldots (1)$$

The experiments were carried out in lime crucibles, and yielded values for a_{SiO_2} in Ca_2SiO_4-saturated slags. Fulton and Chipman[10] investigated a similar reaction using carbon as the reducing agent.

$$(SiO_2) + 2C = \underline{Si} + 2CO \quad \ldots\ldots\ldots\ldots\ldots\ldots (2)$$

Their values for a_{SiO_2} were considerably lower than those of Sanbongi and Ohtani, but agreed well with those obtained theoretically by Richardson.[2] How-

* Liquid (supercooled) CaO and SiO_2

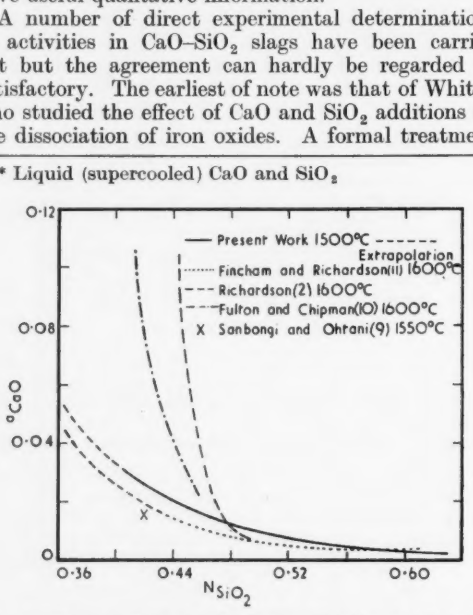

Fig. 1—Comparison of data on activity of CaO in CaO–SiO_2 slags

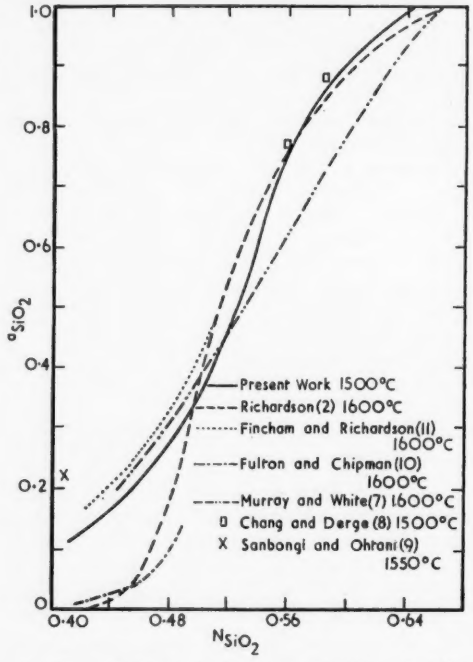

Fig. 2—Comparison of data on activity of SiO_2 in CaO–SiO_2 slags

Table I

COMPARISON OF GAS SULPHURIZING POTENTIALS

Gas Composition		Sulphurizing Potential	
CO/CO_2	S, %	Kelley (A_K)	Richardson and Jeffes (A_{RJ})
1·50	0·86	358	185
3·67	3·08	1800	1430

Values of A derived from the data of St. Pierre and Chipman lie between those of Kelley (A_K) and Richardson and Jeffes (A_{RJ}).

ever, as a result of their experimental investigations of the equilibrium between $CaO–SiO_2$ slags and $H_2–CO_2–SO_2–N_2$ gas mixtures, Fincham and Richardson[11] found it necessary to modify the values given by Richardson for the more basic compositions. The amended figures differed considerably from those of Fulton and Chipman. As can be seen from Figs. 1 and 2, where the results of the various investigations have been compared, the differences appear great enough to justify further examination of this system, especially as in each case some uncertainty exists, arising from either the inherent difficulties of the experimental procedure, or the unreliability of the thermodynamic data used.

EXPERIMENTAL

The experimental procedure was similar to that described previously,[12] $CO–CO_2–SO_2$ gas mixtures being equilibrated at 1500° C with $CaO–SiO_2$ melts contained in small platinum capsules. Suitable compositions were made up from master slags prepared from acid-purified silica sand (99·9% SiO_2) and Analar $CaCO_3$.

Analysis of Slags for Sulphur

Although the evolution method[12] had proved satisfactory for $CaO–Al_2O_3$ slags, difficulty was experienced with $CaO–SiO_2$ slags, since fine grinding, which caused a slight loss of sulphur due to the effect of atmospheric moisture, was necessary to ensure complete decomposition of the sulphide in the slag in acid. Furthermore, in some of the more acid compositions, the analytical error was an undesirably high proportion of the total titration. At this stage, the method of Fincham and Richardson[13] became available (combustion in CO_2 at 1450° C) and was subsequently used. A fresh blast-furnace slag analysed by both methods gave the following results: evolution, 1·18% S; combustion, 1·21% S. The results obtained by combustion with $CaO–SiO_2$ slags are therefore directly comparable with those obtained by evolution with $CaO–Al_2O_3$ slags.

Choice of Gas Composition

The reaction investigated was

$$(CaO) + \tfrac{1}{2}S_2 = (CaS) + \tfrac{1}{2}O_2 \quad \ldots\ldots(3)$$

for which

$$K = \frac{(a_{CaS})}{(a_{CaO}} \cdot \left(\frac{p_{O_2}}{p_{S_2}}\right)^{\frac{1}{2}} = \frac{(a_{CaS})}{(a_{CaO}).A} \quad \ldots\ldots(4)$$

where $A = \left(\frac{p_{S_2}}{p_{O_2}}\right)^{\frac{1}{2}}$, the 'sulphurizing potential' of the gas. This can be calculated from the free energies of formation of the gaseous compounds present in $CO–CO_2–SO_2$ gas mixtures at the experimental temperatures. As has been discussed in Part I,[12] three sets of data are available for this purpose, those of Kelley,[14] Richardson and Jeffes,[15] and St. Pierre and Chipman.[16] On account of the considerable differences between the values of A calculated therefrom for a given gas, as illustrated in Table I, it was originally intended to equilibrate all slags with a gas mixture similar to that used for a standard slag of unit lime activity. Such a slag would have absorbed 2% S from the first gas given in Table I. However, even with almost the highest CaO content possible in a $CaO–SiO_2$ slag which was completely liquid at 1500° C, a_{CaO} was so low that the sulphur content obtained was only 0·064%. It was therefore necessary to use gases of higher sulphurizing potential ($A_K \simeq 1800$). It would have been impractical to equilibrate such gas mixtures with the standard slag, since the corresponding slag sulphur content (about 10%) would have exceeded the saturation limit. Calculated lime activities are therefore dependent on the correctness of the thermodynamic data used. As was discussed in Part I, those of Kelley are preferred. The data of Richardson and

Table II

RESULTS OF GAS–SLAG EQUILIBRIA AT 1500° C USING $CaO–SiO_2$ SLAGS

Slag No.	Original slag composition		M.Pt. (°C)	Inlet Gas			Slag S, %	a_{CaO}	a_{SiO_2}
	CaO	SiO_2		CO/CO_2	SO_2, %	A_K			
*CS*1	35·0	65·0	1470	3·67	3·08	1800	0·038	0·0028	0·985
*CS*1	35·0	65·0	1470	3·69	3·02	1800	0·038	0·0028	
*CS*2	38·0	62·0	1450	3·71	2·90	1790	0·030	0·0023	0·92
*CS*3	42·5	57·5	1500	3·62	3·11	1780	0·048	0·0036	0·77
*CS*4	52·0	48·0	1500	4·70	3·41	2260	0·259	0·015	0·21
*CS*5	53·0	47·0	1490	3·62	3·11	1780	0·259	0·019	0·18
*CS*6	55·4	44·6	1470	3·67	3·08	1800	0·325	0·024	
*CS*6	55·4	44·6	1470	3·69	3·02	1800	0·299	0·022	0·125
*CS*6	55·4	44·6	1470	1·51	0·82	349	0·064	0·024	
*CS*7	56·0	44·0	1500	4·53	3·13	2160	0·348	0·022	0·12

Time of Expts: 3½–4 h. Gas flow = 140–150 ml/min

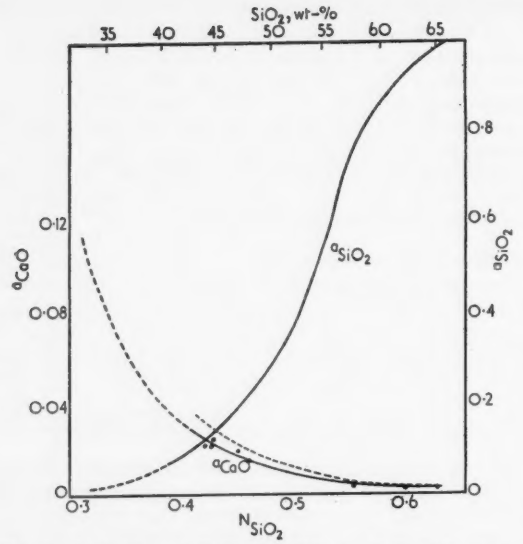

Fig. 3—Activities of CaO and SiO_2 in CaO–SiO_2 slags at 1500° C

Jeffes and St. Pierre and Chipman yield a_{CaO} values about 0·65 and 0·75 times respectively those obtained using Kelley's data, when gases of high sulphurizing potential are used.

Calculation of a_{CaO}

It can easily be derived from equation (4) that

$$a_{CaO} = \frac{\frac{(a_{CaS})}{A}}{\frac{(a^\circ_{CaS})}{A^\circ}} = \frac{\frac{(\%S)\gamma_{CaS}}{A}}{\frac{(\%S^\circ)\gamma^\circ_{CaS}}{A^\circ}} \quad \text{.....(5)}$$

for small slag sulphur percentages, where A°, (a°_{CaS}), $(\%S^\circ)$ and γ°_{CaS} refer to the standard slag. Little is known of the variation of γ_{CaS} with slag composition. It would appear reasonable to assume that at low slag sulphur concentrations, γ_{CaS} would be proportional to that of the same slag at sulphur saturation, which can be calculated if the sulphur solubility is known. Available data[12] indicate that the solubility of sulphur in the standard slag is of the order of 2·5–3·0%, and 3·5–5·5% in CaO–SiO_2 slags, and CaO–SiO_2–Al_2O_3 slags low in alumina. If in the latter case a mean solubility of 4·5% S is taken, a value of 12 is obtained for γ_{CaS} compared with ~16 for the standard slag. Values for a_{CaO} have therefore been calculated using a correction factor of $12/16 = 0{\cdot}75$ for $\frac{\gamma_{CaS}}{\gamma^\circ_{CaS}}$ in equation (5). This does not of course correct for possible variations of γ_{CaS} in CaO–SiO_2 slags with SiO_2 content, for which no data are available. Although γ_{CaS} would be expected to increase with SiO_2 content, an appreciable change is not anticipated, and it will be assumed here that over the range of CaO-SiO_2 slags investigated, γ_{CaS} remains constant.

RESULTS

The results obtained are summarized in Table II and shown graphically in Fig. 3. Since CaO–SiO_2 slags containing 42·4–52·0% CaO are not completely molten at 1500° C, this portion of the curve refers to the supercooled liquid. If no correction for the assumed difference between γ_{CaS} for CaO–SiO_2 slags and the standard slag had been applied, the upper a_{CaO} curve shown in Fig. 3 would have been obtained. The displacement of the curve for the above correction factor of 0·75 for γ_{CaS} is of the same order as that required if the thermodynamic data of Richardson and Jeffes or St. Pierre and Chipman had been used.

Figure 4 shows that, for the same molar fraction of lime, a_{CaO} in CaO–SiO_2 slags is approximately one-third of that in CaO–Al_2O_3 slags, in agreement with the known stability of calcium silicates and aluminates. The comparison can only be carried out over a limited composition range at 1500° C, since N_{CaO} in Al_2O_3-rich liquid CaO–Al_2O_3 slags is approximately equal to N_{CaO} in CaO-rich liquid CaO–SiO_2 slags.

The results obtained are compared with those of other workers in Fig. 1. As a temperature difference of 100° C should cause only a slight alteration in a_{CaO} for the compositions investigated, the agreement with the results of Fincham and Richardson[11] can be regarded as satisfactory, the deviations being in the expected direction. On the other hand, the values of a_{CaO} obtained by Fulton and Chipman[10] and Sanbongi and Ohtani[9] from silica reduction experiments show poorer agreement, lying respectively higher and lower than the present results.* However it should be noted that the agreement between the present results and those of Fincham and Richardson is not entirely unexpected, since

(*a*) the latter workers calculated a_{CaO} with the aid of the free energy change of reaction (3), which

* Fulton and Chipman applied the activity product relationship to the reaction

$$2(CaO) + (SiO_2) = Ca_2SiO_4(s)$$

to obtain a_{CaO} from a_{SiO_2} at Ca_2SiO_4-saturation. The same procedure was used to calculate a_{CaO} at Ca_2SiO_4-saturation from the results of Sanbongi and Ohtani. It should be noted that the latter workers found that a_{SiO_2} increased with fall of temperature. The calculated a_{CaO} values therefore decreased with fall of temperature. These observations are not concordant with the ΔH curve of Fincham and Richardson.[11]

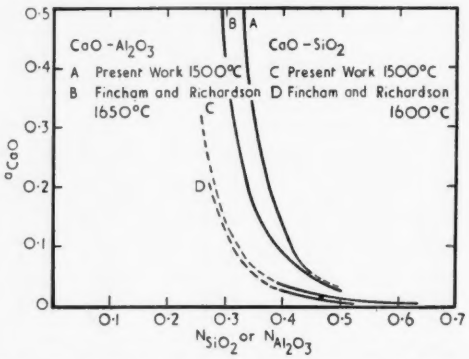

Fig. 4—Comparison of activity of CaO in CaO–SiO_2 and CaO–Al_2O_3 slags

has already been shown to be concordant with results obtained with $CaO–Al_2O_3$ slags using the present experimental procedure (12) and

(*b*) in both cases it was assumed that γ_{CaS} did not vary with slag composition. (If allowance had been made for the expected variation in γ_{CaS} with silica content, slightly flatter a_{CaO} curves would have been obtained.)

A better assessment of the present data may be obtained by deriving a_{SiO_2} from the values of a_{CaO} by means of the Gibbs-Duhem integration. The results so obtained are included in Table II and Fig. 3. Since the values of a_{CaO} obtained using the thermodynamic data of Richardson and Jeffes or St. Pierre and Chipman are an approximately constant proportion (0·65 and 0·75 respectively) of those shown in Table II, the $\frac{N_{CaO}}{N_{SiO_2}}$ /log γ_{CaO} curves differ only in their positions relative to the log γ_{CaO} axis. The derived a_{SiO_2} curves are therefore identical, and independent of the choice of thermodynamic data used to calculate a_{CaO}. Similarly, a_{SiO_2} is independent of the γ_{CaS} correction factor of 0·75 used to relate the results for $CaO–SiO_2$ slags with those for a slag of unit lime activity. It will be seen from Fig. 2 that for the more basic compositions investigated ($N_{SiO_2} = 0·4–0·45$), agreement with the direct a_{SiO_2} determinations of Fulton and Chipman, and Sanbongi and Ohtani is still relatively poor, although in the latter case it is improved if an increase in γ_{CaS} with SiO_2 content is assumed to occur. (An approximately threefold increase in γ_{CaS} from $N_{SiO_2} = 0·40$ to 0·64 would be required to attain complete agreement; this seems unusually high). Such an increase in γ_{CaS} would increase even further the discrepancy between the present results and those of Fulton and Chipman, and the curve shown in Fig. 3 may in fact be regarded as representing minimum values of a_{SiO_2}. Sanbongi and Ohtani obtained a_{SiO_2} in Ca_2SiO_4-saturated slags by comparing the silicon content of iron in equilibrium with these slags with that in equilibrium with silica at the same temperature, having already found that a_{Si} in molten iron–silicon alloys was proportional to the weight percentage of silicon over the relevant range of silicon contents. Fulton and Chipman were unable to use a similar procedure, since in the presence of carbon, silicon carbide separation occurred at silica activities considerably below unity. Their silica activities were therefore calculated using values of γ_{Si} in graphite-saturated iron determined independently.[11] As a fairly lengthy extrapolation from γ_{Si} values obtained at lower carbon contents was required, it is probable that the values of γ_{Si} used were too low at the higher carbon (and lower silicon) contents.

Chemical potential and free energy curves calculated from the present results are shown in Fig. 5. The a_{CaO} curve was extrapolated to 68% CaO with the aid of the Gibbs-Duhem integration curve, and the corresponding a_{SiO_2} values calculated, to obtain the position of the minimum in the free energy curve, which was found to occur at $N_{SiO_2} = 0·37$. The calculated free energy curves of Richardson[2] and Darken[3] show minima at $N_{SiO_2} = 0·46$ and 0·33

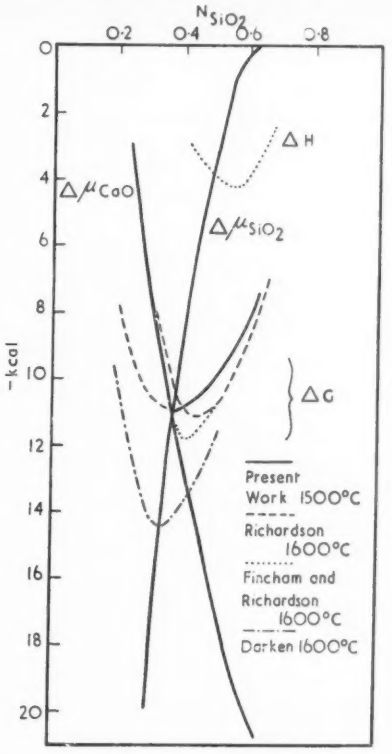

Fig. 5—Free energies of formation and chemical potentials of $CaO–SiO_2$ melts

respectively, although as a result of their gas–slag experimental work, Fincham and Richardson[11] found it necessary to amend the position of the former curve to show a minimum at $N_{SiO_2} = 0·43$. The present value is intermediate, but closer to that of Darken. The agreement with the latter would have been even closer if allowance had been made for a small increase in γ_{CaS} with SiO_2 content of the slag. On the other hand, a more than twofold increase in γ_{CaS} would have led to a minimum at $N_{SiO_2} < 0·33$, which seems improbable. The minimum corresponds to a slag for which $a_{CaO} = a_{SiO_2}$, and its position is related to the relative stability of calcium silicate melts. Its proximity to the composition corresponding to Ca_2SiO_4 is an indication of the high stability of that compound and of the SiO_4^{4-} ion in the liquid slags.

In comparing the free energy curves shown in Fig. 5, allowance for the temperature difference can be made by using the $\Delta H(CaO + SiO_2)$ curve of Fincham and Richardson.[11] This indicates that the effect of a temperature change from 1500° C to 1600° C would be to lower the ΔG(1500° C) curve by about 0·5 kcal. As might be expected from the previous discussion, the agreement with Fincham and Richardson is good, except with regard to the position of the minimum. The agreement with Darken is also good when allowance is made for the difference in standard states.

The present free energy curve indicates a value of $-20{\cdot}2$ kcal for the standard free energy change at 1500° C of the reaction

$$CaO(s) + SiO_2(s) = CaSiO_3(l)$$

Since $CaSiO_3$ does not melt until 1540° C, this value refers to $CaSiO_3$ in the supercooled liquid state. The free energy of formation of solid $CaSiO_3$ can be obtained by applying the activity product relationship

$$\Delta G = -RT \ln a_{CaO} \cdot a_{SiO_2}$$

at compositions saturated with $CaSiO_3$ at 1500° C. A mean value of $-20{\cdot}4$ kcal was obtained, which is well within the error limits of ± 3 kcal assigned to the value of $-21{\cdot}4$ kcal calculated by Richardson, Jeffes, and Withers[1] from available free energy data, and $-22{\cdot}0$ kcal derived from the free energy curve (1600° C) of Fincham and Richardson. A strict comparison in the latter case should take into account the fact that different thermodynamic data were used in the derivation of the ΔG curves. However, since use of the thermodynamic data of Richardson and Jeffes would have lowered the present ΔG curve by only $0{\cdot}5$–$1{\cdot}0$ kcal, it can be seen that the above-noted agreement still holds.

Application of the activity product relationship leads to a value of $\Delta G° = -34{\cdot}0$ kcal at 1500° C for the reaction

$$2CaO(s) + SiO_2(s) = Ca_2SiO_4(s)$$

This may be compared with an approximate value of -30 kcal given by Richardson, Jeffes and Withers and $-34{\cdot}9$ kcal calculated from more recent thermodynamic data by Fulton and Chipman.[10] The agreement with the latter is good, and within the expected accuracy limits.

DISCUSSION

The main uncertainty in the values of a_{CaO} and a_{SiO_2} derived from the results of the present experimental work lies in the lack of knowledge of γ_{CaS} in slags, and in particular of the variation of γ_{CaS} with SiO_2 content in CaO–SiO_2 slags. In the latter case, the expected variation would cause the calculated a_{CaO} and a_{SiO_2} values to be too low at low CaO and SiO_2 contents respectively. The ΔG ($CaO + SiO_2$) curve would therefore be too low at all compositions. However, values derived from this curve for the free energy of formation of $CaSiO_3$ and Ca_2SiO_4 from CaO and SiO_2 are in good agreement with present accepted values and are in fact slightly *less* negative. As the position of the minimum in the free energy curve also appears reasonable, there is good reason to believe that any error in the values given for a_{CaO} and a_{SiO_2} is small.

It will be seen from Fig. 4 that a_{CaO} is small for all compositions more acid than Ca_2SiO_4, but increases rapidly as N_{CaO} increases beyond that corresponding to Ca_2SiO_4. The effect of temperature appears to be comparatively small, only slight increases in N_{CaO} being required to produce the same value of a_{CaO} as the temperature rises. These observations are consistent with the popular method of interpreting slag behaviour in steelmaking slag–metal reactions by assuming the formation of Ca_2SiO_4 when calculating 'base' or 'oxygen-ion' activities. At lower basicities than that corresponding to Ca_2SiO_4, the desulphurizing and dephosphorizing powers of basic steelmaking slags are very poor. Figure 4 also shows that the corresponding rapid increase in a_{CaO} in CaO–Al_2O_3 slags occurs at much lower basicities, and that the value of a_{CaO} is more temperature-dependent. As similar behaviour might be expected in more complex slags, it would appear that the method frequently used of assessing the effect of Al_2O_3 on the base or oxygen ion activity by assuming the formation of $3CaO.Al_2O_3$, or $Al_2O_3^{2-}$ ions, is of dubious value.

The CaO–SiO_2 diagram[18] indicates that the metastable extension of the CaO liquids curve would cut the 1500° C isotherm (corresponding to $a_{CaO} = 1$) at a composition more acid than Ca_2SiO_4. It appears probable that the CaO–Ca_2SiO_4 eutectic point, which has only been estimated approximately, actually occurs at a greater CaO-content than the present accepted value.

Acknowledgments

The authors would like to thank Professor R. Hay for helpful advice and criticism, and B.I.S.R.A. for financial support of this investigation. One of the authors (T.G.M.) also wishes to thank the Ferguson Bequest Fund for financial assistance.

References

1. F. D. Richardson, J. H. E. Jeffes, and G. Withers: *J. Iron Steel Inst.*, 1950, vol 166, pp. 213–234.
2. F. D. Richardson: "The Physical Chemistry of Melts," pp. 75–95: 1953, Institute of Mining and Metallurgy, London.
3. L. S. Darken: "Thermodynamics in Physical Metallurgy," pp. 28–46: 1952, Amer. Soc. Metals, Cleveland, Ohio.
4. C. R. Taylor and J. Chipman: *Trans. Amer. Inst. Min. Met. Eng.*, 1943, vol. 154, pp. 228–247.
5. M. Rey: *Disc. Faraday Soc.*, 1948, vol. 4, pp. 257–265.
6. J. White: *Iron Steel Inst.*, Carnegie Scholarship Memoirs, 1938, vol. 27, pp. 1–75.
7. P. Murray and J. White: *Disc. Faraday Soc.*, 1948, vol. 4, pp. 287–296.
8. Lo Ching Chang and G. Derge: *Trans. Amer. Inst. Min. Met. Eng.*, 1947, vol. 172, pp. 90–120.
9. K. Sanbongi and M. Ohtani: *Sci. Rep. Tôhoku Univ.*, 1952, *A*, vol. 4, No. 1, pp. 59–71.
10. J. C. Fulton and J. Chipman: *Trans. Amer. Inst. Min. Met. Eng.*, 1954, vol. 200, pp. 1136–1146.
11. C. J. B. Fincham and F. D. Richardson: *Proc. Roy. Soc.*, ser. *A*, 1954, vol. 223, pp. 40–62.
12. P. T. Carter and T. G. Macfarlane: *J. Iron Steel Inst.*, 1956 (Part I of present paper).
13. C. J. B. Fincham and F. D. Richardson: *Ibid.*, 1952, vol. 172, pp. 53–55.
14. K. K. Kelley: *Bull. U.S. Bur. Mines*, 1937, No. 406.
15. F. D. Richardson and J. H. E. Jeffes: *J. Iron Steel Inst.*, 1952, vol. 171, pp. 165-175.
16. G. St. Pierre and J. Chipman: *J. Amer. Chem. Soc.*, 1954, vol. 76, pp. 4787–4791.
17. J. Chipman, J. C. Fulton, N. Gokcen, and G. R. Caskey Jr.: *Acta Met.*, 1954, vol. 2, No. 3, pp. 439–450.
18. F. P. Hall and H. Insley: "Phase Diagrams for Ceramists": 1947, *J. Amer. Ceram. Soc.*

Observations on the Mechanical Behaviour of Heat-treated Steel at High Hardness Levels

By
N. H. Polakowski,
Dipl.Ing., Ph.D.

SYNOPSIS

Untempered martensite behaves in many respects like an annealed metal. It has a low elastic limit which can be raised by cyclic stressing; its Meyer index and strain-hardening exponent are high. Despite the high indentation hardness and the internal stresses it contains, fresh martensite work-hardens during plastic deformation although work-softening could have been expected to occur in these conditions.

Tempering up to about 300° C causes the strain-hardening properties to decrease progressively and the elastic limit to rise. The impact fracture energy and ductility at sub-zero temperatures fall to a minimum but they can be improved or otherwise altered by prior cold-working at room temperature.

Most of these facts cannot be explained or accounted for if the commonly held view of virgin martensite being inherently very hard is accepted as an axiom. However, they all find their natural place in an integrated picture if as-quenched steel is visualized as being relatively soft but capable of rapid work-hardening when deformed. Tempering below 300°C is assumed to produce a hardening effect roughly similar to that of cold-working.

A working hypothesis is developed in the paper based on the above premise and incorporating a Cottrell type mechanism involving locking of dislocations by migration of solute carbon atoms. This is then applied to account for various peculiar aspects of the mechanical behaviour of hardened and tempered steel.

1225

THE REASONS FOR the hardness of martensite have been the subject of much speculation and research for a long time and the period prior to 1930 was particularly prolific in various explanatory hypotheses. Some of these have been discarded but one or two survive today, with minor modifications.[1–6] However, none of these concepts is really satisfactory or convincing[6] and indeed, the ultimate reason for the exceptional hardness of fully hardened steel is as obscure today as it was 25 or 50 years ago.

In this paper it is proposed to present a working hypothesis which not only suggests a plausible cause for the high hardness of martensite but also accounts for the changes of this and other mechanical properties of quench-hardened steel taking place upon tempering or plastic deformation, or a combination of both. As will be apparent from the evidence discussed, these changes cannot be fully explained by any one of the existing theories.

ORIGIN OF HIGH HARDNESS OF MARTENSITE

The high resistance of hardened steel to plastic deformation may be interpreted in two ways:

(*a*) It may be assumed that martensite is inherently very hard, this hardness being a direct and immediate result of the heat-treating operation.

(*b*) It could be argued that the as-quenched steel is relatively soft but capable of being strain-hardened very rapidly. The measured high hardness value is thus visualized as a result of certain structural changes induced in the virgin martensite by plastic deformation.

The older hypotheses mentioned above were all based on assumption (*a*). The feasibility of (*b*) was expounded in 1946 by Kishkin,[7] who claimed that the hardness of untempered martensite may be as low as 300–400 B.H.N., but that as a consequence of what he believed to be a carbide precipitation process promoted by plastic flow, the martensite work-hardens severely. Tempering at slightly elevated temperatures was supposed to produce an equivalent effect, and so to increase significantly the initially low hardness of martensite.

Apparently because of the paucity of supporting evidence gathered by Kishkin coupled with the—at first sight—paradoxical character of his theory, this interesting idea virtually slipped into oblivion.*

It will be shown how a modified and expanded version of the ' soft martensite ' concept, in combination with the principles governing the incidence of the work-softening phenomenon,[12] can provide a logical interpretation for a variety of facts not only unexplained hitherto but often not even thought of as being inter-related.

WORK-SOFTENING

The main rules determining the occurrence of this effect were laid down by the author some time ago[12] and several of their applications were described subsequently.[13–15] In view of their importance for the present argument, a brief résumé of the pertinent aspects of the work-softening concept is given below.

A ductile metal containing a system of internal stresses (*ISS*) created by cold-work or heat-treatment will not always harden during subsequent cold deformation. If the latter is of such a type that it tends to produce an *ISS* basically different from that left after the original treatment, transient work-softening will be observed. This will continue until the old *ISS* is disrupted and a new one, characteristic for the ' second ' forming method, begins to emerge. Work- (or strain-) softening is considered to be a manifestation of a partial release of the latent strain energy stored in the metal as a result of the ' first ' cold-working or heat-treating operation.

Hardening of a steel by quenching results in an

Manuscript received 19th September, 1955.

Dr. Polakowski is with La Salle Steel Co., Hammond, Indiana, and at the Department of Metallurgical Engineering, Illinois Institute of Technology, Chicago, U.S.A.

* It was also consistently ignored by Russian authors,[8–10] with the exception of a polemic paper by Kurdyumov.[11] Kishkin restated his case in a recent book written by a group of authors.[45]

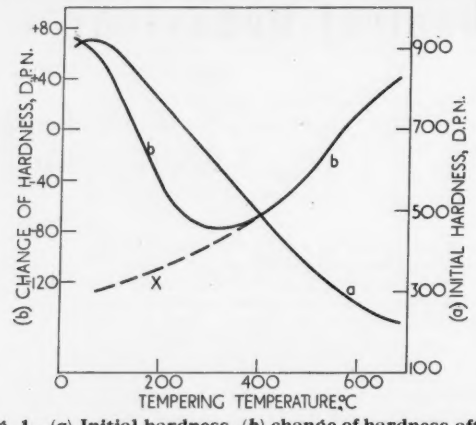

Fig. 1—(*a*) Initial hardness, (*b*) change of hardness after 10–15% compression, of a 0·8% C steel quenched and tempered as indicated[17]

ISS different from one induced by any conceivable cold-working method, if only on account of absence of pronounced directional properties. Consequently cold-working of a heat-treated steel causes strain-softening.[12, 15, 16] The effect is conspicuous at hardnesses above 300 B.H.N. (D.P.H.), it reaches a maximum at about 10–15% strain, and decreases gradually thereafter. The original hardness is restored after about 30–50% deformation. In a single steel, the maximum hardness drop is roughly proportional to the initial hardness in the as-heat-treated condition provided that the latter does not exceed about 600 D.P.H.

In discussing the author's paper,[12] Wilson[17] has demonstrated that at still higher hardness levels the work-softening effect grows gradually weaker and finally disappears altogether. Virgin, or very lightly tempered martensite > 850 D.P.H. strain-hardens when deformed, in a manner similar to that of annealed or normalized steel (Fig. 1).

Untempered martensite is generally thought to contain internal stresses of the highest magnitude. It should have been reasonable to expect, therefore, on the work-softening theory, that curve *b* in Fig. 1 would follow the dashed extension '*x*' rather than turn upwards. Since this is not the case, it is logical to postulate the existence of an additional mechanism which is operative during deformation of martensite tempered below 300° C. This factor is so powerful that it compensates partly (above 600 D.P.H.) or completely (when D.P.H. > 850) for the strain-softening that would have been observed otherwise. Although the intimate details of the mechanism in question are unknown, it is appropriate to suggest its general features so that this and other experimental findings can be analysed and accounted for.

MECHANISM FOR STRAIN-HARDENING OF MARTENSITE : LOW ELASTIC LIMIT OF HARDENED STEEL

The possibility that the fresh supersaturated solid solution of carbon in α-iron may not be inherently very hard was probably realized by Carpenter and Robertson[3] who contended that "... the hardness of martensite is due to the age-hardening change taking place while it forms." But it is obvious that these two steps, namely, formation of martensite and the structural change that hardens it, need not necessarily be simultaneous. The high hardness will also develop if the second process is promoted by mechanical deformation during testing or in service. The latter alternative will be accepted and discussed here as being in better accord with observed facts than the first.

Freshly quenched steel will thus be regarded as being relatively soft, though no attempt will be made at this stage to assess this 'softness' quantitatively. Its matrix is supersaturated with carbon atoms and it also contains many dislocations free to move under an externally applied stress. The initiation of plastic flow is enhanced by the presence of residual stresses of a magnitude dependent on the composition, quenching method, and cross-section of the steel.[18] When flow begins, carbon atoms fixed incidentally in positions of high interaction energy are propelled towards the dislocations where the interaction energy is lower.[19] These atoms anchor the dislocations, thereby obstructing their movement and increasing the resistance of the steel to further deformation. This blocking action is so effective that the rate of latent energy absorption during flow under rapidly increasing resistance is large enough to outweigh the loss of internal energy caused by simultaneous rearrangement of the original *ISS*.

Mild tempering likewise activates a part of the high-energy carbon atoms, so immobilizing a quantity of the existing dislocations. The initiation of flow is thereby impeded, as exemplified by the rising elastic limits, Fig. 2.*

Reheating at increasing temperatures naturally accelerates the process since a higher proportion of the dislocations is being tied up. On the other hand, many of the solute carbon atoms are being used up rather ineffectively 'to fill up the sinks' at individual dislocations and grain sub-boundaries.[19] Consequently, although the elastic range continues to expand, the number of ready-to-migrate carbon atoms available for agitation by cold-work decreases and so

* The question of the existence or otherwise of a 'true' elastic limit is immaterial for the present argument. This term is used for brevity and it may just as well denote a proof stress with a very small specified permanent set (e.g. 0·001%).

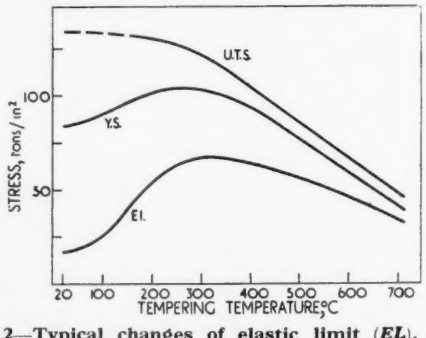

Fig. 2—Typical changes of elastic limit (*EL*), yield stress (*YS*), and tensile strength (*UTS*) of quench-hardened carbon and low-alloy steels on tempering at increasing temperatures[20–22]

does the factor which compensates for the work-softening effect. Evidently, the supply of these atoms is effectively exhausted after tempering in the vicinity of 300° C, a treatment at which a minimum or maximum appear on curve *b* of Fig. 1 and *EL* (or *YS*) of Fig. 2, respectively.

It will be apparent that if the above picture is substantially correct, the rate of work-hardening must be high in untempered martensite and it must decrease progressively during low-temperature tempering of increasing intensity, reaching a minimum after reheating at about 300° C. Tempering between the 300° C region and A_1 results in a gradual fall of the elastic limit, owing to the decomposition of the parent matrix into an inherently softer mixture of ferrite and cementite. A simultaneous relief of internal stresses causes the work-softening effect to weaken and eventually to reverse its sign. When the decomposition is complete, the metal is back in a soft and nearly 'strainless' condition. One would expect, therefore, the rate (or coefficient) of strain-hardening to behave in an opposite manner and to increase progressively as the steel becomes softer upon tempering at increasing temperatures above 300° C. As will be shown later, this is precisely the case.

EFFECTS OF RESIDUAL AND CYCLIC STRESSES ON THE ELASTIC LIMIT OF QUENCH-HARDENED AND/OR COLD-DEFORMED STEELS

It has been customary to ascribe the low elastic limit of fully hardened steel to the action of internal stresses. This intuitive belief originated from the geometrical similarity between the *EL* (or *YS*) curve (Fig. 2) and the familiar relation between ageing temperature and the strength properties of work-hardened steel.[21, 22] Acceptance of this surmise as an axiom has led to the expedient though premature deduction that the gradual increase of the elastic limit upon reheating a hardened steel is caused by a partial relief of internal stress. This opinion, now regarded by the author as essentially incorrect, was

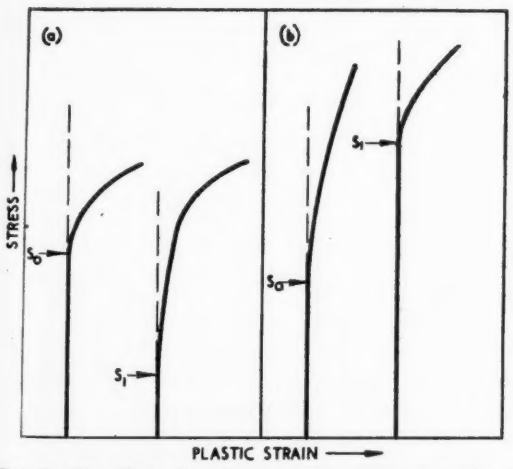

Fig. 3—The effect of cyclic stress upon the proportional (elastic) limit of (*a*) cold-drawn and (*b*) quench-hardened steel. S_0 = original proportional limit; S_1 = proportional limit after cyclic stressing[21]

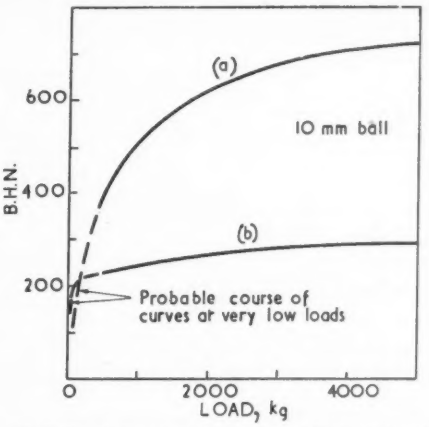

Fig. 4—Relation between test load and Brinell hardness of steel (*a*) in the as-hardened condition, and (*b*) after tempering at 500–600° C [7,27]

previously held by himself,[12] and more recently reaffirmed by Aitchison and Pumphrey,[22] Muir *et al.*,[20] and Kurdyumov.[11]

As is well known, locked-up stresses can be reduced in magnitude by subjecting a metal to cyclic stresses above the primitive elastic limit.[23–25] If the low elasticity were caused by internal stresses in cold-worked and in quench-hardened steels alike, one would expect the changes of mechanical properties induced by fatigue to follow a single pattern irrespective of the hardening procedure used. Yet Aitchison[21] found over 30 years ago that the responses of the two types of material were entirely dissimilar, cyclic stress application *depressing* the elastic limit of the statically work-hardened metal but *raising* it in the one initially quenched (Fig. 3).

These diametrically opposite reactions cannot conceivably be due to a single cause. The present author suggests that the first effect is a manifestation of work-softening, fatigue serving here as the 'second' method of cold-working different from the static deformation used first.[13, 14] The breaking loose of dislocations initially anchored by solute atoms may also act in the same general directions. The other effect conforms with the scheme developed in the preceding section, the solute carbon atoms being activated by the cyclic stress. If the improvement of elasticity of quenched steel were here due principally to stress relief, one could expect on the same grounds a reduced strain-softening effect after tempering at 300° C as compared with the as-hardened condition, in view of the lower level of internal strain energy. But according to Fig. 1, the opposite is the case.

The effect of repeated stress on the elastic limit of fully hardened steel is thus analogous to that observed with annealed metals, such as copper or nickel, under similar conditions.[14]

Internal stresses certainly have a definite influence on the absolute value of the limit of elasticity of hardened steel, but it is very unlikely that they would determine the general shape of the elastic limit versus tempering temperature envelope. This applies to an even greater degree to cold-worked steel, where

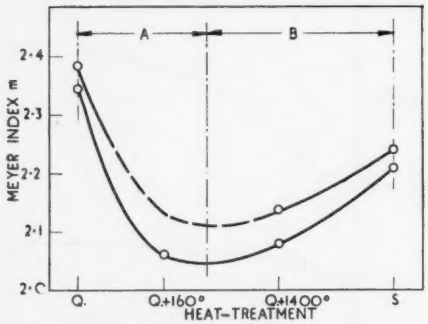

Fig. 5—The Meyer index m of heat-treated steels with 0·6–1·2%C. Q = as quenched, $Q+\ldots$ = quenched and tempered at the temperature shown, S = spheroidized[27]

the course of the 'analogous' envelope is controlled by the progress of strain-ageing.

INDENTATION HARDNESS OF MARTENSITE

On the soft-martensite hypothesis, the high resistance to penetration of hardened steel is explained by the very high rate of strain-hardening of the metal under the indenter, the atomic mechanism of hardening being the same as under the simpler conditions of static or cycling stressing. Tempering below 300°C reduces the capacity for strain-hardening but at the same time increases the inherent resistance of the matrix to deformation. In other words, it is relatively harder to start plastic flow in a tempered than in a fully hardened steel.

In the Brinell test, the plastic strain around the ball impression increases with the applied load so that a plot of B.H.N. *v.* test load represents, in effect, a stress/strain diagram. The two curves in Fig. 4 are typical of the respective behaviours of fully hardened and of tempered steel. As would be expected, the B.H.N. of as-quenched steel is abnormally low when determined at reduced testing loads, owing to the low initial resistance to flow combined with the small plastic strains involved. An increase of pressure and consequent deformation cause the hardness number to rise quickly. However, changes of the test load within broad limits have almost no effect on the B.H.N. of tempered steel, which is not surprising in view of the presence of the work-softening phenomenon.

These two curves are helpful in explaining why the inherent hardness of the undeformed martensite should be less than that measured normally. If it were possible to stop the 'carbon atom hardening' process at an early stage or to prevent it altogether, the upper curve would presumably bend over, forming a fairly sharp knee, and would run considerably below the one actually observed. Its slope, of course, would be greatly reduced.

THE MEYER INDEX OF HARDENED STEEL

The Meyer analysis of ball indentation tests is a convenient means for describing quantitatively the strain-hardening rate of various metals. Annealed copper, aluminium, austenitic steel, and other metals which are characterized by steeply rising stress/strain diagrams also have high Meyer indexes ($2{\cdot}25 < m < 2{\cdot}5$). Severely cold-worked materials usually have nearly horizontal deformation curves approaching in shape those of an ideal elastic–plastic body (*see*, for instance, Figs. 6–8 of Tabor's book[26]). Their m values are close to 2·0, this figure being indicative of zero strain-hardening rate or nearly so.

Turning to heat-treated steels, O'Neill[27] found Meyer's index to be high in as-quenched steel ($m \simeq 2{\cdot}35$), to fall upon tempering, but to rise again after annealing (Fig. 5). Although no attempt was ever made to explain the overall shape of these m-curves, Tabor (*loc. cit.*, pp. 55–60) suggested that the high index of fresh martensite may be a result of test technique rather than a real physical property. However, the preceding discussion of the work-hardening behaviour of hardened steel leads to an opposite conclusion, i.e. that the high Meyer index is a true indication of the high work-hardening rate of fresh martensite. Since the latter is reduced by tempering, even to the extent of being replaced by softening, it is quite natural that m drops. When fully softened, steel again work-hardens during straining and it has, therefore, a high Meyer index, as would be expected.

CHANGES OF LATENT ENERGY DURING WORK-HARDENING AND WORK-SOFTENING

Annealed metals when cold-worked are known to absorb and retain a fraction of the total deformation work in the form of latent strain energy. According to the author's conception, this process should be partially reversible, the metal accumulating latent energy when it progressively work-hardens but releasing some of it under deformation conditions

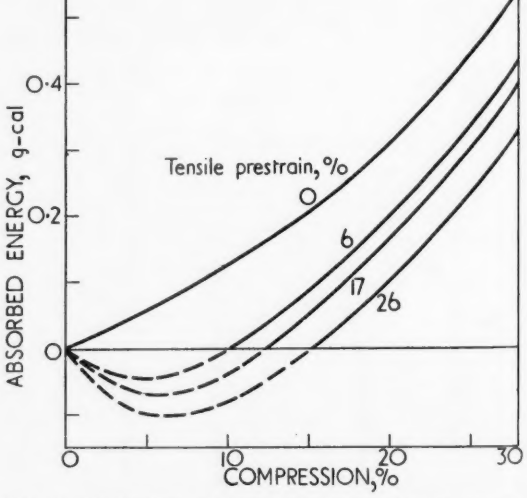

Fig. 6—Absorption of latent strain energy by copper during plastic compression.[28] Note that there is no absorption during the initial stages of compressing prestretched specimens. The dashed portions represent a plausible extension of the original results (added by present author)

which result in work-softening. It was shown[12] that these changes can be imitated on a model which was in turn used to explain the mechanics of the Bauschinger effect. However, no direct experimental support for the thesis could be given at the time.

Degtyarev's work[28] is believed to partly fill up this gap. By using a rather crude but relatively rapid method, he made a large quantity of latent-energy determinations at different stages of cold-working. A set of his results is shown in the upper portion of Fig. 6.

It is seen that annealed copper absorbs latent energy from the very beginning of plastic compression, whilst the prestretched specimens begin to do so at a later stage, depending on the amount of tensile prestrain suffered. Degtyarev said nothing about the energy behaviour at low compressive strains of the initially extended specimens. However, since he committed himself *a priori* to the notion that reversed deformation should continue the work-hardening action of the initial prestrain, it is reasonable to assume that he must have ignored these early stage changes in order not to complicate his own argument.* With this in mind, the graphs have now been supplemented by the dashed (lower) portions which bring the picture to a complete coincidence with the hardness/strain curves obtained from similar experiments.[12]

A comparison between various stress/strain curves recorded in reversed deformation and those of as-annealed metals[12, 29] shows that small prestrains have little effect on the slope of the 'reversed' diagrams whereas large ones >10–15% lower it significantly. This effect is due to the gradual release of latent energy which reduces the external effort needed to maintain plastic flow. Since work-softening depends on the amount of initial pre-strain, and more internal strain energy is released when the initial work-hardening level is higher, a change of slope of the type observed is quite natural.

The same reasoning can be applied to heat-treated steel and it can be expected that as the initial hardness increases due to progressively lowered tempering temperature, the slope of the appropriate stress/strain curves, or 'strain-hardening exponent,' must behave in an opposite manner.

* Degtyarev was obviously aware of the inconsistency of his assumption and results. He therefore conceded that the latter were unexpected but added cautiously that "the initial latent energy absorption was immeasurably small in the prestrained samples."

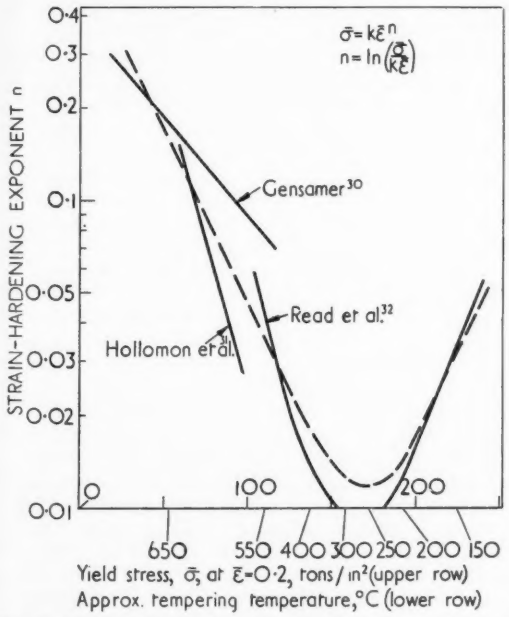

Fig. 7—The strain-hardened exponent *n* in tension and compression tests on steels heat-treated to various strength levels[30–32]

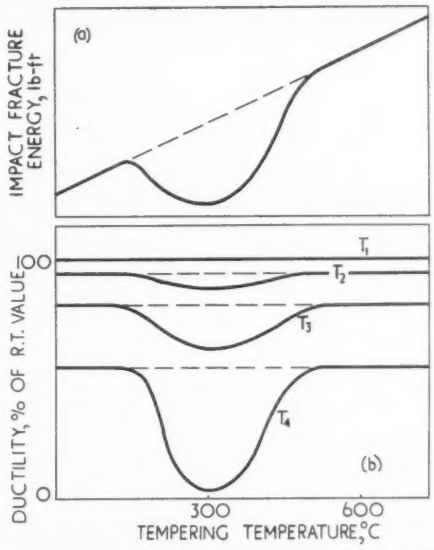

Fig. 8—(*a*) Impact fracture energy and (*b*) ductility at decreasing temperatures ($T_1 > T_2 > T_3 > T_4$; $T_4 \leqslant 0$) of various heat-treated carbon and low-alloy steels (schematic). In the absence of '300° C embrittlement' the pronounced dips would have disappeared, as indicated by dashed lines

THE STRAIN-HARDENING EXPONENT OF HARDENED AND TEMPERED STEEL

As an alternative to Meyer's formula, the strain-hardening properties of metals may also be described by the relation $\sigma = a\epsilon^n$, where σ = actual (true) stress, ϵ = natural (log) strain, a = constant, n = strain-hardening exponent. Except for small strains below 5% or so, this function represents very nearly a straight line when plotted in log/log co-ordinates, n being its slope. Rapidly work-hardening metals have a high n value, and vice-versa.

Strain-hardening exponents obtained in three independent investigations[30–32] are assembled in Fig. 7. Those of Gensamer[30] and of Hollomon and associates[31] were obtained from tension tests on steels at medium strength levels and those of Read *et al.*[32] from compression experiments. Because of the relatively high plasticity of even very hard steels under compressive loads, the latter tests covered a much wider range of heat-treated conditions. Since

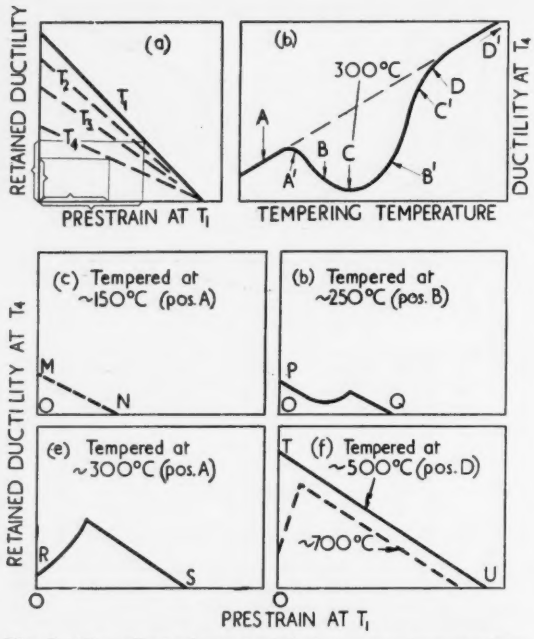

Fig. 9—The effect of prestraining at room temperature T_1 on the residual ductility at reduced temperatures T_2, T_3, T_4. (*a*) Behaviour to be expected in the absence of 300° C embrittlement; (*b*) hypothetical transition of the initial metallurgical conditions *A*, *B*, *C*, *D* into *A'*, *B'*, *C'*, *D'* as a result of cold-working at room temperature T_1; (*c*)–(*f*) break-down of (*b*) into individual diagrams to show the effect of original heat-treatment and increasing prestrains at T_1 on retained ductility at T_4

the power relation between stress and strain does not hold for the initial portion of the curve, the exponent n in Fig. 7 is expressed as a function of σ at $\epsilon = 0{\cdot}2$. The tempering temperatures given at the bottom of the diagram were interpolated from Read's data.[32]

All three curves exhibit identical trends in the medium strength range, n progressively decreasing in each case. In addition, Read's curve reaches a minimum between 250° and 300° C and turns upwards when the tempering temperature is further lowered. According to the same source, this behaviour is typical for a variety of steels and it may be concluded that the strain-hardening exponent obeys the same law as the Meyer index.

In the range of tempering temperatures above 300° C the exponent n behaves as predicted above. After tempering below 300° C, n is apparently governed by the martensite strain-hardening mechanism advanced in the earlier part of the paper, a higher n corresponding to a lower reheating temperature.

IMPACT TOUGHNESS AND DUCTILITY AT LOW TEMPERATURES OF STEELS HEAT-TREATED TO HIGH HARDNESS LEVELS

Tempering of hardened steel at progressively increasing temperatures affects the impact energy value and the ductility at sub-zero temperatures in much the same way as the various mechanical properties already reviewed. That is, both of them exhibit a pronounced minimum in carbon and low-alloy steels tempered in the 250–350° C range, as shown in Fig. 8.

Any complete explanation of these two phenomena would necessarily involve a detailed consideration of the three additional variables, namely triaxiality (in notched bar tests), rate of deformation, and test temperature in relation to microstructure and crystallography of plastic flow and fracture. No attempt in this direction is contemplated in this work, in order not to broaden its scope unduly and to avoid encroaching on a crowded and controversial field. However, it appears that for the purpose in view a strictly phenomenological interpretation of the facts would suffice, and this may be condensed into the following tentative statements:

(i) Each of the three variables amplifies the '300° C embrittlement' effect. Specifically, the impact loading, stress concentration, and reduced testing temperature act so as to reduce the total work to fracture and the ductility (the latter measured by contraction of area at the neck of a fractured specimen[33–35]).

(ii) All three factors tend to raise the elastic limit and yield stress above their static (unnotched, room temperature) value, and even considerably so. At the same time they are supposed to affect the fracture stress to a much lesser degree (*ibid.*). Since the elastic limit and yield stress are inherently very high after tempering in the 300° C range, it seems quite probable that they may be raised by the action of one or more of the factors in question to the point where the yield and fracture stress nearly coincide. In effect, both the ductility and the fracture work would be very low, as is actually observed.

'RHEOTROPIC' ASPECTS OF THE 300° C EMBRITTLEMENT

Ripling and Baldwin[35,36] found that the exceptionally poor ductility at low temperatures of steel tempered at 300° C is to a certain extent strain curable or 'rheotropic.' That is, it can be improved or otherwise altered by subjecting the material to a controlled plastic strain at room temperature prior to testing at sub-normal temperature. Since no explanation of this interesting effect has yet been forthcoming, it may be worthwhile to reconsider it in the light of the hypothesis developed here.

Figure 9*a* illustrates the relation between plastic prestrain at normal temperature T_1 and the retained ductility observed at this or at gradually reducing temperatures ($T_4 < T_3 < T_2 < T_1$). This simple scheme is representative of face-centred-cubic metals as well as of steel tempered above 500° C or so, and in each case a prestrain at T_1 lowers the ductility at T_2, T_3, etc. But this pattern does not apply to 300°C embrittled steel, which behaves in a much more complex fashion, apparently because of the peculiar relation between tempering temperature and low-temperature ductility, Fig. 9*b*. The author submits the following interpretation of the facts.

Changes of residual ductility of structurally unstable alloys occur not only on account of its partial exhaustion by previous permanent deformation (to be called 'strain exhaustion') but also as a result of structural changes taking place during plastic flow. If one considers a steel in heat-treated condition *A*, Fig. 9*b*, progressive straining at room temperature will naturally use up a part of its ductility by regular strain exhaustion. In addition, straining promotes

the carbon-atom hardening process which, according to the general assumption made, will tend to shift A to the right. (It will be remembered that the cold-working of a steel tempered below 300° C is assumed to be substantially equivalent to further tempering at a temperature slightly higher than that used originally.)

The shape of the curve between A and A' would suggest that progressive working should at first increase and then again reduce the sub-zero ductility. However, carbon and low-alloy steels tempered at about 150° C have a very low room-temperature ductility in any case, and only a fraction of this is preserved below −100° C. Taking into account the considerable experimental scatter which is unavoidable in experiments on such hard and relatively brittle materials, as well as strain exhaustion, one cannot expect to obtain reliable and discriminative results in these conditions. For this reason, points M and N, Fig. 9*c*, have been connected by a dashed straight line.

Turning now to the behaviour of a specimen tempered at about 250° C as represented by point B in Fig. 9*b*, deformation at room temperature will not only reduce its ductility by strain exhaustion but will also affect its low-temperature behaviour by displacing B towards C. Hence the low-temperature ductility will rapidly fall because of the combined action of both factors, i.e. strain-exhaustion and carbon-atom hardening, as indicated by the initial falling portion of the curve in Fig. 9*d*, starting from P. Since the room-temperature ductility in (*d*) is substantially higher than in (*c*), it may be possible not only to reach a state corresponding to tempering at C (300° C and minimum low-temperature ductility) but to go beyond that and towards B', in (*b*). The conditions between C and B' correspond to increasing sub-zero ductility and accordingly the curve in (*d*) turns upwards. Eventually it must fall again, of course, because of the exhaustion process which leads finally to fracture at Q.

A specimen tempered initially at 300° C and hence exhibiting a minimum sub-zero ductility to begin with (position C in Fig. 9*b*) will react to deformation at room temperature as shown in Fig. 9*e*. The structural changes caused by cold work at room temperature would tend to shift C from its initial position to the right and towards C', all the intermediate points along the curve corresponding to an improved ductility value. In that way the rising portion of the diagram in (*e*) can be accounted for. Obviously, with strain exhaustion acting at the same time, the curve starting at R is bound to bend over, thereby producing the drooping portion terminating at S.

Finally, a steel hardened and tempered at relatively high temperatures (say 500° C and above) yields a relation of the type shown by a solid line in Fig. 9*f*. The metal structure is gradually approaching a condition of equilibrium and cold-working affects it to a lesser degree. Accordingly, both the normal and sub-zero temperature ductility are controlled essentially only by strain exhaustion, the solid line in (*f*) being identical with any one of those shown in (*a*).

Reference to Ripling and Baldwin's work will demonstrate that their experimental curves are identical with the series (*c*)–(*f*) in Fig. 9. Upon repeating these experiments on a steel in a heat-treated condition intermediate between (*e*) and (*f*) these workers obtained a curve of the type shown dashed in (*f*), as would be expected.

TEMPERING AND THE DUCTILITY OF MARTENSITE: FATIGUE PROPERTIES

Thermal or mechanical treatments which increase the hardness of steel reduce, as a rule, its ductility. Since, according to the theory developed here, low tempering should harden a fully quenched steel, one might expect on the same ground the as-quenched ductility to be higher than after a 250–300° C tempering operation. But this is contrary to what actually happens,[42] and an attempt to account for it is appropriate at this point.

When a freshly quenched steel is plastically deformed, the forced migration of carbon atoms proceeds in an "oriented" manner along the successively formed slip surfaces, thereby producing a maximum hardening effect in the direction of flow and obstructing the latter's progress. The yield stress builds up so rapidly that after a small amount of overall distortion the value of the cohesive strength is reached and failure ensues.

If, on the other hand, the steel is first tempered around 300° C, the structural hardening process comes to an end (and the stockpile of free carbon atoms is exhausted) before the ductility test even commences. The initial yield is naturally higher than in the previous case, but the slip-obstructing carbon atom population is now already tied up uniformly throughout the metal mass instead of being preferentially fed to the active slip areas as deformation proceeds. As a result, flow is less inhibited and more deformation can take place before the fracture stress is reached. The improvement of ductility is thus directly related to the fall of the strain-hardening exponent.

The course of the endurance-limit/tempering-temperature relationship indicates that strain-hardening of martensite is directional by nature. As was shown first by French[43] and later confirmed by Garwood *et al.*,[44] this function too shows a maximum in the vicinity of 250–300° C, the endurance limit being significantly lower before than after reheating. Evidently, the strain reversals retard the expansion of the elastic range so effectively that a crack nucleus has an opportunity to form and propagate before the state referred to in the past as "elastic hysteresis" has time to develop.

Incidentally, this reversibility of strain-hardening is probably the physical reason for the endurance limit being higher under unidirectional or asymmetrical loading than under alternating cyclic loading.

CONCLUSION

In this paper, several remarkable features of the mechanical behaviour of hardened steel have been reviewed, analysed, and correlated by utilizing essentially a single assumption regarding the nature of the hypothetical agent which causes martensite to be hard. It is conceded that the suggested picture of the hardening process (carbon atom migration) is bound to contain at least some errors. For instance, the obvious but unavoidable simplification in the form of the assumed equivalence of deformation and

tempering, with regard to their effects on carbon atom movements in fresh or slightly tempered martensite, is certainly untenable in the long run without some more or less serious modifications. It is felt, however, that this represents a secondary rather than a basic weakness in the main argument; the latter showed its usefulness as an interim measure and may be improved upon as the empirical knowledge in pertinent fields advances.

The microstructure of martensite and its changes during tempering have been thoroughly investigated and repeatedly discussed in the past as well as recently by using mainly the results of microscopic, dilatometric, and X-ray work.[37–42] Yet attempts to relate these to mechanical properties were limited in scope, usually centred on impact energy and, occasionally, ductility in tension.[37, 40–42] In contrast to the above, this paper represents an attempt to generalize a variety of scattered findings on the basis of a self-contained phenomenological theory.

The evidence shown indicates that the frequently invoked analogy between cold-worked and fully hardened steel is quite limited. In particular, the gradual expansion of the elastic range upon reheating is probably caused by a Cottrell-type carbon diffusion process in either case. In all other respects (Meyer's index, strain-softening, rheotrophy, etc.) the mechanical behaviour of work-hardened steel is comparable with that found after quench-hardening followed by tempering in the 300° C range. The latter statement is also supported by Jack,[38] who noticed a qualitative similarity between the anomalous X-ray reflections which accompany cold deformation of carbon steel and those found during the early part of the third stage of tempering (above 260° C).

Acknowledgments

Most of this work was done while the author was employed at La Salle Steel Company, and thanks are due to the Directors for the facilities provided.

References

1. W. Rosenhain: "An Introduction to the Study of Physical Metallurgy," pp. 180–183: 1915, London, Constable and Co.
2. A. Sauveur: " Metallography and Heat Treatment of Iron and Steel," 3rd ed., pp. 251–267: 1926. Cambridge, Mass., The University Press.
3. H. Carpenter and J. M. Robertson: " Metals," vol. 2, pp. 913–914: 1939, London, Oxford University Press.
4. F. Seitz: " The Physics of Metals," pp. 211–212: 1943, New York, McGraw-Hill Book Co., Inc.
5. G. Masing: " Grundlagen der Metallkunde," pp. 86–87: 1951, Berlin, Springer-Verlag.
6. M. A. Grossman: " Principles of Heat Treatment " (revised by E. C. Bain), p. 8: 1953, Cleveland, Ohio, American Society for Metals.
7. S. T. Kishkin: *Izvestya Akademii Nauk U.S.S.R., Otdelenie Tekhnicheskikh Nauk*, 1946, No. 12, pp. 1799–1808.
8. V. I. Arkharov: " Kristallografya Zakalki Stali," 1951, Sverdlovsk, Metallurgizdat.
9. A. P. Gulyaev: " Metallovedenye," 1951, Moscow, Metallurgizdat.
10. N. F. Bolkhovitinov: " Metallovedenye i Termicheskaya Obrabotka," 1952, Moscow, Metallurgizdat.
11. G. V. Kurdyumov: *Zhur. Tekh. Fiz.*, 1954, vol. 24, pp. 1254–1267.
12. N. H. Polakowski: *J. Iron Steel Inst.*, 1951, vol. 169, pp. 337–346.
13. N. H. Polakowski: *Proc. Amer. Soc. Testing Mat.*, 1952, vol. 52, pp. 1086–1097.
14. N. H. Polakowski and A. Palchoudhuri: *Ibid.*, 1954, vol. 54, pp. 701–712.
15. L. Matteoli and B. Andreini: *Met. Ital.*, 1953, vol. 45, pp. 328–337.
16. P. W. Bridgman: " Studies in Large Plastic Flow and Fracture," pp. 185 and 191: 1952, New York, McGraw-Hill Book Co., Inc.
17. D. V. Wilson: *J. Iron Steel Inst.*, 1952, vol. 172, pp. 29–31.
18. H. B. Wishart: (in) " Residual Stress Measurements," pp. 97–128: 1952, Cleveland, Ohio, American Society for Metals.
19 A. H. Cottrell: (in) " Relation of Properties to Microstructure," pp. 131–162: 1954, Cleveland, Ohio, American Society for Metals.
20. H. Muir, B. L. Averbach, and M. Cohen: *Trans. Amer. Soc. Metals*, 1955, vol. 47, pp. 380–399.
21. L. Aitchison: *Carnegie Scholarship Memoirs*, 1923, vol. 12, pp. 113–217.
22. L. Aitchison and W. I. Pumphrey: " Engineering Steels," pp. 88–89: 1953, London, MacDonald and Evans.
23 F. Giesen and R. Glocker: *Z. Metallkunde*, 1938, vol. 30, pp. 297–298.
24. F. Körber: *Stahl u. Eisen*, 1939, vol. 59, pp. 618–626.
25. O. J. Horger and H. R. Neufert: " Fatigue and Fracture of Metals " (ed. W. M. Murray), pp. 103–130: 1952, New York, J. Wiley and Sons.
26. D. Tabor: " The Hardness of Metals," pp. 55–60: 1951, Oxford, Clarendon Press.
27. H. O'Neill: " Hardness of Metals and Its Measurement," pp. 203–205: 1934, London, Chapman and Hall.
28. M. M. Degtyarev: *Zhur. Tekh. Fiz.*, 1950, vol. 20, pp. 440–446.
29. N. H. Polakowski: *J. Iron Steel Inst.*, 1952, vol. 172, p. 373, Fig. 6.
30. M. Gensamer: *Trans. Amer. Soc. Metals*, 1946, vol. 36, pp. 30–60.
31. J. H. Hollomon, L. D. Jaffe, D. E. McCarthy, and M. R. Norton: *Ibid.*, 1947, vol. 38, pp. 807–844.
32. T. A. Read, H. Marcus, and J. M. McCaughey: (in) " Fracturing of Metals," pp. 228–243: 1948, Cleveland, Ohio, American Society for Metals.
33. E. Orowan: Reference 25, pp. 139–167.
34. N. P. Allen: " Mechanical Properties of Metals at Low Temperatures," pp. 1–35: 1952, Washington, D.C., U.S. Department of Commerce National Bureau of Standards.
35. E. J. Ripling: *Bull. Amer. Soc. Test. Mat.*, 1952, Dec., pp. 37–42.
36. E. J. Ripling and W. M. Baldwin, jun.: *Trans. Amer. Soc. Metals*, 1951, vol. 43, pp. 778–805.
37. M. A. Grossmann: *Trans. Amer. Inst. Min. Met. Eng.*, 1946, vol. 167, pp. 39–79.
38. K. H. Jack: *J. Iron Steel Inst.*, 1951, vol. 169, pp. 26–36.
39. I. N. Bogachev and V. G. Permyakov: Otpusk Zakalennoi Stali: 1950, Moscow, Mashgiz.
40. H. Schrader, H.-J. Wiester, and H. Siepmann: *Arch. Eisenhüttenwesen*, 1950, vol. 21, pp. 21–31.
41. B. S. Lement, B. L. Averbach, and M. Cohen: *Trans. Amer. Soc. Metals*, 1954, vol. 46, pp. 851–877.
42. L. J. Klingler, W. J. Barnett, R. P. Frohmberg, and A. R. Troiano: *Ibid.*, pp. 1557–1588.
43. H. J. French: *Trans. Amer. Soc. Steel Treating*, 1933, vol. 21, pp. 899–946 and Fig. 9.
44. F. M. Garwood, H. H. Zurburg, and M. A. Erickson: " Tests and Their Relation to Service," pp. 11–13 and Figs. 4, 5: 1951, Cleveland, Ohio. American Society for Metals.
45. Ya. S. Umanskyi *et al.*: " Fizicheskyie Osnovy Metallovedenya," pp. 669–685: 1955, Moscow, Metallurgizdat.

An Investigation of the System $2FeO.SiO_2$–$3Na_2O.P_2O_5$–$Na_2O.2SiO_2$

By C. Bodsworth, M.Met., A.I.M.

and W. R. Maddocks, Ph.D.

SYNOPSIS

Two quasi-binary systems forming part of the ternary system $2FeO.SiO_2$–$3Na_2O.P_2O_5$–$Na_2O.2SiO_2$ have been investigated, and the results, correlated with data obtained from other sources, have been used to construct a diagram of the ternary system. The form of the quasi-binary diagrams was determined by thermal analysis and the phase fields were confirmed by petrological and X-ray examination. The extent of solid solubility of the binary compounds was not determined.

The ternary system is sub-divided by a eutectiferous quasi-binary join between a stable compound on the sodium-orthophosphate–sodium-disilicate side and fayalite. Since no evidence could be found in X-ray patterns of the existence of stable ternary compounds, it is suggested, on the basis of the data obtained from the quasi-binary systems, that in both subternary regions a ternary peritectic point and a ternary eutectic are formed. 1200

DURING RECENT YEARS experiments on a laboratory scale have shown that a considerable amount of phosphorus and sulphur could be removed from molten steel in steelmaking furnaces using soda-rich slags of controlled compositions.[1, 2] The efficiency of the process has been found to vary markedly with the composition of the slag; it has recently been shown[3] that the optimum removal is obtained when using a slag with a basicity (i.e. ratio bases/acids) of 1·0–1·5.

Whilst the examination of the quantitative application of the process has progressed rapidly, research into the constitution of the slags has not advanced very far. To extend the theoretical basis of the process, a knowledge of the phase associations existing in the solid slag was considered essential, the determination of the relevant phase diagrams of the reactive components being the most obvious means of obtaining these data. It is appreciated that evidence of the existence of a phase combination in the solid slag does not indicate that such phases exist in the liquid state; it is more probable that the latter comprises simple and/or complex ions derived from the participating components, rather than discrete molecules. However, phase-diagram studies can still supply relevant data as follows:

(i) The variation of the temperature of liquid formation with composition
(ii) The presence of regions of immiscibility in the liquid phase
(iii) An indication of the stability of compounds from the slope of their liquidus surfaces
(iv) Activities in the liquid phase can be calculated from accurately determined liquidus surfaces together with heats of formation of the constituents
(v) The interpretation of thermodynamic data for liquid slags by either the ionic or the molecular theories has generally required an assumption of the formation of compounds by the components of the slag, the compounds assumed usually being those known to exist in the solid state.

The laboratory experiments utilized slags containing nine or ten components; of these, ferric oxide, alumina, and sulphur were only minor components. The system Na_2O–SiO_2–P_2O_5 had already been examined[4] and it was decided to extend this by studying the effects of additions of ferrous oxide to this ternary system. The phase associations in the presence of CaO, MnO, and MgO have still to be investigated.

EXPERIMENTS

A molybdenum wire-wound furnace with a closed-end tube was used in the early stages of the experiments. Later an improved form was developed with the element wound on an inner tube, and an inert atmosphere was maintained over the element by sealing an outer annular tube to this with water-cooled rubber ring seals at each end. The upper end of the inner tube was sealed with a sight-glass through which passed the thermocouple and the lower end was closed by a mercury seal to facilitate rapid insertion and rapid cooling of the melts.

A few experiments served to show that the quenching technique was not easily adapted to mixtures containing sodium and ferrous oxides, owing to the water-solubility of the former and the ease of oxidation of the latter. On the other hand, lowering the crucible below the hot zone and quenching with a rapid flow of inert gas was not sufficiently rapid to prevent some crystallization occurring with many of the compositions studied. Consequently, it was decided to use thermal analysis, duplicating arrest points both on heating and cooling.

Synthetic Slags

Ferrous oxide was prepared by the controlled decomposition of pure ferrous oxalate. The combined water was first driven off by heating for 1 h at 150–200° C, and the tube was then continually evacuated and heated to 700° C, at which temperature the CO/CO_2 ratio of the gases evolved is in equilibrium with ferrous oxide. The powder was rendered non-pyrophoric by heating to 1100° C, after all the gas had been exhausted from the tube. The resultant material on analysis corresponded to 99·5–99·8% FeO.

After standing for a period in an evacuated bottle, the ferrous oxide was found to be magnetic, from which it was assumed that part of the ferrous oxide had dissociated according to the reaction

$$4FeO = Fe + Fe_3O_4$$

Manuscript received 29th July, 1955.

Mr. Bodsworth is with the Department of Metallurgy, Liverpool University, and Dr. Maddocks is with the Department of Metallurgy, Sheffield University.

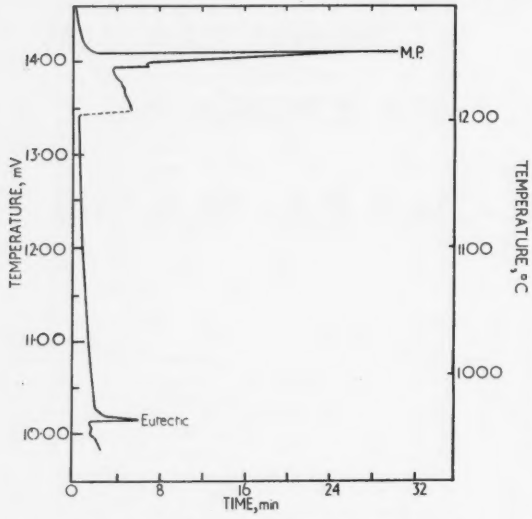

Fig. 1—Inverse-rate cooling curve of melt 9

Carter[5] has shown that metallic iron can reduce sodium oxide with the subsequent loss of metallic sodium at elevated temperatures. The above reaction will, however, go to the left at temperatures in excess of 570° C, leaving no free iron. Application of available free-energy data for the sodium silicates and phosphates indicated that, by placing the slags in the furnace at, say, 900° C and heating until liquid formation was complete, no sodium oxide would be lost. This was substantiated by analysis of the experimental melts.

Sodium disilicate was prepared by the method described by Maddocks and Turkdogan.[4]

Melts were prepared by crushing all materials to pass through a 100-mesh sieve, then drying at 110° C, and weighing after cooling in a desiccator. After mixing in a glass bottle, the charge was transferred to a platinum crucible. The decision to use platinum was made in view of the possibility of loss of soda with iron crucibles, and the danger of contamination from refractory crucibles. It was realized that some iron would be lost from the melts, passing into solid solution in the platinum. The actual gain in the weight of the crucibles between melts was negligible, however, and it was inferred that the change in composition of a melt between the time of the liquidus arrest and complete solidification would be within the limits of analytical error.

All the melts were made in an atmosphere of nitrogen, the gas being passed in turn over heated copper turnings, alkaline pyrogallol, and silica gel. Before the insertion of a melt into the hot zone of the furnace, the tube was thoroughly flushed with nitrogen, the crucible was then raised into the hot zone, and the mercury seal was clamped into position. The flow of nitrogen was maintained for a few minutes to sweep out any air remaining in the tube, and then the flow rate was reduced to hold a slight positive pressure in the tube during the run.

Thermal Analysis

Most melts were duplicated to ensure accuracy and all the arrest points could be reproduced to within ± 3° C. In many cases, after an arrest had occurred during cooling, it was immediately checked by reheating through the arrest temperature, after which cooling was continued. Figure 1 shows the inverse-rate cooling curve for a melt of composition FeO 38·04, Fe_2O_3 2·82, SiO_2 22·87, P_2O_5 9·04, and Na_2O 27·23 mole %. The rate of cooling was increased after the completion of the liquidus arrest at 13·5 m.v. Figure 2 gives the arrests for the composition FeO 5·56, Fe_2O_3 2·35, SiO_2 4·04, P_2O_5 22·02, and Na_2O 66·03 mole %. In all cases the arrest temperature was taken as the peak of the curve.

Silicate and phosphate melts are known to be difficult to crystallize owing to their complex structures of linked tetrahedra in the solid state. Cations with small radii or with a high positive charge do not fit easily into the interstices between the tetrahedra, owing to the lengthening of the cation–oxygen bonds, but tend to disrupt the sheet or chain structures into smaller units more conducive to the crystallization process. This behaviour was evident in these experiments; the primary solidification of all the melts of orthosilicate composition (at which the Si/O ratio is such that the tetrahedra exist as separate, unlinked entities) was completely crystalline at cooling rates of 1° C/min, and even more rapid rates could be used as the phosphate content of such melts was reduced. Conversely the tendency for undercooling and glass formation increased progressively as the content of acid radicles increased beyond the 'ortho' salt

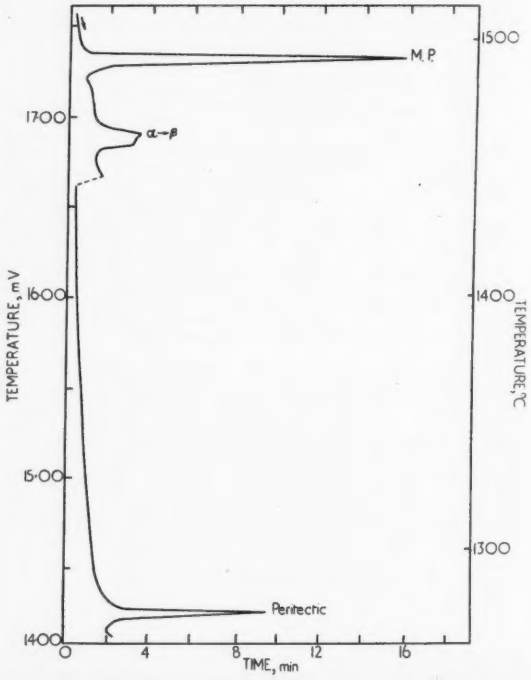

Fig. 2—Inverse-rate cooling curve of melt 15

composition. Thus, in the presence of metasilicates, cooling rates of 0·5° C/min produced some glass in the primary solidification; in some cases the slowest practical cooling rates produced some glass. Arrest temperatures for these melts were determined from a heating curve, after allowing time for crystallization to be completed at 10–20° C below the appropriate eutectic arrest temperature.

Petrological Examination

Investigation of the slags by vertical illumination proved unsuccessful, since the slags were too transparent for detailed study and the marked difference in solubility between sodium salts and fayalite made etching difficult. Petrological examination of crushed crystal fragments gave a qualitative confirmation of the findings by thermal analysis. Refractive indices were determined by immersion in a series of non-volatile liquids of known refractive index and observation of the movement of the Becker line. Crystal shape, cleavage, twinning, interference colours, and extinction angle were determined when possible and were compared with the tabulated data of Winchell[6] and Turkdogan and Maddocks[4] to confirm the range of existence of the phases identified. To ensure that the whole structure was crystalline before examination, small quantities of each melt were annealed below the eutectic temperature as described above.

X-ray Examination

Slag samples crushed to 200 mesh were exposed in a 115-mm powder camera, using an iron target and manganese filter. In view of the water-solubility of the sodium salts present, it was found necessary to mount the specimens in Vaseline on a glass fibre; this method required rather long exposures and gave rise to an appreciable background scattering, but the patterns were sufficiently intense for identification. No attempt was made to make quantitative measurements, the phases present being identified by comparison with patterns of the individual compounds. The standard patterns of all the stable phases were checked where possible with those produced by Beeley and Protheroe,[7] and by Turkdogan and Maddocks.[4]

Analysis

All the slags were analysed in duplicate for ferric and ferrous oxide, silica, and phosphorus pentoxide. Sodium oxide was determined by difference and checked by calculation on the basis of the composition of the sodium salts identified. The compositions of the melts examined are given in Table I.

DISCUSSION OF EXPERIMENTAL RESULTS

The effects of variation in temperature and composition in a 4-component system cannot be portrayed by a 2- or 3-dimensional figure. The temperature variant can, however, be excluded by considering the system at some suitable temperature, e.g. 0° C, and projecting the liquidus surfaces on to this isothermal. The system may then take the form of a regular tetrahedron, bounded by four ternary systems and with the four components occupying the apices of the solid figure. Three of these ternary faces have been reported in whole or in part by previous investigations as follows:

Table I
COMPOSITIONS OF MELTS

Melt No.	Composition, mole %				
	FeO	Fe_2O_3	SiO_2	P_2O_5	Na_2O
1	66·21	0·33	33·46	...	...
2	57·10	1·92	32·11	2·19	6·68
3	53·91	2·59	30·35	3·28	9·87
4	51·49	2·94	29·50	3·97	12·10
5	50·91	2·49	28·76	4·46	13·37
6	49·45	2·41	28·09	5·01	15·04
7	49·05	2·21	26·91	5·48	16·35
8	44·01	3·09	24·61	6·78	21·51
9	38·04	2·82	22·87	9·04	27·23
10	32·99	2·02	18·44	11·64	34·91
11	21·58	5·34	16·59	13·99	42·50
12	22·73	3·92	15·86	14·34	43·15
13	14·31	3·86	12·14	17·41	52·26
14	8·11	3·61	7·85	20·10	60·33
15	5·56	2·35	4·04	22·02	66·03
16	...	...	...	25·00	75·00
17	66·21	0·33	33·46	...	...
18	50·95	2·33	34·50	2·15	10·07
19	36·32	2·92	35·08	4·67	21·01
20	26·47	2·68	35·20	6·42	29·23
21	30·36	2·62	34·94	5·88	26·20
22	24·86	2·25	35·38	6·65	30·86
23	18·86	1·81	35·21	8·04	36·08
24	11·45	2·04	35·18	9·40	41·93
25	...	...	35·14	11·82	53·04
26	30·96	2·89	29·58	7·74	28·83
27	23·54	1·30	47·40	2·65	25·11

The system Na_2O–P_2O_5–SiO_2 was examined by Turkdogan and Maddocks[4] for the region considered to be relevant to dephosphorization under soda slags. The existence of one stable ternary compound ($9Na_2O.\ 2P_2O_5.\ 6SiO_2$) and two ternary peritectic compounds was reported.

Carter and Ibrahim[8] studied the silica-rich portion of the system FeO–Na_2O–SiO_2 and found one stable ternary compound ($Na_2O.FeO.SiO_2$).

The immiscibility region in the system FeO–Na_2O–P_2O_5 was investigated by Oelsen and Wiemer[9]; their results indicate that this region is in the form of a semi-lemniscate, extending from the ferrous oxide corner of the system in the direction of sodium orthophosphate. Within this area the slags separated into an upper layer rich in sodium phosphate and a lower layer rich in ferrous oxide, the two layers being easily identified by a marked difference in colour. The reported limits of the region of immiscibility are possibly in error, since the investigators reported appreciable ferric oxide content in their slags and part of the system was investigated by adding fluoride to the slags to lower the melting points. No evidence of immiscibility has been reported in the binary sides of the system.

The fourth boundary face of the quaternary system has not been investigated, but a region of liquid immiscibility has been reported to exist between silica and phosphorus pentoxide,[10] and the probable limit of this region on the addition of sodium oxide has been indicated.[4]

Quaternary System FeO–Na_2O–SiO_2–P_2O_5

The data from the above investigations have been assembled into a projection figure of the surfaces of

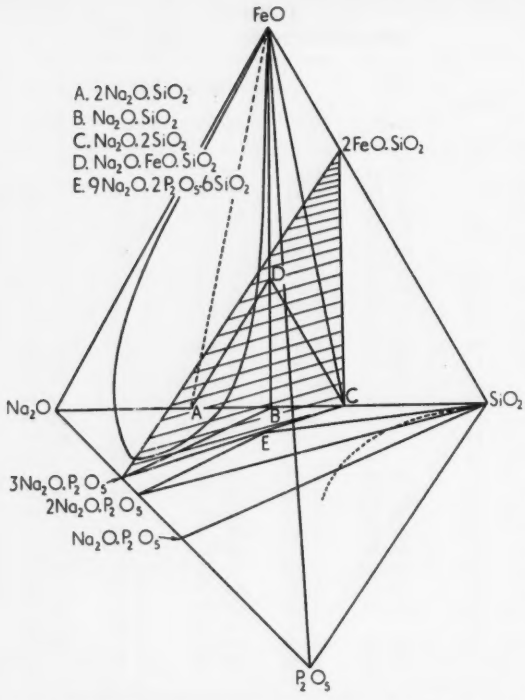

Fig. 3—Phase distribution of boundary faces of FeO–Na_2O–SiO_2–P_2O_5 quaternary system (plane investigated shown shaded)

the quaternary on which the quasi-binary systems and regions of liquid immiscibility are shown (Fig. 3).

The efficiency of soda slags for the removal of phosphorus and sulphur decreases rapidly below a basicity (bases/acids) of 1·0; this is attributed to the effect of silica in decreasing the activity coefficient of sodium oxide in the slag. The activity coefficient of ferrous oxide will likewise be decreased, which is detrimental to dephosphorization; at the same time this should facilitate desulphurization, but the effect of increasing acidity in decreasing γ Na_2O (or alternatively the oxygen ion concentration in the slag) may be expected to more than offset the advantages of decreasing γ FeO. It has been suggested[2] that only 14–15% of phosphorus may be removed at a basicity of 0·5. Examination of the data available at the time this research was begun suggested that the composition of a finishing slag with respect to sodium oxide, silica, and phosphorus pentoxide should lie in the area bounded by $3Na_2O.P_2O_5$–$2Na_2O.SiO_2$–$Na_2O.2SiO_2$. The ferrous oxide contents of these slags rarely exceeded 15%.

Reference to Fig. 3 shows the existence of quasi-binary systems $3Na_2O.P_2O_5$–$Na_2O.2SiO_2$ and 2FeO–SiO_2–$Na_2O.2SiO_2$. It was at once apparent that, if a quasi-binary system existed between $2FeO.SiO_2$ and $3Na_2O.P_2O_5$, a quasi-ternary system might exist bounded by these three systems; this area is shown shaded in the figure. If this proved to be the case, the volume lying to the right of this plane, i.e. richer in silica and phosphorus pentoxide, need not be examined from the point of view of soda slags.

$3Na_2O.P_2O_5$–$2FeO.SiO_2$ System

Thermal analysis was conducted on 16 compositions across this system, and the results, plotted in mole %, are shown in Fig. 4. Pure sodium orthophosphate crystallizes readily in the alpha form at 1585° C and undergoes an allotropic transformation to the beta form at 1474° C. A discontinuity occurs in the liquidus surface at approximately 56·0 mole % $3Na_2O.P_2O_5$. The experimental results indicate that this is due to the formation of a peritectic compound, the simplest molecular formula for which is $6Na_2O.2FeO.2P_2O_5.SiO_2$. The composition of this compound is FeO 18·18, SiO_2 9·09, Na_2O 54·55, P_2O_5 18·18, mole %. This compound melts and also decomposes at 1282° C thus:

$$6Na_2O.2FeO.2P_2O_5.SiO_2. = 2(3Na_2O.P_2O_5) + \text{Liquid}$$

Between 19·8 and 56·0 mole % sodium orthophosphate, the primary solidification is the peritectic compound, the last liquid solidifying by a eutectic separation of fayalite and this compound at 984° C. The liquidus falls very slowly beyond the peritectic point until very close to the eutectic, when the slope of the liquidus increases very rapidly.

Beyond the eutectic point, the liquidus rises smoothly to the melting point of fayalite at 1203° C. This temperature agrees closely with the figure of 1205° ± 2° C reported by Bowen and Schairer.[11]

Since peritectic-type reactions are very susceptible to undercooling, once the approximate composition limits and transformation temperatures had been ascertained, all melts which might be expected to intersect the peritectic horizontal were cooled at a rate of approximately 10° C/h in this temperature range to enable the reaction to be completed. It will also be noted that, for compositions lying just to the left of the peritectic discontinuity, a considerable proportion of the melt solidifies over a small temperature interval owing to the small slope of the liquidus. Here again it was found necessary to retard the rate of cooling to ensure that primary crystallization was

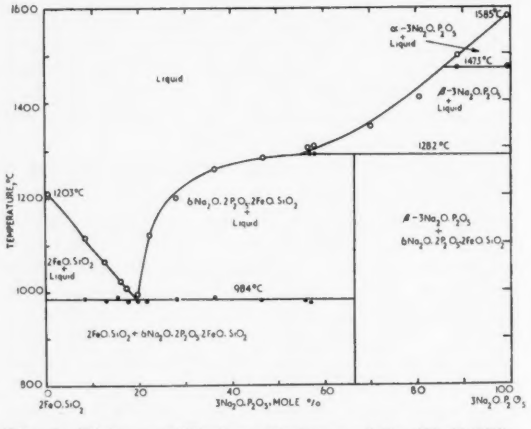

Fig. 4—Phase equilibrium diagram of the $2FeO.SiO_2$–$3Na_2O.P_2O_5$ quasi-binary system

complete. As the proportion of fayalite was increased beyond this stage, an overall rate of cooling of 0·5 to 1·0° C/min. gave satisfactory crystallization.

The $\alpha \rightarrow \beta$ transformation in the orthophosphate-rich melts was found to be sluggish, particularly on heating. It is interesting to note that this transformation in melt 15 (Fig. 4) occurred at approximately the same temperature as in the pure compound, suggesting very limited solid solubility of the terminal compound. No attempts were made to determine the limits of solid solubility in the system; the methods used are not considered sufficiently sensitive to determine such limits accurately. Such indications as were detected from thermal analysis and X-ray line shift pointed to the fact that solubility is probably very restricted.

When the work on this section was begun, it was realized that the immiscibility region studied by Oelsen and Wiemer would probably extend into the quaternary system in the shape of a semi-dome which might intersect the section. Consequently all melts were examined by fracture for indication of any separation, but in no case was any variation in colour apparent. The absence of immiscibility was confirmed by analysing chippings from the top and bottom of melts cooled rapidly from the liquid state. Thermal analysis melts, the compositions of which lay between the orthophosphate end of the system and the peritectic discontinuity, were found to have an appreciable ferric oxide content. This result would be expected if separation into two layers had occurred, one of which was rich in ferrous phosphate, since this compound oxidizes rapidly in air, particularly when ground to a fine powder.[12] The higher ferric oxide content reported here is believed to be due to the longer period that the slags were held at high temperatures in order to complete the peritectic reaction. The gain in weight of the platinum crucibles was insufficient to account for the resultant Fe^{3+}/Fe^{2+} ratio and it is felt that part of the change was due to oxidation within the furnace. In view of this high ferric oxide content, the arrest points on cooling are not necessarily correct. However, when melts of this composition were cooled rapidly from the liquid to below the peritectic temperature and allowed to crystallize, and the arrest points were determined by heating, the arrest temperatures recorded agreed reasonably closely with those obtained during cooling. This does not necessarily imply that the latter melts contained less ferric oxide, but if oxidation were time-dependent, the liquidus arrest on cooling and the peritectic arrest on heating were probably determined at lower ferric oxide content than those found in the melts after the completion of a thermal analysis run.

Support for the range of existence of the phase associations reported above was obtained by petrographic examination. Fayalite crystals were detected in all melts lying to the left of the reported peritectic compound but not beyond this point. Fayalite formed fairly well developed crystals with a faint green or yellow colour and often showed multi-twinning. The crystals were generally tabular, but in several instances a cleavage fragment typical of a (001) section through a barytes type crystal was seen, suggesting orthorhombic symmetry. Under crossed

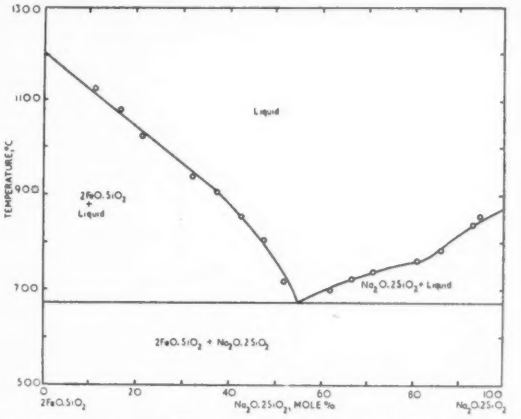

Fig. 5—Phase equilibrium diagram of the $2FeO.SiO_2$–$Na_2O.2SiO_2$ quasi-binary system[8]

nicols, bright interference colours of the second or third order were observed, giving pleochroic haloes in dome-shaped fragments. The refractive index determined by the immersion method was 1·87–1·89.

The high-temperature form of sodium orthophosphate was studied by soaking the compound in a platinum dish at 1550° C and then cooling rapidly by immersing the sides of the dish in a water bath. Crystal fragments were examined immediately after quenching, but the high-temperature form had not been entirely retained; some transformation to the β form had occurred round the grains and round what appeared to be strain cracks. The latter was suggested by the fact that beta deposition occurred in parallel bands crossing several grains. Fairly bright interference colours of the first order were obtained under crossed nicols and a non-straight extinction. This form has previously been reported to be isotropic,[4] but, after studying several melts prepared as described above, the authors are of the opinion that the structure is anisotropic.

The β form, produced by slow cooling in the furnace, was generally of small crystal size and of an irregular shape, so that no safe conclusions can be drawn regarding its crystal symmetry. The interference colours were dark greys of the first order, indicating anisotropy, and the refractive index was found to be between 1·53 and 1·54.

The peritectic compound occurred as colourless, isotropic fragments, which hydrated fairly rapidly on being stood in air. The refractive index was 1·513–1·524, which is less than the mean indices for either the hydrated or anhydrous forms of the orthophosphate.[7, 4]

$Na_2O.2SiO_2$–$2FeO.SiO_2$ System

This system[8] is reproduced in Fig. 5. It is reported to be a single eutectiferous system, the eutectic occurring at approximately 56 mole % $Na_2O.2SiO_2$ and at 675° C.

$Na_2O.2SiO_2$–$3Na_2O.P_2O_5$ System

A stable compound has been reported,[4] of composition $9Na_2O.2P_2O_5.6SiO_2$ melting at 1100° C and a

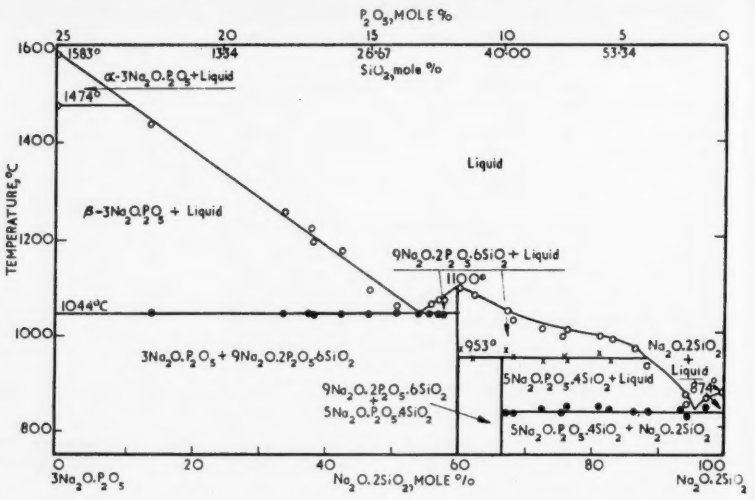

Fig. 6—Phase equilibrium diagram of the $3Na_2O.P_2O_5$–$Na_2O.2SiO_2$ quasi-binary system[4] (Fig. 17 of Ref. 4)

peritectic compound $5Na_2O.P_2O_5.4SiO_2$ which breaks down into the stable compound + liquid at temperatures in excess of 953° C. The complete system also contains two eutectics and is reproduced in Fig. 6.

$2FeO.SiO_2$–$9Na_2O.2P_2O_5.6SiO_2$ System

Examination of these three binary systems shows that, apart from the terminal compounds, only one stable binary compound is present. If it is assumed that no stable ternary compounds occur within the enclosed system, there is a high probability that a 2-phase region would exist between the binary compound and the diametrically opposite terminal compound of the ternary system, i.e. fayalite. Thermal analysis studies of mixtures of these compounds suggested that a quasi-binary system was formed of simple eutectiferous type and is shown, plotted on a mole % basis, in Fig. 7. Both liquidus lines have a small slope near the binary sides, but the slope increases rapidly in the vicinity of the eutectic point, which occurred at 55·5 mole % $9Na_2O.2P_2O_5.6SiO_2$ and at 1012° C. Melts in this series required slow cooling rates to ensure complete crystallization. Cooling rates of the order of 0·3–0·5° C were adopted for all melts, the rate decreasing with decreasing fayalite content.

Petrographic examination showed that the sodium compound hydrated very readily in air. The grains were small and of irregular shape, so that the habit could not be deduced, but the sections examined appeared to be isotropic, indicating cubic symmetry. Crystals of the pure compound were colourless in transmitted light, but in the presence of fayalite the thicker fragments frequently exhibited a pale green colour. This was probably due to a thin film of fayalite which formed round the grains during the eutectic reaction. The refractive index was between 1·513 and 1·524.

Ternary System $3Na_2O.P_2O_5$–$Na_2O.2SiO_2$–$2FeO.SiO_2$

On the basis of the data quoted for the foregoing quasi-binary systems (summarized in Table II), an attempt has been made to define the fields of existence of the liquidus surfaces in this system. The ternary diagram may be divided into two parts, meeting in the quasi-binary system $2FeO.SiO_2$–$9Na_2O.2P_2O_5.6SiO_2$. Within either of these regions, alternative constructions are possible:

(i) One or more stable ternary compounds may be formed
(ii) A ternary peritectic point could result from the intersection of two liquidus discontinuities, one originating from a binary peritectic reaction and the other from a eutectic gutter.

To determine which of the two constructions was applicable, two melts were prepared of compositions corresponding roughly to the centre of each region and slowly cooled. X-ray patterns were obtained, and compared with the standard patterns of the appropriate boundary compounds, and no extra lines were found. It was therefore assumed that no ternary compounds exist in the system. On this basis a probable form of the diagram based on hypothesis (ii) above has been constructed and is shown in Fig. 8. The initial phases separating on each of the liquidus surfaces are indicated.

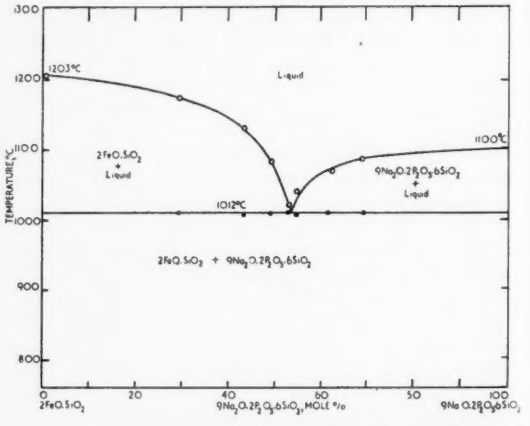

Fig. 7—Phase equilibrium diagram of the $2FeO.SiO_2$–$9Na_2O.2P_2O_5.6SiO_2$ quasi-binary system

Table II

THE TERNARY SYSTEM $2FeO.SiO_2$–$3Na_2O.P_2O_5$–$Na_2O.2SiO_2$

Type	Phases	Temp., °C	Composition, mole % FeO	Na_2O	P_2O_5	SiO_2
	$2FeO.SiO_2$–$3Na_2O.P_2O_5$ Quasi-binary System					
Melting	α–$3Na_2O.P_2O_5$, liquid	1583	0·00	75·00	25·00	0·00
Inversion	α–$3Na_2O.P_2O_5$, β–$3Na_2O.P_2O_5$, liquid	1474	0·00	75·00	25·00	0·00
Peritectic	β–$3Na_2O.P_2O_5$ = $6Na_2O.2P_2O_5.2FeO.SiO_2$, liquid	1282	29·33	42·00	14·00	14·67
Eutectic	$6Na_2O.2P_2O_5.2FeO.SiO_2$, $2FeO.SiO_2$, liquid	984	53·47	14·85	4·95	26·73
Melting	$2FeO.SiO_2$, liquid	1203	66·67	0·00	0·00	33·33
	$2FeO.SiO_2$–$9Na_2O.2P_2O_5.6SiO_2$ Quasi-binary System					
Melting	$9Na_2O.2P_2O_5.6SiO_2$, liquid	1100	0·00	53·04	11·82	35·14
Eutectic	$9Na_2O.2P_2O_5.6SiO_2$, $2FeO.SiO_2$, liquid	1012	29·67	29·44	6·56	34·33
Melting	$2FeO.SiO_2$, liquid	1203	66·67	0·00	0·00	33·33
	$3Na_2O.P_2O_5$–$Na_2O.2SiO_2$ Quasi-binary System[4]					
Melting	α–$3Na_2O.P_2O_5$, liquid	1583	0·00	75·00	25·00	0·00
Inversion	α–$3Na_2O.P_2O_5$, β–$3Na_2O.P_2O_5$, liquid	1474	0·00	75·00	25·00	0·00
Eutectic	β–$3Na_2O.P_2O_5$, $9Na_2O.2P_2O_5.6SiO_2$, liquid	1044	0·00	55·30	13·25	31·45
Melting	$9Na_2O.2P_2O_5.6SiO_2$, liquid	1100	0·00	53·04	11·82	35·14
Peritectic	$9Na_2O.2P_2O_5.6SiO_2$ = $5Na_2O.P_2O_5.4SiO_2$, liquid	953	0·00	39·74	3·85	56·41
Eutectic	$5Na_2O.P_2O_5.4SiO_2$, $Na_2O.2SiO_2$, liquid	838	0·00	35·57	1·37	63·06
Melting	$Na_2O.2SiO_2$, liquid	874	0·00	33·33	0·00	66·67
	$2FeO.SiO_2$–$Na_2O.2SiO_2$ Quasi-binary System[5]					
Melting	$2FeO.SiO_2$, liquid	1203	66·67	0·00	0·00	33·33
Eutectic	$2FeO.SiO_2$, $Na_2O.2SiO_2$, liquid	675	29·33	18·67	0·00	52·00
Melting	$Na_2O.2SiO_2$, liquid	874	0·00	33·33	0·00	66·67

According to this construction, the liquidus discontinuity caused by the formation of the binary peritectic compound $6Na_2O.2FeO.2P_2O_5.SiO_2$ intersects the liquidus gutter from the eutectic on the sodium disilicate binary side in a ternary peritectic point. A liquidus gutter falls from this point to intersect eutectic gutters falling from the quasi-binary sides in a ternary eutectic. Two 4-phase planes exist in this part of the system, one at the temperature of the ternary eutectic point and the other at the ternary eutectic temperature. The former is bounded by the compounds $6Na_2O.2FeO.2P_2O_5.SiO_2$–$3Na_2O.P_2O_5$–$9Na_2O.2P_2O_5.6SiO_2$ and the ternary peritectic point, and the latter by $6Na_2O$.

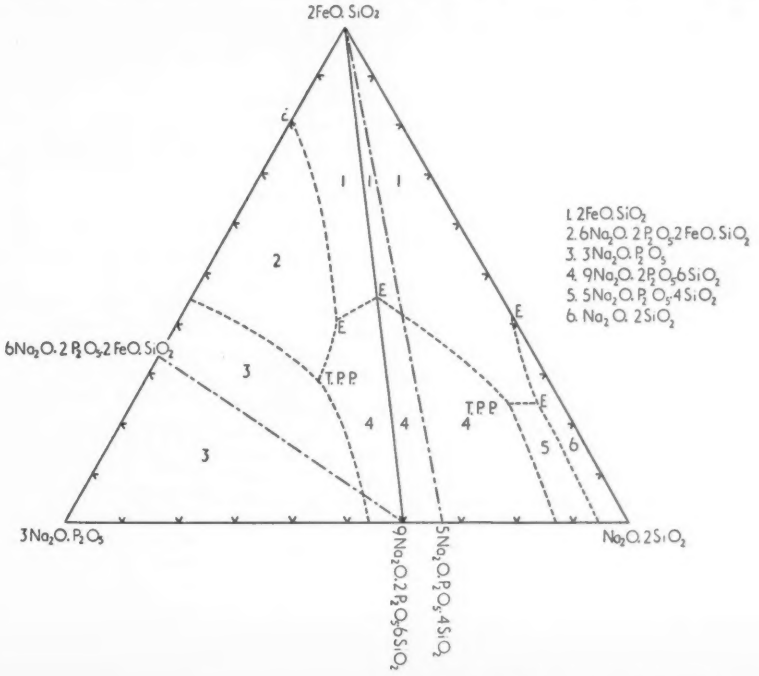

Fig. 8—Phase equilibrium diagram of the $2FeO.SiO_2$–$3Na_2O.P_2O_5$–$Na_2O.2SiO_2$ ternary system

$2FeO.2P_2O_5.SiO_2$–$2FeO.SiO_2$–$9Na_2O.2P_2O_5.6SiO_2$, assuming negligible solid solubility within the system. From this construction the range of existence of sodium orthophosphate for equilibrium conditions at room temperature is limited by the 2-phase join $6Na_2O.2FeO.2P_2O_5.SiO_2$–$9Na_2O.2P_2O_5.6SiO_2$, but, with rates of cooling too rapid for completion of the peritectic reaction, sodium orthophosphate may be present in all slags whose composition lies within the limits of the ternary peritectic 4-phase plane.

A similar construction has been assumed for the sodium disilicate side of the system, with 4-phase planes bounded by $9Na_2O.2P_2O_5.6SiO_2$–$2FeO.SiO_2$–$5Na_2O.P_2O_5.4SiO_2$ and the ternary peritectic point, and by $Na_2O.2SiO_2$–$2FeO.SiO_2$–$9Na_2O.2P_2O_5.6SiO_2$. The room-temperature range of existence of $9Na_2O.2P_2O_5.6SiO_2$ is limited by the 2-phase join $2FeO.SiO_2$–$5Na_2O.P_2O_5.4SiO_2$ in equilibrium, but may occur for any composition within the area covered by the former 4-phase plane with more rapid cooling.

A notable feature of this ternary system is the comparatively low melting points found. Whilst the temperatures of the two ternary eutectic planes have not been closely determined, they are believed not to exceed 800° C.

Acknowledgments

The authors wish to acknowledge the help given to them by Dr. W. B. Rotsey, in conducting some of the experiments. They are also grateful for the many helpful discussions which they have held with their colleagues at Sheffield and in particular with Professor J. White.

One of the authors (C.B.) appreciates the financial assistance given to him in the form of a Goodwin Fellowship by the Cutlers Company in Hallamshire.

References

1. W. R. Maddocks and E. T. Turkdogan: *J. Iron Steel Inst.*, 1949, vol. 162, pp. 249–264.
2. W. R. Maddocks and E. T. Turkdogan: *Ibid.*, 1952, vol. 171, pp. 128–141.
3. W. B. Rotsey: Private communication.
4. E. T. Turkdogan and W. R. Maddocks: *J. Iron Steel Inst.*, 1952, vol. 172, pp. 1–15.
5. P. T. Carter: *Ibid.*, 1950, vol. 166, pp. 321–322.
6. A. N. Winchell: Synthetic Minerals under the Microscope, New York.
7. P. R. Beeley and H. T. Protheroe: *J. Iron Steel Inst.*, 1951, vol. 167, pp. 141–157.
8. P. T. Carter and M. Ibrahim: *Transactions of the Society of Glass Technology*, 1952, vol. 36, pp. 142–163.
9. W. Oelsen and H. Wiemer: *Mitt. Kaiser Wilhelm Inst. Eisenforsch.*, 1942, vol. 24, pp. 167–210.
10. R. L. Barrett and W. J. McCaughey: *American Mineralogist*, 1942, vol. 27, pp. 680–695.
11. N. L. Bowen and J. F. Schairer: *Amer. J. Sci.*, 1932, vol. 24, pp. 177–213.
12. J. W. Mellor: "A Comprehensive Treatise of Inorganic and Theoretical Chemistry," vol. 14, p. 393: 1935, London, Longmans, Green.

Laboratory Production of Cylindrical Alumina Crucibles of $5\frac{1}{2}$ Litres Capacity

By

Vaughan H. Stott, D.Sc., F.I.Ceram.

SYNOPSIS

A description, with adequate detail for non-specialists, is given of a method of forming cylindrical alumina crucibles of $5\frac{1}{2}$ l. capacity and of a convenient gas-furnace for firing them. 1345

CYLINDRICAL CRUCIBLES having an internal diameter of 6 in. ($15\frac{1}{4}$ cm), an external diameter of 7 in. ($17\frac{3}{4}$ cm), an internal height of 12 in. ($30\frac{1}{2}$ cm), and a thickness at the bottom of $\frac{13}{16}$ in. (2 cm), are in use at the National Physical Laboratory for the melting of iron and ferrous alloys in a controlled atmosphere by means of induced electric currents of high frequency. Such crucibles are rather large for production in the laboratory, and it is thought that the relatively simple procedure which has been found to be effective warrants description.

PREPARATION OF MIXTURE

The crucibles are formed by tamping a mixture of two parts by weight of crushed fused alumina which has passed through a sieve having 90 meshes/in., and one part by weight of finely ground calcined alumina. This mixture is made slightly damp by the addition of water containing about 4% of ammonium alginate. In this mixture the fused alumina, graded as stated, is a commercial product. The calcined alumina is also a commercial product in the unground state. It is ground wet for 5 h in a laboratory edge-runner mill of which the original muller and bowl have been replaced by a muller and bowl made of aluminium. At first this method of grinding scores the muller and bowl, and the abraded aluminium reacts with the water and produces aluminium hydroxide. After much use, the metal parts are greatly hardened by embedded alumina and by cold work, and the proportion of aluminium hydroxide produced becomes small. To make the tamping mixture, the ground product is dried and the resulting cake is lightly ground in a Wedgewood mortar and passed through a sieve having 20 meshes/in. The material is then mixed with the fused alumina in a rotating stoneware jar driven by two supporting horizontal steel rollers wrapped with rope. The speed of longitudinal mixing is greatly increased by the insertion of a wooden rod of such length as to

Manuscript received 20th July, 1956.
Dr. Stott is with the National Physical Laboratory.

rest diagonally in the jar. The speed of rotation of the jar is that which produces the normal cascading action of a ball mill. When mixing is complete, the rod is removed and the solution of ammonium alginate is added. Rotation of the jar now converts the material into balls, the mean diameter of which is larger, with a greater proportion of liquid to solid, and a greater viscosity of the solution of ammonium alginate. After a little practice, a glance at these balls tells the operator whether the mixture is suitable for tamping. It is usual to start with too little liquid, and gradually to add more until the balls have a mean diameter of about 1 in. The mixture, after being rubbed through a sieve having 4 meshes/in., is ready for use.

FORMING THE CRUCIBLES

A section through the axis of the mould for tamping is shown in Fig. 1. The main metal parts are made from an alloy of 96 parts by weight of aluminium and 4 parts of copper. Contamination of the inner wall of the crucible by abrasion of this alloy is harmless because copper oxide volatilizes at the usual firing temperatures. The core *C* is a sliding fit in the block *B*, round which is a three-part sleeve *S*, the divisions being longitudinal. The three parts are held together by steel bands which can be tightened or loosened by worm-drives. The core is fixed to the square plate *P* by a steel screw working in a flanged steel sleeve riveted to the core. The crucible is formed upside down as indicated in Fig. 1. The circular plate *R*, shown at the top of the figure, is not in use at this stage. When assembling the apparatus, the inner surface of the block *B* must be coated with a film of tallow applied with a rag. This greatly reduces the risk of trouble which may arise from the entry of alumina between the core and the block during the withdrawal of the untapered

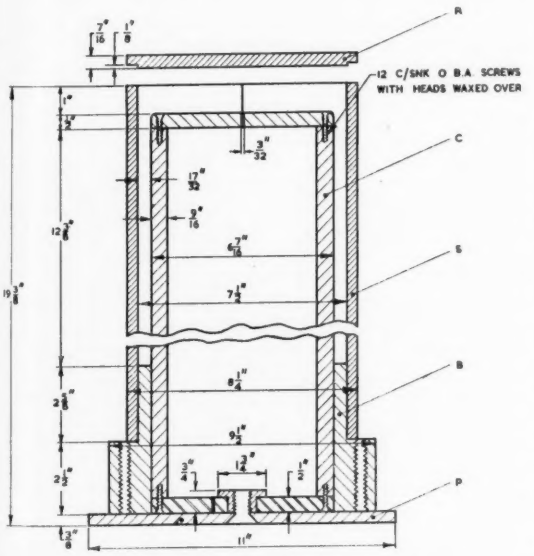

Fig. 1—Crucible mould: axial section

core. In connection with arrangements for twisting the core before its withdrawal, there is a correct range of angular positions of the core with respect to the block *B*. It is desirable to place a paper annulus on that part of the block *B* which is between the core and the sleeve *S*, in order to prevent adherence of the crucible to the block. It is also necessary to insert a paper liner to prevent the crucible from sticking to the sleeve *S*. Single-sided varnished paper 0·006 in. thick is used with the varnish on the inside. Before use it is re-rolled so that the varnished surface is on the outside, and it is then left in a warm place until the next day. When placed in the sleeve *S* with the varnished surface on the inside and an overlap of about an inch, there is little difficulty in adjusting it with the aid of a rod so that it fits snugly the inside of the sleeve. The paper should be cut so that it projects an inch or more above the top of the sleeve. To facilitate even feeding of the alumina round the circumference of the crucible, a finned aluminium cone is fixed centrally on the top of the core by means of a pin, attached to the bottom of the cone, which enters the air vent in the core. This cone may be made by creasing a circular sheet of aluminium 13 in. in diameter, a small hole being first made in the centre; otherwise, the operation would not be possible for a sheet of finite thickness. Twelve fins, measuring 1 in. from the inside to the outside, are convenient, the fins being squeezed tighter until the diameter of the bottom of the cone is correct. After the sheet has been creased, the central hole becomes the top of the slightly truncated cone and is closed with a cork. The material is fed on to this cone with a scoop, alternate scoopfuls being a right angle apart in the horizontal plane because, although it is easy to pour centrally with respect to possible displacements to the right or to the left, it is difficult to judge what is happening in front and behind. Reasonably accurate feeding is necessary because the tamping tool affects a large area at a stroke. The tool consists of a brass tube 16 in. long, of outside diameter $7\frac{1}{4}$ in., and of wall thickness $\frac{3}{64}$ in. At the top, two handles, each consisting of a brass tube 3 in. long and of 1 in. external diameter, are inserted a short distance through holes in the main tube, and fixed to it by soldering, flanges being attached to produce a strong joint. At the bottom end of the main tube, vertical saw-cuts are made $\frac{3}{4}$ in. high, dividing the bottom of the tube into six parts. Horizontal cuts are made $\frac{3}{4}$ in. above the bottom edge so as to cut out three alternate sections, and leave three sections projecting downwards. In the latter sections, vertical saw-cuts $\frac{3}{4}$ in. high and $\frac{3}{4}$ in. apart are made. The three projecting parts are then bent inwards so that the bottom edges move about $\frac{1}{8}$ in. towards the centre of the tamping tool, and the saw-cuts are filled with solder. When using the tamping tool the three turned-in parts produce an effective wedging action and there is no danger of tearing the paper inside the sleeve *S*. During tamping, the tool must be rotated at regular intervals in such a way that the whole circumference of the wall is well tamped. The removal of sections from the bottom of the tamping tool is not essential, but it has been found that the effects of slightly uneven feeding

of the alumina mixture may be practically eliminated by this practice combined with a measure of acquired skill. It is of great importance that only small quantities of material should be added at a time, for otherwise, uneven density may result from 'bridging'. When tamping approaches the level of the horizontal part of the core, a small piece of paper is placed over the air vent and tamping is continued with an ordinary tool until the material projects a trifle above the end of the sleeve *S*. The projecting part of the paper liner is now cut away with a razor blade and the material is smoothed off at the level of the sleeve. The circular plate *R*, of aluminium alloy, is now laid on the tamped material and is tapped into position, the lower projecting part being an easy fit in the paper-lined sleeve. No difficulty is experienced in thus compressing the tamped material another $\frac{1}{8}$ in. for this purpose. The next operation is to invert the whole apparatus in order to permit the extraction of the core; for this purpose the apparatus is first placed on a support somewhat smaller than the square plate *P*. The plate *P* has a clearance hole near each corner through which four long rods can be passed, these rods acting as the legs of a table, and the table top being a plate of aluminium alloy similar to the plate *P*. The two plates are clamped together by screwing nuts on the rods below the plate *P*. The rods do not extend above the top plate; they are screwed into this plate so that they are flush with the upper surface and are locked by nuts beneath the plate. When the apparatus has been inverted, so that the crucible is the right side up, this temporary clamping arrangement is dismantled, and the main apparatus, with the plate *R* at the bottom, rests on what was the upper clamping plate. The plate *P* is now removed, being released by removal of the central screw.

Before extracting the core, it is desirable to twist it with respect to the sleeve. For this purpose a piece of channel steel is fixed diametrically on the core by means of two bolts which screw into the top plate of the core. Two blocks of metal are bolted to diametrically opposite parts of the piece *B*, and these blocks carry bolts which can be screwed so as to press on the piece of channel steel and thus rotate the core through a small angle. It is because of the need for this small rotation, which reduces the friction between the core and the formed crucible, that at an earlier stage the core must be set in a suitable angular position with respect to the block *B*. The core, having been slightly rotated, must next be withdrawn; to do this, the twisting-gear is removed and a circular steel plate $\frac{9}{32}$ in. thick with three tubular legs of $\frac{3}{4}$ in. external diameter, of 0·07 in. wall thickness, and $19\frac{1}{4}$ in. long, is placed with its legs resting on the block *B*. Each end of a leg is threaded and a bolt secures the top to the steel plate. A bolt screwed in the lower end has its head turned to a radius in order to produce an approximate point contact with the block *B*. A steel boss fixed to the centre of the plate is drilled and provided with a $\frac{5}{8}$-in. Whitworth thread through which is screwed a steel rod 21 in. long. The bottom end of this rod is screwed into the core, which can then be extracted by rotating a nut above the steel plate with a ratchet-spanner while the legs of the plate are held firmly by a second person. The air vents at each end of the core prevent the bottom of the crucible from being damaged by the considerable suction produced on raising the core. Vents are not usually necessary in the case of a tapered core.

After removal of the core, the block *B* must be removed from the split sleeve *S*. The bands clamping the sleeve are slightly slackened, the upper band somewhat more than the lower one, and the block is lifted slightly by means of a screwdriver which can be inserted in three places where a little metal has been removed from the sleeve for this purpose. The extra slackness of the upper clamp, as compared with the lower one, permits the removal of the block by hand after the first small movement with the screwdriver. The clamps are next taken from the sleeve, the three parts of which are then separated from the crucible. It is at this stage that the value of the plate *R* becomes apparent, for, whilst it is just possible to make a crucible without it, there is in such a case a great danger of damaging the crucible with an edge of one of the parts of the sleeve. The paper annulus on the top of the crucible and the paper round the crucible may now be removed, the paper being bent backwards and peeled off tangentially. After drying in a warm place, the crucible is strong enough to be lifted by the hands, which should be placed round the crucible at the bottom.

FIRING

Firing is normally carried out in a recuperative natural-draught gas-furnace,* the linear shrinkage after firing at 1700° C for 4 h being one-fifteenth. A much cheaper and smaller furnace may be used for firing to 1625° C, a temperature quite sufficient for most purposes for which the crucibles are likely to be used. The burner used with this furnace is of the 'injector' type† and uses air at 75 lb/in². The air jet has a diameter of $\frac{11}{64}$ in. as compared with $\frac{1}{4}$ in. for the standard burner. The smaller jet is used for convenience in control, because the larger jet would permit the furnace to reach its normal maximum temperature at a relatively low pressure of air. The maximum gas consumption of the burner, using the smaller air jet, is about 600 ft³/h. For the construction of the furnace, alumina refractories were made and were fired to 1800° C in another furnace‡ lined with equally high-fired refractories. This system would appear to have no beginning, but it is feasible to line the first furnace needed with a cement consisting of four parts of fused alumina to pass through a sieve having 90 meshes/in., one part of finely-ground calcined alumina, and water as needed. The furnace should be fired slowly the first time to, say, 1700° C. After cooling, the shrinkage cracks in the alumina cement should be patched, and the furnace may then be fired to 1800° C, further patching being necessary on cooling. After this quite a long life may be expected from such a furnace provided that cracks in the lining are regularly patched. The

* V. H. STOTT: *Bulletin of the British Refractories Research Association*, 1941, No. 60, p. 1.

† V. H. STOTT: *Trans Ceram. Soc.*, 1938, vol. 37, p. 353.

‡ V. H. STOTT: *Trans. Brit. Ceram. Soc.*, 1940, vol. 39, p. 1.

advantage of using a lining of alumina bricks is that this tends to distribute the cracks so that no single crack is as wide as one which may form in a monolithic lining. However, the difference in reliability between the two methods of construction is not great for furnaces of the size under consideration. Returning to the description of the furnace for firing crucibles, this furnace is of the type in which the hearth is heated directly from below. Figure 2 shows a horizontal section of the furnace just above the third course. The flame from the burner impinges on the alumina pillars which support the hearth, passes up the flue at the back, and enters the rectangular furnace chamber which is 16 in. high. The flame leaves through an opening $1\frac{1}{2}$ in. square at the top of the chamber and at the middle of the front. The pillars supporting the hearth are cylindrical, 1 in. high and 1 in. in diameter, and are made of four parts fused alumina passing through a sieve having 90 meshes/in., and one part of finely-ground calcined alumina; they are fired for 1 h at 1800° C. All pure alumina ware used in the furnace has the same composition and firing treatment. The pillars stand on commercial bricks, 9 in. × $4\frac{1}{2}$ in. × 3 in., containing 90% of alumina. These bricks form a rectangle $13\frac{1}{2}$ in. × $22\frac{1}{2}$ in., and round this rectangle, in the same course, the bricks are of sillimanite. The course below, which is the first, consists of insulating bricks. The dimensions of the inside of the furnace in plan are 8 in. × 15 in. The first of the two courses forming the hearth consists of alumina tiles 4 in. × 2 in. × $\frac{1}{2}$ in., laid as stretchers as shown dotted in Fig. 2. The second course consists mainly of similar tiles laid as headers in such a way as to break the joints. Some smaller tiles are necessary to complete the upper course of the hearth. The opening surrounding the nozzle of the burner is 2 in. square, and, $7\frac{1}{2}$ in. from the front of the furnace, the passage splays out horizontally and the roof slopes downwards so as to fit the gap of 1 in. which is the height of the pillars supporting the hearth. This arrangement entails the production of special alumina bricks, but their shapes are quite simple. The furnace chamber is lined to the top with 70% alumina bricks round which are sillimanite bricks with insulating bricks on the outside. The roof consists of unmortared bricks which are laid after charging the furnace, and removed in order to empty the furnace. Stretchers containing 70% alumina cover the chamber to within $1\frac{1}{2}$ in. of the front, where an opening $1\frac{1}{2}$ in. square is left for the exhaust gases, cut bricks being used on each side of the opening. The 70% alumina bricks are surrounded by sillimanite bricks, and these by insulating bricks. The next course contains sillimanite bricks immediately above the furnace chamber and the last course contains only insulating bricks. The joints in the brickwork are broken by small displacements backwards and sideways, and the exhaust gases have an unimpeded exit in a vertical direction. The brickwork immediately in front of the flue is arranged so that an optical pyrometer may be sighted from a suitable distance at an angle of rather less than 45° to the horizontal. It is convenient for the furnace to be built on a low steel structure provided with small wheels. For tying the brickwork a 2 in. × $\frac{1}{4}$ in. angle-iron pillar is fixed to each corner. In each pillar two horizontal slots, one near the top and one near the bottom, are cut a short distance into the angle, and each slot carries a horizontal rectangle of steel plate $2\frac{1}{2}$ in. × 1 in. × $\frac{3}{8}$ in. which projects equally on either side of the slot at an angle of 45° to a side of the furnace. These plates are pulled together by means of steel rods $\frac{1}{4}$ in. in diameter by means of adjustable couplings with right-handed and left-handed threads, and swivelling connections are used between the rods and the rectangular plates. The rods, couplings, and swivels are standard parts stocked by garages. The couplings are not normally adjusted during the running of the furnace, but may need occasional tightening.

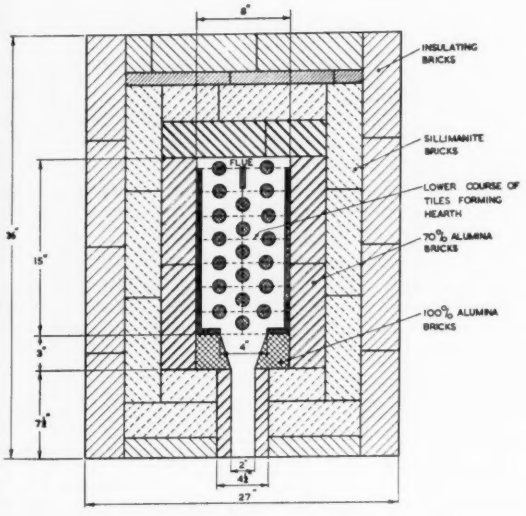

Fig. 2—Gas furnace: section just above third course

The furnace holds two crucibles bedded on coarse fused alumina powder. It is lighted in the morning, and the maximum temperature is reached and held for the required time the next day, no adjustments being made during the night. The temperature is not normally allowed to exceed 1625° C because too high a temperature above the hearth, combined with a still higher temperature below, involves a risk of distortion of the hearth in spite of the closeness of the supports. During the early stages of firing, heat does not penetrate the hearth quickly, and the flame is cooled and extinguished by the time it reaches the flue at the back. This protects the ware from the risk of cracking, but a large well-ventilated room is necessary.

Acknowledgments

The apparatus described was developed in connection with the programme of research of the National Physical Laboratory, and this paper is published by permission of the Director of the Laboratory.

The author acknowledges the valuable co-operation and suggestions of Mr. A. A. Hatcher.

Sinter-plant Assessment Trials at Margam

By C. Lang

and H. Bates

STEEL COMPANY OF WALES, LTD.

SYNOPSIS

A sinter-plant assessment trial has been carried out at the Margam Works of the Steel Company of Wales Ltd. Particular attention has been given to the measurement of air volumes at the fan. The leakage volume between the strand and the fan has been measured and amounts to approximately 40% of the total fan air at the normal sintering suctions. The average sintering air requirement per ton of raw mix, after correction for the plant leakages and for cooling air, was estimated at 28,400 ft³ (S.T.P.). A brief assessment of the straight-line coolers was also made. 1377

THE ASSESSMENT TRIAL carried out at Margam sinter plant of the Steel Company of Wales was a continuation of the policy of assessing sinter-plant performance to provide a basis for increasing the output of existing plant and for the design of new equipment. The techniques used throughout the trial were based as far as conditions allowed on the work done in previous assessments* and results should therefore be comparable between the Margam plant, which was of German design and construction, and those obtained on Dwight-Lloyd machines of British design.

The trial lasted ten consecutive working days, during which time normal assessments were made, the final dustcatcher was calibrated to give the fan airflows, and the leakage of air into the plant was measured. When possible, assessments were made over periods of 2 or 3 h, the major variables measured being airflow, fan inlet temperature and suction, strand suction, and input of raw material. The running of the plant was left in the hands of the plant operator, any variation in mix composition, etc. being made by him.

Throughout the trials the team enjoyed the fullest co-operation from the Sinter Plant Management and the staff of the Margam Fuel Department, and also the use of equipment from the Fuel Department.

DESCRIPTION OF PLANT

The sinter plant at Margam consists of two Dwight-Lloyd sintering machines. The plant was built by the Lurgi Gesellschaft für Chemie und Hüttenwesen m.b.H. and came into commission in 1954—No. 1 strand in June and No. 2 strand in November. Each machine is 8 ft 3 in. wide with an effective length of 117 ft, giving a grate area of 968 ft². There are 19 windboxes, the first and last being half the length of the remainder. The plant flow sheet is shown in Fig. 1 and a diagrammatic side elevation in Fig. 2.

Sinter Materials

The ores, previously screened to $-\frac{3}{8}$ in., are delivered to a 50,000-ton fine-ore stockyard. The ores are stockpiled under cover in four groups: soft, Swedish, siliceous, and concentrates. Recovery from the stockyard is by means of an overhead crane with a 9-ton ore-capacity grab. There are 12 bunkers in line, each of 1000 tons capacity, all feeding on to one large conveyor belt. A small-capacity bunker to which the dustleg fines and spillage are returned also feeds on to the ore-gathering belt. Feed rates are set by a movable-belt weigher and are controlled by adjustable ploughs and skirts on the feeder tables.

The total feed rate of materials on this belt is continuously measured by a cradle-type belt weigher.

Coke and flue dust enter the plant by a separate system. Coke is screened at $\frac{1}{2}$ in., the oversize not being used at present in the sinter plant; the undersize is rescreened at $\frac{1}{8}$ in. The $-\frac{1}{2}+\frac{1}{8}$ in. fraction is crushed in a double-roll crusher, mixed with the $-\frac{1}{8}$-in. screened fraction, and conveyed to two 130-ton capacity bunkers. Flue dust is held in three 1000-ton capacity bunkers.

The return fines $-\frac{3}{8}$ in. are discharged from the screens into a 340-ton capacity bunker, one for each machine. Similarly, the hearth layer of $+\frac{5}{8}$–1-in. sinter is discharged into 250-ton capacity bunkers.

The return-fines feed rate is measured by a cradle-type belt weigher, and flue dust and coke are added, the coke being discharged on to the main belt by Schenck constant-weight feeders fitted two to each bunker. The feed rate of return fines plus flue dust plus coke is measured on a further cradle-type weigher before these materials join the main ore stream.

Mixing and Feeding

Mixing is carried out in two stages. A primary mixer of the tapered-drum type, 25 ft long × 10–15 ft dia., is installed at ground level and takes the combined feed. Water is normally added in this mixer automatically but during the period of investigation, owing to a faulty valve, the mixer was operated dry. The mix falls on to an uprising conveyor and is transported to the top of the sinter building where it is discharged by conveyor and chutes alternately into the two machine surge hoppers. The discharge to the surge hoppers can be controlled automatically or manually. A vibrating screen situated over the surge hoppers removed any oversize material, which is then allowed to fall on top of the sinter cake on the strand. The undersize falls into the surge hoppers,

*E. W. Voice *et al.*, *J. Iron Steel Inst.*, 1953, vol. 175, pp. 97–152; R. F. Jennings *et al.*, *ibid.*, pp. 267–277.

Paper IM/S/23/56 of the Sinter Committee of the Ironmaking Division of the British Iron and Steel Research Association, received on 5th November, 1956. The views expressed are the authors' and are not necessarily endorsed by the Committee as a body.

Mr. Bates is on the staff of the Association's Ironmaking Division at the North East Coast Laboratories; Mr. Lang, who was formerly with the Division, is now with the U.K. Atomic Energy Authority.

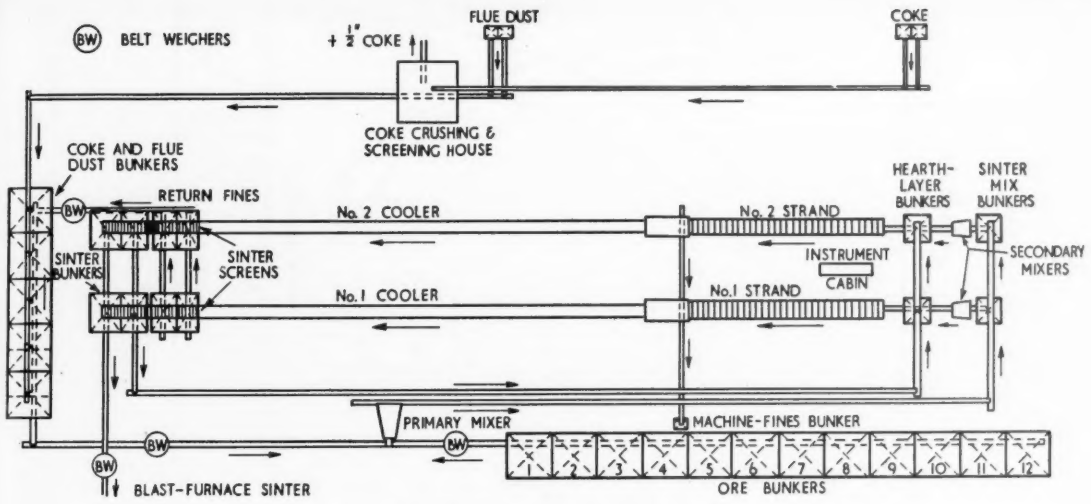

Fig. 1—Flow diagram of Margam sinter plant

which are of 100 tons capacity. The mix from these hoppers passes by a roll feeder to the secondary mixers.

The secondary mixers are of the drum type, 17 ft long by 7 ft dia., with an internal rotating paddle. Water is added at the feed end of the mixer through a spray pipe. The wet mix is then taken by conveyor to a small-capacity bunker situated above the strand roll feeder. Machine No. 2 differs from No. 1 in that the conveyor is arranged to swing from side to side to improve distribution in the bunker. The hearth-layer sinter is elevated on a separate conveying system to two surge hoppers.

Sinter Machines

The raw sinter mix is fed from the small holding bunkers, by a 4 ft 3 in. dia. roll feeder, on to a slightly inclined back plate against which it settles at its angle of repose . Situated ahead of the roll feeder is the hearth-layer surge bin which feeds the hearth layer directly on to the grate bars. The depth of the hearth layer is controlled by a cut-off plate. A small-diameter roll, immediately ahead of this position, presses any displaced grate bars back into position, so giving a flat grate surface. The maximum bed height including hearth layer is $12\frac{3}{4}$ in., but during the trials the total bed height was 11 in. including a hearth layer of $1\frac{1}{2}$ in. The ignition hoods are of the normal semicircular-hood type, 4 ft 3 in. long by 8 ft 3 in. wide, supplied with blast-furnace gas enriched with 6% coke-oven gas.

Each strand is made up of 92 pallets, 8 ft 3 in. wide and 3 ft $3\frac{3}{8}$ in. long. Each pallet is fitted with four pairs of rollers. The outer rollers are used for carrying the pallet back on the return journey and also carry part of the weight of the pallet during sintering. The inner rollers engage on the head and discharge wheels of the machine. During sintering the pallets slide on a fixed track on each side of the windboxes. This track is made up of replaceable steel strips, and the joint with the pallets is made air-tight by a cushion of grease which is fed continuously to the whole sliding surface from four automatic grease presses. Grease consumption is 3·55 oz per ton of sinter. The track is relieved of part of the weight

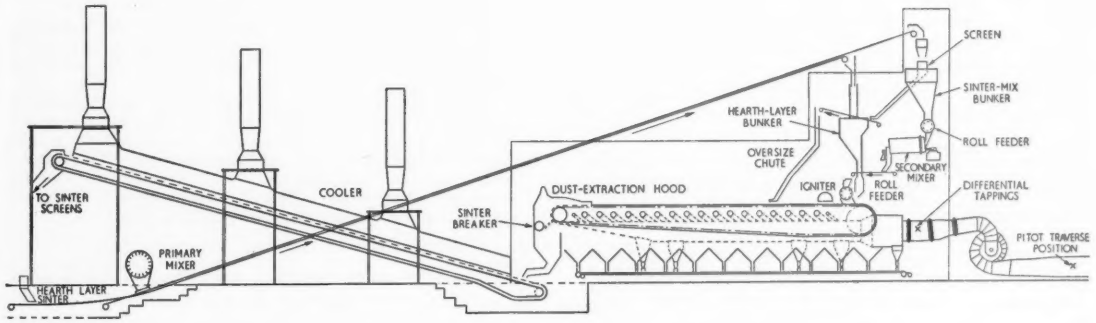

Fig. 2—Diagrammatic side elevation of Margam sinter plant

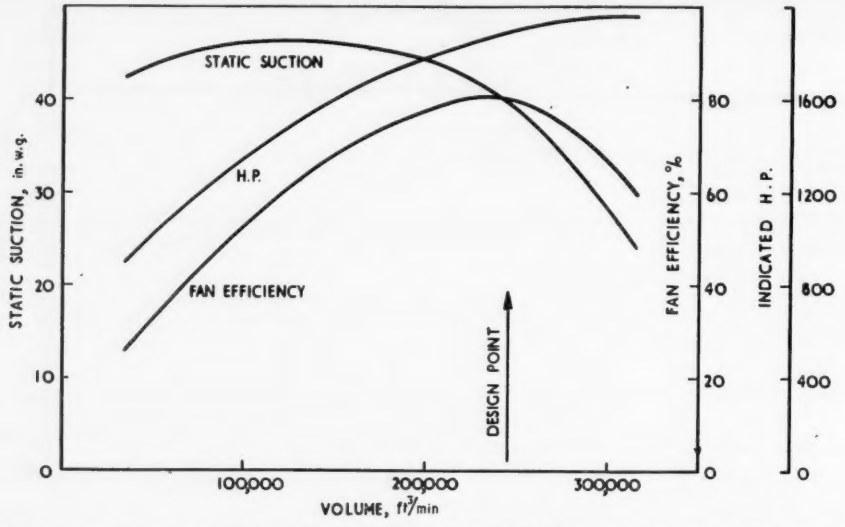

Fig. 3—Margam sinter plant fan characteristic. Fan speed 1437 rev/min, fan inlet temp. 150° C

of the pallets by means of rails on which the outer rollers rest. In No. 2 machine the rails are mounted on vulcanized rubber and can be adjusted in height to take up to 90% of the weight of the pallets. Strand speeds are controllable between 5 and 15 ft/min. The sinter is discharged into a claw-type sinter breaker and falls from here on to a Schenck vibrating feeder which feeds the sinter cooler. No screening takes place at this point.

The windlegs are connected via two alternative types of dustcatcher to a common main. Windlegs 1, 16, 17, 18, and 19 contain multiclone dustcatchers, and the rest Lurgi *S*-type dustcatchers. Each windleg is fitted with butterfly valves after the individual dustcatchers, and these are used when starting up. The dust collected in the dustcatchers is discharged from time to time on to a belt which also collects spillage, and is then conveyed to the machine fines hopper by a bucket elevator. The common waste-gas main has an expansion-chamber dustcatcher before the fans.

The fans are of a backward-bladed type driven by 2650-h.p. motors through fluid couplings and are rated at 245,000 ft³/min at 40 in. w.g. suction and 150° C. Figure 3 shows the makers' estimated performance curve for the sinter-plant fans when running at 1437 rev/min and with a fan inlet temperature of 150° C. The fan outlets enter a chimney common to the two machines.

Sinter Cooling and Screening

The Lurgi cooler is of the straight-line steel conveyor type, 212 ft long × 4½ ft wide with 12-in. sides, and elevates the sinter from ground level to the screen house situated above the holding bunkers (Fig. 2). Three extraction fans are installed at intervals along a hood which covers the cooler. Sealing between the hood and conveyor is by steel flaps. These are being replaced by composite flaps with rubber seals but there were some gaps of up to 3 in. where this modification had not been completed. The fans are each rated at 110,000 ft³/min at 130° C and 2 in. w.g. and driven by 85-h.p. motors. Cold air is drawn through slots in the conveyor and passes through the bed of broken sinter. The cooled sinter is discharged down a chute to horizontal vibrating screens. The product is screened to give four fractions: $-\frac{3}{8}$ in. for return fines, $+\frac{5}{8}$ in.–1 in. for hearth layer, $+\frac{3}{8}$–$\frac{5}{8}$ in. and + 1 in. for blast-furnaces.

Plant Instrumentation

All the instruments are grouped together in a pressurized cabin placed between the two strands, and the instruments are normally viewed from outside the cabin:

(1) Suction gauges—vertical edgewise gauges indicate the suction at all windboxes, at the fan inlet, and the stack draught.

(2) Temperature indicators—all the windboxes are equipped with thermocouples and a multi-point switch allows any couple from windboxes 1–12 to be selected for indication. Windboxes 13–19 and waste-gas temperatures are recorded on two charts.

(3) Strand speed is indicated and recorded in feet per minute.

(4) Cooling conveyor speed is indicated and recorded in feet per minute.

(5) Gas volumes at the ignition hood are indicated and recorded. Air volume and pressure is indicated.

(6) The sinter-fan power consumption in kilowatts is indicated.

(7) In addition to the above instruments, the weights of raw materials entering and of blast-furnace sinter leaving the plant are measured by cradle-type weight meters installed at convenient positions. These indicate, record, and integrate the weight of material passing. The coke constant-weight feeders indicate and integrate the weights delivered.

Plant Controls

All control switches for conveyors, feed tables, mixers, etc. are situated in a control cabin on the strand floor in front of a comprehensive mimic diagram indicating exactly which machinery is working. Trip wires are provided on all conveyors, and stop and

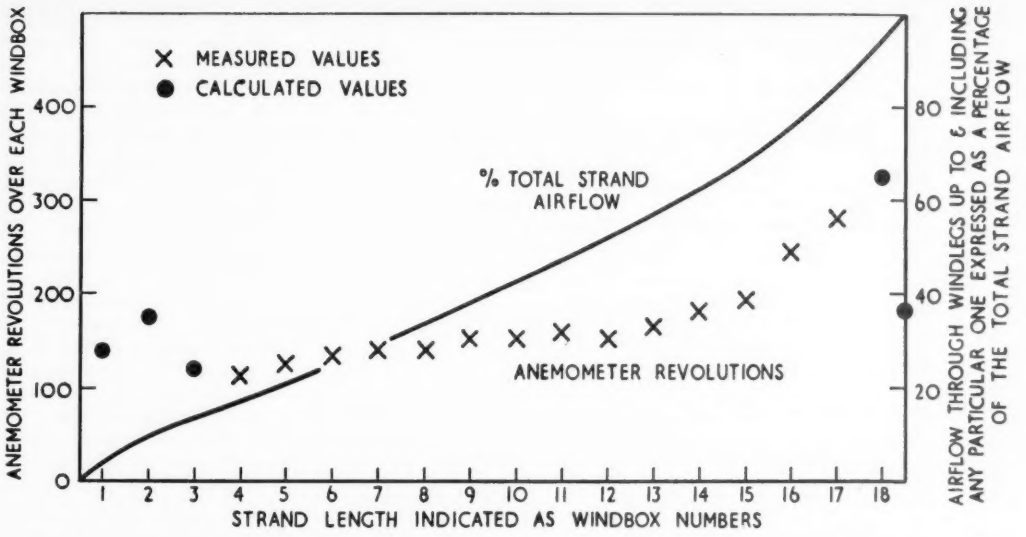

Fig. 4—Average results from 8 runs made with an anemometer along the Margam No. 2 strand

reset buttons for all plant equipment are placed in accessible positions.

Strand and cooler variation controls for speed, suction, etc. are positioned outside the instrument cabin adjacent to the respective strand. Speaker microphone intercommunication systems covering 120 points are used throughout the Ore Preparation Plant.

TRIAL CONDITIONS AND MEASUREMENTS

The assessment was made under normal operating conditions on No. 2 strand, the mix composition used being controlled by the plant operator, depending on the ores available. Bed height was maintained constant at $9\frac{1}{2}$ in. of raw mix over $1\frac{1}{2}$ in. of hearth layer of $+\frac{5}{8}$–1-in. sinter. Measurements of the following variable were made:

(1) Volume of air at the fan.
(2) Air temperature and suction at the fan inlet.
(3) Raw-mix feed rate and composition.
(4) Strand speed.
(5) Windleg suction and temperature (from plant instruments).
(6) Bed segregation.
(7) Percentage of moisture and carbon in the mix.

Various ores were used during the trial and have been grouped according to type under the headings.

(1) *Soft*: (a) *Screening*: Santander, Keloucha, Ouenza, Zaccar.
(b) *Purchased*: Sierra Menera Fines, BeniSaf Smalls.
(2) *Swedish:* Kiruna, Gelliväre, Grängesberg.
(3) *Siliceous:* Gelliväre H, May-sur-Orne, Moncorvo.
(4) *Concentrates:* Sierra Leone, Sydvaranger.

The mix composition was very variable throughout the trial, although all four groups were present in all mixes. Flue dust and screened magnesian limestone were used in the mixes when sufficient stocks of these had been accumulated to ensure a reasonable run.

EXPERIMENTAL PROCEDURE

Fan Air-flow Measurement

As no provision has been made at Margam sinter plant for airflow measurement, it was decided to calibrate the final dustcatcher, through which all the air passes to the fan, as a measuring device to give the total airflow at the fan. Four tests were carried out at varying fan airflows and the differential pressures produced across the dustcatcher were measured. The air volume flowing was measured by a Pitot traverse in the main after the fan. During the tests the strand was cold and empty and the windleg valves were fully open so that the volume of air flowing remained steady. The variation in fan airflow was achieved by manipulating the twin butterfly valves in the fan inlet mains.

From the results a calibration curve was drawn which enabled the total air volume at the fan to be obtained in cubic feet per minute at S.T.P., from the differential pressure across the dustcatcher and the fan inlet temperature.

Windleg Air-flow Measurement

Because of the complicated design of the windlegs it was impossible to find a suitable point for pitot traversing to obtain individual windleg airflows, and so the following method was adopted. A 9-in. dia. steel tube 1 ft long, inside which was fixed a combined anemometer and integrating revolution counter, was placed on top of the moving sinter cake. The volume of air drawn through the tube per unit time was proportional to the anemometer revolutions; therefore, provided that the strand speed was kept constant, the volume of air flowing through each windleg would then be proportional to the revolutions over the corresponding windbox. During the trial eight successful runs were made along the strand. As the general air flow patterns (plotted as anemometer revolutions) showed consistent trends, although the hottest wind-

Table I

RESULTS OF TRIALS

Date (1955) Time	30/9 A.M.	30/9 P.M.	2/10 9.30 to 10.15	2/10 10.30 to 12.00	2/10 2.30 to 5.00	4/10 9.30 to 10.00	4/10 2.30 to 4.00	4/10 4.30 to 6.45	6/10 9.15 to 10.15	6/10 10.45 to 12.15	6/10 2.00 to 2.30	6/10 2.30 to 4.15
Average bulk density, lb/ft³	122	118	113	116	115	113	113	111	108·5	103	114	110
Bed height, in. (total)	11	11	11	11	11	11	11	11	11	11	11	11
Strand speed, in./min	116	108	92	104	88	73	78	101	94	97	92	100
Tonnage input raw mix, tons/h	203	189	152	176	147	121	128	166	148	146	153	160
Hottest windbox No.	17	17	17	17	16	17	17	17	16	17	17	18
Maximum windbox temp., °C	429	392	396	438	261	235	215	314	311	374	310	365
Time to last windbox, min	12·1	13·0	13·3	13·5	16·0	19·2	18·0	13·8	15·0	14·6	15·3	14·0
Time to hottest windbox, min	11·1	11·9	14·9	12·4	13·8	17·6	16·5	12·6	13·4	13·4	14·0	13·6
Average suction sintering windboxes, in. w.g.	32·3	28·6	31·7	31·2	36·3	38·6	41·0	30·7	30·0	31·6	35·2	28·4
Average suction cooling windboxes, in. w.g.	22	18	21	19	23	30	6·5	24·0	18	19·4	32·0	17·0
Ignition gas, ft³/min	87,000	86,000	90,000	90,000	90,000	90,000	90,000	90,000	85,000	86,000	87,000	87,000
Sinter fan power consumption, kW	1530	1572	1460	1482	1461	1425	1520	1472	1450	1428	1510	1510
Average suction all windlegs, in. w.g.	31·3	27·5	31·4	30·0	33·7	37·7	40·5	30·0	27·2	30·0	34·9	27·3
Fan inlet suction, in. w.g.	40·4	39·2	40·9	40·0	44·3	45·3	46·6	40·8	38·9	39·9	42·0	38·3
Fan inlet temp., °C	182	196	181	198	139	121	103	179	184	182	148	185
Fan volume, ft³/min (S.T.P.)	159,000	157,000	157,000	156,000	148,000	147,000	145,000	157,000	155,000	148,000	150,000	160,000
Leakage airflow, ft³/min (S.T.P.)	65,200	64,500	65,700	65,000	68,000	68,600	69,500	65,600	64,300	65,000	66,500	64,000
Airflow through strand, ft³/min (S.T.P.)	93,800	92,500	91,300	91,000	80,000	78,400	75,500	91,400	90,700	83,000	83,500	96,000
Fan air per ton raw mix, ft³ (S.T.P.)	47,000	49,800	62,000	53,100	60,500	73,000	68,000	56,800	62,900	60,900	58,800	60,000
Bed air per ton raw mix, ft³ (S.T.P.	27,700	29,400	36,000	31,000	32,600	38,800	35,400	33,000	36,800	34,100	32,800	36,000
Apparent permeability, B.P.U.	75·1	75·6	73·7	74·2	66·3	65·0	63·1	73·8	75·0	70·6	69·4	78·0
Average bed permeability, B.P.U.	51·8	55·1	50·3	51·4	42·2	38·7	35·7	51·6	54·5	46·9	43·2	57·5
Estimated sintering airflow, ft³/min (S.T.P.)	79,700	78,600	77,600	77,300	60,800	66,000	64,200	77,700	69,000	70,500	71,000	90,600
Estimated cooling airflow, ft³/min (S.T.P.)	14,100	13,900	13,700	13,700	19,200	11,800	11,300	13,700	21,700	12,500	12,500	5400
Estimated sintering air per ton, ft³	23,600	25,600	30,700	26,400	24,800	33,000	30,000	28,100	28,000	29,000	27,800	34,000
Estimated cooling air per ton, ft³	4100	4400	5300	4600	7800	5800	5400	4900	8800	5100	5000	2000
Estimated sintering permeability, B.P.U.	47·3	50·0	46·5	46·6	35·7	35·4	32·9	47·4	45·4	42·3	39·8	54·5
Estimated cooling-zone permeability, B.P.U.	113·4	126·4	93·5	120·4	91·4	79·3	57·0	104·8	119·7	109·1	80·1	154·4
$\frac{1}{4}$-in material in raw mix, %	62·7	67·4	69·4	62·7	66·5	66·4	59·5	74·0	70·5	72·5	68·2	64·9
Moisture in raw mix, %	5·0	5·5	6·5	6·2	6·2	7·0	7·0	6·2	6·4	6·3	5·8	6·9
Soft ore in mix, %	17·0	...	14·9	14·0	24·4	...	10·7	13·6	18·2	20·6	18·8	22·8
Sredish in mix, %	15·9	...	16·0	14·3	12·6	No	9·8	10·1	13·4	12·0	14·4	14·3
Siliceous in mix, %	8·2	...	12·0	10·7	8·0	Figures	9·8	5·2	4·3	7·8	8·1	5·4
Concentrates in mix, %	17·9	No	13·1	11·7	13·7	...	23·3	20·8	18·6	18·2	21·6	15·8
Limestone in mix, %	0·9	Figures	...	...	...	...	1·3	1·3	1·7	2·9	...	2·6
Returned fines in mix, %	3·9	...	6·0	6·3	8·7	...	5·6	6·8	1·5	5·3	7·2	7·8
Flue dust in mix, %	26·8	...	25·0	27·5	28·0	34·8	28·5	30·8	26·6	20·6	23·8	23·8
Coke in mix, %	4·5	...	8·7	11·5	...	...	6·7	6·8	1·6	7·3	...	1·8
	4·8	...	4·3	4·0	4·5	3·9	4·3	4·3	5·3	5·2	6·1	5·7

box varied from No. 16 to No. 18, the results were averaged and are shown in Fig. 4. Owing to obstructions over both ends of the strand it was impossible to obtain anemometer readings for windboxes 1, 2, 3, 18, and 19, and in order to complete Fig. 4 the necessary results had to be calculated. As the S.T.P. airflow through any particular windleg should be proportional to the root pressure drop across it after temperature correction, the corrected pressure drop across each windleg was plotted against the distance along the strand. The resultant curve was found to be similar in trend to that obtained from the average anemometer readings. From this it was assumed that a unit S.T.P. airflow through *S*-type dustcatchers (Nos. 2–15) and multiclones (Nos. 16, 17, and 18) produced a similar root pressure drop. Furthermore, as the windlegs and multiclones on windboxes 1 and 19 are half-size, it was assumed that a unit S.T.P. airflow through them would produce twice the root pressure drop. Using the above two assumptions, airflows for windboxes 1, 2, 3, 18, and 19 were then calculated in terms of anemometer revolutions. The completed curve (Fig. 4) for airflow along the strand bears a distinct resemblance to that obtained when using foreign-ore mixes on the B.I.S.R.A. experimental sinter box which in the authors' opinion further substantiates the above assumptions. Also shown in Fig. 4 is a curve giving the cumulative airflow up to any particular windlegs as a percentage of the total strand airflow. From this curve and a knowledge of the total strand airflow it is possible to obtain an estimate of the airflow through any particular part of the bed.

Temperature and Suction

Waste-gas temperature and static suction at the fan airflow measuring point were measured by an unsheathed chromel/alumel thermocouple and water manometer. All other tem-

peratures and suctions were obtained from the plant instruments.

Mix Compositions

Hourly readings of the raw feed rate from each ore feeder table were obtained by placing a tray on the gathering belt and allowing it to pass under the feeder table concerned. Three tray passes were made at each table to reduce errors due to variability of the feed. A daily composite sample of each raw material was collected for size analysis. Coke, return fines, and flue-dust feed rates were obtained from the individual belt weighers installed on the plant. From these individual feed rates the percentage of each constituent in the mix was calculated on a 'dry mix' basis.

Tonnage Input of Raw Mix to the Strand

The use of the plant belt weighers for measuring the tonnage input of raw mix to the strand over short periods of time is subject to error because the installed belt weighers weigh the common mix to both strands and each strand has a surge hopper with a capacity of about 1 hour's supply of raw mix. It was decided, therefore, that a more reliable figure for raw-mix tonnage input would be that calculated from the bulk density of the mix on the strand, the strand speed, and the bed height. Measurements of the bulk density were made hourly by filling a 1-ft³ box with raw mix shovelled from a position in front of the cut-off plate.

Strand Speed

Although the strand speed was indicated and recorded in feet per minute, during assessment periods strand speed was measured every 15 min by timing the pallets past a given point with a stop-watch.

Raw Mixtures

The sample of raw mix taken for the measurement of the bulk density was later analysed for size grading and carbon content and a separate 1000-g sample taken at the same time was dried and reweighed to give the percentage moisture in the raw mix fed to the strand.

Segregation of the Raw Feed on the Strand

A specially constructed multi-shovel was used to take samples simultaneously from five vertical levels in the bed. Three sampling positions were chosen along the face of the bed before the cut-off plate and the samples obtained were analysed to give the variation in size grading, carbon content, and percentage moisture both across the bed and vertically through it.

OBSERVATIONS AND RESULTS

The trials at Margam were carried out during the period 27th September to 6th October, 1955. Two days were spent in checking the belt weigher, calibrating the final dustcatcher to give the fan airflow and determining the plant leakage at varying suction. Normal plant assessments were made on four days and a further day was spent on sinter cooler tests.

The four assessment days have been subdivided into periods during which conditions were markedly different, giving trial periods varying from ½ h to 3 h. Average conditions observed over these trial periods are shown in Table I, together with the derived data calculated from the basic equations:

(*a*) Air requirements per ton of raw mix

$$V = \frac{60F}{I} \text{ ft}^3/\text{ton (S.T.P.)}$$

(*b*) Permeability $P = \frac{F}{A}\left(\frac{h}{s}\right)^{0.6}$ B.P.U.

where F = Airflow, ft³/min (S.T.P.)
A = Area of strand, ft²
I = Material input rate, tons/h
h = Depth of bed (before ignition), in.
s = Suction, in. w.g.

Strand Utilization

In general the hottest windbox during the trial was No. 17 and thus two windboxes were used for cooling on the strand. As the first and last windboxes are only half-size, the length of strand used for sintering was therefore 92%, and the corresponding percentage of the total bed airflow used for sintering from Fig. 4 was 84%.

Air Requirements per ton of Raw Mix

The accurate measurement of windleg airflows at Margam was found to be impracticable, and the total

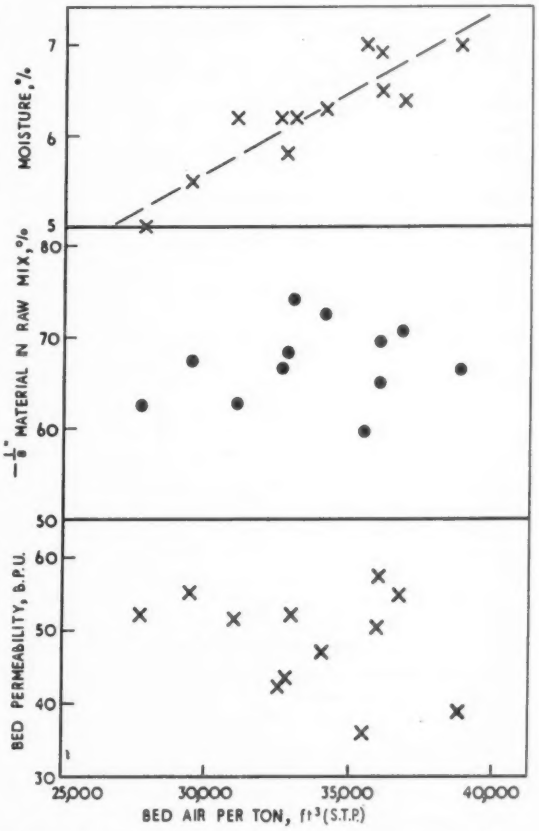

Fig. 5—Bed airflow per ton of raw mix: some of the possible correlations

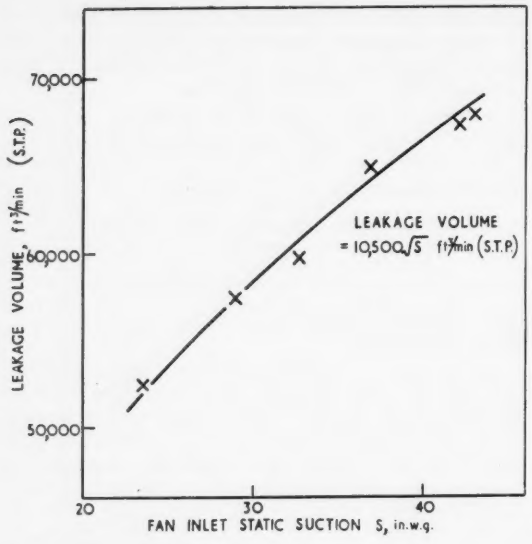

Fig. 6—Plant leakage at varying fan inlet suctions: results obtained on a cold strand sealed with brown paper

fan airflow has been used to calculate the quantity termed ' fan air per ton '. This is the specific volume of air measured at the fan per ton of raw mix fed to the strand. Measurement of the plant leakage (*see* below) enabled the actual airflow through the strand to be calculated and hence the specific volume referred to as ' bed air per ton of raw mix '. During the trial, however, sintering was always completed before the mix reached the end of the strand and therefore the quantities termed ' fan and bed air per ton ' include a certain proportion of cooling air. Since the hottest windbox was known, estimated figures for the sintering and cooling airflows, as a percentage of the total strand airflow, were obtained from Fig. 4. These figures are only an approximation and the quantities calculated from them have therefore been termed ' estimated ' values and their inclusion in the report is only to give an indication of the order of sintering and cooling air per ton. Fan, bed, and estimated air per ton figures and the corresponding mix compositions are shown in Table I.

The fan air per ton, which included a variable amount of leakage depending on the fan inlet suction, ranged from 47,000 to 73,000 ft³ for all the mixes investigated. Bed air per ton figures which exclude this leakage show a variation between 27,700 and 38,800 ft³. Over the 12 assessments during the trial the bed air averaged 33,600 ft³/ton of raw mix passing over the strand, 75% of the results being within ± 10% of this value, and the average estimated sintering air per ton of raw mix fed to the strand was 28,400 ft³.

The only definite correlation obtained between the bed air per ton and the many variables examined was in the case of percentage moisture in the raw mix fed to the strand. Figure 5 shows some of the variables plotted against the bed air per ton and suggests that the bed air per ton increases with increasing moisture content in the mix.

It was considered therefore that apart from any variations caused by the percentage of moisture in the mix, the bed air per ton was independent of the other operating variables experienced, and that the fan air per ton increased with increasing fan inlet suction owing to the greater leakage incurred.

Plant Leakage

The procedure used in a previous assessment trial, of covering the strand completely with stout brown paper, was used for the measurement of leakage at Margam. Variation of the suction under the strand was achieved by manipulating the twin butterfly valves in the fan inlet mains. The temperature, static suction, and differential pressure at the final dustcatcher were measured to calculate the leakage volume in cubic feet per minute (S.T.P.). As the suction along the strand is not constant during normal plant operation, it was decided to obtain the relationship between the leakage air volume and the fan inlet suction measured in inches water gauge. All fan inlet suctions throughout the trial were measured at a point after the final dustcatcher, in the short section of main immediately before the fan.

Measurement of the leakage airflow was made at varying fan inlet suctions after a maintenance shutdown with the plant cold and the strand stationary. Before beginning the test, however, the strand was moved through two full revolutions to get the seals fully lubricated with grease. The results obtained

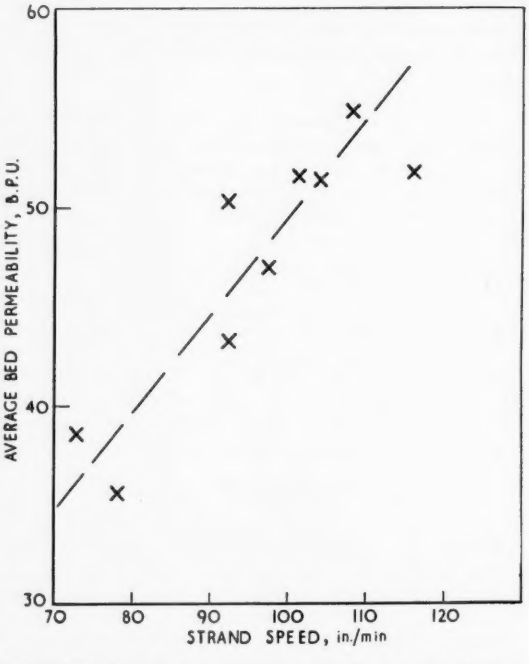

Fig. 7—Relation between strand speed and average bed permeability for assessment when sintering was completed over No. 17 windbox

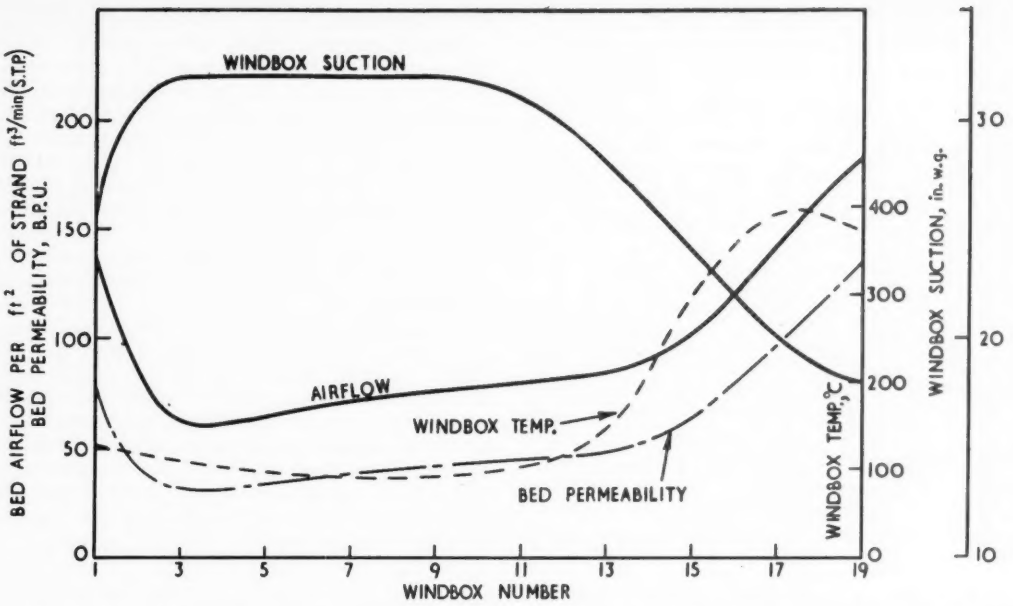

Fig. 8—Typical operating data measured on Margam No. 2 machine during assessment period 'P.M. 30.9.55'

are shown in Fig. 6, from which the leakage airflow is given by the expression:

$$\text{Leakage airflow} = 10{,}500\sqrt{\text{Fan inlet suction}} \quad \text{ft}^3/\text{min (S.T.P.)}$$

A further brown-paper test was carried out at constant fan inlet suction with the strand moving to find if there was any variation in the leakage airflow.

Table II
RAW MATERIALS SIZE VARIATION

Constituent*		'As-received' Size Grading, wt-%		
		+ ½ in.	+ ⅛ in.	− ⅛ in.
Swedish ores	Av.	10·3	33·3	66·7
	Max.	13·3	39·9	77·5
	Min.	6·1	22·5	60·1
Soft ores	Av.	10·2	31·3	68·7
	Max.	14·2	33·3	70·0
	Min.	6·3	30·0	66·7
Siliceous ores	Av.	7·6	24·2	75·8
	Max.	11·8	37·5	83·6
	Min.	5·4	16·4	62·5
Magnesian limestone	Av.	14·8	41·7	58·3
	Max.	16·8	46·8	64·3
	Min.	13·0	35·7	53·2
Machine fines	Av.	9·0	35·0	65·0
	Max.	12·6	43·7	76·2
	Min.	6·0	23·8	56·3
Return fines	Av.	1·2	28·1	71·9
	Max.	1·4	38·9	87·7
	Min.	0	12·3	61·1
Coke	Av.	2·1	27·0	63·0
	Max.	2·6	48·8	75·3
	Min.	0	24·7	51·2
Raw mix	Av.	5·9	32·8	67·2
	Max.	10·8	43·0	85·2
	Min.	3·3	14·8	57·0

* Concentrates not determined.

Measurements were made at 15-s intervals while the fan inlet suction was kept constant at 42 in. w.g. and the strand speed was approximately 5 ft/min. The strand was moved a total distance of about 9 ft and the maximum variation obtained in the leakage airflow was ± 1%.

In the absence of a method for measuring the variation which might be caused by having the plant hot instead of cold, the results shown in Fig. 6 have been taken as representative of continuous operation.

The leakage given by Fig. 6 includes the leakage at the pallet seals, over the dead plates at each end of the strand, and all the air leaking into the dustcatching system and air main to the fan. It is interesting to note, however, that during the test and throughout the assessment periods there were no indications of air passing through the pallet grease seals, whereas numerous leaks could be detected around the flanges and seals of the windlegs, dustcatchers, and dustlegs. It was also noted that in the above leakage tests the suctions in the first and last windboxes were almost identical with the fan inlet suction. This would seem to indicate that the leakage over the dead plates was low. It was also observed that suction in individual windboxes during the trials altered appreciably from one to the next, which would also seem to indicate little leakage between adjacent windboxes.

Permeability

The specific permeabilities shown in Table I were calculated from the permeability equation:

$$P = \frac{F}{A}\left(\frac{h}{s}\right)^{0\cdot6}$$

using the following data:

Table III
RESULTS OF BED SEGREGATION TESTS

Position		Left-hand Side, % + ⅛ in.		Centre, % + ⅛ in.		Right-hand Side, % + ⅛ in.	
Top	5	31·0		32·8		27·8	
	4	32·2		36·5		28·0	
	3	29·6		36·0		35·3	
	2	33·5		41·6		39·3	
Bottom	1	30·5		38·3		37·3	
		Mois., %	C, %	Mois., %	C, %	Mois., %	C, %
Top	5	6·5	3·47	6·0	3·95	6·0	3·73
	4	6·5	4·48	6·5	3·88	6·0	4·60
	3	6·5	4·74	5·5	4·33	6·0	4·10
	2	7·0	4·56	6·5	3·77	5·5	4·44
Bottom	1	6·5	4·43	7·5	3·76	6·0	6·86

Permeability	*F*	*A*	*h*	*s*
Apparent	Total fan air	Total strand area	11 in.	Fan inlet suction
Average bed	Bed airflow	Total strand area	11 in.	Av. strand suction
Estimated sintering	Est. sintering airflow	Strand area up to hottest windbox	11 in.	Av. strand suction up to hottest windbox
Estimated cooling	Est. cooling airflow	Strand area after hottest windbox	11 in.	Av. strand suction after hottest windbox

None of these specific permeabilities appeared to show any correlation with the process variables examined, including mix moisture content, raw mix composition and percentage $-\frac{1}{8}$-in. material in the raw mix. This apparent lack of correlation could be due to changes in mix composition from one assessment period to another.

Figure 7, however, which shows average bed permeability plotted against strand speed, suggests that an increase in the average bed permeability is followed by an increase in the strand speed. Figure 8 shows typical curves of the average conditions, including the average bed permeability measured during an assessment period.

Raw Materials Size Variation

The daily composite samples obtained from the tray samples were sieved at $\frac{1}{4}$ in. and $\frac{1}{8}$ in.; there was a negligible quantity of $+\frac{1}{2}$-in. material and the materials were too wet to sieve at $\frac{1}{16}$ in. The average maximum and minimum values are given in Table II, together with those obtained on the samples of the raw mix taken for bulk density measurements.

It will be noted that the materials were relatively fine with only a small fraction $+\frac{1}{4}$ in. The return fines contained a large proportion of very fine material, mostly unsintered concentrates. The magnesian limestone was slightly coarser than the other materials and was obtained by screening the crushed limestone used at the blast-furnaces; only a small percentage was used in the sinter mix. The relatively high proportion of $+\frac{1}{8}$-in. coke suggests that the coke crushers were not working very efficiently.

Bed Segregation

Samples were obtained simultaneously at five vertical levels in the bed by use of a multi-shovel. Three positions across the bed were sampled one after another: 1 ft from the left-hand side, at the centre, and 1 ft from the right-hand side of the pallet. Since the proportion of $+\frac{1}{4}$-in. material in the mix was extremely small, the samples were sieved at $\frac{1}{8}$ in. The average results obtained from six tests are given in Table III. In addition, one set of samples were analysed by the Steel Company of Wales Ltd. for moisture and carbon content and these are included in the table.

It would appear from Table III that the left-hand side receives slightly finer material than the right-hand side and centre, the centre being coarser. The left-hand side also appears to have little vertical segregation, whereas the other possitions do show a tendency to have coarser material at the bottom. Moisture is fairly evenly distributed, but the carbon content is higher at the side positions than the centre, and is slightly lower at the top of the bed, possibly because about 30% of the coke breeze was $+\frac{1}{8}$ in. during the trial periods.

Sinter Cooling

The sinter coolers are designed to cool the entire output of sinter from the strands. The cooled sinter is then screened immediately on discharge from the cooler into various fractions, which are then held in storage bunkers before despatch by rubber belt to the required destination.

The temperature of sinter entering and leaving the coolers was measured by dropping about 20 lb of sinter into a lagged calorimeter containing 60 lb of water. The rise in temperature was noted and the average temperature of the sinter calculated, assuming the specific heat of sinter to be 0·22. Six tests were carried out in each trial. Access problems made it extremely difficult to obtain representative samples of the sinter, especially at the discharge from the coolers where the sinter passed immediately on to the screens. The larger lumps were naturally the hotter and on breaking open after cooling were often found to be red-hot at the centre.

The values obtained were:

Entering Cooler	
Range of av. temperature, °C	300–500
Mean temperature, °C	400
Leaving Cooler	
Two fans working:	
Range of av. temperature, °C	100–400
Mean temperature, °C	270
Three fans working:	
Range of av. temperature, °C	80–200
Mean temperature, °C	140

No attempt was made to size the sinter entering or leaving the cooler, but two samples of sinter removed from the blast-furnace transfer belt gave the following size analyses:

	$-\frac{1}{2}$ in.	$+\frac{1}{2}-1$ in.	$+1$ in.
No. 1	18·0	18·0	64·0
No. 2	23·5	12·6	63·9

CONCLUSIONS

The assessment trial on the Margam No. 2 strand has shown that the airflow at the fan per ton of raw

mix passing over the strand varied from 47,000 to 73,000 ft³ (S.T.P.). The bed air per ton increased with increasing moisture content in the raw mix from 27,700 ft³ (S.T.P.) per ton with 5·0% moisture to 38,800 ft³ (S.T.P.) with 7·0% moisture; the average estimated sintering air was 28,400 ft³ (S.T.P.) per ton of raw mix.

Leakage volume was measured and found to be proportional to the square root of the fan inlet suction. Over the normal range of plant operation the leakage was approximately 40% of the total airflow at the fan. The results suggest that most of this leakage occurred at the windlegs and dustcatchers and there was no evidence of leakage through the pallet grease seal.

During the trial the average length of strand used for sintering was 92% and the corresponding proportion of total bed air used for sintering was 84%.

Average bed permeabilities varied from 35 to 57 B.P.U., an increase in permeability being accompanied by an increased strand speed, but changes in the mix bulk density obscured the relationship between raw-material input rate and permeability. Although the material input rate could be increased by improving the strand utilization, it is thought that the sinter coolers are already working near their maximum capacity and that any increase in the quantity or temperature of the sinter output from the strand would result in excessive heat at the discharge of the cooler. The coolers could be modified, however, in order to increase their capacity.

PLANT MODIFICATIONS

Since the assessment trials certain modifications have been carried out and others are under consideration.

Coke-breeze Preparation Plant

The feeder systems of both roll crushers have been modified and improved quality and quantity have resulted. The following outputs at the respective gradings are possible.

Crusher set to produce % − ⅛ in.	*Tons per hour per Crusher at that Setting*
95	9·9
91	12·2
87	15·9
81	20·3
75	24·4

The plant is now run to produce the necessary coke for sintering at the best possible grading, and a rod mill is on order to augment production.

Cooling Conveyor

The rubber side seals have been installed and form an efficient air seal. Consideration is being given to the modification of the present cooler feeding system to hot-screen the return fines before cooling the furnace-size sinter.

Ignition

The calorific value of the mixed gases burnt at the ignition hood has been increased to 156 B.t.u./ft³ by altering the ratio of blast-furnace to coke-oven gas to 5·88 : 1. The effect of this has been to improve sinter quality to reduce the return/machine fines circulating load to approximately 25%.

The Alcoholic-Iodine Method for the Extraction of Inclusions from Steel

By J. E. Garside, M.Sc.Tech., Ph.D., F.R.I.C., F.I.M., M.Inst.F., T. E. Rooney, A.M.C.T., and J. J. J. Belli, M.Sc.

SYNOPSIS

This paper reviews the development of the alcoholic-iodine method for the determination of oxides in steel since its first use in 1927 and describes the various separation techniques evolved since that date. The apparatus and procedure used by the authors, which incorporate all the improvements and modifications resulting from the previous investigations, are described, and details are given of the preparation of samples and the analysis of the residues.

Total oxygen results by the iodine method agree reasonably well with those obtained by vacuum-fusion analysis, but the great advantage of the iodine method is that the distribution of oxides may be determined and in addition the inclusion compounds are available for identification. The application of the alcoholic-iodine method to various types of steel is discussed. 1300

THIS METHOD was devised originally as a method of determining oxide and total oxygen contents in steels but, in researches carried out at the Northampton Polytechnic, London, particular attention has been given to the identification of individual inclusion compounds by X-ray diffraction analysis.

In order to appreciate the value of this technique as a method of investigation, one should be aware of previous work, and an historical survey is therefore given below describing modifications to the original method and the manner in which this technique has developed.

HISTORICAL DEVELOPMENT OF THE ALCOHOLIC-IODINE SEPARATION METHOD

Original Method

The method dates back to 1927 when Willems[1] first used an alcoholic-iodine solution to dissolve out the metallic constituents of a steel sample, filtering

Paper SM/C/191/55 of the Physical Chemistry of Steelmaking Committee of the Steelmaking Division of the British Iron and Steel Research Association, received on 29th March, 1956. The views expressed are the authors', and are not necessarily endorsed by the Committee as a body.

Dr. Garside and Mr. Rooney, formerly with Northampton Polytechnic, are now with Borough Polytechnic, London. Mr. Belli was formerly with Northampton Polytechnic, London.

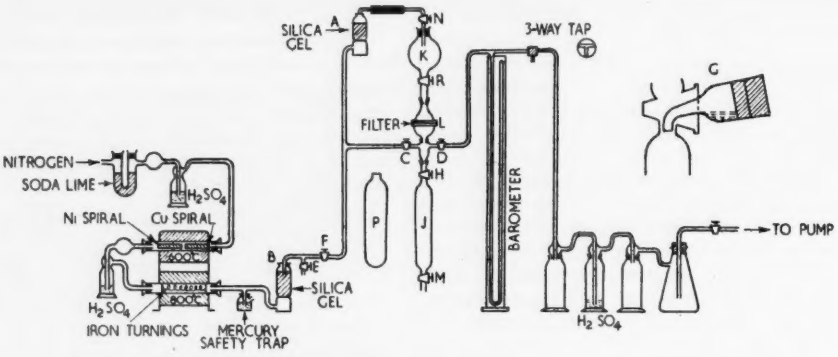

Fig. 1—Apparatus for the ' churning ' method

through an ultra-filter to retain the fine particles of non-metallic material which remained. This technique was elaborated by B. A. Bannister, in a thesis at Sheffield University, and introduced to the National Physical Laboratory by Dr. C. H. Desch. The modified apparatus and procedure used at the National Physical Laboratory were described by Rooney and Stapleton[2] in 1935 and became known as the ' churning method'. This apparatus is illustrated in Fig. 1.

The main innovations were a small mercury safety trap for the nitrogen stream, the silica-gel tower at *A*, and the dry purification train for the nitrogen instead of the alkaline pyrogallol used by Bannister. The efficiency of the gas purification train is important to the success of the method in eliminating all traces of moisture from the nitrogen. Removal of traces of oxygen is an additional safeguard.

Carbon dioxide and moisture were removed from the nitrogen stream by soda-lime and concentrated sulphuric acid respectively, after which the gas passed through a combustion tube kept at 600° C and containing spirals of copper and nickel gauze. After passing through another sulphuric acid bottle it entered a second combustion tube containing iron filings at 800° C and finally entered the apparatus by way of the silica-gel tower and the tap *F*.

The sample, in the form of millings, was prepared carefully in a special milling machine after a cleaning cut to remove any effects of surface corrosion. The millings were immediately dried in a stream of nitrogen. A portion was placed in the weighing bottle *G*, weighed, and transferred through the tap *H* into the reaction vessel *J*; the bottle was then reweighed. A slow stream of nitrogen was passed through the by-pass *E* into the reaction vessel placed in a horizontal position and continued overnight to displace the air and thoroughly dry the vessel and contents.

Seventy grams of pure, dry iodine, previously stored over silica-gel, was placed in the tap-funnel *K* and dissolved in 600 ml of pure methyl alcohol. (Pure synthetic methanol was found to be more reliable than ethyl alcohol, after two or three distillations over metallic calcium.)

The iodine solution was filtered through either a Cella ultra-filter or a No. 50 Whatman filter that had been dried after soaking in methanol. This was fitted between the flanges at *L*, smeared with vaseline and held together with spring clips, and laid on a perforated glass disc. The filter was washed several times with methanol with slight suction and the filtrate was collected in *P*. With the apparatus assembled as shown and with taps *R*, *H*, *M*, and *C* closed, a slow stream of nitrogen was allowed to enter through the tap *N* with *D* closed. Taps *R* and *H* were opened and the iodine solution filtered into the reaction vessel with slight suction. The vessel was disconnected and fitted securely into a felt-lined wooden box which was mounted on trunnions and slowly revolved by means of a small geared motor. The contents were churned in this way until all the steel had dissolved, usually in 2–3 h.

The used filter was now replaced by one freshly prepared and the reaction vessel was fitted above it in place of the funnel *K*. Tap *H* was opened to admit nitrogen, tap *M* was opened, and the liquid filtered with slight suction into the vessel *P*. The reaction vessel was washed three or four times with methanol, drained, and disconnected. The filter was washed with methanol until free from iodine and dried under greater suction; the residue was black or dark grey. After the edges contaminated with iodine had been trimmed off, the filter and contents were ignited in a small platinum crucible and weighed.

The method described by Bannister involved the evacuation and washing out of the apparatus with dry nitrogen, to remove traces of moisture, before each operation. The procedure described above is simpler, quicker, and safer. Filtration of the iodine solution took about 20–30 min and filtration of the reaction liquid about 40–50 min.

Between 7 g and 8 g of millings was used, giving 5–20 mg of residue. Bannister recommended colorimetric methods for the analysis of these small amounts of material, but these were found to be unsatisfactory by Rooney and Stapleton for traces of alumina. They also experienced difficulty in the estimation of small amounts of silica, in the presence of relatively large amounts of iron oxide, by the hydrofluoric acid method. Fusion of the residue with sodium carbonate was found to involve some attack on the crucible.

The most recent analytical procedure described in the report was as follows. The residue was digested with concentrated hydrochloric acid and the insoluble portion was filtered off, ignited, and weighed. Silica

was determined by evaporation with hydrofluoric acid and sulphuric acid; the residue was fused with a little sodium carbonate, dissolved in hydrochloric acid, and added to the main filtrate. Iron was determined with ' cupferron ' reagent, aluminium by means of ammonium benzoate,[3] and manganese with bromine and ammonia. The use of a micro-balance was almost essential for the small weighings involved.

Modifications in the Separation Technique

As a result of experience with the alcoholic-iodine method of several investigators, some modifications had been made by 1937 to decompose sulphides etc. during the separation and to bring the calculated value for total oxygen closer to that obtained by the vacuum-fusion method.

Churning Method—Some improvements in the described technique have been noted by Rooney, Stevenson, and Raine,[4] including the continuation of churning, after solution of the steel, for 20 h in the case of steels containing less than 0·1% sulphur and up to 40 h for higher sulphur contents. This was to ensure the complete decomposition of sulphides. The residue was ignited gently at first and then at 1000° C until constant in weight.

In the case of steels with more than 0·02% sulphur the Rooney and Stapleton churning method was found to give much higher calculated oxygen values than the vacuum-fusion method. Experiments on the effect of churning time on the weight of separated residue showed that the weight decreased with increasing time, becoming constant for a churning period of 40 h on a steel containing 0·17% sulphur. It is fairly certain that the effect of prolonged churning is to decompose sulphides present, as the greatest reduction is in the iron and manganese contents, sulphides of which elements are expected in steels containing appreciable sulphur. If undecomposed, these sulphides will be ignited to and reported as oxides of iron and manganese in the residue analysis, resulting in a high total oxygen value.

Stirring Method—This method was designed by Rooney and Stapleton and described by Rooney, Stevenson, and Raine.[5]

The reaction vessel used was similar to the newer apparatus illustrated in Fig. 2 and the operation of the apparatus was also similar to that described later.

The samples were prepared as previously described, in the form of fine millings. The anhydrous methanol was distilled twice over calcium before use. The iodine solution was prepared from 70 g of ' Analar ' iodine, previously dried over silica-gel, in 600 ml of methanol. About 6 g of iodine per gram of steel was sufficient for complete solution.

The Cella filters were stored in a 1% solution of formaldehyde, excess moisture being removed with filter paper and the filter then soaked in methanol and again blotted before use. The Whatman papers were dried in a steam oven for ½ h and then immersed in alcohol before use.

The stirring apparatus was designed in order to facilitate the maintenance and control of temperature during the separation process. It was not found practicable to maintain a high enough temperature with the churning apparatus to decompose all the sulphides. This was apparently effected with the stirring apparatus above about 59° C, as a residue of constant weight was formed between 59° and 61° C. The stirring method was found to give a slightly lower total residue than the churning method with somewhat smaller iron and manganese percentages.

From the results of these experiments it was realized that the stirring method was the best all-round separation technique and most of the subsequent work on the alcoholic-iodine method was carried out in this way.

Analysis of Non-metallic Residues Obtained by the Iodine Method

The scheme of analysis described fully in 1937[6] is outlined as follows:

(i) Separation and determination of silica by evaporation twice with concentrated hydrochloric acid and then evaporation of the filtered residue, with hydrofluoric acid and a drop of sulphuric acid (concentrated)

(ii) Precipitation of iron, titanium, and zirconium with ' cupferron ' and determination of (*a*) Fe_2O_3, colorimetrically using thioglycollic acid, (*b*) TiO_2, colorimetrically with hydrogen peroxide, and (*c*) ZrO_2, gravimetrically by precipitation as the phosphate

N.B. The residue from (i), after extraction with sodium carbonate and a little potassium chlorate, is dissolved in a small amount of sulphuric acid and added to the filtrate for (ii)

(iii) Precipitation of aluminium and chromium using 8-hydroxy-quinoline or ammonium hydroxide and determination of (*a*) Al_2O_3, colorimetrically with ' aluminon ' (ammonium aurine tricarboxylate) and (*b*) Cr_2O_3, colorimetrically using diphenylcarbazide

(iv) Precipitation of manganese by means of bromine and ammonium hydroxide and subsequent determination of Mn_3O_4 by the volumetric bismuthate method, or colorimetrically using potassium periodate.

This procedure was designed for the analysis of residues weighing not more than 10–12 mg. A microchemical balance was preferred for weighing. Either paper pulp filters or No. 42 papers were used. The residue was ignited gently at first, then at 1000° C in a tared platinum crucible. A blank determination using similar amounts of filter was also carried out.

The following observations were made concerning the calculation of individual and total oxygen contents:

(i) Iron and manganese exist in the ignited residue as Fe_2O_3 and Mn_3O_4, but in the steel most probably as FeO and MnO respectively

(ii) The very small amounts of Cr_2O_3, ZrO_2, and TiO_2 found in the residues from carbon steels are separated probably as carbides and ignited to oxides; they are therefore disregarded for the purpose of determining total oxygen contents

(iii) Discrepancies occur in the sum of the estimated contents of SiO_2, Fe_2O_3, and Mn_3O_4 and Al_2O_3 with respect to the total ignited residue content, partly due perhaps to the influence of other elements such as phosphorus and sulphur.

Improvements in the Alcoholic-Iodine Stirring Method

By 1939 it had been established that the use of samples in the form of thin discs, instead of millings, and of deoxidized iodine solution reduced the contamination of the residue by phosphorus.[7] Deoxida-

tion was effected by boiling the iodine solution with a stream of pure, dry nitrogen passing through. As oxygen is soluble in methanol to an appreciable extent, even at ordinary temperatures, this deoxidation practice is desirable as a safeguard against the possible oxidation of metallic and non-metallic constituents during the separation process. No advantage was found in the use of hydrogen for deoxidation instead of nitrogen.

A number of solvents other than alcohol have been used, such as acetone, benzene, and carbon tetrachloride, but with unsatisfactory results, mainly on account of the insolubility of iron iodide. Variation in the concentration of the iodine solution was also found to produce no improvement in the method.

It was discovered that with normal carbon steels sulphides were decomposed with the precipitation of sulphur, which was removed from the residue by subsequent ignition. Strongly carbide-forming elements, such as chromium, titanium, and vanadium, and probably molybdenum, were found to interfere with the method when present in quantity.

It has been stated by Rooney[8] that the addition of up to 0·5% of water to anhydrous methanol caused no increase in the amount of P_2O_5 retained in the residue. However, the addition of water caused an increase in the amount of FeO retained, while the other constituents were practically unaffected.

There seems to be little advantage in distilling methanol over calcium more than once before use if the original density is about 0·7919 g/ml at 25° C. One distillation reduces the density to about 0·7917 g/ml corresponding to 99·8% methanol.

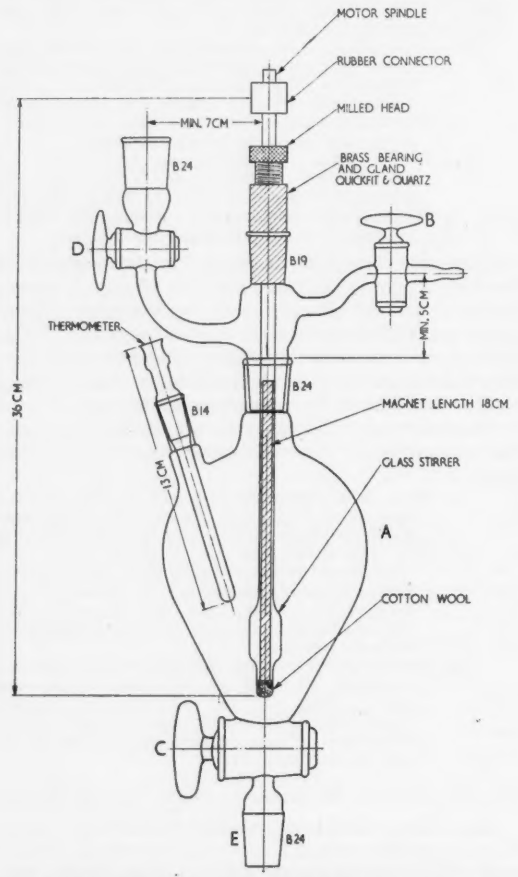

Fig. 2—Reaction vessel used in the 'stirring' method

Composition of Residues from High Carbon and Phosphorus Steels

The Fe_2O_3 and P_2O_5 contents of the ignited residues from the alcoholic-iodine method depend somewhat on the carbon content of the steel. Rooney has suggested that the method is useful only for low- and medium-carbon steels (less than 0·43%) owing to the low solubility of cementite, Fe_3C, in the iodine solution and the subsequent retention of carbide in the separated residue.

High FeO and P_2O_5 values, as compared with those from other methods, can be explained by assuming that the carbides and phosphides of iron are not completely decomposed by alcoholic-iodine and are to some extent retained in the residue, being subsequently ignited to Fe_2O_3 and P_2O_5. Another explanation is that of Speight[9] postulating the complete decomposition of carbides and phosphides, with the formation of soluble iodides of iron, free carbon, and either free phosphorus or phosphorus iodide. The phosphorus or phosphorus compound is then assumed to be hydrolysed, either by a trace of water or by the alcohol itself, to an oxide or oxyacid of phosphorus. The free carbon present may then absorb these phosphorus compounds, together with iron and other soluble constituents of the alcoholic solution, and so carry them into the residue on filtration. It was thought that, whilst washing with alcohol or alcoholic-iodine solution will cause only a slight removal of these absorbed compounds, treatment of the unignited residue with another reagent solution, e.g. ammonium tartrate, might remove them from the residue. Actual treatment by refluxing with 10% ammonium-tartrate solution was found to give a considerable reduction in weight of the ignited residue. The calculated FeO content was greatly reduced, but the P_2O_5 content only slightly so. The calculated total oxygen value after treatment, ignoring the P_2O_5, was nearer to that determined by vacuum fusion. This seems to support the method of treatment but does not necessarily prove the validity of Speight's theory.

The Presence of Alumina in the Residue

Speight has suggested that aluminium compounds are also absorbed by free carbon, leading to high alumina contents in the residue. It was shown by Rooney[10] that the decomposition of aluminium carbide in a sample of aluminium is slow and may be incomplete even after prolonged treatment with alcoholic iodine. The results obtained by Rooney with the iodine method on three aluminium steels showed that the alumina percentage in the ignited residue corresponded to an oxygen value much greater than that from vacuum-fusion. Some undecomposed aluminium nitride was found in an unignited residue. After treatment of the separated residue with sodium carbonate and dilute sulphuric acid, a total oxygen

value was obtained that was more consistent with the vacuum-fusion value.

Effect of Surface Oxygen Films

Experiments conducted by Sloman and Rooney[11] have shown that the amount of surface oxygen on a disc-type steel sample is not appreciably greater than that on a massive sample. The use of this disc-type sample in preference to millings was recommended for alcoholic-iodine determinations of total oxygen. The air-formed film on millings is of a much higher order and definitely vitiates results by the alcoholic-iodine method, especially on low-carbon steels.

Examination of Rimming and Alloy Steels by the Alcoholic-Iodine Method and Identification of Compounds in the Residues by X-ray Methods[12]

Satisfactory total oxygen results were obtained in 1943 on three rimming steels, containing more than 0·15% carbon, using the standard iodine method. The residue, separated from a low-carbon rimming steel by a modified method, in which no external heat was applied and the temperature rose to only 31° C, was found to contain manganese sulphide, MnS. Low total oxygen results were obtained by both the standard and modified procedures for a basic Bessemer steel (C 0·04%), probably owing to the partial solubility of small particles of iron and manganese oxides in the iodine solution. MnS was again found in the residues. Heat treatment of this steel produced a tendency for the retention of cementite in the residue from the modified method.

Identification of the above compounds was achieved by the X-ray powder diffraction method. Previous attempts with this method had been unsuccessful, even after the removal of carbon from the residue by low-temperature ignition. However, an X-ray examination of the unignited residue from the heat-treated basic Bessemer steel revealed the presence of considerable quantities of MnS and Fe_3C. MnO was also detected in the residue from this steel with no heat treatment.

The amount of MnS in a residue was estimated by an evolution method. When present in considerable amounts, Fe_3C was separated by magnetic means. Later work on the identification of compounds in iodine residues has confirmed the usefulness of the X-ray powder diffraction technique.

For example, the co-operative examination of a Ni–Cr steel[13] has revealed the presence of MnS, rhodonite ($MnO.SiO_2$), and quartz, as the principal constituents of the residues from both alcoholic-iodine and acid separations. These findings were corroborated by the results of fractional vacuum-fusion and chemical analysis. The ratio of MnO : SiO_2 obtained from analysis results corresponded to that in a silicate of the rhodonite type. Microscopic examination of the steel confirmed the above results and revealed the presence also of some inclusions of alumina.

The agreement in these results demonstrates the similarity in the inclusion compounds separated by the low-temperature alcoholic-iodine method and those actually present in the steel. This emphasizes the mildness of the attack of alcoholic iodine on steel.

Table I

CHEMICAL ANALYSIS OF (65° C) RESIDUES

Material (Steel)	Total Oxygen, %	
	Calculated	Vacuum-fusion
Basic open-hearth	0·011	0·010
Basic electric-arc	0·009	$0·003_5$
Basic Bessemer, heavily-killed, (Al)	0·005	0·004
Arc-weld 1	0·092	Not determined
Arc-weld 2	0·072	Not determined
Arc-weld 3	0·125	Not determined
Arc-weld 4	0·116	Not determined
Arc-weld 5	0·095	Not determined

Examination of Mild-steel Arc-weld Deposits

A co-operative examination of the representative selection of weld deposits, made by Rooney, Sloman, and Schofield[14] in 1945, included the results of the analyses of residues separated by the alcoholic-iodine stirring method. The chemical analyses of residues separated at 65° C showed that the major oxide constituent was usually silica. There was great variation in the FeO content, the MnO content was always high (more than 0·09%), and only very small amounts of Al_2O_3 and TiO_2 were found.

The results of X-ray examination of residues separated at 30° C showed the main inclusion compounds to be $(Mn,Fe)O.SiO_2$ $(Fe,Mn)O$, $2(Mn,Fe)O.SiO_2$ and MnS. The X-ray diffraction pattern obtained for $(Mn,Fe)O.SiO_2$ was slightly displaced with respect to both natural and synthetic rhodonite, probably because of the variable amount of iron found in this silicate.

All the low-temperature residues gave a positive chemical test for sulphur. It can be seen that the presence of the above inclusion phases is supported by the analysis of the high-temperature residues.

The chemical analyses of residues from two mild-steel weld deposits, laid down by an automatic process, showed the main oxide constituents to be SiO_2 and MnO. X-ray examination of the low-temperature residues resulted in the identification of a rhodonite-type silicate and MnS.

Some Recent Results with the Alcoholic-Iodine Method

A recent investigation into the effect of the deoxidation of molten iron–oxygen alloys with titanium by Evans and Sloman[15] has demonstrated the suitability of the iodine separation method for the isolation of mixed Ti–Fe oxides. Constituents ranging from α–Ti_2O_3 and TiO_2 to ilmenite, $FeO.TiO_2$, and Fe_3O_4 were identified by the X-ray diffraction analysis of residues separated at 30° C. The authors suggested that the positive identification of inclusions of this type is possible only by the X-ray crystallographic analysis of the separated non-metallic constituents. The microscopical appearance of these inclusions was found to vary radically with a small departure from strictly stoichiometric composition.

Rooney[16] has quoted the results given in Table I for a number of fully-killed steels and for some mild-steel arc-weld deposits.

The agreement between the iodine and vacuum-fusion values for total oxygen is just as reasonable as

Table II
RESULTS OF X-RAY EXAMINATION OF (30° C) RESIDUES

Material (Steel)	Compounds Identified
Basic open-hearth	Manganese sulphide (MnS) and Fe_3C
Basic electric-arc	MnS
Basic Bessemer, heavily-killed, (Al)	MnS, aluminium nitride, and Al_2O_3
Arc-weld 1	Ilmenite, ($FeO.TiO_2$)
Arc-weld 2	Rhodonite, ($MnO.SiO_2$) and MnS
Arc-weld 3	($MnO.SiO_2$) and MnS
Arc-weld 4	Ferrous oxide and (Fe, Mn)O*
Arc-weld 5	Tephroite, ($2MnO.SiO_2$)

* This is an iron-rich solid solution; a manganese-rich solid solution is indicated by placing the symbol for manganese before that for iron.

Note: The usually small phosphorus contents were calculated to P_2O_5, and included for the total oxygen values given in Table I.

that between individual vacuum-fusion values, excepting for the basic electric-arc steel. For each steel there is a definite correlation between the calculated oxide distribution and the identified oxide constituents.

Applications of the Alcoholic-Iodine Method

Rooney[16] has commented as follows on the applications of the alcoholic-iodine method : experience has shown that difficulties occur, particularly with alloy steels, owing to the incomplete decomposition of the steel by the iodine solution. With carbon steels the following difficulties arise:

(i) With steels containing the oxygen in the form of MnO or a solid solution (Mn,Fe)O, the oxide is soluble in the alcoholic-iodine solution. Examples are basic Bessemer steels with low carbon content and mild-steel arc-welds containing inclusions of a manganiferous type, e.g. silicates such as tephroite, $2MnO.SiO_2$, and free MnO.

(ii) Good results have been obtained on steels with as much as 0·6%C, but the probable upper limit is about 0·4% C. Even with 0·4% C the oxygen determinations can be too high compared with vacuum-fusion results. This occurs with a basic electric-arc steel containing a fair proportion of ' residuals.'

(iii) With higher carbon contents there may be some difficulty in decomposing the iron carbide. There is also the risk of absorption of some elements by the free carbon produced during the decomposition. Aluminium nitride, when present in quantity, may not be completely broken down, and aluminium carbide is also suspect in this respect. It is believed that aluminium is easily absorbed by free carbon.

When alcoholic-iodine results are suspect, some improvement can be obtained by treating the residue before ignition and before analysis with a specific reagent. For example, if the unignited residue contains undecomposed aluminium compounds, treatment with hydrochloric acid may dissolve such compounds.

With steels of the type described in (i) above, attempts have been made to reduce the solubility of MnO in the iodine solution by altering the *p*H of the solution by adding a suitable reagent, but without success.

Small amounts of MnO have been obtained by keeping the temperature below 30° C during separation, and have been identified by X-ray diffraction. Other compounds identified by X-ray diffraction are:

Silicates: Fayalite, rhodonite, tephroite
Oxides: FeO, (Fe,Mn)O, MnO, Al_2O_3, TiO_2, $FeO.TiO_2$
Sulphides: MnS, FeS, PbS
Silica; Iron carbide; Aluminium nitride.

Examination in this way can provide useful information and is usually successful for mild-steel arc-weld metal. In this case the alcoholic-iodine method has been useful in determining the true manganese and silicon contents of the weld steel.

Techniques for Alcoholic-Iodine Separation Recommended by the Authors

The apparatus and procedure adopted, as detailed hereafter, are those described in 1952[16] which incorporate all the improvements and modifications resulting from the detailed investigation of the method over the previous 15 years or so. The main changes from the previous techniques are the elimination of the nitrogen purifying train and of the distillation of the methanol over calcium. Nitrogen can now be obtained sufficiently free from oxygen, although it is still dried before use and A.R. methanol has been found to be sufficiently dry for immediate use.

The reaction vessel is similar to that used in earlier work, but with the addition of a re-entrant tube carrying a thermometer; it is illustrated in Fig. 2.

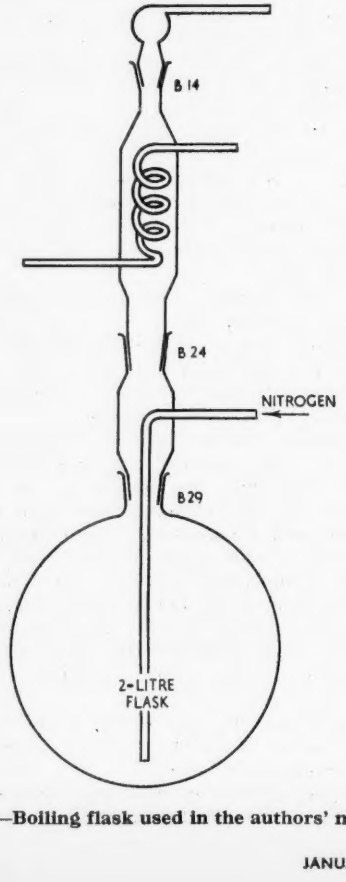

Fig. 3—Boiling flask used in the authors' method

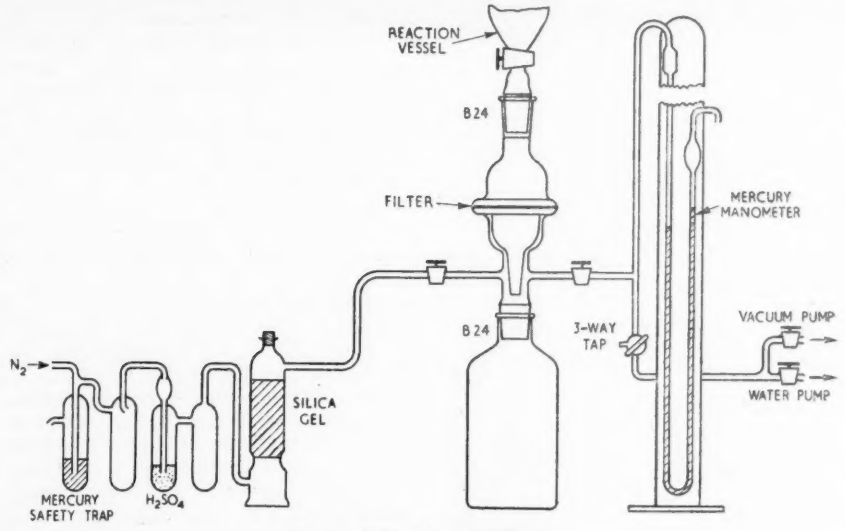

Fig. 4—Filtration apparatus

Preparation of Samples

The preparation of samples may vary according to the size and shape of the material to be examined. Usually the sample is first cleaned with carbon tetrachloride to remove oil, grease, etc. The next step is to remove the surface layer sufficiently to eliminate any contamination due to oxide scale and other adherent material. Slices about 1 mm thick comprising the whole cross-section are sawn off with a small hack-saw. If necessary, these slices may be cut into pieces small enough to pass through the neck of the reaction vessel. The pieces are then scrubbed with carbon tetrachloride and dried in a desiccator.

In the case of steel rod or wire, about $\frac{1}{8}$ in. in diameter or less, the sample is cleaned with coarse emery paper, wiped with carbon tetrachloride, smoothed with fine emery paper, and again cleaned with carbon tetrachloride. The rod or wire is then cut into small pieces, cleaned with carbon tetrachloride, and dried in a desiccator.

Samples should be used as soon as possible to avoid any contamination due to corrosion, etc.

Separation Procedure at 65° C

Pure iodine (65 g), previously dried by storing over phosphorus pentoxide, is dissolved in 600 ml of dry A.R. methanol (several batches of this solution are usually made up and stored in a dry Winchester bottle.) The solution when freshly prepared sometimes contains a fine suspension which inhibits filtration. It is therefore allowed to stand for several days and carefully decanted during filtration, using a Whatman No. 542 hardened paper.

The filtered solution is placed in the ' boiling ' flask (Fig. 3) fitted with a nitrogen delivery tube and reflux condenser, and the flask is placed on a sand bath on a small electric hot-plate. The solution is brought to the boil, allowed to cool, reboiled, and finally allowed to cool with the nitrogen still bubbling through. This is the ' deoxidation ' proeedure, after which the flask is stoppered and kept free from air until required.

Just over 10 g of the prepared sample is placed in the reaction vessel *A* and the stopper carrying the stirring gear, etc. is fitted. The ground-glass joints are lubricated with Apiezon grease *L*. The glass stirring paddle contains a cobalt-steel magnet. The space between the stem of the paddle and the brass gland is sealed with Apiezon sealing compound *Q*. The reaction vessel is evacuated twice and refilled with nitrogen each time, after which 600 ml of iodine solution are poured in through the large-bore tap, avoiding undue contact with air.

The small-bore tap *B* on the reaction vessel is connected to the nitrogen supply and the large-bore tap is left slightly open. A slow stream of nitrogen is passed through. The vessel is placed inside a small casing, heated by means of a carbon filament lamp, and a temperature of 65° C is maintained during the reaction. The temperature is measured with a thermometer placed in the re-entrant tube. Stirring is effected with the glass paddle which is connected to the spindle of a small motor by a piece of rubber pressure tubing. When all the sample has dissolved, the reaction vessel is fitted to the filtration apparatus illustrated in Fig. 4. The complete solution of the steel is observed by lifting the paddle containing the magnet.

A dried 7-cm Whatman paper, No. 542, is fitted between the ground-glass flanges of the filtering apparatus, previously greased with Vaseline and held together by spring clips. The apparatus is evacuated below the main tap *C* of the reaction vessel and then filled with nitrogen. The main tap is opened and the liquid filtered using slight suction from a water pump and at the same time admitting nitrogen above the liquid in the reaction vessel. A mechanical pump is used for the evacuation.

The filter and reaction vessel are well washed with methanol and the filter is sucked dry. It is then removed from the flanges and the top flange is wiped

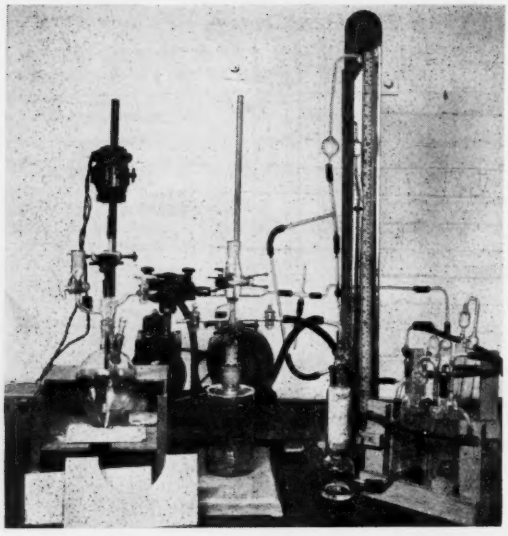

Fig. 5—Reaction vessel and separation apparatus

with a small piece of filter paper to remove the small amount of residue adhering to it. Complete solution of the sample is effected in about 3½–4½ h.

Separation Procedure at 30° C

A similar procedure is adopted, except that the temperature is kept just below 30° C with occasional heating if necessary. The complete decomposition of the sample is effected in about 4½–5½ h depending on the size of the pieces. As the residue in this case is to be used only for X-ray diffraction analysis, decomposition of all the steel is not essential. Any small remaining pieces are pulled up on the magnet and held above the liquid surface during filtration. Complete recovery of the residue is not necessary for the same reason.

A photograph of the reaction vessel and separation apparatus is shown in Fig. 5.

Chemical Analysis of Residues Extracted at 65° C

The purpose of the analysis is to determine the distribution of oxygen amongst the oxide inclusions and also the total oxygen content of the inclusion material, which is taken to be the actual content of the steel itself. Sulphides and carbides are decomposed at 65° C and are not separated with the oxides. The analysis procedure is described briefly below.

The filter and residue are ignited in a small weighed platinum crucible, gently at first and then for about 15 min at 950–1000° C, after which the crucible is cooled and reweighed. The residue is brushed carefully in a small beaker, covered with small amounts (about 5 ml) of concentrated hydrochloric acid, and the solution is evaporated twice. It is then taken up in about 15 ml of dilute hydrochloric acid, warmed, and filtered warm through a Whatman No. 40 paper. The filter is washed and ignited in a platinum crucible, cooled, and weighed. The residue consists of silica contaminated with probably some alumina and oxides of manganese and iron. Silica is determined by evaporation with hydrofluoric acid and a drop of sulphuric acid, in the usual way by loss of weight. The oxides remaining in the crucible after ignition are dissolved by fuming with a little sulphuric acid, and the solution is added to the main filtrate.

Iron and titanium in the filtrate are precipitated in cold acid solution with ' cupferron.' The precipitate is filtered off, ignited, and weighed, and the residue digested with sulphuric acid. Iron is determined by precipitation as ferrous sulphide, in ammoniacal solution to which a small crystal of citric acid has been added, and the precipitate is filtered quickly from the hot solution with only slight washing. Titanium is obtained by difference, and also by a second precipitation with ' cupferron ' as a check. (Iron is weighed as Fe_2O_3 and the titanium as TiO_2.)

Concentrated nitric acid (10 ml) is added to the filtrate from the first ' cupferron ' precipitation, and the solution is evaporated to a syrup to destroy organic matter. The solution is diluted and made alkaline with a small excess of ammonia, re-acidified with hydrochloric acid, and aluminium and chromium precipitated with ammonia. As the precipitate is probably contaminated with manganese, it is filtered off, washed, redissolved in dilute hydrochloric acid, and reprecipitated as above. It is ignited and weighed and then fused in the crucible with a little sodium carbonate and a few crystals of potassium chlorate. The fusion is dissolved in hot water and acidified with sulphuric acid. Chromium is determined colorimetrically with diphenylcarbazide reagent and any phosphorus determined as phosphomolybdate. The aluminium is obtained by difference.

Manganese in the filtrate from the ammonia precipitate is determined by means of bromine and ammonia and weighed as Mn_3O_4. Any phosphorus in the filtrate is determined as phosphomolybdate.

Of the elements determined, the iron is calculated to FeO, aluminium to Al_2O_3, manganese to MnO, chromium to Cr_2O_3, titanium to TiO_2, and phosphorus to P_2O_5. The total oxygen content of the steel is obtained by adding together the oxygen fractions of these oxides and usually agrees, in the case of mild-steel weld metal, with the total oxygen obtained by vacuum-fusion, within reasonable limits.

Acknowledgments

The authors wish to make grateful acknowledgment of grants from the British Iron and Steel Research Association and the British Welding Research Association, which have enabled two of them (T. E. Rooney and J. J. J. Belli) to take part in the investigations reported here.

References

1. F. Willems: *Arch. Eisenhüttenwesen*, 1927–8, vol. 1, p. 655.
2. T. E. Rooney and A. G. Stapleton: *J. Iron Steel Inst.*, 1935, vol. 131, No. I, pp. 249–254.
3. P. G. Ward: *J. Inst. Metals*, 1927, vol. 37, p. 89; I. M. Kolthoff, V. A. Stenger, and B. Moskovitz: *J. Amer. Chem. Soc.*, 1934, vol. 56, pp. 812–815.
4. T. E. Rooney, W. W. Stevenson, and T. Raine: Seventh Report on the Heterogeneity of Steel Ingots, *Iron Steel Inst. Spec. Rep.* No. 16, pp. 109–112: 1937.
5. *Ibid.*, pp. 112–113.
6. *Ibid.*, pp. 117–123.

7. T. E. Rooney: Eighth Report on the Heterogeneity of Steel Ingots, *Iron Steel Inst. Spec. Rep.* No. 25, pp. 150 and 156: 1939.
8. T. E. Rooney: *J. Iron Steel Inst.*, 1943, vol. 148, No. II, p. 255p.
9. G. E. Speight: *Ibid.*, pp. 260p–261p.
10. T. E. Rooney: *Ibid.*, pp. 273p–277p.
11. H. A. Sloman and T. E. Rooney: *Ibid.*, pp. 327p–340p.
12. T. E. Rooney and F. W. Jones: *Ibid.*, pp. 340p–348p.
13. T. E. Rooney: *Ibid.*, 1948, vol. 160, pp. 410–412.
14. H. A. Sloman, T. E. Rooney, and T. H. Schofield: *Ibid.*, 1945, vol. 152, No. 2, pp. 127p–153p.
15. E. Ll. Evans and H. A. Sloman: *Ibid.*, 1953, vol. 174, pp. 318–324.
16. T. E. Rooney: Private Communication to the Solid Steel Study Group of the B.I.S.R.A. Gases and Non-Metallics Sub-Committee, Nov., 1952.

Letters to the Editor

The Identification of Microscopic Spherical Inclusions in Electric-Furnace Steel

A RECENT REPORT* of fatigue tests on electric and open-hearth furnace steels showed that the life of high-tensile steels under fatigue tests was considerably reduced by the presence of microscopic spherical inclusions, which were found mainly in basic electric-arc steel. This note describes the identification, by conventional X-ray diffraction techniques, of the inclusions in a sample of electric-arc ball-race steel.

Material

The inclusions were found in a sample from a batch of a carbon–chromium steel to B.S. Specification En.31; this is a British basic electric-arc normal-procedure steel having the composition C 0·94%, Si 0·23%, S 0·030%, P 0·023%, Mn 0·44%, Ni 0·18%, Cr 1·35%, Fe balance. They were *non-deformable*, that is, they had remained spherical throughout the rolling process used to produce the bar from which the samples were taken. Other types of inclusion are elongated during the rolling process; these are described as *deformable* and are less detrimental to the fatigue strength of the steel. The latter class, which includes sulphide inclusions, is present to some degree in all commercial samples of steel, but the spherical non-deformable inclusions appear to be unique to basic electric-arc normal-procedure steels.

The steel used was heat-treated to a nominal hardness of 750 D.P.N. The results of tests carried out with a Wöhler-type fatigue machine on the two samples from

* P. H. Frith, " Fatigue Tests in Rolled Alloy Steels made in Electric and Open-Hearth Furnaces," *Iron Steel Inst. Spec. Rep. No.* 50, 1954.

Table I
RESULTS OF FATIGUE TESTS

Reverse Bending Stress, tons/in²	Broken after Cycles	Hardness in Critical Section of Test Pieces after Test, D.P.N.
±45	13,261,000	752
±50	382 000	726
(±55)	(20 000 000)	(760)

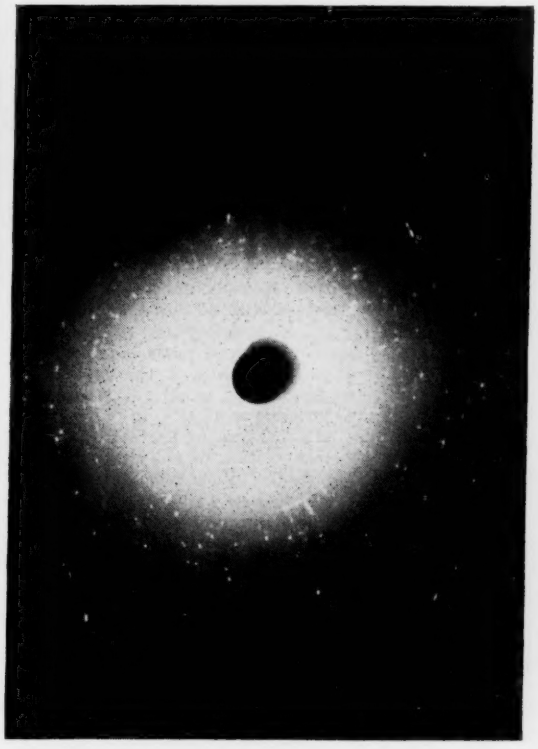

Fig. 1—Laue photograph, stationary specimen, cylindrical film. Exposure 48 h at 40 kV and 15 mA to unfiltered copper radiation

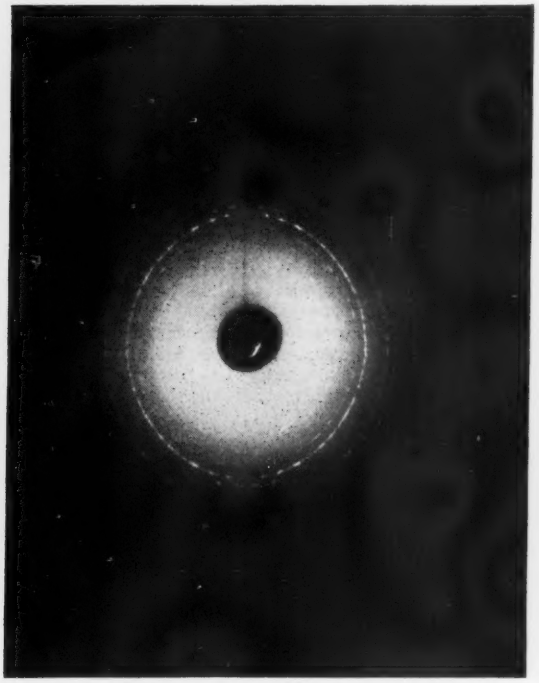

Fig. 2—As Fig. 1, but specimen rotated and exposure increased to 80 h to Ni-filtered CuK_α radiation

which the identified inclusions were taken are given in Table I; the figures in parentheses refer to a typical sample of identical material free from *spherical* inclusions.

Small spherical inclusions, first revealed by micro-radiography, were present in sizes up to about 0·0015 in. (38μ) in diameter in a concentration of about 25,000 per cubic inch.

Since the expansion coefficient of the steel is greater than that of the inclusion material, the inclusions, on cooling from the melt, behave as filled cavities with a stressed skin. These produce local concentrations of stress when an external stress is applied, and were shown by Frith to be present at the point of commencement of fracture in most broken Wöhler fatigue-test sections. Thus their exclusion from the steel is of the greatest importance.

Isolation of Inclusions

Some of these inclusions were loosened by progressive polishing and etching with a 20% solution of bromine in methanol. Electron diffraction micrographs taken of a number of these gave similar diffraction patterns, showing that they were of the same material. The largest inclusion found, 40μ in diameter, was stuck to the end of a glass fibre 0·1 mm in diameter mounted in a fine glass capillary, ¼ in. standing proud. This was facilitated by practising with the mounting of titania spherulites; a simple 'micro-manipulator', described below, was used.

The inclusion was placed near the edge of a microscope slide in the focal plane of a low-power objective. The glass capillary carrying the fibre was then stuck horizontally, with a separation of about 0·02 in., normal to the edge of a second slide, and with the fibre protruding over the edge. This was then placed next to the former slide, and moved until the tip of the fibre, dipped into a 20% solution of Canada balsam in xylene, appeared out-of-focus immediately above the inclusion. The fibre was then gently depressed until the inclusion was picked up, and allowed to dry undisturbed.

Identification

The specimen was mounted in a standard 9-cm dia. Unicam single-crystal X-ray diffraction camera, using a 0·25-mm dia. collimator. Great care was taken in aligning the collimator, inclusion, and scatter trap to give the best possible diffraction-to-background ratio. A Laue photograph (Fig. 1) with a 48-h exposure showed the inclusion to be polycrystalline, but a rotation photograph with increased exposure (Fig. 2) was necessary to provide the data for comparison with the A.S.T.M. index. Agreement to within 0·01 Å was obtained for the lattice-spacing parameters of the five strongest lines of the fayalite lattice.

Conclusion

The present work, together with the electron micrography information, which would be unnecessary if a number of X-ray diffraction photographs of different inclusions had been made, shows that the great majority of spherical inclusions were of the mineral fayalite (ferrous ortho-silicate $2FeO.SiO_2$).

That such inclusions are only present in steels made by the basic electric-arc furnace technique shows that the inclusions must have been introduced at this stage, for the starting materials are common to all processes. It is not possible to make any further suggestions, for the whole process is most complex, and worthy of close investigation.

I am grateful to Mr. R. S. Sharpe of the Bristol Aeroplane Company for assistance in publishing this letter.

R. M. GLAISTER

University of Bristol,
H. H. Wills Physics Laboratory,
Royal Fort,
Bristol 8

21st June, 1956

Rapid Solution of Oxygen in Molten Iron-oxide Slags

THE FOLLOWING EXPERIMENTS were performed to find out whether the rate of solution of oxygen in molten iron-oxide slags is high. About 6g of iron oxides (84·5% FeO, 15·5% Fe_2O_3), contained in a small recrystallized alumina crucible, was placed in an electrically heated recrystallized alumina tube in an atmosphere of nitrogen. After holding the sample in nitrogen for about 5 min to fuse, pure oxygen was introduced into the reaction tube at a rate of 180 ml/min through a ¼-in. dia. alumina tube placed immediately above the crucible. After a specified time of reaction, the crucible and its contents were dropped on to a water-cooled copper block at the bottom of the reaction tube. The slag was then analysed for ferrous and ferric iron contents.

The results were as follows:

Time of Reactions, min	Slag Analysis, wt-%			
	FeO	Fe_2O_3	Al_2O_3*	(FeO)†
0	84·5	15·5	0	84·5
2	39·3	45·6	15·1	28·7
5	24·6	54·5	20·9	9·9
10	21·2	57·7	21·1	6·3
15	17·8	59·1	23·1	1·5

* By difference.
† % FeO left in solution after allowing for the formation of $FeO.Al_2O_3$.

At 1550° C iron oxide reacts with the alumina crucible very rapidly as indicated by the above results. When the equilibrium is established, the system at 1550° C will consist of spinel $FeO.Al_2O_3$ solid solution and oxygen at 1 atm pressure. The percentage of (FeO) given in the last column of the table is the difference between the total ferrous oxide content of the slag (second column) and the ferrous oxide required to form $FeO.Al_2O_3$ with all the alumina present. The results show that the alumina content, and hence spinel content, of the mixture increases with time very rapidly at first and then at a much lower rate.

In one experiment a mixture of ferric oxide, ferrous oxide, and alumina (the amounts of the latter two oxides being adjusted to give the spinel $FeO.Al_2O_3$) was heated in an alumina crucible at 1550° C in pure oxygen at 1 atm pressure. After 30 min of heating no change was observed in the composition of the mixture. This is concordant with the results in the table above, which show that after 15 min ferrous oxide in solution, i.e. (FeO), is very small, indicating approach to equilibrium.

Since Fe_2O_3 and spinel have high melting points, it is thought that the initially liquid wüstite becomes partially or totally solid at 1550° C immediately after the introduction of oxygen into the system. The rate of oxygen solution in these slags decreases appreciably after the first 2 min of reaction, presumably owing to the formation of a solid phase.

E. T. TURKDOGAN
D. J. GOODWIN

British Iron and Steel Research Association,
Chemistry Department,
140, *Battersea Park Road,*
*London, S.W.*11.

8th October, 1956

AFFILIATED LOCAL SOCIETIES

Sheffield Metallurgical Association

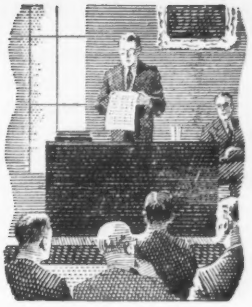

Production Control Quantometer for Steelworks Analysis

By D. Manterfield, F.I.M., and W. S. Sykes

SYNOPSIS

This paper details the use of a direct-reading spectrometer for routine analysis in a steelworks.

The principles involved are given and a description of the instrument and its scope. Iron is used as an internal standard for steel analysis and the instrument calibrated against standard samples of known composition.

The results obtained on residual elements, low and high alloy concentrations are equal in accuracy to those obtained by chemical methods, and the speed of analysis gives strict control over steelmaking. 1208

Introduction

WITHIN THE LAST 15 years or so spectrographic methods of analysis have been used to supplement and, in some cases to replace, the traditional wet chemical methods of analysis in steelworks. The earlier development work using spectrographic technique has been progressively described by various workers.[1–5] A method for low-alloy steels was recently published as an Iron and Steel Institute Special Report.[6]

Spectrographic methods using photographic technique have been used for many years as routine in many steelworks laboratories for control and other purposes with much success. By this means more rigid control could be exercised in the manufacturing processes.

In the post-war era it became apparent that still more rapid and economical methods of analysis were desirable. In photographic spectrography most time is taken in processing the photographic plate and measuring the line densities. In addition, the accuracy of results is affected by plate characteristics, and errors in processing and density measurements.

Although direct-reading methods received attention for some years, it is only since about 1945 that practical instruments have been developed commercially in the U.S.A. and later in Europe.[7–10] This development has been made possible by improved excitation units giving greater variation in the type of discharge according to analytical requirements; by the development of multiplier photo-tubes with a high amplification factor, and by improvements in grating spectrographs which have advantages when direct photoelectric recording is employed. In principle the photographic plate is replaced by a number of multiplier photo-tubes placed behind the focal plane of the spectrometer. On the focal plane are corresponding exit slits through which the selected element beam is isolated and directed to the cathode of the phototube.

Measurement of the resultant photo-currents can be made by several methods. With the instrument described here, these outputs are integrated for about 20 s, the photo-currents being allowed to charge condensers in the recording unit. Subsequent measurement consists of reading the charge on each condenser in turn. Selected iron lines are used as internal standards for steel analysis. A schematic diagram of the system is shown in Fig. 1.

ANALYTICAL REQUIREMENTS

It should be stated that each direct-reading instrument is designed to a specific type of alloy or other material, usually to meet recurrent analytical requirements. The Quantometer to be discussed was acquired for production control in the manufacture of plain carbon and low-alloy steels, and for a research programme to assess its potentialities for the analysis of high-alloy steels, sinters, and slags. The specification upon which it is designed covers the determination of P, Si, Mn, Ni, Cr, Sn, Cu, Mo, Al, V, Ti, Pb, and B in steels, and of SiO_2, Fe, CaO, P_2O_5, MnO, MgO, Al_2O_3, and F in slags and sinters.

In designing a particular instrument the selection of spectral lines for the desired elements depends upon several factors, including the range of concentration of the element. These in turn determine the type of

Paper presented to a joint meeting of the Sheffield Metallurgical Association and The Iron and Steel Institute on 6th December, 1955.

Mr. Manterfield is Chief Chemist with Steel, Peech and Tozer, where Mr. Sykes is Chief Spectrographer.

excitation required, and the number of channels, photo-tubes, and integrators. In this Quantometer there are 30 multiplier photo-tubes for 45 channels, and 16 integrators for the 30 tubes.

The selected spectral lines, ranges covered, groups, and types of excitation are given in Table I.

DESCRIPTION AND AUXILIARIES

The Quantometer is housed in a separate room 20 ft × 15 ft in the spectrographic section of the laboratories. The temperature is maintained at 70° ± 2° F, and the relative humidity at 50 ± 5%, by an air-conditioning plant. Adjoining the spectro-

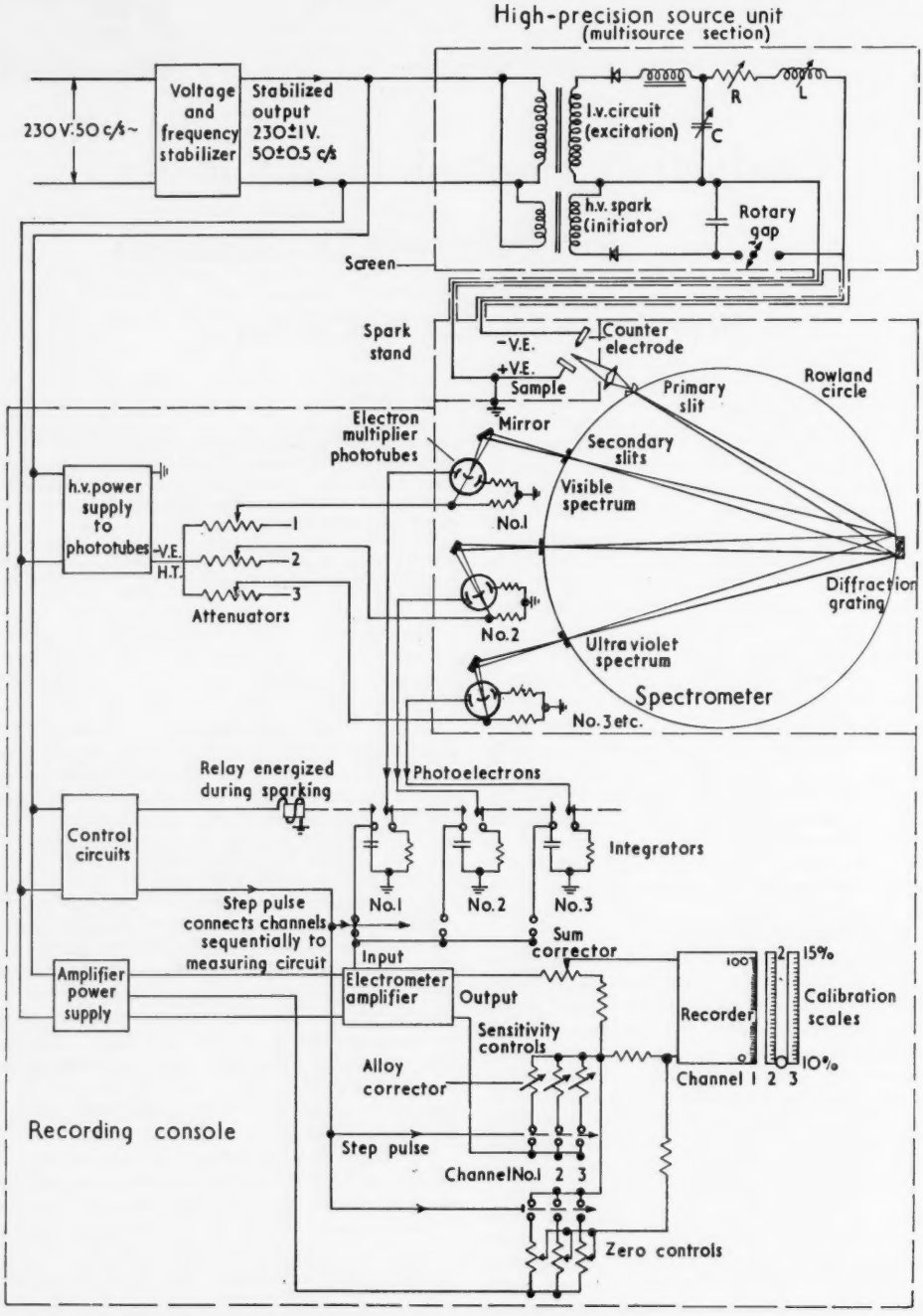

Fig. 1—Simplified schematic diagram of Production Control Quantometer

graphic rooms, facilities are available for sample delivery and preparation.

The Production Control Quantometer consists of the source unit, the spectrometer, and the recording console. The source unit is the Applied Research Laboratories 5700 Controlled Multisource, providing various excitations from low-voltage arc to low-voltage spark as required by the analytical programme.

To ensure stability of power supply, a Schindler motor generator set is available, the output of which is electronically controlled, any change of voltage or frequency being corrected within 4 cycles. An alternative supply from the mains is available via a Zenith stabilizer as a standby.

The spectrometer cabinet contains a 1·5-m spectrometer covering a range of 2000–7000 Å. The grating is ruled 24,400 lines/in. and the dispersion is 6·95 Å/mm in the first order and 3·5 Å/mm in the second order. Three slit frames carrying the slits to isolate the required spectral lines are on the Rowland circle. These slit frames are capable of external adjustment to ensure alignment with the spectral lines. On each frame is a selected iron line which serves as ' monitor ' for this alignment. Sited near the grating is a tungsten-filament lamp which is automatically operated between analysis runs to keep the photo-tubes in a fatigued state. This lamp also serves the purpose of checking optical alignment and circuit performances.

The excitation stand is mounted on the spectrometer unit, the electrode supports being water-cooled. A gauge is attached for adjustment of a 3-mm gap between sample and counter electrode.

The spectrometer unit has thermostatically controlled heater elements incorporated to maintain additional precise temperature conditions.

The recording console contains integrators, the measuring circuits for the photo-currents, the power supplier, the attenuators controlling the photo-tube sensitivities, the amplifier, and a Leeds Northrup recorder. Included also in this unit are the timing and switching mechanisms and zero and sensitivity controls for each channel. The integrator units each

Table I

SPECTRAL LINES, RANGES (%), AND GROUPS

Element	Spectral Line	C, Low- and High-alloy Steels		Slags and Sinters		Monitors
		A Low-voltage spark 1	B Low-voltage arc 1	D Low-voltage spark 3	E Low-voltage arc 3	F Low-voltage spark 1
P	2149·1	...	...	0·5–8·0 A 5·0–20·0 B	...	...
Cu	2192·6	0·5–1·5	...	...	...	...
Ni	2316·0	0·1–1·5 A 1·0–5·5 B	...	...	...	...
Fe	2368·8	...	...	...	...	Monitor 2
Fe	2395·6	...	...	0·1–5·0 A	...	...
Si	2516·0	0·5–2·5	0·01–0·5	5·0–40·0 A 15·05–20·0 B	...	...
Cr	2677·2	0·1–1·5 A 1·0–4·0 B	...	...	...	...
Fe	2714·4 Internal standard	...	...	...	...	Internal standard 1
Cr	2862·6	15·0–30·0 C	...	...	...	...
Al	3082·2	...	...	0·3–8·0 A 8·0–25·0 B	...	...
Mo	3170·3	0·2–1·2	0·01–0·5	...	...	...
Cu	3274·0	...	0·01–0·5	...	...	...
Ni	3414·8	...	0·01–0·5	...	...	...
Fe	3930·3	...	...	...	...	Monitor 3
Al	3961·3	...	0·005–0·5	...	...	...
Cr	4254·3	...	0·01–0·5	...	...	...
P	2149·1 × 2	...	0·01–0·2	...	...	...
V	4379·8	...	0·005–0·5	...	...	...
Fe	4404·8	...	Internal standard	...	...	...
Ca	4435·0	...	...	16·0–22·0 A 30·0–60·0 B	...	...
Li	4972·0	...	...	Internal standard	Internal standard	...
B	2496·8 × 2	...	0·0002–0·01	...	...	...
Mg	5183·6	...	...	2·0–10·0	0·3–3·0	...
F	5291·0	...	...	...	...	...
Fe	2739·5 × 2	...	...	2·0–12·0 B 10·0–40·0 C	...	...
Pb	2833·1 × 2	...	0·005–0·35	...	...	...
Mn	2933·1 × 2	0·5–2·5	0·01–0·5	1·0–15·0	...	...
Fe	3047·6 × 2	...	...	...	...	Monitor 4
Ti	3242·0 × 2	...	0·005–0·3	...	...	...
Sn	3262·3 × 2	...	0·005–0·5	...	...	...

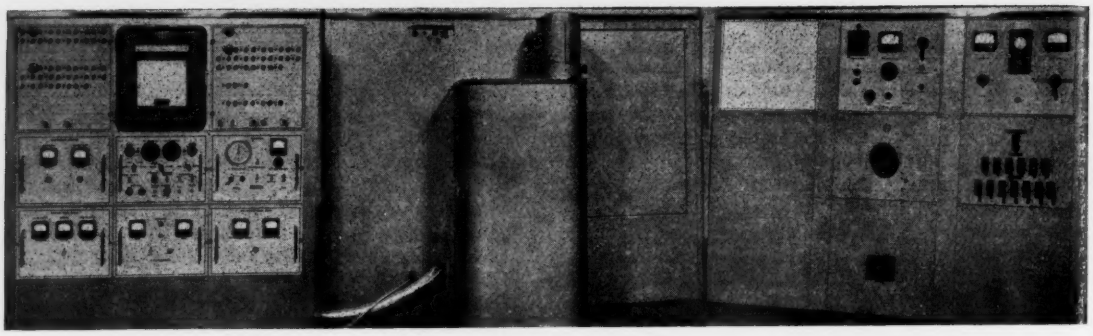

(*a*) Source unit (*b*) Spectrometer (*c*) Recording console

Fig. 2—Complete Quantometer

contain two matched 1·0 μF condensers with a high dielectric constant. For analysis, only one of these is used but both are required for calibration.

During an analytical run, the photo-currents from each tube in circuit charge their respective condenser. The iron internal standard condenser also charges and is connected directly to the amplifier and recording circuits. The recorder reading is traced during the exposure. Integration time is controlled by the time required for this charge to register the full scale of the recorder. At full-scale reading of this internal standard the excitation is automatically terminated. A micro-switch operates and each condenser in the group in turn is connected to the measuring circuit at intervals of 2·6 s. The potential of each is recorded and the readings related to percentage concentration by pre-calibration. The complete instrument is illustrated in Fig. 2.

Calibration for Residuals and Low Alloys

During installation, critical adjustment of the optical system, the individual slits, and slit frames is carried out. Using the test lamp as a light source, final tests are made of electrical reproducibility which should not vary more than 0·5% on 20 consecutive runs.

Actual calibration is entirely based on homogeneous and accurately analysed standards which cover the required percentage ranges. Square bars of at least 1 in. section × 2 in. long are the most suitable size of standard.

In commencing calibration, two standards having concentrations near to the upper and lower limits of the range are selected for each element. Using the specified excitation conditions, an integration is carried out to charge one of the two integrator condensers for the low value and a second integration to charge the other condenser with the high value. The zero control for the channel in question is then adjusted to give a recorder reading near zero for the low concentration and the sensitivity control to give a reading near the top of the scale for the high concentration. This procedure is carried out for each element.

On satisfactory completion of these high and low adjustments the selected number of standards to cover the full range is carried through in turn and the recorder readings are noted. From these readings and the known composition, working curves are prepared for conversion of recorder readings to percentage concentration on unknown samples.

For routine check calibration, which is carried out at least once each shift in routine practice, it is not necessary to use a full range of standards. It is sufficient to use a high- and low-concentration standard for each element being determined. These can be combined in specially prepared pairs of standard samples.

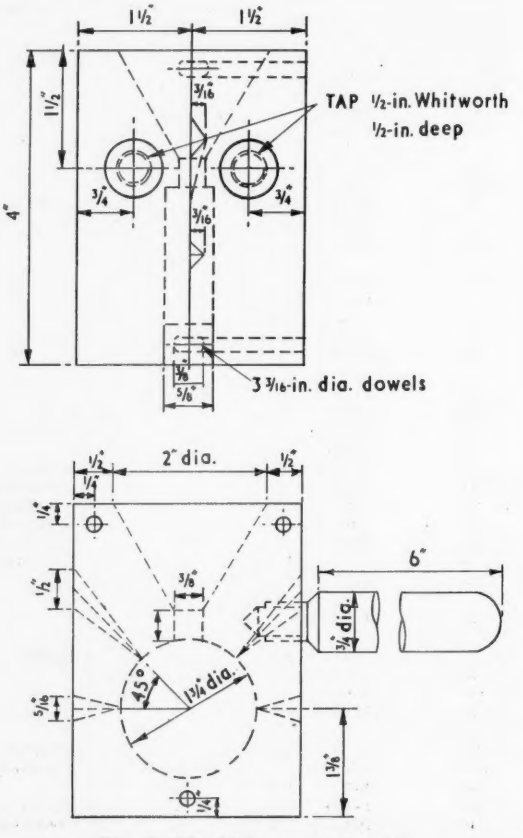

Fig. 3—Mould for cast samples

Application

Attention was first given to low-alloy steels and residual elements in plain carbon steels. The excitation conditions used are:

	Group A Low Alloys	Group B Residuals
Type of discharge	Spark-like	Arc-like
Peak secondary voltage	1000 V	1000 V
Capacitance	10 μF	50 μF
Inductance	120 μH	430 μH
Resistance	5 Ω	50 Ω
Sample	Positive	Positive
Counter electrode	120° cone graphite	120° cone graphite
Gap	3 mm	3 mm

A pre-integration time of 5 s and integration time of 20 s are used for each group.

Samples

In the literature of spectrographic analysis there is some difference of opinion as to the best type of sample to give the highest accuracy and reproducibility. Although the electrode support stand on the Quantometer is water-cooled, it is evident that a minimum size of sample is required to avoid thermal effect. In addition, sufficient area should be available for several successive excitations.

After some trials with pencil and wedge samples a coin or disc type was developed which gave a sample 1·75 in. dia. × 0·625 in. thick. A diagram of the mould used is given in Fig. 3. This type of sample gives good reproducibility on successive excitations. Typical standard deviation figures are given in Table II.

Table II
REPRODUCIBILITY TESTS

Type and No. of Discharges	Element	Concentration, %	Standard Deviation, %
10 spark-like	Ni	2·46	1·8
	Mo	0·98	1·25
10 arc-like	Ni	0·066	2·4
	Cr	0·08	1·6
	Sn	0·032	5·7
	Cu	0·172	1·4
	Mo	0·012	5·9

It cannot be too strongly emphasized that good, sound samples are essential. Routine bath samples are killed with a minimum amount of Al wire before casting. This addition is kept at less than 0·05% by weight, as excess Al has been found to cause third-element interference, particularly with Ni and Cu, when arc-like excitation is used for residual elements.

For final pit samples, 1-in. square forged bars have proved satisfactory.

Table III
COMPARATIVE RESULTS BY QUANTOMETER, PHOTOGRAPHIC, AND CHEMICAL METHODS: RESIDUAL ELEMENTS

Number	Type of Sample	N	Cr	Sn	Cu	Mo	Q = Quantometer S = Spectrograph C = Chemical
16/1169 Bath	Coin	0·10	0·04	0·021	0·16	0·02	Q
		0·09	0·06	0·02	0·16	0·02	S
		0·10	0·07	0·03	0·15	0·03	C
16/1162 Bath	Coin	0·07	0·07	0·026	0·15	0·02	Q
		0·09	0·06	0·02	0·16	0·02	S
		0·09	0·065	0·025	0·15	0·015	C
16/1176 Bath	Coin	0·15	0·04	0·02	0·14	0·04	Q
		0·16	0·04	0·02	0·14	0·05	S
		0·17	0·04	0·01	0·13	0·05	C
19/9443 Bath	Coin	0·04	0·04	0·021	0·12	0·14	Q
		0·04	0·03	0·02	0·13	0·14	S
		0·07	0·04	0·01	0·11	0·165	C
22/7098 Bath	Coin	0·08	0·16	0·024	0·27	0·02	Q
		0·08	0·14	0·025	0·28	0·02	S
		0·09	0·16	0·03	0·29	0·05	C
39/5704 Pit	Forged	0·12	0·03	0·031	0·28	0·02	Q
		0·14	0·03	0·025	0·25	0·01	S
		0·12	0·06	0·03	0·29	0·04	C
35/4319 Pit	Forged	0·17	0·05	0·020	0·25	0·01	Q
		0·13	0·05	0·02	0·24	0·01	S
		0·16	0·06	0·01	0·24	0·02	C
36/2922 Pit	Forged	0·23	0·08	0·028	0·23	0·03	Q
		0·26	0·09	0·03	0·24	0·04	S
		0·24	0·12	0·02	0·24	0·04	C
33/4624 Pit	Forged	0·10	0·04	0·052	0·24	0·01	Q
		0·07	0·06	0·05	0·22	0·01	S
		0·10	0·05	0·04	0·215	0·015	C

The difference in the forged and cast samples has not been found highly significant when dealing with residual and low-alloy concentrations. Efficient sample preparation certainly contributes to the accuracy of results obtained. One surface of the sample is ground flat using a horizontal grinder and finished on a band-facing machine using a belt of 150 grit. This preparation occupies about 2 min.

ROUTINE TESTS

After preparation of the working curves, the technique was applied to routine control. In the early stages a proportion of the figures were checked by the photographic instrument and a number were checked chemically. The agreement was within the usual tolerance of chemical methods. It was established that at least two sparks for residual elements and three for low-alloy steels should be tentative routine practice.

Attention was first centred upon Ni, Cr, Sn, Cu, Mo, and Si, as these were the elements determined in routine practice. A series of representative bath and pit samples was then selected from routine practice and analysed by the Quantometer, the photographic instrument, and by chemical methods. Selections of comparable results are given in Tables III and IV.

Other Elements

Owing to insufficiency of standards and samples, less work has been done on the other elements for which channels are available.

The S.S.11–17 series of spectrographic standards for residual elements was available and has been used for some of this work. Some of the figures issued are tentative, as the chemical figures are still being checked by a B.I.S.R.A. Analysis Committee. Table V gives the quantometric figures for Al, V, and B on this series; Mn was also recorded but these figures only cover a small range and further work is still required on this element; P is also a special item on the research programme still to be completed.

High-alloy Steels

It will be apparent that a different technique will be required for calibration of the instrument for high-alloy steels owing to the wide variation in Fe content. The method finally adopted was based on that recommended by the Applied Research Laboratories. Compensation is made for variation in the iron content by use of the calibrated dial, known as the 'alloy corrector dial,' which is fitted to the Fe (internal standard) channel. In practice this implies previous knowledge of the approximate iron content, but in routine use this knowledge is available within the requisite tolerance. The excitation conditions were the same as for low alloys.

Table IV

COMPARATIVE RESULTS BY QUANTOMETER, PHOTOGRAPHIC, AND CHEMICAL METHODS: LOW ALLOYS

Number	Type of Sample	Ni	Cr	Sn	Cu	Mo	Si	Q = Quantometer S = Spectrograph C = Chemical
16/1250 Bath	Coin	3·15	0·04	0·018	0·13	0·05	...	Q
		3·20	0·06	...	0·14	...	...	S
		3·16	0·05	...	0·16	...	...	C
16/1185 Bath	Coin	0·80	0·09	0·018	0·12	0·02	...	Q
		0·82	0·07	...	0·14	...	...	S
		0·80	0·08	...	0·13	...	...	C
16/1245 Bath	Coin	0·08	3·89	0·022	0·13	0·49	...	Q
		0·06	3·81	...	0·14	0·48	...	S
		0·09	3·91	...	0·10	0·50	...	C
16/1173 Bath	Coin	0·07	0·03	0·022	0·10	0·87	...	Q
		0·05	0·05	...	0·14	0·89	...	S
		0·08	0·05	...	0·11	0·90	...	C
16/1251 Pit	Forged	1·49	1·02	0·022	0·12	0·26	0·330	Q
		1·53	1·04	0·020	0·14	0·24	...	S
		1·55	1·01	...	...	0·29	0·315	C
16/1257 Pit	Forged	3·26	0·10	0·019	0·12	0·02	0·200	Q
		3·25	0·08	0·020	0·14	0·03	...	S
		3·22	...	...	...	...	0·192	C
16/1282 Pit	Forged	0·12	4·72	0·026	0·14	0·54	0·470	Q
		0·08	4·83	0·02	0·15	0·55	...	S
		...	4·72	...	...	0·57	0·490	C
17/7535 Pit	Forged	2·46	0·79	0·018	0·10	0·55	0·280	Q
		2·43	0·79	0·02	0·13	0·51	...	S
		2·43	0·75	...	...	0·51	0·275	C
19/9447 Pit	Forged	2·81	0·86	0·018	0·07	0·52	0·310	Q
		2·79	0·83	0·02	0·10	0·53	...	S
		2·80	0·85	...	...	0·51	0·295	C

Table V
RESULTS ON S.S. SPECTROGRAPHIC STANDARDS

No.	Mn		Al		V		B	
	Quantometer	Issued Figure	Quantometer	Issued Figure	Quantometer	Issued Figure	Quantometer	Issued Figure
SS11	0·42	0·47	0·01*	0·01	Trace	Trace	0·010	0·019
SS12	0·48	0·48	0·06*	0·06	0·013	0·01	0·0037	0·004
SS13	0·47	0·48	0·045	0·06	0·05	0·05	0·0018	0·002
SS14	0·51	0·51	0·035	0·04	0·02	0·02	0·008*	0·008
SS15	0·48	0·49	0·02	0·03	0·057	0·06	0·001*	0·001
SS16	0·51	0·48	0·03	0·03	0·057	0·07	0·0047	0·006
SS17	0·51	0·50	0·012	0·02	0·11	0·12	Trace	Trace

* Samples used for calibration. For Mn and V, private standards were used.

DETAILS OF CALIBRATION

For calibration and test purposes 45 samples of widely varying alloy content were obtained. The major alloy elements covered ranges of Cr 10·0–24·0%, Ni 7·0–15·0%, and Mo 1·6–3·0%, with an iron content of 50·0–90·0%. Some of the samples also contained smaller amounts of Ti, Nb, or V.

As Cr was the major alloying element and, in this research programme, the one for which the highest accuracy was desired, the initial calibration was based on this element.

In principle, the calibration is in three stages: the construction of a primary Cr graph, calibration of the alloy corrector dial, and construction of working curves for the ranges to be covered. For the first two stages, which are interrelated, it is necessary to have a minimum of five samples of known analysis, three of which should have a similar Fe content but varying Cr, and two or more with similar Cr content and varying Fe. One of these samples can be common to both groups.

Six samples were used in this series:

	Fe, %	Cr, %
1	68·21	23·82
2	67·72	17·28
3	67·96	10·06
4	49·10	23·54
5	76·78	14·2
6	86·0	12·5

Samples 1, 2, and 3 with similar Fe content were used to construct the primary Cr graph illustrated in Fig. 4.

Calibration of the alloy corrector dial was next carried out by preparation of an Fe correction curve using samples 1, 4, 5, and 6. This is illustrated in Fig. 5.

Working curves were next prepared to cover the full range of Cr content in the samples available. The earlier calibration and the construction of these curves were carried through using straight Ni–Cr steels, a suitable selection being made from the series. In order to ensure highest accuracy, two curves were prepared covering ranges 7·0–15·0% Cr, and 14·0–21·0% Cr respectively. The samples were sparked using the alloy corrector dial setting appropriate to each sample and graphing recorder reading against Cr percentage direct. Typical curves are shown in Fig. 6.

A further selection of Ni–Cr steels containing Nb, Ti, and/or Mo, and some straight Cr steels was carried through and the results referred to the Ni–Cr steel graph. Straight Cr steels plotted with the Ni–Cr and

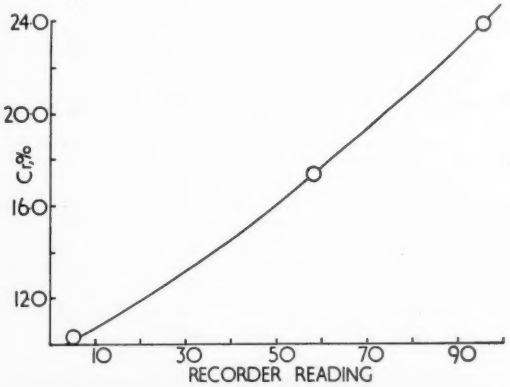

Fig. 4—Primary Cr graph for high Cr steels

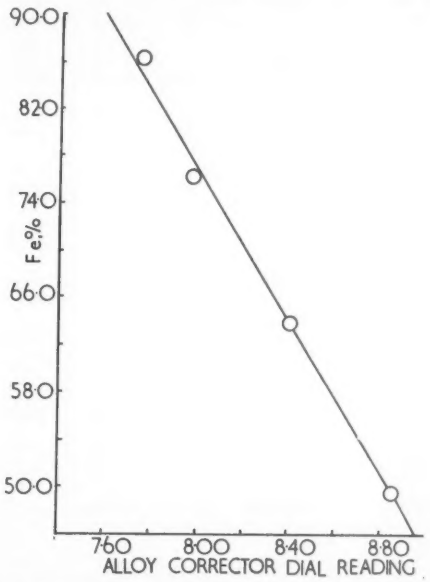

Fig. 5—Iron correction curve for high Cr steels

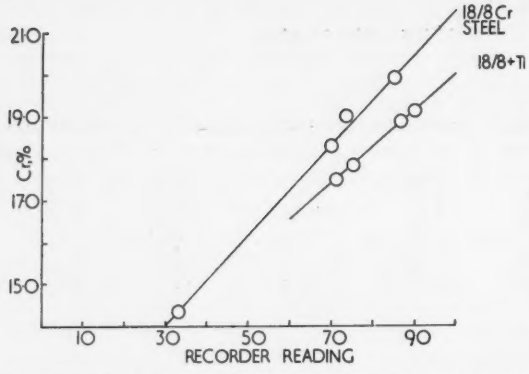

Fig. 6—Typical Cr working curves for stainless steels

Nb at the 1% level had no apparent influence on the Cr determinations. Ti (0·20–1·0%) and Mo (0·30–2·8%) both influenced the results, and separate graphs were necessary. The line for Ti-bearing samples is shown in Fig. 6.

Other Elements

Although this instrument was not designed for extensive analysis of high-alloy steels it was decided to extend the investigation as far as possible to include Ni, Si, Mn, and Mo. No channel was available for Nb and insufficient standards for Ti. It was found possible to extend the Ni range to 15%, to close a gap in the Cr range between 5% and 15% and to extend the range for Mo to 3·2%. The Si and Mn channels in use for low-alloy steels could be used for this series.

The necessary working curves were prepared from suitable samples in the series.

PROCEDURE FOR ROUTINE ANALYSIS

The samples used for calibration and test were all of known analysis. For routine work where the true analysis is not known, an additional step was necessary which involved the use of the 'sum corrector' incorporated in the instrument.

The type of steel under test is usually known. The alloy corrector dial is first adjusted to an approximation of Fe content and an analysis through at this setting. The sum of Si, Mn, Ni, Cr (C etc.), and Fe (as set on the alloy corrector dial) is then obtained. If the total is 100% then the recorded values are correct. If the total deviates from 100% by $\pm 2\%$ or less, the 'sum corrector' is set to the value of the sum total, and by means of the recycle switch, the values are recorded again. The sum corrector automatically multiplies each value by $100/x$ where x equals the sum. If the first total deviates by more

Table VI

COMPARATIVE RESULTS BY QUANTOMETER AND CHEMICAL METHODS: HIGH ALLOY STEELS

Type	No.	C	Si	Mn	Ni	Cr	Mo	Ti	Nb	Q = Quantometer C = Chemical
13% Cr	E3604	...	0·31	0·48	...	14·1	...	...	...	Q
RR229		0·25	0·30	0·49	0·27	14·06	...	...	...	C
18% Cr	C799	...	0·41	0·58	...	17·25	...	...	...	Q
SF.18		0·15	0·37	0·60	1·85	17·20	...	...	...	C
C Cr	C846	...	0·67	0·62	...	13·57	...	...	...	Q
		2·21	0·66	0·57	0·10	13·60	...	...	...	C
12/12 NiCr	D168	...	0·39	0·56	12·38	13·08	...	...	...	Q
SF.21		0·08	0·42	0·54	12·28	13·00	...	...	...	C
20% Cr	D312	...	0·53	0·55	10·10	19·76	...	...	...	Q
SF.620		0·06	0·54	0·58	9·90	19·56	...	...	...	C
18/8	C828	...	0·49	0·46	10·02	19·10	...	...	...	Q
SF.620		0·06	0·49	0·47	10·0	18·80	...	...	...	C
18/8 MoTi	F4160	...	0·67	0·61	9·50	18·50	1·58	...	...	Q
SF.25		0·06	0·72	0·62	9·48	18·48	1·72	0·42	...	C
18/8 Mo	C827	...	0·47	0·43	8·80	18·44	2·50	...	...	Q
SF.35		0·07	0·47	0·45	8·96	18·44	2·81	...	...	C
18/8 Ti	F4180	...	0·64	0·53	8·24	18·19	...	...	...	Q
SF.22		0·06	0·70	0·55	8·22	18·40	...	0·60	...	C
18/8 Ti	C813	...	1·40	0·75	8·11	18·70	...	...	...	Q
SF.23		0·08	1·35	0·73	8·32	18·72	...	0·64	...	C
18/8 Nb	B7384	...	0·54	0·52	9·30	18·60	...	...	...	Q
SF.26		0·07	0·63	0·54	9·18	18·40	...	...	0·98	C
—	F641	...	0·43	0·61	6·70	15·4	...	...	...	Q
		0·18	0·44	0·56	6·72	15·26	0·18	...	...	C

than ± 2% from 100% it is necessary to run the sample through again with a new setting of the alloy corrector dial.

As a test of the accuracy of the instrument and the method employed, a further series of 12 unknown samples was analysed. The final results and corresponding chemical analyses are given in Table VI.

Comment on Results

For residual elements and low alloys the accuracy is well within the limits required and the figures compare very favourably with the slower traditional chemical methods. For high-alloy steels the Ni and Cr results are highly satisfactory. Several Si and Mn figures and the two Mo results show some discrepancy. It should be stated, however, that these latter elements on high-alloy steels hardly come within the terms of reference for the research programme and insufficient standards were available.

PRODUCTION CONTROL

The instrument has now been in use for several months for routine control almost 24 h daily. From every charge a melting sample is sent from the melting shops to the spectrographic laboratory by pneumatic tube. The transit time is 4 min from the Templeborough Shop and rather less from the Rotherham Melting Shop. The sample is prepared by grinding and finishing which occupies 2 min. A single sparking and recording occupies 1 min. Transmission of a written record of the results back to the melting shops by a further electronic instrument takes less than 2 min. The whole operation from taking of the sample to receipt of results is thus completed in 10 min or less.

At the start of each shift or when necessary, the routine calibration with high and low standards and checking of the monitors is carried out. The time required for this procedure naturally varies with the adjustments to be made and the number of standards. In our case the time is not more than 15 min.

Use is made of these figures for production control. Some plain carbon steel specifications now include maximum limits for certain residual elements. In addition there is a special schedule of maximum residuals depending upon the steel quality and purpose. Any casts exceeding these maxima can quickly be diverted to less rigorous specifications with less dislocation of melting shop or mill programmes. For low-alloy steels, earlier addition of alloying materials can be made and a further sample sent down for check on these additions, thus giving more precise control.

The final pit samples are also checked for the relevant elements, and numerous other miscellaneous samples are also analysed. At present about 500 reported determinations are put through per day and this will be increased as further use is made of the Quantometer.

The adoption of production control by this instrument at Steel, Peech and Tozer will undoubtedly assist the production rate, as has already been done at the electric furnace plant. It also gives closer control over steelmaking conditions and composition of the final products. Finally, it relieves the analytical load on the chemical section of the laboratories.

References

1. F. Twyman and A. Harvey: *J. Iron Steel Inst.*, 1932, No. II, pp. 397–407.
2. F. Twyman and A. A. Fitch: *Ibid.*, 1930, No. II, pp. 289–300.
3. F. G. Barker: *Ibid.*, 1939, No. I, pp. 211p–245p.
4. H. T. Shirley and E. Elliott: *Ibid.*, 1943, No. I, pp. 299p–337p.
5. H. T. Shirley, E. Elliott, and J. Meeds: *Ibid.*, 1947, vol. 157, pp. 391–409.
6. Spectrographic Analysis of Low-Alloy Steels, *Iron Steel Inst. Spec. Rep.* No. 47, 1952.
7. M. F. Hasler and H. W. Dietert: *J. Opt. Soc. Amer.*, 1944, vol. 34, No. 12, pp. 751–758.
8. M. F. Hasler, R. W. Lindhurst, and J. W. Kemp: *Ibid.*, 1948, vol. 38, No. 9, pp. 789–799.
9. A. Argyle: *J. West Scotland Iron Steel Inst.*, 1954–55, vol. 62, pp. 27–44.
10. Ramsden: *B.N.F.M.R.A.*, Reports RRA. 959, RRE. 390.

N E W S

Announcements and News of Science and Industry

THE IRON AND STEEL INSTITUTE

Special Reports

Combustion and Heat Transfer in an Open-hearth Furnace

The latest addition to the Special Report series of the Institute is entitled " Combustion and Heat Transfer in an Open-Hearth Furnace," by S. W. Pearson, M. W. Thring, and J. H. Chesters. This report describes a large-scale trial carried out on a Templeborough furnace with a team consisting of groups from Steel, Peech and Tozer, the Research and Development Department of the United Steel Companies Ltd., the University of Sheffield, and the British Iron and Steel Research Association.

The previous Templeborough trials, reported in Special Report No. 37 (1946), emphasized the necessity for aerodynamic studies, continuous roof-temperature measurement, and the maintenance of the highest practicable furnace pressure. The shift from producer gas to oil firing in the last ten years has added new objectives, e.g. the determination of optimum nozzle size, steam/oil ratio, and burner direction. The work of the International Flame Radiation Committee at Ijmuiden has given preliminary answers to some of the questions, whilst the theory of heat transfer initially expounded in Special Report No. 37 has been developed to a point where calculated melting times and fuel consumptions are of the same order as those found in practice. The main purpose of the present trial was to measure as many factors as possible, leaving only one free parameter in each verifiable part of the calculation; this could then be determined from the observed result and the value thus obtained used with some confidence in future calculations. A subsidiary objective was the comparison of flow pattern and mixing in model and furnace.

The Report, No. 59 in the series, is fully illustrated with diagrams and photographs and is bound in cloth with stiff board covers. Copies are available from the Offices of the Institute, price 37*s*. 6*d*. (Members 25*s*.).

Proceedings of the Forgemasters' Meeting, 1954

In October, 1954, The Iron and Steel Institute held a joint meeting with the National Forgemasters' Association and La Chambre Syndicale de la Grosse Forge Française. Technical Sessions were held in London at which nine papers on forging theory, practice, and plant were presented and discussed. The remainder of the Meeting comprised visits to the English Steel Corporation Ltd., Thos. Firth and John Brown Ltd., and Hadfields Ltd., in Sheffield.

The Proceedings at the Technical Sessions are shortly to be published as a Special Report, which will be No. 60 in the series.

NEWS OF MEMBERS

Dr. **M. L. Becker** has relinquished his position as Head of the Metallurgy Division of the British Iron and Steel Research Association and taken an appointment as Technical Director of the Chrome Alloying Co., Ltd., Hatfield, and of Diffusion Alloys Ltd., London Bridge House, S.E.1.

Mr. **Tom Bishop**, Editor of *Metal Treatment*, is leaving Industrial Newspapers Ltd. in January to join the metallurgical staff of John Miles and Partners (London) Ltd.

Mr. **D. R. Brown** has been appointed Director of the Blast Furnace Division of the Power-Gas Corporation Ltd.

Dr. **R. D. Carter** has been appointed Technical Manager of the Wire Mill Division of British Insulated Callender's Cables, Ltd., Prescot, Lancashire.

Mr. **D. Howell Davies** has left the R.T.S.C. Laboratories to join B.I.S.R.A. at their South Wales Laboratories as a Scientific Officer.

Mr. **W. H. Glaisher** has left B.I.S.R.A. and is now on the Management Training Staff of the British Iron and Steel Federation at Hoyle Street, Sheffield.

Dr. **A. T. Green,** O.B.E., Director of Research of the British Ceramic Research Association, was the recipient of a Special Annual Insignia Award in Technology of the City and Guilds of London Institute in 1956.

Dr. **T. A. Henderson** is at present on leave in England from Rho-Anglo Mine Services Ltd., Kitwe, Northern Rhodesia. He is retiring later this month to take up the position of Chief of the Metallurgical Study Section of Rhokana Corporation Ltd., N'Kana.

Mr. **A. M. Horsfield** has transferred from the London headquarters of the British Welding Research Association to the Association's Engineering Research Laboratories, Abington Hall, near Cambridge.

Mr. **J. H. John** has retired from his position as Chairman and Director of the Bynea Steel Works Ltd., Loughor, Swansea, owing to ill-health.

Mr. **W. M. May** has been awarded the degree of B.Sc. (Met.) at Durham University, and has also passed the L.I.M. examination.

Mr. **H. W. Morgan** has been appointed Joint Managing Director of the Bynea Steel Works Ltd., and other companies in the group.

Mr. **D. Morris** has graduated from the Royal School of Mines with First Class Honours in Metallurgy, and is now Personal Assistant to the Foundry Superintendent at APV-Paramount Ltd., Crawley.

Mr. **E. H. Parfrey** has transferred to the Nuclear Power Branch of the Central Electricity Authority.

Mr. **B. N. Prasad** has joined the technical staff of the South Durham Steel and Iron Co., Ltd., in the General Laboratory.

Mr. **R. W. Ruddle** is relinquishing his appointment as Head of the Melting and Casting Section of the British Non-Ferrous Metals Research Association on 31st January, 1957, and is taking up the post of Technical Manager with Foundry Services Inc., Columbus, O., U.S.A., an associate company of Foundry Services Ltd., Birmingham.

Mr. **C. Storey** has left the Research and Development Department of the United Steel Companies Ltd. to take

up a position as Ceramic Engineer with the Consett Iron Co., Ltd.

Mr. **B. Sweeney** has left the B.I.S.R.A. Sheffield Group to become Research Metallurgist with the Permanent Magnet Association, Sheffield.

Mr. **F. V. Wright** has joined W. S. Atkins and Partners as Manager of their Birmingham office.

Mr. **E. J. Wynne** has been awarded the degree of B.Sc. of Durham University.

Obituary

Mr. **Vivian Westgarth Davison,** B.MET. (*elected* 1935), on 28th April, 1955.

Mr. **Edward Houghton** (*elected* 1905), of Chesterfield, on 30th October, 1956.

Mr. **Harold Maltby Long,** O.B.E. (*elected* 1938), of Montreal, Canada, on 20th February, 1956.

CONTRIBUTORS TO THE JOURNAL

J. J. J. Belli, M.SC.—At present with H.M. Forces.

Mr. Belli studied chemistry at University College, Swansea, and graduated B.Sc. (Hons.) in 1952. He was granted a Research Scholarship by the Northampton Polytechnic, London, where he has been engaged on research into the constitution of inclusions in steel. He was awarded the degree of M.Sc. by London University as a result of a thesis dealing with the nature of inclusions.

J. E. Garside, M.SC. TECH., F.R.I.C., F.I.M., M.INST.F.—Principal, Borough Polytechnic, London, S.E.1.

Dr. Garside was educated at the Central High School for Boys, Manchester and the College of Technology (Faculty of Technology), University of Manchester. From 1924 to 1931, he was a foundry apprentice with Metropolitan-Vickers Electrical Co., Ltd., Manchester, and in 1934 graduated as B.Sc. with 1st Class Honours in Applied Chemistry. He became M.Sc. Tech. in 1935 after metallurgical research on acoustical resonance in steels. In 1944, he was awarded the degree of Ph.D. by London University for research into the physical chemistry of solutions.

Dr. Garside, who is a Constantine Medallist of the Manchester Association of Engineers, was Assistant Lecturer in Metallurgy at Coventry Technical College from 1935 to 1937; he became Lecturer in, and later Head of, the Department of Applied Chemistry at Northampton Polytechnic in 1937, and was appointed Principal of Borough Polytechnic in 1956.

A. M. Godridge, M.SC.—British Coal Utilisation Research Association, Leatherhead, Surrey.

Mr. Godridge was educated at Reading School and the University of Reading. Since 1952 Mr. Godridge has been employed in the Physics Department of B.C.U.R.A. on problems mainly associated with the measurement of gas temperature.

D. Manterfield, F.I.M.—Chief Chemist, Steel, Peech and Tozer, Sheffield.

Mr. Manterfield was educated at the Central Secondary School and the Applied Science Department of Sheffield University. After a brief period with Vickers Ltd. (now English Steel Corporation Ltd.) he joined Steel, Peech and Tozer as a metallurgical chemist. He was appointed Works Chemist in 1930, and became Chief Chemist of the laboratories in 1947. Mr. Manterfield, who is a Fellow of the Institution of Metallurgists, has served as Chairman of the B.I.S.R.A. Raw Materials, Slags and Refractories Analysis Sub-committee, and is Chairman of the United Steel Companies Chemists Sub-committee.

T. E. Rooney, A.M.C.T.—Borough Polytechnic, London, S.E. 1.

Mr. Rooney studied metallurgy at the Manchester School of Technology (now the College of Technology), from 1902 to 1905 and was awarded the Associateship of the College. He subsequently became Assistant Chemist and Metallurgist with W. T. Glover and Co., Ltd., and later Chief Chemist and Metallurgist with Berger, Peacock and Co., Ltd. For 38 years he was a member of the staff of the Department of Metallurgy and Metallurgical Chemistry of the National Physical Laboratory. For many years he was a Fellow of the Royal Institute of Chemistry. Since his retirement from the N.P.L., Mr. Rooney has been engaged on research work on inclusions in steel at the Northampton and the Borough Polytechnics, London.

S. W. K. Shaw, B.SC.—National Gas Turbine Establishment, Farnborough.

Mr. Shaw was born at Sheffield in 1929 and educated at Buxton College and Sheffield University. He graduated with Honours in Physics in 1950 and joined the Department of Metallurgy, where he carried out work on the formation of carbide in Cr–V steels under Professor Quarrell.

W. S. Sykes—Chief Spectrographer, Steel, Peech and Tozer, Sheffield.

Mr. Sykes was educated at Hipperholme Grammar School, near Halifax, and Ackworth School, near Pontefract. In 1920 he joined the laboratory staff of the Denaby and Cadeby Collieries as an apprentice chemist. He continued his apprenticeship the following year in the laboratory of John Firth and Sons Ltd. In 1923 he joined the staff of Steel, Peech and Tozer as a steelworks chemist. Mr. Sykes transferred to the laboratory's spectrographic section in 1941, and was appointed Chief Spectrographer in 1949.

G. G. Thurlow, M.SC.(ENG.), A.M.INST.F., GRAD.I.MECH.E.—British Coal Utilisation Research Association, Leatherhead, Surrey.

Mr. Thurlow graduated at the University of Bristol in Mechanical Engineering in 1945 and joined the Technical

J. E. Garside

A. M. Godridge

S. W. K. Shaw

G. G. Thurlow

Department of the Bristol Aeroplane Co. (Engine Division), working on problems associated with engine cooling. In 1947 he joined the British Coal Utilisation Research Association, studying the occurrence of deposits and corrosion on the fire-side of water-tube boilers. The work included investigations on industrial and pilot plant. In 1950 he was awarded the degree of M.Sc. for work on regenerative air preheaters.

Since 1953 Mr. Thurlow has been in charge of a team engaged in heat-transfer studies, chiefly concerned with heat flow from flames in furnaces and boilers. A principal part of this programme has consisted of a study of flame and waste-gas temperatures.

INSTITUTE OF METALS

The Metallurgical Engineering Committee of the Institute of Metals is holding an all-day Informal Discussion on "Degreasing" in the University, Edgbaston, Birmingham, on Wednesday, 27th February, 1957. The meeting will be open to both members and non-members. Those who would like to be present should notify the Secretary of the Institute of Metals, 17 Belgrave Square, London, S.W.1, as early as possible.

EDUCATION

Awards for Essays and Papers on Corrosion Science

The Education Panel of the Corrosion Group, with the approval of the Council of the Society of Chemical Industry, last year established a competition designed to encourage those who are still in the early stages of their career to take an interest in corrosion science and to express their ideas in writing. With the support of industrialists interested in the application of corrosion science in industry, a prize of the value of 25 guineas will again be awarded this year for an essay or paper on any aspect of corrosion of metals and its prevention.

Essays are invited from persons aged not more than 27 years on the closing date. A length about 4000 words is suggested, but reasonable latitude is allowable.

The closing date for receipt of entries is 31st March, 1957. Further details from:

Corrosion Group Essay Competition,
c/o Society of Chemical Industry,
14 Belgrave Square,
London, S.W.1.

United Steel Lectureship in Statistics

The United Steel Companies, Ltd. have agreed to assist the University of Sheffield to create an independent Department of Statistics. Dr. G. H. Jowett, formerly lecturer in statistics at the university, has been appointed head of the new department and took up his new duties at the beginning of the current academic session. Dr. Jowett's post carries the rank of senior lecturer and will be known as "The United Steel Lectureship." Before joining the university, Dr. Jowett was a member of the staff of United Steel's Research and Development Department.

National Council for Technological Awards

The National Council for Technological Awards now has its own premises at 9, Cavendish Square, London, W.1 (telephone: MUSeum 1978).

NEWS OF SCIENCE AND INDUSTRY

New British Standards

A revised edition of B.S. 1328 "*Methods of sampling water used in industry*" covers requirements for the sampling and physical testing of water for industrial purposes. It deals with the size of samples, with containers and their labelling, and with sampling of water of the following types: raw water, treated or softened water, feed water, boiler water, condensate and distillate, water from vessels under reduced pressure, and water for the determination of dissolved oxygen. The Standard costs 6*s*.

Another Standard which has been revised is B.S. 500 "*Steel railway sleepers for flat bottom rails*," first published in 1933. The revised edition was produced to provide for the change in practice in ordering railway sleepers; it deals with steel quality, provision of test samples, templates, and gauges, methods of manufacture, cleaning and dipping, and inspection during manufacture, and costs 3*s*. 6*d*.

Two new Standards for cast iron have also been issued recently. A new edition of B.S. 1452 "*Grey iron castings*" (price 4*s*.) incorporates certain results obtained from publication of the 1948 edition; these include the introduction of the transverse test instead of the tensile test for control and regularity of product, the introduction of a test sample in place of very large test bars for large or heavy castings, and amendment of the deflection requirement in the transverse test. A graph given as an Appendix shows the strength to be expected in different running thicknesses of the same casting. B.S. 2789 "*Iron castings with spheroidal or nodular graphite*" is a new Standard to cover this recently developed type of iron and costs 3*s*. 6*d*.

The important B.S. 1121 "*Methods for the analysis of iron and steel*" has been revised to some extent, and a new part has been issued. The revised parts are 14 "*Determination of copper in iron and steel*" and 25 "*Determination of vanadium in iron, steel and ferro-vanadium*"; the new part is 36 "*Absorptiometric determination of copper in iron and steel.*" Parts 14 and 36 cost 2*s*. and Part 25 2*s*. 6*d*.

Copies of all the Standards mentioned can be obtained from the British Standards Institution, Sales Branch, 2 Park Street, London, W.1.

Quantometer for Stocksbridge

A new and complex instrument at the Stocksbridge works of Samuel Fox and Co., Ltd., is cutting the time taken to analyse samples of stainless steel from 1 h to 15 min. Known as a Quantometer, the Swiss-made instrument provides direct readings of the elements contained in a steel sample in as little as 4 min, although it takes several minutes extra to prepare the sample for examination and a little longer to convey it from the melting shop to the laboratory.

When a cast of over 70 tons of stainless steel was made in the large electric furnace at Stocksbridge recently, the Quantometer was called in to help with the final analysis of this massive quantity of special steel just before it left the furnace, something which has never been possible before because of the time factor.

The United Steel Companies Ltd. installed the first Quantometer at their Steel, Peech and Tozer branch early in 1955. Details of this instrument, which is in routine use, are given in a paper on p. 105 of this issue of the *Journal*.

British Timken at Daventry

The foundation stone of the Daventry factory of British Timken Ltd. was laid in June, 1954, and the works is now in full production. It was specifically designed for the manufacture of the heavier tapered roller bearings; the smaller types are made at the Company's works at Duston, Northampton.

The layout of the Daventry factory is in the form of an **E**; the arms of the **E** are respectively preparation, heat-treatment, and finishing bays. The layout is such

that expansion, which is already in progress, will be relatively easy. A large proportion of the production at Daventry is of bearings for four-high, blooming and slabbing, plate, billet, section, and rod mills. The bearings are made of case-hardening high-nickel steel which provides the hard wear-resisting surface and tough shock-resistant core necessary for the conditions the bearings must work under.

Double Duo Mill for Kayser Ellison

A 10¼-in. double duo rolling mill has recently been installed by Kayser, Ellison and Co., Ltd., of Sheffield. The mill, of four stands, with provision for a fifth, was built by Brightside Foundry and Engineering Co., Ltd.

Corrigendum

In the paper "The Occurrence of Sigma-Phase in a High-Chromium–Nickel Steel," by L. Pryce, H. Hughes, and K. W. Andrews (*J. Iron Steel Inst.*, 1956, Nov., vol. 184, pp. 289–301), the reference letters (*a*), (*b*), (*c*), (*d*), and (*e*) alongside Figs. 1 and 2 should read from bottom to top, and not from top to bottom as in the printed version. Thus on Fig. 1 (p. 292), the top row of micrographs should be marked (*e*)—i.e. water-quenched after 4 h at 1250° C.

DIARY

3rd Jan.—INSTITUTE OF METALS (London Local Section)—"The Metallurgical Challenge of Nuclear Power," by Dr. H. K. Hardy—17 Belgrave Square, London, S.W.1, 6.30 P.M.

3rd Jan.—LEEDS METALLURGICAL SOCIETY—"Some High-temperature Properties of Copper Alloys," by Dr. J. P. Dennison—Large Chemistry Lecture Theatre, The University, Leeds, 7.15 P.M.

7th Jan.—CLEVELAND INSTITUTION OF ENGINEERS—"Visit to Russia," by Dr. T. P. Colclough and F. Kennedy—Cleveland Scientific and Technical Institution, 6.30 P.M.

7th Jan.—INSTITUTE OF BRITISH FOUNDRYMEN (Sheffield and District Branch)—"Foundry Maintenance," by G. J. Jenkins—Sheffield College of Commerce and Technology, Pond Street, Sheffield, 1, 7 P.M.

8th Jan.—INSTITUTE OF METALS (Oxford Local Section)—"Gases in Metals," by Dr. C. E. Ransley—Cadena Café, Cornmarket Street, Oxford, 7 P.M.

8th Jan.—INSTITUTION OF ENGINEERING INSPECTION—"The Inspection of Electrodeposits," by N. A. Tope—Coventry Technical College, 7.30 P.M.

8th Jan.—INSTITUTION OF ENGINEERING INSPECTION—Film: "A Century of Engineering Tool Development" (English Steel Corp. Ltd.)—Leeds Church Institute, Albion Place, Leeds 1, 7.30 P.M.

8th Jan.—INSTITUTION OF ENGINEERING INSPECTION—"The Manufacture, Testing, and Inspection of Springs," by C. Harris—Grand Hotel, Broad Street, Bristol, 7.30 P.M.

8th Jan.—SHEFFIELD METALLURGICAL ASSOCIATION—Annual General Meeting of the Methods of Analysis Group—B.I.S.R.A. Laboratories, Hoyle Street, Sheffield 3, 7 P.M.

9th Jan.—SOCIETY OF CHEMICAL INDUSTRY (CORROSION GROUP)—"Corrosion Problems in Nuclear Power Production," by A. B. McIntosh—14 Belgrave Square, London, W.1, 6.30 P.M.

10th Jan.—EBBW VALE METALLURGICAL SOCIETY—"Symposium on Skin Passing," by F. W. Lewis, J. B. Davies, E. L. Sullivan, and F. G. Rees—Lecture Room, Richard Thomas and Baldwins Ltd., Ebbw Vale, 7.15 P.M.

10th Jan.—STAFFORDSHIRE IRON AND STEEL INSTITUTE—"Extrusion and Its Modern Applications," by A. B. Graham—Star and Garter Royal Hotel, Wolverhampton, 7.30 P.M.

14th Jan.—INSTITUTION OF ENGINEERING INSPECTION—"Quality Control," by A. D. McGregor—Royal British Hotel, Dundee, 7.30 P.M.

14th Jan.—INSTITUTION OF PRODUCTION ENGINEERS (Sheffield Section)—"Material Handling," by D. H. Outwin—Grand Hotel, Sheffield, 6.30 P.M.

14th Jan.—LINCOLNSHIRE IRON AND STEEL INSTITUTE—"The Influence of Modern Trends in Ironmaking on the Energy Balance of the Ironworks," by J. Szczeniowski—North Lindsey Technical College, Scunthorpe, 7.30 P.M.

15th Jan.—INSTITUTE OF METALS (South Wales Local Section)—"Fatigue," by P. L. Teed—Department of Metallurgy, University College, Singleton Park, Swansea, 6.45 P.M.

15th Jan.—SHEFFIELD METALLURGICAL ASSOCIATION—Annual General Meeting of the Refractories Group—B.I.S.R.A. Laboratories, Hoyle Street, Sheffield 3, 7 P.M.

16th Jan.—INSTITUTE OF WELDING—"Fabrication of Power Station Plant," by W. G. Brown—Cleveland Scientific and Technical Institution, 7.30 P.M.

16th Jan.—MANCHESTER METALLURGICAL SOCIETY—"Physical Chemistry in Extraction Metallurgy," by Dr. F. D. Richardson—Central Library, Manchester, 6.30 P.M.

18th Jan.—INSTITUTION OF ENGINEERING INSPECTION—"Practical Welding Inspection," by J. Taylor—Neath Public Library, 7.30 P.M.

21st Jan.—NORTH EAST METALLURGICAL SOCIETY—"The Industrial Development of Tees-side," by J. C. H. Booth—Constantine Technical College, Middlesbrough, 7.15 P.M.

21st Jan.—SHEFFIELD SOCIETY OF ENGINEERS AND METALLURGISTS—"The Work of the Department of Metallurgy, Sheffield University," by Professor A. G. Quarrell—Engineering Lecture Theatre, St. George's Square, Sheffield, 7.30 P.M.

22nd Jan.—INSTITUTION OF PRODUCTION ENGINEERS—"Precision Casting," by J. S. Turnbull—Cleveland Scientific and Technical Institution, 7 P.M.

22nd Jan.—NEWPORT METALLURGICAL SOCIETY (joint meeting with INSTITUTE OF BRITISH FOUNDRYMEN)—"The Mechanism of Solidification of Cast Iron," by H. Morrogh—Whitehead Iron and Steel Institute, Newport, 7 P.M.

22nd Jan.—SHEFFIELD METALLURGICAL ASSOCIATION—Annual General Meeting—B.I.S.R.A. Laboratories, Hoyle Street, Sheffield 3, 7 P.M.

23rd Jan.—INSTITUTION OF ENGINEERING INSPECTION—"General Principles of Steel Wire Drawing," by Dr. R. Goodacre—Birmingham Exchange and Engineering Centre, 7.30 P.M.

28th Jan.—INSTITUTE OF BRITISH FOUNDRYMEN (Sheffield and District Branch)—Annual Dinner—Royal Victoria Hotel, Sheffield.

30th Jan.—INSTITUTE OF BRITISH FOUNDRYMEN (London Branch)—"High-duty Iron-castings Production," by C. R. van der Ben—Constitutional Club, Northumberland Avenue, London, W.C.2, 7.30 P.M.

30th Jan.—MANCHESTER METALLURGICAL SOCIETY—"The Preparation of Germanium and Silicon for use in Semiconductor Devices," by S. E. Bradshaw—Central Library, Manchester, 6.30 P.M.

4th Feb.—CLEVELAND INSTITUTION OF ENGINEERS—"Road versus Rail," by S. C. Pearson—Cleveland Scientific and Technical Institution, 6.30 P.M.

4th Feb.—INSTITUTE OF BRITISH FOUNDRYMEN (Sheffield and District Branch)—"Some Aspects of the CO_2 Process," by I. Reese and D. H. Snelson—Sheffield College of Commerce and Technology, Pond Street, Sheffield 1, 7 P.M.

4th Feb.—INSTITUTE OF WELDING (Sheffield and District Branch)—"Metal Spraying," by R. Wallwork—Grand Hotel, Sheffield, 7.15 P.M.

5th Feb.—SHEFFIELD METALLURGICAL ASSOCIATION—"Spectrography," by M. Z. de Lippa—B.I.S.R.A. Laboratories, Hoyle Street, Sheffield 3, 7 P.M.

5th–8th Feb.—NATIONAL METALLURGICAL LABORATORY OF INDIA—Symposium on Mineral Beneficiation and Extractive Metallurgical Techniques—Jamshedpur.

7th Feb.—INSTITUTE OF METALS (London Local Section)—"Beryllium," by B. Kjellgren—17 Belgrave Square, London, S.W.1, 6.30 P.M.

7th Feb.—LEEDS METALLURGICAL SOCIETY—"Fuel Ash Corrosion Problems," by Professor A. Preece—Large Chemistry Lecture Theatre, The University, Leeds, 7.15 P.M.

8th Feb.—NORTH EAST COAST INSTITUTION OF ENGINEERS AND SHIPBUILDERS—"Ceramic Materials for High-temperature Gas Turbines," by T. H. Blakeley—Mining Institute, Newcastle-upon-Tyne, 6.15 P.M.

TRANSLATIONS SERVICE

(The previous announcement was made in the December, 1956, issue of the *Journal*, p. 465).

TRANSLATIONS AVAILABLE

No. 515 (Russian). N. K. LEONIDOV: "The New Russian 2000-m³ Blast-furnace." (*Stal*, 1956, No. 2, pp. 115–124).

TRANSLATIONS IN COURSE OF PREPARATION

(German). O. EMICKE and K.-H. LUCAS. "Factors Influencing the Accuracy of the Rolling of Sheet and Strip. Their Control by Experiment and by Calculation." (*Neue Hütte*, 1956, vol. 1, Mar., pp. 257–274).

(German). W. KAFKA. "A New Method of Electrode Control with Magnetic Amplifiers." (*Stahl u. Eisen*, 1956, vol. 76, 5th Apr., pp. 381–387; Discussion, pp. 387–389).

ABSTRACTS OF CURRENT LITERATURE AND BOOK NOTICES

Iron and Steel Manufacture and Related Subjects

CONTENTS

	PAGE
Abbreviations and List of Periodicals	118
Ores—Mining and Treatment	123
Fuel—Preparation, Properties, and Uses	123
Temperature Measurement and Control	124
Refractory Materials	124
Iron and Steel, General	124
Blast-Furnace Practice and Production of Pig Iron	125
Treatment and Use of Slags	125
Production of Steel	126
Production of Ferro-Alloys	127
Foundry Practice	127
Reheating Furnaces and Soaking Pits	129
Heat-Treatment and Heat-Treatment Furnaces	129
Forging, Stamping, Drawing, and Pressing	130
Rolling Mill Practice	130
Machinery for Iron and Steel Plant	131
Lubrication	132
Welding and Flame-Cutting	132
Machining and Machinability	134
Cleaning and Pickling	134
Protective Coatings	135
Powder Metallurgy	135
Ferrites, Cermets, and Carbides	136
Properties and Tests	136
Metallography	141
Corrosion	144
Analysis	147
Industrial Uses and Applications	149
Historical	150
Economics and Statistics	150
Miscellaneous	150
Book Notices	150
New Publications	152

ABBREVIATIONS AND LIST OF PERIODICALS EXAMINED BY THE ABSTRACTING SERVICE

Abhandlungen der **Braunschweigischen wissenschaftlichen Gesellschaft** (Brunswick)
Acciaio e Costruzioni Metalliche (Milan)
Acciaio Inossidabile (Milan)
Acero y Energia (Barcelona)
Acier Stahl Steel (Brussels)
Aciers Fins et Spéciaux Français (Paris)
Acta Crystallographica (London)
Acta Metallurgica (Toronto)
Acta Physica Polonica (Warsaw)
Acta Polytechnica (Stockholm)
Acta Technica (Budapest)
Advancement of Science (London)
Advances in Physics (London)
Aeroplane (London)
Aircraft Engineering (London)
Aircraft Production (London)
Alloy Castings Bulletin (New York)
Alloy Metals Review (Widnes)
Alluminio (Milan)
Aluminium (Düsseldorf)
Aluminium Development Association, Information Bulletin (London)
American Ceramic Society Bulletin (Columbus, Ohio)
American Foundrymen's Society, Preprint (Chicago)
American Gas Association Monthly (New York)
American Institute of Mining and Metallurgical Engineers (New York)
Blast Furnace, Coke Oven & Raw Materials Committee, Proceedings
Electric Furnace Steel Conference Proceedings
Proceedings National Open-Hearth Committee
Proceedings Symposia Series
American Iron and Steel Institute (New York)
Annual Statistical Report
Contributions to the Metallurgy of Steel
Steel Products Manual
American Journal of Physics (New York)
American Journal of Science (New Haven, Conn.)
American Society for Metals (Cleveland, Ohio)
Preprint
Review of Metal Literature
American Society for Testing Materials (Philadelphia)
Bulletin
Preprint
Special Technical **Publication**
Anais da Academia Brasileira de Ciencias (Rio de Janeiro)
Anais Associacao Brasileira de Quimica (Sao Paulo)
Anales de la Asociacion Quimica Argentina (Buenos Aires)
Anales de la Real Sociedad Española de Fisica y Química (Madrid)
Anales de Mecanica y Electricidad (Madrid)
Analyst (London)
Analytica Chimica Acta (New York and Amsterdam)
Analytical Chemistry (Washington)
Annales des Mines (Paris)
Annales de la Société Scientifique de Bruxelles (Brussels)
Annual Proceedings of the Sheet and Strip Metal Users' Technical Association (London)
Annual Report of the Smithsonian Institution (Washington)
Annual Review of Physical Chemistry (Stanford, California)
Anvil (Sheffield)
Applied Mechanics Reviews (New York)
Applied Research Laboratories, Reports (Glendale, Calif.)
Applied Scientific Research (The Hague)
Archiv für das Eisenhüttenwesen (Düsseldorf)
Archiwum Elektrotechniki (Warsaw)
Arkiv för Kemi (Stockholm)
Arkiv för Mineralogi och Geologi (Stockholm)
Arts et Manufactures (Paris)
Atomics (London)
Atti della **Accademia** Nazionale dei **Lincei**, Classe di Scienze Fisiche, Matematiche e Naturali (Rome)
Memorie
Rendiconti
Australasian Engineer (Sydney)
Australian Journal of Applied Science (Melbourne)
Australian Journal of Chemistry (Melbourne)
Australian Journal of Physics (Melbourne)
Australian Machinery and Production Engineering (Sydney)
Automation in Industry (London)
Automation Progress (London)
Automobile Engineer (London)
Avtomaticheskaya Svarka (Kiev)

B.C. Professional Engineer (Vancouver)
B.H.P. Review (Melbourne)
Ball Bearing Journal (Luton)

Battelle Technical Review (Columbus, Ohio)
Beama Journal (London)
Bell Laboratories Record (New York)
Bell System Technical Journal (New York)
Bell Telephone Magazine (New York)
Bell Telephone System Technical Publication (New York)
Berg- und hüttenmännische Monatshefte (Vienna)
Bibliographical Bulletin of Welding (Paris)
Blad för Bergshandteringens Vänner (Stockholm)
Blast Furnace and Steel Plant (Pittsburgh)
Board of Trade Journal (London)
Boletim da Associação Brasileira de Metais (São Paulo)
Boletim da Sociedade Geológica de Portugal (Oporto)
Boletin Minero e Industrial (Bilbao)
Brennstoff–Warme–Kraft (Dusseldorf)
British Cast Iron Research Association, Journal of Research and Development (Birmingham)
British Coal Utilisation Research Association, Monthly Bulletin (London)
British Coke Research Association, Technical Papers (London)
British Constructional Steelworks Association (London)
Publications
British Dental Journal (London)
British Electrical and Allied Industries Research Association, Reports (London)
British Engine Boiler and Electrical Insurance Co. Ltd. (Manchester)
Technical Report
British Engineering (London)
British Foundryman (Manchester)
British Iron and Steel Research Association, Reports (London)
British Journal of Applied Physics (London)
British Productivity Council (London)
Publications
British Standards Institution (London)
British Standards
Handbook
Specifications for Aircraft Materials
British Steel Founders' Association (Sheffield)
B.S.F.A. Bulletin
British Steelmaker (London)
British Welding Journal (London)
Brown-Boveri Review (Baden)
Bulletin de l'Académie Polonaise des Sciences (Warsaw)
Classe Quatrième
Classe Troisième
Bulletin of the British Scientific Instrument Research Association (London)
Bulletin de Cercle d'Etudes des Métaux (St. Etienne)
Bulletin of The Geological Institutions of The University of Uppsala (Uppsala)
Bulletin of The Geological Survey of Great Britain (London)
Bulletin de L'Institut Polytechnique de Jassy (Jassy)
Bulletin of the Institute of Metal Finishing (London)
Bulletin of the Institution of Metallurgists (London)
Bulletin of the Institution of Mining and Metallurgy (London)
Bulletin of Ohio State University Engineering Experiment Station (Columbus, O.)
Bulletin of the School of Mines and Metallurgy, University of Missouri (Minneapolis)
Bulletin des Sociétés Chimiques Belges (Brussels)
Bulletin of The Technical University of Istanbul (Istanbul)
Bulletin Téchnique de la Société Française des Constructions Babcock & Wilcock (Paris)

Calore (Milan)
Canada Department of Mines and Technical Surveys, Mines Branch (Ottawa)
Technical Paper
Canadian Journal of Chemistry (Ottawa)
Canadian Journal of Physics (Ottawa)
Canadian Journal of Technology (Ottawa)
Canadian Metals (Toronto)
Canadian Mining Journal (Quebec)
Canadian Mining and Metallurgical Bulletin (Montreal)
Castings (Sydney)
Centre de Documentation Sidérurgique, Circulaires d'Informations Techniques (Paris)
Centre d'Études Supérieurs de la Sidérurgie (Metz)
Les Cahiers du CESSID
Ceramics (Leighton Buzzard)
Chaleur et Industrie (Paris)
Chartered Mechanical Engineer (London)
Chemical Age (London)
Chemical Engineering (New York)
Chemical Engineering and Mining Review (Melbourne)
Chemical and Engineering News (Washington)
Chemical Engineering Progress (New York)
Chemical & Process Engineering (London)
Chemické Listy (Prague)
Chemisch Weekblad (Amsterdam)
Chemist-Analyst (Phillipsburg, N.J.)
Chemistry and Industry (London)
Chimica e Industria (Milan)
Chimie Analytique (Paris)
Chimie et Industrie (Paris)
Chrome Dur (Paris)
Ciencia y Tecnica de la Soldadura (Madrid)
Circular of the National Bureau of Standards (Washington)
Circular of Ohio State University Engineering Experiment Station (Columbus)
Claycraft (London)
Coke and Gas (London)
Coke Review (London)
Collection of Czechoslovak Chemical Communications (Prague)
Colliery Guardian (London)
Colonial Geology and Mineral Resources (London)
Colorado School of Mines, Quarterly (Golden, Colorado)
Commonwealth Engineer (Melbourne)
Comptes Rendus Hebdomadaires des Séances de l'Académie des Sciences (Paris)
Congrès du Groupement pour l'Avancement des Méthodes d'Analyse Spectrographique (Paris)
Corrosion (Houston, Texas)
Corrosion et Anti-Corrosion (Paris)
Corrosion Prevention and Control (London)
Corrosion Technology (London)
Corrosione (Rome)
Coventry Engineering Society Journal (Coventry)
Czechoslovak Heavy Industry (Prague)

Dansk Teknisk Tidsskrift (Copenhagen)
Davy and United Engineering (Sheffield)
Demag News (Duisburg)
Department of Scientific and Industrial Research (London)
Miscellaneous Reports
Discussions of the Faraday Society (London)
Documentation Métallurgique (Paris)
Doklady Akademii Nauk S.S.S.R.
Draht (English edition) (Coburg)
Draht (German edition) (Coburg)
Dyna (Barcelona)

ESAB Revue (Göteburg)
E.S.C. News (Sheffield)
Echo des Mines (Paris)
Edgar Allen News (Sheffield)
Eidgenossische Materialprüfungs- und Versuchsanstalt für Industrie, Bauwesen und Gewerbe, Berichte (Zürich)
Electrical Engineer and Merchandiser (Melbourne)
Electrical Journal (London)
Electrical Review (London)
Electrical Times (London)
Electronic Engineering (London)
Electroplating and Metal Finishing (London)
Elektrotechnik (Prague)
Elektrotechniski Vestnik (Ljubljana, Yugoslavia)
Elektrowärme Technik (Mindelheim)
Elliott Journal (London)
Endeavour (London)
Engenharia, Mineração e Metalurgia (Rio de Janeiro)
Engineer (London)
Engineer and Foundryman (Braamfontein, Johannesburg)
Engineering (London)
Engineering and Boiler House Review (London)
Engineering Journal (Montreal)
Engineering and Mining Journal (New York)
Engineers' Digest (London)
English Electric Journal (Stafford)
Escher-Wyss News (Zürich)

F & G Rundschau (Köln-Mülheim)
First Iron Works Association, Gazette (Saugus, Mass.)
Fizika Metallov i Metallouedenie (Moscow)
Fonderia Italiana (Milan)
Fonderie (Paris)
Forschung auf dem Gebiete des Ingenieurwesens (Düsseldorf)
Forschungsberichte des Wirtschafts- und Verkehrsministeriums Nordrhein-Westfalen (Köln and Opladen)
Foundry (Cleveland)
Foundry and Metal Treating (Sydney)
Foundry Trade Journal (London)
Fuel (London)
Fuel Economy Review (London)

Fuel Society Journal (Sheffield)
Fulmer Research Institute (Stoke Poges)
Special Report
Translations

G.E.C. Journal (London)
G.E.C. Telecommunications (Coventry)
Galvano (Paris)
Gas Council (London)
Research Communication
Gas Times (Watford)
Gas World (London)
Gazzetta Chimica Italiana (Rome)
General Motors Engineering Journal (Detroit)
Génie Chimique (Paris)
Génie Civil (Paris)
Geologiska Föreningens Förhandlingar (Stockholm)
Giesserei (Düsseldorf)
Giesserei Technisch Wissenschaftliche Beihefte (Düsseldorf)
Giessereitechnik (Berlin)
Gjuteriet (Stockholm)
Glückauf (Essen)
Government Mechanical Laboratory Bulletin (Tokyo)

Härterei-Technische Mitteilungen (Stuttgart)
Hutnické Listy (Prague)
Hutnik (Prague)
Hutnik (Poland)

IVA Ingeniörs Vetenskaps Akademien (Stockholm)
Illinois University Engineering Experiment Station (Urbana)
Circular
Bulletin
Indian Journal of Physics (Calcutta)
Industria y Química (Buenos Aires)
Industrial Chemist (London)
Industrial and Engineering Chemistry (Washington)
Industrial Finishing (Leighton Buzzard)
Industrial Gas (Leighton Buzzard)
Industrial Heating (Pittsburgh)
Industrial Heating Engineer (London)
Industrie Nationale (Paris)
Ingegneria Meccanica (Milan)
Ingenieria e Industria (Buenos Aires)
Ingeniörs Vetenskaps Akademien, Handlingar (Stockholm)
Inspection Engineer (London)
Institut pour l'Encouragement de la Recherche Scientifique, Comptes Rendus de Recherches (Brussels)
Institut Mashinovedeniya, Trenie i Iznos v Mashinakh (Moscow)
Institute of British Foundrymen, Paper (Manchester)
Institute of Fuel, Advance Copies (London)
Institute of Petroleum, Review (London)
Institute of Vitreous Enamellers (Ripley, nr. Derby)
Bulletin
Institution of Gas Engineers, Communications (London)
Instituto del Hierro y del Acero (Madrid)
Instituto de la Soldadura, Publicacíon (Madrid)
Instituto Sperimentale dei Metalli Leggeri, Relazione Annuale (Milan)
Instituto Nacional del Carbon Boletin Informativo (Oviedo)
Instrument Engineer (Luton)
Instrument Practice (London)
International Union of Crystallography (Utrecht)
Structure Reports
Iron Age (New York)
Iron and Coal Trades Review (London)
Iron and Steel (London)
Iron and Steel Engineer (Pittsburgh)
Iron and Steel Institute, Special Reports (London)
Izvestiya Akademii Nauk S.S.S.R., Otdelenie Khimicheskikh Nauk (Moscow)
Izvestiya Akademii Nauk, S.S.S.R., Otdelenie Teknicheskikh Nauk (Moscow)
Izvestiya Akademii Nauk S.S.S.R., Seriya Fizicheskaya (Moscow)

Jernindustri (Oslo)
Jernkontorets Annaler (Stockholm)
Journal of the American Ceramic Society (Columbus, Ohio)
Journal of the American Chemical Society (Washington, D.C.)
Journal of the American Society of Naval Engineers (Washington, D.C.)
Journal of the American Water Works Association (New York)
Journal of the American Zinc Institute (New York)
Journal of Applied Chemistry (London)
Journal of Applied Mechanics (New York)
Journal of Applied Physics (New York)
Journal of The Australian Institute of Metals (Victoria)
Journal of the Birmingham Metallurgical Society (Birmingham)
Journal of the British Institution of Radio Engineers (London)
Journal of The British Nuclear Energy Conference (London)
Journal of the British Shipbuilding Research Association (London)
Journal of Chemical Physics (New York)
Journal of the Chemical Society (London)
Journal de Chimie Physique (Paris)
Journal of Dental Research (Baltimore)
Journal of the Electrochemical Society (Baltimore)
Journal du Four Electrique (Paris)
Journal of the Franklin Institute (Lancaster, Pa.)
Journal of the Indian Chemical Society (Calcutta)
Journal of The Indian Institute of Science (Bangalore)
Journal d'Informations Techniques des Industries de la Fonderie (Paris)
Journal of the Institute of Australian Foundrymen (Melbourne)
Journal of the Institute of Fuel (London)
Journal of the Institute of Metals (London)
Journal of the Institute of Petroleum (London)
Journal of the Institution of Automotive and Aeronautical Engineers (Melbourne)
Journal of the Institution of Electrical Engineers (London)
Journal of the Institution of Engineers, Australia (Sydney)
Journal of the Institution of Heating and Ventilating Engineers (London)
Journal of the Institution of Locomotive Engineers (London)
Journal of the Institution of Production Engineers (London)
Journal of The Iron and Steel Institute (London)
Journal of the Junior Institution of Engineers (London)
Journal of The Liverpool Engineering Society (Liverpool)
Journal of Mechanical Laboratory (Tokyo)
Journal of the Mechanics and Physics of Solids (London)
Journal of Metals (New York)
Journal of the Optical Society of America (New York)
Journal of Petroleum Technology (Dallas, Texas)
Journal of the Physical Society of Japan (Tokyo)
Journal de Physique et le Radium (Paris)
Journal and Proceedings of the Royal Society of New South Wales (Sydney)
Journal of Research of the National Bureau of Standards (Washington, D.C.)
Journal of the Royal Aeronautical Society (London)
Journal of the Royal Artillery (London)
Journal of the Royal Institute of British Architects (London)
Journal of the Royal Institute of Chemistry (London)
Journal of the Royal Microscopical Society (London)
Journal of the Royal Society of Arts (London)
Journal of the Royal Statistical Society (London)
Journal of Scientific and Industrial Research (New Delhi)
Journal of Scientific Instruments (London)
Journal of the Scientific Research Institute (Tokyo)
Journal of the Society of Glass Technology (Sheffield)
Journal of The South African Institute of Mining and Metallurgy (Johannesburg)
Journal and Transactions of the Society of Engineers (London)
Journal of the West of Scotland Iron and Steel Institute (London)

Kohászati Lapok (Budapest)

Laboratoria N.V. Philips' Gloeilampfabrieken, Separaat (Eindhoven)
Lastechniek (The Hague)
Light Metal Age (Chicago)
Light Metals (London)
Liteĭnoe Proizvodstvo (Moscow)
Lithgow Journal (Glasgow)

Machine Design (Cleveland, Ohio)
Machine Shop Magazine (London)
Machinery (Brighton)
Machinery Lloyd (London)
Man and Metal (London)
Manchester Association of Engineers, Preprints (Manchester)
Maschinenbau und Wärmewirtschaft (Vienna)
Maschinenwelt und Elektrotechnik (Vienna)
Materials and Methods (New York)
Mechanical Engineering (New York)
Mechanical Handling (London)

Mechanical **World** and Engineering Record (London)
Memoirs of the **Faculty** of **Engineering Kyoto University** (Kyoto)
Memoirs of the **Faculty** of **Engineering Kyushu University** (Fukuoka)
Memoirs of The **Faculty** of **Science Kyushu** University (Fukuoka)
Memoirs of the **Faculty** of **Technology, Tokyo Metropolitan University** (Tokyo)
Memoirs of The **Geological Survey** of Great Britain (London)
Memoirs of the **Geological Survey** of **India** (Calcutta)
Mémoires de la Société des **Ingénieurs Civils** de **France** (Paris)
Mémorial de l'**Artillerie Française** (Paris)
Metaalinstitut T.N.O. (Delft)
Publication
Metal Age (London)
Metal Bulletin (London)
Metal Finishing (New York)
Metal Finishing Journal (London)
Metal Industry (London)
Metal Progress (Cleveland, Ohio)
Metal Treating (New Rochelle, N.Y.)
Metal Treatment and Drop Forging (London)
Metalen (The Hague)
Metall (Berlin)
Metalloberfläche (Munich)
Metallurg (Moscow)
Metallurgia (Manchester)
Metallurgia **Italiana** (Milan)
Metallurgical Reviews (London)
Métallurgie et la **Construction Mécanique** (Paris)
Metals **Review** (**Cleveland**, Ohio)
Metalurgia si **Constructia** de **Masini** (Bucharest)
Metalurgia y **Electricidad** (Madrid)
Metalworking Production (London)
Métaux–Corrosion–Industries (Paris)
Metropolitan **Vickers Gazette** (Manchester)
Microtecnic (Lausanne)
Midwest Engineer (Chicago, Ill.)
Mine and **Quarry Engineering** (London)
Mineralogical Magazine (London)
Mining, Electrical and **Mechanical Engineer** (Manchester)
Mining Engineering (New York)
Mining Journal (London)
Mining Magazine (London)
Mitteilungen aus dem **Max-Planck-Institut** für **Eisenforschung** (Düsseldorf)
Modern **Castings** (Des Plaines, Ill.)
Modern **Foundry** (Melbourne)
Modern Metals (Chicago)
Murex Review (Rainham, Essex)

Nachrichten aus der **Eisen-Bibliothek** der **Georg Fischer** Aktiengesellschaft (**A.G.**) (Schaffhausen)
National **Bureau** of **Standards** (Washington, D.C.)
Miscellaneous Publication
Technical News Bulletin
National **Physical Laboratory** (Teddington)
Notes on Applied Science
Report
National **Science Foundation Translations** (Washington)
Nature (London)
Neue Hütte (Berlin)
New Scientist (London)
New Zealand Engineering (Wellington)
New Zealand Journal of **Science** and **Technology** (Wellington)
Nickel Bulletin (London)
Nippon Kinzoku Gakkai-Si (Sendai)
Non-Destructive Testing (Evanston, Ill.)
Norsk Geologisk Tidsskrift (Oslo)

Oil Engine and Gas Turbine (London)
Operational Research Quarterly (London)
Optima (Johannesburg)
Osaka University, Faculty of **Engineering Technology Reports** (Osaka)
Overseas Engineer (London)

PACT (Prevention des Accidents Contrôles Techniques Hygiene et Maladies Professionnelles) (Paris)
Paliva (Prague)
Peintures, Pigments, Vernis (Paris)
Philippine Geologist (Manila)
Philips Research Reports (Eindhoven)
Philips Technical Review (Amsterdam)
Philosophical Magazine (London)
Philosophical Transactions of the **Royal Society** (London)
Physical Review (New York)
Planseeberichte für Pulvermetallurgie (Reutte, Tyrol)
Plating (Jenkintown, Pa.)
Post **Office Electrical Engineers' Journal** (Epsom)
Powder Metallurgy Bulletin (Yonkers, N.Y.)
Prace Instytutów Mechaniki (Warsaw)
Prace Instytutów Ministerstwa Hutnictwa (Stalinogrod)
Pratique du **Soudage** (Brussels)
Precision Metal Molding (Cleveland)
Proceedings, American Gas Association (New York)
Proceedings of the **American Society** for **Testing Materials** (Philadelphia)
Proceedings of the **Annual Convention** of the **American Electroplaters' Society** (Jenkintown, Pa.)
Proceedings, Australasian Institute of **Mining** and **Metallurgy** (Melbourne)
Proceedings of the **Cambridge Philosophical Society** (London)
Proceedings, Chemical Engineering Group (London)
Proceedings, Diesel Engine Users' Association (London)
Proceedings of the **Durham Philosophical Society** (Durham)
Proceedings of the **Ebbw Vale Metallurgical Society** (Ebbw Vale)
Proceedings of the **Indian Academy** of **Sciences** (Bangalore)
Proceedings of the **Indiana Academy** of **Sciences** (Greencastle, Ind.)
Proceedings of the **Institute** of **Australian Foundrymen** (Melbourne)
Proceedings of The **Institute** of **Vitreous Enamellers** (Ripley, nr. Derby)
Proceedings of the **Institution** of **Electrical Engineers** (London)
Proceedings, Institution of **Mechanical Engineers** (London)
Proceedings of the **Institution** of **Mechanical Engineers, Automobile Division** (London)
Proceedings of the **Japan Academy** (Tokyo)
Proceedings of The **Leeds Philosophical** and **Literary Society** (Leeds)
Proceedings of the **Lincolnshire Iron** and **Steel Institute** (Scunthorpe)
Proceedings, Metal Powder Association (New York)
Proceedings of the **Physical Society** (London)
Proceedings of the **Royal Canadian Institute** (Toronto)
Proceedings of the **Royal Institution** of Great Britain (London)
Proceedings of the **Royal Society** (London)
Proceedings of the **Royal Society** of **Edinburgh** (Edinburgh)
Proceedings of the **Society** of **Experimental Stress Analysis** (Cambridge, Mass.)
Proceedings of the **South Wales Institute** of **Engineers** (Cardiff)
Proceedings of the **Staffordshire Iron** and **Steel Institute** (Walsall)
Process Control and **Automation** (London)
Product Engineering (New York)
Product Finishing (London)
Products Finishing (Cincinnati)
Pro-Metal (Berne)
Przeglad Odlewnictwa (Cracow)
Przeglad Techniczny (Warsaw and Lodz)
Publications de l'**Association** des **Ingénieurs** de la **Faculté Polytechnique** de **Mons** (Mons)
Publications de l'**Institut** de **Recherches** de la **Sidérurgie** (St. Germain-en-Laye)
Publications Scientifiques et **Techniques** du Ministère de **L'Air** (Paris)
Purdue University, Engineering Experimental Department (Lafayette, Ind.)
Engineering **Extension Series**
Engineering **Research Series**

Quarterly Journal of **Mechanics** and **Applied Mathematics** (Oxford)
Queensland Government Mining Journal (Brisbane)

Radex Rundschau (Radenthein)
Railway Gazette (London)
Railway Steel Topics (Sheffield)
Recherche Aéronautique (Paris)
Records of the **Geological Survey** of **India** (Calcutta)
Recueil des **Travaux Chimiques** des **Pays-Bas** (The Hague)
Refractories Journal (London)
Regional Technical Meetings of the **American Iron** and **Steel Institute** (New York)
Report of The **Government Mechanical Laboratory** (Tokyo)
Reports of the **Scientific Research Institute** (Tokyo)
Research (London)
Research Association of **British Paint, Colour** and **Varnish Manufacturers' Review** (Teddington)
Review of **Scientific Instruments** (New York)
Reviews of **Modern Physics** (New York)
Revista de **Ciencia Aplicada** (Madrid)
Revista de **Quimica Industrial** (Rio de Janeiro)
Revue de l'**Aluminium** (Paris)
Revue de la **Faculté** des **Sciences** de l'**Université** d'**Istanbul**
Revue Générale de **Mécanique** (Paris)

Revue de l'Industrie Minérale (St. Etienne)
Revue d'Informations de la Fédération Royale des Associations Belges d'Ingénieurs (Brussels)
Revue de Métallurgie (Paris)
Revue du Nickel (Paris)
Revue des Produits Chimiques (Paris)
Revue de la Soudure (Lastijdschrift) (Brussels)
Revue de la Société Royale Belge des Ingénieurs et des Industriels (Brussels)
Revue Technique Luxembourgeoise (Luxembourg)
Revue Universelle des Mines (Liége)
Rheology Bulletin (New York)
Roll'schen Eisenwerke A.G. (Gerlafingen, Switzerland)
Mitteilungen
Werkzeitung
Royal School of Mines Journal (London)
Rudarsko-Metalurski Zbornik (Ljubljana)

S.A.E. Journal (New York)
Schweissen und Schneiden (Brunswick)
Schweisstechnik (Vienna)
Schweizer Archiv für Wissenschaft und Technik (Solothurn, Switzerland)
Science Abstracts (London)
Science and Engineering (Calcutta)
Science Reports of the Tôhoku University (Sendai, Japan)
Science Reports of the Research Institutes, Tôhoku University (Sendai, Japan)
Scientific Lubrication (Broseley, Shropshire)
Scientific Proceedings of the Royal Dublin Society
Sheet Metal Industries (London)
Shipbuilder and Marine Engine-Builder (Newcastle-upon-Tyne)
Silicates Industriels (Brussels)
Slévárenství (Prague)
Soudage et Techniques Connexes (Paris)
South African Mechanical Engineer (Johannesburg)
Spectrographic News Letter (Glendale, Calif.)
Stahl und Eisen (Düsseldorf)
Stainless Steel Review (London)
Stal' (Moscow)
Stanki i Instrument (Moscow)
Statens Provningsanstalt (Stockholm)
Berättelse
Meddelande
Steam Engineer (London)
Steel (Cleveland, Ohio)
Steel Processing (Pittsburgh)
Steel Review (London)
Steelways (New York)
Structural Engineer (London)
Suiyokwai-Shi, Transactions of the Mining and Metallurgical Alumni Association (Japan)
Sulzer Technical Review (Winterthur)
Sumitomo Metals (Osaka)
Sveriges Geologiska Undersökning, Arsbok (Stockholm)
Svetsaren (Gothenburg)
Swansea and District Metallurgical Society, Advance Copies (Gorseinon)
Swiss Technics (Lausanne)

Technical Reports of The Engineering Research Institute, Kyoto University (Kyoto)
Technik (Berlin)
Technique et Humanisme (Liège)
Techniques et Civilisations (St. Germain-en-Laye)
Technische Mitteilungen (Rheinhausen)
Technische Mitteilungen Krupp (Essen)
Tecnica e Industria (Buenos Aires)
Tecnica Metalúrgica (Barcelona)
Teknillisen Kemian Aikakausilehti (Helsinki)
Teknisk Tidskrift (Stockholm)
Teknisk Ukeblad (Oslo)
Tetsu-to-Hagane (Tokyo)
Tidsskrift for Kjemi, Bergvesen og Metallurgi (Oslo)
Times Review of Industry (London)
Tin and its Uses (Greenford)
Tisco (Jameshedpur)
Tokyo University, Journal of the Faculty of Engineering (Tokyo)
Torch (London)
Transactions of the American Foundrymen's Society (Chicago)
Transactions of the American Institute of Electrical Engineers (New York)
Transactions of the American Institute of Mining and Metallurgical Engineers (New York)
Transactions of the American Society of Mechanical Engineers (New York)
Transactions of the American Society for Metals (Cleveland, Ohio)
Transactions of The Australian Institute of Metals (Victoria)
Transactions of the British Ceramic Society (Stoke-on-Trent)
Transactions of the Canadian Institute of Mining and Metallurgy (Montreal)
Transactions of the Danish Academy of Technical Sciences (Copenhagen)
Transactions of the Faraday Society (London)
Transactions of the Indian Institute of Metals (New Delhi)
Transactions of the Institute of Marine Engineers (London)
Transactions of The Institute of Metal Finishing (London)
Transactions of the Institution of Chemical Engineers (London)
Transactions of the Institution of Engineers and Shipbuilders in Scotland (Glasgow)
Transactions, Institution of Gas Engineers (London)
Transactions of the Institution of Mining Engineers (London)
Transactions of the Institution of Mining and Metallurgy (London)
Transactions of the Institution of Naval Architects (London)
Transactions of the Liverpool Engineering Society (Liverpool)
Transactions, Manchester Association of Engineers (Manchester)
Transactions of the Mining, Geological and Metallurgical Institute of India (Calcutta)
Transactions of the Newcomen Society (London)
Transactions of the North East Coast Institution of Engineers and Shipbuilders (Newcastle-on-Tyne)
Transactions of the Royal Canadian Institute (Toronto)
Transactions of the Royal Society of Canada (Ottawa)
Transactions of the Society of Automotive Engineers (New York)
Transactions of the Society of Instrument Technology (London)
Transactions of the South African Institute of Electrical Engineers (Johannesburg)

United Effort (Pittsburg)
United Nations—Economic Commission for Europe (Geneva)
Quarterly Bulletin of Steel Statistics for Europe
United States Bureau of Mines (Washington, D.D.)
Bulletin
Information Circular
Mineral Industry Survey
Minerals Yearbook
Report of Investigations
United States Geological Survey, Bulletin (Washington)
Usco Magazine (Pretoria)
Usine Nouvelle (Paris)

Vacuum (London)
Vakuum Technik (Berlin)
Varilna Tehnika (Ljubljana)
Värmländska Bergsmannaföreningens Annaler (Filipstad, Sweden)
Verein deutscher Ingenieure Zeitschrift (Düsseldorf)
Vestnik Mashinostroenniya (Moscow)
Vickers Magazine (London)

Waseda University, Report of the Casting Research Laboratory (Tokyo)
Welder (Waltham Cross)
Welding Journal (New York)
Welding and Metal Fabrication (London)
Welding Research Council, Welding Research Council Bulletin Series (New York)
Werkstoffe und Korrosion (Mannheim)
Werkszeitung der Schoeller-Bleckmann Stahlwerke (Vienna)
Western Metals (Los Angeles)
Wild-Barfield Heat-Treatment Journal (Watford, Herts)
Wire Industry (London)
Wire Production (London)
Wire and Wire Products (Stamford, Conn.)

Yearbook of the American Iron and Steel Institute (New York)
Yearbook of the Coke Oven Managers' Association (London)
Yearly Proceedings of the Association of Iron and Steel Engineers (Pittsburgh)

Zastita Materijala (Belgrade)
Zavodskaya Laboratoriya (Moscow)
Zeitschrift für Erzbergbau und Metallhüttenwesen (Stuttgart)
Zeitschrift für Metallkunde (Stuttgart)
Zhurnal Analiticheskoi Khimii (Moscow)
Zhurnal Fizicheskoi Khimii (Moscow)
Zhurnal Prikladnoi Khimii (Moscow)
Zhurnal Tekhicheskoi Fiziki (Moscow)
Zváranie (Bratislava)

ORES—MINING AND TREATMENT

Babbitt's Contribution to Reserve Mining Company's Taconite Operations. R. J. Linney. (*Iron Steel Eng.*, 1956, **33**, March, 73–75). This article describes mining operations at the Reserve Mining Co. at Babbitt. The Company produces a concentrate which runs from 80 to 85%— 325 mesh and which has an average Fe content of 64·5%. The concentrate is processed in a pelletizing plant.—M. D. J. B.

The Phase $CaO \cdot 2Fe_2O_3$ in the System CaO–Fe_2O_3 and its Importance as a Binder in Ore Pellets. J. O. Erdström. (*Jerkontorets Ann.*, 1956, **140**, 2, 101–115). [In English]. An investigation was made to clarify conditions governing the existence of the phase $CaO \cdot 2Fe_2O_3$ and a check was made of the equilibrium conditions prevailing within the parts of the system CaO–Fe_2O_3 which contain more than 50 Mol.% Fe_2O_3. The studies were made on briquettes of calcium oxalate and Fe_2O_3 powder containing various impurities. The effects of adding CaO on pellet strength are discussed.—G. G. K.

Recent Developments—Sintering and Pelletizing. E. N. Hower and J. A. Anthes. (*Iron Steel Eng.*, 1956, **33**, Feb., 60–65). The authors describe recent improvements in the manufacture of sinter on straight line travelling grate sinter machines and in the manufacture of pellets produced on revolving discs. A recent development: The sintering of pellets using only external fuel is described.—M. D. J. B.

Sinter Plant Assessment Trials at Margam. C. Lang and H. Bates. (*J. Iron Steel Inst.*, 1957, **185**, Jan., 86–95). [This issue].

Microradiography Applied to the Study of Sintered Iron Ores. J. M. Bermudez de Castro y Mosquera, J. M. Fuster Casas, and J. A. Boned Sopena. (*Inst. Hiero Acero*, 1956, **9**, Jan., 75–91. *Special Number*). [In Spanish]. Comparative photo-micrographs and photo-microradiographs illustrate this study of the structures and constituents of various Spanish ores and a series of sinters made from them. The sinters were lime-free or had had lime or quick-lime additions in various amounts made to them. The influence of the lime: silica ratio on the type of silicate formed, and many other mineralogical features of the sinters are discussed. (22 references).—P. S.

FUEL—PREPARATION, PROPERTIES, AND USES

Comparison of Various Thermal Methods of Assessing Lignite Quality on an Energy Basis. J. Jilek. (*Paliva*, 1956, **36**, (3), 73–77). [In Czech].

Complexes in Coal. J. Schuyer. (*Chem. Week.*, 1956, **52**, Mar. 31, 234–240). [In Dutch]. This issue is devoted entirely to a Symposium held at Leyden in Nov. 1954 on the Chemistry of Complex Compounds. The particular paper indicated shows that small crystalline areas occur in pit coal which are formed by tiny groups of aromatic lamellæ, arranged parallel to each other, consisting of large numbers of carbon atoms. The electrical and optical properties of pit coal indicate that these crystallites in the anthracite stage, which may be regarded as molecules having a high linkage energy, are of the nature of charge-transfer complexes the latter being connected with prevalence of the aromatic lamellæ.—F. R. H.

The Size-Reduction and Sample-Division of the Moisture Sample of Coke for General Analysis. R. A. Mott and R. W. Turner. (*Yearbook Coke Oven Man. Assoc.* 1956, 358–380).

Expansion Pressure of Carbon. R. Baukloh, O. Knacke and W. Löscher. (*Arch. Eisenhüttenwesen*, 1956, **27**, Feb., 95–99). Experiments on the splitting effect of carbon are described. Capillaries of steel (18% Cr, 8% Ni), copper and quartz were filled with iron oxide and exposed to a stream of carbon monoxide. The diffusion of gas is discussed as the factor determining the rate of cleavage of the capillaries. The Boudouard constants were measured at 500° C. The theory of the expansion pressure of carbon, and the most important thermodynamic and kinetic conditions involved, are considered.—A. C.

Kinetic Study of Coal Carbonization in the Plastic Zone. D. Fitzgerald. (*Fuel*, 1956, **35**, Apr., 178–183). Changes taking place in the apparent viscosity of coal while in the plastic state are interpreted in terms of the kinetics of the reactions taking place.—B. G. B.

Some Special Features in the Formation of Basic Types of Structure of Metallurgical Coke. B. A. Onusaitis. (*Izvest. Akad. Nauk SSSR, Otdelenie Tekn. Nauk*, 1956, (4), 85–93). [In Russian]. The mechanism of the formation of coke from coal blends and its influence on the coke structure is discussed. Two basic coke structures are considered: monolithic—when the whole mass of a blend forms gel, and conglomerate—when only a part of the blend passes through the gel state. In the latter case gel either forms the skeleton of the whole mass of coke or acts as a binder of the individual components of a blend. The importance of the rate of shrinkage of individual components as a factor influencing coke strength and possible methods of influencing the rate of shrinkage are discussed.—V. G.

New Ways of Estimating Coke Strength by Sizing and Rattler Tests. F. Wesemann, U. Graf, and R. Wartmann. (*Stahl u. Eisen*, 1956, **76**, Feb. 9, 133–145). The development and characteristics of various strength testing methods are reviewed. A fundamental approach is attempted, leading to a new criterion and its diagrammatic representation. The measurement of uniformity and the accuracy of sample tests are discussed, and the effects of transport and rattling time considered. The validity and sensitivity of the new criterion are evaluated, and results compared with those of other test methods.—A. C.

The Production and Properties of Lignite High-temperature Coke. E. Rammler and G. Bilkenroth. (*Neue Hütte*, 1956, **1**, Feb., 226–234). At the "Mátyás Rákosi" Coking Plant at Lauchhammer a lignite high temperature coke is produced from briquettes (size 0–1 mm, moisture, 10–11%, crushing strength 180–200 Kg/cm²) and graded as follows: + 45 mm, 30–45 mm, 20–30 mm, 3–20 mm, and 0–3 mm. The first two of these grades account for 75–80% of total production and are used mainly in low shaft furnaces.—L. J. L.

Production of Metallurgical Coke from Lorraine Coal. A. Ferry. (*Chaleur et Ind.*, 1956, **37**, Mar., 59–64). Until recently very little Lorraine coal was used for producing metallurgical coke, owing to its unsatisfactory properties. Three methods, outlined here, using various mixtures of coal, are now used. They are the Carling process, the method developed by the experimental station at Marienau, and the selective crushing process, (Sovaco system).—T. E. D.

Investigations on the Manufacture of Metallurgical Coke from High-Volatile Venezuelan Coals. R. Wasmuht and C. Abramski. (*Glückauf*, 1956, **92**, Feb. 4, 150–160). The various deposits of coal in Venezuela are discussed, their properties described, and an account given of experiments made to produce metallurgical coke suitable for the blast furnace from high-volatile coals by blending and admixture with coke breeze, etc.—L. D. H.

The Mechanism of Thermochemical Transformation of Iron Pyrites during Coking of Coals and Coal Blends. K. P. Medvedev. (*Izvest. Akad. Nauk SSSR, Otdelenie Tekn. Nauk*, 1956, (4) 75–84). [In Russian]. Using additions of pyrites containing radioactive sulphur the dependence of the sulphur elimination and the distribution of remaining sulphur between sulphide and organic sulphur on the temperature of carbonization and the coal rank was investigated. On the basis of results obtained, the mechanism of the reactions involved is postulated.—V. G.

Observations on the Measurement of the Absolute Density of Coke. C. G. Thibaut and P. Vigneron. (*Centre Doc. Sidér., Circ. Inform. Techn.*, 1956, **13**, No. 2, 341–344). The density of finely ground samples is determined by immersion in water, benzene and toluene. The influence of grinding on results obtained by IRSID at Thionville on 5 different cokes are reported. Reproducibility is possible with any grain size less than 200μ.—T. E. D.

The Present State and the Tasks of Microscopy in Coke Research. K. Beneš and P. Dvořák. (Paliva, 1956, 36, (2), 36–39). [In Czech].—P. F.

Heavy Fuel Oil Gasification for Metallurgical Furnaces. (*Iron Coal Trades Rev.*, 1956, **172**, Apr. 27, 497–499). A system of oil gasification, which numbers among its advantages a high thermal conversion efficiency and applicability to single-furnace operation, has been developed in France. The principle of the gasifier and its control are described, and experience gained at two works is discussed.—G. F.

Experiences in Purging. H. E. Ferguson. (*Iron Steel Eng.*, 1956, **33**, May, 130–136). The author discusses various methods of preventing the formation of flammable mixtures of fuel gas and air in large chambers or mains by interposing an inert or non-combustible gas.—M. D. J. B.

TEMPERATURE MEASUREMENT AND CONTROL

Standardizing Equipment for Sonic Suction Pyrometers. J. Maulard. (*Res. Aéronautique*, 1956, No. 49, Jan.-Feb., 27–30). An apparatus is described capable of generating gas at temperatures up to 1200° C by burning propane under controlled conditions. The gas stream is suitable for standardizing suction pyrometers.—B. G. B.

New Thermocouple for Service in Reducing Atmospheres. C. L. Guettel. (*Metal Progress*, 1956, **69**, Apr., 89–90). Two new base-metal thermocouple alloys which are more resistant to the corrosive attack of reducing gas and which maintain their thermal EMF longer than conventional base-metal thermocouples are described.—B. G. B.

Thermocouple Immersion Errors. J. M. Berry and D. L. Martin. (*Amer. Soc. Test. Mat. Spec. Tech. Pub.* 178, 1956, 5–12). Two types of errors in thermocouples used in electric furnaces are discussed. The first type occurs when an heterogeneous portion of a thermocouple is subjected to a temperature gradient. The second is related to conduction of heat to or from the hot junction of the thermocouple. The extent of these errors and their minimization are discussed.—B. G. B.

Optical Cinematographic Pyrometry in the Comparisons of Brightness. R. Chion. (*Compt. Rend.* 1956, **242**, Jan. 9, 232–234). A process is described for surface exploration of samples heated by high-frequency high power induction.

Measurement of Stress-Relieving Temperatures of Some Power Plant Steels. J. D. Murray. (*Metal Treatment and Drop Forging*, 1956, **23**, Apr., 131–134). A laboratory method is described in which a torsional stress is applied and the specimen heated at constant strain. Elastic strain and hence remanent stress is then measured. A mild steel and four alloy steels are described.

Effect of Current and Atmospheres on Arc Temperatures. G. M. Gordon, O. A. Cotter, E. R. Parker. (*Welding J.*, 195s, Feb., 109s–112s). The problems involved in the measurement of arc temperatures are discussed.—U. E.

REFRACTORY MATERIALS

Tests on the Dry Crushing of Sinter Dolomite. P. Delong. (*Stahl u. Eisen*, 1956, **76**, Mar. 22, 333–334). The working of an old crushing mill is compared with that of a new type, and the particle sizes attained are also compared. The effect of the tar admixture on the breaking load of the crushing mills is discussed.—A. C.

Experimental Measurement of the Apparent Density of Non-tarred Dolomite. de Hedouville. (*Centre Doc. Sidér., Circ. Inform. Tech.*, 1956, **13**, (1), 125–132). The bulk density of a number of synthetic mixes of dolomite is measured. The effect of size distribution on the density is discussed. Some results are shown graphically.—T. E. D.

Influence of the Quality of Portland Cement Clinker on the Initial Strength and Hardening of Blast-Furnace Cements. L. Blondiau. (*Silicates Indust.*, 1956, **21**, Jan., 13–19; Feb., 74–81). Portland cement clinker is a powerful catalyst of the hydration and setting processes in blast-furnace cements. An attempt was made to use a special type of clinker saturated with lime in order to reduce the amount of clinker addition and simultaneously improve the strength of the cement by this means. No significant improvements were obtained.

Effect of Firing Temperature on the Properties of Fireclay Brick. G. R. Eusner and W. S. Debenham. (*Amer. Ceram. Soc. Bull.*, 1956, **35**, Apr., 151–154). Five brands of fireclay brick were fired to various temperatures, and the properties of each determined. It was concluded that careful control of firing temperature is desirable; spalling sensitivity is not related to other properties; increased firing temperature improves slag resistance.—D. L. C. P.

Foundry Furnace Refractories. W. R. Jaeschke. (*Canad. Metals*, 1956, **19**, Mar., 36–42). The properties of the refractory materials in current use in foundry furnaces are discussed. It is considered that furnaces are being operated close to the limit of the refractory linings.—B. G. B.

Reactions Between Aluminium Oxide and Carbon. The Al_2O_3–Al_4C_3 Phase Diagram. L. M. Foster, G. Long, and M. S. Hunter. (*J. Amer. Ceram. Soc.*, 1956, **39**, Jan., 1–11). A phase diagram is proposed; reaction products were investigated and implications in the field of ceramics considered. Because of the reactivity of aluminium carbide and all the intermediate compounds with moisture and oxygen, use of refractories based on the system Al_2O_3–Al_4C_3 must be limited to applications where these agents are excluded. The behaviour of high alumina refractories in the presence of carbon is explained.—D. L. C. P.

Phase Equilibria at Liquidus Temperatures in the System MgO–FeO–Fe_2O_3–SiO_2. A. Muan and E. F. Osborn. (*J Amer. Ceram. Soc.*, 1956, **39**, Apr., 121–140). Data were obtained for the temperature range 1159–1775° C and with oxygen pressures ranging from 1 to $10^{-8.9}$ atm. Applications of the phase diagrams to steel plant refractories problems is indicated (e.g. stability of magnesite bricks; effect of iron oxide adsorption).—D. L. C. P.

Present Trends in the Evaluation of Mechanical Strength of Refractory Products at High Temperatures. J. Baron. (*Met. Ital.*, 1956, **48**, Jan., 10–14). [In Italian]. The mechanical strength of silica products at high temperatures can be determined by load tests provided the rate of heating of the sample is consistent with its size. The results are described of 2 sets of tests, one carried out according to French specifications, the other with French standard refractories, but with a rate of heating reduced to 1° C per min at temperatures above 1550° C. Both tests give the same results to within ± 10° C for the temperatures of failure. Details are also given of creep tests at constant temperature. Results obtained with two Cowper recuperator collars confirm Dale's law provided the products are homogeneous. The author establishes that under very severe conditions creep depends on porosity, while under less severe conditions creep depends on refractoriness. (8 references).—M. D. J. B.

Laboratory Production of Cylindrical Alumina Crucibles of 5½ litres capacity. V. H. Stott. (*J. Iron Steel Inst.*, 1957, **185**, Jan., 82–85). [This issue].

IRON AND STEEL—GENERAL

France's Contributions to Metallurgy. G. Bastien. (*Rev. Mét.*, 1956, **53**, May, 321–331). A lecture at the Congress of the American Metallurgical Societies. A short historical account of iron and steel and non-ferrous metallurgy is presented.

The Iron and Steel Industry in Austria. (*Usine Nouvelle*, 1956, **12**, Mar. 22, 29). The activities of the two principal iron and steel groups, namely Alpine Montan and Voest, are outlined. Oxygen refining is mentioned, and some details are given of its use at the Voest works in Linz.—T. E. D.

Arctic Iron. I.—Development of the Mo i Rana Steelworks in Norway. (*Elect. Rev.*, 1956, **158**, 4 May, 703–710). A general description is given of the new Mo i Rana iron and steelworks of A/S Norsk Jernwerk in northern Norway. This is a fully integrated plant, capable at present of producing about 170,000 tons of rolled products annually, to be expanded eventually to half a million tons. Ore is at present imported, but when the ore preparation plants are complete, local deposits will be used. The layout and electrical equipment are described.—L. D. H.

Arctic Iron.—II. Power for Production at Mo i Rana. (*Elect. Rev.*, 1956, **158**, 11 May, 753–759). The construction and operation are described of the Rossago hydroelectric scheme for the present and future supply of power to the Mo i Rana iron and steelworks.—L. D. H.

Arctic Iron. III—World's Largest Electric Pig-Iron Furnaces. (*Elect. Rev.*, 1956, **158**, 18 May, 841–845). The construction and operation of the 20MW electric pig-iron furnaces installed at Mo i Rana are described.—L. D. H.

In the Algerian Metallurgical Industry. (*Usine Nouvelle*, 1956, **12**, Apr. 12, 27–29). Production of the metallurgical, engineering and electrical industries in Algeria are tabulated and discussed.—T. E. D.

Improving the Utilization of Capacity at the Dzerzhinskii Works. G. È. Tsukanov. (*Stal'*, 1955, (10), 867–870). [In Russian]. The Dzerzhinskii works was rebuilt after its destruction during the war and is now one of the largest metallurgical enterprises in the southern region of the U.S.S.R. In this article the growth in production of sinter, pig iron, steel, and rolled products and the measures by which the increases were secured are analysed, most attention being given to iron making. The blast furnaces work with high top pressure, constant humidity blast and cooling of the gases in the throat; self-fluxing sinter is extensively used and attention is given to coke quality. The increase in rolled products output is attributed mainly to improved pass design.

Australian Steel-Using Industries. (*Engineer*, 1956, **201**, June 8, 645). This article reviews the great post-war expansion programme of the Australian iron and steel industry. Developments in producing and consuming industries are discussed.—M. D. J. B.

BLAST-FURNACE PRACTICE AND PRODUCTION OF PIG IRON

Blast Furnace Erection Poses Many Problems. J. F. Zeigler. (*Iron Steel Eng.*, 1956, **33**, April, 141–150). This paper discusses the problems encountered in planning, designing and erecting a 28 ft 9 in. furnace at Bethlehem on a site once occupied by a 19 ft furnace. The job took 174 days to complete.—M. D. J. B.

The New Blast Furnace at Donawitz is Blown in. (*Maschinenwelt Elektrotechnik*, 1956, **11**, Jan., 1–2). The dimensions and operating conditions are given of the new blast furnace at Donawitz, which is intended for a daily production of 750–850 tons.—L. D. H.

The Latest SECIM Installations. E Goué. (*Centre Doc. Sidér., Circ. Inform. Techn.*, 1956, **13**, No. 4, 745–764). The following are described with the aid of diagrams: two wire drawing trains; a rolling mill plant for special steels; a complete plant in Paz del Rio, comprising coke ovens, blast furnace, three Thomas converters, power station, wire-drawing equipment and rolling mill; a rolling mill plant in Chimbote, Peru.—T. E. D.

Some New Experiences With Rammed Carbon Linings Used for Blast-Furnace Bottoms and Hearths obtained from Works and Laboratory Tests. J. Dobrý. (*Hutnické Listy*, 1956, **11**, (5), 307–313). [In Czech]. Laboratory tests and examination of samples of rammed linings from a furnace blown-in 5 years ago and now out of commission showed that a rapid deterioration of the carbon by graphitization, coking, and attack by carbon dioxide took place at the high temperatures occurring in the furnace. Some discrepancies between the laboratory and full-scale test results are discussed.—P. F.

Axial Blowers for Furnace Blast. (*Engineer*, 1956, **201**, April 13, 336–339). The demands of the gas turbine for high component efficiencies have brought about a great advance in axial compressor techniques. The characteristics of these compressors which call for accurate matching to various applications are described in this article.—M. D. J. B.

Merits of Various Fuels for Smelting in Blast and other Furnaces. F. Lüth. (*Stahl u. Eisen*, 1956, **76**, Mar. 22, 317–322). After comparing smelting processes the author discusses problems in the charging of small blast furnaces with fuels other than coke, the effect of the size of ore and coke particles, and the results of smelting tests in a small blast furnace using coke–coal mixtures. Carbon consumption and the effect of hydrocarbons in the volatile constituents are also considered.—A. C.

Effects of Coke Quality on Blast Furnace Operation. E. W. Stahl and V. B. Mancke (*Blast Furn. Steel Plant*, 1956, **44**, Apr., 385–390, 397). The results of a blast furnace trial carried out at the Johnstown plant of Bethlehem Steel Co., U.S.A. are described. Two furnaces were used and cokes from two different sources were employed on these furnaces for alternate 3 to 4 week periods. The properties of the cokes are discussed in relation to the differences found in blast furnace performance.—B. G. B.

Temperature Control in the Blast Furnace Hearth by the Physical and Chemical Properties of the Slags in the Smelting of Pig-Iron. W. W. Michailow. (*Neue Hütte*, 1956, **1**, Feb., 235–237). The principal factor determining hearth temperature is the temperature at which primary slag attains a completely liquid state. A slag of optimum viscosity is obtained by careful temperature control of the burden. The presence of magnesium in the slag makes for fluidity but sulphur in the pig iron may inhibit this. Magnesium has a favourable effect on the production of cold chemical pig iron.

Thermal Mechanism inside the Blast Furnace. J. Givaudon. (*Compt. Rend.*, 1956, **242**, Jan. 9, 258–261). Comparison of six furnaces yielded a simple relation between heat evolved in the different zones.

Process of Pre-refining of Pig Iron by Injections of Oxygen-enriched Air into the Blast Furnace Hearth. K. Kanamori. (*Rev. Mét.*, 1956, **53**, Apr. 305–310). The process of desulphurization is described with the object of making use of chrome- and nickel-containing ores. Experiments on an experimental furnace are described.

Novel Interpretations of the Combustion Process of Coke in the Blast Tuyeres of Furnaces. I. P. Bardin, L. M. Zyljew, M. J. Ostrouchow, and L. S. Chodak. (*Neue Hütte*, 1956, **1**, Feb., 238–244). Recent investigations in the USSR, U.S.A., and Great Britain (Burns) are summarized. Deviations from "classical" theory are interpreted. Combustion in front of blasting tuyeres was found to occur not in a stationary layer of coke, but in a turbulent motion of coke particles. Coke combustion is characterized by chemical factors, i.e. kinetics, and by physical factors, dependent on the power of the jet. The extent of the combustion zone in the blast furnace has been shown to depend far more on the physics of the process than on combustion velocity.—L. J. L.

The Production of Pig Iron with a Low Manganese Content. A. Bichler. (*Hutnické Listy*, 1956, **11**, (3), 148–150). [In Czech]. Experiments on the use of low Mn pig-iron in the Molotov Steelworks in Třinec in the production of open-hearth steel with a 60% liquid charge show that reduced manganese contents lead to economies. A drop of 0·1% in the manganese content was found to facilitate a reduction of the amount of coke used in the open hearth furnace by ½%. Steel quality is unaffected.—P. F.

Advances in Electric Methods of Iron Making. H. Walde. (*Elektrowärme Techn.*, 156, **6**, Sept.-Oct., 161–167). The scope, performance, and likely future developments of low-shaft furnaces, Lubatti furnaces etc. are reviewed.—P. F.

The Pre-refining of Pig Iron in the Ladle by Means of Pure Oxygen. P. Leroy and L. Septier. (*Met. Ital.*, 1956, **48**, Feb., 61–67). [In Italian]. The authors discuss the results of experiments carried out on pilot plant at the IRSID laboratories. The techniques adopted are described and details of the plant at Mondeville are given. The authors claim that the process described is workable on an industrial scale for all irons with a Si content above 0·35%.—M. D. J. B.

Use of Non-Coking Coals in the Electric Melting of Pig Iron. F. C. Collin. (*Inst. Hierro Acero*, 1956, **9**, Jan., 1–5. *Special Number*). [In Spanish]. The author draws attention to the advantages of the electric smelting furnace in its ability to utilize non-coking coals; a fact of great importance to countries which lack suitable coals for blast furnace operation. An illustrated review of this type of furnace is given together with a brief account of its operation and a discussion of the most suitable types of non-coking coals and other raw materials.—P. S.

TREATMENT AND USE OF SLAGS

Phase Relationships in the System CaO–Al_2O_3–P_2O_5. P. E. Stone, E. P. Egan, jun., and J. R. Lehr. (*J. Amer. Ceram. Soc.*, 1956, **39**, Mar., 89–98). Primary fields of crystallization in the system, at temperatures from 900° to 1600° C, were determined by the method of quenching, and results are given in diagrams and tables.—D. L. C. P.

The System Iron–Phosphorus–Calcium. R. Vogel and H. Klose. (*Arch. Eisenhüttenwesen*, 1956, **27**, Jan., 75–76). General tests were carried out to give an overall conception of equilibrium conditions in the zone Fe–Fe_2P–Ca_3P_2–Ca. These were performed on a thermal basis.—A. C.

Thermodynamics of Slag Systems. Part I—The Thermodynamic Properties of CaO–Al_2O_3. Part II—The Thermodynamic Properties of CaO–SiO_2. P. T. Carter and T. G. Macfarlane. (*J. Iron Steel Inst.*, 1957, **185**, Jan., 54–66). [This issue].

Tests on Heaped Concrete from Metallurgical Foamed Slag. K. Wesche. (*Stahl u. Eisen*, 1956, **76**, Jan. 12, 27–30). The properties of the concrete are enumerated. The production, storage, and testing of concrete cubes is discussed. Test results are given and evaluated.

An Investigation of the System $2FeO$, SiO_2–$3Na_2O$, P_2O_5–$Na_2O.2SiO_2$. C. Bodsworth and W. R. Maddocks. (*J. Iron Steel Inst.*, 1957, **185**, Jan., 75–82). [This issue].

Improvements in the Quality of Slag Cements Containing Clinker, and Some Perspectives for its Future. P. Dournauls. (*Silicates Indust.*, 1956, **21**, March, 123–125). Properties of various types of cements are reviewed. In many applications slag cements can replace Portland cement. The advantages of clinker cements are outlined. These can be made at the building site, so that it might prove economical in future to have "mobile cement factories", assuming further developments in the quality of these cements.—P. F.

PRODUCTION OF STEEL

Manpower Requirements in the Iron and Steel Industry. H. Euler. (*Stahl u. Eisen*, 1956, **76**, Jan. 12, 31–39.) The situation in Summer 1955 is reviewed, giving consideration to the distribution of labour and its shortages. Trends at the end of 1955 and the prospects up to 1957 are discussed.

Recent Developments in European Steel Practices. H. B. Emerick. (*Iron Steel Eng.*, 1956, **33**, March, 105–108). The author describes new practices in basic Bessemer and basic O.H. steelmaking, desiliconization with oxygen, the desulphurization of iron with solid lime, developments with the low-shaft blast furnace and the oxygen Linz and Donawitz steelmaking process.—M. D. J. B.

Kaiser Expansion to Ladle 450,000 More Tons into Steel-hungry West. *Western Metals*, 1956, **14**, June, 53–54). An account of proposed extensions, with a diagram of the oxygen steelmaking unit.

Industrial Results Obtained with Cylindrical Converters with Shallow Baths and Large Diameter Bottoms. N. Gombert and J. de Hedouville. (*Centre Doc. Sidér., Circ. Inform. Tech.*, 1956, **13**, (1), 157–168). Detailed dimensions of 13T, 19T and 30T converters at three different works are given. The effects of design, blowing area, and bath depth on performance are briefly discussed.—T. E. D.

Foreign Experiences with the Use of the Oxygen Lance in Converter Practice. V. Chvátal. (*Hutník*, (Prague), 1956, **6**, (1), 14–18). [In Czech].

Converter Bottom Effects from Cooling Down. P. Delong. (*Stahl u. Eisen*, 1956, **76**, Mar. 22, 334–335). The harmful effects of cooling down on the life of converter bottoms are discussed. A diagram is given showing the variation in bottom thickness with number of melts before and after cooling down.—A. C.

On the Carbon Uptake of Liquid Steel treated with Coke in the Ladle. L. Šmrha and M. Böhm. (*Hutnické Listy*, 1956, **11**, (3), 143–148). [In Czech]. The effect of carburization on the gas content of the ingots, the yield per ingot, and on the segregation contours was studied. Except with intense carburization, gas content and ingot yields are not materially affected, but a displacement of the segregation zone was shown to take place. Sulphur prints were used; statistical methods were employed throughout.—P. F.

Open Hearth Furnace Control. E. Whitehead. (*Instrument Practice*, 1956, **10**, Jan. 44–48; discussion 48–50). Advantages and difficulties of open hearth pressure, fuel supply and temperature control are discussed. Difficulties of obtaining the full benefit of pressure control due to air infiltration, mainly from furnace doors, are pointed out. The advantage of the floating mode of control in avoiding " hunting " is mentioned.—L. D. H.

The Influence of Pressure in the Open-Hearth Furnace on its Thermal Efficiency. V. Parma. (*Hutník*, 1956, **6**, (5), 130–133). [In Czech]. Recent work in this field is discussed, with special reference to Soviet work. The desirability of automatic pressure-control is emphasized.—P. F.

The Direct Measurement of Total Heat in Open-hearth Furnaces. A. M. Godridge and G. G. Thurlow. (*J. Iron Steel Inst.*, 1957, **185**, Jan., 46–53). [This issue].

Instrumentation and Automatic Control of Open-Hearth Furnaces. F. J. Cunningham. (*Instrument Eng.* 1956, **2**, Apr. 11–19). A description of recent examples of automatic-control schemes. Centralized control and instrument panels housed in pressurized cubicles are described.

Nitrogen in Metal in the Process of Acid Open-Hearth Smelting. M. M. Karnaykhov and A. Kh. Urazigil'deev. (*Izvest. Akad. Nauk SSSR, Otdelenie Tekn. Nauk.*, 1956, (4), 126–128). [In Russian]. Changes in the nitrogen concentration during the production of acid O.H. carbon and alloy steels were investigated. It was found that the concentration of nitrogen in steel is independent of the type of acid process. Acid open hearth slag is practically impermeable to nitrogen. The concentration of nitrogen in steel during boiling decreases due to its simultaneous evolution with carbon monoxide. The proportion of nitrogen so removed depends on its initial concentration in steel and the amount of removed carbon. On tapping, the concentration of nitrogen in steel increases.—V. G.

Thermal Conditions for the High Speed Operation of Open-Hearth Furnaces. I. M. Koburneev. (*Stal'*, 1955, (10), 895–904). [In Russian]. O.H. operating experience at a Soviet works where large increases in productivity and decreases in fuel consumption have been obtained recently is analysed and views on the effects of various operating factors are put forward. It is concluded that in general, modern furnaces still have large reserves of productivity and fuel economy. For optimal operation the activity of the flame must always be maintained by eliminating organizational stoppages, improving combustion and decreasing the thermal resistance of the bath. The waste-gas temperature and oxygen contents are basic factors and should be used for the automatic regulation of combustion. Some simple design modifications for improving operation are listed.—S. K.

Distribution of Sulphur between Liquid Iron and Slag in the Basic Open-Hearth Furnace. K.-F. Lüdemann. (*Neue Hütte*, 1955, **1**, Dec., 78–96). The published work of this subject is reviewed; the characteristics of the melts, and the effects of slag composition and temperature on sulphur distribution are discussed.—L. J. L.

Studies on Ball-bearing Steels. III. M. Ueno and Y. Nakano. (*Tetsu to Hagane*, 1955, **41**, Nov., 1179–1184). [In Japanese]. In steel made in the basic electric arc furnace, cementite readily goes into solution; in that made in the acid open-hearth, it does not do so at temperatures $< 850°$, but does so rapidly $> 850°$. In the former steels there are many nonmetallic inclusions; nevertheless they are stable in the austenitic state. Their quenching behaviour is sluggish.

Production of High Nitrogen Steels. V. F. Zackay, E. R. Morgan, and J. C. Shyne. (*Trans. Amer. Inst. Min. Met. Eng.*, 1956, **206**; *J. Met.*, 1956, **8**, Feb., Section 2, 216). Possible alternatives to pressure melting methods of producing high nitrogen steels are briefly discussed. They include centrifugal casting and mechanical capping as in low-carbon rimming-steel practice. Mechanical properties of the steels produced are given.—G. F.

Nickel-Free and Low Nickel Austenitic Stainless Steels. D. J. Carney. (*Reg. Tech. Meet. Amer. Iron Steel Inst.*, 1955, 103–113; *Blast Furn. Steel Plant*, 1955, **43**, Dec., 1377–1380). The United States Steel Corporation has investigated the possibility of producing a nickel-free austenitic steel with mechanical properties similar to those of 18/8 steels. Structural diagrams are presented showing that a completely austenitic steel at 1260° C can be produced with chromium contents above 17% and little or no nickel, by using manganese contents of 15% and nitrogen up to 0·5%. Data illustrating the excellent mechanical propertiesof the new steels are given.

Restoration of Plug-Bottom Moulds by Deposition. N. I. Pavlovtseva. (*Stal'*, 1955, (10), 942–945). [In Russian]. The defects developed by top and bottom pouring plug bottom ingot moulds are analysed and the influence on mould life of depositions by welding on cast iron at suitable points is considered. In general, iron deposition raised the life by 15–25 fillings, the following being the optimal conditions: careful removal of oxides from local defects with an acetylene flame; preliminary heating to 600–700° C before the deposition; iron electrodes 8–10 mm in diameter to be cast from iron treated in the ladle with magnesium or aluminium; the deposited metal should not contain a free-cementite structure. The treatment can be repeated until the whole inside of the mould is covered with a common crack-network.

Fifty Years of Progress in Electric Furnace Steelmaking. H. J. Stagg. (*Metal Progress*, 1956, **69**, Apr., 49–55). The development of this branch of steelmaking is reviewed. It is now possible to produce steel at lower cost than in open hearth furnaces.—B. G. B.

Problems in Supplying Power to Electric Furnaces. G. E. Duerr. (*Iron Steel Eng.*, 1956, **33**, Jan., 67–70). The author discusses the best means of supplying power to electric furnaces and shows how proper design can help in meeting the high peak loads and in reducing load swings. The proper selection of equipment is also discussed.—M. D. J. B.

Recent Developments in Alloy and Special Steels in Great Britain. T. Bishop. (*Iron Coal Trades Rev.*, 1956, **172**, Apr. 6, 303–312). The advances referred to are concerned with high-strength low-alloy structural steels, boron and rare-earth additions, leaded alloy steels, corrosion and heat resistance, alloy conservation in stainless steels, cladding, steels for high-temperature service, tool and high-speed steels, manganese steel, and magnet steels.—G. F.

Hot Work Die Steels. E. A. Loria. (*Metallurgia*, 1956, **53**, Mar., 119–121). The properties of hot work die-steels are discussed in relation to their use in other high temperature conditions particularly in aircraft.—B. G. B.

Recent Developments in the Use of Nickel in Special Steels. M. Ballay. (*Mét. Constr. Mécan.* 1956, **88,** Feb., 95–105). The state of perfection now attained by heat treatment processes has enabled the development of steels containing less nickel for constructional purposes. An increasing amount of nickel is being used in stainless type steels. Constructional steels, stainless and heat-resisting steels and magnetic materials are considered, particular reference being made to the alloy composition and use of nickel.—B. G. B.

Titanium Steels and Cast Irons. (*Génie Civil*, 1956, **133,** May 1, 173–175; May 15, 192–194). An account is given of deformation in ageing in steels containing carbon, nitrogen, and oxygen and of the stabilizing action of titanium. The second part discusses microstructure and gives dilatometric curves and tables of mechanical properties for titanium-containing grey irons. Anti-corrosive effects are briefly indicated.

Studies on the Boron-treated Spring Steel TS50B60. I. Y. Yasuda and K. Suzuki. (*Tetsu to Hagane*, 1956, **42,** Feb., 105–110). [In Japanese]. Various properties of this boron-treated chromium steel, viz. non-metallic inclusions, transformation points, hardenability, quenching cracks, grain growth and decarburization etc. on heating, were determined and compared with those of SUP6 Si–Mn steel, SAE5160 Mn–Cr steel and SAE 6150 Cr–V steel.—K. E. J.

Ingot Mould Manufacture at Kaiser Steel. J. B. Klukkert. (*Iron Steel Eng.*, 1956, **33,** April, 73–79). This paper describes the standard ingot mould production methods applied at Fontana and discusses some of the problems unique to a new and rapidly expanding plant. Certain special practices have been developed to meet special specifications.—M. D. J. B.

Volume Changes in Cast Iron Steelworks Moulds. J. Přibyl. (*Hutník*, 1956, **6,** (4), 106–113). [In Czech]. The nature of the volume changes leading to "growth", and premature incrustation of ingot moulds are considered with reference to recent publications. Possible methods of alleviating these effects, and relevant researches to be carried out are discussed.—P. F.

Temperature Drop in Pouring Ladles. V. Paschkis. (*Amer. Found. Soc. Preprint*, 1956, No. 43). The factors affecting heat losses from ladles are reviewed and the results of calculations on the losses from ladles of 150 and 16,000 lb holding capacity are presented and discussed. The variables studied included lining thickness, nature of metal (steel or cast iron), the presence or absence of a cover, and the extent of preheat given to the ladle and cover. Among the conclusions reached are that preheating the ladle is essential, but preheating the lid does not seem to be important, and that there is a critical lining thickness beyond which no further gain can be expected.—B. C. W.

Electric Hot-Topping of Steel Ingots: Recent Developments in Sweden. (*Iron Coal Trades Rev.*, 1956, **172,** Apr. 20, 435–437). Details are given of a modification of the Kellogg hot-topping process now used in Sweden, in which heat is supplied to the hot-top by a D.C. arc from a water-cooled graphite electrode with power input up to 60 kW. The apparatus and its operations are described, and the effect on the ingot is discussed. An estimate of the economics is given.—G. F.

Oxygen in Steel During the Process of Syphon Casting. V. A. Mchedlishvili and A. M. Samarin. (*Izvestiya Akademii Nauk SSSR, O.T.N.*, 1956, No. 3, 106–110). [In Russian]. The results of an investigation of changes in the oxygen content of steel during its deoxidation, casting, and rolling are described.—V. G.

Experiences of Continuous Casting and Subsequent Hot Working of Ingots. F. Leitner. (*Inst. Hierro Acero*, 1956, **9,** Jan.-Mar., 258–266). [In Spanish]. Details are given of the continuous casting equipment at Breitenfeld, Austria. A fixed mould is used, with an oscillating stream, to produce billets (up to 130 mm dia.) and slabs (275 mm × 65 mm) in various carbon steels. Casting conditions are discussed with reference to structure and segregation and examples are given of the structure, quality, and type of hot-worked product. The advantages of such plant for works which do not desire heavy equipment for hot-working are emphasized.

The Technology of Multiple Continuous Casting. R. Baake and H. Rosahl. (*Neue Hütte*, 1956, **1,** Mar., 293–303). Development of the Freital continuous casting plant, where 3 billets of 6 m length are cast. Cooling and casting control depending on the surface temperature of the billet, steel distribution, the correlation between flow velocity, steel quantity, vent diameter in the distributor, bath level, mould capacity, and ladle charge are described.—L. J. L.

Zone Liquation and Mechanical Properties as Observed in a Section through a Forging Blank taken from a 110 Ton Ingot. L. Šmrha. (*Hutnické Listy*, 1956, **11,** (6), 363–370). [In Czech]. It is shown on the basis of analysis of samples taken from a basic O.H. 1·4% Cr, 0·15% Mo, 0·2% V steel that the liquation of phosphorus was greater than the segregation of sulphur. The order of liquation being: carbon, phosphorus, sulphur. The effect of sulphides, and the relation between liquation, and contraction and ductility are discussed.—P. F.

Statistical Control of Yield in the Casting and Rolling of Steel. M. Spreux. (*Centre Doc. Sidér., Circ. Inform. Techn.*, 1956, **13,** No. 4, 735–743). A simple graphical discussion on the frequency curve is presented.—T. E. D.

Abrasive Wheels Simplify Steel Billet Cutting. V. E. Lysaght. (*Iron Age*, 1956, **177,** Feb. 16, 99–101). The use of abrasive cut-off machines for sizing alloy steel billets by Crucible Steel Co. of America is described. The 26 inch diameter rubber-bonded abrasive wheels can wet cut 8 × 8 inch billets.—D. L. C. P.

PRODUCTION OF FERRO-ALLOYS

Notes on Industrial Research on Ore Reduction. Application to the Production of 75% Ferrosilicon. A. Palazzi and F. Rinaldi. (*Rev. Mét.* 1956, **53,** Feb. 92–104). Trials on a 6000 kVA furnace are described, extending over a month. The effect of ground quartz was investigated.

Manufacture of Ferro-Molybdenum and Molybdenum Alloys at the Langelath Works of the Climax-Molybdenum Co. (*J. Four Elect.*, 1956, **65,** Jan.-Feb., 13–14). An account of the techniques used at this works in Colorado, U.S.A. is given. The ore is washed and roasted. The molybdenum oxide is later volatilized by further heat treatment. The purified oxide is then reduced by reaction with silicon for the production of ferro-molybdenum.—B. G. B.

FOUNDRY PRACTICE

Modern Facilities Incorporated in New British Foundry. V. Delport. (*Foundry*, 1956, **84,** Jan., 94–99). A description is given of the lay-out, equipment and foundry practice at the new foundry of W. and T. Avery Ltd. at Tame Bridge, nr. Walsall.—B. C. W.

Casting Facilities Prominent in New Westinghouse Pilot Plant. K. L. Mountain. (*Foundry*, 1956, **84,** Jan., 100–103). The new pilot plant at Blairsville, Pa., which is designed to process both wrought and cast alloys, is described with particular reference to the foundry facilities and practice.

The Control of Castings from the Point of View of the Foundryman. Boucher. (*Usine Nouvelle*, 1956, **12,** Feb. 23, 37–38). All aspects of quality and size control are briefly discussed.—T. E. D.

You can Reduce Noise in Your Foundry. E. R. Lund and W. O. Hanson. (*Amer. Found. Soc. Preprint*, 1956, No. 144). The steps taken to reduce the noise level in a foundry cleaning room are summarized.—B. C. W.

Labour Reserves in Foundries in the Ural Mountains. A. A. Gorschkow. (*Giessereitechn*, 1956, **2,** 155–159; *Liteinoe Proizvodstvo*, 1955, 1–6). A description is given of the exploitation of "untapped resources" in a foundry. This proceeds in two stages: rationalization of the use of labour, equipment, and funds, followed by mechanization and automation.—L. J. L.

Some Aspects of Dust Suppression in Foundries. C. M. Stoch. (*Amer. Found. Soc. Preprint*, 1956, No. 178). The methods available for preventing or controlling the formation of dust are reviewed and a detailed account is given of the work carried out by B.S.C.R.A. on local exhaust systems applied to grinding machines. Modifications to ensure improved dust control on pedestal grinding machines are described, and a discussion is given of the dust flow characteristics of swing frame grinders. Observations and trials conducted on a number of exhaust systems are presented and the experimental work carried out on the development of a combined integral and booth system is reviewed.

Views on Modern Sand Preparation Equipment. G. Lindgren. (*Gjuteriet*, 1956, **46,** No. 3, 33–38). [In Swedish]. After discussing the functions and suitability of the various components in a modern sand treatment plant—such as sand

coolers, magnetic separators, screens, mixers, dosing and wetting equipment—the author gives details of a suggested completely automatic plant with a capacity of 25 m^3/h.

Cooling of Foundry Sands. G. Martin. (*Foundry*, 1956, **84**, Feb., 98–103). The cooling of individual sand grains and bulk sand is considered as a heat transfer problem and experimental results on different methods of sand cooling are summarized and discussed. It is concluded that if cold sand is required it is necessary to install special equipment and the various possible systems are then reviewed. The practical requirements for cooling core sand, steel foundry sand, and iron foundry sand are finally outlined.—B. C. W.

Moulding Technique with Cement Bonded Sands. L. Barbero Luna and J. Tallada Cabello. (*Inst. Hierro Acero*, 1956, **9**, Feb., 146–168. *Special Number*). [In Spanish]. The history, advantages, and disadvantages of cement sand moulding are discussed, after which the results of a series of laboratory tests are described. The moulding technique in use at the Manises (Valencia) plant is illustrated by means of examples, the possible defects such sands are likely to cause are mentioned briefly, and the production of steel and bronze castings by this method is discussed.—P. S.

Dry Reclamation of Foundry Sand. H. W. Zimnawoda. (*Foundry*, 1956, **84**, Mar., 114–120). The reclamation of used foundry sands by pneumatic scrubbing is discussed in detail. The aspects covered are the principles of operation, the lay-out of alternative systems and the costs of reclamation.

Methods of Sand Regeneration in Foundries and Their Significance. B. Kamenický. (*Slévárenství*, 1956, **4**, (3), 74–79). [In Czech]. The causes of recent increases in the specific sand consumption in Czechoslovak foundries are ascribed mainly to incomplete sand regeneration. Available methods and their respective scopes are discussed, with special reference to Soviet electrostatic separator methods.

Does Sand Testing Give Us the Facts? R. W. Heine, E. H. King, and J. S. Schumacher. (*Amer. Found. Soc. Preprint*, 1956, No. 152). The lack of correlation between mould hardness developed in the standard AFS ramming device, and that produced by jolting or squeezing, is discussed and related to the work done on the sand. The factors affecting the work done in compacting sand and sand density are considered and it is concluded that laboratory tests will correlate better with foundry results if 2 or 4 lb weights with a 2 in. drop are used in preparing sand specimens. However the standard 14 lb, 2 in. ramming procedure is regarded as a useful method for comparing the properties of sands at high densities where the data are most reproducible.—B. C. W.

Investigations on the Influence of Granulation on the Compressibility and the Works Behaviour of Foundry Sands. F. Hofmann. (*Giesserei*, 1956, **43**, Mar. 1, 105–108). The preparation of test mixtures and the methods of investigation are first described. The dependence of the following properties on the granulation was investigated: compressibility, permeability, porosity, green strength and compressibility after prior consolidation. The behaviour of sand during casting is considered; including the behaviour of quartz sand at high temperatures and the simultaneous effect of expansion and the degree of compression.—R. J. W.

The Construction of a Diesel Motor Pattern Outfit. W. Hagedorn. (*Giesserei*, 1956, **43**, Mar. 1, 119–120). The manufacture of patterns and core boxes for the crank case of a large Diesel motor is described in detail. The seven different types of pattern or core box required are dealt with separately and illustrated with sketches.—R. J. W.

Risering of Steel Castings. H. F. Bishop and W. H. Johnson. (*Foundry*, 1956, **84**, Feb., 70–74; Mar., 136–141). The methods used to calculate the location and dimensions of risers for steel castings are summarized and the necessary data are presented in graphical form. The application of the methods to several commercial-type castings is then described in detail.—B. C. W.

Gating for Shell Moulding Castings. M. R. Hincheliffe. (*Metal Ind.* 1956, **88**, Jan. 27, 63–65). An account of difficulties met with is presented, with an account of the layout of runners and gates and the problems of feeding heads.

Examples of the Use of the Core-moulding Method. W. Hagedorn. (*Giesserei*, 1956, **43**, Apr. 12, 193–195). The advantages of the core-moulding method are first discussed. A detailed description is then given of the manufacture of a pressure collecting pipe (manifold) with cooling fins and also of a motor cylinder by the core-moulding process.—R. J. W.

Core Making With CO_2 Process. F. M. Scaggs. (*Amer. Found. Soc. Preprint*, 1956, No. 164). Experiences with the CO_2 process for making cores at the Oklahoma Steel Castings Co. Inc., Tulsa, Oklahoma, are briefly described.—B. C. W.

Advantages of the CO_2 Process. K. Götz. (*Giessereitechn.*, 1956, **2**, June, 139). Three examples of casting by the CO_2 process are given, and the resultant benefits enumerated. They include low cost, absence of scale formation, improved flow conditions, less waste, greater accuracy of casting, and ease of operation.—L. J. L.

Casting with Carbon-Dioxide Hardened Sands. (*Mech. World*, 1956, **136**, Feb. 54–56). The use of sodium silicate bonded sands hardened by carbon dioxide in the production of moulds and cores is described.—D. H.

Applications of the Carbon Dioxide Sodium Silicate Moulding Process in Machine and Hand Moulding. F. Dubielzig. (*Giessereitechn.*, 1956, **2**, June, 134–137). The theory of the process is explained at length; examples are given for its application in machine moulding and hand moulding (ships' sirens); its economies are discussed, and some drawbacks are mentioned.—L. J. L.

The Development of the CO_2 Process in the VEB Steelworks Silbitz-Rasberg. F. Sedlacek. (*Giessereitechn.*, 1956, **2**, June, 124–130). Examples of the successful application of the moulding process employing sand with sodium silicate binders hardened with carbon dioxide are given; the operation of the method at Silbitz-Rasberg is described (200,000 idlers for tractors were produced by the process in 1954); and the investigation, and elimination by pre-heating, of the needle hole porosity from which the process suffered are discussed.

Changes in the Technique of Producing Wheel Hubs Brought About by the Application of the CO_2–Sodium Silicate Process. K. Haake and E. Pfitzmann. (*Giessereitechn.*, 1956, **2**, July, 153–154). The application of the method to one particular problem is discussed in considerable detail. Casting the hubs standing up rather than in the horizontal position helped.

The Use of Plastics as Core Binders. J. Ornst. (*Giessereitechn.*, 1956, **2**, Mar., 54–56). *Slévárenství*, 1955, **3**, 236–239). Foreign operating experience is surveyed. Phenolic-formaldehyde, urea-formaldehyde, and melamin-formaldehyde resins are discussed. Sand composition, the effect of clay, of starch, and dextrin, and of the moisture content, are examined. Drying, characteristics after drying, and practical applications are described.—L. J. L.

Novel Core Binders in the Peoples' Republic of Poland. J. Buciewicz and T. Rzepa. (*Giessereitechn.*, 1956, **2**, Jan., 11–15). The prices of commercially available binders are listed; the uses of urea resin 121 and the engineering characteristics of cores containing it are described. The properties of Oil "ST", a by-product of the cellulose industry containing from 30 to 35% of unsaturated vegetable oils, from 60 to 65% abietic acid and dihydioabietic acid, and up to 5% of water, are discussed. Experiments to determine the hygroscopicity of cores are described. Results are compared with those obtained in tests with linseed oil.—L. J. L.

Testing the Dryness of a Foundry Mould with the Aid of an Electrical Bridge. E. A. Glozman. (*Zavodskaya Laboratoriya*, 1955, **21**, (11), 1386–1388). [In Russian]. In the procedure described the dryness of mould mixtures is found from the electrical resistance between two stainless-steel electrodes inserted in them.—S. K.

Casting Tolerances as Affected by Automation in the Machine Shop. E. L. Buchman. (*Amer. Found. Soc. Preprint*, 1956, No. 103). Some of the problems in casting tolerances and quality control which arise in an automatic machine shop are discussed in general terms.—B. C. W.

The Production of Cast Iron Water Ducts. V. Čáp. (*Hutník*, 1956, **6**, (4), 98–102). [In Czech]. The development of casting techniques is surveyed and an account is given of modern methods used in Czechoslovakia to-day.—P. F.

The Napier Investment Foundry. (*English Elec. J.*, 1956, **14**, March 13–19). An illustrated account of the process used.

The Settling Head Casting Process. H. Schiegner. (*Giessereitechn.*, 1956, **2**, July, 146–150). By employing the settling head gating method, liquid steel will be saved, yield efficiency will be improved, the amount of material in circulation will be reduced, and casting of better quality will be obtained. The method is described, and practical examples of its use are given.—L. J. L.

On the Hydrodynamic Theory of Centrifugal Casting. M. M. Chepinoga. (*Izvestiya Akademii Nauk SSSR, O.T.N.*,

1956, No. 3, 92–105). [In Russian]. A theoretical study of the flow of liquid in a rotating cylinder is given. Experimental and theoretical results differed by no more than 20%.—V. G.

Shell Moulding. J. Cañameras Gonzalo. (*Inst. Hierro Acero*, 1956, **9**, Jan., 6–22. *Special Number*). [In Spanish]. A comprehensive, illustrated, review of the technique of shell moulding is given. The foundry methods are discussed together with the economic considerations.—P. S.

Porosity Licked as 3000 lb Cast Oil Well Cylinder is Poured on Side. C. J. Bradley. (*Western Metals*, 1956, **14**, Mar., 58–59).

Where Castings in Ceramic Molds Fit into Your Products. (*Precision Met. Mold.*, 1956, **14**, Apr., 40–41). The advantages of the split ceramic mould process are listed and typical products of the process illustrated.—D. H.

Continuous Casting of Cast Iron Bars. G. J. Shaw. (*Metal Treatment and Drop Forging*, 1956, **23**, May, 165–170; June, 233–236). Casting machines are considered, mould materials and design, mechanism of solidification, and closed and open systems. Experiments are described and structures and defects arising from conditions of casting are described and illustrated.

Cleaning Process for Castings. (*Engineer*, 1956, **202**, July 6, 25). A process is described for cleaning iron or steel castings of sand, rust, grease, and scale, in readiness for machining, plating, enamelling, brazing etc. Cleaning is carried out in a salt bath, which acts catalytically when activated electrically.—M. D. J. B.

Shell Moulding Practice. D. F. Bailey. (*Metal Ind.*, 1956, **88**, June 22, 520–522; June 29, 544–547). Core blowing and mould blowing are described and the production and use of coated sands, with notes on runner systems, pouring methods, and shell assembly processes.

Shell Forming: Some Like it Hot, Some Like it Cold. A. F. MacConochie (*Steel*, 1956, **138**, Feb. 27, 128–132). The processes and rival advantages of hot and cold forming of shells are considered. Forging is favoured by experience and cost, but in war-time expansion, cold forming offers conservation in manpower, metal and mill capacity. The hot cupping, cold-forming process has advantages.—D. L. C. P.

REHEATING FURNACES AND SOAKING PITS

Multi-Zone Steel Re-Heating Furnace. Uniform Heating and Simplified Maintenance. (*Engineering*, 1956, **182**, July, 20, 82–83). This article describes a re-heating furnace which consists essentially of three units, each with different heat and atmosphere conditions but operating as one continuous pusher-type furnace. The furnace described is used for heating blooms and billets.—M. D. J. B.

Use of a Protective Heat-Resisting Section Before a Needle Recuperator. B. L. Poletaev and A. A. Sorokin. (*Stal'*, 1955, (10), 945–947). [In Russian]. An account is given of tests on the recuperator of a continuous furnace dealing with flue and air-temperatures of 850° and 200° C respectively. The cast iron needle recuperator was found to fail mainly through thermal shocks produced by interruptions of mill operation or increases in operating rates. These shocks were largely eliminated by introducing a pre-cooling section made of heat-resisting steel (0·14% C, 0·57% Mn, 0·50% Si, 33·15% Cr, 0·22% Ni, 0·019% S, 0·035% P), in which the temperature was reduced by 200–300° C. With the protective section the air temperature could be safely increased from 200 to 360–390° C.—S. K.

HEAT-TREATMENT AND HEAT-TREATMENT FURNACES

Some Aspects of Furnace Doors, Construction and Operation. J. E. Hyler. (*Steel Processing*, 1956, **42**, Mar., 163–166; Apr., 225–228). Heat-treating furnaces are dealt with, and controls and hoist mechanisms are described and illustrated.

A Commercial Heat Treating Furnace Installation. J. P. Benedict. (*Metal Treating*, 1956, **7**, Mar.-Apr., 2–3). A bottom-opening furnace operating from 250°–2275° F and capable of handling a 5000 lb load is described. Loading and unloading is hydraulic and the furnace is divided into 6 zones recording temperatures every 90 s by a 6-point recorder. The furnace is gas fired through 16 burners.

Stress-Relieved 200 ft up. (*Chem. Eng.*, 1956, **63**, Apr., 132–134). The way in which a 25 ft diameter, 71 ft high tower section was heat-treated after erection is briefly described.—T. E. D.

Heat Treatment with Controlled Atmosphere. (*Mét. Constr. Mécan.*, 1956, **88**, Mar., 261–267). The different types of gas atmospheres used in practice and the design of gas generators are discussed. Examples of commercial equipment are shown.—B. G. B.

Automatic Carbon Control for Batch-type Furnaces. T. N. Duncan. (*Steel Processing*, 1956, **42**, May, 283–287). An account of work at Tulsa Winch.

Heat Treatment of Grey-Cast Iron. A. H. Rauch and J. B. Peck. (*Amer. Found. Soc. Preprint*, 1956, No. 25). The heat treatment of grey cast irons is briefly discussed and the results of end-quench hardenability tests on alloyed and unalloyed irons are reported. Microhardness tests on as-quenched and quenched and tempered grey iron samples with different R_c hardness showed that the hardness of the matrices was essentially the same. Results to show the effect of tempering on the tensile strength, flexural strength, impact resistance, modulus of elasticity and hardness of an unalloyed iron are presented and discussed.—B. C. W.

Hardening High-Speed Steel. (*Engineer*, 1956, **201**, June 15, 685). A brief description is given of a furnace designed for hardening precision high-speed steel tools. The furnace is made by the Electric Resistance Furnace Co., Weybridge.

Commercial Bright Hardening of Stainless Steels. (*Canad. Metals*, 1956, **19**, Apr., 51–52). An account of a high temperature, gas-fired muffle furnace for the heat treatment of stainless steel parts in a controlled atmosphere is presented. The furnace operates at temperatures between 1650 and 1950° F and handles 60 lb of material/hour.—B. G. B.

Effect of Alloying Elements on the Boundary Hardenability of Case-Hardening Steels. H. U. Meyer. (*Stahl u. Eisen*, 1956, **76**, Jan. 26, 68–78). The author discusses the behaviour of case-hardened components in the light of their surface hardness, structure, and hardness distribution over the section. He considers indices of these properties obtained from boundary hardenability, enlarging on the concept of boundary hardenability itself and methods for its determination. Investigations of the boundary hardenability of certain American and German case-hardening steels are described. The effects of carbon and alloying elements are indicated and compared with effects on the hardenability of the basic material.

Micro-cracks in Case Hardened Steel. A. H. Rauch and W. R. Thurtle. (*Metal Progress*, 1956, **69**, Apr., 73–76). Micro-cracks which occur in high carbon steels or cases are principally dependent on the grain size established by heat treatment and are independent of quenching rate, alloy content or method of carburizing or carbo-nitriding.—B. G. B.

Piston Pins are 100% Surface Hardened for Better Service. R. E. Haislip. (*Steel Processing*, 1956, **42**, Feb., 107–110). The process is described and compared with the previous pack carburizing process.

The Use of Shot Peening to Reduce Weight. W. R. Berry (*Inst. Mechanical Eng.*, 1956, Preprint, pp. 11). An account of work on spring leaves with the object of increasing working stress and so reducing weight. It is considered that a saving of 20–25% can be attained.

Applications of the Cathode Ray Oscillograph to the Recording of Temperature-Time Curves during Rapid Hardening. R. Bigot and R. Faivre. (*Rev. Mét.*, 1956, **53**, Feb. 131–138). Experiments on nickel are described using the extremely rapid response of the instrument to study the effects of the quenching liquids used.

Carbonitriding Small Parts. J. McMullen and D. R. McHarg. (*Metal Treatment and Drop Forging*, 1956, **23**, May, 179–184). Plant for treatment of calculating machine parts is described and the resulting structures are illustrated. Bright hardening and gas carburizing are dealt with, giving weights, temperatures and atmospheres.

Reduction of Heat Consumption in Annealing of Cast Steel. G. Prieur and G. Fechner. (*Stahl u. Eisen*, 1956, **76**, Jan. 26, 78–81). The change effected in heat consumption after an examination of the process is described. Heat consumption diagrams and their significance are discussed and the effect of annealing time indicated. The effects of output and unit weight are also considered. The construction of a new annealing furnace is described.

Tempering in Liquid and Gaseous Media. Z. Hostinský. (*Reports of Czechoslovak Foundry Research, Appendix to Slévárenství*, 1956, **4**, (3). [In Czech]. The research was aimed to elucidate the possibility of replacing annealing pots by annealing directly in a protecting atmosphere consisting principally of nitrogen with small amounts of carbon monoxide and dioxide, or in a salt bath made from a mixture of barium chloride and borax. The former method was used in the range 900–950° C, the latter in the range 1000–1100° C. The cast iron was of the 2·41% C, 1·13% Si type, inoculated with either, Fe-Si, Al, Mg–Fe–Si or boron. The use of the oxygen lance in the ladle stage was studied, and the course of graphitization was examined. The most efficient means of reducing the first graphitization period was found to be annealing at 1000–1050° C; at higher temperatures, lamellar graphite was precipitated. Boron was found to be the most and manganese and aluminium the least efficient inoculating agents amongst those tested. The characteristics of the second hardening period, the effect of inoculating in the ladle, hardening of the castings prior to annealing, and the strength of the castings are discussed. Annealing without annealing pots is judged to be economically and metallurgically superior to conventional methods.—P. F.

FORGING, STAMPING, DRAWING, AND PRESSING

Current Studies of Large Forgings. A. O. Schaefer. (*Metal Progress*, 1956, **69**, Apr., 63–67). An account is given of co-operative research work in America to find the cause (and cure) of brittle fracture and establish inspection methods whereby potentially dangerous forgings can be identified.

Resistance Heating Boosts Forging Efficiency. (*Iron Age*, 1956, **177**, Feb. 16, 108–110). A German, semi-automatic production line for flanged rear-wheel axles is described. Parts are heated by an electrical resistance method, before upsetting and friction forging. There are advantages in quality and requirements.—D. L. C. P.

Origin and Prevention of Flake-Formation in Forgings on Cooling. R. Hřivňák. (*Hutník* (*Prague*), 1956, **6**, (3), 71–76). [In Czech]. A survey is made of principles and methods related to the avoidance of flaking, with special reference to Soviet practice.—P. F.

Automatic Press Line for the Production of Wheel Discs. (*Machinery*, 1956, **88**, Apr. 13, 461–466; *Steel Processing*, 1956, **42**, Mar., 146–148, 178–179). The Clearing Machine Corporation, U.S.A. have recently completed a production line for the manufacture of motor-car wheel-discs at Dunlop Rim and Wheel Co., Coventry. The line consists of four individual presses, the first of 275 tons and remainder of 600 tons capacity. Four pressing operations are performed, the process being completely automatic.—M. A. K.

Modern Applications of Hydraulic Power to Presswork. O. Kühner. (*Sheet Metal Ind.*, 1956, **33**, Mar., 167–172; from *Blech*, 1955, June, 1559).

Some Aspects of the Use of Ferritic Chrome Iron in Sheet Form. J. N. Edwards and A. A. Pearson. (*Sheet Metal Ind.*, 1956, **33**, Jan. 17–24). An account is given of the use of 17% Cr sheet by Morris Motors Ltd., with a section on corrosion resistance.

Cut Blanking Costs with Simplified Design. F. Strasser. (*Iron Age*, 1956, **177**, Mar. 15, 83–86). Hints on the planning and operation of metal-blanking are given, based on shop experience.—D. L. C. P.

Ford Operating New Cleveland Stamping Plant. (*Steel Processing*, 1956, **42**, Jan. 37–41, 50). An illustrated account of the plant and processes is presented.

Automation's Effect on Quality Requirements in the Steel Industry. R. Guthrie. (*Iron Steel Eng.*, 1956, **33**, March, 116–119). The author discusses the effects of automation in body stamping plants and the changes that the Ford Steel Division has found necessary in order to produce the type of product the internal customers want.—M. D. J. B.

Inspection of Hob Cutters. (*Report of Government Mechanical Laboratory*, No. 25, 1956, (Tokyo), pp. 71).

Gearmotors Guide Pipe through Heat Treating Line. J. W. Brinks. (*Iron Steel Eng.*, 1956, **33**, Feb. 125).

Seamless Pipe for the Oil Fields. C. C. Crawford. (*Iron Steel Eng.*, 1956, **33**, March, 96–99). The author describes the sequence of operations in the manufacture of tubes at the Seamless Tube Mill—Colorado Fuel and Iron Corp. The heating and piercing of billets, rolling in the plug mill, reeling, sizing and reducing are discussed as well as quality and size specifications.—M. D. J. B.

Studies in Cold-Drawing—III. Determination of Friction Coefficient. H. Majors. (*Trans. Amer. Soc. Mech. Eng.*, 1956, **78**, Jan., 79–87). Average coefficients of drawing friction were determined for forward and reversed drawing of 0·2% C steel using Sachs' theory and compared with measurements using resistance-wire strain gauges on the outer die surface to determine die pressures. Die profiles were determined by plastic castings. A series of dies were used to provide true reductions of rod area up to 0·76 at drawing speeds of 2 i.p.m.—D. H.

A Method of Abrasion Measurement in Wire Drawing with Activated Dies. W. Dahl and W. Lueg. (*Stahl u. Eisen*, 1956, **76**, Mar. 8, 257–261). A review of the literature is given before describing the experiments performed. (The dies were activated at Harwell). The drawing tests, the preparation of the solution of wear debris, the measurement of activity and the autoradiographic photography employed are described. The calculation of the quantity abraded and the enlargement of the die is outlined.—A. C.

Extrusion of Metals. G. A. Moudry. (*Iron Steel Eng.*, 1956, **33**, March, 79–83). After describing briefly the development of extrusion techniques for aluminium, the author discusses the practicability of extruding steel and titanium. It appears that steel can be extruded at speeds much higher than aluminium and with lower pressures. The principal difficulties are the high extrusion temperature of steel, about 2300° F, and the bad effects on the die blocks.—M. D. J. B.

New Applications of "Fibrage Integral". P. Verot. (*Pamphlet of Compagnie des Ateliers et Forges de la Loire, Usine de Saint-Chamond*). A general account is given of the production of crankshafts and propellor hubs by the continuous grain-flow process.

Plastic Working of Metals. W. S. Wagner. (*Trans. Amer. Soc. Mech. Eng.*, 1956, **78**, Feb., 401–406). Plastic working of metals is discussed in general terms. The significance of the thermoplastic and crystoplastic states is explained, the relationship between work hardening and deformation hardness mentioned and one method of estimating deformation strength from true strain given. The effect of ageing on plastic working is discussed briefly.—D. H.

Plastic Metal-working. E. V. Crane. (*Trans. Amer. Soc. Mech. Eng.*, 1956, **78**, Feb., 413—415). The author gives a short discussion of some practical and theoretical aspects of plastic working.—D. H.

ROLLING-MILL PRACTICE

Factors Affecting the Accuracy of Rolling in the Hot Rolling of Sheets and Strips and their Control by Experiment and Calculation. O. Emicke and K. H. Lucas. (*Neue Hütte*, 1956, **1**, Mar., 257–274). Static bending tests with chilled rolls and alloy steel rolls in a 1000 ton press showed good agreement with results calculated by the Caswell method. A diagram for the graphical determination of roller bending and heating in plate rolling mills is given. Caswell's formulæ and the author's experimental results were used to determine elastic deformation of rollers in three-high and four-high rolling stands. The latter were found to be superior. Roller bending was formed to constitute two-thirds of total elastic deformation.—L. J. L.

A Note on the Calculation of Roll Force and Torque in Hot Mills. R. B. Sims. (*Davy-United Engineering*, 1956, **1**, April, 2–8, 24). Equations are derived and tested and deviations noted.

Residual Stresses in Double-Pour, Cast Iron Work Rolls. A. M. DiGioia, jun. and C. F. Peck, jun. (*Iron Steel Eng.* 1956, **33**, March, 58–61). The authors describe an experimental method for determining residual stresses in double-pour, alloy cast iron work rolls. Residual stresses are studied by measuring the surface strains of the rolls experimentally. The physical properties of specimens cut from four different rolls are examined.—M. D. J. B.

Roll Grinding and Roll Grinding Wheel Application. W. Pope. (*Iron Steel Eng.*, 1956, **33**, May, 125–128). The author describes various types of roll grinding machines and discusses their relative merits.—M. D. J. B.

The Effect of Macrostructure on the Life of Cast-Iron Rolls for Use in Cold Rolling of Strip. M. Šourek. (*Hutník*, 1956, **6**, (4), 113–117). [In Czech]. An account is given of methods used and experiences gained in the Králův Dvůr

Metalworks in the cold-rolling of steel strip and in assessing the criteria of quality of the rolls used.—P. F.

Formulæ for the Determination of the Dimensions of Squares and Rhombs. M. Casas Bayer. (*Inst. Hiero Acero*, 1956, **9**, Jan., 23–27. *Special Number*). [In Spanish]. In order to help the roll designer to specify passes for hot rolling steel to a square or diamond section formulæ are given which, for vertex angles of 91 to 145° give the lengths of the vertical and horizontal diagonals, and the pass height and width as a function of the thickness, corner radii, and roll separation of the pass.—P. S.

The Planetary Rolling Mill and its Control Equipment. (*Usine Nouvelle*, 1956, **12**, Feb. 9, 30–31). The action of a planetary mill is explained and the advantages are examined. Some details are given of the first planetary mill to be put into use. It is installed at Ductile Steels Ltd., Wolverhampton, and commenced operations in 1953. The chief electrical contractors were English Electric. The mill can reduce steel 44·4 mm thick to 1·01 mm in a single pass.—T. E. D.

Pittsburgh Steel's New Hot and Cold Strip Mill at Allenport, Pa. H. A. Long and J. C. Peth. (*Iron Steel Eng.*, 1956, **33**, Jan., 57–66). A description is given of the new 66 in. semi-continuous hot strip mill and of the new four-strand tandem cold mill at Pittsburgh Steel. Technical data are given on the layout, capacities, motors, finishing lines and ancillary equipment.—M. D. J. B.

Steel Co. of Wales Extend their Works. First Continuous Annealing Plant in Europe. (*Engineering*, 1956, **182**, July 13, 45–46). This article describes the new 4-high, five-stand, cold-reduction rolling mill at the new Velindre Works of the Steel Co. of Wales. The mill will cold-roll strip at speeds of up to 5000 ft per minute for subsequent processing into tinplate.—M. D. J. B.

Automatic Thickness Control on Five-Stand Tandem Cold Reduction Mill. (*Engineer*, 1956, **201**, March 16, 258–259). This article describes an X-ray gauge system to obtain closer, continuous control of cold reduction mills producing sheet and strip. The system developed by the U.S. Steel Corp. and the G.E.C. consists of two portions: a coarse system utilizing an X-ray gauge between stands 1 and 2, a regulating system to operate the screw-down motor on stand 1, and a vernier system utilizing an X-ray gauge after stand 5 and a regulating system to vary stand 5 motor speed to effect gauge control.

Industrial Television at Steel Rolling Mill. (*Electronic Eng.*, 1956, **28**, Aug., 349). The installation at the Steel Company of Wales is shown.

High-Speed Five-Stand Tandem Cold Strip Mill. (*Engineer*, 1956, **201**, April 13, 342–343; April 20, 378–379). A new 5-stand tandem cold strip mill installed at the Ebbw Vale works of Richard Thomas and Baldwins, Ltd., is designed to operate at a maximum speed of 5000 ft per min. It is intended for reducing hot rolled steel strip down to tin plate gauge up to 38 in. wide. The ingoing gauge of strip is up to 0·140 in. maximum, the minimum outgoing gauge being 0·006 in.—M. D. J. B.

Production, Technical, and Economic Problems in the Production of Transformer Steel. J. Dušek. (*Hutnické Listy*, 1956, **11**, (3), 129–132). [In Czech]. A survey is made of the present state of development of the technology of transformer sheet production by both hot and cold rolling processes.

Specification for Cold-Rolled Strip Steel. G. Molinder. (*Sheet Metal Ind.*, 1956, **33**, 203–204, 214). An account of Swedish work at Munkfors is given. Tolerances and testing methods are discussed. A method for appraisment of surface finish is referred to and, generally, the improvement of products while specifications tend to remain fixed is considered. A short discussion on hardness testing is appended.

Control Systems Using Non-Contacting Thickness Gauges. W. E. Van Horne. (*Iron Steel Eng.*, 1956, **33**, Feb., 96–100). This paper describes some of the uses of non-contacting gauges and accessory equipment for continuously and automatically performing production control functions in the manufacture of cold-rolled strip and electrolytic tinplate.—M. D. J. B.

The Cold Roll Forming Process: A Rapid and Accurate Method for Producing a Wide Variety of Shapes. (*Automobile Eng.*, 1956, **46**, Jan., 34–36). A review is made of the method of producing roll-formed sections. Machines consisting of a number of stands, each having a pair of forming rolls, are now available for the forming of steel strip up to 0·156 inches thick × 30 inches wide. The machines described in this article were made by the Yoder Company of America.

New Concepts in Drive Systems for Hot Strip Mills. H. N. Snively and R. J. Moran. (*Iron Steel Eng.*, 1956, **33**, April, 101–109). The authors discuss modern mill drives with such features as individual rectifiers, magnetic amplifier regulators, twin drives with individual armature loops, and individual motors to roller table rolls. It is claimed that these features result in maintenance savings, more flexible operation and better load balance and control.—M. D. J. B.

Present Position in the Development of the Electrical Aspect of Newly Equipped Reversing Mill Trains. K. Müller-Trimbusch. (*Stahl u. Eisen*, 1956, **76**, Feb. 23, 201–211). The author reviews the state of rectifier development and electrical requirements in steelworks. He compares the advantages and disadvantages of rectifier installations. Reversing switchgear and regulating techniques are considered. He discusses the various types of drive, the interaction between speed and torque, and the question of reversing time. Frequency distributions of rolling time are given. Twin drive with rectified supply is considered. The incidence of breakdowns is discussed and frequency distributions of causes are given. The electrics of auxiliaries are also dealt with. The author finally calls on past experience in outlining possible future developments.—A. C.

Present Position in the Development of the Mechanical Aspect of Newly-Equipped Reversing Mill Trains. W. Dehne. (*Stahl u. Eisen*, 1956, **76**, Feb. 23, 192–201). The purpose of this review is stated to be, not the enumeration of the advantages of the new installations, but the consideration of their shortcomings and the unfulfilled aspirations of mechanical plant engineers. Such discussion is felt to be in the interest of future development. Technical points are dealt with in some detail, and the need for collaboration between plant manufacturers and users is stressed. So many unsolved problems exist, it is thought, that a plant engineering research establishment is becoming necessary.—A. C.

Electrical and Mechanical Requirements in Single Stand Reversing Mill Trains. E. Wilms. (*Stahl u. Eisen*, 1956. **76**, Feb. 23, 185–192). The author considers the reversing mill train as a connecting link between steelworks and finishing trains. The rolling programme; quality and quantity requirements as deciding factors in the construction and layout of a train; the fundamentals of operation; the main motor requirements in relation to the rolling programme and capacity; torque and reversing speed; the twin drive; requirements on mill housings with respect to clearances, roll change, and roll wear; screwdown speed and accuracy; automatisation; manipulators; and roller table speed and control are among the subjects discussed. The need for measuring devices as operational aids and in the furtherance of research is urged.

Electrical Equipment for Auxiliary Drives of Hot Strip Mills. S. H. Williamson. (*Iron Steel Eng.*, 1956, **33**, Jan., 94–104; Feb., 68–75; Mar., 84–93). A review of what is to-day considered good practice in the selection of motors and control drives. Some of the special requirements of the various drives are considered, together with engineering reasons for selecting particular systems. The duty requirements of auxiliary drives are tabulated and slab pushers and squeezers, guides, roughing mill tables, shears, loopers, and screwdowns are reviewed, and finally requirements for flying shears, runout tables, coilers and conveyors are considered with technical and operational data.—M. D. J. B.

MACHINERY FOR IRON AND STEEL PLANT

Power Systems Chicago District—U.S. Steel. K. E. Dinius. (*Iron Steel Eng.*, 1956, **33**, May, 98–102). This article describes the measures developed by the Chicago District electric generating stations to cope with the expanding power requirements and production changes. The power system has a capacity of 385,000 kW and generates both 25 and 60 cycle frequencies.—M. D. J. B.

Design Factors for Steel Mill Tractors. J. A. Draxler. (*Iron Steel Eng.*, 1956, **33**, March, 100–104). This article describes the broad requirements of mobile handling equipment for use in steel mills. Fork lift trucks of various types are described as well as straddle carriers, ram trucks and coil handling trucks.—M. B. J. B.

Shock Loading Effects in Overhead Travelling Cranes—Review of Dynamic Stress Allowances. E. Lightfoot. (*Engineering*, 1956, **181**, April 6, 169–173). A description

is given of tests carried out on three lattice-type E.O.T. cranes to study the effects of shock loading on the structures. (8 references).—M. D. J. B.

Rectifier Equipment Supplies D.C. Power in Steel Plants. C. S. Hague. (*Iron Steel Eng.*, 1956, **33,** May, 84–91). This article describes the major types of rectifiers now being applied to steel mill service and reviews their salient characteristics. The principal applications described are:—250 volt constant potential supply for auxiliary drive motors; 700 volt supply for main drive motors; 6 to 36 volt supply for tinning lines and cleaning lines.—M. D. J. B.

Steel Works Locomotives—Diesel or Steam? M. D. J. Brisby and J. H. Turnbull. (*Engineer*, 1956, **201,** June 29, 746–748). The authors discuss the operating capabilities of diesel and steam shunting locomotives and show that despite the higher first cost of the diesel, the lower operating costs, coupled with the greater shift and yearly availabilities, make it no longer possible for the steamer to compete.

A Stabilized D.C. Crane Hoist Control. K. S. Kuka. (*Iron Steel Eng.*, 1956, **33,** Feb., 86–95). This paper describes a new hoist control scheme which is designed to give a simple and more straightforward main motor power circuit having the most desirable speed-torque characteristics, which at the same time gives a simple control circuit.—M. D. J. B.

LUBRICATION

Effect of Lubricant on Pitting Failure of Ball Bearings—Experimental Results for Various Fluids. F. T. Barwell and D. Scott. (*Engineering*, 1956, **182,** July 6, 9–12). The authors describe experiments carried out at the Mechanical Engineering Research Laboratory to assess the effect of the lubricant on fitting failure. Simple apparatus was used with conventional ball bearings as test specimens.—M. D. J. B.

WELDING AND FLAME-CUTTING

General Developments in Welding Techniques during the last 25 years. F. Rapatz and A. Schmidt. (*Schweisstechn.*, 1956, **10,** Jan-Feb.-March, 9–14). Testing is included.

Butt Welding of High Pressure Pipelines. (*Inst. Petroleum, I.P. Rev.*, 1956, **10,** May, 147–148). An account of the Burton automatic process.

The Arc Welding of 2·25% Cr–1·0% Mo Alloy Steel Pipe. J. Bland. (*Welding J.*, 1956, **35,** April, 181s–194s). A significant correlation was found to exist between hardness and ductility and between hardness and tensile strength, for heat-treated 2·25% Cr–1·0% Mo alloy steel pipe and 2·25% Cr–1·0% Mo alloy weld deposits.—U. E.

Carbon-Dioxide-Shielded Consumable Electrode Arc Welding. G. R. Rothschild . (*Welding J.*, 1956, Jan., 19–29). It is shown that the process will give sound welds on mild steel provided that a close control of variables is exercised and that the electrode contains sufficient manganese and silicon.—U. E.

Moisture and its Effects in Carbon Dioxide Welding of Steel. R. W. Tuthill. (*Welding J.*, 1956, **35,** April, 330–333). It is shown that for good welding practice, the moisture content in carbon dioxide should be kept as low as is practical.—U. E.

Properties and Applications of Low-Hydrogen Iron-Powder Electrodes. D. C. Smith, W. G. Rinehart, D. C. Helton. (*Welding J.*, 1956, **35,** April, 341–347). Two commercial groups of low-hydrogen electrodes having 30 and 50% iron powder in their coatings were tested along with three brands of conventional E7016 electrodes and results compared. Tables, charts, and photographs show results obtained on efficiencies, burn-off and deposition rates, tensile, and yield strengths, ductility, Charpy-Vee impacts and horizontal-vertical-, and flat-position welding. The mechanical properties to those of the conventional E7016 electrodes.—U. E.

Mechanical Properties of Butt Joints Brazed with BAg-1, BAg-3, and BCu Filler Metals. G. Hansel. (*Welding J.*, 1956, **35,** April, 211s–216s). The room temperature, impact, tensile, and fatigue properties of brazed butt joints are discussed.—U. E.

Some Applications of Projection Welding. P. Jonges. (*Lastechn.*, 1956, **22,** 6L, July, 106–112). [In Dutch]. This is a description emanating from the Philips Telecommunicatie Industrie, Hilversum, of the development of this welding method claimed to be suitable for the series and mass production of small mechanical parts enabling more welds to be made simultaneously with mutual tolerance remaining within 0·008 in. provided correctly constructed tools, presses, and assemblies are adopted. Details and examples of the process are discussed in conjunction with numerous diagrams and illustrations.—F. R. H.

The Welding of Alloy Steel Lips of Dredger Buckets. J. J. Besteman. (*Lastechn.*, 1956, **22,** Jan., 8). [In Dutch]. In order to reduce the draft of a dredger under construction, a large number of light weight buckets were made with welded Mg-steel lips. The method of welding adopted is described and the results of tensile tests on the buckets are given.

Rivetting and Welding. W. P. Kerkhof. (*Lastechn.*, 1956, **22,** Mar., 38–44). [In Dutch]. This is a paper read on 28 Oct., 1955, before the Bond voor Materialienkennis in which the author answers critically the statements made in the Dutch publication *Bedrijf en Techniek* (22.X.1955), concerning the relative merits of rivetted and welded constructions. Numerous illustrations appear in the text of the use of both methods in structural, industrial and civil engineering and in shipbuilding. The author concludes that without welding many projects would be impossible of execution.—F. R. H.

Transient Problems with High-Flux Density-Transformers in Welding Applications. R. C. Mierendorf. (*Welding J.*, 1956, **35,** March, 236–243). It was found that hypersil transformers can be used with success in welding applications with almost all types of control equipment. Magnetizing transients may be predicted when the characteristics of the welding transformer are available and the power factor of the welding transformer will determine the optimum initiation angle.

Recommendations Regarding the Minimum Requirements to be Met by Ordinary Carbon or Low-Alloy Carbon Manganese Structural Rolled or Forged Steels so that they may be Suitable for Electric Arc Welding. (*Soudage Techn. Connexes*, 1956, **10,** Jan.-Feb., 7–11). It is suggested that steels should be divided into four qualities from the welding viewpoint. Minimum acceptable thicknesses and chemical requirements are indicated, and testing is outlined.—T. E. D.

The Development and Investigation of High-Tensile High-Impact Electrodes. G. S. Wepfer. (*Welding J.*, 1956, **35,** March, 229–235). Electrodes of E12015, Grade 260, MIL-E-986B, specification were tested. Tensile properties were found to be adequate, impact properties were low, and not satisfactory in the stress-relieved condition. The same result was obtained with Mn–Mo electrodes of E9015 and E10015 type, but E9015 was below the minimum strength levels of T-1 steel requirements for yield and tensile strength. The influence of size and weld-metal density on mechanical properties and impact values was studied. An electrode containing 3·5% nickel and 0·50% molybdenum was developed which will meet the required tensile and impact properties of T-1 steels.—U. E.

Effect of Individual Coating Ingredients on Surface Tension of Iron Electrodes. T. H. Hazlett and E. R. Parker. (*Welding J.*, 1956, **35,** March, 113s–114s). The surface tension of iron electrodes was measured by the drop geometry method. Average surface tension values in atmospheres of nitrogen, argon, and helium, were found to be 829, 829 and 836 dyne per centimeter, respectively.—U. E.

Testing and Inspection of Materials and Welded Work for Hydraulic Power Plants. W. Stauffer and A. Keller. (*Escher Wyss News*, 1956, **29,** 35–48). Specifications and testing methods are detailed, with microstructures.

Method of Evaluating the Fluidity of the Welding Bath. A. A. Erokhin. (*Zavodskaya Laboratoriya*, 1955, **21,** (12), 1466–1468). [In Russian]. In the method described the fluidity of the molten metal in open or submerged-arc welding is estimated from the weight of metal which splashes out when the work is suddenly inverted to empty the bath. Apparatus for effecting this is outlined.—S. K.

The Behaviour of Spot Welds Under Stress. J. F. Rudy, R. B. McCauley, R. S. Green. (*Welding J.*, 1956, Feb., 65s–71s). An investigation was made of the existence of a relationship between four spot-welding parameters, limited to spot welds in 11 gauge Armco iron. It was found that spot welds fail by either a shear, intermediate or tear system of failure. The macro-geometry of the weld cross-section is decisive. The four parameters, failure system, weld strength, macro-geometry of cross-section and sectioned spot shear test observations are related.—U. E.

The Practical Application of the Slide Rule "Schweisstechnik". J. Titscher. (*Schweisstechn.*, 1956, 10 April, 53–57). A number of practical uses of the slide rule described in *Schweisstechnic*, August, 1955, are discussed. With the help of this slide rule

the weight of the weld seam, welding time and oxygen consumption can be determined accurately.—U. E.

The Horton Spheroid. C. Arne and R. V. McGrath. (*Lastechn.* 1955, **21**, Nov., 218–220). [In Dutch]. An illustrated general description of the two welded—nearly spherical and flattened—types of spheroidal containers used for the storage of volatile petroleum products under pressure and made by the Chicago Bridge & Iron Company.—F. R. H.

Quality of the Seam in Tubes Produced by the Resistance Method. B. D. Zhukovskiĭ, L. I. Zil'bershtein, and F. D. Manevich. (*Stal'*, 1955, (11), 1011–1015). [In Russian]. In the investigation of the influence of various factors on the quality of the seam in tubes resistance-welded with A.C. it was possible to establish: (*a*) the dependence of the periodic heterogeneity of the seam on the welding speed; (*b*) the possibility of reducing this heterogeneity by increasing the power supplied to the edges being welded; (*c*) the existence of a certain welding speed (for a given current frequency) at which increased power supply fails to reduce heterogeneity. Tubes welded at 27–29·5 m/min with a current frequency of 50 hertz have satisfactory seams, but higher speeds lead to periodic variations in seam strength.—S. K.

Electric Arc Welding. Its Defects and How to Avoid Them. (*Acciaio Inossid.*, 1955, **22**, Sept.-Oct., 161–173; Nov.-Dec., 209–225). [In Italian]. This paper describes in detail the techniques for welding stainless steels, discusses the various types of welding defects and suggests means of avoiding these. Special attention is given to the problems of penetration, excessive heating, slag inclusions, porosity and cracks. Details are also given of the types of electrodes available for welding stainless steels. (15 references).—M. D. J. B.

The Influence of Weld Faults or Fatigue Strength with Reference to Butt Joints in Pipe Lines. R. P. Newman. (*Trans. Inst. Marine Eng.*, 1956, **68**, June, 153–172) An account is given of tests on welded 6 in mild steel pipe in alternating plane bending. The effect of the root zone of welds is shown to be predominant and no correlation between radiographic appearance and fatigue behaviour is possible. Discussion follows.

Hot Cracking of Stainless Steel Weldments. P. P. Puzak, W. R. Apblett, W. S. Pellini. (*Welding J.*, 1956, Jan., 9s–17s). A number of heats and forgings of 347 and 304 stainless steels were investigated. It is deduced that hot cracking of the base metal results from the liquation of fusible segregates located at the boundaries of grains which adjoin the fusion line of the weld proper, and due to the high strain concentrations, the cracks extend into the weld metal.—U. E.

Hot Cracking of Austenitic Chromium Nickel Welds. W. Hirsch and H. W. Fritze. (*Schweissen u. Schneiden*, 1956, **8**, March, 81–85). An investigation was made of the cause of hot cracking in welded austenitic chrome-nickel steel. It is shown that the tendency to hot cracking is due to liquid phases being present at the grain boundaries shortly before final solidification of the weld metal. The effect of the structure, grain-size and alloying elements such as niobium on hot cracking is discussed.—U. E.

On Macro Non-Uniformity of the Chemical Composition of Welds. G. L. Petrov. (*Izvest. Akad. Nauk SSSR, Otedelenie Tekn. Nauk*, 1955, (9), 137–153). [In Russian]. Chemical non-uniformity of welds was investigated. It is concluded that this non-uniformity caused by technological factors can be reduced to a minimum by improving welding materials and practice. On the boundaries between welds and solid metal, changes in the chemical composition can reach 0·05–0·3 mm in depth, depending on the composition of welding and welded metals.

The Influence of Porosity in Welded Butt Joints. B. Lauterburg. (*Lastechn.*, 1956, **22**, Jan., 2–6, Feb. 26–30). [In Dutch]. This article is a translation of a report on an investigation conducted in Switzerland. It discusses at length the static adhesion, brittle fracture risk, fatigue resistance and the influence on these characteristics exerted by tiny cavities (porosity) in the weld.—F. R. H.

A New Product—A Welding Paint. J. Hardy. (*Prat. Soud.*, 1955, **9**, May, 80–83). [In French]. The author describes a process to be used with soft welds of tin and lead tin alloys in which the surfaces to be welded are painted with a special cleaning agent containing a tin alloy. This can be applied by brush or spray gun.—M. D. J. B.

High-Temperature Furnace Brazing. D. M. Davey and K. C. Randle. (*Metal Treatment and Drop Forg.*, 1955, **22**, Dec., 501–505). A method of brazing without using a flux is described. The process involves the use of a protective atmosphere of burnt town's gas, dissociated ammonia, or hydrogen, depending on the metal or alloy being brazed. The process can be carried out in batch or continuous type furnaces provided they are reasonably "gas-tight". The compositions of several brazing alloys are quoted and examples of the method and its applications are discussed. (5 references).

A Test Block for Welding Gray and Nodular Cast Irons. W. A. Schumbacker A. L. Schaeffler. (*Welding J.*, 1956, Feb., 91s–99s). A simple test is described with which to discriminate the many welding procedures and filler metals available for welding grey and nodular castings.—U. E.

Rapid Determination of Ferrite in Austenitic Welds. (*Engineering*, 1956, **182**, Aug. 3, 143). A note on the Elcometer.

The Brittle Behaviour of Welded Structures. Goëau. (*Centre Doc. Sidér., Circ. Inform. Tech.*, 1956, **13**, No. 2, 361–376). Brittle fracture and methods of testing are surveyed in detail, mentioning the low temperature failure of a number of American welded merchant ships. Quality, as indicated by resilience, impact and explosion tests, is discussed, in particular where a line of weld metal is applied to the test piece. Compatability of weld metal and base is also examined and testing techniques are described.—T. E. D.

Dependence of Steel Weld Properties on Lattice Structure. J. Henschkel. (*Welding J.*, 1956, Feb., 82s–90s). The difference between true fracture stress and yield stress from the tensile tests and the energy absorbed in the impact tests were simultaneously related to test temperature to show that the low temperature ductile-to-bubble transition temperature exists with either type of test. Unnotched tensile specimen data for plain low-carbon and austenitic Cr–Ni-steel welds, deposited with several arc processes were examined. It was found that for Cr–Ni steel welds the low temperature true fracture and yield stresses are divergent and for such metals the transition temperature is below that usually explored.

Weld Distortion, especially with Deep Penetration Electrodes. H. Pflug. (*Schweissen u. Schneiden*, 1956, **8**, April, 115–122). The shrinkage and distortion of welds made with deep penetration electrodes is discussed. It is shown that distortion is greater than shrinkage with a 10 mm thick butt-welded test plate. The method of Anders and Kohlhaupt for measuring distortion was used and it is found that distortion along the longitudinal axis of the weld seam is independent of the type of electrode, welding current and width of groove, but dependent on the position of the resultant shrinkage forces away from the centroidal axis.—U. E.

High Speed Welding of Steel Compressor Cases. C. F. Stephenson and R. A. Stone. (*Welding J.*, 1956, Feb., 113–121). The application of inert-gas metal-arc welding to the production of an hermetic line of compressors for room air-conditioners and refrigeration is discussed.

Controlled Low-Temperature Stress Relieving of Pressure Vessels. T. W. Greene and C. R. McKinsey. (*Welding J.*, 1956, **35**, March, 145s–152s). Controlled low-temperature stress relieving is accomplished by progressively and simultaneously heating two 6 in. wide bands, one on each side of the weld, to 350°–400° F, while keeping the weld relatively cool. The longitudinal expansion of the heated bands stretches the weld plastically, and when temperature equilibrium is established, weld stresses have been reduced. This process was applied to three large propane storage tanks of ASTM–A212 steel. The results showed that residual welding stresses were reduced to very low values on all seams without significant distortion.—U. E.

The Functions and Education of Welding Engineers. R. G. Braithwaite, J. A. Dorrat, S. M. Reisser, R. M. Watts, F. Clark, L. W. Derry, L. Wimpenny, and F. Brooksbank. (*Brit. Welding J.*, 1956, **3**, May, 159–178). A number of papers discussed at the conference held 16th to 18th Sept., 1956. I.—The Functions of the Welding Engineer in Industry; II.—Welding in Higher Technical Education—Present Situation; III.—The Education of Welding Engineers in other Countries; IV.—Some Proposals for Improving Higher Education in Welding.—U. E.

International Institute of Welding. Recommendations of Commission. IX.—Behaviour of Metals subjected to Welding. A. Audigé. (*Brit. Welding J.*, 1956, **3**, June, 246–254). Results are presented obtained from an investigation of notch toughness of full-quality ship steels by means of key-hole and **V**-notch Charpy tests.—U. E.

Recent Publications on Preheating for Welding and Local Heat Treatment for Working. (*Schweissen u. Schneiden*, 1956, **8**, March, 92–97). A review is given of recent literature on the practice and effect of preheating for welding and cutting. (167 references).—U. E.

Welding Clad Steel. W. H. Funk. (*Iron Steel Eng.*, 1956, **33**, May, 104–107). The various precautions which must be taken when welding clad steels are discussed. Particular importance is given to the selection of proper electrodes and to the preparation of the joint.—M. D. J. B.

A New Approach to the Automatic Welding of Alloy Steels. E. Smith and P. Jerabek. (*Welding J.*, 1956, **35**, March, 244–247). The application of automatic and semi-automatic processes to the welding of alloy steels of heavy thickness is described.—U. E.

Welding of High-Strength Stainless Steels for Elevated-Temperature Use. J. J. Vagi and D. C. Martin. (*Welding J.*, 1956, **35**, March, 137s–144s). Welding tests on stainless steels indicate that AMS5643, AMS5528, and AMS5616 stainless can be welded under conditions of high restraint, using the inert-gas-shielded tungsten-arc process. To obtain reasonable elongations, it is necessary to solution-anneal as part of the post-welding heat treatment (1700° F to 1900° F, depending on the alloy). Preliminary tests on AMS5735 stainless steel showed that this steel is extremely sensitive to hot cracking. X-ray diffraction and metallographic studies show the presence of a low-melting grain-boundary film.—U. E.

A Weld Cracking Susceptibility Test for Sheet Materials. J. S. Boudreau. (*Welding J.*, 1956, **35**, April, 164s–168s). The test consists of applying a measurable, steady, tensile load to a sample of sheet stock while an inert-arc weld is made normal to the axis of loading, without filler being added. Good correlation was obtained and the known weldability of certain materials. Photographs of the equipment, specimens and test results are given.—U. E.

Rupture Properties of Inconel Weldments at 1400, 1600, and 1800° F. D. A. Scott. (*Welding J.*, 1956, **35**, April, 161s–153s). It was found that at 1400° F, 100% joint efficiency is obtained at all rupture lives. At 1600° F 100% joint efficiency is obtained only up to 500 h rupture lives, dropping to 80–85% at 10,000 h. At 1800° F metal-arc joint efficiencies are 75 and 85% at 500 h and 85 and 100% at 10,000 h rupture lives, inert gas weldments in fine grained Inconel are 95% at all rupture lives.—U. E.

Permeability and Crack Sensitivity of Stainless Welds. J. L. Lang, and C. Wright. (*Welding J.*, 1956, **35**, March, 225–228). The problems encountered in obtaining crack-free stainless steel weld deposits of low magnetic permeability are presented. Factors affecting crack sensitivity and permeability of stainless weld deposits on base metal types 302 and 304 as well as methods of evaluation are discussed. A modified type 308 electrode consistently produced sound welds with a magnetic permeability rating of less than 2·0μ.

Prevention of Weld Scaling of Plain and Alloy Steels by Protective Gases. K. Boeckhaus. (*Schneissen u. Schneiden* 1956, **8**, Jan., 17–19). The use of a protective gas (80% pure nitrogen/20% hydrogen mixture) in welding plain and alloy steel is discussed. The gas was applied to welding a pipeline by means of the oxyacetylene process and clean smooth weld was obtained.—U. E.

Fabrication of Crosshead Beams for the World's Largest Forging Press. V. M. Nigring. (*Welding J.*, 1956, Jan., 9–18). The fabrication of very large crosshead beams by the submerged arc welding process is discussed.—U. E.

Weld-Brazing in the Repair Shop. G. Boucher. (*Usine Nouvelle*, 1956, **12**, Feb. 23, 89–90). Weld-brazing is defined and compared with welding. Its applications and advantages in the repair of cars, agricultural equipment, etc., are outlined.—T. E. D.

Ceramic Brazing Jigs Cut Cycle Time, Raise Output. H. Schwartz. (*Iron Age*, 1956, **177**, Jan. 12, 71–73). The advantages and use of ceramic jigs for positioning parts during brazing are described. They are thermally stable and allow tolerances down to $\pm$ 0·005 in.—D. L. C. P.

Studies on Flame Cutting Procedure. K. Teske. (*Schweissen u. Schneiden*, 1956, **8**, April, 122–129). The flame cutting procedures are discussed. Preheating up to 1150° C should be carried out for pure iron and up to 1230° C for steel of increasing carbon content. It is assumed, as the temperature of 3600° is never reached during flame cutting that the iron forms ferrous oxide and the upper limit of cutting speed is about 4000 mm/min. The normal cutting speed is about $\frac{1}{4}$ less than the upper limit.—U. E.

Powder Cutting, E. T. Casey. (*Metal Ind.*, 1956, **88**, Jan. 13, 23–27). An account of the oxygen–iron powder cutting process for stainless steels.

MACHINING AND MACHINABILITY

Study on High-Speed Machining. H. Takeyama, T. Murai, and E. Usui. (*J. Mech. Lab.*, 1955, **9**, Nov., 249–256). Chip formation and plastic flow in the shear zone have been investigated photographically and great differences were observed at various cutting speeds. From these records and from a study of the chips, empirical formulæ relating cutting speed, chip thickness ratio and shear and rake angles were derived. These agree very well with practical data.—J. G. W.

Materials for High and Very High Cutting Speeds. C. Agte and R. Wehner. (*Neue Hütte*, 1956, **1**, July, 421–424). Processes for the production of ceramic oxide plates, of cermets (containing metallic additives), and of newly-developed oxide carbide ceramic plates are described. The metal newly developed at Immelborn consists mainly of titanium carbide, an iron and nickel and chromium alloy being used as binder. Tests have shown that this hard metal can be used for cutting steel at very high cutting speeds.

Electric Spark Machining. W. Ullmann. (*Dansk Tekn. Tidsskrift*, 1956, **80**, No. 2, 49–56). In Danish]. A review of the principles of electro-arc and spark machining is followed by details of the design and applications of the Agietron machine. Examples are shown of typical machining operations.—G. G. K.

The Electro-Erosion Method of Metal Working. V. Hermoch. (*Elektrotechnik*, 1956, **11**, (1), 12–15). [In Czech]. Methods of utilizing electrical discharges in metal working, particularly in the case of hard metals, are surveyed, and their scope is discussed.—P. F.

Present Position and Future Possibilitiies of Electro-erosion and Spark Machining. M. Bruma. (*Schweiz. Arch. Wiss. Techn.*, 1956, **22**, Jan., 18–22). A general description is given of the phenomenon of electro-erosion with a brief theoretical basis. The factors of importance to the process are outlined and its advantages stated. In particular the machining of fragile pieces and very hard materials may be carried out by this method. Future developments especially in France, are commented on.—J. R. P.

Observations on Electro-erosive Machining from the Point of View of the Works Engineer. G. Fefer. (*Schweiz. Arch. Wiss. Techn.*, 1956, **22**, Feb., 48–49). A brief summary of the different methods of spark production is given, leading to a description of the Sparcatron unit.—J. R. P.

Electronic Control of Metal-Working by the Electro-Erosion (Spark) Method. M. Promberger. (*Elektrotechnik*, 1956, **11**, (2), 42–48). [In Czech]. Electronic equipment developed by the Czechoslovak Institute for Metal-working Gear is shown, and its mode of application, scope, and circuits are considered.—P. F.

Problems and Bottlenecks of European High Grade Steel Manufacture. Grinding—a Timely Theme. R. Sachers. (*Maschinenwelt Elektrotechnik*, 1956, **11**, Mar., 59–63). Methods of increasing grinding efficiency and output, with particular reference to automatic grinding are described.

New Carbide Tool Drills Cast Iron Ten Times Faster. (*Iron Age*, 1956, **177**, Feb. 9, 87–89). The Starbore drill is a carbide tipped tool which will bore precision holes at up to 60 in. per min in cast iron and 20 in. per min in steel. A coolant is fed through the tool.—D. L. C. P.

CLEANING AND PICKLING

Cleanability and Oil-Spreading Rates. A. L. Bisio, H. B. Linford, and E. B. Saubestre. (*Indust. Eng. Chem.*, 1956, **48**, Apr. 798–801). A study of metal surface preparation for finishing processes has been made and an oil-spreading rate test developed which is correlated with optimum cleaning conditions.

The Finish That Fits. (*Steel*, 1956, **138**, Feb. 13, 92–94). Finishes in which stainless steels are available are specified. Details of various finishing operations are tabulated.

Production Barrel Finishing. A. Polucha (*Metal Finishing*, 1956, **54**, Feb., 57–64). Plant, layout, equipment and

methods for barrelling ferrous and non-ferrous alloys are given.—A. D. H.

Developments in Shot Blasting Strip Steel. K. R. Keska. (*Iron Steel Eng.*, 1956, **33**, March, 65–72). This article describes modern shot blasting cleaning equipment and techniques particularly when used on hot rolled pickled steel, which is to be coated with paints, oxides or metallic coatings. Centrifugal blasting is used and the types of shot described are cast iron shot, cast iron grit, malleablized iron shot, steel shot and clipped wire.—M. D. J. B.

Safety Precautions with Cleaning Solutions. H. Allen. (*Product Finishing*, 1956, **9**, Feb., 61–62). Safety measures are recommended for solvent and alkaline degreasing systems.

The Sodium Hydride Process for Descaling Metals. N. L. Evans. (*Corrosion Techn.*, 1956, **3**, Feb., 47–51). The author sketches the development of the process and then details the equipment and operational technique involved in the modern application of this descaling method. The advantages of the process are outlined and the precautions necessary when handling and storing sodium are dealt with.—L. E. W.

Developments in Scalebreaking and Continuous Pickling Lines. J. I. Greenberger. (*Iron Steel Eng.*, 1956, **33**, May, 69–76). This paper reviews the development and background of the scalebreaker as well as its engineering principles. It shows the advantages of applying the scalebreaker to continuous pickling lines and provides solutions to the problems of scalebreaking and increased mechanical pickle zone speeds.—M. D. J. B.

Considerations on the Pickling of Iron and Steel. K. A. V. Oeteren-Panhäuser. (*Metalloberfläche*, 1956, **10**, Feb., 49–53; Mar., 81–85). An account is given of the chemical processes taking place during pickling, and methods of pickling are described and compared.—L. D. H.

Pickling Processes Reviewed. 3—Treating Ferrous Materials. D. J. Fishlock. (*Product Finishing*, 1956, **9**, Jan., 72–85, 124). The author gives a comprehensive review of the chemistry of pickling using mineral acids. Hydrogen embrittlement, electrolytic pickling and chemical polishing and brightening methods are described. Methods are given for the control of pickling operations and the methods of treatment of waste pickle liquor at the Trostre Works of the Steel Company of Wales are outlined.—A. D. H.

Dollars Down the Drain. (*Steel*, 1956, **138**, Feb. 6, 136–142). The problems of liquid waste disposal are considered and suggestions made for economical or effective treatment.

PROTECTIVE COATINGS

The Finish of Steel Structures in Metal Works. L. Bierner. (*Stahl u. Eisen*, 1956, **76**, Mar. 22, 335–344). Finish in metal works structures is discussed from the standpoints of the expenditure entailed and the protection afforded. Criteria of the utility, effectiveness, and life of a finish are considered.

Today's Wide Range of Treatments Provides a Comprehensive Service for Metal Finishing. R. H. Warring. (*Indust. Finishing*, 1956, **9**, Jan., 322–323, 325–326, 328, 330). A general review of processes and materials is given, with tables of proprietary and other methods.

Effect of the Walls of Electrolytic Cells on Current Distribution. F. Hine, S. Yoshizawa and S. Okada. (*J. Electrochem. Soc.*, 1956, **103**, Mar., 186–193).—A. D. H.

An Isotope Effect in Molten Metals. A Lunden. (*Tek. Tidskrift*, 1956, **86**, May 8, 453–454). [In Swedish]. Details are given of the isotope effects observed when a direct current is passed through mercury and other metals, tests having been undertaken using indium to establish the temperature-dependence of this effect. The author gives details of Klemm's theory of ionic mobility and discusses isotope displacement in solid metals.—G. G. K.

A New Development in Metal Cladding. G. Durst. (*J. Met.*, 1956, **8**, Mar., 328–333). Details are given of the development and principles of a new three-step process of metal cladding involving cold bonding. The three stages of the process are: (1) thorough cleaning of the surfaces; (2) mechanical deformation sufficient to cause substantial areas of the mating surfaces to approach within atomic distances; and (3) growth of the cold-bonded interface into a substantially continuous bond by sintering. The kinetics of the bonding process are discussed.—G. F.

Stress in Electrodeposited Coatings. J. B. Kushner. (*Metal Finishing*, 1956, **54**, April, 48–51, 57). An elementary explanation of the effects of stresses is followed by an account of their effects in plating practice.—A. D. H.

The Anodic Etch in Preparation for Plating. F. G. Brune and V. L. McEnally, jun. (*Plating*, 1956, **42**, Sept., 1127–1132). The use of an anodic etch in an $MgSO_4$–H_2SO_4 solution is described which has been used to obtain good adhesion of nickel on plated parts. It is suggested that an adsorbed aqueous film protects the chemically clean surface during rinsing and transport before plating.—A. D. H.

Investigations on Cathodic Polarization in Bright Electrolytic Baths. R. Weiner and G. Klein. (*Metalloberfläche*, 1956, **10**, Jan. 17–21). Current density–cathode potential measurements unexpectedly showed that frequencies of positive and negative potential displacements were the same; the effect on the properties of the deposit was studied.—L. D. H.

Notes on the Use of Water for Cleaning and Electroplating. E. Engler. (*Products Finishing*, 1956, **20**, (4), Jan., 38–46, 50). The use of chelating agents for the removal of metal impurities, water softening, and detoxification of waste liquors are briefly considered.—A. D. H.

Evaporators Used in Plating Solution Recovery. (*Products Finishing* 1956, **20**, Jan., 76–78, 82). Boiling at reduced pressure is used to concentrate zinc cyanide wash liquors. The plant is briefly described.—A. D. H.

Plating Thickness by the Attenuation of Characteristic X-Rays. P. D. Zemany and H. A. Liebhafsky. (*J. Electrochem. Soc.*, 1956, **103**, Mar., 157–159). The X-rays reflected by a metal are diminished in intensity by absorption in the layer of electroplated metal. It is shown for iron deposits on silver and zirconium that this principle can be used to measure the thickness of the film.—A. D. H.

Bright Nickel Plating. E. Lütter. (*Metal Ind.*, 1956, **89**, July 27, 65–67). A translation from "Metallwaren—Ind. und Galvanotechn.," reviewing processes and test methods.

A Description of the Automatic Nickel–Chromium Plating Line in Operation at the Luton Works of Vauxhall Motors Ltd. (*Metal Finishing J.*, 1956, **2**, Jan., 5–12, 22). A detailed account is given of the layout of the plant, methods used and early difficulties encountered in the process which involves 22 consecutive operations.—A. D. H.

Lanolin—As a Temporary Protective. H. Silman. (*Corrosion Techn.*, 1956, **3**, May, 138–140, 153). The author stresses that the indiscriminate application of oil to metal parts to inhibit corrosion, can have adverse effects. Many of the disadvantages are overcome when lanolin is used instead and the author outlines the properties of lanolin, compares it with other coating materials, and indicates the various grades of lanolin available and the improvements achieved by incorporating a soluble chromate.—L. E. W.

High-Temperature Ceramic Coatings. (*Corrosion Prevention and Control*, 1956, **3**, Mar., 40–42). This article describes the work of the research laboratories of the Ryan Aeronautical Co., of San Diego, on ceramic-coating large, thin-walled jet structures, welding through ceramic coatings and flame-spraying refractory materials.—L. E. W.

Enamelling Used to Protect Aircraft Materials. P. Midol. (*Corrosion et Anticorrosion*, 1956, **4**, Feb., 60–66). Enamelling of stainless steel in aircraft engines increases the life of the parts, enables cheaper steel to be used, and can lead to improved performance. The method of coating with refractory enamels is outlined. The low conductivity of the enamels reduces the temperature of the base metal by 50° to 80° C, and at the same time the coating protects against corrosion by O_2, V_2O_5, SO_2, SO_3, and $CO + CO_2$.

Quantitative Study of the Opacifying Crystals in Titania Enamels Using the X-ray Spectrometer. R. E. Cowan. (*Amer. Ceram. Soc. Bull.*, 1956, **35**, Feb., 53–56). The effect of magnesia and phosphate additions on the crystallization of four titania enamels was studied by X-ray diffraction.

POWDER METALLURGY

The Mechanism of Densification during Sintering of Metallic Particles. G. C. Kuczynski (*Acta Met.*, 1956, **4**, June, 58–61). Mechanisms of pore shrinkage during sintering are compared, and it is concluded that volume diffusion with sinks at grain boundaries is the most probable.—A. D. H.

Remarks on the Granulation of Cast Iron, E. M. Onitsch-Modl and R. Mitsche. (*Powder Met. Bull.*, 1956, **7**, Apr., 134–137). The preparation, with the effects of pre-disintegration, and the effects of chemical composition are described.

Powder Metallurgy Permits Air Cooling of Turbine Blades. R. W. A. Buswell, I. Jenkins, and E. R. Perry. (*Metal Progress*, 1956, **69**, Mar., 52–56). The manufacture of turbine blades with a multiplicity of small holes running the full length of the blade for cooling purposes is described. The blades are produced by powder metallurgy and cadmium wires are incorporated into the pressing and the cadmium is later evaporated off prior to sintering.—B. G. B.

FERRITES, CERMETS AND CARBIDES

Cermets. (*Génie Civil*, 1956, **133**, Mar. 1, 92–95). A general review is given with very brief accounts of the mechanical properties and their adjustment, the kinds of powdered mixtures used, and the mechanism of compaction. Schematic representations of mechanisms and structures are shown with a short account of practical methods and the products formed.

An Investigation of Boride Cermets. J. A. Stavrolakis, H. N. Barr, and H. H. Rice. (*Amer. Ceram. Soc. Bull.*, 1956, **35**, Feb., 47–52). An investigation of manganese boride cermets and silicon–boron cermets is reported. Promising strength and oxidation resistance are noted.—D. L. C. P.

Studies on Ferrites. VII, Effect of Heating Temperature on Microstructure. T. Takei, M. Sugimoto and F. Arai. **VIII, Effect of As_2O_3 on the Properties of Zinc-Nickel Ferrite.** M. Sugimoto, S. Okamoto and T. Takei. **IX, Zinc-Nickel Ferrite having Low Temperature Coefficient of Permeability.** S. Kobayashi, S. Okamoto, M. Sugimoto, and T. Takei. (*Rep. Sci. Res. Inst.*, 1956, **32**, May, 56–60, 61–64, 65–69). [In Japanese].

On the Individuality of the Double Carbide FeWC and its Character as Limited to the Type Fe_nW_nC. W. Freundlich, A. Chrétien, and F.-A. Josien. (*Compt. Rend*, 1956, **242**, Apr. 23, 2157–2159). Tests are described proving the stoichiometric exactness of the composition, and its status as the limit of the $(FeW)_nC$ series. X-ray results are confirmatory.

Reactions between Solids in the Carbon–Iron–Tungsten System. Preparation in a Pure Condition of a Double Carbide FeWC. A. Chrétien, W. Freundlich, and F.-A. Josien. (*Compt. Rend.*, 1956, **242**, Mar. 19, 1619–1621). Cementite was reacted with W_2C. Five reactions were distinguished, two of which formed the double carbide.

PROPERTIES AND TESTS

Electronic Control System Regulates Over Long Distances. (*Iron Steel Eng.*, 1956, **33**, May, 153–154). The article describes a new method by which industry can select from a series of 21 standard components the best electronic control system to regulate push-button manufacturing operations from remote points. The components are manufactured by the Sparks-Withington Co.—M. D. J. B.

Timing the Operation of Control Systems Associated with Rotating Equipment. C. Cuthbert and D. A. Picken. (*Proc. Inst. Elect. Eng.*, 1956, **103**, *Part A*, Apr., 112–117; discussion 117–120). The operation of various control systems associated with rotating equipment can be timed to better than one-thousandth of a second with the system described. A piece of teledeltos paper is attached to the rotating surface, and a stylus is connected to an a.c. circuit so that a voltage of about 170v (r.m.s.) is applied. When the voltage applied is above 160v (instantaneous) a series of dashes will be drawn in the paper i.e. 100 per sec. By measuring the distance between corresponding points, the speed of the rotating surface can be determined. By applying further styli to the paper, the actuation of various control devices can be indicated.—L. D. H.

New Color System Identifies Steels. (*Western Metals*, 1956, **14**, June, 64). J. T. Ryerson and Son's new system is given.

Surface Inspection of Hot Rolled Coil Rod and Bars. W. C. Campbell. (*Iron Steel Eng.*, 1956, **33**, May, 55–57). Some examples are discussed of testing practices as they apply to hot rolled rod and bars in coil form for use in cold heading and cold forming such products as bolts and nuts.—M. D. J. B.

The Mass Transfer Properties of Various Metals and Alloys in Liquid Lead. J. V. Cathcart and W. D. Manly. (*Corrosion*, 1956, **12**, Feb., 43–47). The relative resistance to mass transfer in liquid lead of 24 metals and alloys were measured using quartz thermal convection loops with the hot leg at 800° C and the cooler leg at 500° C. Alloys which exhibited a higher resistance to mass transfer than their pure metal constituents included several stainless steels, 2% silicon–14% chromium–iron alloy and a 50% molybdenum–iron. Nickel was on the whole deleterious. The formation of intermetallic compounds is believed to favour resistance to mass transfer.—J. F. S.

Elastic Stress Distribution in Specimens Composed of Layers of Material. L. Föppl. (*Forsch. Ingenieurwesens*, 1956, **22**, (2), 63–69). To investigate the elastic properties of rock beds photoelastic tests were performed on circular discs having the boundary of two layers along a diameter. When a load is applied parallel to the disc surface and normal to the boundary, stress discontinuities are found at the latter and the distribution of stress is complex. If a vibrating load is applied the discontinuties do not occur, provided that the boundary layer is very nearly perpendicular to the direction of the applied load, and the strain amplitude in the disc gives a measure of the elastic properties of the composite material.—J. R. P.

An Approximate Method for Determining the Temperatures Reached in Steady Motion Problems of Plane Plastic Strain. J. F. W. Bishop. (*Quart. J. Mech. Appl. Math.*, 1956, **9**, June, 236–246). Cold extrusion is used as an example of a numerical and graphical method.

Quantum Theory of Cohesive Properties of Solids. P.-O. Löwdin. (*Advan. Phys.*, 1956, **5**, Jan., 1–172). Information concerning cohesive and elastic properties of simple ideal crystals is derived from quantum mechanics; metals of Group I are considered according to cellular, linear combination of atomic orbitals, and statistical methods. (326 references).—K. E. J.

Can Specimen Size Affect Tensile Testing. E. Dugger, A. Brisbane. (*Iron Age*, 1956, **177**, Mar. 22, 82–85). An investigation to determine how the accuracy of tensile strength measurements is affected by specimen size is reported. Unnotched specimens show no effect, but for notched specimens, it is shown that as the outside diameter of the specimen increases the ratio of notched strength to unnotched strength decreases for all strength levels.—D. L. C. P.

Observations on the Mechanical Behaviour of Heat-treated Steel at High Hardness Levels. N. H. Polakowski. (*J. Iron Steel Inst.*, 1957, **185**, Jan., 67–74). [This issue].

Methods of Producing Thin Metallic Films by Vapour Condensation. E. C. Crittenden, jun. and R. W. Hoffman. (*J. Phys. Radium*, 1956, **17**, March, 179–183). A description is given of the following:—purity of material, protection from chemical reaction with residual gas after deposition, crystal size and preferred orientation, crystal imperfections, mechanical stress, roughness, and agglomeration.—E. E. W.

The Manufacture of Fine Steels and Physical Science. A. Michel. (*Mét. Constr. Mécan.*, 1956, **88**, Feb., 87–93). The application of physical measurements to the study of fine steel manufacture is discussed. Particular reference is made to the work of I.R.S.I.D. who have used electron microscopical, ultrasonic, creep, X-ray, and radioactive techniques.

Physical Tests Aid Plant Maintenance. (*Chem. Eng. Mining Rev.*, 1956, **48**, Jan. 10, 115–116). Methods of detection of corrosion, cracks, and high-stress areas are briefly referred to, with methods of coating thickness measurement.

Application of Electrical Analogy for the Solution of Problems in Elasticity. V. Cadambe and S. G. Tewari. (*J. Sci. Indust Res.*, 1956, **15B**, March, 107–111). A circuit diagram and the technique of measuring the potential distribution for solving the Laplace equation are described. The results compare favourably with those obtained by Timoshenko.

Investigation of the Behaviour of Metals under Deformation at High Temperatures. Part III—The Deformation, Microstructure, and Form of Carbides in a 0·15% C, 0·5% Mo Steel in Creep Tests. C. H. M. Jenkins, and E. A. Jenkinson. (*J. Iron Steel Inst.*, 1957, **185**, Jan., 23–46). [This issue].

Control of Residual Stress in Practice. G. Sachs. (*SAE Transactions*, 1955, **63**, 628–641). A discussion of macrostresses due to chemical and mechanical load, season cracking, and preventive and strengthening and other treatments.

The Fatigue of Metals. (*Papers presented at the Institution of Metallurgists, Ninth Refresher Course, Llandudno*, Oct., 1955). **Fundamental Considerations on the Fatigue of Metals.** J. Holden. (pp. 3–39). The author traces briefly the history of the recognition of fatigue and then proceeds to discuss the fundamental relationships involved. The function of S–N

curves is reviewed with many examples; the physical changes occurring during fatigue are discussed and the various fatigue mechanisms that have been advanced are considered. Metallographic and X-ray structural observations on fatigued samples, and the effects arising from work-hardening and crystal imperfections are described in some detail. As a result of this review of the fundamentals involved in fatigue, the author advances a working hypothesis and also indicates in which directions of investigation further emphasis should be placed. (49 references). **The Effect on Fatigue of Notches, Surface Finishes, etc.** G. Forrest. (pp. 40–81). The author surveys the behaviour of materials with respect to notches and surface finishes and concludes that such behaviour is related to so many variables that it is still not possible to estimate with certainty the strength of complicated engineering components from laboratory-scale fatigue tests. In arriving at this conclusion the author discusses in detail the theoretical principles involved in, and empirical data obtained from, notch sensitivity tests, and consider such factors as size effect, notch sensitivity variation, elastic and non-elastic behaviour, non-propagating cracks, mean and residual stresses, etc. Similarly in the case of surface finish, the factors discussed include special surface finishes, e.g. nitriding, shot blasting, cores with strong and soft coatings, etc. (24 references). **The Structural Aspects of Aircraft Fatigue.** P. B. Walker. (pp. 82–104). The author gives an account of the work done in the structural field to combat fatigue in aircraft. External and internal loading patterns, geometric and applied stress concentrations, combined and superimposed stress raisers, static strength and plasticity, and pressure cabin fatigue are all discussed and related to the problems arising in aircraft design. **Corrosion Fatigue.** R. B. Waterhouse. (pp. 105–131). The author defines corrosion fatigue and recalls some of the general features of corrosion. The characteristics of corrosion fatigue are described and the results of experimental investigations are presented and discussed. The author concludes with a consideration of fretting corrosion and points out that corrosion and fretting have a far greater influence on fatigue strength than merely the production of pits in the surface which act as stress raisers. **Effect of Temperature on Fatigue Properties.** P. H. Frith. (pp. 132–148). The types of machines and test procedures for fatigue measurements both at elevated temperatures and at temperatures below atmospheric are described in some detail. The effects of temperatures below atmospheric on the fatigue properties of various alloys are outlined and then the effects of elevated temperatures are dealt with in considerable detail. Magnesium, aluminium, copper, non-austenitic ferrous, austenitic ferrous, nickel, and cobalt alloys are discussed. The author concludes with a brief consideration of the relationship between creep and fatigue. Much data is presented in tabular form. (35 references).—L. E. W.

A Theory of Fatigue—Damage Accumulation in Steel. D. L. Henry. (*Trans. Amer. Soc. Mech. Eng.*, 1955, **77**, Aug., 913–918). The author presents a simple theoretical model for predicting the change in endurance limit resulting from the accumulation of overstressing cycles at moderate levels of overstrain and moderate degrees of fatigue damage.—D. H.

Some Factors Affecting the Fatigue Strength of Steel Members. C. W. Gadd, J. O. Anderson, and D. Martin. (*SAE Transactions*, 1955, **63**, 362–372). Work on crankshaft design is described, with an appendix on measurement of fillet stress by means of wire strain gauges and the use of Lubriplate.

Methods of Determining Fatigue Strength at High Temperatures. B. I. Aleksandrov. (*Zavodskaya Laboratoriya*, 1955, **21**, (11), 1357–1364). [In Russian]. A survey is presented of methods developed outside the U.S.S.R. for high-temperature fatigue-testing.—S. K.

A Machine for Electronically Controlled Fatigue, and its Applications. M. Russenberger. (*Inst. Hierro Acero*, 1955, **8**, Nov., 618–624. *Special Number*). [In Spanish]. After a brief consideration of fatigue testing, the advantages of resonance testing are discussed. An electronically controlled Amsler machine is illustrated, with details of the equipment including that for high and low temperature testing.—P. S.

Method of Observing the Alternating Cyclic Load of Hydraulic-Pulsating Testing Machines. I. M. Roĭtman. (*Zavodskaya Laboratoriya*, 1955, **21**, (11), 1378–1380). [In Russian]. The incorrect results often obtained with existing methods of operating the valve in the registering system of devices for measuring alternating cyclic loads produced by hydraulic pulsators are considered, and an improved method is described. The method is based on changing the rate of rotation of the valve in such a way that the frequency with which the manometers are connected to the working space of the cylinder differs by a certain amount from the pulsator frequency. A variable cyclic load or only its limiting values can be observed or recorded.—S. K.

Resonance Apparatus for Fatigue-Testing Materials at High Temperatures. A. V. Antonovich. (*Zavodskaya Laboratoriya*, 1955, **21**, (2), 231–234). [In Russian]. In the apparatus described, a flat test-piece is secured at one end and caused to vibrate in resonance to electromagnetic excitation. The free end of the test-piece forms one plate of an air-dielectric condenser, the other being a fixed plate. The signal from this condenser is suitably amplified and recorded. At the first signs of failure the amplitude of the test-piece oscillation decreases, giving a sharp break on the recording. The test-piece is situated in a furnace with closely-controlled temperature.—S. K.

Measuring Installation with a Magnetic Amplifier for Resistance Strain-Gauges. G. N. Slavaskiĭ. (*Zavodskaya Laboratoriya*, 1955, **21**, (11), 1382–1384). [In Russian]. The use of a magnetic amplifier for dealing with signals from a series of resistance strain-gauges is described. Special attention is given to amplifier characteristics.—S. K.

The Statistical Interpretation of Fatigue Tests. F. Gatto. (*Alluminio*, 1955, **24**, Nov.-Dec., 543–554). **Application of Statistical Analysis to the Interpretation of Fatigue Tests.** (555–460). Statistical methods of calculation and graphical treatment are described and illustrated with trials on steels, etc.

Crack Formation and Stress Concentration Effects in Direct Stress Fatigue. N. E. Frost. (*Engineer*, 1955, **200**, Sept. 30, 464–467; Oct. 7, 501–503). The author describes a series of reversed direct stress fatigue tests carried out on V-notched cylindrical specimens of aluminium alloy, and shows that there is a minimum nominal stress below which cracks do not form, but that between this value and the nominal stress at the fatigue limit of the notched specimens, non-propagating cracks are always formed.—M. D. J. B.

Field Testing of Diesel Locomotive Axles. R. A. Moreau and L. Petersen. (*Proc. Soc. Exper. Stress Anal.*, 1955, **13**, Dec., 27–38). Fatigue cracking is considered, the effects of track curvature and irregularities appearing to be responsible.

Creep and Creep-Rupture Tests. (*Metal Progress*, 1955, **68**, Aug. 15, 175–184). A comprehensive review of this subject is presented. Test machines and specimens are described together with full details of carrying out creep tests. Rupture strengths, application of data on creep and rupture and relaxation tests are considered. The influence of intermittent load and temperature and dynamic creep and fatigue properties are described. Most creep data are determined under simple uniaxial tension but creep under compression, shear, bending, bearing, and multiaxial loading is also considered.—B. G. B.

Installation for Testing the Long-Term Strength and Creep of Metals in an Ionizing-Gas Atmosphere. E. K. Gordeeva, T. K. Marinets, N. N. Tikhodeev, and L. I. Tushinskiĭ. (*Zavodskaya Laboratoriya*, 1955, **21**, (4), 487–488). [In Russian]. An apparatus is described in which prolonged high-temperature tests can be be carried out at 25–800° C in any gas except oxygen. Hollow test-pieces are used inside which the gas is ionized.—S. K.

Experiments on the Rapid Determination of the Speed of Long-Term Creep. V. S. Ivanova. (*Zavodskaya Laboratoriya*, 1955, **21**, (4), 476–478). [In Russian]. Of attempts to develop rapid methods of determining the rate of long-term creep, the most promising were those based on the relation between the value of the plastic deformation and the service-time of the metal. The present article describes the treatment and comparison of data obtained in four different laboratories using one such method (that of I.A. Oding). Numerous creep curves of austenitic steels at 550–700° C and of pearlitic steels at 480–550° C were dealt with. The results show that testing times of 1500–2500 h are satisfactory.—S. K.

Characteristics of the Plasticity of Metals during Creep. V. S. Ivanova. (*Zavodksya Laboratoriya*, 1955, **21**, (2), 212–216). [In Russian]. A new criterion of hot strength is proposed. This is the potentiality for plasticity which approximately characterizes the extent of plastic deformation taking place in the first and second stages of creep. This can rise and fall with length of service depending on other criteria. For

metals with a large reserve of plasticity, extrapolation of the long-term strength from 2000–3000 h to 100,000 h can lead to substantial error because of the decreasing cross-sectional area of the test piece. It is suggested that the new characteristic is a specific value for parts working under creep conditions. Discussion on this is invited editorially.

Tests Probe Limits of Controlled Shot Peening. W. W. Safee. (*Iron Age*, 1956, **177**, Mar. 1, 76–79). Tests into the effect of shot peening metal surfaces on surface finish and fatigue are described. Shot peening improves the fatigue properties of unpolished and notched specimens. The degree of improvement depends on surface finish and notch radius; the sharper radius and the rougher surface show greatest improvement.—D. L. C. P.

Creep in Torsion. P. Ya. Boguslavskii. (*Izvest. Akad. Nauk SSSR, Otdelenie Tekn. Nauk*, 1956, (4), 151–152). [In Russian]. An approximate method of treatment of data on creep of springs is described. Calculated deformations of copper and steel spring agreed well with the experimental results.—V. G.

On the Exact Measurements of Strains in Creep Testing. L. Jeníček and K. Fritsche. (*Hutnické Listy*, 1956, **11**, (4), 237–241). [In Czech]. Two newly developed models of double telescopes for the observation of both fiducial marks on specimens used in creep tests are described, and the possibility of developing them further for the automatic recording of creep curves in industrial creep testing is discussed.—P. F.

Barium Titanate Accelerometers and Strain Gauges. (*Engineer*, 1956, **201**, April 20, 382–383). This article describes miniature accelerometers and strain gauges using barium titanate transducers suitable for vibration testing developed by the G.E.C., London.—M. D. J. B.

Creep and Stress-Rupture Tests on Molybdenum–Vanadium Weld Metal and Welds in Molybdenum–Vanadium Steel using Vanadium-bearing Electrodes. R. P. Kent. (*Metal Treatment and Drop Forging*, 1956, **23**, May, 193–202). A detailed account is given of a long series of tests on weld and parent metal. Two different electrodes were used.

Creep and Rupture Test Pyrometry. C. R. Wilks. (*Amer. Soc. Test. Mat. Spec. Tech. Pub.* 178, 1956, 19–31). The practices used at the American Brake Shoe Co. creep laboratory are described. The temperature control which has been achieved and the techniques used for the calibration of thermocouples are explained. The results of tests carried out to measure the errors of temperature measurement caused by contamination are discussed.—B. G. B.

Temperature Recording in Creep Testing. (*Electronic Eng.*, 1956, **28**, Aug., 332). A note on the use of the Servograph Mk. II.

Creep-Rupture by Vacancy Condensation. E. S. Machlin. (*Trans. Amer. Inst. Min. Met. Eng.*, 1956, **206**; *J. Met.*, 1956, **8**, Feb., Section 2, 106–111). The author examines quantitatively the proposition that the voids produced at grain boundaries in a creep test are a result of vacancy condensation, and puts forward a theory of creep-rupture. A number of experiments to evaluate the vacancy condensation mechanism further are proposed.—G. F.

Industry Learns From a Turbine Spindle Failure. R. G. Matters, R. E. Lochen, J. A. Dedinas, and H. K. Ihrig. (*J. Met.*, 1956, **8**, Mar., 317–324). An investigation of the failure of a large low-pressure turbine spindle indicated that thermal cracks and flakes in radial planes near the centre of the forging were the cause of rupture, lack of hydrogen diffusion appearing to be the basic factor. The application of new testing techniques and changes in production practice resulting from the investigation are described.—G. F.

The Study of Fracture Surface Markings. C. F. Tipper. (*J. Iron Steel Inst.*, 1957, **185**, Jan., 4–9). [This issue].

A Contribution to the Study of Micro- and Macro-Hardness Testing. E. Aseni Alvarez-Arenas and H. Perez Vazquez. (*Inst. Hierro Acero*, 1956, **9**, Jan., 35–58. *Special Number*). [In Spanish]. After a brief account of the factors which influence the determination of micro-hardness, a comprehensive study of the results of tests on eleven different metals and alloys is reported. The Meyer curves reveal the differences caused by mechanical and electropolishing, especially in the softer alloys, and emphasize that electropolishing is essential for loads of less than 1 kg. With reference to macro-hardness testing, Kick's law is shown to be valid only for loads that exceed 5 kg. Photomicrogaphs of the alloys and experimental data are included. (34 references).—P. S.

Foreign Experiments and Reflections on the Brittle Fracture Sensitivity of Steel. K. Rühl. (*Arch. Eisenhüttenwesen*, 1956, **27**, Feb., 107–118). A review is given of literature concerned with the effect of wall thickness and chemical composition on the brittle fracture sensitivity of structural steel, and with evidence from ISA, Schnadt and Charpy impact bending tests, van der Veen notched-bar bending tests, and Kommerell bending tests on built-up welded joints. The origin and propagation of brittle fracture is discussed.

Dispersion and Discrimination in Various Tests of Brittle Fracture Sensitivity in Steel. H. Knüppel and K. E. Mayer. (*Arch. Eisenhüttenwesen*, 1956, **27**, Jan., 25–33). The results of a statistical examination of tests for the determination of brittle fracture sensitivity are given. The results of notched bar impact bending tests on 85 killed and unkilled unalloyed basic converter steels and 17 killed and unkilled unalloyed Siemens–Martin steels are compared with those of DVM and Schnadt tests, and also with those of Kuntze impact tension and Kahn–Imbembo impact bending tests. The repeatability of the various methods is discussed, and the dependence of their results on the analysis of the melt is indicated.—A. C.

Zone Melting. W. G. Pfann. (*Chem. Eng. News*, 1956, **34**, March 26, 1440–1443). In an account of the process it is mentioned that iron and other metals can be purified by zone melting and that low-temperature embrittlement in steel is reduced to below — 196° C by this means.

The Fight Against Wear, New Methods and New Materials. (*Usine Nouvelle*, 1956, **12**, Feb. 2, 93–94). The use of low temperature treatment (— 75° C), the Durgi process, sulphurization, electrolytic deposits, hard metal spraying, sintered hard metals and boron carbide as means of reducing wear, are outlined.—T. E. D.

Effect of a Circular Field on the Magnetization of Steel. V. Sanchez-Giron Nuñez. (*Inst. Hierro Acero*, 1956, **9**, Feb., 222–227. *Special Number*). [In Spanish]. The author reports an experimental study of the effect of a circular D.C. standing magnetic field superimposed on the longitudinal magnetizing field. The effect of this circular field is to increase the permeability in weak magnetizing fields, and decrease it in strong ones. The hysteresis losses and coercive force decrease in proportion to the increase in the circular field strength. (11 references).—P. S.

ERRATUM

Abstracts, March 1956, p. 324. "Domains of Reverse Magnetization in Ferro-Magnetic Salts." T. G. Nilan and W. S. Paxton. For "Salts" read "Metals".

Comments on the Theory of Magnetic Properties of Thin Films and of Fine Grains. L. Néel. (*J. Phys. Radium*, 1956, **17**, March, 250–255). For powdered iron, the variation of the coercive field against grain size is interpreted by supposing the energy spent during a hysteresis cycle is used only for the irreversible production of the system of "Walls." For other metals this does not hold. Several tests are described.—E. E. W.

Behaviour of Ferromagnetics under Strong Compression. F. D. Stacey. (*Canad. J. Phys.*, 1956, **34**, Mar., 304–311). The effect on iron is strongly dependent on carbon content and thermal history. Steels may show negative or positive coefficients, but magnetization of pure iron and high-carbon steels is increased while in mild steels, it is decreased in general.

Examination by Magnetic Powders. Some Considerations Concerning the Standardization of the Test. R. Castra. (*Centre Doc. Sidér., Circ. Inform. Techn.*, 1956, **13**, No. 4, 787–795). Standardization of the magnetic powder method is discussed with reference to magnetization by passing a current through the test piece, and magnetizing by means of a coil.—T. E. D.

The Law of Approach to Saturation of a Monocrystal of FeSi in the Three Principal Crystallographic Directions. H. Danan. (*Compt. Rend.*, 1956, **242**, Feb. 6, 748—750).

The Demagnetization of Magnetite and α–Fe_2O_3 by Alternating Fields. (Mlle.) F. Rimbert. (*Compt. Rend.* 1956, **242**, Feb. 13, 890–893). The distinction is pointed out between isothermal remanent magnetization and thermo-remanent magnetization. Curves for both are given.

Intradomain Magnetic Saturation and Magnetic Structure of γ-Fe_2O_3. W. E. Henry and Mary J. Boehm. (*Phys. Rev.*, 1956, **101**, Feb. 15, 1253–1254). A sample motion ballistic method was used for direct measurements of magnetic moments. The average moment for γ-Fe_2O_3, which was found to be 1·18 Bohr magnetrons per iron atom, supports preferential distribution of iron vacancies on octahedral sites in a spinel structure.—E. E. W.

Measurement of the Electrical and Magnetic Properties of Thin Films at Low Temperature. A. van Itterbeek. (*J. Phys. Radium*, 1956, **17**, March, 241–249). A brief report is given of measurements on, and the properties of, nickel, tin, and iron films at low temperatures. A new technique is described for film manipulation.—E. E. W.

High Frequency and Electronics in the Service of Metallurgy. C. Freteur. (*Usine Nouvelle*, 1956, **12**, Feb. 9, 25–29). A account is given of the use of induction heating in the U.S.A., and its advantages are examined. Its use in rolling mills is described and the short high-frequency heating times are compared with heating times in oil-fired furnaces in a number of specific cases. Applications quoted include its use in manufacturing track-links, cylinder liners and induction-welded tubes.—T. E. D.

Measurement of Casting Thickness by Use of Pulsed Eddy Currents. D. L. Waidelich. (*Nondestructive Test*, 1956, **14**, May-June, 14–16). A Thyratron pulser with circuit and probe is described, with their application to clad metals.

Method of Investigating the Wear of Case-Hardened Steel Used for Making Gear Wheels. L. M. Fel'dman and M. A. Balter. (*Zavodskaya Laboratoriya*, 1955, **21**, (12), 1501–1503). [In Russian]. A machine is described with the aid of which the friction and loading conditions which the working surfaces of gear wheels undergo are closely approximated. The machine consists essentially of four touching rolls with their axes parallel. One roll is the test-piece and the others are disposed symmetrically about it. Gear wheels are mounted eccentrically on the roll shafts, causing stress and friction on the test-piece during rotation. The method was used for an alloy steel, the test-pieces being case-hardened to a depth of 1·8 mm and then subjected to different heat treatments.—S. K.

Formation and Breakdown of Welded Bridges between Surfaces in Friction. M. P. Levitskii. (*Doklady Akad. Nauk S.S.S.R.*, 1953, **92**, (4), 797–798). A theoretical approach is formulated.

Magnetostrictive Effects in an Antiferromagnetic Hematite Crystal. Helen M. A. Urquhart and J. E. Goldman. (*Phys. Rev.*, 1956, **101**, Mar. 1443–1450). The magnetostrictive distortions in a natural single crystal are closely related to the parasitic magnetization in the region of the transition near − 25° C where the antiferromagnetic axis spontaneously shifts its crystallographic direction by 90°.—E. E. W.

Determination of the Quantity of Residual Austenite by the Magnetic Method. Yu. A. Geller. (*Zavodskaya Laboratoriya*, 1955, **21**, (2), 177–181). [In Russian]. In the investigation described the effects of various factors on the results of magnetic determinations of austenite in carbon steels and steels alloyed with carbide-forming elements (chromium, vanadium and tungsten) were studied, mainly the change in the magnetic saturation of the standard and specimen produced by the carbides present and by change in the composition of the solid solution (martensite and ferrite). Improved methods of calculation, not subject to these effects, are developed and applied to several steels.—S. K.

Determination of Austenite Content from the Magnetic Saturation. A. A. Popov and R. Sh. Shklyar. (*Zavodskaya Laboratoriya*, 1955, **21**, (6), 677–685). [In Russian]. Problems involved in the magnetic investigation of the kinetics of the decomposition of super-cooled austenite are discussed. The effects on the accuracy of magnetometric phase-composition investigations of the type of apparatus, choice of standard, method of calculating the quantity of ferromagnetic or paramagnetic components, test-piece dimensions and temperature measurement are considered. In isothermal and thermokinetic studies of austenite decomposition strict control of test-piece temperature is essential. Best results are obtained with test-pieces in the form of plates 0·3–0·5 mm thick to whose surface the thermocouple is welded directly.

Determination of Residual Austenite by the Magnetic Method. V. G. Permyakov. (*Zavodskaya Laboratoriya*, 1955, **21**, (6), 685–686). [In Russian]. Some notes are presented on factors influencing the accuracy of magnetometric residual-austenite determinations, the most important is said to be the choice of the standard.—S. K.

Quality Control through Nondestructive Testing with Eddy Currents. L. A. Cosgrove. (*Non-Destructive Test.*, 1955, **13**, Sept.-Oct., 13–15). An instrument is described which can be used for the study of surface flaws, improper heat treatment and sorting (of mixed aluminium alloys).–A. H. M.

The Determination of Core Losses with Epstein's Differential Apparatus. V. S. Giron Nuñez. (*Inst. Hierro Acero.*, 1955, **8**, Oct.-Dec., 797–804). [In Spanish]. Core loss figures are given in W/kg for B_m values ranging from 5000 to 15,000 gauss and a frequency of 50 c.p.s. for four different sheet materials of Spanish and German manufacture. A 25 cm Epstein apparatus was used for standardization and comparative tests performed with the differential circuit. The effect of gap distances of 0·20 to 1·0 mm between the sides of the square were also studied and indicated that the greater B_m the greater the error; the effect of differing gaps is also discussed.—P. S.

The Variation in the Conductivity and Melting-Point of Iron Oxide as a function of its Composition. J. Aubry and F. Marion. (*Compt. Rend.*, 1955, **241**, Dec. 14, 1778–1781). Non-stoichiometric lower oxides of iron show linear variation of electrical conductivity with composition but the fusion temperature is changed very little.

ABC's of Ultrasonic Inspection. E. F. Weller, Jun. (*S.A.E. Transactions*, 1955, **63**, 177–191). The inspection of long rods, bars, and bolts is included.

Ultrasonic Flawplotting Equipment—A New Concept for Industrial Inspection. R. W. Buchanan and C. H. Hastings. (*Non-Destructive Test.*, 1955, **13**, Sept.-Oct., 17–25). The results are presented of an evaluation of the "Watertown Arsenal Ultrasonic Flaw Plotting Equipment", a device which gives plan and cross-section view pictorial presentation of flaw images, and a manually operated search scanner capable of coping with a wide range of specimen geometry.

Detection of Flaws in Jet Engine Parts by Ultrasonics. M. J. Bratt and V. I. E. Wiegand. (*Non-Destructive Test.*, 1955, **13**, Sept.-Oct., 45–47, 59). The authors illustrate the effectiveness of ultrasonic inspection in realizing large savings in a jet engine manufacturing plant.—A. H. M.

Ultrasonic Testing of the Size of Graphite Inclusions in Grey Iron. N. V. Khimchenko and V. N. Prikhod'ko. (*Zavodskaya Laboratoriya*, 1955, **21**, (12), 1468–1471). [In Russian]. The replacement of metallographic by ultrasonic methods for the determination of the size of graphite inclusions in grey cast iron is described. The apparatus used works in the frequency range 0·35–5·6 mega Hertz, which is sufficient for the normal range of graphite inclusion sizes. Both reflection and transmission methods were used and the respective experimental conditions are discussed. Results are given in terms of "structural coefficients" from which inclusion dimensions can be derived. The method has been verified by comparison with metallographic results. Combined with magnetic methods the ultrasonic method developed is recommended as a non-destructive test procedure. It is also suitable for spheroidal-graphite iron.—S. K.

Some Applications of Ultrasonic Testing to Large Forgings. A. De Urioste Haya. (*Inst. Hierro Acero*, 1955, **8**, Oct.-Dec., 765–781). [In Spanish]. After an account of the principles and practice of ultrasonic testing, an illustrated account of the results of such tests, applied to forgings and ingots, is given. It is emphasized that experience and a suitable technique are desirable, and that reflection methods are to be preferred. (25 references).—P. S.

Application of Nondestructive Testing in the Manufacture of Aviation Gas Turbine Engines. F. W. Rohde. (*Nondestructive Test.*, 1956, **14**, May-Jun., 26–28). Raw materials, parts during manufacture and assembly and during operation and service are considered.

Central Diffraction of X-rays by Metals. J. Blin. (*Publications Scientifiques et Techniques du Ministère de l'Air*, 1956, No. 311). A complete description of the method and underlying theory.

Practical Methods for Attaining Constant Sensitivity and Density in Industrial Radiography. K. G. Roberts. (*Trans. Amer. Found. Soc.*, 1955, **63**, 669–674).

Constant Potential Radiography of Steel at 2 Mev. S. S. Stacey. (*Non-Destructive Test.*, 1955, **13**, July-Aug., 29–32). Data is presented which illustrates the versatility of the Van de Graaf 2 Mev constant potential X-ray generator. The unit under review is installed at the Foster Wheeler

Corp. Plant, Pennsylvania. Penetrating power, scattering factor, and angular coverage of beam are discusssed. The equipment permits the use of simple direct techniques free from the inconveniences caused by secondary radiation, and it gives the radiologist films characterized by high degrees of sensitivity and definition. (2 references).—P. M. C.

Method of X-ray Structural Analysis with a Narrow Beam. B. A. Movchan. (*Zavodskaya Laboratoriya*, 1955, **21**, (6), 699–702). [In Russian]. The use of a narrow beam for the X-ray structural analysis of small regions of metallographic specimens is considered. With the method used the smallest irradiated area was 0·02–0·03 mm in diameter. The technique can be used for studying the structures of the boundary and central regions of crystals, the structures of various types of cracked and fractured surfaces and of crystal-structure changes produced by different forms of mechanical action. A photograph obtained of the surface of a pearlitic iron after wear by the narrow-beam method is compared with one taken with an ordinary wide-beam technique.—S. K.

Field Evolution of Industrial Xeroradiography. G. M. Taylor and G. H. Tenney. (*Non-Destructive Test.*, 1955, **13**, Nov.-Dec., 12–17). The authors give data for the Xeroradiographic process on sensitivity, resolution, and technique for a variety of X-ray machines and metals. Some special characteristics of this method are given and a comparison made with data obtained by conventional radiography.

New Method for the Projections of Crystal Structures using X-Ray Interference. H. Seemann. (*Z. Metallkunde*, 1955, **46**, Sept., 722–730). A system using three exposures, and requiring no calculations after tracing systems of hyperbolic curves, is described and applied to a monoclinic hydrocarbon crystal, (coronene).

Residual Stresses in Welded Structures and their Measurement. H. Muir and J. S. Hoggart. (*Australasian Eng.*, 1955, **48**, Dec., 46–50). After a discussion of origin and magnitude, the methods of measurement of stresses are considered. X-Ray methods are described, and finally the effects of residual stress are briefly reviewed.

Soft X-Ray Absorption of Thin Films of Iron and Iron Oxide. D. E. Carter and M. P. Givens. (*Phys. Rev.*, 1956, **101**, Mar. 1, 1469–1472). During tests on the absorption of films of iron and iron oxide (170–340Å) it was found that the absorption edge of iron was at 225Å and that of iron oxide at 218Å.—E. E. W.

Dilatometric Behaviour of Pure Iron. P. Lehr. (*Compt. Rend.*, 1956, **242**, Jan. 30, 632–635). Differential curves are plotted up to transformation temperature, and structure changes correlated. Hysteresis is not eliminated by very slow temperature change.

High Speed Quenching Dilatometer. F. E. Martin and R. H. Raring. (*Trans. Amer. Inst. Min. Met. Eng.*, 1956, **206**; *J. Met.*, 1956, **8**, Feb., Section 2, 191–195). A high-speed gas quenching dilatometer employing an electrical micrometer tube is described. It can be used for determining transformation temperatures for maximum cooling rates as great as 5000° F per s and is believed to give satisfactory results for transformation progress for cooling rates up to 2800° F per s, making it useful for studying transformations in low alloy steels.—G. F.

The Activation Energies of Viscous Flow and Self-Diffusion in Molten Metals. A. Hrbek. (*Hutnické Listy*, 1956, **11**, (3), 164–167). [In Czech). Experimental data and theories relating to self-diffusion and viscosity in liquid metals are surveyed. The activation energies for both processes are evaluated from data giving the temperature dependence of the viscosity in the case of Na, Al, K, Fe, Cu, Zn, Ag, Cd, Sn, Sb, Au, Hg, Pb, and Bi. The equation $Q = C_V \cdot T_m$, relating the activation energy Q, identical for both processes, to the specific heat at constant volume and the melting temperature, is derived. This is applicable also to non-metals, e.g. water.

Spectroscopic Analysis Using Rontgen Fluorescence. O. Werner. (*Arch. Eisenhüttenwesen*, 1955, **26**, Dec., 721–737). The fundamentals of the method and the equipment needed for production and measurement of Röntgen fluorescent radiation are reviewed. Examples of qualitative and quantitative analysis of metals are given. The range of utility of the method is discussed.

Radiography of Small Castings with High Cobalt or Nickel Contents. E. A. Burrill. (*Non-Destructive Test.*, 1955, **13**, May-June, 19–21). The difficulties associated with the radiographic inspection of aircraft components containing up to 65% cobalt or nickel are related. It is then shown that the X-rays from the recently available 1 million volt Van de Graff generator can be effectively utilized for this class of work. In a single exposure, the details in ¼ and 1 inch thicknesses can be observed with adequate sensitivity (1 to 2%). The relatively low equipment cost and short exposure time make this type of X-ray facility economical not only for very special types of castings, but also for more conventional components.—P. M. C.

Use of Gamma-Rays for Testing Castings and Welded Joints at the Kuznetsk Metallurgical Combine. V. V. Ivanov and A. P. Pavlovskiĭ. (*Zavodskaya Laboratoriya*, 1955, **21**, (11), 1353–1356). [In Russian]. After extensive trials in 1951 gamma-ray defectoscopy was widely adopted at the Kuznetsk combine for testing steel castings, welds and works equipment, and the accumulated experience is reviewed in this article. It has been found that for thicknesses of 5–200 mm defects whose size is 3–5% of the thickness are satisfactorily revealed. The sensitivity when irradiating welds and articles up to 80 mm thick is greater with ^{60}Co than with ^{192}Ir as the source. The gamma-ray testing laboratory and equipment are briefly described.—S. K.

A Scintillation Count-Rate Meter for Gamma Radiation. J. G. Morse and A. W. Kneibler, Jun. (*Nondestructive Test.*, 1956, **14**, May-Jun., 30–32). Directions for the construction of the counter are given.

Radiation Effects on Materials. W. Riezler. (*Stahl u. Eisen*, 1956, **76**, Jan. 12, 14–18). The action of electron, γ-, and X-radiations, slow and fast neutrons, and fast ions is described, as well as the construction of the leading apparatus for the generation of these radiations. The effect of radiation on the properties of polyethylene, and the evolution of defects, foreign atoms, and disturbed zones (or "spikes") in metallic materials are discussed.

Tasks and Problems in Non-Destructive Testing of Materials. K. Schreier. (*Maschinenwelt Elektrotechnik*, 1956, **11**, Mar., 78–80). The range of application of various techniques for the non-destructive testing of materials are outlined briefly, particular attention being paid to X-ray and γ-ray apparatus, and ultrasonic testing.—L. D. H.

Guiding Principles for the Execution of Non-Destructive Tests on Heavily Stressed Arc Welded Steel Structures. B. Schuil. (*Lastechn.*, 1956, **22**, Feb., 21–24, Mar., 45–47). [In Dutch]. In the absence of other authoritative guiding principles, the author has summarized the various non-destructive methods of testing which have been published in the literature. The paper concludes with a table assessing the utility of the various methods touched upon. (16 references).—F. R. H.

Development of The New Post-Emulsion Fluorescent Penetrant Inspection. F. W. Rohde. (*Non-Destructive Test.*, 1955, **13**, May-June, 27–33). The use of fluorescent penetrant oils for revealing surface defects on subsequent examination under black light is discussed. Due to improper process control, human failings, and the limiting sensitivity of the penetrant, the process is not 100% foolproof. A further refinement, the post-emulsion process, in which the components are immersed in an emulsifier following the penetrant is described. Specifications with very detailed instructions for the correct application of various fluorescent penetrants and subsequent examination are given.—P. M. C.

A Method of Automatic Measurement of Specific Heat. T. Hirone, S. Maeda, I. Tsubokawa, and N. Tsuya. (*Sci. Rep. Res. Inst. Tohoku Univ.*, 1953, **A5**, Dec., 513–519). An automatic recording apparatus for the measurement of the specific heat of alloys and compounds is described.—J. G. W.

Measurement of Thermal Conductivity of Building Materials. H. Weibull. (*Stat. Provn. Medd.*, 1955, 117, pp. 21). A method is described in which materials are sandwiched between standard plates.

High Temperature Thermal Conductivity of Gases. A. J. Rothman and L. A. Bromley. (*Indust. Eng. Chem.*, 1955, **47**, May, 899–906). Measurements on N_2, CO_2, A, and N_2–CO_2 mixtures up to 775° C are reported.

Apparatus for Determining Coefficients of Thermal Expansion Over a Wide Temperature Range. S. F. Burlakov and M. I. Korolev. (*Zavodskaya Laboratoriya*, 1955, **21**, (11), 1390–1392). [In Russian]. Accurate data for constructing dilatometric curves for the temperature range −160– + 800° C can be obtained in protective atmospheres with the aid of the apparatus described.—S. K.

Dilation Measurements of Steel Sphere and Rock Deformations at Kemano, B.C. G. A. Brewer. (*Proc. Soc. Exper. Stress Anal.*, 1955, **13**, Dec., 63–78).

The Viscosity of Molten Metals. M. van den Brandhof. (*Metalen*, 1956, **11**, April 15, 153–160). [In Dutch]. This article is a general review on the viscosity of molten metals and alloys with special reference to their fluid moulding. A brief description is also given of the usual measuring methods together with the results obtained with Pb–Bi alloys when using a sphere-oscillation viscometer.—F. R. H.

A Study of the Influence of High-melting Elements on Self-diffusion of Iron using Radioactive Isotopes. S. Z. Bokshtein, V. A. Kazakova, S. R. Kishkin, and L. M. Mirskiĭ. (*Izvestiya Akademii Nauk SSSR., O.T.N.*, 1955, **12**, 18–27). [In Russian]. The dependence of the coefficient of self-diffusion of iron in iron–nickel alloys on temperature for various contents of nickel, molybdenum, niobium, titanium, and vanadium was investigated. Specimens of alloys in the form of plates were electroplated on one side with radioactive iron Fe^{59}, and heated *in vacuo*. The diffusion of iron was followed by measuring the integrated radioactivity of a layer removed from the specimen investigated.—V. G.

Effect of Stresses on Hydrogen Diffusion in Steel. F. de Kazinczy. (*Jernkontorets Ann.*, 1955, **139**, 11, 885–892). [In English]. Hydrogen flow through a cylindrical steel tube subject to axial tensile stress was measured. Up to the yield point the flow increased almost proportionally to the stress: 0·25% for 1 kg/mm². Equations show that this is due almost entirely to increased solubility in the lattice, which indicates the hydrogen diffuses homogeneously through the lattice in annealed steel. When the sample was subjected to plastic deformation the increase in flow was greater, especially at high stresses. This may be due to stress multiplication in certain zones, probably along the slip planes.—G. G. K.

Effect of Hydrogen introduced into Steel on the Phenomenon of Deferred Rupture. P. Bastier and P. Amiot. (*Compt. Rend.* 1955, **241**, Dec. 14, 1760–1762). Steels are less susceptible to deferred fracture according as they are nearer physicochemical, structure, and mechanical equilibrium. Variations occur according to whether saturation with hydrogen is carried out before or after stress is applied.

The Effects of Alloying Additions on the Properties of Carbon Steels. A. G. Gardner. (*Machinery*, 1955, **87**, Nov. 11, 1143–1146). The limitations of low-cost carbon steels can only be overcome by the addition of alloying elements, these allow higher strength characteristics to be developed with less drastic hardening treatments. The characteristics of each of the commonly employed elements is discussed and their influence on the properties of the final alloy steel is considered.

Strength and Plastic Properties of Structural Steels Alloyed in a Complex Manner. M. P. Bruan and E. E. Maistrenko. (*Izvest. Akad. Nauk. SSSR., Otdelenie Tekn. Nauk*, 1955, (6), 119–126). [In Russian]. Two groups of chromium, manganese nickel steels containing 1·3–1·7% and 2·3–2·7% of nickel respectively were additionally alloyed with small quantities of one or more of the following elements: vanadium, tungsten, titanium, and niobium and the influence of this additional alloying on the mechanical properties of steels produced was investigated. The results obtained are discussed.—V. G.

An Improvement in Properties of Chromium Manganese Silicon Steel By An Additional Alloying. M. P. Braun. (*Izvest. Akad. Nauk SSSR, Otdelenie Tekn. Nauk*, 1955, (5), 119–122). [In Russian]. Changes in properties of steel containing 0·23–0·28% of carbon, 1·3–1·4% of chromium, 1·2–1·4% of manganese and 1·0–1·1% of silicon, additionally, alloyed either with one of the following elements: tungsten, titanium, niobium, vanadium, boron, nickel, or with tungsten + titanium + nickel were investigated. The experimental results are given in the form of diagrams.—V. G.

Steels Containing Tungsten. F. Javier Mariñas. (*Met. Elect.*, 1955, **19**, Jun., 62–71). [In Spanish]. A review is given of the steels which contain tungsten as a major alloying element. The principal effects of tungsten upon the properties and microstructure of steel are discussed and the beneficial effects of chromium additions are indicated. A short account of the five main types of tungsten steels is also given.—P. S.

Boron in Quenched and Subsequently Drawn Steels and in Casehardening Steels. F. Eidmann-Jesnitzer and H. Kahle. (*Neue Hütte*, 1956, **1**, May, 322–332). Results of experiments are reported to confirm that boron essentially merely serves to increase hardening capacity. Fundamental differences in German and American practice are discussed. Economies in alloying elements reported from the U.S.A. cannot be attributed solely to boron. The use of boron steels in Germany would appear to be justified in exceptional cases only.

Contributions to the Study of Diffusion of Carbon and Nitrogen in α-Iron by Measurements of Internal Damping. L. Guillet and B. Hockeid. (*Rev. Mét.* 1956, **53**, Feb. 122–130). The heats of activation for C and N diffusion in α-iron are deduced from measurements over a range of frequencies and conclusions are drawn from these values.

Investigation on the Development of Low-Carbon Low-Alloy Steels with Electrolytic Manganese. S. Visvanathan, S. N. Anant Narayan, and P. K. Chakravarty. (*Tisco*, 1956, **3**, Jan., 19–38). The authors discuss briefly the properties of the case and core of case-hardening steels and indicate the general requirements of such steels. The influence of nickel and chromium is considered and the development of manganese case-hardening steels is reviewed. The use of boron as an alloying element is also considered. The authors then describe their experimental work which consisted of making six new compositions and comparing the properties with two German standard manganese and three nickel based case-hardening steels. The results are presented and discussed. (51 references).—L. E. W.

The Use of Molybdenum in Steel and its Development Potentialities. (*Usine Nouvelle*, 1956, Jan., 21–23). Production of molybdenum ores, research into widening the field of application of molybdenum, and the important part played by its stable price are dicussed. The advantages of its use in ordinary, stainless, tool and special steels are considered. Uses of molybdenum metal are indicated, and molybdenum disulphide in lubricants is mentioned.—T. E. D.

Comparable Tool Steel Brand Charts. (*Iron Age*, 1956, **177**, Mar. 8, 169–184). Tables are given which classify many U.S. produced tool steels under A.I.S.I. designations; the names and suppliers of each brand are given. In other tables the chemistry, physical properties, forging and heat treating data for each type is listed.—D. L. C. P.

Relaxation of High Tensile-Strength Steel Wire for Use in Prestressed Concrete. G. McLean and C. P. Siess. (*Amer. Soc. Test. Mat. Bull.*, 1956, Jan., No. 211, 46–52). A test method is described for measuring the relaxation of highly stressed steel wires. Typical results obtained on 28 specimens of 4 types of wire are discussed.—B. G. B.

Choice, Properties and Behaviour of High Temperature Materials. J. I. Nish. (*J. Inst. Eng. Australia*, 1956, **28**, Apr.-May, 109–116). Creep and other properties at high temperatures are discussed and steels and other materials are tabulated and discussed.

The Performance of High Strength Pressure-Vessel Steels. J. H. Gross and R. D. Stout. (*Welding J.*, 1956, **35**, March, 115s—119s). Six high strength steels were given extensive mechanical tests for determining their applicability to pressure vessels. It was found, as expected, that both at room and elevated temperatures their strength was considerably greater than that of A201 plain carbon steel. Somewhat greater cracking tendency was observed. Notch toughness was found to be equal to or better than that of A201 steel.

METALLOGRAPHY

Filtering Apparatus for Study of Liquid–Solid Equilibrium in Alloy Systems. L. A. Willey. (*Trans. Amer. Inst. Min. Met. Eng.*, 1956, **206**; *J. Met.*, 1956, **8**, Feb., Section 1, 263–264). The author describes an apparatus for separating liquid and solid metal phases by filtration through a porous carbon disc. It has been used for equilibrium studies in alloy systems in the range 185–800° C.—G. F.

Some Aspects of the Metallography of Stainless Steel and Stainless-Steel Weldments. G. V. Smith. (*Welding J.*, 1956, **35**, May, 456–462). The metallography of stainless steel and stainless steel welds is discussed. It is shown that better micrographs can be obtained when using several etchants in turn. In some cases microhardness and X-ray diffraction tests are useful for differentiating several microconstituents in these steels.—U. E.

On a Replica Method for Optical Microscopy and its Use in Non-destructive Testing. A. van Effenterre, P.-A. Jacquet, and E. Mencarelli. (*Compt. Rend.*, 1956, **242**, May 7, 2355–2357). A nitrocellulose lacquer (not described) is used, with or without previous electropolishing. The method is the subject of a patent application.

The Scope of Electron Reflection Micrography in the Study of the Structure of Metals. A Delong, V. Drahoš, L. Bezděk, and D. Růžička. (*Hutnické Listy*, 1956, **11**, (6) 355–363). [In Czech]. The new Czechoslovak table-model electron microscope, adaptable to reflection microscopy with resolutions of 400Å, is used in a study of structures, mostly pearlitic, of carbon steels, as a function of carbon content. Cementite coagulation and other phenomena were observed, and are illustrated by 35 micrographs.—P. F.

Test for Determination of Ionic and Metallographic Characteristics of Grey Pearlitic Cast Iron by Anodic Oxidation. A. Roos. (*Rev. Mét.*, 1956, **53**, Mar., 170–178). Diffusion coefficients are measured for Cr, Co, Mn, and Ni. Combination of alloying elements with positive and negative coefficients yields oxidation-resisting metals. Silicon greatly affects the diffusion coefficients, and resistance to abrasion is correlated with ionic diffusion coefficients.

The Oxidation in Air of Ferrous Alloys Employed as a Metallographic Etch. A. Scortecci and C. Durand. (*Inst. Hierro Acero*, 1956, **9**, Feb., 169–175. *Special Number*). [In Spanish]. A brief account is given of the technique of air oxidation of metallographically prepared specimens in order to colour and accentuate differences in phase etc. Examples of the fields in which this method is useful are reviewed. (42 references).—P. S.

Polymorphism of Iron at High Pressure. D. Bancroft, E. L. Peterson, and S. Minshall. (*J. Appl. Phys.*, 1956, **27**, Mar., 291–298). Under certain conditions, propagation of compressive waves, generated in Armco iron and in mild steel by high explosive, occur with three stable shocks which are characterized by abrupt and possibly quasi-discontinuous change of pressure. Investigations have shown that these shocks are consistent with the hypothesis of a polymorphic transition in iron at about 0·13 megabar.—E. E. W.

Determination of Differences in the Structure of Cast-Iron by Means of Colour Photography. G. Aubrion. (*Giesserei*, 1956, **43**, Apr. 26, 203–210). The task of the most important conventional etching agents and of the special oxidizing etching agents is first considered with reference to colour photography. The composition of the oxidizing etching agents is then described, (*a*) for agents oxidizing at high temperatures, and (*b*) for agents used cold. The solidification process in cast iron is surveyed: coloured reproductions are shown of the micrographs. The results of examining various types of cast-iron after a special etch are then described.—R. J. W.

Some Effects of Micro-Segregation. Variation in Hardenability across Alloy Steel Billets. H. Allsop. (*Metal Treatment and Drop Forging*, 1956, **23**, Mar., 105–110). A comprehensive review of structures and their possible causes is presented in an address to the Sheffield Metallurgical Association.

Semi-Automatic Polishing of Very Hard Metallographic Specimens. Z. Ministr. (*Hutnické Listy*, 1956, **11**, (3), 154–160). [In Czech]. A special holder for the simultaneous polishing of 12 samples on a rotary-disc machine was developed, together with diamond and boron carbide pastes of suitable grain size for application to very hard materials. Very satisfactiory performance of the machine and the pastes was recorded.—P. F.

On Determination of Non-metallic Inclusions in Chromium Steel by Hot H_2SO_4 Method. S. Mackawa and M. Ebihara. (*Tetsu to Hagane*, 1956, **42**, Feb., 121–126). [In Japanese]. To obtain reproducible results by the Gakushin method, quenching is often necessary to avoid formation of carbide which would not be decomposed by $KMnO_4$ treatment. Water quenching is desirable for cutting specimens, but vacuum quenching may be used for drilling specimens. If the C and Cr contents are less than 0·7 and 1·0%, respectively, quenching is not necessary; it must be done, however, with 13% Cr steel and 18–8 stainless steel to avoid formation of TiC.—K. E. J.

On the Dynamics of Phase Growth. P. L. Chambré. (*Quart. J. Mech. Appl. Math.*, 1956, **9**, June, 224–233). Equations are derived for the growth of a solid into a surrounding supercooled fluid. Difference of densities of liquid and solid phases are taken into account and convection effects are included.

Kinetics of Solidification. K. A. Jackson and B. Chalmers. (*Canad. J. Phys.*, 1956, **34**, May, 473–490). The kinetic theory of freezing and melting is developed from the concept of atom movements between solid and liquid and nucleation is then considered. Agreement with observation is obtained in that supercooling is proportional to equilibrium temperature, surface free energy per atom is half latent heat, and the amount of supercooled liquid has little effect on the temperature of homogeneous nucleation.

Modes of Growth of Cementite in Constituents formed by Isothermal Transformation in a 12% Mn Hypereutectoid Steel. A. Kohn, J. Plateau, and G. Pomey. (*Compt. Rend.*, 1956, **242**, Jan. 9, 256–258). Optical and electron microscopical and X-ray examination is described and the structures illustated. Lamellar structures are produced which grow by two different processes.

Ordering of Atoms in the σ Phase. J. S. Kasper and R. M Waterstrat. (*Acta Crystallographica*, 1956, **9**, Mar., 289–295) Ordering of component atoms in the σ phases Fe–V, Ni–V, and Mn–Cr was studied by neutron diffraction. Definite evidence of ordering was found in all three systems. These results, with some X-ray investigations, enable a generalization to be made regarding the scheme of the ordering for binary σ phases of the first row transition elements.—T. E. D.

Electrolytic Polishing of Steel and Cast Iron Metallographic Sections in a Chromic–Phosphoric Electrolyte. L. P. Zaĭtseva. (*Zavodskaya Laboratoriya*, 1955, **21**, (4), 443–447). [In Russian]. An account is given of the use of a chromic–phosphoric electrolyte (88% H_3PO_4, 12% CrO_3) for electrolytic polishing and etching of metallographic sections of carbon and alloy steels and of cast irons. The effect is similar to that of alkaline sodium picrate solutions. Polishing without etching is secured by intensive stirring of the electrolyte; otherwise light etching takes place except with austenitic steels, for revealing the structure of which electrolytic etching in different electrolytes which dissolve the oxide film on the polished surface is required.—S. K.

Studies of the Determination of Non-Metallic Inclusions in Iron and Steel. I. Determination of Non-Metallic Inclusions in Plain Carbon and Silicon Steel. H. Gotô and T. Watanabe. (*Sci. Rep. Res. Inst. Tohokû Univ.*, 1953, **A5**, Dec., 505–512). Comparing the hot nitric acid, electrolytic and chlorine methods for the determination of non-metallic inclusions in iron and steel, the author found that the chlorine method was the most convenient and accurate.—J. G. W.

Influence of Forging on Phosphorus Segregation in Steel. A. Kohn and J. Doumerc. (*Metal Treatment and Drop Forging*, 1955, **22**, Sept., 387–394; *Steel Processing*, 1956, **42**, Jan., 13–19). An autoradiographic study. Steel containing 0·42% C and 0·21% P was used and the segregation is expressed as the ratio of phosphorus in dendrite axis to that in interdendritic spaces. This "degree of heterogeneity" may be about 4 and is reduced to 2·5 in 64 h at 1100° C or to 1·5 in 64 h at 1200° C. Forging reduces the heterogeneity to a micro-scale but facilitates homogenization.

Several Experiments Concerning the Production of Single Iron Crystals by the Recrystallization Method. M. Yamamoto and R. Miyasawa. (*Sci. Rep. Res. Inst. Tohoku Univ.*, 1953, **A5**, Dec., 493–504). Round bars, 3 to 5 mm dia., were prepared from 0·065 to 0·13% C steels and heated to 1000° C in moist hydrogen. The greater part of the carbon was removed during heating up. The decarburization velocity was inversely proportional to the specimen diameter; grain growth was moderate. Specimens treated thus for two days showed maximum grain growth when subsequently stretched 4% and annealed at 880° C for two or three days. The higher the purity of the materials, the greater the grain growth.—J. G. W.

Metals, Perfect and Imperfect. T. E. Allibone. (*Found. Trade J.*, 1955, **98**, June 23, 667–675). The present state of knowledge of metal crystals is reviewed. Among the aspects discussed are crystal growth, grain boundaries, the formation of slip bands, dislocations in crystals, impurities in metals and the production of very pure metals.—B. C. W.

Principal Physical Factors in Crystallization. V. I. Danilov. (*Stal'*, 1955, (10), 909–913). [In Russian]. In this article the general theory of crystallization based on experimental data for organic compounds and easily fusible metals is outlined and its relevance to the crystallization of steel is examined. Modern theories on the formation of centres of crystallization and the growth of crystals do not, it is concluded, contradict the concepts of the successive crystallization of the steel ingot and the importance of heat-removal. In studying the mechanism of the formation of the ingot structure due weight must be given to the kinetics of crystallization, connected with the effects of supercooling and of impurities in crystal nucleation and growth.—S. K.

Crystallization of Super-Cooled Metal Alloys. W. Geller and H. Garbeck. (*Arch. Eisenhüttenwesen*, 1955, **26**, Oct., 611–621). The authors discuss nucleation and crystal growth, the effects of foreign nuclei on the super-cooling of pure metals and alloys, and thermal and metallographic investigations of super-cooled alloys developing normal eutectics and solid solutions. The mode of solidification of super-cooled melts is compared with the behaviour of melts solidified by rapid cooling without super-cooling.—A. C.

A Theory of Regular Short-range Order. E. Scheil and F. Wegener. (*Z. Metallkunde*, 1955, **46**, Sept., 658–668). A thermodynamic study of order–disorder in three-phase systems is given. Solution theory is used with allowance for disequilibrium.

The Recrystallization Diagram. G. G. Kromrey. (*Neue Hütte*, 1955, **1**, Dec., 104–112). A critical discussion of Czochralski's recrystallization diagram is followed by the description of a new diagram which, it is claimed, is more in accord with practice.—L. J. L.

Variation in Preferred Orientation and Modulus of Elasticity in Cold Drawn Music Spring Wire. H. C. Burnett and C. J. Newton. (*Wire and Wire Prod.*, 1955, **30**, Nov., 1375–1376, 1408–1410). Preferred orientation and Young's Modulus of cold-drawn music wire were found to change together, with maximum values occurring for a reduction in area of approximately 58 per cent. The ultimate tensile strength exhibited no such maximum. It is thought that the change of modulus is caused by the development of preferred orientation. The "maximum" in the latter refers to the fraction of (110) alignment.—J. G. W.

Phase Transformations in Austenitic Manganese Steel. K. H. v. Klitzing in collaboration with E. Wesselhöft. (*Arch. Eisenhüttenwesen*, 1955, **26**, Dec., 755–759). Microscopical investigations were carried out on austenitic steel containing 0·45% C and 12·6% Mn after deformation, annealing, and low-temperature cooling in a current of air. Both etched and unetched specimens were examined.

The Surface Relief Effect due to Bainite Transformation Observed by Hot Stage Microscopy. K. Tsua, T. Mitsuhashi, and Y. Sakami. (*J. Mech. Lab.*, 1955, **9**, Nov., 243–248). Relief markings were observed in the hot-stage microscope during the formation of bainite corresponding to the dotted line of carbide in the upper bainite structure and to the acicular structure of lower bainite. Relief effects were also caused by the Widmanstätten figure of ferrite in various carbon and alloy steels. The relation between the relief markings and etched structures is discussed.—J. G. W.

Comparative Reliability of Methods of Evaluating the Alpha-Phase in Stainless Steel. N. K. Ipatov. (*Zavodskaya Laboratoriya*, 1955, **21**, (2), 198–199). [In Russian]. The relation between alpha-phase determinations in ladle samples of stainless steels and in the rolled product are discussed and experiments aimed at the study of this relation are described. Alpha-phase determinations were made on 200 heats, using samples from 140 × 140 mm rolled blanks and from forged castings 80 mm in diameter cast in a fireclay tube, and were compared with those obtained by the use of a nomogram involving the titanium, chromium, nickel, carbon, and manganese contents of the steel. The results obtained with ladle samples are judged to be most suitable and reliable for production-control conditions.—S. K.

Study of High Chromium Steels. II. On the Anomaly of α-Solid Solution of Fe–Cr System at High Temperatures. Y. Imai and K. Kumada. (*Sci. Rep. Res. Inst. Tohoku Univ.*, 1953, **A5**, Dec., 520–532). The effect of prolonged annealing of steels containing 15 to 74% chromium was studied by measurements of hardness, dilatation and magnetic properties. Inflexions in the change of properties with chromium content were found at about 25 and 35%.—J. G. W.

Peritectic Reactions in Ternary Metal Systems. A. Prince. (*Metal Treatment and Drop Forg.*, 1955, **22**, Nov., 485–489, 34 Adv.). The author reviews peritectic reactions which may occur in ternary systems. (See author's complementary article, *idem.*, 1955, **22**, May, 193–201). Two cases of four phases co-existing in a ternary system are considered, viz.: (1) the phases disposed at the ends of straight lines which intersect at some point, and (2) one phase exists within a triangle formed by the other three phases. (3 references).

The Nature of Spottiness in a Chromium–Molybdenum–Aluminium Nitriding Steel. V. D. Oreshkin. (*Stal'*, 1955, **15**, (1), 69–70). Spottiness in rolled specimens appears to be due to segregation associated with non-metallic inclusions. The dark zones are enriched in carbon but not in S or P, and no correlation with sulphur content was found. The spots are mainly of pearlite and are harder than the basic structure. The inclusions consist mainly of alumina.

Mechanics and Kinetics of Diffusionless Martensite Formation. H. Knapp and H. Dehlinger. (*Acta Met.*, 1956, **4**, May, 289–297). [In German]. Empirical studies of martensite formation exclude nucleation although the distortion energy/mol. tends to infinity with decreasing nuclear size. By assuming the presence of a preformed nucleus a theory of martensite growth is developed using dislocation theory.

Transformations of Iron–Chromium Alloys near Equi-atomic Proportions. G. Pomey and P. Bastien. (*Rev. Mét.* 1956, **53**, Feb., 147–160). The order–disorder and α–σ transformations are investigated and compared in very pure alloys. Thermomagnetic, dilatometric, metallographic, and other observations are used and correlated. Discussion is reported.

Separation of Carbon from Supersaturated Solution in α-Iron During Precipitation. W. Pitsch and K. Lücke. (*Arch. Eisenhüttenwesen*, 1956, **27**, Jan., 45–54). The authors discuss the dependence of the damping and electrical resistance of supersaturatedly dissolved and separated carbon in α-iron. They describe the progress of separation at 90–170° C in strained and unstrained wires after quenching from 710° C. The results of experiments are considered in terms of various separation theories for both the strained and unstrained states.—A. C.

Solubility of Oxygen in Molten Iron containing Titanium. B. K. Lyandis and A. M. Samarin. (*Doklady Akad. Nauk. S.S.S.R.*, 1955, **101**, (2), 325–326). Data are given for 1600° C and 1650° C with a discussion of the deoxidation mechanism by titanium.

Contribution to the Study of Grain Boundaries and Sub-Boundaries in Steels. L. Habraken and P. Cuvelier. (*Métaux–Corrosion–Indust.*, 1956, **31**, Mar., 105–125). The development of boundaries in pure iron, carbon steels, and alloy steels has been studied with the aid of the electron microscope. The standard structures and development of structures during iso-thermal and non-uniform heat treatments are described with the help of photo-micrographs. The influence of creep on the structure of boundaries between crystals is also considered.—B. G. B.

Lattice Imperfections. W. Dekeyser. (*Silicates Indust.*, 1956, **21**, Feb., 61–68). The nature and role of vacancies and other point imperfections, dislocations, and imperfections in ionic crystals associated with an excess or deficiency of electric charge are considered in outline. With the exception of dislocations, imperfections found in lattices are also of importance in amorphous bodies, i.e. in the vitreous state.

Recrystallization Phenomena in Pure Metals. C. de Beaulieu. (*Chim. Ind.*, 1956, **75**, Apr., 740–747). The results obtained from the study of the properties of ultra-pure aluminium and iron are discussed.—B. G. B.

On a New Mechanism of the Precipitation of Vanadium Carbide. F. Králík. (*Hutnické Listy*, 1956, **11**, (4), 230–233). [In Czech]. The experiments, carried out on a boiler steel containing 0·13% C, 0·49% Mn, 0·26% Si, 0·017% P, 0·019% S, 0·15% Cu, 0·08% Ni, 0·5% Cr, and 0·28% V, showed that vanadium carbide may be precipitated by two distinct mechanisms. In both cases the carbide precipitates from the solid solution, but in the initial martensitic structure the dispersion hardening, accompanied by the formation of V_4C_3, takes place in the supersaturated solution while during reprecipitation in bainitic structures a progressive dissolution of the cementite present occurs, and the vanadium carbide is formed from ferrite. The rate of precipitation is about 10 times slower in the latter case.—P. F.

Theory of Orientated Crystallization, (Epitaxis), Effects of Temperature of the Support and Supersaturation. G. Blisnakov. (*Compt. Rend.*, 1956, **242**, Jan. 30, 656–657). Mathematical expressions are derived.

Sigma Phase Formation in Stainless Steels. H. O. Werme. (*Jernkontonets Ann.*, 1956, **140**, 1, 47–74). [In Swedish]. Details are given of a literature survey on sigma phase formation in chromium and chromium–nickel steels, with special reference to some of the most common types of steel. Sections deal with its influence on mechanical properties at room or high temperatures, its effect on corrosion characteristics, and metallographic methods of identifying this phase.

On the Morphology of the Brittle Phase in Transformer Steels. J. Ježek. (*Hutnické Listy*, 1956, **11**, (3), 139–143). [In Czech]. The formation and dissolution of a globular precipitate of a non-ferrous phase associated with brittleness was studied in a 4% Si transformer steel by means of electron-micrography.—P. F.

The Formation of Carbide in Low-carbon Chromium–Vanadium Steels at 700° C. S. W. K. Shaw and A. G. Quarrell. (*J. Iron Steel Inst.*, 1957, **185**, Jan., 10–22). [This issue].

Calorimetric Study of the Austenite: Pearlite Transformation. W. C. Hagel, G. M. Pound, and R. F. Mehl. (*Acta Met.*, 1956, **4**, Jan., 37–46). A high temperature, recording, constant heat-flow calorimeter was used to measure the specific heats of austenite and pearlite in eutectoid carbon and alloy steels, over the range 400°–850° C. The addition of 0·8% C increases specific heat relative to pure iron but the addition of up to 2% Mn, Mo, or Co or variation of the interlamellar spacing had little effect. The enthalpy and free energy of the transformation are calculated from the calorimetric data.—A. D. H.

Cementite Morphology in Pearlite. F. C. Frank and K. E. Puttick. (*Acta Met.*, 1956, **4**, Mar., 206–210). [In English]. The growth patterns of pearlite revealed by electron microscopy are discussed in terms of the geometry of growth, diffusion and surface energy factors. It is concluded that the lamellar nature of pearlite is a result of anisotropy in the ferrite–cementite interface.—A. D. H.

The Morphology of Precipitates in Titanium-Stabilized Stainless Steels. V. Číhal and J. Ježek. (*Hutnické Listy*, 1956, **11**, (3), 151–154). [In Czech]. Results of an electron-micrographic study of carbide-formation and decomposition in titanium-stabilized 18/8 steel are discussed. Decomposition of the titanium carbides at temperatures of the order of 850° C is the main cause of intercrystalline corrosion; the carbide precipitated being $Cr_{23}C_6$. The shapes and X-ray diffraction patterns of the various carbides isolated are considered. The phenomenon of "knife-edge attack" is elucidated in terms of the mechanisms studied.—P. F.

A Study of Austenite Transformations Occurring on Slow Cooling. B. Šesták. (*Hutnické Listy*, 1956, **11**, (5), 299–307). [In Czech]. A self-recording dilatometer suitable for use with cooling rates as high as 10° C/s, giving an amplification of length changes of up to 1000× is described. Results obtained with it on a ledeburitic 1·94% C, 12·8% Cr steel on continuous cooling are given.—P. F.

Investigation of the Isothermal Decomposition of Austenite and Martensite in Unalloyed Steels in the Temperature Range 100–400° C by Method of Deposit from Solution. H.-K Görlich and H. Goossens. (*Arch. Eisenhüttenwesen*, 1956, **27**, Feb., 119–126). A description is given of the method of deposit from solution for the isolation of structural components for electron microscopical examination. The examination of the isothermal decomposition of austenite, the decomposition of martensite, the indication of hexagonal ϵ-iron carbides, the process of transformation of ϵ-iron carbide in cementite, and the determination of the lattice parameters of hexagonal ϵ-iron carbide are discussed.—A. C.

Propagation of Lüder's Bands in Steel Wires. J. C. Fisher and H. C. Rogers. (*Acta Met.*, 1956, **4**, Mar., 180—185). [In English]. The rate of propagation of Lüder's band-fronts in SAE 1020 steel wire was studied visually through the cracking of a brittle lacquer. At 24°, 0° and − 78° C it was found that the velocity V was given by: $\log V = C - D/\sigma T$. Where σ = applied stress, T = absolute temperature and C and D are constants.

On the Mechanism of the Action of Alloying Elements on the Eutectoid Reaction. N. T. Gudcov and J. Čadek. (*Hutnické Listy*, 1956, **11**, (4), 199–207). [In Czech]. The paper represents an abridged version of a doctoral thesis dealing with the carbide phases of products of the isothermal decomposition of austenite in four tungsten steels in the range 600–700° C, as well as with the carbide phase obtained on prolonged heating of the decomposition products in the same temperature range. The results can be summarized as follows: (1) The important function of kinetic processes indicated by the frequent formation of metastable transitional carbide phases was established, and it was found that the formation of cementite is not necessarily an indispensable stage even if cementite is one of the stable carbide phases of the steel. (2) In a 0·41% C, 1·59% W steel the stable carbide phase consists of a mixture of WC and Fe_3C, but in the eutectoid reaction the carbide formed is $M_{23}C_6$, where M may represent more than one metal, i.e. Fe and Mo. This phase was not, on the other hand, observed on prolonged heating of martensite. (3) In the case of a 0·43% C, 4·28% W steel the stable carbides are cementite and WC, but in the isothermal decomposition of austenite the formation of a granular eutectic containing M_6C was first observed, and only after a certain amount of this phase had been formed was the formation of a lamellar eutectoid with carbide observed, the formula being $M_{23}C_6$. Cementite formed in the initial period of the austenite decomposition of this steel disappears rapidly, but forms again in specimens heated for 2000 hours. (4) Similar results were obtained with a 0·42% C, 9·01% W steel, the stable carbide phases of which are WC and M_6C. (5) The rate of segregation of tungsten in austenite in the vicinity of the pearlite/austenite phase boundary is considerably more rapid than the rate of partition of tungsten between the components of the ferrite–carbide mixture. The formation of pearlite is related to this segregation. The carbide $M_{23}C_6$, which is formed in the process of the decomposition of the austenite, may contain less tungsten than the cementite formed during the decomposition of martensite in the same steel. It follows from this that the limited solubility of tungsten in cementite is not responsible for the fact that the latter does not immediately transform into $M_{23}C_6$. (6) The complexity of the observed reactions shows that the interpretation of the mechanism requires the taking into account of kinetic and thermodynamic processes.—P. F.

On the Position of the Ferrous Oxide Region in the Iron–Oxygen Diagram. J. Aubry and F. Marion. (*Compt. Rend.*, 1956, **242**, Feb. 6, 776–779). Measurements by three methods: analysis, solid reaction, and conductivity, show the limits to lie between $Fe_{0.946}O$ and $Fe_{0.875}O$.

Comparative Study of Reversible Oxidation Equilibria and Chemosorptions on Iron–Chromium Alloy Surfaces. J. Moreau and J. Bénard. (*Compt. Rend.*, 1956, **242**, Mar. 26, 1724–1726). Conditions for the stability of oxide layers can be investigated by the method described, in which microscopical observations are made after heating in controlled hydrocarbon–moisture atmospheres. An intermediate striated condition has been observed.

Contribution to the Study of Iron–Cobalt Alloys. J. Papier. (*Compt. Rend.*, 1956, **242**, May 14, 2455–2457). The face-centred form is metastable and cold work changes it, in part at least, to the body centred form stable even at high temperatures.

Interpretations of the Instability of Invar and of Reversible Ferro-nickels. E. Josso. (*Compt. Rend.*, 1956, **242**, Apr. 23, 2148–2150). Chevenard's theory is applied on the assumption that the carbide phase is not cementite but a percarbide.

The Isolation of Silicon Nitride from a Commercial 4% Silicon Steel. H. A. Sloman. (*Metallurgia*, 1956, **53**, Mar., 135–136). A short note reporting this isolation is presented. The conditions of formation and importance from the analytical aspect are briefly considered.—B. G. B.

A Model Metallographic Laboratory. S. J. Majka. (*Canad. Metals*, 1956, **19**, Mar., 54–58; Apr., 56–63). A detailed account of the design and facilities of the general purpose metallographic laboratory at the Ontario Research Foundation is presented.—B. G. B.

CORROSION

The Mechanism of the Corrosion of Steel. A. Hache. (*Corrosion et Anticorrosion*, 1956, **4**, Apr., 115–125). A laboratory study of corrosion of steel by distilled water, salt solution and sea water is described, and results are quoted concerning corrosion as a function of time, volume of solution, salinity and temperature. The necessity of field work is mentioned, and after an outline of the type of work carried out at marine corrosion stations, the interdependence of this work and laboratory work is indicated.—T. E. D.

Filiform Corrosion of Polished Micro Specimens. T. Geiger. (*Schweiz. Arch. Wiss. Techn.*, 1956, **22**, Jan., 16–17). Filiform corrosion occurs on polished microspecimens of nodular iron. Micrographic illustrations are given. The damage may be avoided by storage in a desiccator.—J. R. P.

Nomograph for Corrosion Rate Calculations. H. K. Bass, Jun. and R. V. Andrews. (*Corrosion*, 1956, **12**, Jan., 20–21).

The Conductometric Method Applied to the High Temperature Oxidation of Iron. George C. Fryburg. (*Corrosion*,

1956, **12,** Feb., 40–42). Using ribbons of pure iron 0·001 to 0·002 in. thick and a current of 50 mA the oxidation of iron at 600° C has been successfully studied and the results compared with gravimetric methods.—J. F. S.

Corrosion Testing at High Temperatures. N. D. Greene, Jun. (*Chem. Eng.*, 1956, **63**, Apr., 175–180). The problems involved in selecting materials for use at high temperatures are examined. Testing methods, including a critical examination of three methods, and application of test results are discussed.—T. E. D.

The Oxidation of Iron in the Range 400°–700° C. J. Païdassi. (*Acta Met.*, 1956, **4**, Mar., 227–229). [In French]. A letter in which the effect of variations in experimental technique on the measurement of the kinetics of the oxidation of iron are pointed out. Gravimetric and metallographic methods were used to obtain the data.—A. D. H.

ERRATUM

Abstracts, March 1956, p. 330. "The Prevention of Metallic Corrosion by Inhibitors." A. Bukowiecki. For "1955, **21,**" read "1954, **20.**"

Corrosion in Welded Constructions. H. G. Zelders. (*Lastechn.*, 1956, **22,** 6L, July, 101–105). [In Dutch]. In this article the author explains how the different forms of corrosion, namely surface, intercrystalline, stress, and crack corrosion, also that due to spotting and pitting, occur in welded structures, going on to indicate the measures that may be adopted for their prevention. Numerous diagrams and micrograms of welds appear in the text. (16 references).

A New Atmospheric Cycling Test for Corrosion Study. T. J. Nussdorfer and D. O. White. (*Amer. Soc. Test. Mat. Bull.*, 1956, May, No. 214, 61–65). The apparatus described was designed to simulate the daily variations in atmospheric conditions and was used to evaluate the efficacy of volatile corrosion inhibitors and preservative oils used in reciprocating and turbojet engines. Qualitative agreement of this laboratory method with field results was obtained.—B. G. B.

Mathematical Studies on Galvanic Corrosion. V. Calculation of the Average Value of the Corrosion Current Parameter. J. T. Waber, J. Morrissey, and J. Ruth. (*J. Electrochem. Soc.*, 1956, **103,** Feb., 138–147). A detailed mathematical analysis is made of the current density in alloys containing two phases. The conclusion that current density is greatest when the phases are in equal proportions agrees with experimental observations.—A. D. H.

On the Pitting of Electro-Polished Surfaces of Steels. J. Ibarz Aznarez and S. Feliu Matas. (*Rev. Cienca Apl.*, 1956, **10,** Jan.-Feb., 22–29.) [In Spanish]. The development of pitting during the electro-polishing of steels is discussed, and a study of the behaviour of stainless steel in phosphoric acid and citric-sulphuric acid baths is reported. The characteristic ring-like appearance of the pits is illustrated. It is concluded that pitting is related to the presence of stationary bubbles on the surface leading to accelerated corrosion. Evidence is given which indicated that carbide particles are favoured points for the formation of stationary bubbles.

High Temperature Hydrogen Sulphide Corrosion. E. B. Backensto, R. D. Drew, and C. C. Stapleford. (*Corrosion*, 1956, **12,** Jan., 22–32). Corrosion rates are given for carbon, low chrome, and stainless steels exposed to hydrogen–hydrogen sulphide atmospheres. The range of conditions studied was 0·002 to 1·0% H_2S by volume, 500–1300° F and 0 to 500 psig hydrogen pressure. Corrosion resistance increased with chromium content above 5% of chromium. Less than this had no effect on the corrosion rate. Flaky scale formed on all specimens whenever the corrosion rate rose above 0·01 to 0·02 inches per year. Maxima in the corrosion rate–temperature curves occurred at 1000° F for the stainless steels rising to 1200° F for 0–5% chromium steels. Corrosion rates increased with the hydrogen sulphide partial pressure but not so noticeably for longer term tests especially at the higher pressures. The effects of other variables are briefly considered. Tests on aluminium coated steel gave promising results. It is suggested that hydrogen sulphide corrosion in the petroleum industry can be minimized by reducing the hydrogen sulphide in the process streams, by the use of chrome–nickel steels or by aluminium coatings.—J. F. S.

The Study of Corrosion in Urban Marine Conditions. B. Callame. (*Corrosion et Anticorrosion*, 1956, **4**, Mar., 81–89). With a view to assisting in the standardization of corrosion testing (French and international), conditions and seasonal variations at various testing stations are compared. La Rochelle, Toulon, Antibes, Brest, Côte d'Ivoire, Bordeaux, Abidjan, and stations in Britain and the rest of the world are included.—T. E. D.

The Investigation of an Unusual Cause of Ship-bottom Pitting. R. P. Devoluy. (*Corrosion*, 1956, **12,** Jan., 49–54). On two separate occasions severe pitting occurred on parts of hulls which had only received an anti-fouling paint. In both cases the ships had been exposed to sulphide forming waters. Panel tests confirmed that these two factors present together can cause considerable damage. Bilge keel block areas are liable to receive only anti-fouling paint if this is sprayed on after brush application of the anti-corrosive paints.

Corrosion Problems at Stanlow Refinery. D. H. Nicholson. (*Corrosion Prevention and Control*, 1956, **3,** Feb., 37–39). The author outlines the causes of corrosion at this refinery and then shows how the problems have been dealt with in the distillation, catalytic cracking and Teepol plants. Special reference is made to graphite softening and to the problems arising from hydrogen sulphide formation.—L. E. W.

Internal Casing Corrosion in Sour Oil Wells. J. A. Caldwell and M. L. Lytle. (*Corrosion*, 1956, **12,** Feb., 23–26). The injection of an oil/inhibitor or a paraffin/oil/inhibitor mixture into the tubing casing annulus appears to be a cheap and effective method of reducing corrosion.—J. F. S.

Effects of Water Quality on Various Metals. L. Streicher. (*J. Amer. Waterworks Assoc.*, 1956, **48,** March, 219–238). Exposure tests on small metal panels are described. Treated waters from various sources were used and recommendations are given for the reduction of corrosion difficulties.

Contribution to the Study of Steel Corrosion in Salt Solutions. A. Hache. (*Rev. Mét.*, 1956, **53,** Jan. 76–80). Studies on sodium chloride solutions show the amount of dissolved oxygen to be the factor controlling the corrosion of immersed steel specimens. Discussion is reported.

Corrosion Tests on Aluminium Alloys. E. M. J. Mulders, W. G. R. de Jager, J. W. Boon. (*Metaalinstituut TNO Publn.*, 25c–3rd.Interim Report, 58 pp., Feb., 1956). [In Dutch]. This third interim report gives the results obtained with the 4th and 5th test series since the issue of the 2nd interim report together with the results found so far with the 6th test series still proceeding. Uses with steel are included.—F. R. H.

All-Glass Multiple-Test Apparatus for Corrosion Testing of Stainless Steels. J. V. Alger, E. C. Roberts, R. P. Lent, and G. W. Anderton. (*Amer. Soc. Test. Mat. Bull.*, 1956, May, No. 214, 57–60). The apparatus described is designed for evaluating the susceptibility to intergranular corrosion and corrosion resistance of stainless steels by the boiling nitric acid method.—B. G. B.

Corrosion Resistance and Mechanical Properties of Cr–Ni–Mn Stainless Steels. R. A. Lula and W. G. Renshaw. (*Metal Progress*, 1956, **69,** Feb., 73–77). The corrosion resistance and mechanical properties of two A.I.S.I. Types 201 and 202 steels are discussed and shown to be excellent for many structural applications in corrosive environments. A modified alloy with more chromium and nickel may be necessary to resist the more severe applications in the chemical industry.

Low Temperature Corrosion by Flue-Gas Condensates. R. W. Kear. (*Corrosion Techn.*, 1956, **3**, Feb., 59–63; Mar., 78–80; April, 125–127). The author discusses the formation, variation of concentration, rate of condensation and corrosive effects of sulphuric acid, and then deals with the physical and chemical methods of assessing the corrosiveness of flue-gas. This is followed by a description of some industrial studies of corrosion by sulphur oxides in industrial appliances; sulphuric acid corrosion in domestic applicances and chimneys, and flue-gas corrosion by chlorine compounds and oxides of nitrogen. Corrosion studies conducted in B.C.U.R.A. laboratories in relation to such problems are outlined. The author concludes with the methods of reducing corrosion by such means as fuel selection, addition of 'inerts', etc. (135 references).—L. E. W.

The Measurement of Soil Corrosivity. I. T. Rosenqvist. (*Tek. Tidskr.*, 1956, **86**, Mar. 13, 229–231). [In Norwegian]. After describing cases of severe corrosion experienced with steel piling in Norway, the author explains the mechanism of

the depolarization process and points out the Russian and American observations have been based on soils which were largely oxidized and in equilibrium with the atmospheric oxygen, so that use of their corrosion criterion (corrosivity = f(1/log of resistance) may lead to unfavourable results if deeper layers of soil are involved. A new equation is presented for such a case and details are given of actual measurements with a special corrosion probe to establish the relationship between e.m.f. and the soil's content of oxidizing substances.—G. G. K.

The Station for Study of Marine Corrosion and Fouling in the Central Tropics. V. Romanovsky. (*Peintures, Pigments, Vernis*, 1956, **32**, Apr., 309–313). An account of the experimental station and work being carried out at Abidjan under tropical conditions is given. Considerable differences have already been found between the efficacy of protective coating as tested at Abidjan and at La Rochelle.—B. G. B.

An Investigation into the Air-heater Corrosion of Oil-fired Boilers. B. Lees. (*J. Inst. Fuel*, 1956, **29**, April, 171–175). Methods which have been applied to reduce corrosion and fouling of the air heaters in the oil-fired boilers at Bankside generating station are described. More superheater tubes were installed to allow the optimum combustion conditions to be used while obtaining the required superheat.—D. L. C. P.

The Problem of Corrosion in Petroleum Refining. E. J. M. Tait. (*Corrosion Prevention and Control*, 1955, **2**, Dec., 25–30, 44; 1956, **3**, Mar., 29–33). The author separates corrosion in the refining industry into two main types, namely, external and internal, and indicates the corrosive environments and methods of control. Internal corrosion is dealt with in terms of heaters, vessels, etc. Typical examples of failure due to corrosion in heat exchange equipment, catalytic cracking units, chemical treating plant and in general ancillary equipment are given, and the preventive measures taken are outlined.—L. E. W.

Corrosion Problems on the Texas Gulf Coast. A. D. Rust. (*Corrosion Techn.*, 1956, **3**, May, 134–137; June, 185–190). The author is concerned primarily with corrosion and associated subjects as encountered at the two plants of the Dow Chemical Co., Freeport, Texas. The steps taken to prevent atmospheric and sea-water corrosion, and the surface preparations for, and the part played by, painting are described in some detail.—L. E. W.

New Experiments and Discoveries on Corrosion by Cooling Water and Anti-Freeze in Motor Cars. A. Bukowiecki. (*Schweiz. Arch. Wiss. Techn.*, 1956, **22**, March, 65–74). Experiments on the corrosion of metals by water and mixtures of anti-freeze and water are described. Effective corrosion-inhibitors in water are sodium chromate and sodium orthophosphate and emulsive oils. For ethylene glycol and water anti-freeze mixtures the most useful inhibitors are borax and triethanolamine phosphate/sodium mercaptobenzothiazol mixtures. A mixture of benzoate and sodium nitrite may also be used. Water chlorination reduces the anti-corrosive action of these inhibitors.—J. R. P.

Corrosion of Car Bodies; A Résumé of American Investigations. J. A. Edwards. (*Automobile Eng.*, 1955, **45**, Dec., 550–552). Tests are described in which the composition of rusts, and the extent of rusting were determined for several types of sheet steel, after normal exposure and artifical corrosion tests. It is shown that high carbon content reduces corrosion, but such steels cannot be used for car bodies because of their poor forming characteristics. The search for a cheap steel with good forming properties and improved corrosion resistance continues.—P. M. C.

Effects of Softened Water on Equipment. L. E. Tabor. (*J. Amer. Waterworks Assoc.*, 1956, **48**, March, 239–246). Tests on stainless steels are included in an account of corrosion in water systems. They were regarded as unsuitable on the grounds of cost and difficulty of machining in comparison with manganese bronzes.

Progress Report of Task Group T-4F-1 on Water Meter Corrosion. (*Corrosion*, 1956, **12**, Jan., 77–80).—J. F. S.

Acceleration of the Dissolution of Iron in Sulphuric Acid by Ferric Ions. H. C. Gatos. (*J. Electrochem. Soc.*, 1956, **103**, May, 286–291). The role of Fe^{+++} in accelerating the solution of iron in sulphuric acid was quantitatively studied.

The Determination of the Effect of a New Grass Killer on Application Equipment. J. A. Kelly, W. J. Falkenstein, and J. P. Carr. (*Corrosion*, 1956, **12**, Feb., 35–39). Aqueous solutions of sodium 2 : 2-dichloropropionate had a slight but negligible effect on the materials, including iron, steel, stainless steel, and galvanized steel, used in the construction of agricultural field sprayers.—J. F. S.

Some Observations on Assessing the Corrosion Behaviour of Tinplate. W. E. Hoare. (*Sheet Metal Ind.*, 1955, **32**, Mar., 176–178, 188). An apparatus is described for study of the possibility of obtaining useful comparative data on the corrosion behaviour of various lots of tinplate.—A. H. M.

Corrosion Aspects of Liquid Metals in Nuclear Engineering. (*Corrosion Prevention and Control*, 1956, **3**, Mar., 35–36, 56) This article is a summary of a paper presented at the Nuclear Engineering and Science Congress held recently in Cleveland, Ohio. A comparison is made between sodium, lithium and lead as heat-transfer media from the corrosion aspect.—L. E. W.

On the Titanium Stabilization of 18/9 Cast Stainless Steels. R. Pospíšil and R. Štefec. (*Hutnické Listy*, 1956, **11**, (4), 218–225). [In Czech]. A metallographic study of the intercrystalline corrosion resistance of the steels, accompanied by weld-tests and intercrystalline corrosion tests (utilizing bending tests on specimens boiled in standard mixtures of sulphuric acid and copper sulphate), showed that stabilization is possible in the same manner as in forged steels of similar composition. The Ti/C ratio should be greater than unity; even if it is as high as 10 no deterioration of the stabilizing effect is observed.—P. F.

On the Intercrystalline Corrosion of Cr–Ni Steels. V. Číhal and M. Pražák. (*Hutnické Listy*, 1956, **11**, (4), 225–230). [In Czech]. Electrolytic corrosion studies of 18/8 steel showed that intracrystalline corrosion depends on the amount of chromium carbides which have precipitated, and on the oxidation reduction potential of the electrolyte. The reduction in the chromium concentration in the vicinity of the carbides leads to a change in this potential near grain boundaries, the potential being displaced to more positive values. In the limiting case the passivation potential of the grain boundaries equals that of an Fe–Ni alloy. The results were compared with standard corrosion tests.—P. F.

Segregation in Titanium-Stabilized Austenitic Chrome Nickel Steel and its Connection with Intercrystalline Corrosion. K. Bungardt and G. Lennartz. (*Arch. Eisenhüttenwesen*, 1956, **27**, Feb., 127–133). Analytic and radiographic investigations were carried out on steel containing 0·07% C, 17·5% Cr, 0·4% Mo, 0·013% N, 10·4% Ni, and 0·47% Ti with the object of determining the effect of quenching temperature and duration on the separation process during subsequent heat treatment between 500 and 800° C. Interest was also taken in the susceptibility to intercrystaline corrosion. At 500° C there was no marked separation of titanium or chromium carbides. The latter reached a maximum at 600° C and was inhibited at higher temperatures by the increased simultaneous formation of titanium carbide. For longer quenching times the separations occurred more slowly during subsequent heat treatment.—A. C.

Hot Corrosion in Commercial Hypochlorite of 18/8 Ti, 18/8 and 18-Ti Welded Stainless Steels. C. Bighi and G. Pancaldi. (*Met. Ital.*, 1956, **48**, Feb., 73–81). [In Italian]. Rapid corrosion tests carried out in hypochlorite are described. The tests were conducted by using samples with flat or curved surfaces under different dipping conditions. The products of corrosion going into solution in the etching bath are determined by colorimetric methods. Results affecting the iron, chrome, nickel and titanium are examined and the behaviours of the sheets are discussed. (26 references).—M. D. J. B.

Erosion of Steel by Hot Gases. M. J. Fraser and A. A. Burr. (*J. Electrochem. Soc.*, 1956, **103**, Apr., 224–231). The use of a vent-plug device has allowed simulation of service conditions in a laboratory test for studying the behaviour of Armco iron and carbon and alloy steels when exposed to hot gases produced by an explosion. During erosion up to five surface layers are produced and X-ray and metallographic evidence for the retention of austenite is put forward.

Studies of the Effect of Titanium on Resistance of 18% Cr 9% Ni Steels to Intercrystalline Corrosion. V. Číhal and R. Pospíšil. (*Hutnické Listy*, 1956, **11**, (5), 284–289). [In Czech]. A study was made of the effect of various heat-treatments in the range 550–700° C. Titanium carbide begins to decompose at higher temperatures, while chromium carbides precipitate, rendering the steel susceptible to intracrystalline corrosion. The amount of ferrite which decomposes to give the brittle sigma-phase increases with the amount of titanium present in excess of stoichiometric quantities, necessary for

carbide formation, above 800° C. Reprecipitation of the thermochemically more stable TiC is controlled by the rate of diffusion of the titanium, which is less than that of chromium. The detrimental effect of high stabilization temperatures can be avoided by a stabilization heat-treatment in the range 850–950° C, when finely dispersed precipitates of titanium carbide already begin to form. The titanium content of the steels investigated varied from 0 to 0·8%. Electronmicrographic evidence of the structural changes is shown.

A Study of Protective Criteria on a Pipe Section in a Uniform Environment. L. P. Sudrabin. (*Corrosion*, 1956, **12,** Feb., 16–22). Tests using a 3 in. steel pipe coupled to zinc plates on its surface indicate that the potential gradients of the smaller local corrosion cells are not discernable by surface potential measurements. The tests indicate that while a potential of − 0·85 volts with respect to a remote copper–copper sulphate reference electrode is sufficient to protect bare iron against long line currents, the same potential must be achieved with respect to an electrode over the pipeline or close to the pipe surface of intermediate corrosion currents or local cell corrosion currents respectively are to be suppressed. In some circumstances the potential measured at the surface can be used to deduce the potential adjacent to the pipe.—J. F. S.

Warragamba Pipeline. (*Commonwealth Eng.*, 1956, **43,** Feb., 203–206; Mar. 239–242, from *Sydney Water Board Journal*, 1955, Oct.) The construction, laying, and protection are described.

Cathodic Protection. J. W. Boon. (*Metalen*, 1956, **11,** May 31, 219–225). [In Dutch]. The article touches on the electrical and electro-chemical approach to cathodic protection and also the galvanic method under applied currents. Reference is made to the reactions occurring at the anodes and cathodes while the advantageous and disadvantageous secondary effects are discussed. A practical method of cathodic protection of a pipe line in conjunction with galvanic anodes is described.—F. R. H.

Cathodic Protection and Shipping—Practical Considerations. A. W. Hubbard. (*Corrosion Prevention and Control*, 1956, **3,** June, 47–49). The author indicates the increasingly successful applications of cathodic protection to tanker cargo/ballast compartments and then discusses and compares the merits of the impressed current and sacrificial anode systems from the practical viewpoint.—L. E. W.

Induced Alternating Current Used for Cathodic Protection of a Coated Pipe Line. S. J. Bellassai. (*Corrosion*, 1956, **12,** Jan., 17–19). In a salt marsh near a.c. high-voltage transmission lines, the induced a.c. current in the soil has been rectified and used to protect cathodically a 6½ in. diameter coated steel pipeline. A graphite groundbed and selenium rectifier stack were used.—J. F. S.

Final Report on Four Annual Anode Inspections. N.A.C.E. Technical Unit Committee T-2B on Anodes for Impressed Current. (*Corrosion*, 1956, **12,** Jan., 63–74). Data on anode lives have been obtained from four test ground beds. In these the following anodes were installed for up to four years: steel, carbon and graphite, each in natural soil and in carbonaceous backfills. Graphite anodes in a carbonaceous backfill were best. Full details of anode performance, ground bed resistance and total current for the period of the test are to be published separately. Detailed recommendations, based both on the tests described and on the experience of committee members, are made concerning the installation of anodes, the selection of ground bed sites and the use of various backfills.

Systematic Investigation of the Efficiency of a Vapour Phase Inhibitor in Preventing the Corrosion of a Series of Common Metals. W. Paul. (*Werkstoffe Korrosion*, 1956, **7,** Apr., 189–198). The standard short-period accelerated test devised in America for testing the efficiency of vapour phase inhibitors has been applied to a similar product made in Germany. Its effect on nine different metals and alloys was investigated. Cast iron was completely protected only when the iron was in contact with paper impregnated with the inhibitor but mild steel suffered no corrosion either under these circumstances or when the inhibitor was merely present in the surrounding atmosphere. In view of the occasional use of cadmium coatings on steel, it is noteworthy that, in contrast with the other metals tested, cadmium was attacked by the inhibitor. The results are illustrated with colour photographs.—J. C. H.

The Influence of Nitrogen-Containing Organic Inhibitors on the Electrode Potential of Steel in Sulphuric Acid. R. N. Ride. (*J. Electrochem. Soc.*, 1956, **103,** Feb., 98–107). The electrode potential and corrosion rate of mild steel in NH_2SO_4 containing thirteen organic inhibitors were studied. From hydrogen over-voltage considerations it is postulated that the inhibitor is mainly adsorbed on the already present hydrogen film. Inhibitions is considered to result from hindrance of the anodic dissolution process accompanied at higher inhibitor concentrations by an increase in hydrogen overvoltage.—A. D. H.

Correlation of the Results Obtained with Corrosion Inhibitors in the Laboratory and in the Field. G. E. Purdy and W. J. Ries. (*Corrosion*, 1956, **12,** Jan. 33–38). Examples are given of three applications of a laboratory test to evaluate inhibitors for use in crude oil–brine systems. Field observations over a number of years are correlated with inhibitor concentration and with the earlier laboratory work. The principal factors influencing internal corrosion in oil wells are reviewed.—J. F. S.

Recent Research on Anticorrosive Bottom Compositions. H. J. Adams and J. C. Hudson. (*Corrosion Prevention and Control*, 1956, **3,** June, 41–45). The authors review recent researches on various anticorrosive media used to protect the submerged parts of a steel hull. Typical anticorrosive compositions are tabulated and their applications and effectiveness are discussed . The authors conclude with a brief discussion of metallic coatings.—L. E. W.

Corrosion Research Laboratories—9: The Corrosion Committee of the A.B.E.M. D. Bernane. (*Corrosion Techn.*, 1956, **3,** Mar., 72–75). The author describes the development of the organization and then outlines past and current investigations in relation to the applications of paints as corrosion preventives.—L. E. W.

ANALYSIS

Microanalytic Investigation in Iron Research. W. Koch and H. Malissa. (*Arch. Eisenhüttenwesen*, 1956, **27,** Jan., 13–24). The various domains of microanalysis are reviewed. Accuracy and sensitivity, the significance of surface reactions, the experimental apparatus and its use are discussed. Detailed attention is paid to the methods of weighing, heating up, heat treatment and decomposition. Separation by the various techniques of decanting and filtration, pouring, extraction, evaporation and electrolysis is considered, and determination by the methods of photometry, titration, polarography and spectrographic examination is described.

The Alcoholic Iodine Method for the Extraction of Inclusions from Steel. J. E. Garside, T. E. Rooney, and J. J. Belli. (*J. Iron Steel Inst.*, 1957, **185,** Jan., 95–103). [This issue].

Pouring and Preparation of Test Samples for the Quantometric Analysis of Cast Iron. V. Pavanelli. (*Met. Ital.*, 1956, **48,** Jan., 40–42). [In Italian]. Results are given of comparative quantometric tests carried out on chilled iron. Samples with constant structures are claimed to have been obtained independently from cooling periods, reproducibility is claimed to have been improved and the calibration curve of silicon has been standardized both for grey and malleable cast irons.—M. D. J. B.

A Semi-Micro Method for the Determination of Carbon in Iron and Steel. P. H. Scholes. (*Metallurgia*, 1956, **53,** Mar., 129–131). An apparatus based on the micro technique for the determination of carbon and hydrogen in organic materials is described. A detailed account of the operational procedure is given, together with typical results for standard steels.

Determination of Small Carbon Content in α-Iron by Measurement of Damping. W. Wepner. (*Arch. Eisenhüttenwesen*, 1956, **27,** Jan., 55–59). The author first reviews the fundamentals of the method of determining small quantities of dissolved elements by measurement of damping. He then describes the test rig and the preparation of specimens, and reports measurements on 1–4 mm iron wires containing 0·002–0·03% C, 0·003% Si, 0·002% Mn and P, 0·011% S, 0·002% Al, 0·001% Cr and Cu, 0·0008% N, 0·001% Ni and 0·016% O. The relation between phase angle and carbon content is indicated. Accuracy of the method, sources of error, and the upper limit of determination are discussed.

Determination of Aluminium in 75–80% Ferrosilicon. F. Baldi and R. Passeri. (*Met. Ital.*, 1956, **48,** Jan., 8–14). [In Italian]. The authors describe a method of analysing powdered materials by mixing them with a conducting agglomerant, forming them into small tablets and using a

rotating electrode. A critical examination of the phenomena which occurred during emission shows up irregularities which may appear when determining the calibration curves, due to variations in intensities emitted by the various components. (10 references).—M. D. J. B.

The Use of Complexones in Chemical Analysis. I. Colorimetric Determination of Iron with Complexone III. P. Schneider and J. Janko. (*Chemické Listy*, 1956, **50**, (6), 899–902. [In Czech].

Determination of Free and Carbide Carbon in Austenitic Chromium–Nickel Steel. N. M. Popova and L. V. Zaslavskaya. (*Zavodskaya Laboratoriya*, 1955, **21**, (11), 1285–1288). [In Russian]. An account is given of the investigation of the state of carbon in two steels (0·50, 0·73% C; 20·8, 20·6% Cr; 18·5, 20·5% Ni; 0·55, 0·50% Mn, respectively) after hardening and tempering at different temperatures. Treatment of the anodic carbon residue with hydrogen peroxide removed free carbon leaving chromium carbide undecomposed. Combined carbon was determined in this latter, free carbon then being found by difference from the total carbon. Results obtained were compared with the quantities of bromothymol blue absorbed by the carbide of the solid solution during the adsorption of this dye by the carbide residue. The comparison was satisfactory and the further investigation of the adsorption method is recommended.—S. K.

Luminescence Analysis of Non-Metallic Inclusions. N. F. Leve and S. S. Sandomirskaya. (*Zavodskaya Laboratoriya*, 1955, **21**, (6), 711–712). [In Russian]. An account is given of an investigation of the possibility of applying luminescence analysis to the study of non-metallic inclusions. Using an ultra-violet microscope and source the luminescence of natural minerals and synthetic compounds approximating in composition to non-metallic inclusions and of non-metallic inclusion from carbon steels were studied. It was shown that a number of non-metallic inclusions (including corundum and silicates) produce primary luminescence differing in colour and intensity. The method was applied to the study of inclusions separated from a rimming steel.—S. K.

Perchlorate Method for the Determination of Chromium in Steels. P. F. Agafonov. (*Zavodskaya Laboratoriya*, 1955, **21**, (11), 1311–1312). [In Russian]. Two variants of the perchlorate method for the determination of chromium in steel are described. One is for low-chromium the other for high chromium steels and they have been checked on standard samples containing 0·80–1·68 and 8·90–25·79% Cr, respectively.—S. K.

Use of Perchloric Acid for the Determination of Chromium in Steels. N. V. Belogorskaya. (*Zavodskaya Laboratoriya*, 1955, **21**, (11), 1313). [In Russian]. In the method briefly described losses of chromium during its determination in steels by the perchlorate method are avoided by trapping chromium chlorides.—S. K.

Rapid Determination of Cobalt In Steels. F. Velasco and J. Hontoria. (*Inst. Hierro Acero*, 1956, **9**, Feb., 176–182. *Special Number*). [In Spanish]. A rapid and fairly accurate spectrophotometric method for the determination of cobalt is described. The blue colour with ammonium thiocyanate is extracted with *cyclo*hexanone in a centrifuge; Beer's law is obeyed. No previous separation of the other elements is necessary, iron interference is avoided by ammonium citrate and disodium phosphate, copper with potassium iodide and sodium thiosulphate. The method, which takes less than one hour, is detailed. (16 references).—P. S.

Amperometric Determination of Copper and Nickel in Alloy Steels with Rubeanic Anhydride. Kh. Ya. Levitman and Z. A. Krivchik. (*Zavodskaya Laboratoriya*, 1955, **21**, (4), 397–399). [In Russian]. Based on experiments with mixed solutions, an amperometric method has been developed by which copper and nickel present together in alloy steels can be determined. Rubeanic anhydride is used as the precipitating reagent.—S. K.

Potentiometric Method of Determining Large Quantities of Manganese. D. A. Pchelintsev. (*Zavodskaya Laboratoriya*, 1955, **21**, (11), 1307–1309). [In Russian]. The potentiometric method described gave satisfactory results for manganese determinations in manganese ores and ferromanganese with 52–88% Mn.—S. K.

Use of the Method of Ion-Exchange Chromatography in the Determination of Molybdenum in Steels and Ores. I. P. Alimarin and A. M. Medvedeva. (*Zavodskaya Laboratoriya*, 1955, **21**, (12), 1416–1418). [In Russian]. The use of cation-exchange resins in the presence of hydrogen peroxide for the separation of molybdenum from iron and other elements is the basis of the method described for molybdenum determination in steels and ores. The hydrogen peroxide prevents the sorption of molybdenum by forming permolybdic acid, but iron, copper, nickel, manganese and small quantities of titanium are sorbed. Tungsten and vanadium are not separated from molybdenum. Results for standard samples of a steel (0·31% Mo) and iron ores (0·31–1·28% Mo) are presented, showing satisfactory agreement.—S. K.

Method of Determining Phosphorus in Ferrophosphorus. I. M. Engalÿchev and N. M. Bekker. (*Zavodskaya Laboratoriya*, 1955, **21**, (12), 1443–1444). [In Russian]. The effects of various factors during the solution of ferrophosphorus on the results of phosphorus determinations were studied and a procedure for such determinations developed.—S. K.

Photometric Determination of Tin in Iron and Steel. I. Studies of Colour Reactions of Stannous Salts with Cacotheline. H. Gotô and Y. Kakita. (*Sci. Rep. Res. Inst. Tohoku Univ.*, 1953, **A5**, Dec., 554–560). Photo-electric measurements of the reaction between cacotheline and stannous solution reduced by aluminium in a stream of carbon dioxide showed some interference from the ions of iron, antimony, chromium, silver, mercury, tungsten, molybdenum, vanadium, and titanium.—J. G. W.

Analytical Determination of Trace Constituents in Metal Finish Effluents. IX. The Determination of Free Chlorine in Effluents. E. J. Serfass, R. F. Muraca, and D. G. Gardner. (*Proc. Ann. Conv. Amer. Electroplaters' Soc.*, 1956, 1–2). A colorimetric method using *o*-tolidine reagent is described for the determination of 5–50 p.p.m. Cl.

Organization of a Laboratory for the Analysis of Gases in Metal. A. G. Atlasov and Yu. D. Labut'ev. (*Zavodskaya Laboratoriya*, 1955, **21**, (2), 253–254). [In Russian]. The layout of apparatus in a laboratory specially constructed for the vacuum-fusion and vacuum-heating analysis of gases in metal is illustrated and some suggestions are made.—S. K.

Determination of Hydrogen in Steel. Analysis of Gas extracted from Samples in a Vacuum at 500–1100° C. J. Marot. (*Rev. Mét.*, 1955, **52**, Dec., 943–960). In a study to determine optimum temperature it was found that while 600° is suitable for steel with a high H_2 content, higher temperatures and analysis of the extracted gases are necessary where the content is low. At 900–1000° 95% extraction is achieved and it appears that part of the hydrogen cannot be removed.

Determinations of Nitrogen in Blast Furnace Pig Iron. (Mlle.) M. Hanin and E. Jaudon. (*XXVIII Congreso Internacional de Quimica Industrial, reprint*). Apparatus for determination by vacuum fusion is described. **Nitrogen in Pig Irons.** (Mlle.) Hanin, Pontet, and E. Jaudon. (Reprint 1955, pp. 4). [In French]. An account of a comparison of chemical methods of determination with the authors' vacuum fusion method, with a discussion of possible resistant nitrides in relation to the differences between the values found.

On the Determination of Nitrogen in Steels. R. Suarez Acosta. (*Inst. Hierro Acero*, 1956, **9**, Jan.-Mar., 315–319). [In Spanish]. A review is given of the various methods for the determination of gases in steel with particular reference to the determination of nitrogen by chemical and vacuum fusion methods. The vacuum fusion method used by the author is described and illustrated.—P. S.

Determination of Hydrogen-Ion Concentration in Nickel-Plating Electrolytes by the Potentiometric Method. E. I. Ishutchenko, V. S. Ogienko, and V. G. Shipunova. (*Zavodskaya Laboratoriya*, 1955, **21**, (2), 164). [In Russian]. A brief account is given of a modified electrode arrangement.—S. K.

Control of the Reduction of Iron Oxides by Carbon by use of Differential Thermal Analysis. B. Dobovišek. (*Rudarsko-Metalurski Zbornik*, 1955, No. 4, 229–238). Reduction curves are obtained for pure ferric oxide, hæmatites, magnetite, limonite, siderites, and chamosite.

Mercurometric Determination of Iron in Ores. D. N. Finkel'shtein and G. N. Kryuchkova. (*Zavodskaya Laboratoriya*, 1955, **21**, (4), 403–405). [In Russian]. An account is given of an investigation of the use of the mercurometric method for the determination of iron in iron and other ores. The titration is best carried out in 0·01–2·2 N sulphuric acid: nitric acid has no effect if pure, and the titration is rapid. Perchloric and hydrochloric acids in concentrations up to three times that of iron and chloride up to 0·005 N have no effect. The effects of other ions are also considered.

Results for a wide variety of ores show the accuracy to equal that of the dichromate method.—S. K.

The Use of Carbon Dioxide Instead of Oxygen in the Determination of Sulphur in Ores. A. V. Dobrzhanskiĭ and V. I. Sakunov. (*Zavodskaya Laboratoriya*, 1955, **21**, (4), 399–400). [In Russian]. The low results of determinations of sulphur in ore by oxidation in oxygen or air followed by uncorrected iodine titration were shown to be due to oxidation of sulphur dioxide to trioxide. The oxidation of the dioxide occurs in the cold parts of the tube, especially if the walls are contaminated with iron. This is avoided by oxidizing with carbon dioxide. Sulphide-sulphur is converted to the dioxide at 1100–1200° C, the temperature for sulphide being 1300° C. This method gave satisfactory results with a wide variety of iron and other ores, sinter, and coke ash.—S. K.

Photoelectric Methods of Emission-Spectrum Analysis. L. D. Kondrasheva, I. V. Podmoshenskiĭ, and V. K. Prokof'ev. (*Zavodskaya Laboratoriya*, 1955, **21**, (12), 1446–1455). [In Russian]. The literature on instruments of the "quantometer" type is surveyed. The various makes are discussed and the theory of the method is outlined.—S. K.

Spectrophotometric Determination of Chromium following a Chromatographic Separation. A. J. Blair and D. A. Pantony. (*Anal. Chim. Acta.*, 1956, **14**, June, 545–552).

New Spectrographic Equipment. E. Raiteri. (*Met. Ital.*, 1956, **48**, Jan., 35–36). [In Italian]. A brief description is given of a grid-type spectrograph and a new arc and condensed spark generator, recently installed at the Fiat Auto-Avio Research Laboratories. The advantages of the equipment and the results obtained are discussed.—M. D. J. B.

Production Control Quantometer for Steelworks Analysis. D. Manterfield and W. S. Sykes. (*J. Iron Steel Inst.*, 1957, **185**, Jan., 105–113). [This issue].

A Rapid Method of Determining Tungsten in Steels by Means of Secondary X-Rays. J. Drahokoupil. (*Hutnické Listy*, 1956, **11**, (4), 233–237). [In Czech]. The applicability of the method was examined on steels containing 4, 9, and 18% tungsten. It was found to be accurate and rapid enough to be used for control of the tungsten content of steels during melting. A determination takes about one minute. An extension of the method to the simultaneous rapid determination of several alloying elements is discussed.—P. F.

The Use of Radioactive Isotopes in Metallurgical Research. S. M. Makin. (*Metal Treatment and Drop Forging*, 1956, **23**, April, 127–130). Autoradiography, activation analysis, and the uses of α- and β-rays are briefly surveyed.

Liquid Emulsion Autoradiography of Metals. J. C. Bokras and P. C. Rosenthal. (*Trans. Amer. Inst. Min. Met. Eng.*, 1956, **206**; *J. Met.*, 1956, **8**, Feb., Section 1, 286–288). The authors have adapted the liquid emulsion autoradiographic technique used in biological science to the study of metals. The results of a study of the distribution of carbon–14 in pure iron after various treatments are discussed.—G. F.

Rapid Analysis of a Mixture of Dolomite and its Components. M. Gibaud and M. Geloso. (*Peintures Pigments Vernis*, 1956, **32**, Apr., 306–308). The use of a thermo-balance for the analysis of dolomite is described. It enables the lime, magnesia and total CO_2 contents to be measured.—B. G. B.

Oxygen Determination by Combustion in Bomb. J. W. Whitaker, R. N. Chakravorty and A. K. Ghosh. (*J. Sci. Indust. Res.*, 1956, **15B**, Feb., 72–77). The apparatus and method are described together with the results of experiments on oxygen determination in fuels and some organic compounds.—E. E. W.

Rapid Determination of the Moisture Content of Coal and Coke. W. Radmacher and P. Mohrhauer. (*Glückauf*, 1956, **92**, 4th Feb., 166–170). Moisture in coal or coke is determined by treating with a solution of zinc chloride, the vapour pressure of which has been lowered by admixture with lithium chloride. The solution is filtered after about 20 minutes, and the decrease in density is a measure of the moisture taken up from the fuel. The moisture content is derived from a calibration curve. In the case of coke, the sample was broken down to < 5 mm particle size, and the air removed by evacuation before the determination. Satisfactory results are claimed.—L. D. H.

Effect of Sampling Tube Material on Dew Point Measurements. P. C. Kirby. (*Metal Treatment and Drop Forging*, 1956, **23**, Apr., 153–155). The tubes described are intended for measurements of furnace atmospheres. Rubber and Vinyl tubing are considered.

The Sampling of Commercial Gases, Particularly Coke Oven Gas. P. Michaelis. (*Glückauf*, 1956, **92**, Mar. 3, 264–271). This is a survey of methods for the direct and indirect sampling of gas. General principles are discussed, and specific methods are described for long-period and spot samples.

Vapour Phase Chromatography. S. W. Green. (*Indust. Chem.*, 1956, Jan., 24–28). The underlying principles and the relevant apparatus of the two types of vapour-phase chromatography are described.—E. E. W.

Radioactive Isotopes and their use in Materials Testing. G. Freyer. (*Technik*, 1956, **11**, Jan., 19–22). Principles of the use of radioactive isotopes are outlined, and some examples of applications are quoted in the testing of castings and welds for soundness, of thickness of materials, and of wear, surface cracks etc.—J. G. W.

The Application of Radioactive Isotopes in Metallurgy and Metallography. A. Hentsch. (*Neue Hütte*, 1956, **1**, July, 413–419). Practical examples of the use of radioactive isotopes are given mainly from the Anglo-Saxon literature. The formation of surface films in flotation processes, prospecting for ores, investigation of blast furnace processes, sulphur determination, slag reactions, phosphorus distribution, determination of changes caused in the properties of materials by radiation, etc. are briefly mentioned.—L. J. L.

Spectrographic Determination of Silica. J. W. Anthony, R. J. Chandler, W. B. Huckabay, and C. T. Kenner. (*Analy. Chem.*, 1956, **28**, Apr., Part I, 470–473). A spectrographic method is developed for the quantitative determination of silica in high concentrations using germanium metal as an internal standard. The procedure was tested on analysed samples of siliceous shales, cherts and other high-silica rocks.

A New Semimicro-Kjeldahl Method for the Determination of Nitrogen in Coal. M. Dermel and L. Strauch. (*Bulletin Scientifique, Conseil des Academies de la RPF Yougoslavie*, 1956, **2**, Mar., 104).

A Rapid and Precise Method for the Determination of Oxygen in Certain Gases. L. Silverman and W. Bradshaw. (*Anal. Chim. Acta*, 1956, **14**, June, 514–526). A method is described for blanketing atmospheres for liquid metals. The re-oxidation of a sodium anthraquinone–2-sulphonate solution is followed spectrophotometrically.

INDUSTRIAL USES AND APPLICATIONS

Wrought Steel: Its Choice and Applications for the Mining Industry. T. G. Bradbury. (*Canad. Min. Met. Bull.*, 1956, **49**, Mar., 167–174). Reasons for choice of specific alloy steels for various mining equipment parts are given, together with summaries of the properties of the steels suggested.

Use of Special Steels in Equipment for Power Stations. R. Rath. (*Mét. Constr. Mécan.*, 1956, **88**, Feb., 131–150). A comprehensive account of the use of alloy steels in various parts of power stations is presented. The metallurgical problems presented by the conditions of service are first discussed and the reasons for the selection of particular alloy steels are explained. American developments of martensitic chrome-steels and austenitic nickel-chrome steels are reviewed, attention being paid to the efficient welding of these steels and avoidance of the sigma phase and creep failure. Recent power station construction in France and Germany is also discussed. The increasing operating temperature of steam turbines and the associated metallurgical problems are reviewed. (26 references).—B. G. B.

Limit Design of Compressed Bars. E. Bölcskei. (*Acta Techn.*, 1956, **14**, (3–4), 377–400). [In English]. The statical design of compressed bars on the basis of their load carrying capacity is treated theoretically starting with an eccentrically loaded bar. Thus it is possible to show that the carrying capacity of a bar of plastic material depends on the loading process, which also accounts for the contradictory results obtained by a number of workers who treated this problem previously.—P. F.

Special Steels and Prestressed Concrete. P. Guyon. (*Mét. Constr. Mécan.*, 1956, **88**, Feb., 177–193). Various techniques used for prestressed concrete construction are described. The conditions of service of the steel wires and their metallurgical properties are discussed. Having been stressed, the wire is maintained at constant length and decrease in tension is to be avoided in subsequent service.—B. G. B.

Influence of the Type of Steel on the Cost of Gears and Pinions. O. G. d'Estaing (*Mét. Constr. Mécan.*, 1956, **88**, Feb.,

169–175). The selection of alloy steels for the construction of gears and pinions with particular reference to the balance between cost of steel and metallurgical suitability is discussed.

The Development of Metal-Bonded Carbon Bearings. H. B. Nudelman, C. H. Sump, and W. C. Troy. (*Amer. Soc. Test. Mat. Bull.*, 1956, Apr., No. 213, 62–69). The development of a water lubricated bearing material capable of use in water at temperatures of 200° F and above is described. A 70% cobalt, 30% chromium alloy matrix with carbon additions of 60 to 70% by volume is recommended for future bearing development work.—B. G. B.

Illustrated Review of the Use and Role of Special Steels in the Construction of Hydraulic Machines. J. Narcy. (*Mét. Constr. Mécan.*, 1956, **88,** Feb., 153–159). The metallurgical problems presented by the conditions of service of hydraulic turbines are discussed and the type of steels used in practice and the reason for their selection are considered. Various techniques used for increasing the wear resistance of turbine parts are described; these include welded, hard chrome and thick nickel coatings.—B. G. B.

Designing of Ferritic Steel Steam Tubing for High Pressures and Temperatures. H. Haferkamp. (*BWK*, 1956, **8,** July, 333–336). Design data are discussed. It is shown that it is possible to use ferritic steels at high pressures up to 530° C.

Symposium on Exhaust Valve Life. (*Symposium Rept. Inst. Mechanical Eng. Automobile Division*, Preprint, 1956). **Experimental Work on Exhaust Valve Life at Thornton Research Centre,** P. W. Bedale and R. Graham (3–13). A bench test correlating with lives found in practice was developed. **Exhaust Valve Life in Small Industrial Gasoline Engines.** D. Downs. (14–22). Tests on 5 engines are described. Water-cooled engines failed in 210–270 hours and air-cooled in 65–80 hours due to valve stem sticking. Fuel additives and lubricants were investigated. **Performance of Vehicle Engines on Heavily-Leaded Fuels,** R. W. Long, (23–27). **Aero-Engine Exhaust Valve Development,** J. E. Morgan (28–36). **Exhaust Valve Life—Some Metallurgical and Mechanical Considerations.** R. D. Mogford and F. A. Ball (37–43). Corrosion fatigue and hot strength are considered. Tests are given and a basis for development of suitable alloys is discussed.

Economic but Safe Pressure-Vessel Construction. J. J. Murphy, C. R. Soderberg, and D. B. Rossheim. (*Welding Res. Council Bull. Ser.*, 1956, No. 27, May, 11–39). Current requirements of pressure-vessel codes are reviewed and basic principles for revision of the ASME pressure codes are suggested. Fatigue test results obtained from Illinois University tests and Ecole Polytechnique Model vessel tests are reported. The effect of stresses on the design of pressure vessels is discussed.—U. E.

Further Progress in Permanent Magnet Materials. (*Instrument Practice*, 1956, **10,** Apr., 337). An announcement is made of the introduction of three new semi-columnar permanent magnet materials by the Permanent Magnet Association—L. D. H.

HISTORICAL

The Ancient Exploitation of Iron in Berry. A. J. Kerleroux. (*Techn. Civil.*, 1956, **5,** No. 2, 68–76). Archaeological findings connected with iron making in the Berry region of Gaul are briefly described, with photographs.

The History of the Tropenas Process. E. H. Simons. (*Engineer*, 1956, **201,** March, 9, 247–249). The author gives a brief description of the Tropenas steel making process and its first application in Britain in the works of Edgar Allen and Co. in Sheffield in 1890.—M. D. J. B.

High Permeability Steel Castings. An Historical Note. E. N. Simons. (*Elect. Rev.*, 1956, **158,** 10 Feb., 231–232). The early development of the production of dynamo magnet steel castings by Messrs. Edgar Allen is described.

ECONOMICS AND STATISTICS

Industrial Italy. (*Usine Nouvelle*, 1956, Jan., 3–7). The production index has risen from 100 in 1938 to 194 in June 1955. Iron and steel production and raw materials consumption figures are quoted. The Cornigliano steelworks is described. Production is 1600 t/day. Fiat, Innocenti, (Lambretta), and Olivetti organizations are also described.

Economic Development and Technical Progress in the Soviet Iron and Steel Industry. (*Usine Nouvelle*, 1956, Jan., 25–28). The impressions of the British members of the international delegation to Russia are reported.—T. E. D.

Progress in Production. S. J. Cort. (*Iron Steel Eng.*, 1956, **33,** May, 142–144). The author describes the various developments and measures taken to increase production in the U.S.A. since 1949.—M. D. J. B.

MISCELLANEOUS

Atomic Energy and the Steel Industry. P. Comte. (*Mét. Constr. Mécan.*, 1956, **88,** Feb., 123–129). A short assessment of the influence of atomic energy on the Industry in the future is made. The use of radio-active isotopes, produced in piles for non-destructive testing is briefly considered.—B. G. B.

Fundamentals of Chlorine Metallurgy. B. Estberger. (*Tek. Tidskr.*, 1956, **86,** May 8, 445–449). [In Swedish]. Details are given of the theory of the chemical thermodynamics of chlorine metallurgy, followed by its industrial applications such as reduction of chlorides with other metals, use of chlorine for refining metals, and the chlorination of metallic oxides and sulphides.—G. G. K.

New Formulæ Concerning Sedimentation. J. M. Dunoyer. (*J. Chim. Phys.*, 1956, **53,** Apr., 352–358). Rate of sedimentation as a function of the dimensions of the solid particles is studied in the case of spherical particles in laminar and non-laminar flow.—T. E. D.

Crushing and Mixing Under Controlled Conditions—A New Principle Theoretically Developed. M. S. Frenkel. (*Engineering*, 1956, **182,** July 13, 41–42). The author describes a simple fundamental principle which meets all the requirements of a continuous crusher for various materials. It is claimed that the crusher gives uniformity of crushing combined with uniform mixing.—M. D. J. B.

Beryllium. (*Tek. Tidskrift*, 1956, **86,** Apr. 17, 371–374). [In Swedish]. The article reviews world resources of beryllium; its chemical properties and methods employed in the U.S.A. for producing it; mechanical properties and its treatment by vacuum casting, sintering and continuous casting; and the manufacture of beryllium alloys, and its use as a construction material in nuclear reactors.—G. G. K.

BOOK NOTICES

BAKER, J. F. "*The Steel Skeleton.*" Volume I. "*Elastic Behaviour and Design.*" La. 8vo, pp. xi + 206. Illustrated. Cambridge, 1954: The University Press. (Price 50*s.*).

BAKER, J. F., M. R. HORNE, and J. HEYMAN. "*The Steel Skeleton.*" Volume II. "*Plastic Behaviour and Design.*" La. 8vo, pp. xii + 408. Illustrated. Cambridge, 1956: The University Press. (Price 63*s.*).

For nearly thirty years a considerable amount of research effort has been spent in the United Kingdom on design in structural steel. During this time Professor Baker has taken a prominent part, for the first seven years with the Steel Structures Research Committee and subsequently under his own direction. These two volumes, arranged chronologically, give an authoritative account of the whole of the research work and enable a broad view to be obtained of all the stages. They give a clear exposition of the theory, test procedure and results combined with a most interesting narrative of causes, events and effects.

The first volume shows how the empirical regulations of the various countries throughout the world had grown out of the elementary conception of pin-jointed beams and pin-jointed single-storey columns, and the inconsistencies which existed between various specifications. Some of the notable events and work dealt with are the Code of Practice 1931, the new data on live loads in offices and wind pressure and the Perry Robertson strut formula—with the author's comments on the Code's anomalies—the full-size building tests, methods of stress analysis of building frames with semi-rigid beam-to-stanchion connections, the tests on connections used in practice and finally the "Recommendations for Design." Professor Baker very ably makes a well informed commentary on the general disregard of the Committee's recommendations, the later empirical

solution, and the third revision of B.S.449:1948 with its possibly dangerous clauses.

Although with further experience, if that had been obtained, the load factors could have been reduced, the authors show that collapse design can give the greatest economy, and this is the subject of the second volume. This includes the early tests on model portal frames and stanchions; the simple theory; the postulation of general principles, fundamental theorems and methods of analysis in plastic design, together with relevant problems such as initial yield and subsequent shake-down to purely elastic conditions. Whereas the advantages of the plastic theory for designing stanchions for single-storey building has been established, the full and simultaneous application to the design of continuous stanchions and beams has proved intractable, and the authors frankly state that "anything approaching a general method of design seems far away." It is to be hoped that, in time, a satisfactory method will eventuate. There is a full discussion on a suitable load factor to cover various loading conditions, and the volume concludes with interesting descriptions of completed structures designed by this method, and two appendices.

All structural engineers will wish to study these volumes to become acquainted with the ideas discussed here, and will look forward to subsequent text books, suggested by Professor Baker, which have a didactic approach without the historical background and reasoned argument.—J. S. Terrington.

Chalmers, Bruce and R. King (Editors). "*Progress in Metal Physics*, Volume 6." La. 8vo, pp. viii + 354. Illustrated. London and New York, 1956: Pergamon Press, Ltd. (Price 70*s*.).

A glance at the contents list testifies to the judicious editorial choice of subjects for inclusion into the present volume. The six reviews are topical and well written; they should satisfy a wide circle of readers.

The study of the effects of hydrostatic pressures on the electrical resistivity of metals and metalloids generally entails considerable experimental difficulties, but it can fully compensate for these by a wealth of fundamental data on the electronic structure, specific heats, and other properties of the solid state. A. W. Lawson's treatment of this subject is well composed, clear, to the point.

The fundamental role of dislocations in crystal growth and, what may be regarded as its opposite, in the evaporation of metals, has created a real demand for an up-to-date review of the mechanisms of evaporation. This is well met by O. Knacke and I. N. Stranski. Perhaps the emphasis of the paper should have been rather more on the scope of modern techniques in this field, primarily the use of tracer atoms, rather than on the work of the early pioneers.

R. F. Mehl and W. C. Hagel record considerable progress in the understanding of the classical problem of the nature of the austenite/pearlite reaction, but leave the reader in no doubt as to how much still remains unexplained.

The curious, much debated phenomenon of the growth of metal whiskers is discussed by H. K. Hardy, and recent advances in the understanding of creep in metals are well surveyed by A. H. Sully, who succeeds in clearing away much of the confusion due to loose thinking in a subject weighed down heavily by out-of-date approaches.

Finally, P. B. Hirsch provides a most competent review of the nature of the mosaic and macromosaic found in metals. Russian investigators have paid considerable attention to this subject in recent years, both in experimental work and in attempting to relate the dimensions of the mosaic to the applied stress in deformed metals. Many readers would, no doubt, have appreciated the inclusion of a critical assessment of this work.

Whilst, beyond all doubt, the volume will fully maintain the high reputation established for itself by this series, one or two points on the debit side deserve to be mentioned. First, the captions to figures are often inadequate; it is irritating to the reader to find numerous micrographs (e.g., in chapter VI) the legends to which specify neither the original source nor the magnification. Secondly references to work carried out after 1954 are practically non-existent. This is quite serious in a book coming off the press late in 1956.—P. Feltham.

Houdremont, Eduard. "*Handbuch der Sonderstahlkunde*." Dritte, verbesserte Auflage. Unter Mitarbeit von Hans-Joachim Wiester. La. 8vo, illustrated. Erste Band, pp. xvi + 1–874; Zweiter Band, pp. vii + 875–1538. Berlin, Göttingen, Heidelberg, 1956: Springer Verlag: Düsseldorf: Verlag Stahleisen m.b.H. (Price (two volumes) DM. 220.–).

These are two excellent volumes and fortunately for the English reader their style is such that they can be sufficiently understood by any metallurgist with an elementary knowledge of German. A minor criticism is that the name and subject indexes, both of which are adequate, appear only at the end of the second volume, and it is often convenient for both to be at the end of each volume.

Special steels are defined as iron and steel alloys whose special properties are due either to their composition, their method of manufacture or their heat-treatment. There is a certain amount of theory in the volumes, but practical information predominates and is so detailed that for many years to come they will be of great value to all makers of special steels and iron alloys and to metallurgical laboratories attached to engineering establishments.

A two-page introductory section is followed by one dealing with the structure, the mechanical, the physical and the chemical properties of pure iron and of a number of very low-carbon iron alloys, and concluding with particulars of a few of their uses.

Then follows a section dealing with the practical use of the iron–carbon thermal equilibrium diagram in annealing, hardening and general heat-treatment, and concluding with particulars of the technical uses of plain carbon steels. One interesting point discussed is the difference that formerly existed between English and German crucible steels; English crucible steels were characterized by a low silicon content (0·1 to 0·2%) and consequently the depth of hardening was less than that of German crucible steels, which usually contained about 0·4 to 0·6% silicon.

There is next an interesting section which deals in a somewhat novel manner with the alloying elements that are added to iron, and it is followed by sections dealing at length with manganese, nickel, chromium, tungsten, molybdenum, vanadium, cobalt, and silicon steels, respectively. The section devoted to chromium steels is typical of them all. The author first deals in general with the iron–chromium system and with carbon–iron–chromium alloys, and then goes on to discuss the influence of nickel and of manganese on chromium steels. He next considers chromium tool steels, structural steels and the physical properties of chromium steels and the influence of chromium upon the chemical properties of a number of corrosion-resisting alloys containing chromium. He does indeed deal with some alloys that contain no iron such as the nickel-chromium and the nickel-chromium-molybdenum heat-resisting alloys.

Other sections deal with aluminium, copper, oxygen, nitrogen, hydrogen, sulphur and phosphorus, lead, titanium and even with niobium and tantalum, and the rare earths in steel.

The section "Aluminium in steel" is particularly comprehensive and covers a consideration of the system iron–aluminium, carbon–iron–aluminium and iron–nickel–aluminium, and it is in this section that the modern iron–nickel–aluminium permanent-magnet alloys are described. A great deal of information about permanent-magnet alloys is also to be found in the section devoted to cobalt steels.

Indeed, in the confines of this short review, it is not possible to convey the scope of these two volumes, and one can but say that the author appears to have omitted nothing.—J. Ferdinand Kayser.

Levin, Ernest M., Howard F. McMurdie and F. P. Hall. "*Phase Diagrams for Ceramists*." (Fifth compilation]. La. 8vo, pp. [ii +] 286. Illustrated. Columbus, Ohio, 1956: The American Ceramic Society. (Price $10).

Some years ago Dr. Herbert Insley remarked somewhat ruefully to the present reviewer that, when he and Dr. F. P. Hall first prepared a compilation of phase diagrams for the American Ceramic Society, they appeared to have taken on a job for life. Be that as it may, the first issue, which appeared in 1933, was followed by revised and enlarged versions in 1938 and 1947 by the same authors and by a short supplement in 1949 by H. F. McMurdie and F. P. Hall. The new issue, although Dr. Insley's name

no longer appears on it, follows the pattern of its predecessors in presentation and arrangement and contains 800 diagrams as compared to 507 in the 1947 edition. The most recent of these are from papers published in 1955, but, since these and most of the diagrams representing 1954 are from American sources, it would appear that the authors did not continue their search of the foreign literature beyond 1952–53. Amongst the newer diagrams we noted a number relating to polycomponent oxide systems which are important to the technology of metallurgical slags, and to halide systems, which have been the object of some attention in recent years as possible alternatives to oxides and sulphides for use as containers for reactive metals in the liquid state. Recent interest in the hydrothermal synthesis of minerals is reflected in the number of new diagrams for systems containing water as a component.

In addition to the actual phase diagrams the book also contains an extremely useful and concise introductory section dealing with the theory of phase diagrams, an explanatory note on the differences between the Geophysical and International Temperature Scales, which are still the source of some confusion in the literature, and a comprehensive alphabetical index to the systems included in the compilation, the latter replacing the tabular form of index used in the earlier versions. Like its predecessors, the new edition will undoubtedly be regarded as indispensible not only by ceramists but by all who are concerned in any way with the high-temperature behaviour of non-metallic inorganic materials.—J. WHITE.

MEETHAM, A. R. "*Atmospheric Pollution—Its Origins and Prevention.*" Second revised edition. 8vo, pp. ix + 302. Illustrated. London and New York, 1956: Pergamon Press. (Price 63*s.*).

This edition is an attempt to bring up to date a work written before 1952, for the purpose of helping the fight against atmospheric pollution in this country.

Since the original publication the occurrence of the London Smog at the end of 1952, and its sequel, the Beaver Report and the Clean Air Act, have raised the subject out of the rut it was then in, and one would therefore have expected, when the need for a new edition arose, that the author would have made a more complete revision of the text that has taken place.

With the exception of the additional Chapter XVI, which deals adequately enough with the newer sources of pollution arising from the greater use of liquid fuel and the potentialities of nuclear reactions, only minor modifications have been introduced. As the sub-title indicates that not only the origin of pollution was to be dealt with but also its prevention, reference could have been made to such developments as have taken place since the initial publication, and the impending new legislation, the introduction of improved and new methods of preventing dust from reaching the atmosphere, the production of more types of instruments to detect the presence of smoke, to quote only a few, could have been referred to in a more prominent manner, even if it had meant a reshuffling or shortening of those parts of the book having only a side connection with the main subject.

The author can be further criticized for not having eliminated some of the obvious imstakes that occurred in the first edition. On the other hand, he can be thanked for the inclusion of the supplementary bibliography.—NEIL H. TURNER.

NEW PUBLICATIONS

AKADEMIK ZDENĚK BĂZANT. "*Slovník Stavebné Mechaniky a Příbuzných Oborů v Pěti Rečích.*" Dictionary of Structural Mechanics. 8vo, pp. 251. Praha, 1953: Nakladatelstoí Československé Akademie. Věd. (Price 28*s.*).

AMERICAN INSTITUTE OF MINING AND METALLURGICAL ENGINEERS. "*Nuclear Metallurgy.*" A Symposium on Behavior of Materials in Reactor Environment, February 20, 1956, arranged by Nuclear Metallurgy Committee. (Institute of Metals Division Special Report Series No. 2). La. 4to, pp. [ii +] 94. Illustrated. New York, 1956: The Institute. (Price $3.75).

BARWELL, F. T. "*Lubrication and Bearings.*" 8vo, pp. xi + 292. Illustrated. London, 1956: Butterworths Scientific Publications. (Price 50*s.*).

BOËTHIUS, BERTIL, AND ÅKE KROMNOW. "*Jernkontorets Historia.*" Del III. "*Jernkontoret och Tekniken Före Götstålsprocesserna.*" Part 1, text; Part 2, supplement. La. 8vo, illustrated. Part 1, pp. xvi + 547; Part 2, pp. 213. Stockholm, 1955: Jernkontoret.

BRITISH STANDARDS INSTITUTION. B.S. 468: 1956. "*Solid Rolled Steel Railway Wheels and Disc Wheel Centres.*" 8vo. pp. 13. London, 1956: The Institution. (Price 3*s.*).

BRITISH STANDARDS INSTITUTION. B.S. 874: 1956. "*Definitions of Heat Insulating Terms and Methods of Determining Thermal Conductivity.*" 8vo. pp. 22. London, 1956: The Institution. (Price 5*s.*).

CHAMBRE SYNDICALE DE LA SIDÉRURGIE FRANÇAISE." *Sidérurgie Française. Sidérurgie Sarroise. Annuaire*, 1956." La. 4to, pp. 277. Paris, 1956: Les Éditions M. Colomb.

FINNISTON, H. M. and J. P. HOWE. "*Progress in Nuclear Energy.*" Series V. "*Metallurgy and Fuels.*" 8vo, pp. viii + 785. Illustrated. London, New York, 1956: Pergamon Press. (Price £7 7*s.*).

FREDE, LUDGER. "*Fachkunde für Former.*" 8vo, pp. vii + 167. Illustrated. Weinheim/Bergstrasse, Berlin, 1956: Verlag Julius Beltz.

"*Gmelins Handbuch der Anorganischen Chemie.*" Achte völlig neu bearbeitete Auflage. System-Nummer 28: "*Calcium.*" Teil B, Leiferung 1: "*Technologie.*" La. 8vo, pp. viii + 264. Illustrated. Weinheim/Bergstrasse, 1956: Verlag Chemie, GmbH. (Price DM. 147.–).

INTERNATIONAL LABOUR OFFICE. "*Production and Employment in the Metal Trades. The Problem of Regularisation.*" Studies and Reports, New Series. No. 44. pp. 121. (Price 7*s.* 6*d.*).

INTERNATIONAL UNION OF THEORETICAL AND APPLIED MECHANICS. "*Colloquium on the Deformation and Flow of Solids*, Madrid, September 26–30, 1955." Edited by R. Grammel. La. 8vo, pp. xii + 324. Illustrated. Berlin, Göttingen, Heidelberg, 1956: Springer-Verlag. (Price DM. 37.50).

KNIPP, ERWIN. "*Die Gegossenen Metallischen Werkstoffe.*" Zahlentafeln über Zusammensetzungen, Eigenschaften und Verwendungszwecke von Grauguss, Temperguss, Stahlguss, Schwermatallen, Leichmetallen und Lagermetallen. 8vo, pp. 173. Düsseldorf, 1956: Giessserei-Verlag.

KRISHNAN, M. S. "*Iron Ores of India.*" 8vo, pp. [xi +] 177. Illustrated. Calcutta, 1955: Indian Association for the Cultivation of Science. (Price 10*s.* 6*d.*).

LANSE, H., and KOHLHAAS, R. "*Über die Wärmeleitfähigkeit von Stählen bei hohen Temperaturen*" *I. Teil.* "*Literaturbericht*" (Forschungsberichte des Wirtschaft —und Verkehrsministeriums Nordrhein-Westfalen, No. 263.). 4to, pp. 37. Köln und Opladen, 1956: Westdeutscher Verlag. (Price DM. 10.70).

LE BRETON, H. "*Défauts des Pièces de Fonderie.*" Tome 1: "*Défauts dus au Mode de Solidification de l'Alliage Coulé.*" (Collection Technologie de Fabrication, 14.) La. 8vo, pp. 284. Illustrated. Paris, 1956: Editions Eyrolles. (Price 3045 fr.).

THE PHYSICAL SOCIETY. "*Reports on Progress in Physics.*" Vol. XIX (1956). Executive Editor, A. C. Strickland. La. 8vo, pp. [iv +] 367. Illustrated. London, 1956: The Society. (Price 50*s.*).

PROCHAZKA, JINDŘICH. "*English-Czech* and *Czech-English Dictionary.*" Fifteenth revised and enlarged edition. Sma. 8vo, pp. [iv +] 599. London, 1952: George Allen and Unwin, Ltd. (Price 25*s.*).

"*Russian–English Glossary of Metallurgical and Metal-Working Terms.*" Editorial Director, Paul W. Howerton; Compiler, Alexander Akhonin. La. 8vo, pp. iii + 175. (Mimeographed). Cambridge, Massachusetts, 1955: Center for International Studies, Massachusetts Institute of Technology. (Price 8*s.* 6*d.*).

UDY, MARVIN J. "*Chromium.*" American Chemical Society. Monograph No. 132, in 2 Volumes). 8vo. Each volume, pp. 450. Illustrated. New York, 1956: Reinhold Publishing Corp. (Price, each volume $11; together $19.50).

F. B. GEORGE, B.Sc.

FRANK BERNARD GEORGE served with the army from 1917 to 1918. After demobilization he joined Swan Hunter of Wallsend as an engineering apprentice. He graduated from Durham University with the degree of B.Sc. in mechanical engineering, and in 1924 joined the Steel Company of Canada. Later that year he moved to the U.S.A. where he worked for the Inland Steel Corporation, but in 1925 he returned to the United Kingdom to join Consett Iron Company Ltd., his present company, as Assistant Mill Manager. He became Mill Manager in the following year, and Works Manager in 1939. He was promoted successively to Works Development Manager in 1946, to General Works Manager in 1951, and to his present position as Director and General Manager in 1956.

Mr. George joined The Iron and Steel Institute in 1928. He has been a member of the Cleveland Institution of Engineers for a number of years, and was elected President for the 1956–1957 Session; as such he serves as an Honorary Member of Council of The Iron and Steel Institute during his term of office.

F. B. George, B.Sc.,

Honorary Member of Council, 1956–1957